

AD-A032 801

ARMY ELECTRONICS COMMAND FORT MONMOUTH N J
PROCEEDINGS OF INTERNATIONAL WIRE AND CABLE SYMPOSIUM (25TH) HE--ETC(U)
NOV 76

F/G 17/2

UNCLASSIFIED

NL

1 OF 5
ADA032801





ADA 032801

1952 Silver Jubilee 1976

IWCS



COPY AVAILABLE TO DDC DOES NOT
PERMIT FULL-SCALE PRODUCTION

Proceedings of the Twenty-fifth International wire and
cable symposium 16th, 17th, 18th, November 1976

Cherry Hill Hyatt House, Cherry Hill, N.J.



SPONSORED BY THE
U.S. ARMY ELECTRONICS COMMAND
FORT MONMOUTH, N.J.

DISTRIBUTION STATEMENT A
Approved for public release;
Distribution Unlimited

UNCLASSIFIED

SECURITY CLASSIFICATION OF THIS PAGE (When Data Entered)

REPORT DOCUMENTATION PAGE		READ INSTRUCTIONS BEFORE COMPLETING FORM
1. REPORT NUMBER N/A	2. GOVT ACCESSION NO.	3. RECIPIENT'S CATALOG NUMBER
4. TITLE (and Subtitle) Proceedings of the 25th International Wire and Cable Symposium 1976		5. TYPE OF REPORT & PERIOD COVERED Final 16-18 November 1976
		6. PERFORMING ORG. REPORT NUMBER N/A
7. AUTHOR(s) Various Chairman: Elmer F. Godwin		8. CONTRACT OR GRANT NUMBER(s) None
9. PERFORMING ORGANIZATION NAME AND ADDRESS Xmsn & Electromech Dvc Team (DRSEL-TL-ME) Electronic Technology & Dvc Lab USA Elcts Command, Ft. Monmouth, NJ		10. PROGRAM ELEMENT, PROJECT, TASK AREA & WORK UNIT NUMBERS Proj. Element: 62705A Proj./Task: 1S7 62705 AH94 W1 01; Work Unit #: 012C8
11. CONTROLLING OFFICE NAME AND ADDRESS Xmsn & Electromech Dvc Team (DRSEL-TL-ME) Electronic Technology & Dvc Lab USA Elcts Command, Ft. Monmouth, NJ		12. REPORT DATE November 1976
14. MONITORING AGENCY NAME & ADDRESS (if different from Controlling Office) Same as 11 above.		13. NUMBER OF PAGES 431
		15. SECURITY CLASS. (of this report) UNCLASSIFIED
		15a. DECLASSIFICATION/DOWNGRADING SCHEDULE N/A
16. DISTRIBUTION STATEMENT (of this Report) Approved for Public Release: Distribution Unlimited.		
17. DISTRIBUTION STATEMENT (of the abstract entered in Block 20, if different from Report)		
18. SUPPLEMENTARY NOTES Proceedings of technical papers presented at 25th International Wire and Cable Symposium sponsored annually by the US Army Electronics Command.		
19. KEY WORDS (Continue on reverse side if necessary and identify by block number) Aerospace electronics, cable design, cable evaluation, cable manufacture, cable materials, cable performance, electronic wiring, fiber optics, inter-connections, military electronics, telephone communications, wire insulation, wire materials.		
20. ABSTRACT (Continue on reverse side if necessary and identify by block number) The International Wire & Cable Symposium is the only symposium of its kind in the world. The proceedings include fifty-seven (57) papers in the field of electrical and electronic wire and cable, covering design, materials, testing, evaluation, connections, splicing, installation, applications, fiber optics, manufacturing, and processing.		

DD FORM 1 JAN 73 1473

EDITION OF 1 NOV 65 IS OBSOLETE

UNCLASSIFIED

SECURITY CLASSIFICATION OF THIS PAGE (When Data Entered)

6

8

**PROCEEDINGS OF
25th INTERNATIONAL
WIRE AND CABLE
SYMPOSIUM** (25th)

**Sponsored by
U.S. Army Electronics Command**

Held at

**Cherry Hill, New Jersey, on
November 16, 17 and 18, 1976**

11 Nov 76

12 429p.

DDC
RECEIVED
NOV 29 1976
RECEIVED

A

**APPROVED FOR PUBLIC RELEASE; DISTRIBUTION
UNLIMITED**

ACQUISITION	
HTG	
DIS	
MAIL ROOM	
POSTAL	
BY	
EXTENSION	
DATE	
A	

037620

B

25th INTERNATIONAL WIRE AND CABLE SYMPOSIUM

SYMPOSIUM COMMITTEE

Elmer F. Godwin, Co-Chairman, USAECOM (201-544-2770)
Milton Tenzer, Co-Chairman, USAECOM (201-544-4834)
Marta Farago, Northern Telecom Ltd.
F. M. Farrell, 3M Company
Joseph M. Flanigan, Rural Electrification Administration (REA)
James Kanely, Superior Continental Corp.
Irving Kolodny, General Cable Corp.
Sherman Kottle, Dow Chemical U.S.A.
Joe Neigh, AMP Inc.
Frank Short, Belden Corp.
George H. Webster, Bell Laboratories

TECHNICAL SESSIONS

Tuesday, 16 November 1976

9:30 a.m. Session I: Tutorial on Telecommunication — Yesterday, Today
and Tomorrow
2:00 p.m. Session II: Cable Design
2:00 p.m. Session III: Cable Materials I

Wednesday, 17 November 1976

9:00 a.m. Session IV: Cable Testing and Evaluation
9:00 a.m. Session V: Connections, Splicing and Installation
2:00 p.m. Session VI: Cable Applications
2:00 p.m. Session VII: Fiber Optics

Thursday, 18 November 1976

9:00 a.m. Session VIII: Cable Materials II
9:00 a.m. Session IX: Cable Manufacturing and Processing I
2:00 p.m. Session X: Cable Materials III
2:00 p.m. Session XI: Cable Manufacturing and Processing II

PROCEEDINGS

Responsibility for the contents rests upon the authors and not the Symposium Committee or its members. After the symposium all the publication rights of each paper are reserved by their authors, and requests for republication of a paper should be addressed to the appropriate author. Abstracting is permitted, and it would be appreciated if the symposium is credited when abstracts or papers are republished. Requests for individual copies of papers should be addressed to the authors. Extra copies of the Proceedings may be obtained from the Symposium Chairman, US Army Electronics Command, ATTN: DRSEL-TL-ME, Ft. Monmouth, NJ, 07703. (One to three copies \$10.00 each; four to ten copies \$8.00 each; eleven copies and above \$5.00 each). Copies may also be obtained for a nominal fee from the National Technical Information Service (NTIS), Operations Division, Springfield, Virginia, 22151.

Copies of papers presented in previous years may also be obtained from the National Technical Information Service. Papers from the first 24 years, with their AD numbers are catalogued in the "KWIC Index of Technical Papers, Wire and Cable Symposium (1952-1975)," December 1976 (AD-A027558).



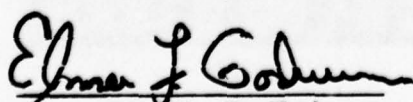
MESSAGE FROM THE CO-CHAIRMEN

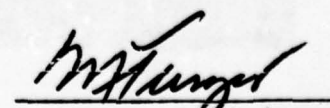
Your Co-Chairmen heartily welcome you to the 25th International Wire and Cable Symposium. The symposium last year was the most successful one held to date, with the largest attendance (over 1350) of any previous symposium. It was a very successful meeting as evidenced by the crowded and at times standing room only space available during many of the technical sessions. The Committee received many compliments from attendees and supporters with respect to the technical sessions and the new location for the symposium.

This year's symposium represents our silver anniversary and the Committee is looking forward to a very exciting and enthusiastic meeting. The response to the "Call for Papers" was tremendous and sixty technical papers are scheduled for presentation. This Silver Anniversary Symposium will also feature an opening session with a panel of experts who will contrast the enormous progress made in wire and cable technology during the past twenty-five (25) years with an even greater potential for the next twenty-five.

Committee members Joseph M. Flanigan of the Rural Electrification Administration (REA) and James Kanely of Superior Continental Corp. are retiring from the Committee after three years of outstanding service. Joe and Jim contributed significantly to the success of the Committee's mission. On behalf of the rest of the Committee your Co-Chairmen wish to thank them both for their efforts and valuable contributions to the wire/cable industry and wish them well in their future activities.

Your Co-Chairmen once again gratefully acknowledge the unstinting efforts of our Committee members and the unqualified cooperation of representatives of the many industrial organizations and government activities in attendance at these very successful symposia. We look forward to the continued enthusiastic support by members of the wire and cable industry and the dedicated support of our Committeemen to ensure comparable success in future years.


E. F. GODWIN, Co-Chairman


M. TENZER, Co-Chairman

Committee Members 1952 - 1976

COMMITTEE MEMBERS SHOWN

- 1 I. Stoneback
- 2 H. Wuerth
- 3 F. Willis
- 4 H. Kingsley
- 5 J. Robb
- 6 C. Wyman
- 7 B. Levinson
- 8 B. Jore
- 9 L. Tomlinson
- 10 R. Blain
- 11 H. Kitts
- 12 G. Hamburger
- 13 E. Burrough
- 14 J. McBride
- 15 J. Perkins
- 16 R. Devany
- 17 M. Caine
- 18 F. Scoville
- 19 J. Ruskin
- 20 M. Tenzer
- 21 F. Oberlander
- 22 S. Luques
- 23 R. Watt
- 24 F. Horn
- 25 J. Spergel
- 26 M. Suba
- 27 M. Lipton
- 28 E. Wolff
- 29 L. Dunlop
- 30 L. Gumina
- 31 J. Kirk
- 32 E. Godwin
- 33 G. Heller
- 34 W. Smith
- 35 L. Frisco
- 36 J. Hager
- 37 A. Averill
- 38 M. Farago
- 39 I. Kolodny
- 40 J. Kanely
- 41 S. Kottle
- 42 G. Webster
- 43 J. Neigh
- 44 R. Spade
- 45 E. Short
- 46 S. Montgomery
- 47 J. Roache
- 48 J. Flanagan
- 49 R. Mildner
- 50 M. Noble
- 51 W. Rigling
- 52 F. Harden



COMMITTEE MEMBERS NOT SHOWN

- R. Graharr
H. Weber
A. Maibau
G. Forsber
W. Crater
P. Grogan
E. Love
E. Merrill
A. McKea
R. Houliha
W. Acton
W. Bracke
L. Kent
B. Tyrell
L. Marrin
L. Adelso
G. Lohsl
J. Roark
D. Stewa
J. Toome
W. Smith
R. Solom
C. Hatch



Guest Speaker Mr. Lee Oberst, Vice President, New York Telephone Company

HIGHLIGHTS OF THE 24th INTERNATIONAL WIRE AND CABLE SYMPOSIUM

November 18, 19, 20, 1975
Cherry Hill Hyatt House, Cherry Hill, N.J.



Panel Members—Tutorial Session: Messrs. V. Sielert, General Telephone and Electronic Corp.; G. Landis, Allendale Insurance and E. J. Coffey, Underwriters Laboratories, Inc.



Co-Chairmen with Committee Members. Standing left to right: J. Hager, Northern Petrochemical Co.; I. Kolodny, General Cable Corp.; G. Heller, Tensolite Co.; J. Kanely, Superior Continental Corp.; F. M. Farrell, 3M Company; G. Webster, Bell Laboratories; J. Flanigan, REA; J. Neigh, AMP Inc. and seated Martha Farago, Northern Telecom, Ltd.



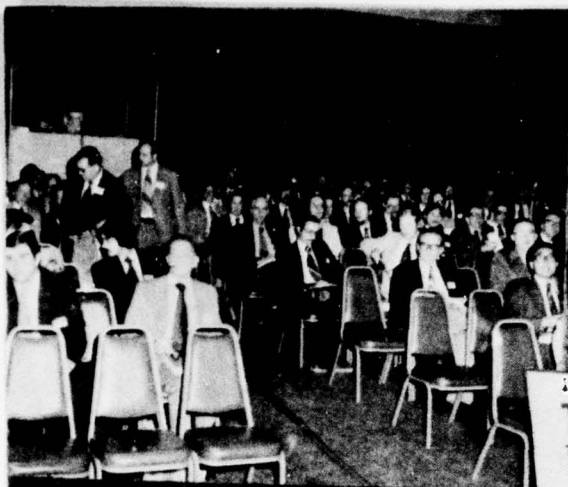
Award Winners (1975) — T. S. Choo, 3M Company, Outstanding Technical Paper; and J. Wimsey, IJS Airforce, Best Presentation



Awards presented by the symposium co-chairmen to G. Webster (left), Bell Laboratories for Best Presentation (1974); D. Doty (2nd right), AMP Inc. for Outstanding Technical Paper (1974); G. Heller (2nd left) Tensolite Co. and J. Hager (right) Northern Petrochemical Co. Certificates of Appreciation for serving three years on the Symposium Committee.

Candid Scenes at the 24th IWCS





TECHNICAL SESSIONS

TUESDAY, NOVEMBER 18

SESSION I 9:30 am - 12:00 pm TUTORIAL ON WIRE AND CABLE CONSIDERATIONS IN TIMES HUNTERDON & CUMBERLAND ROOMS

SESSION II 2:15 pm - 5:15 pm RELIABILITY CONSIDERATION IN CABLES GLOUCESTER ROOM

SESSION III 2:15 pm - 5:15 pm MANUFACTURING & PROCESSING HUNTERDON ROOM

WEDNESDAY, NOVEMBER 19

SESSION IV 9:15 am - 12:15 pm CABLE APPLICATIONS I GLOUCESTER ROOM

SESSION V 9:15 am - 12:15 pm CABLE DESIGN HUNTERDON ROOM

SESSION VI 2:15 pm - 5:15 pm TESTING & EVALUATION GLOUCESTER ROOM

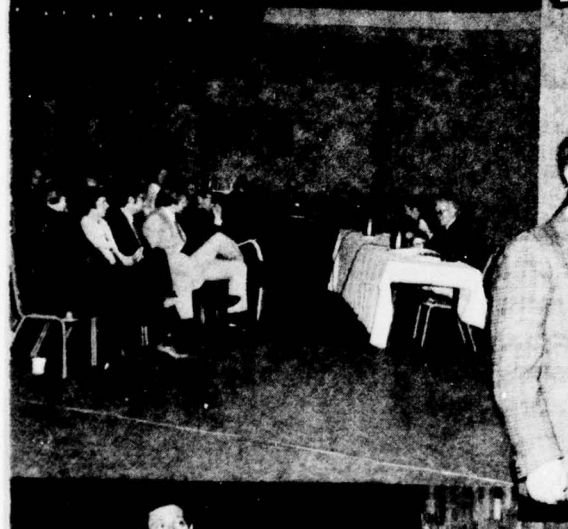
SESSION VII 2:15 pm - 5:15 pm CABLE MATERIALS I HUNTERDON ROOM

THURSDAY, NOVEMBER 20

SESSION VIII 9:15 am - 12:15 pm CABLE APPLICATIONS II GLOUCESTER ROOM

SESSION IX 9:15 am - 12:15 pm CABLE MATERIALS II HUNTERDON ROOM

SESSION X 2:15 pm - 5:15 pm WATERPROOF CABLE HUNTERDON ROOM





AWARDS

Outstanding Technical Paper

- | | |
|---|------|
| H. Lubars and J. A. Olszewski, General Cable Corp.—"Analysis of Structural Return Loss in CATV Coaxial Cable" | 1968 |
| J. B. McCann, R. Sabia and B. Wargotz, Bell Laboratories—"Characterization of Filler and Insulation in Waterproof Cable" | 1969 |
| D. E. Setzer and A. S. Windeler, Bell Laboratories—"A Low Capacitance Cable for the T2 Digital Transmission Line" | 1970 |
| R. Iyenger, R. McClean and T. McManus, Bell Northern Research—"An Advanced Multi-Unit Coaxial Cable for Tool PCM Systems" | 1971 |
| J. B. Howard, Bell Laboratories—"Stabilization Problems with Low Density Polyethylene Insulations" | 1972 |
| Dr. H. Martin, Kabelmetal—"High Power Radio Frequency Coaxial Cables, Their Design and Rating" | 1973 |
| D. Doty, AMP inc.—"Mass Wire Insulation Displacing Termination of Flat Cable" | 1974 |
| T. S. Choo, Dow Chemical U.S.A.—"Corrosion Studies on Shielding Materials for Underground Telephone Cables" | 1975 |

Best Presentation

- | |
|--|
| N. Dean, B.I.C.C.—"The Development of Fully Filled Cables for the Distribution Network" |
| J. D. Kirk, Alberta Government Telephones—"Progress and Pitfalls of Rural Buried Cable" |
| Dr. O. Leuchs, Kabel and Metalwerke—"A New Self-Extinguishing Hydrogen Chloride Binding PVC Jacketing Compound for Cables" |
| S. Nordblad, Telefonaktiebolaget LM Ericsson—"Multi-Paired Cable of Nonlayer Design for Low Capacitance Unbalance Telecommunication Network" |
| N. Kojima, Nippon Telegraph and Telephone—"New Type Paired Cable for High Speed PCM Transmission" |
| S. Kaufman, Bell Laboratories—"Reclamation of Water-Logged Buried PIC Telephone Cable" |
| R. J. Oakley, Northern Electric Co., Ltd.—"A Study into Paired Cable Crosstalk" |
| G. H. Webster, Bell Laboratories—"Material Savings by Design in Exchange and Trunk Telephone Cable" |
| J. E. Wimsey, United States Airforce—"The Bare Base Electrical Systems" |

CONTRIBUTORS

- Abbott Industries, Inc.**
Leominster, Massachusetts
- Aktieselskabet**
Nordiske Kabel- og Traadfabriker
Copenhagen, Denmark
- Alcan Aluminum Corporation**
Alcan Cable Division
Atlanta, Georgia
- Allied Chemical Corporation**
Morristown, New Jersey
- Alpha Associates, Inc.**
Woodbridge, New Jersey
- AMP Incorporated**
Harrisburg, Pennsylvania
- The Anaconda Company**
Aluminum Division
Louisville, Kentucky
- Anaconda Telecommunications**
Overland Park, Kansas
- Anchorage Telephone Utility**
Anchorage, Alaska
- ARCO Polymers**
Philadelphia, Pennsylvania
- Arnold Field Associates**
Hackensack, New Jersey
- Arvey Corporation**
Jersey City, New Jersey
- ATO-CHIMIE (M. NURY)**
Orthez, France
- Austral Standard Cables Pty. Limited**
Melbourne, Victoria, Australia
- Autometrix**
Dayton, Ohio
- Baker Industries, Inc.**
Hartselle, Alabama
- Belden Corporation**
Geneva, Illinois
- Berk-Tek, Inc.**
Reading, Pennsylvania
- BICC Telecommunication Cables Ltd.**
Prescot, Merseyside, England
- The Boeing Company**
Wichita, Kansas
- Boston Insulated Wire and Cable Company, Ltd.**
Hamilton, Ontario, Canada
- Brand-Rex Company**
Willimantic, Connecticut
- Buchanan Crimp Tool Products**
Union, New Jersey
- Burndy Corporation**
Norwalk, Connecticut
- Cable Consultants Corporation**
Larchmont, New York
- Cable Equipment Corporation**
New York, New York
- Cables de Comunicaciones, S.A.**
Zaragoza, Spain
- Cabot Corporation**
Boston, Massachusetts
- Camden Wire Co., Inc.**
Camden, New York
- Canada Wire and Cable Limited**
Winnipeg, Manitoba, Canada
- Canadian Industries Limited**
Brampton, Ontario
- Campbell Technical Waxes Limited**
Crayford, Kent, England
- Carlew Chemicals Ltd.**
Montreal, Quebec, Canada
- R. E. Carroll, Inc.**
Trenton, New Jersey
- Cary Chemicals, Inc.**
Edison, New Jersey
- Central Tool & Machine Co.**
Bridgeport, Connecticut
- Cerro Communication Products**
Freehold, New Jersey
- Cerro Wire & Cable Co.**
Division of Cerro Marmon Corporation
Maspeth, New York
- Chase & Sons, Inc.**
Randolph, Massachusetts
- Chemplast, Inc.**
Wayne, New Jersey
- Cimco Wire & Cable Inc.**
Division of E-B Industries Inc.
Allendale, New Jersey
- Citcom Systems, Inc.**
New York, New York
- Cities Service Company**
Chester Cable Operations
Chester, New York
- Columbia Cable & Electric Corp.**
Brooklyn, New York
- Columbia Research Corporation**
Gaithersburg, Maryland
- Continental Wire & Cable Corp.**
York, Pennsylvania
- Copperweld Bimetals Division**
Glassport, Pennsylvania
- Crompton & Knowles Corporation**
Davis-Standard Division
Pawcatuck, Connecticut
- Dainichi-Nippon Cables, Ltd.**
Osaka, Japan
- Dardanio Manuli S.p.A.**
Brugherio (Milano), Italy
- Dart Industries Inc.**
Paramus, New Jersey
- Devcon Corporation**
Telephone & Power Products Division
Danvers, Massachusetts
- Diamond Shamrock Chemical Company**
Cherry Hill, New Jersey
- Dodge Fluorglas Division**
OAK Materials Group
Hoosick Falls, New York
- The Dow Chemical Company**
Midland, Michigan
- Dow Corning Corporation**
Midland, Michigan
- Dussek Bros. (Canada) Limited**
Belleville, Ontario, Canada
- Easy Heat/Wirekraft**
Rolling Prairie, Indiana
- Eastman Chemical Products, Inc.**
Kingsport, Tennessee
- Easy Heat — Wirekraft**
Rolling Prairie, Indiana
- Economy Cable Grip Co., Inc.**
South Norwalk, Connecticut
- Edmands Division Wanskuck Company**
Providence, Rhode Island

Elco Corporation
El Segundo, California
Electroconductores, C.A.
Caracas, Venezuela
The Electron Machine Corporation
Umatilla, Florida
Electronized Chemicals Corporation
(Burlington Operations Division)
Burlington, Massachusetts
The Entwistle Company
Hudson, Massachusetts
Exxon Chemical Company U.S.A.
Houston, Texas
Fabrics Manufacturing Limited
Trenton, Ontario, Canada
Felten & Guillaume Carlswerk AG
Bereich Nachrichtenkabeltechnik NK
Köln, Germany
Firestone Plastics Company
Pottstown, Pennsylvania
Formulabs Industrial Inks Inc.
Escondido, California
Foster Grant Company, Inc.
Subsidiary of American Hoechst Corporation
Leominster, Massachusetts
The Fujikura Cable Works, Ltd.
Tokyo, Japan
The Furukawa Electric Company Limited
Chiyoda-ku, Tokyo, Japan
Gary Chemicals, Inc.
Edison, New Jersey
Gavitt Wire & Cable Division
Brookfield, Massachusetts
General Cable Corporation
Colonia, New Jersey
General Electric Company
Silicone Products Department
Waterford, New York
General Engineering U.S.A., Ltd.
Stratford, Connecticut
GGG Hatfield Communication Products
Cranford, New Jersey
Duncan M. Gillies Co., Inc.
West Boylston, Massachusetts
Glenair, Inc.
Glendale, California
W. L. Gore & Associates, Inc.
Newark, Delaware
W. R. Grace & Company
Hatco Plastics Division
Brooklyn, New York
Great American Chemical Corporation
Fitchburg, Massachusetts
GTE Automatic Electric (Canada) Ltd.
Toronto, Ontario, Canada
GTE Lenkurt
San Carlos, California
GTE Service Corporation
Stamford, Connecticut
HABIA K/B
Krivsta, Sweden
Hardman Incorporated
Belleville, New Jersey
Heany Industries Inc.
Scottsville, New York
Hercules Incorporated
Scott Wise Industries
Crowley, Louisiana

Hercules Incorporated
Wilmington, Delaware
Hewlett-Packard
Palo Alto, California
High Voltage Engineering Corp.
Burlington, Massachusetts
Hitachi Cable Limited
Tokyo, Japan
Hitemp Wire Division — ALI
Covina, California
Hudson Wire Company
Ossining, New York
Icore Wire & Cable
Santa Barbara, California
Independent Cable, Inc.
Hudson, Massachusetts
International Business Machines Corp.
Rochester, Minnesota
International Wire Products Co.
Wyckoff, New Jersey
ITT Electro-Optical Products Division
Roanoke, Virginia
Judd Wire Division
Turners Falls, Massachusetts
Kenrich Petrochemicals, Inc.
Bayonne, New Jersey
Lamart Corporation
Clifton, New Jersey
Larabee Wire, Inc.
Camden, New York
S.A. Lignes Telegraphiques et Telephoniques
Conflans Sainte Honorine, France
Lowe Associates, Inc., J. J.
Reels and Tape Division
Bedford Hills, New York
Madison Wire & Cable Company
South Lancaster, Massachusetts
Maillefer S.A.
Ecublens-Lausanne, Switzerland
Mark-Mor Tool & Die Company, Inc.
Allenwood, New Jersey
J. Frank Market & Sons, Inc.
Norristown, Pennsylvania
Micro-Tek Corporation
Cinnaminson, New Jersey
3M Company
TelComm Division
St. Paul, Minnesota
Monsanto Industrial Chemicals Co.
St. Louis, Missouri
The Montgomery Company
Windsor Locks, Connecticut
S. R. Morrow Company
Chatham, New Jersey
MSP Industries Corporation
East Heat/Wirekraft Division
Rolling Prairie, Indiana
H. Muehlstein & Co., Inc.
Greenwich, Connecticut
Nesor Alloy Corporation
West Caldwell, New Jersey
New England Printed Tape Company
Pawtucket, Rhode Island
Nippon Telegraph and Telephone
Public Corporation
Tokai, Ibaraki-ken, Japan
NKF KABEL B.V.
Delft, Holland

N.L. Industries

Hightstown, New Jersey

Nonotuck Manufacturing Company

South Hadley, Massachusetts

Northern Petrochemical Company

Des Plaines, Illinois

Northern Telecom Limited

Montreal, Quebec, Canada

The Okonite Company

Providence (Rumford), Rhode Island

Olex Cables Limited

Melbourne, Victoria, Australia

Omni Chemical Corporation

Lyndhurst, New Jersey

Oy Nokia Ab

Helsinki, Finland

The Pantasote Company of N.Y., Inc.

Passaic, New Jersey

Pennwalt Corporation

Philadelphia, Pennsylvania

Penreco

Butler, Pennsylvania

PFD/PENN Color, Inc.

Doylestown, Pennsylvania

Phalo Corporation

Shrewsbury, Massachusetts

Phelps Dodge International Corporation

New York, New York

Phillips Cables Limited

Brockville, Ontario, Canada

Phillips Chemical Company

Pasadena, Texas

Pirelli USA Representative Corp.

New York, New York

Plastics Division

Pasadena, Texas

Plastoid Corporation

New York, New York

Plymouth Rubber Co., Inc.

Canton, Massachusetts

Plymouth Wire & Cable Company

Worcester, Massachusetts

Polymer Services Inc.

East Brunswick, New Jersey

Ets. Pourtier Pere & Fils

Romainville, France

Prestolite Wire Division

Port Huron, Michigan

Radiation Dynamics, Inc.

Westbury, New York

Radix Wire Company

Euclid, Ohio

Raychem Corporation

Menlo Park, California

Reichhold Chemicals, Inc.**Cooke Division**

Hackettstown, New Jersey

Revere Corporation of America

Wallingford, Connecticut

G. Whittfield Richards Co.

Philadelphia, Pennsylvania

The Rochester Corporation

Culpeper, Virginia

Rockbestos: Products**Cerro Wire & Cable Company****Division of Cerro-Marmon Corp.**

New Haven, Connecticut

John Royle & Sons

Paterson, New Jersey

St. Joe Minerals Corporation

Monaca, Pennsylvania

Santech Incorporated—Ware Division

Toronto, Canada

Shell Chemical Company

Houston, Texas

Siemens Corporation, CED

Iselin, New Jersey

Soltex Polymer Corporation

Houston, Texas

Southwest Chemical & Plastics Company

Seabrook, Texas

Southwire Company

Carrollton, Georgia

Standard Electrica, S.A.

Maliano (Santander Espana)

Standard Elektrik Lorenz AG

Stuttgart, West Germany

Sterling/Davis Electric

Wallingford, Connecticut

Storm Products Co.

Inglewood, California

Sumitomo Electric Industries, Ltd.

Yokohama, Japan

Sun Chemical Corporation,**Facile Division**

Paterson, New Jersey

Superior Continental Corporation**Cable Division**

Brownwood, Texas

Albert H. Surprenant Inc.

Jaffrey, New Hampshire

Syncro Machine Company

Perth Amboy, New Jersey

Tamaqua Cable Products Corporation

Schuylkill Haven, Pennsylvania

Technical Coatings Co.

Nutley, New Jersey

Teknor Apex Company

Pawtucket, Rhode Island

Tektronic, Inc.

Beaverton, Oregon

Teledyne Thermatics

Elm City, North Carolina

Teledyne Western Wire & Cable

Los Angeles, California

Telefonaktiebolaget L M Ericsson**Telephone Cables Division**

Alvsjö, Sweden

Telephone Cables, Ltd.

Dagenham, Essex, England

Tenneco Chemicals, Inc.

Piscataway, New Jersey

Tensolite Company**Division of Carlisle Corporation**

Tarrytown, New York

A. E. Tetsche Co., Inc.

Arlington, Texas

TFE Industries

Warwick, Rhode Island

Thermax Wire Corporation

Flushing, New York

Times Wire & Cable Company

Wallingford, Connecticut

Torpedo Wire & Strip Inc.

Pittsfield, Pennsylvania

Trea Industries Inc.
East Greenwich, Rhode Island
Ube Industries, Ltd.
Tokyo, Japan

Union Carbide Corporation
New York, New York

Uniroyal, Incorporated
Chemical Division

Naugatuck, Connecticut

U. S. Steel Corporation
Electrical Cable Division

Worcester, Massachusetts

Videx Equipment Corporation
Paterson, New Jersey

Wardwell Braiding Machine Company
Central Falls, Rhode Island

The Ware Chemical Corporation
Bridgeport, Connecticut

The Ware Chemical Corporation
Stratford, Connecticut

Western Electric Company
Kearny, New Jersey

Whitmor Wire & Cable Corporation
North Hollywood, California

Wilson Products Company
Division of Dart Industries, Inc.

Neshanic, New Jersey

Wireonics Products Company
Winnetka, Illinois

Witco Chemical Corporation
Sonneborn Division

New York, New York

Wyre Wynd, Incorporated
Jewett City, Connecticut

Wyrrough and Loser, Inc.
Trenton, New Jersey

TABLE OF CONTENTS

Tuesday, November 16, 1976 — 9:30 am Hunterdon and Cumberland Rooms

SESSION I: Tutorial — Telecommunication — Yesterday, Today and Tomorrow

Chairman: Irv Kolodny, General Cable Corp.

Panel Members:

Dr. M. C. Biskeborn, Phelps Dodge
F. W. Horn, Cable de Comunicaciones S.A.
J. R. Apen, Bell Laboratories
Dr. G. D. Wallenstein, Consultant
H. Jones, GT&E International
R. Briskman, COMSAT General

Tuesday, November 16, 1976 — 2:00 pm Gloucester Room

SESSION II: Cable Design

Chairman: George Webster, Bell Laboratories

THE INTERNATIONAL TELEPHONE CABLE MARKET,
*F. W. Horn and M. Villari, Cables de Comunicaciones
S.A., Spain* 1
FINITE ELEMENT ANALYSIS OF CABLES, *A. D. Carl-
son, Naval Underwater Systems Center* 12
DESIGN GUIDES FOR FINE-WIRE CABLE, *H. E. Miller,
Honeywell, Inc.* 17
IMPROVED PAIR TO PAIR UNBALANCE FOR PAPER
INSULATED CABLES WITH UNIT-TWIN CONSTRUC-
TION, *G. I. B. Vermont, Olex Cables Limited, Austrab*
..... 21
A STATISTICAL MODEL FOR CALCULATION OF
CROSSTALK IN A BALANCED PAIR CABLE, *N. Holte,
Electronics Research Laboratory, Norway* 25
CUSTOMIZED GAS FEEDER PIPE FOR PRESSURIZ-
ING AND MONITORING TELEPHONE CABLE, *M. R.
Dembiak and W. Purkert, Western Electric Company*
..... 32

Tuesday, November 16, 1976 — 2:00 pm Hunterdon Room

SESSION III: Cable Materials I

Chairman: Marta Farago, Northern Telecom, Ltd.

ALUMINUM OXIDE INTEGRATED THIN FILM INSULA-
TION FOR ALUMINUM WIRE AND STRIP CONDUCT-
ORS, *H. D. Walker, Permaluster, Inc.* 36
CONTINUOUS CERAMIC FIBER REFRACTORY IN-
SULATION, *K. A. Karst, 3M Company* 42
LOW LOSS POLYETHYLENE FOR THE INSULATION
OF SUBMARINE COAXIAL CABLE, *I. H. Kishi, Y.
Yamazaki, T. Nagasawa, H. Takashima, H. Fujita, and I.
Tsurutani, Ube Industries, Ltd., Japan* 47
ENERGY SAVINGS AND PRODUCT COST EF-
FICIENCY THROUGH THERMOPLASTIC ELAS-
TOMERS, *W. H. Korcz, Shell Development Company*
..... 56

CONTAMINANT TRACE GAS TESTING OF LEAD-
STABILIZED POLYMERIC COMPOUNDS, *J. P. Franey
and T. E. Graedel, Bell Laboratories* 63
PROCESSING STABILITY OF SEVERAL POLYMERS,
C. C. Swasey, Sandoz Colors & Chemicals 68

Wednesday, November 17, 1976 — 9:00 am Gloucester Room

SESSION IV: Cable Testing and Evaluation

Chairman: James Kanely, Superior Continental

RF LEAKAGE MEASUREMENTS DIRECTED TOWARD
ACHIEVING ELECTROMAGNETIC COMPATIBILITY, *L.
Radar, The Boeing Company* 74
STRUCTURAL RETURN LOSS PERFORMANCE
EVALUATION OF MATERIALS AND ELEMENTS FOR
HIGH QUALITY COAXIAL CABLES, *R. Mathieu, Y.
Peltier, and A. J. Ghazi, Societe Anonyme de
Telecommunications, France* 82
EFFECT OF PAIR UNBALANCE ON CARRIER
FREQUENCY INSERTION LOSS AND CROSSTALK IN
MULTIPAIR CABLE, *A. F. Judy and J. J. Refi, Bell
Laboratories* 91
CHARACTERIZATION OF CROSSTALK IN TWISTED
PAIR TELEPHONE CABLES WITH NONMATCHED
TERMINATIONS, *J. C. Issacs, T. F. McIntosh and T. D.
Nantz, Bell Laboratories* 100
EFFECTS OF CABLE UNBALANCES ON POWER IN-
DUCED CIRCUIT NOISE, *M. L. Brewer, REA and H. P.
Price, Central Telephone Company* 108
RODENT BITING PRESSURE AND CHEWING ACTION
AND THEIR EFFECTS ON WIRE AND CABLE SHEATH,
*N. J. Cogelia, Bell Laboratories; G. K. Lavoie and J. F.
Glahn, US Department of the Interior* 117

Wednesday, November 17, 1976 — 9:00 am Hunterdon Room

SESSION V: Connections, Splicing and Installation

Chairman: Joe Neigh, AMP, Incorporated

CONNECTORIZED EXCHANGE CABLE SPLICING
(CONES), *D. R. Frey and A. G. Hardee, Bell
Laboratories* 125
SPLICING METHOD USING HEAT-SHRINKABLE
TUBES FOR SUBMARINE LOCAL CABLES, *Y. Kubota
and S. Yamakawa, Nippon Telegraph & Telephone
Public Corporation, Japan* 129
SHIELD BONDING CONNECTORS, *L. Ance and H. M.
Hutson, REA* 138
ENVIRONMENTAL EFFECT OF TELEPHONE FACILI-
TIES, *M. N. Evans, Southern New England Telephone*
..... 143
THE CABLE ENTRY SYSTEM, *Dr. J. E. Godts, Martin
Marietta Aerospace* 149
INFERRING DUCT-RUN GEOMETRY FROM CABLE-
TENSION DATA: A CASE HISTORY, *A. L. Hale and M.
R. Santana, Bell Laboratories* 152

Wednesday, November 17, 1976 — 2:00 pm
Gloucester Room

SESSION VI: Cable Applications

Chairman: Joseph M. Flanigan, Rural Electrification Administration

FILLED CABLE FOR AERIAL INSTALLATION, L. Molleda and E. Used, Compania Telefonica Nacional de Espana, Spain	158
EXTENDED FIELD TRIALS ON CONDUCTIVE PLASTIC SHEATHED TELECOMMUNICATION CABLE IN A TRUNK NETWORK, P. Calzolari and Dr. M. B. Forleo, Industrie Pirelli, Italy, and G. Cosimi and E. Fucini, S.I.P. — Societa Italiana per l'Esercizio Telefonico p.A., Italy	174
VARIOUS KINDS OF NEW PAIR TYPE CABLES FOR LOCAL BROADBAND NETWORK SYSTEMS, K. Oshima, Nippon Telegraph & Telephone Public Corporation; J. Niwa, The Furukawa Electric Co., Ltd; S. Hiramatsu, Sumitomo Electric Industries, Ltd. and T. Maruoka, The Fujikura Cable Works, Ltd., Japan	185
NEAR END CROSSTALK PROPERTIES OF COMPARTMENTALIZED PCM CARRIER SYSTEM CABLES, A. P. Gabriel, J. Peveler and J. J. Woods, General Cable Corporation	199
THE DEVELOPMENT OF SUPER HIGH TEMPERATURE WIRE AND CONNECTORS FOR GENERAL PURPOSE AEROSPACE APPLICATIONS, F. D. Bayles and M. A. Dudley, Canada Wire and Cable Ltd.	207
ALUMINUM WAVEGUIDE WITH ALUMINUM OXIDE DIELECTRIC LINING, Dr. F. Krahn, Felten & Guilleaume Carlswerk AG, West Germany	216

Wednesday, November 17, 1976 — 2:00 pm
Hunterdon Room

SESSION VII: Fiber Optics

Chairman: Milton Tenzer, US Army Electronics Command

TESTING OF TENSILE STRENGTH OF OPTICAL FIBER WAVEGUIDES, C. Kao, M. Maklad and T. Reed, ITT Electro-Optical Products Division	223
FIBER OPTIC CABLES FOR LOCAL DISTRIBUTION SYSTEMS, J. C. Smith, ITT Electro-Optical Products Division and M. Pomerantz, US Army Electronics Command	226
OPTICAL FIBER CABLE FOR T1 CARRIER SYSTEM, J. A. Olszewski, Dr. A. Sarkar and Y. Y. Huang, General Cable Corporation	235
A REVIEW OF OPTICAL FIBER CONNECTOR TECHNOLOGY, J. F. Dalglish, Bell Northern Research Ltd., Canada	240
DEVELOPMENT OF A ROBUST OPTICAL FIBER CABLE, AND EXPERIENCE TO DATE WITH INSTALLATION AND JOINTING, N. S. Dean, BICC Telecommunication Cables Limited, England and R. J. Slaughter, BICC Research & Engineering Limited, England	247

Thursday, November 18, 1976 — 9:00 am
Gloucester Room

SESSION VIII: Cable Materials II

Chairman: F. Farrell, 3M Company

WEATHERABILITY OF BLACK POLYETHYLENE—PREDICTABLE?, W. F. Jensen, Jr., and J. N. Jones, E. I. duPont de Nemours & Co.	257
PREDICTION OF POLYETHYLENE AGING BY ISOTHERMAL DIFFERENTIAL SCANNING CALORIMETRY, Dr. D. L. Davidson, Union Carbide Corporation	265
PREDICTING FRACTURE, CREEP, AND STIFFNESS CHARACTERISTICS OF CABLE JACKETS FROM MATERIAL PROPERTIES, G. M. Yanizeski, E. D. Nelson and C. J. Alosio, Bell Laboratories	272
HIGHLY FIRE-RETARDANT NAVY SHIPBOARD CABLES, M. A. DeLucia, Naval Ship R&D Center	281
A TEST METHOD FOR MEASURING AND CLASSIFYING THE FLAME SPREADING AND SMOKE GENERATING CHARACTERISTICS OF COMMUNICATIONS CABLE, J. R. Beyreis, J. W. Skjordahl, Underwriters Laboratories, S. Kaufman, and M. M. Yocum, Bell Laboratories	291

Thursday, November 18, 1976 — 9:00 am
Hunterdon Room

SESSION IX: Cable Manufacturing and Processing I

Chairman: Frank Short, Belden

THE NATURE OF WATER IN SUBMARINE CABLE CORE AND ITS RELATIONSHIP TO DIELECTRIC LOSS, J. H. Daane, H. E. Bair, G. E. Johnson and E. W. Anderson, Bell Laboratories	296
CORROSION STUDIES ON SHIELDING MATERIALS FOR UNDERGROUND TELEPHONE CABLES PART II: CORROSION PROTECTION FOR FILLED CABLES, K. E. Bow and L. G. Colter, Dow Chemical USA	302
DEVELOPMENT OF CABLE WITH GAS-STOPPAGE DAM BY POLYETHYLENE MOLD PROCESS, M. Azuma, Y. Oishi, K. Fuse and M. Oda, The Furukawa Electric Co., Ltd, Japan	312
THE USE OF BLOWING AGENT CONCENTRATES IN THE MANUFACTURE OF TELECOMMUNICATIONS CABLES, T. C. Hodgson, D. B. Carefoot and G. F. Gouthro, Santech Incorporated, Canada, and S. M. Beach, Phillips Cables Limited, Canada	317
A NEW METHOD FOR RING COLOR CODING OF PLASTIC INSULATED WIRES, K. Kimmich — Standard Elektrik Lorenz AG, West Germany	323
A NEW TECHNIQUE FOR PERMANENT AND NON-ABRASIVE MARKING OF PLASTIC CABLE SHEATHS, Dr. J. Hennig, SEL — Standard Elektrik Lorenz AG, West Germany	328

Thursday, November 18, 1976 — 2:00 pm
Gloucester Room

SESSION X: Cable Materials III

Chairman: Sherman Kottle, Dow Chemical USA

DEVELOPMENT OF FIRE-STOPPING MATERIALS FOR WIRING SYSTEM, <i>M. Ishibashi, H. Kobayashi and M. Makiyo, the Fujikura Cable Works, Ltd., Japan</i>	333
NEW TYPES OF INTUMESCENT MATERIALS AND THEIR APPLICATION TO A FIRE PROTECTION OF CABLES, <i>T. Yabuki, Y. Koide, T. Kaide and M. Takada, Dainichi-Nippon Cables, Ltd., Japan</i>	340
RADIATION CURABLE POLYOLEFIN COMPOUNDS FOR FLAME RETARDED WIRE & CABLE INSULATION, <i>M. F. Maringer, J. W. Biggs and P. E. Pinnow, US Industrial Chemicals Co.</i>	350
FILLED VINYL JACKET COMPOUNDS, <i>J. A. Falter and P. C. Warren, Bell Laboratories</i>	356
FLAME RESISTANT — LOW SMOKE CABLE JACKET DEVELOPMENTS, <i>W. D. Jones, Uniroyal Chemical Division</i>	362

Thursday, November 18, 1976 — 2:00 pm
Hunterdon Room

SESSION XI: Cable Manufacturing and Processing II

Chairman: Irv Kolodny, General Cable Corporation

PLASTIC INSULATING OF TELEPHONE CONDUCTORS AT 10,000 to 15,000 FPM, <i>A Cueto, M. Cubero and A. Garvalena, Cables de Comunicaciones S.A., Spain</i>	370
COMPUTER CONTROL OF HIGH SPEED WIRE COATING LINES, <i>V. L. NeNir, Northern Telecom Limited, Canada</i>	380
A UNIQUE MONITORING SYSTEM FOR EXPANDED WIRE INSULATIONS, <i>T. S. Dougherty, Western Electric Company</i>	387
NOVEL EXTRUSION PROCESS FOR ROBUST HIGHLY EXPANDED POLYETHYLENE INSULATED COAXIAL CABLES, <i>T. Nakahara, A. Tsukamoto, H. Shimba, F. Suzuki T. Miyaziri, and M. Yuto, Sumitomo Electric Industires, Ltd., Japan</i>	394
EXTRUSION OF FLAT MULTI-WIRE COMPUTER CABLE, <i>C. J. Fetner, Jr., IBM — International Business Machines Corporation</i>	402
SPACE-SAVING TELEPHONE WIRE EXTRUSION LINES WITH VERTICAL COOLING AND SHARED AUTOMIZED REEL TAKE-UP, <i>S. Nordblad, Telefonaktiebolaget L M Ericsson, Sweden</i>	408

THE INTERNATIONAL TELEPHONE CABLE MARKET

By

F.W. Horn and M. Villarig
Cables de Comunicaciones S.A.
Zaragoza, Spain

Abstract

The extremely complex international telephone cable market is the result of historical and technical influences. The authors have systematically classified world-wide product requirements and analyzed current and future trends. The demand placed on the engineering function of a potential supplier and the case for international standardization is explored.

Introduction

The international telephone cable market is extremely complex in terms of its diversity with regard to product configuration, design and characteristics. Uniformity does not exist in the domestic markets of most countries and much less so internationally. The supplier who attempts to operate in this market will more than likely be unable to find more than a faint resemblance between what he customarily manufactures and what most tenders will require. The consumer, on the other hand, encounters a bewildering variety of products, each different in some or many ways, yet all presented by appropriately sincere marketing people as better than their competitors' product.

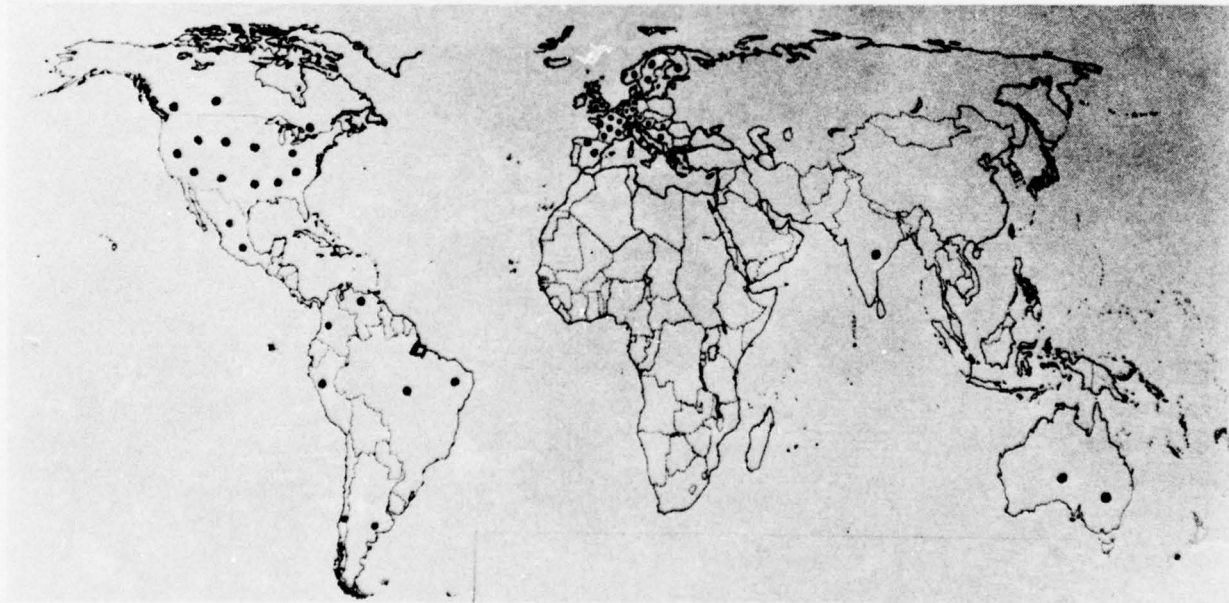
Historical, technical and even political influences have created the current situation, which in many respects promises to become even more complex. The authors have provided an overview of the market. Specifications in use by geographical areas, current and future tendencies in the market and explore the case for standardization.

Configuration of the international telephone cable market

Logically, the term *market*, suggests consumers and suppliers. More specifically, however, by *international market* we focus on geographical areas which via tenders or other means generate a demand outside of their own borders and on the other hand the various countries capable of supplying such demand: the exporting countries.

Whereas at first glance it would appear that the importing countries are the less developed and the exporting countries the most highly industrialized, this generalization is an oversimplification as we will see later on.

In figure 1 we show a world map which graphically



World map showing location of the principal manufacturers of telephone cable

Figure 1

locates the principal manufacturers of telephone cable.

It should be kept in mind while studying the map that the major companies are identified by a single dot located in the geographical location of their headquarters. Multi-plant companies are represented with a single dot although some will have perhaps 10 plants. As an example the United States, which has a large geographical extension compared to other countries, has many plants whereas only 10 dots are shown on the map (Fig.1).

Geographical Areas of Specifications Influence

Both in producing and consuming countries alike, definite tendencies can be detected with respect to the principal origins of the product standards employed.

It is not our intention to catalog all of the world's countries and individual markets along with their product requirements. For our purposes it is sufficient to identify the four primary tendencies in telephone cable specifications from which have evolved practically all of the existing designs of universal acceptance. These cable standards are:

- a) German - V.D.E.
Verband Deutscher Elektrotechniker
- b) English - B.P.O.
British Post Office
- c) French - P.T.T.
Postes Telegraphiques et Telephoniques
- d) United States - R.E.A.
Rural Electrification Administration

It must be remembered that the areas of influence are not clearly defined and some countries use more than one set of specification and possibly different specifications for the various classes of communication cable.

With respect to the R.E.A. standard the vast majority of telephone cable produced in the U.S.A. is manufactured by Western Electric Co. for the Bell System. Although these specifications are not available outside the Bell System the R.E.A. specifications are very similar. Also in the U.S.A. there is considerable exchange of information and most manufacturers produce basically the same types of cable and with very similar transmission characteristics.

The group of countries which base their requirements upon one of the four standards above constitute what we refer to later as AREAS OF INFLUENCE. Figure 2 shows a world map indicating approximate AREAS OF INFLUENCE.

The creation of these areas of influence are due fundamentally to 3 reasons:

a) Historical motives:

The colonial influence has played an important role in establishing a base or starting point and some countries still require almost identical specifications to the original versions.

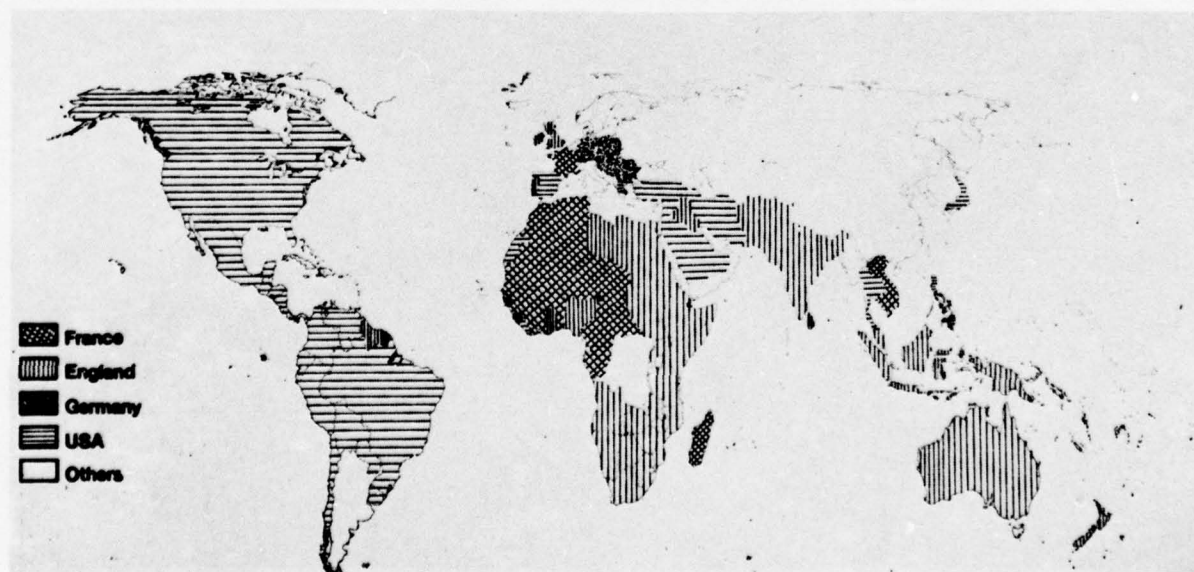
The similarity of specifications in ex-colonial areas can readily be understood as a natural result of a cultural and technical influx resulting in telephone networks similar to the source country.

b) Political Influence:

Political influence has often been the traceable factor in the determination of standards. In using the term *political influence* we should hasten to make clear that no negative inference is intended. Moreover, it is clear that developing countries have obtained badly needed financial and technical assistance from industrially developed countries. It is logical to expect that under such circumstances the assisting areas' standards were adopted.

c) Technological and Economic Influences:

Some areas have long standing technological pres-



World map showing areas which utilize the various cable specifications

Figure 2

tige in general, which may or may not be deserved with respect to telephone cables. Nevertheless it is apparent that technical image was a persuasive factor in their norms having been adopted. Also, highly developed countries which lead in technological advancements and volume of internal telephone system size can often present convincing advantages from the technical and economic standpoints to standardize on their products.

Current Tendencies for Telephone Cable Standards

Unfortunately, the apparent political need to create a "new image" in developing countries or ex-colonial states (now sovereign nations) often results in "do-it-yourself" standards. The inescapable impression is that several technicians got together, each with copies of specifications from various countries, and proceeded to put together the most stringent requirements from each in hopes of obtaining a "super" product. The pressure upon many of the above technicians to assume the responsibility for changing the standards overnight makes it easy to understand cases such as the above. This is especially true where the technicians' zest and/or concern over the effect upon his career in the event that he is later proved wrong results in over engineering, inertia and patch work specifications.

Actually all of us in the industry know that the opposite is usually the case. Specifications often cannot be mixed together unjudiciously. The consumer is far better off determining the characteristics he desires after studying the alternatives offered by the professionals in the cable business and making a final decision insisting that the manufacturer limits himself to a standard mass-produced product. The result is a lower price, a higher standard of quality especially with regard to uniformity, longer useful life, etc. which often is not the case with "specials".

Analysis of the product - The Telephone Cable

Although the end use is essentially identical in all countries, to act as a transmission vehicle, we can observe an extensive variety both quantitative and functional. This is obvious keeping in mind the various influences already mentioned.

Whereas this diversification of standards exists in many products, it is usually associated with consumer products and not to be logically expected of a product which is expected to be interconnected and perform the same function.

Nevertheless, the differences manifest themselves not only from the standpoint of construction features but also with respect to their transmission characteristics.

A) Analysis of the construction of Telephone Cables

1. Conductor

All of the standards agree on electrolytic, annealed copper with or without tinning.

Some production of aluminium conductors exists in the U.S.A., U.K., Japan, Australia, France and others. However copper, by far, is the most prevalent material used.

2. Gauge

The same cannot be said for the wire gauge where we list the following types:

2.1 Metric gauges:

These are commonly found in the areas of French and German influence and in some cases the U.K. areas. The most common metric sizes used are: 0.4, 0.5, 0.8, 1.0, 1.2 and 1.3.

2.2 AWG Gauge

These are typical of the U.S.A. areas of influence and the most common gauges are:

AWG	Ø MM
28	0.32
26	0.405
24	0.51
22	0.64
19	0.91

Note that in the U.S.A. areas the 0.8 mm. gauge is not common while it is widely used in the French and German areas.

3. Insulation:

3.1 Plastic Insulation:

In general, most consumers specify polyethylene for its superior characteristics with respect to mutual capacitance in various densities (low, medium, high), foam, etc. PVC is employed in some cases such as switch-board cable for example, but not usually for the bulk of exchange area cables.

Other types of insulations such as polypropylene seems to be used only in the U.S.A.

3.2 Paper Insulation:

Generally there are two basic types in use:

a) Paper ribbon - applied helically or longitudinally.

This type is common in the French, German and English areas of influence, and to a lesser extent in the U.S.A.

b) Paper pulp-paper manufactured directly onto the wire on a continuous basis.

This type of insulation is commonly employed in the U.S.A., Canada, Spain and Japan.

4. Conductor Assembly:

There are two basic types of conductor assembly:

4.1 Pairs - These are used fundamentally in the U.S.A., Canada and Spain. They are also used in the U.K. areas to a lesser extent and in other areas where high frequency is used or low cross talk is desired.

4.2 Quads - These are used particularly in the French and German areas and normally are produced as "star" or "DM" quads (Dieselhorst-Martin).

5. Color Codes:

In similar cable types there seems to be no uniformity of the colors for the identification of the pairs or quads. In each of the areas of influence which have been discussed, all of the color codes are different. As a matter of fact the difference in colors, degree of opaqueness, etc. varies considerably even within a particu-

lar area of influence.

6. Core Construction:

There are two types:

6.1 Concentric layer Core Construction

In this area there are several variations:

- Reverse layer construction
- Staggered Layer Construction
- Oscillated construction

These cores may or may not have separating tapes between layers.

In cables made up of pairs this type of construction is generally not used for cables over 25 pairs. These cores are typical of the V.D.E. quadded cables regardless of the number of quads.

6.2 Unit Construction:

This type of core is predominant in the standards of the U.S.A., French and English areas, although the number of elements per unit are different.

Whereas the U.S.A. and U.K. specifications generally follow multiples of 25 (25 pairs, 50 pairs, 100 pairs), the French P.T.T. uses a multiple of 7: 7 and 14 quads per basic unit and 56 or 112 quads per composite unit.

7. Core Wrap Tapes

If the conductor insulation is paper or paper pulp the core wrap tape is paper applied helically.

If the conductors are plastic then a great variety of core wrap tapes are available. These can be Mylar (registered Dupont trade mark), polyester, plastic, rubber or any combination of these materials. They can be embossed or corrugated and in two or more layers. They are applied longitudinally or helically.

8. Cable Sheaths:

Basically there are two groups of sheaths:

8.1 Sheaths which include lead:

With various alloys, anticorrosion protections, armoring, etc.

These sheaths are commonly specified by the

V.D.E., B.P.O. and French P.T.T. These sheaths have practically gone out of use in the U.S.A., Canada and Spain.

8.2 Sheaths which do not include lead:

The most usual types are: Alpeth, Stalpeth, Alpeth FPA, PAP, PASP, ALVYN, GLOVER, etc.

These sheaths are used almost exclusively in the U.S.A. areas and to a lesser extent in the U.K. and French areas.

The metallic screens or protection which are used in these cables are aluminium, coated aluminium, steel and copper. They are applied helically or longitudinally, the latter either smooth or corrugated.

9. Filled and Unfilled Cables:

Filling of the air space in the cable core with petrolatum or special blends of a petrolatum base started in the 60's and is used to a large extent in the U.K., U.S.A. and Germany.

We have however been unable to determine if filled cable is used in the French area other than on an experimental basis.

Figure 3 is a summary table of cable standards.

B) Analysis of Transmission Characteristics:

A detailed listing of the differences in this area would occupy more space than can be logically allowed. Therefore, we will restrict this part of our comparison to mutual capacitance in view of this being the primary parameter, which determines the cable design characteristics.

As can be expected there is little uniformity in the mutual capacitance specified by the various consumers.

Whereas either paper, pulp or plastic insulated paired cables fundamentally are of 52 nF/Km in the U.S.A. areas, in the areas of U.K. influence this value is usually higher: 53, 56 and 59 nF/Km and not alike for all gauges.

Quads do not coincide in mutual capacitance either. While VDE specifies 36 and 42 nF/Km for paper insulated conductors the French P.T.T. sets a maximum value of 57 nF/Km.

Plastic insulated quads are another matter with aver-

DETAILS OF CONSTRUCTION SPECIFICATIONS	CONDUCTORS	GAUGE	INSULATION		CABLE ELEMENTS	COLOR CODE	CORE FORMATION		CORE WRAP TAPE	SHEATHS		
			PLASTIC	PAPER			CONCENTRIC LAYERS	UNITS		PAPER CABLE	PLASTIC CABLE	FILLED CABLE
B.P.O.	Copper	METRES 0.4, 0.5, 0.63, 0.9	Polyethylene Solid and cellular	Helical paper tape	Pairs and quads	Their own	up to 100 pairs	Multiples of 25 pairs 25, 50 and 100	Paper plastic Textile	Lead anticorrosive armor	Metal and plastic	Widely used
R.E.A.	Copper	A.W.G. 26, 24, 22, 19	Polyethylene Polypropylene solid or cellular	Paper or wood pulp	Pairs	Their own	up to 25 pairs	Multiples of 25 pairs 25, 50 and 100	Paper plastic	Stalpeth PASP	Metal and plastic	Widely used
P.T.T.	Copper	METRES 0.4, 0.5, 0.6, 0.8	Polyethylene solid	Helical paper tape	Star and DM quads	Their own	Up to 14 quad:	Multiples of 7 quads 7, 14, 56 and 112	Paper plastic textile	Lead anticorrosive armor	Metal and plastic	Experimental only
V.D.E.	Copper	METRES 0.4, 0.6, 0.8	Polyethylene solid and cellular	Helical paper tape	Star and DM quads	Their own	All sizes	-----	Paper plastic Textile	Lead anticorrosive armor	Metal and plastic	Widely used

Summary of Cable Standards

Figure 3

age values of 50 and 52 nF/Km with a maximum of 57 nF/Km by the P.T.T. 41 nF/Km average and 46 nF/Km maximum by the B.P.O. and maximums of 50 and 55

nF/Km by the V.D.E.

Figure 4 provides a summary of the above differences.

GAUGE	PAPER PAIRED CABLES								PAPER QUADDED CABLES							
	VDE		BPO		PTT		REA		VDE		BPO		PTT		REA	
	Med.	Max.	Med.	Max.	Med.	Max.	Med.	Max.	Med.	Max.	Med.	Max.	Med.	Max.	Med.	Max.
0.4	-	-	53	60	-	-	52+4	61	36	36	-	-	52.5	57.5	-	-
0.5	-	-	53	60	-	-	52+4	61	-	-	-	-	52.5	57.5	-	-
0.6	-	-	53	60	-	-	52+4	61	38	42	45	48.6	52.5	57.5	-	-
0.8	-	-	-	-	-	-	-	-	38	42	-	-	52.5	57.5	-	-
									34*	38*						
0.9	-	-	59	64	-	-	52+4	61	34*	38*	41	44.3	-	-	-	-
			38.5*	41.5*												
1.27	-	-	-	-	-	-	-	-	35	39.2	41	44.3	-	-	-	-

GAUGE	POLYETHYLENE PAIRED CABLES								POLYETHYLENE QUADDED CABLES							
	VDE		BPO		PTT		REA		VDE		BPO		PTT		REA	
	Med.	Max.	Med.	Max.	Med.	Max.	Med.	Max.	Med.	Max.	Med.	Max.	Med.	Max.	Med.	Max.
0.4	-	-	53	60	-	-	52+4	61	50	50	-	-	52.5	57.5	-	-
0.5	-	-	53	60	-	-	52+4	61	-	-	-	-	52.5	57.5	-	-
0.6	-	-	56	59	-	-	52+4	61	45	50	47	-	52.5	57.5	-	-
0.8	-	-	-	-	-	-	-	-	50	55	-	-	52.5	57.5	-	-
0.9	-	-	59	62	-	-	52+4	61	-	-	41+2	46	-	-	-	-
1.27	-	-	-	-	-	-	-	-	-	-	41+2	46	-	-	-	-

* Long distance cables

MUTUAL CAPACITANCE (nF/Km)

Figure 4

The Case for International Standardization

We have just examined the International Telephone Cable Market and from the standpoint of cable norms have observed that its fundamental characterization is a myriad diversification of the product within a basic uniform end use in terms of function. It is clear that even with a summarised analysis of the current requirements for this product a pattern of complete inconsistency surfaces. We are cognizant of the difficulties and obstacles which would be involved in any program to standardize this product. As a matter of fact, it would appear to be impossible at first glance even to the most interested of advocates of such an undertaking.

Despite the many factors which have made other, equally difficult and apparently impossible objectives impractical in other eras, the fact is that many are now a reality. As an example, who would have thought a few years ago that the metric system would be adopted despite high initial expense and public resistance in the U.K.? Nevertheless, despite all of the difficulties encountered, this program is well on its way to becoming a reality in the not too distant future.

In our opinion standardization would have the following advantages which would benefit manufacturer and user alike.

- Obtain a scientific structurization of telephone cables which would benefit the professionals engaged in this activity.
- Cut the costs for telephone cable manufacturers reducing the capital outlay required, improve utilization of the manufacturing processes, reduction of changeovers, scrap, stock requirements and permit longer production runs, to name a few.
- As a consequence of the above and the obvious investment economies for the consumer, the telephone administrations could reduce their own stock, simplify training and eliminate problems of interconnections.
- Reduce lead time for acquisition of products and in general providing more "agility" for the industry in general.

e) While it is advantageous to encourage development and improvement of the product, standardization can focus and concentrate these efforts on the basic problems and eliminate marketing "Gimmicks".

f) Greater competition in the international marketing as we would all be speaking the same "language".

In summary, the objectives would be directed towards an orderly system with many obvious economic and technical advantages. All of this can be obtained, we are convinced, without limiting development efforts or causing overly restrictive conformity keeping in mind the highly competitive nature of this market.

The logical steps to achieve this objective in our opinion may follow the two successive phases discussed in the following section.

1. Standardization - The first step:

The initial phase would seem to have been within incumbency of the C.C.I.T.T. (International Consultative Telegraph and Telephone Committee) (Plenary Assembly of 1972) which has dedicated scant attention to the subject of telephone cable. In any case, the recommendations of the proceedings have restricted itself to minimum requirements of transmission characteristics, i.e:

G.321 Electrical characteristics of the star quad cables enabling 12, 24, 36, 48, 60 or 120 telephone carrier channels on each pair of a quad.

G.331 Electrical characteristics of coaxial pairs type 2.6/9.5 mm.

G.342 Electrical characteristics of coaxial pairs type 1.2/4.4 mm.

G.521 Bare wires on overhead and mixed lines:

- a) Loading of bare wire on overhead lines
- b) Establishing the bare wire on overhead lines

G.522 The use of different types of electrical information on cables employed at voice frequency.

Even in the above, the recommendations are of insufficient detail and in some cases would appear to require up-dating.

The problem stated above is in direct contrast with the thoroughness, in general, with which other areas of transmission are covered.

Perhaps the most complete references concerning cable are contained in volume IX series L recommendations, discussing cable sheaths in general historical terms without treating the topic of standards.

In our opinion, telephone cables constitute in themselves, a sufficiently important item to warrant a volume exclusively on the subject. In such a volume the principal standards in existence could be included and perhaps recommendations by this important organization could be included for the various end uses in the industry. A starting point which may not represent an overly conflictive area of agreement would appear to be standardization of gauges, color codes, core formation, sheaths, etc. and some of the principal materials used in the manufacture of the product.

2. Standardization - The second step

Acceptance by the various administrations of the standards proposed by the C.C.I.T.T:

This second step presents the most severe stumbling block to realize this objective and can effectively block any progress in such a program. Obviously, the obstacles to acceptance of any recommendations will depend upon the type of recommendations involved. The ability of the specific producing or consuming areas to adapt to such standards, tradition, nationalistic interests, economic considerations, technical considerations, differences of opinion based on the above or any number of other reasons which in the consideration of the administrations would bear sufficient persuasive weight.

In short, we are amply convinced that the road to standardization contains many perils and practical considerations which limit the likelihood of success in the near future.

Characteristics of Requirements

Working without standardization causes many problems as discussed below. All of these influence the cost of the product for the consumer.

1. Requirements which do not affect performance:

This condition exists not only with respect to the types in existence in the industry but also with respect to the diversity within a functional type.

As discussed previously, this is due to the various influences which affect the standards or specifications. This results in serious difficulties for the prospective manufacturer who encounters several orders of an almost identical type but is unable to combine the orders to obtain more economical run quantities, improve his efficiency, reduce stock, waste, etc. Consider as an example, orders for identical cables in every respect except; that one is 0.64 mm (22 AWG) and others are 0.6 mm. or; identical gauge, insulation, color codes, etc. but different core formations. It is easy to visualize the unfortunate circumstances which are often the result of insignificant differences and the resulting excessive costs for producer and consumer alike.

2. Inertia in the market:

Often the market is surprisingly slow to accept change. Improvements and new developments are difficult to introduce with some consumers who insist upon certain designs only because they have *always* used them. For the supplier, it is frustrating to encounter consumers who have automatically discarded anything which represents change. Certain designs which have been in use for 40 years continue to be required despite their having been declared obsolete in most administrations as much as 20 years ago.

Perhaps an example is the requirements of paper-lead cable whereas paper pulp-Stalpeth has replaced the former in the U.S.A. and other countries as long ago as 25 years. Without entering into a commercial debate or endorsement for one product over another, it is generally conceded that paper-pulp-Stalpeth possesses many advantages not the least of which is cost. As a minimum, one would expect consumers to insist upon the latest technological and economical benefits for their organization.

The matter of selection of one product over another

is most certainly the sole responsibility of the consumer and our comment is not directed at this fundamental and logical decision making process, but instead, we are concerned with disregard *a priori* due to market inertia.

The Suppliers situation in the International Market

We have discussed the varied nature of the specifications in a proceeding section and the effect upon the supplier.

As an illustration of the difficulties which a supplier might face in the international market we can indicate that our firm has over 1200 different cable variations in its sales catalog and comparatively is a rather small company. Furthermore, we often encounter tenders which we are unable or unwilling to manufacture because unusual specifications, obsolete designs, or unsound requirements by the consumer which we deem could adversely reflect upon us.

For a supplier to be able to quote on any given requirement from the international market he must possess an extremely extensive range of machinery, much of which he will utilize sporadically. Obviously, there is little justification for such a massive outlay in terms of investment for a few hours of production each year. It is a fundamental tenet of business that investments which depend solely upon export business must be weighed carefully because of the inherent uncertainty of a consistent supply of business.

An interesting situation is the fact that the conditions which are discussed in the preceding section concerning inertia of the market provide a certain amount of regular business for suppliers with obsolete equipment which can be pressed into service for occasional duty. The situation in which such companies find themselves is disturbing for them for obvious reasons: technologically they are in a negative cycle unable to renew the installations for fear of losing customers, and, of course concerned with respect to the future and the effect of any sudden end to the "inertia factor".

The supplier who intends to deal in the international market can review the section "Analysis of the Product" and easily determine in advance that he will be unable to meet all requirements. Obviously, he must sacrifice substantial "areas of influence" which he will be unable to supply. With respect to the areas which on the surface appears to be similar, the supplier can expect that his organization's engineering competence and manufacturing flexibility will be tested to its limits.

The requirements for entry into this market are:

Flexibility and adaptation to the market:

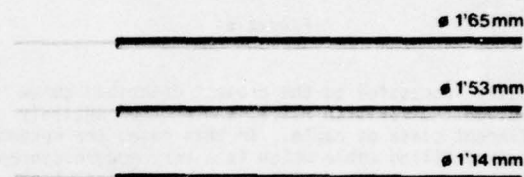
Often the "small" differences between the supplier's standard products and the customer's requirement involves major modifications to equipment and often must be performed in record time.

The usual initial approach is to attempt to convince the customer that a suitable alternative construction, often of a better design, can meet his requirements. In the event that the supplier is unsuccessful, his equipment must be modified to meet the design commitments. In the majority of cases, the solution is a compromise between the two approaches.

As examples of the above, we can cite two case histories where customers had a specific need requiring the modification of a standard product and of the manufacturing equipment.

one example involved pulp insulated Stalpth sheathed cable and was a joint project with General Cable Corporation. The Iran Telephone Company had modified their specifications to pulp insulated cable with a Stalpth sheath in preference to spiral wrapped paper with a lead sheath. However, TCI wanted a lower capacitance value than the normal 52 nF/Km. (0.083 mF/mile). After detailed study it was determined that 40 nF/Km. (0.064 mF/mile) would be established as average mutual capacitance. Anyone familiar with pulp machines immediately recognizes the difficulties of putting additional pulp on 0.6 mm (approx. 22 AWG) wire. In essence it required a pulp ribbon width similar to that which is used in 19 AWG pulp in the U.S.A.

Figure 5 shows the sizes of the low capacitance (40 nF/Km) pulp as compared to the normal pulp insulated conductor (52 nF/km).



COMPARISON OF STANDARD 19 AND 22 GAUGE PULP WITH LOW CAPACITANCE .6MM. FURNISHED FOR IRAN

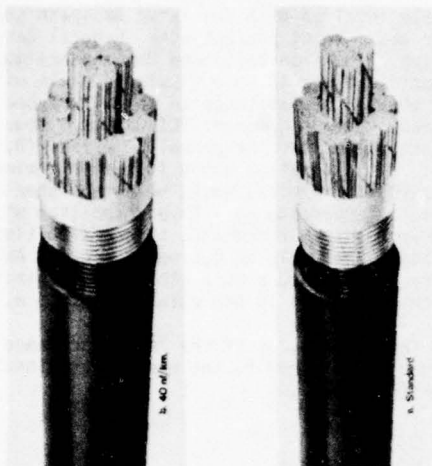
Figure 5

To retain the inherent economical advantage of pulp it was necessary to run the machine with 60 conductors instead of the 30 conductors simultaneously produced in the case of 19 AWG. Pulp machines are among the least flexible in the industry having been designed for a production of 13 million feet of conductor per day for days on end provided no production scheduling changes are required. It is apparent that such machines do not lend themselves to the development of prototype cables.

All of the above including the design of the cable, issuance of specifications, modifications of machinery, etc. had to be accomplished in less than thirty days including the completion of a sample manufacturing program. In the ensuing two years, thousands of reels of cable were shipped without a single quality reject. Fortunately, even the prototype cable met all target requirements and formed part of the shipments.

Figure 6 shows the completed cables for Iran as compared to the standard design.

In the case of export business long delivery lead time must be allowed to meet schedules. Customs and transportation difficulties can frequently occur and costly scrap and penalties can easily result under the pressure of tight schedules. The normal problems associated with regular domestic business can be compounded many times over when dealing internationally.



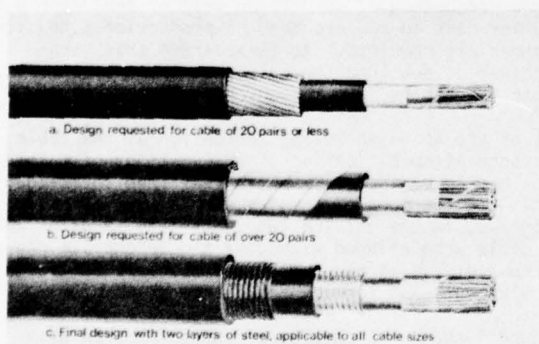
Comparison of 600 pair 0.6 mm. Standard Construction and 40 nf Km. design

Figure 6

Equally successful to the project described above involved the Pakistan P.T.T. and another entirely different class of cable. In this case, the customer required filled cable which is a very modern concept but this was combined with a very primitive sheath and armor involving two helically applied steel tapes. Spiral taping is slow and many modern plants including ours have not purchased this type of equipment.

A joint-technical meeting between Pakistan engineering personnel and our research and development group determined that longitudinal corrugated steel was equal to spiral tape from the standpoint of ruggedness. Nevertheless, the customer would not yield on the requirement that two steel tapes be used. The final design selected was essentially an ASP sheath with another unsoldered corrugated longitudinal protection and final sheath of polyethylene.

Figure 7 shows the designs requested compared to the one which was finally agreed upon.



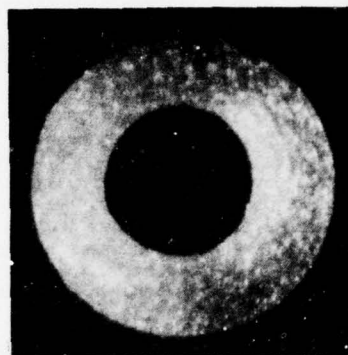
Designs requested as compared to compromise design

Figure 7

Alternative insulation materials were also studied at the same time to compensate the increase in material costs of the sheath described above.

Low density foam insulation was not acceptable and yet was the only foam polyethylene material readily available in Spain. The selection of another polyethylene was made and this led to a rather novel way of adding the expanding agent. Wilson Company and CCSA entered into a joint development project with the result being color chips that included the blowing agent.

Using this technique yielded a very uniform insulation as can be seen by the next figure.



Magnified cross-section of Foam Insulation

Figure 8

In the two examples given above, a total of ten processes were modified and specific equipment developed to produce the order. If these projects are occurring simultaneously with dozens of other orders involving similar adaptations, the dependence upon the human ingenuity within a given organization is of prime importance.

Future growth of the International Telecommunications Market

1. Projection:

Based upon hypothetical calculations utilizing logical consumptions one must conclude that the future of this market is enormous.

Although telephony does not monopolize all of the world requirements for communications, its proportion in comparison to other users is sufficient so that we can restrict our calculations to this field. Rather than estimating the amount of cable required it is simpler to consider that the future requirements in terms of telephones is roughly proportional to the amount of cable required.

Therefore, we should examine the number of telephones installed world wide at the beginning of 1973, which is the latest date for which statistics are available.

Continent or Area	Million Telephones	Telephones per 100 Population
North America	142.1	61.3
Central America	3.4	3.4
South America	6.7	3.3
Europe	106.1	16.0

Continent or Area	Million Telephones	Telephones per 100 Population
Africa	3.7	1.0
Japan	34.0	31.5
Rest of Asia	10.2	0.5
Australia and Pacific Islands	6.4	29.4

If we accept the figure shown for North America, a telephone for each 1.6 of population as a possible statistic world wide, then we would require 2.287 million additional telephones distributed in the following manner:

Continent or Area	Approximate requirement no. of Telephones
Central America	60 millions
South America	120 "
Europe	400 "
Africa	370 "
Japan	34 "
Rest of Asia	1,296 "
Australia and Pacific Islands	7 "

However, if we consider that:

- The world population increases at a rate of 2% annually.
- The population of the rest of the world (excluding North America) was approximately 3500 million (1973).
- The number of telephones installed in the rest of the world was 171 million (1973).

and assuming that the rest of the world increases the number of telephones installed per year at an increase of 12%, to achieve the goal of 1 telephone per 1.6 population we would calculate the following:

$$\frac{3.500 (1.02)^t}{1.6} = 171 (1.12)^t$$

t = no. of years required

Solving the above equation would indicate that to meet the objective would require 27 years. In effect this level would be achieved shortly after the year 2,000.

The number of telephones installed in the rest of the world would be: 3734 million. Subtracting the telephones already installed (171 million), 3563 million new telephones would have to be installed.

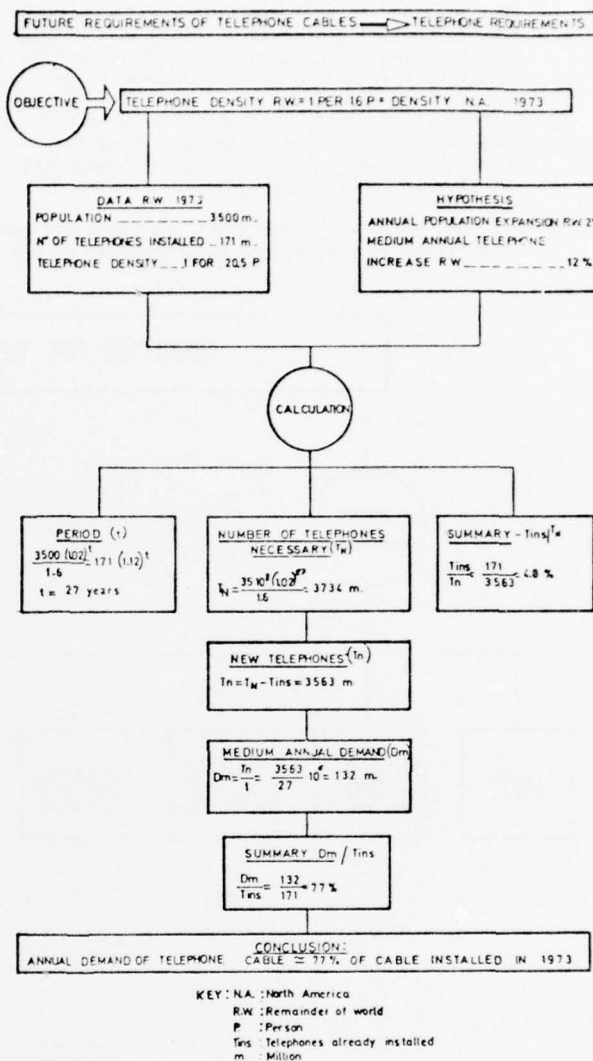
This implies an average annual requirement of 132 million telephones the equivalent of 77% of those which were already installed in 1973.

The installation effected in 100 years of telephony in the rest of the world represents 4.8% of the future requirements if we accept the density (telephone/population) ratio given.

Continuing the idea of proportion between telephones and cables, we can estimate on a very rough basis that:

- The telephone cable installed in the rest of the world up to 1973 represents only 4.8% of its requirements to the year 2,000.
- If this objective were to be reached by the year 2,000, the average annual consumption for the rest of the world represents 77% of the cables already installed and in service up to 1973.

This information is shown in figure 9.



Calculation of telephone demand

Figure 9

2. Product Requirements - Current and future market tendencies:

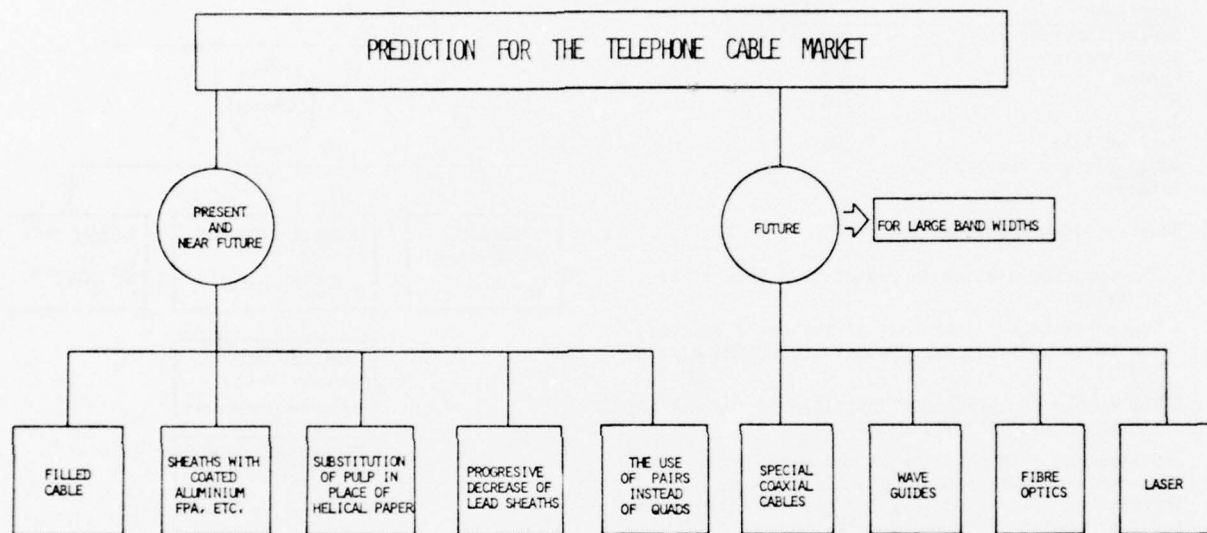
- It is apparent that many of the consumers are specifying filled cables or at least demonstrating an interest in this type of cable with the increasing desire to bury cable.
- In non-filled plastic insulated cables there is an interest in FPA, Glover, etc. sheaths which employ copolymer coated aluminium screens.
- Pairs have gained in acceptance in comparison to quads due to:
 - a) Reduction of the use of "phantom circuits"
 - b) Elimination of the cost differential between the two, and
 - c) Increase in PCM or other high frequency applications.

- A reduction in the use of lead for sheaths is evident with the "age of plastic" gaining in acceptance by consuming areas apparently as a result of economics and by observing that highly developed countries have made a successful transition.
- Paper/pulp, a continuous tube of paper manufactured directly onto the conductor has gained acceptance in many areas over the conventional spiral wrap paper insulation.
- PVC, having a higher dielectric constant and poorer dissipation factor than polyethylene, is now

only used for special applications for exchange area cable insulation.

For obvious reasons, the objective of the summary was to describe current and immediate future trends observed. In general, the interest in video phones, special coaxial cables, wave guides, fiber optics, laser, etc. is restricted to areas with supply capabilities within its borders. International market interest in these areas is considered to be on a long range basis in terms of commercial applications.

This projection is summarized in the final figure.



Present and future trends

Figure 10

ACKNOWLEDGEMENTS

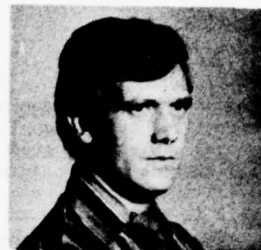
The authors appreciate the collaboration of all those people who have helped with their advice and suggestions.

REFERENCES

1. German - V.D.E.
Verband Deutscher Elektrotechniker
2. English - B.P.O.
British Post Office
3. French - P.T.T.
Postes Telegraphiques et Telephoniques
4. United States - R.E.A.
Rural Electrification Administration
5. "Comunicaciones Eléctricas" - Volume 49/2 - 1974
6. "Libro Verde del CCITT" (Asamblea Plenaria 1972)



Frank W. Horn is currently Director of Research and Development for Cables de Comunicaciones, S.A. in Zaragoza, Spain. An honor graduate in Electrical Engineering from the University of Colorado, he has been actively involved in the telecommunications field for over 50 years. Mr. Horn was associated with Bell Laboratories for over 45 years where he was responsible for the development of most of the cable in use today. The recipient of numerous awards, he also has many technical papers to his credit. Mr. Horn is the author of the book "Cable Inside and Out".



Manuel Villarig has a degree in telecommunications engineering from the E.T.S.I.T. (Escuela Técnica Superior de Ingenieros de Telecomunicación) of Madrid and is Manager of Cable Design and Engineering with Cables de Comunicaciones, S.A. in Zaragoza, Spain. Mr. Villarig joined CCSA immediately upon graduation and started as a process technician. His assignments have included engineering projects related to the plant start-up and he was also assigned various special projects in process and product engineering until 1973 when he was promoted to his present position.

FINITE ELEMENT ANALYSIS OF CABLES

Arthur D. Carlson
New London Laboratory
Naval Underwater Systems Center
New London, CT 06320

Summary

A structural analysis technique employing the theory of finite elements has been applied to several multiconductor armored cables with good results. The interactions of all the cable components, that is, the armor, conductor, filler materials, etc., are determined when the cable is subjected to an axial load, and in one case to a hydrostatic pressure as well. The analytical results include the stress, strain, and relative motion of each cable component; for example, the radial deformation and stress level in the covering of a copper conductor can be determined as well as the stress in the principal load carrying members. With this kind of detailed information, one now has the basis for postulating the life of a cable.

This analysis technique is not restricted to rotationally symmetric geometry. In fact, it is geometrically independent, and therefore permits its application to practically all possible designs. It is also possible to consider nonlinear problems, such as those caused by elastic-plastic stress states, large deformation, and creep.

Introduction

It is clear that a detailed understanding of the interaction and relative importance of the constituents (armor, insulation, wire diameter, etc.) of a cable is needed before a predictable reliability determination can be made. If a designer had this information and the means to vary parameters in the design, he would understand and thereby be able to control and build into a cable any desired performance. This paper will discuss how the theory of finite elements, a structural analysis technique, has been applied to several cable designs and what new insights result. Also, the formulation of the problem of stresses induced in a cable as it goes over a sheave is outlined.

Before proceeding to the discussion of the technique and a comparison of the analytical results with some experimental results, let us first define what is implied by the terms "structure" and "mathematical model." A structure connotes anything composed of organized or interrelated elements. This could mean, for example, a bridge, a chair, an automobile or a cable. Structure, then, has an extremely broad meaning. One usual connotation of the term math model appears to be that one must, in effect, know certain solution information beforehand and construct a set of modeling equations (a mathematical model) that will predict the measured or apparent results, which in turn permits the extrapolation of measured results to a point beyond; we prefer to call this process a curve fitting technique. The second connotation, which is the meaning in this report, is that a mathematical model can be developed to describe the system (structure) without knowing what the response will be. Thus, the solution of the resultant equations of motion, with the problem boundary conditions, will describe the total response, thereby providing new insight into the physical nature of the problem and showing the interaction of the problem variables.

The analysis of several cable designs is presented along with experimental results that at least partially attest to the correctness of the math models.

NASTRAN was used as the analysis tool for these results, but one is not limited to this program only. It is not necessary to prove the validity of the finite element theory as this has already been done in the literature and in practice.

The cables to be considered are not the usual wire rope designs, but rather specialized designs to fit particular undersea requirements. These requirements are a combination of mechanical and electrical factors. There are some current methods for handling wire rope designs that are apparently quite adequate. The theory of finite elements will be applied to cables where these techniques are not appropriate. The cables and the theory presented in this paper are, for the most part, covered in references 1, 2, and 3.

Math Model I

The cross section of the cable considered as model I is shown in figure 1. The Kevlar-29 is in a parallel lay, whereas the electrical conductors (copper with an ethylene-propylene rubber jacket) are twisted triads with a period of one inch. This configuration is covered with a neoprene jacket. The cable is to be subjected to an axial load (which will be 8100 lb) and hydrostatic pressure (of 4535 psi). It is desired to determine the stress and deformation of the Kevlar-29 rather accurately. It is acceptable that the degree of accuracy in the remaining components will be less.

Because of symmetry, only one quarter of the cross section requires mathematical modeling. The quarter segment to be modeled is shown in figure 1 and is the area included within the x-y quadrant. A decision must now be made regarding the length of the cable to be modeled. The determining factor for this particular cable was the pitch of the conductors. It was considered necessary to model at least two complete rotations of the triad. Longitudinally then the math model was two inches. With this length, enough of the helix is far enough away from the boundaries of the math model so as not to be affected by them. This point will be discussed in more detail in a later part of the text.

The finite element math model in the plane of the cable normal to the longitudinal axis is shown in figure 2. The Kevlar-29 longitudinal fibers were modeled with three-dimensional finite elements. Note that continuity across each finite element boundary is satisfied, hence the assemblage of finite elements models the Kevlar as a continuum. Because the Kevlar-29 has a very different modulus of elasticity in the longitudinal (z direction) and lateral directions (x-y plane), this orthotropic nature has to be considered. This effect is easily accounted for within the NASTRAN program in a straightforward manner, in that the material properties in the orthogonal directions are input parameters.

Now that the interactions of the Kevlar-29 with itself have been accounted for, the interactions between the Kevlar-29 and the surrounding electrical conductors is considered. This interaction would be due to the hydrostatic load as well as the axial load. The radial interaction between these two constituents

is modeled with scalar finite elements, more particularly, springs. These are designated as K_1 in figure 2. The magnitude of K_1 is determined experimentally by placing one of the conductors on a rigid surface, loading it on the opposite side and plotting a force deflection curve from which a spring constant can be found. Figure 3 shows a typical test setup for finding the spring constant. A similar procedure is used to find an equivalent spring to simulate the radial force interaction between the conductors. A typical test setup is shown in figure 4. This interaction is modeled by spring K_2 shown in figure 2.

The last constituent to be considered is the neoprene coating. This is not particularly important from an axial strength point of view but it does contribute to the radial squeeze on the conductors. Three-dimensional wedge finite elements were used here and are shown in figure 2. Since the Kevlar-29 and neoprene are three-dimensional finite elements, they have a dimension of length which is normal to the radial plane. The length of each element is dependent on the length of the helix of the electrical conductor in the sense that the radial contact between the spring K_1 is a function of the helix period. Spring K_1 represents the continuous radial contact force between the Kevlar and the ethylene-propylene rubber covering the copper, but concentrated at discrete points. The length of each three-dimensional element was 0.33 inch and was based on a helix period of one inch.

The conductor was modeled with bar finite elements (3 per helix) which can withstand tension, compression, bending, and torsion. A three bar approximation is rather crude for finding the detailed state of stress in the conductor, but because we were more interested in the state of stress in the Kevlar at this particular point, this approximation was accepted. If a more detailed state of stress was desired, more bar elements would have been used. A detailed examination of the finite element math model of figure 2 will show a slightly different arrangement of the triad spacing, and the depth of the neoprene. This slight adjustment was done for ease of modeling. The measured triad stiffness is, in effect, smeared along the outer circumference of the Kevlar-29. The triad and neoprene approximations are minimal from a stiffness point of view, which is important since this is the parameter which determines the load transfer. If one wanted a detailed stress picture of the triads and neoprene many more finite elements would be used to model these two components. A picture of the complete three-dimensional model is shown in figure 5.

Boundary Conditions

The question now to be addressed concerns the boundary conditions the structure is to be subjected to. In the actual cable, any plane normal to the longitudinal axis is assumed to move as a plane. To simulate this effect, the boundary of the math model at $Z=0$ (see figure 5) is restrained from any movement in the axial (Z direction) but is free to move in all other directions. The boundary at the top plane of the model (figure 5) is given an enforced displacement. That is, each node point which is the junction of intersecting finite elements is moved a unit distance in the Z direction, but is free to respond in all other directions. The distance used was 0.010 inch. These boundary conditions simulate the axial elongation. The hydrostatic pressure load is simulated by applying a load at each node point on the outermost circumference in the radial direction and in the Z direction on the top and bottom surfaces. The pressure used was 4535 psi.

Results for Cable I

Maximum values of stress in the cable members for an axial load of 8100 lb (correspond to 0.010 inch axial displacement) and the state of stress due to the combined effects of the axial and hydrostatic load of 4535 psi are given in table 1.

TABLE 1

Material	Axial Load (8100 lb)			Axial Load plus Hydrostatic Pressure (4535 psi)		
	σ_x psi	σ_y psi	σ_z psi	σ_x psi	σ_y psi	σ_z psi
Kevlar-29	314	-309	49,000	-5510	-5510	48,700
Neoprene	101	106	106	-6620	-6835	-6,701
Copper Conductor			-2			--59
Conductor-Conductor Interaction in Radial Direction (K_2)	-6.4 psi			-1266 psi		
Kevlar-29-Conductor Interaction in Radial Direction (K_1)	-9.5 psi			-5209 psi		

The addition of the hydrostatic pressure has a negligible effect on the state of stress in the Kevlar-29. In either case, the stress levels were within the problem tolerance. The other cable constituents experienced a marked change in stress due to the addition of the hydrostatic load. No problem is foreseen for the copper conductor, but one could be envisioned for the insulation covering of the conductor where the maximum compressive stress is on the order of 5200 psi compression. This state of stress may be high enough to cause a creep problem, which may, if it occurs, cause the conductor insulation to become egg shaped. This, in turn, may affect the electromagnetic characteristics in a negative manner. As mentioned, this model is not fine enough to give detailed states of stress in the conductor insulation, but since a problem may exist, a new more detailed math model could be built and analyzed.

Math Model Validation

These stress results are, of course, calculated values. One must accept them with the same level of acceptance that is given to the math model and the theory of finite elements. A test was conducted on the cable to compare its axial elongation-axial force characteristics with the calculated values. These results are shown in figure 6. The important characteristic of this plot is the similar slopes of the analytical and experimental load-strain curves. From approximately 6000 to 16,000 lb they are reasonably parallel. The offset is due, we believe, to the voids and slack which are in the real cable, for which no modeling was done. Because these voids are random and not easily controlled, and diminish after an initial loading, there does not appear to be any compelling reason to consider them. Because the load-deformation characteristics of the finite element model and the test were essentially the same, we consider the math model to be a reasonable representation of the real cable. Other information available from the model was the relative motion of each constituent.

Math Model II

A second cable configuration is shown in figure 7. This cable also demonstrates a convenient radial symmetry with respect to the center. The strength members (fiberglass) with a helical period of 20 inches provide the necessary strength to counteract the axial forces (figure 7). The center copper conductor is surrounded by polyethylene. The fiberglass strands are wrapped about the polyethylene core which is imbedded in a foamed polyethylene cover.

Due to the symmetry of this structure, only a quadrant of the cross section was modeled (figure 8). The type of finite elements chosen for the various material constituents are as follows:

- * Copper conductor - This material located at the center was modeled by the use of four CWEDGE (NASTRAN) elements for each plane (figure 8). These are three-dimensional finite elements and yield stress-strain results in the x, y, z directions. The total length of the model was seven inches. The material was assumed to be isotropic with a Young's modulus of 17.6×10^6 psi and a Poisson's ratio of 0.3. In the finite element model (figure 9), this designates the area surrounded by the grid points 0, 10, 11, 12, 13, and 14.

- * Polyethylene - This section of material was modeled with the use of the CHEXA2 elements, also three-dimensional finite elements. The Young's modulus for this isotropic element was 1.8×10^5 psi and the Poisson's ratio was 0.48 (nearly incompressible). This material is indicated by elements 5 through 8.

- * Fiberglass - This cable component was modeled as a rod element for the anticipated tensile load. Since the period of the helical lay is 20 inches, it was assumed for this model of 7 inches that the rod is essentially in a parallel lay configuration. This assumption was used as a first approximation since the polyethylene core is only 0.2 in. in diameter. The stiffness of the fiberglass in the horizontal plane is accounted for with springs acting in the radial and circumferential direction. The stiffness of these springs was determined experimentally (as it was for model I) and are denoted as K_1 and K_2 .

- * Foamed polyethylene - The covering material was modeled with the use of the CHEXA2 elements, a three-dimensional, isotropic finite element. The elements are numbered 9 through 16 in figure 9.

- * The circumferential stiffnesses of the fiberglass-polyethylene interactions and the radial stiffness of the fiberglass alone were determined by the usual implementations of experiments. This method was described in the discussion of the first math model (figures 3, 4). The resulting stiffnesses are modeled in the form of CELAS1 (spring) elements.

Boundary Conditions

In the bottom plane ($Z=0$) of the model, all grid points were mathematically fixed (no displacement). The top plane of the model was forced to displace 0.1 inch in the axial direction.

Due to the modeling of only one quarter of the cable section, appropriate boundary conditions were substituted. Namely, all displacements in the radial and axial direction along the cut were allowed. All the displacements orthogonal (circumferential displacements) to the cut were not allowed.

Results for Cable II

From the computed results it was determined that about 20% of the total tensile force was taken up by the center conductor. A much larger portion of the force was distributed among the fiberglass strands (75%). The remaining 5% of the load was taken up by the foamed polyethylene and the internal polyethylene. This was approximately the desired load distribution.

Math Model Validation

The modeled cable was tested in the laboratory. The cable length was nine feet with each cable end properly potted and fitted into end grips. A tensile load was applied through a hydraulic actuated load cell. The axial displacements were measured to within $1/32$ of an inch. The cable specimen was loaded to 850 lb and then unloaded to approximately 80 lb. The experimental curve is shown in figure 10. The initial loading segment on the experimental curve (from the origin to point A) is attributable to the internal adjustment (reorientation) of the cable component. It required a certain amount of preload for this structure to behave as an elastic continuum due to internal voids. Once material continuity is established, the cable responds in an elastic manner. Both the loading and unloading curves display the same slope on the force-strain (F-e) plane.

Cable Model Variations of Cables I and II

Two different cable configurations have been analyzed and the load distribution and component deformations have been found. If any of these results do not fit within a particular material or system boundary, it is a straightforward process to change the model, make another computer run and evaluate the new configuration. For example, if in the second cable, 20% of the axial load being carried by the copper conductor is too much (perhaps it raises the stress level to yield), one could change the material or geometrical characteristics of the foamed polyethylene to determine if a new axial load sharing could be made. Another variation might be to change the size and/or position of the fiberglass strands.

The two cables we have discussed have had convenient geometries in that their symmetry could be taken advantage of, and the minimum number of degrees of freedom, i.e., equations of motion were required to solve the problem. Degrees of freedom are, in general, related to problem size, which is related to model setup time and computer run time, all of which are related to cost. Symmetry, however, is not a requirement for the implementation of the finite element application to a problem. In fact, the strength of the method is its nonreliance on symmetry. A nonsymmetrical design would simply require a more complicated model.

Linear and Nonlinear Problems

The two cables previously discussed fit within the theory of elasticity, i.e., the stress is elastic and the displacements are small. For an axially applied load the first condition that is usually violated is that of elastic stress. The stress levels can easily be above the yield point, well into the plastic zone. This nonlinearity can be accounted for in some finite element computer programs. Strains of the order of 5% to 10% may be considered with some finite element codes.

A further theoretical complication can be added to a problem which occurs when the deflection

of the structure is large. Deflection defined here is a movement of the structure in space, over and above a large strain in a material. A physical situation which is described by this action is the bending of a cable over a sheave. If during this bending the stress exceeds the yield point, we have a combined elastic-plastic, large deflection problem. Work is currently underway to solve this problem.

The problem on time-dependent material effects (creep) can also be considered within the finite element context. A number of codes are available to handle such problems. It may, in some cases, be harder to get the actual material creep data than to compute the effects.

Conclusions

The results of two different finite element analyses have been presented along with some supporting test work to verify the models. With this technique, new insight into the interaction of the cable constituents can be found and the design adjusted "on paper" if the performance is not within a given specification. Although not discussed in this paper, several other cable designs subject to different performance require-

ments have been analyzed, the resultant designs built, and they have performed well in the field.

The nonlinear problems of elastic-plastic stress states, large deflection, and creep problems can also be considered. Such nonlinearities complicate the analysis and add to the computing costs, but nevertheless are amenable to solution in some cases.

References

1. A. D. Carlson, M. A. Tuccio and R. G. Kasper, "A Finite Element Stress Analysis of a Multi-conductor Armor Cable," *Marine Technology Society Journal*, vol. 7, no. 7, Oct-Nov 1973.
2. R. G. Kasper, "The Mechanical Response of an Electromechanical Array Cable Subject to Dynamic Forces," Tenth Annual Conference, Proceedings of Marine Technology Society, 23-25 Sept 1975.
3. R. G. Kasper, "A Correlation Study Between Experimental and Finite Element Analysis of Various Electromechanical Cables," NUSC Technical Memorandum No. EM-31-75, 8 May 1975.

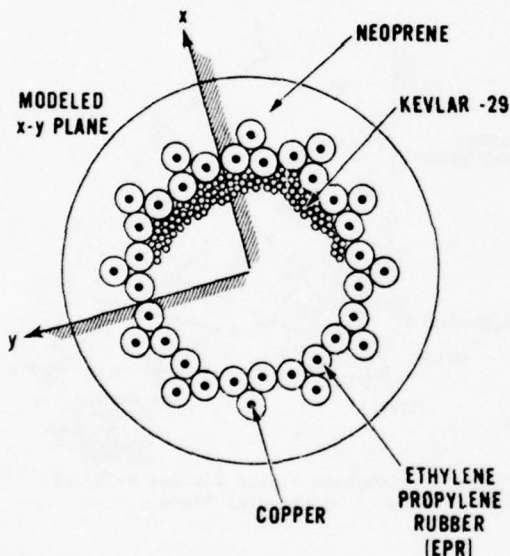


Figure 1. Kevlar-29 Multiconductor Cable

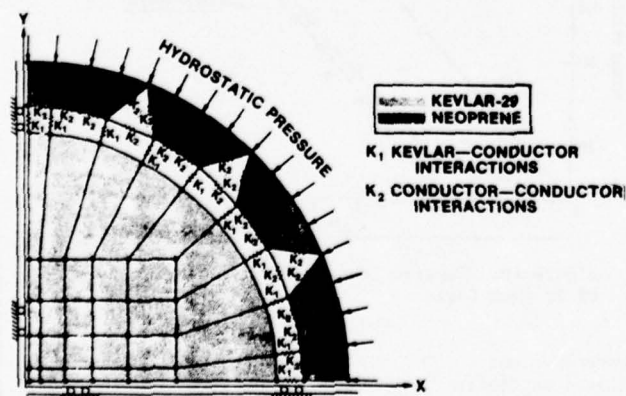


Figure 2. Finite Element Model of Kevlar-29 Cable in Horizontal Plane

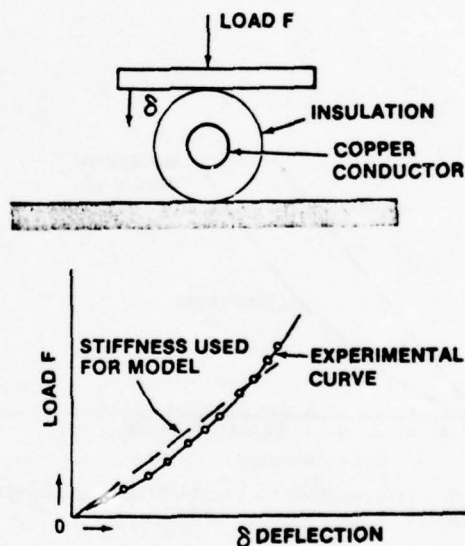


Figure 3. Experimental Method for Finding Stiffness of Conductor

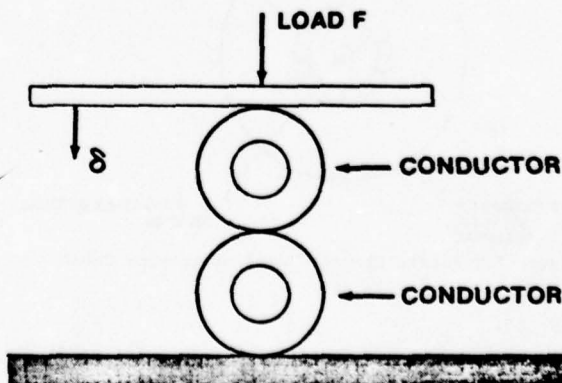


Figure 4. Experimental Method for Finding Stiffness Between Conductors

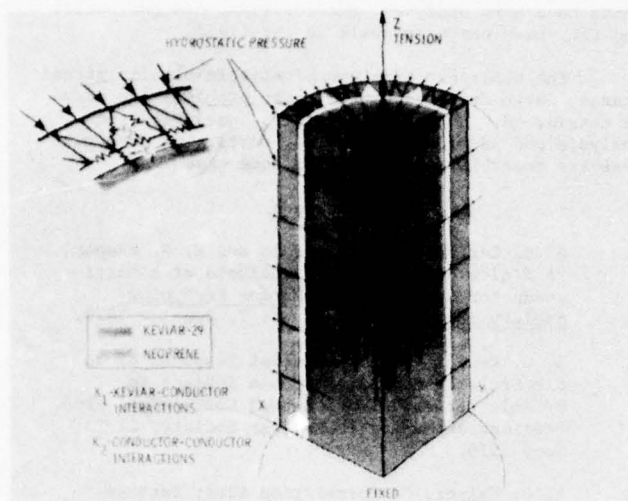


Figure 5. Three-dimensional Math Model of Kevlar-29 Multiconductor Cable

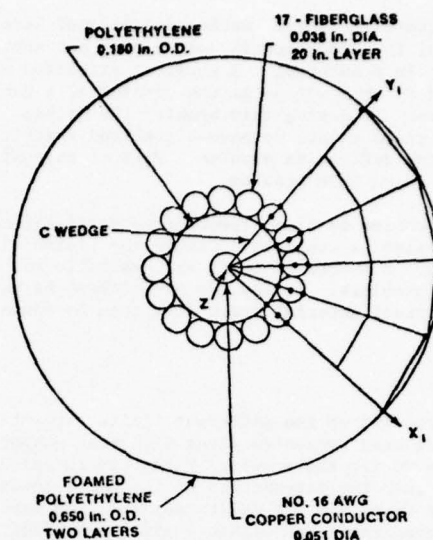


Figure 8. Initial Finite Element Model of Buoyant Cable

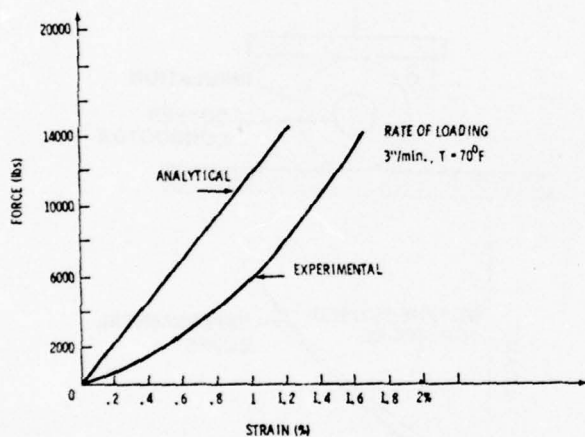


Figure 6. Tension Test vs Finite Element Analysis of Kevlar-29 Multiconductor Cable

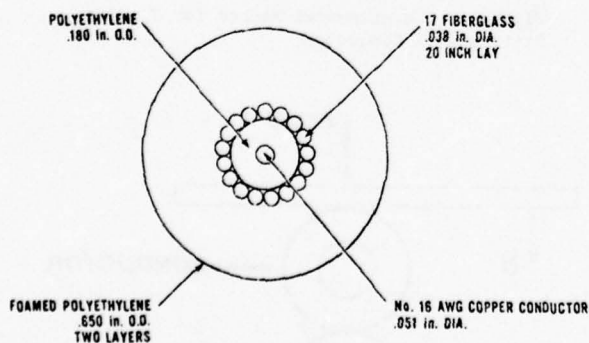


Figure 7. Finite Element Model of Buoyant Cable

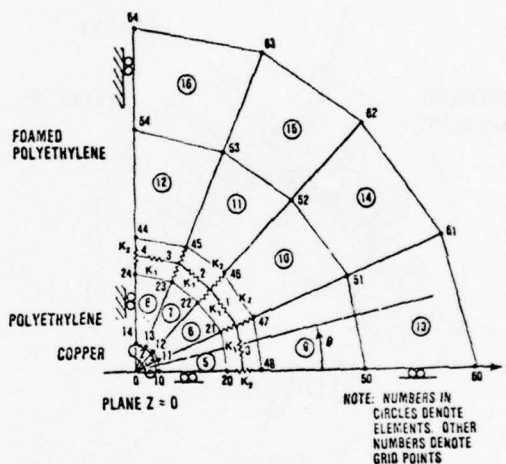


Figure 9. Complete Finite Element Model of Buoyant Cable in Horizontal Plane

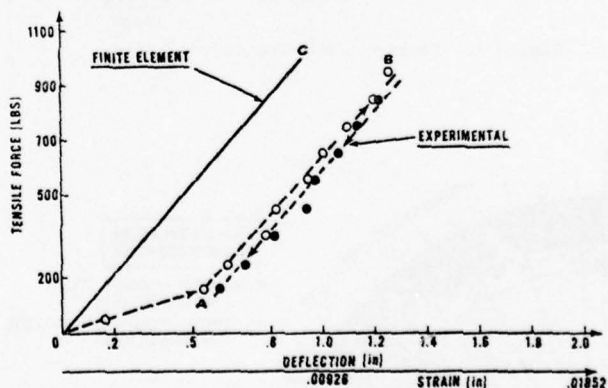


Figure 10. Tension Test vs Finite Element Analysis of Buoyant Cable

BIOGRAPHY

Head of the Engineering Mechanics Staff at the Naval Underwater Systems Center, New London Laboratory, New London, CT. Has concentrated on finite element applications for the last seven years on problems ranging from machine structures and cables to acoustic and electromagnetics. Has worked in private industry and government for a total of 17 years.

DESIGN GUIDES FOR FINE-WIRE CABLE

by

H. E. Miller

Honeywell Inc., G&APD
Minneapolis, Minn. 55413

Abstract

The electronics industry trend toward smaller packaging concepts has led to the need for design guides for flat rather than round fine-wire cable used in applications needing wire sizes AWG #30 or smaller. The cable guides presented include data on conductor characteristics, primary insulation, insulated conductor groupings, and shielding. Also discussed are conductor grouping configurations, cable jacketing and materials available and cable packaging at termination points. Conductor characteristics include hardness, tensile strength, and elongation as related to cable strength and configuration, and a review of the various conductor materials available such as copper ETP, copper OFHC, and copper alloys. Also included are kinds of strand plating (coating) available and the number of strands per conductor. Primary insulations cover various insulating materials and their thicknesses. Selection of the number of conductors depends on the overall cable configuration and this is part of the design considerations on insulated conductor grouping. Shielding requirements are reviewed along with the selection criteria on insulated conductor grouping. Selection of jacket materials is related to the packaging of the cable termination points in order to have compatibility between the connector used, and potting or encapsulating system required for the cable system. Cable flex life versus cable flexibility is determined by the particular application requirements.

Introduction

The trend toward smaller packaging concepts within the electronics industry has created the need for design guides in the application for fine-wire cable. These types of cables are used in applications needing wire sizes that are AWG #30 diameter or smaller and have a flat shape rather than round.

A typical cable has a silicone or polyurethane jacket over the cable components. The cable components are unshielded singles, twisted pairs, twisted triplets and twisted sextuplets. The cross section of this cable is rectangular (flat) and the components are equally spaced and vertically centered across this jacket material. The shield is the braid design, which is normally found on round-wire cable components. A cable will consist of two or more of the above components in the jacket. The conductor strands are size AWG #50 wires (0.001-inch diameter), silver coated (plated) or bare copper (no coating), bunched in groups of 64 or 66 to form a conductor of size AWG #32 insulated with 0.003 to 0.005-inch wall Teflon-TFE or Teflon-FEP. No cable component has more than one conductor size throughout.

These cables are not described in government or industrial documents (specifications). This information is available only from vendor literature.

This design guide containing all the variables that must be considered and which are interrelated has been developed to provide a tool for planning this kind of cable.

Design Guides

A design guide (Table 1) for cable planning provides an outline approach for selection of cable parts. Included in this list are the number of conductors; conductor size, material and finish; conductor insulation; grouping of insulated conductors and the method of shielding they may need. The above completes the cable plan up through the cable component stage.

The next item in the plan is the component configuration, which may be considered group arrangement for a flat rectangular-type cross-section cable. The final cable item is its jacket.

The final items in the list are related to the cable as it becomes part of a cable assembly. These are connector and method of termination of the conductor, bend radius control, encapsulating or potting material and size of this section, and any special requirements for the cable or cable assembly.

TABLE 1
CABLE PLANNING GUIDE LIST

BASIC CABLE PART	
Number of Conductors	
Conductor	
Size	No. of Strands
AWG	
30	7 19 25
32	7 19 64
34	7 19
36	7 25
38	7
Material	
Copper, ETP Copper, OFHC Copper, Alloy	
Finish (Plating on Strands)	
None Silver Tin	
Insulation (Primary)	
TFE - (Teflon) FEP - (Teflon) ETFE - (Tefzel) PVF ₂ - (Kynar) Other	

TABLE 1 CONCLUDED

CABLE COMPONENTS	
<u>Grouping of Insulated Conductor.</u>	
Single	
Pair	
Triple	
Quad	
Other	
<u>Shielding</u>	
Braid	
Serve	
Metallized Plastic (with Drain Wire)	
CONFIGURATION	
Flat (Rectangular)	
Round	
Other	
Group Arrangement	
JACKET	
Material	
FEP - (Teflon)	
TFE - (Teflon)	
Polyurethane/Silicone	
Other	
CABLE ASSEMBLY	
Special Requirements	
Connector and Cable Termination	
Bend Radius Control	
Encapsulation Material	
CABLE HANDLING	

Basic Cable Part

By using the guide list it is possible to review the options that are available for the cable build. This list is helpful when establishing the kind of cable a particular application will need.

Number of Conductors

The first item to consider is how many conductors the cable will have. If an exact number is not known, a close approximation will start the cable construction plan.

Conductor Size

Since most cables have stranded conductors, the size or sizes of conductor in the cable is the next item to consider. After the size has been selected, the number of strands that are available for the particular size can be selected. Conductor size and number of strands used are often variables subject to many outside influences in actual practice. For example, if a conductor size, AWG #32, with 19 wires of AWG #44 is selected but later it is found that the cable vendor to be selected normally works only with AWG #32 conductor with seven wires of AWG #40, a change to fewer strands might be in order to avoid a situation where the vendor would be working with an unknown as far as his experience is concerned. Table 2 lists the possible lead-wire options; for comparison, Table 3 lists standard lead-wire options.

TABLE 2

FINE-WIRE CABLE SIZE

Conductor		Strand		
AWG	Diameter (in.)	Number	AWG	Diameter (in.)
30	0.0120	7	38	0.0040
		19	42	0.0025
		25	44	0.0020
32	0.0093	7	40	0.0031
		19	44	
		64	50	0.0010
34	0.0075	7	42	
		19	46	0.0016
36	0.0060	7	44	
		25	50	
38	0.0042	7	46	

TABLE 3

STANDARD LEAD-WIRE CABLE SIZE

Conductor		Strand		
AWG	Diameter (in.)	Number	AWG	Diameter (in.)
18	0.0480	7	26	0.0159
		19	30	0.0100
20	0.0380	7	28	0.0126
		19	32	0.0080
22	0.0300	7	30	
		19	34	0.0063
24	0.0240	7	32	
		19	36	0.0050
26	0.0190	7	34	
		19	38	0.0040
28	0.0150	7	36	
30	0.0120	7	38	

Conductor Material

The most common material used for conductor wires is copper electrolytic tough pitch (ETP). The wire-wrap wire industry uses the copper-OFHC (oxygen-free high conductivity) for its single-strand conductor because it has a higher degree of ductility than copper-ETP. For other higher-strength applications, a copper alloy material may have to be considered for conductor wires but availability could be a problem if the wire sizes are less than AWG #40. For example, if an AWG #36 conductor is selected it is possible that the cable application may require the strength of a copper alloy, but for size AWG #36 (seven strands of AWG #44) the wire is not available. Since it may not be possible to go to a larger-size conductor, the compromise would be to use a conductor with hard wire instead of annealed wire. This change could raise the tensile strength value from

32,000 psi to over 40,000 psi which would not be as high as that of copper alloy which is 55,000 psi, but it would offer an improvement of almost 25 percent. Selecting a conductor AWG #36 with 25 wires of AWG #50 is a way to obtain a hard wire through the normal wire drawing operation.

Conductor Finish

The common finishes (plating) on conductor wires are tin and silver. Nickel and gold are sometimes used but only in special applications. In AWG #30 gage or finer, with FEP-Teflon insulation, quite often no plating is used, only the bare copper wires. The guide list has three finish conditions - none (bare), silver and tin. This finish can depend on the kind of conductor primary insulation used. If a TFE-Teflon is selected for the conductor insulation, the wire finish will be silver because the tin will not take the process temperatures that are required for sintering the TFE. Also, if a bare copper wire conductor is used with the TFE-Teflon insulation, the copper wire would oxidize enough during the sintering process of the TFE so that soldering of the completed insulated conductor would be very difficult. In contrast to this, the FEP-Teflon will work with any of the three finish conditions: none, silver and tin.

Conductor Insulation

There are more than 10 common conductor insulating systems for leadwire which go into cables. For work with fine conductor wires, the systems have been mainly related to the fluorocarbon group. The conductor insulations used in these fine-wire cables have been FEP and TFE (both Teflon types). Their temperature ratings are 200°C and the wall thickness of the insulations is usually in the range of 0.003 to 0.005 inch (often noted as 3 to 5 mils) for those applications in which the conductor size range is AWG #30 to AWG #38. Two other fluorocarbon insulations are listed in the guide list, ETFE (Tefzel) and PVF₂ (Kynar). Their temperature ratings are 150°C and 130°C, respectively. Generally, the wall thickness for these two insulations would be 0.005 inch or more. At this point the basic building block of the cable is complete--the insulated conductor.

Cable Components

The next step in the cable plan is to determine the number of single conductors, twisted pairs, twisted triples, twisted quads, etc., that are needed for the completed cable. Also, the component function will determine whether or not it is to be shielded. For example, if a cable has six components - two singles, two pairs and two triples - and all of these components need shielding, then the appropriate checks and numbers would be entered on the guide list form. The space geometry in which the cable is to be located determines the type of shield used. A served shield only requires half the thickness of a braid shield for any given shield wire diameter. A metallized plastic (shield) with a drain wire requires even less thickness.

The shield coverage normally varies from 85 percent to near 100 percent. The serve and metallized plastic shields approach the 100 percent coverage while the braid shield will typically have 85 to 90 percent coverage. The wire size of the braid and serve shields for the cable applications in this discussion is typically AWG #42. The finish on this shield wire is tin, silver and gold flash. Normally, the length of lay (number of twists per inch) for a cable component group is a function of the total diameter of the conductors in the cable component, but if the cable is used

in a sharp bend application, the normal length of lay will need to be shorter, or more twists per inch, and the uniformity of these twists becomes more significant.

Cable Jacket

The configuration of the group or groups that are to be jacketed will have some influence on the geometry of the cross section of the jacket and this may determine whether the cable can be flat or round. For example, a group of cable components such as two shielded single conductors, two shielded twisted pair conductors and two shielded twisted triple conductors may be arranged as single, pair, triple, triple, pair, and single across the rectangular cross section of a flat cable. These arranged components could be then jacketed with silicone rubber or polyurethane. The silicone rubber jacket material will be more flexible than the polyurethane material. The typical jacket thickness is 0.015 to 0.020 inch for most flexible-type flat cables. The TFE and FEP are both jacketed materials that can be used for flat cable constructions. The FEP is used more often for jacketing material than the TFE. This cable may be dispensed as a bulk item and cut to needed length or it may become a component in a cable assembly or assemblies.

Cable Assembly

The items, special requirements, connector and cable termination, bend radius control, encapsulation material which is at the connector-cable interface, are all interrelated and need to be examined with the cable assembly end use to decide which one or ones will be compromised for the benefit of the particular cable assembly situation. For example, special requirements, such as treatment of Teflon insulation for bonding or post cure of silicone rubber for off-gas improvement, are the kind of requirements that influence the sequence of the processing which involves cable termination into a connector. The post-cure temperature for the silicone rubber jacket may be such that the jacket will need to be post cured prior to assembly into the connector because the temperature would damage the solder joints. Even an item such as the ability to rework must be considered in the selection of a potting or encapsulating compound for the connector-cable interface (commonly referred to as connector back potting).

The cable packaging technique can influence the length of potting at the connector cable interface because this length can complicate the bend radius situation. In compact packaging the longer connector back potting forces bends in cables that exceed 90 degrees, where the shorter length tends to allow bends of less than 90 degrees. Keeping the cable from exceeding the bend radius adds to the life of the cable conductor wires. See Table 4 for minimum bend radius for copper wires. The hardness of the wire improves the bend radius for the particular size. These are a few areas that need documenting as the cable is designed. Also, these items need monitoring during the particular device build, inspection, and testing because any problems developing in the cabling during the life of the device will need as much baseline data as possible to aid in establishing the failure modes of the particular problem. Radiography (x-ray) is a useful tool for this monitoring, but cost always becomes a challenge for this kind of activity.

TABLE 4

TYPICAL MINIMUM BEND RADIUS

Size		Condition	
AWG	Diameter (in.)	Annealed	Hard
50	0.0010	0.850	0.213
44	0.0020	1.700	0.425
36	0.0050	4.250	1.063
32	0.0080	6.800	1.700
30	0.0100	8.500	2.125

The minimum bend radius for copper wire to reach yield stress is:

$$R_{\min} = \frac{Ed}{2S_y}$$

R_{\min} is minimum bend radius

E is Young's modulus = 17×10^6

d is wire diameter

S_y is yield stress

Cable Flex Life and Flexibility

Cable flex life is related to the strength, size and condition (temper) of the material in the conductor strand. In theory, an annealed strand of a given material will have a longer fatigue life than a strand in the hard condition, but in practice the hard strand will restrict the sharpness of bend which tends to result in a longer flex life for the cable. Generally, flex life is increased by use of a large number of fine (small) strands. In applications requiring a large number of flexes during the life of the cable, the bend radius of the particular conductor size in relation to the overall "assembly-cable package" is more important than the conductor strand condition and size. For more detail on the size-bend radius relationship, see Table 4.

The cable flexibility is related to the size and condition (temper) of the material in the conductor strand. For the most cable flexibility, the annealed condition of the strand is desired. If flexibility and flex life are both desired, some flexibility may need to be traded for the added flex life by increasing the hardness of the conductor strand.

Cable Handling

In larger cables, cable handling during assembly, inspection and testing of any particular device is a parameter that normally does not cause much concern, but cables with conductors in sizes AWG #30 or smaller need more surveillance. Handling is a parameter that requires more attention as cables become smaller. If a failure does occur in a cable assembly with these smaller conductors, the normal failure analysis techniques are unsuitable because procedures for examining failed hardware packages containing these cables frequently are the cause of new failures in these delicate systems. In general, mechanical stripping techniques for failure analysis of this size cable are not recommended.

Conclusions

A guide system is an adaptable tool for planning a cable. The guide system is most effective when it is tailored to promote the size (range) cable desired. Cabling is too complex to attempt to have an all-inclusive one for all the conductor sizes available. Throughout this discussion on using the guide list, various optional parameters in this kind of cable construction are explained. In summary, users of finer wire cable (conductors AWG #30 or smaller) need to be prepared to modify techniques that they have associated with larger cable because the two are different in size, strength and handling characteristics.

References

1. "Copper Wire Tables," U.S. Department of Commerce - National Bureau of Standards, February 1966.



Herbert E. Miller is an Engineer in the Plastics Lab of the Materials and Process Engineering Department, Government and Aeronautical Products Division, Honeywell, Inc., Minneapolis, Minnesota. For the past 10 years he has been engaged in the material and process applications for the Division, with the wire and cable specialty as a major assigned activity. He holds a B.A. degree (1949) in Physics from Gustavus Adolphus College, St. Peter, Minnesota.

IMPROVED PAIR TO PAIR UNBALANCE FOR PAPER INSULATED CABLES
WITH UNIT-TWIN CONSTRUCTION.

by

G. I. B. Vermont
Olex Cables Limited
Melbourne, Australia.

ABSTRACT

This paper describes the development to produce larger (100 pair) Units with low capacitance unbalance, maintaining a "layer-type construction and "uni-directional" flexibility.¹

It is shown that capacitance unbalance between adjacent pairs can be expressed, for design purposes, by the equation -

$$\text{UNBALANCE (RMS) pF/500 m} = K_1 \times \text{Longer Lay} + K_2 \times F + K_3$$

where F is a function of the two twist lengths under consideration and K_1 to K_3 are constants, and can be obtained from statistical analysis of normal production.

Using a lay-scheme based on this equation, 36% of the MAXIMA (highest unbalance of each one of the 100 pairs to any other pair in a Unit) occurs between pairs in different layers and is a function of the direct capacitance between the wires of the pairs involved. A technique is, therefore, developed to reduce the direct layer to layer capacitance without affecting the "uni-directional" construction of the Unit.

INTRODUCTION

In any communication cable network, symmetric pair cables comprise a most significant component of all installations. The designs adopted for these have evolved over many years, from an interaction between manufacturing techniques, transmission performance requirements, materials technology, costs and associated line-equipment developments. As the requirements for information flow increases, new types of cables may be developed, but the large investment in existing plant demands a higher utilisation of it by extending the frequency range transmitted and, in consequence, a continuous re-appraisal of the manufacturing technique is necessary to facilitate longer term exploitation without incurring re-equipment.

AUSTRALIAN BACKGROUND.

Symmetric pair cables most commonly used are either of quad or of twin construction, the type depending on tradition, environment and of individual Telecommunication Authorities forward planning activities, which takes into account the economic evaluation of all aspects constituting the totality of a system. It is not the objective of this paper to consider or equate the advantages and disadvantages

of either quad-layer or unit-twin type cables. An efficient and quality conscious manufacturer, with strong Technical and Design expertise, can accommodate either system and will be instrumental in introducing techniques which will enhance the transmission properties for higher utilisation.

Telecom Australia has made a choice of Unit-twin construction. This decision was based on a comparison of costs related to diametric gains and field-balancing penalties of quads versus cross-talk standard obtainable with random jointing within units without additional balancing of twins. It was considered that Unit construction will give added potential for high-frequency operation, by allowing the separation of go and return circuits into well defined segments of the same cable.

DEVELOPMENTS IN UNIT CONSTRUCTION.

The original Unit construction consisted of cables made up from 51 and 102 pair Units employing four main lays (twist-lengths) in each Unit; two alternating in the odd layers and the other two in the even layers. It can be looked at as being a 2 by 2 matrix and is often referred to as such. It is obviously a simple construction but the economics, which can be introduced by faster and more modern lay-up techniques (e.g. bunching), tend to destroy the Capacitance Unbalance characteristics, since any movement in the relative position of any pair would bring pairs of identical nominal lay into immediate adjacency. To reduce the chances of this happening, the construction has been revised to contain a 3 x 3 matrix of lay-combinations, i.e., each layer contains three different lays alternating and the same lays will re-occur in every third layer only. The necessity of a "Marker-pair" in each layer for pair identification, and the variation of number of pairs in the layers, has led to the eventual requirement of these being of different lay lengths and to an actual 4 x 3 matrix. Cross-talk objectives have also led to the reduction of the maximum value of capacitance unbalance which is allowed in any Unit, and the present limits (max.) are:

150 pF/500 metres for 19 AWG (20 lb or .9 mm)
190 pF/500 metres for 22 AWG (10 lb or .64mm)
230 pF/500 metres for 26 AWG (4 lb or .4 mm)

There is also an additional requirement, which states that the RMS value of all significant combinations of Pair to Pair Unbalances should be less than 20% of the maximum specified value.

REALISATION OF REQUIREMENTS.

Traditionally it was accepted that (until the advent of computerised testing) unbalances which may give concern occur within a layer between immediately adjacent pairs. If these were kept under control the cable was deemed to be acceptable and, with manual testing, the one hundred such combinations were tested only in a 100 pair Unit.

As the specification requires the layers to be separated by a binder, and since the distance between the cabling points of each layer is defined by the unitising machine used, certain pairs in adjacent layers remain close to each other throughout the Unit length.

A typical configuration is given in Figure 1.

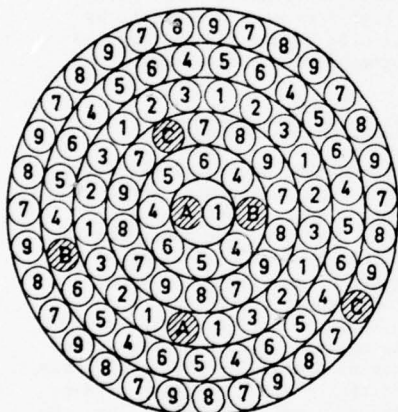


FIG.1
TYPICAL LAY-SCHEME
OF A 100 PAIR UNIT
(A,B,C ARE MARKERS)

It was, therefore, realised that at least nine of the lays (taking the "marker-lays" as less significant from the frequency distribution of combinations) have to be selected to be completely compatible with each other to avoid the occurrence of inadmissible unbalance. This represents thirty-six (36) possible lay combinations and, if the marker pairs are also treated in the same way, the number of combinations to be analysed rises to sixty-six. The frequency of combinations occurring in a 100 pair Unit is given in Figure 2, which is restricted to "significant" combinations only, i.e., to those which can be immediately adjacent with conventional unitising techniques.

ESTABLISHMENT OF LAY-SELECTION

Using data generated on previous production, a task was set to establish the relationship between two twin lays and the resulting Pair to Pair capacitance unbalance performance. It was found that, for any

combination, a normal distribution did exist when those were separated according to twinning machine types used. It was assumed that the factors which may influence the end result will be determined by:

- The length of lay
- The difference between the lays
- The type of machine used

In accordance with these logical assumptions, an equation of the form -

$$\text{Unbalance (RMS) pF/500 m} = K_1 \times \text{longer lay} + K_2 \times F + K_3$$

was proposed, where F is a function of the two twist lengths under consideration and K_1 to K_3 are constants to be determined by statistical analysis of normal production. The formula is an interaction of variables and, in establishing the constants, the work was modelled on a mathematical treatment of several variances.²

The proposed formula has given a satisfactory agreement with practical results (within ± 5 pF) and lead to the following conclusions:

- The validity is limited to the lay-range of approximately 2 to 6 inches. (50 to 150 mm)
- K_1 is positive, but is also a function of the conductor gauge; heavier conductors can tolerate a longer lay.
- K_2 and K_3 are negative and complimentary.

If K_2 is large, K_3 is small, and vice versa, and are really a measure of lay-consistency. With machines providing a consistent lay, the lay-difference is very significant (K_2 is large), whilst a large K_3 indicates uncontrolled variations and, from the design point of view, is less desirable - "Rogues" are more likely to occur.

	A	B	C	1	2	3	4	5	6	7	8	9
A	/	1	0	3	0	0	5	3	3	1	1	1
B		/	0	2	2	1	3	0	1	2	2	2
C			/	2	1	2	3	3	2	3	0	1
1				/	6	6	9	11	9	6	5	5
2					/	6	8	8	8	6	6	5
3						/	8	8	7	5	6	6
4							/	10	9	13	14	14
5								/	10	16	14	12
6									/	12	14	13
7										/	14	13
8											/	14
9												/

FIG.2
FREQUENCY DISTRIBUTION
OF "SIGNIFICANT" COMBINATIONS
100 PAIR UNIT
(REF. FIG.1)

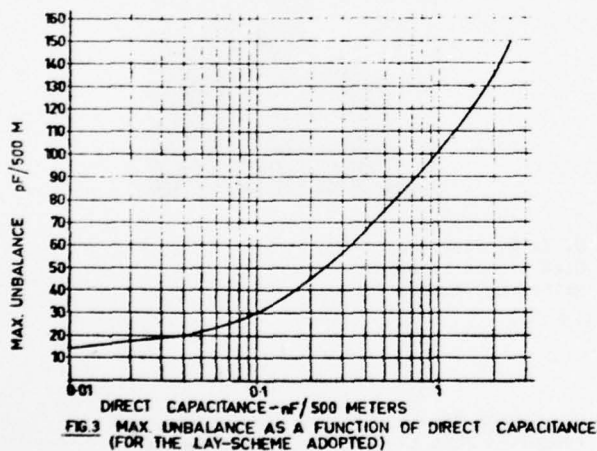
/// WITHIN LAYER IMMEDIATE ADJACENCY

FURTHER DEVELOPMENTS.

With the aid of the established relationship, appropriate lay-schemes were designed for use, and have given very satisfactory results for 26 and 22 AWG cables. The number of high performance combinations required for 19 AWG was just not available within the lay-ranges obtainable and a certain amount of grading, according to the frequency distribution of occurrence, was necessary to reduce the chances of high Pair to Pair unbalance.

Computer-controlled testing has provided the facility to more closely examine all significant unbalances. An analysis revealed that 36% of the maxima, i.e., the maximum unbalance of each individual pair to any other pair in the Unit (100 values for a 100 pair Unit) did occur between pairs in adjacent layers and not within a layer.

This analysis has also established an additional relationship, which connects the maximum unbalance obtained for any combination with that of the direct capacitance between the wires of the pairs under examination. (Figure 3)



The direct capacitance distribution between a pair in one layer against the pairs in the adjacent layer immediately above it, has been plotted in Figure 4 (Curve A).

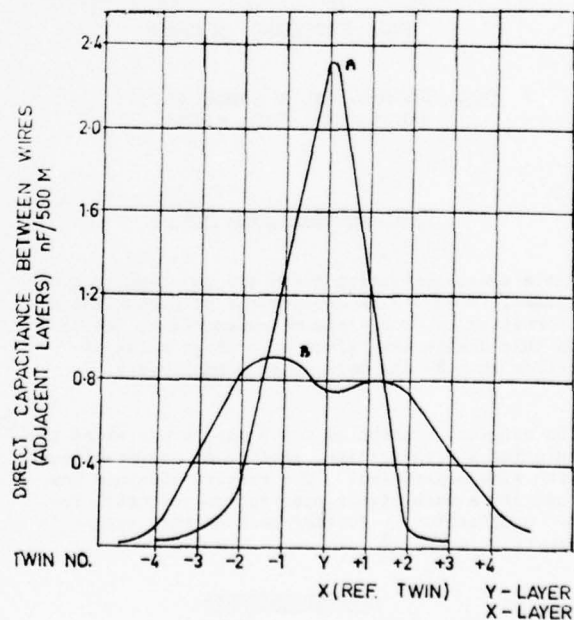
When the results of these two are compared, it is evident that a significant reduction of the possible maximum values between pairs in adjacent layers can be accomplished if the peaks are eliminated or, at least, diminished.

A periodic limited displacement of every second layer is within the plant capability, without affecting the essentially uni-directional nature of unitisation to maintain the flexibility required at the later process of combining the Units into a single cable. Its effect on direct capacitances between the pairs in different layers is, however, appreciable, as shown by 'Curve B' in Figure 4. The three worst values are reduced and the maximum reduction amounts to a 40% better unbalance for the formerly critical combination.

There is a penalty to be paid, as about four previously low direct capacitances are now increased, but the increase still places these combinations into a 50% cell at the worst, which should be quite acceptable. This process of 'improvement' is accorded to every single pair in its layer to layer situation, hence the overall benefit is very significant.

An optimisation of the lay-scheme is now possible, and the number of combinations with primary importance is reduced to nine (three in each layer), with some added emphasis on particular "marker" lays, as indicated in Figure 2.

The treatment of the other combinations, using the formula established, is still necessary but some relaxation in the required RMS value is permissible, due to the reduction of the direct capacitances occurring.



The results obtained for cables using this design and method on routine production is shown in Figure 5. For cables using either 19 or 26 AWG conductors, the curves are inseparable on the graph. However, it must be mentioned that the Twinning machines used for 26 AWG cables are of simple design and least costly. On more sophisticated machines, the effect of conductor gauge is clearly indicated as the lay-schemes used are identical. Curves A. and C. represent all combinations, whilst B. and D. are restricted to "significant combinations" only.

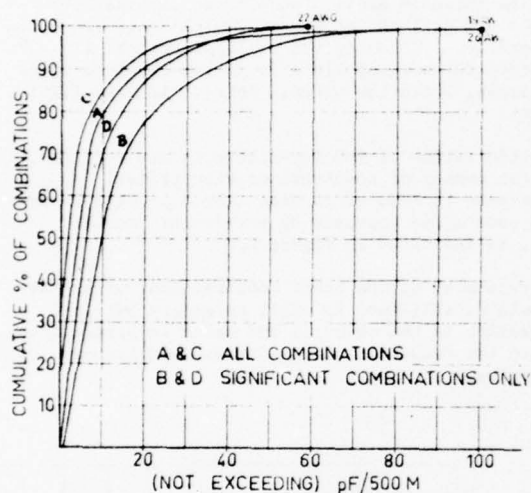


FIG 5 DISTRIBUTION OF CAPACITANCE UNBALANCE (FINAL DESIGN)

HIGH FREQUENCY PENETRATION

Cable characterisation tests are an on-going programme, in step with development of transmission techniques. Cross-talk measurements at 780 KHz on this design have given an average value of better than 80 db. between adjacent layers.

The original concept of 3 x 3 matrix was aimed at ensuring a predetermined section of bearer-circuits with wide separation. The results obtained now indicate a much higher penetration potential for PCM utilisation. Further work on this aspect is now in progress. ³

ACKNOWLEDGEMENTS

Credits are due to Mr. Paul Rumpf, formerly Development Engineer with Olex Cables Limited, who carried out a substantial part of the work for the verification of the formula on which lay-selection is based.

The author wishes to thank Olex Cables Limited for their kind permission to publish this paper.

REFERENCES

1. Nordblad, S. S. - "Multi-paired cable of non-layer design for low capacitance unbalance telecommunications network." (International Wire & Cable Symposium, 1971.)
2. Wigg, H. H. - "Geometrical Distortion in a T.V. Raster." (Paper presented at the I.R.E. (Aust.) Convention, 1963.)
3. Rheinberger, M. A. - "Transmission in Communication Cables." (Seminar on Power and Communication Cables, Institute of Engineers (Aust.) 1976.)



G. I. B. Vermont.
Olex Cables Limited,
Melbourne, Australia.

Mr. George Vermont was born in Hungary, and graduated from the Royal Military Technical Academy, Budapest, as Dux of the Academy.

After World War 2 he was awarded a scholarship to gain British qualifications at the University of London (B. Sc. Eng.). He was then employed by Standard Telephones & Cables, as Design Engineer in their Coaxial Cable Plant in London.

In 1956 he emigrated to Australia, accepting an appointment with the Australian Post Office, Long Line Equipment Section, at their headquarters. In 1960 he joined Olympic Cables Pty. Limited, to assist in the manufacture of the Sydney - Melbourne Coaxial Cable Project, and is now Technical Manager of Olex Cables Limited, which was formed by the merger of Olympic and Nylex Cables.

A STATISTICAL MODEL FOR CALCULATION OF CROSSTALK IN A BALANCED PAIR CABLE

by

Nils Holte

Electronics Research Laboratory
Trondheim - Norway

SUMMARY

Previous calculations of crosstalk in balanced pair cables predict much better crosstalk performance than measured in practical cables. It is generally assumed that the difference is due to production tolerances and cabling effects. In order to take unavoidable production tolerances into account, a statistical model is used for crosstalk calculations. Thus it is possible to optimize crosstalk performance in a cable having realistic deviations from ideal geometry.

The coupling functions between the transmission lines in the cable are calculated, assuming ideal geometry and TEM-propagation of waves, and the coupling functions are expressed as generalized Fourier series. The deviations from ideal geometry produce angle- and amplitude modulation of each term in the Fourier series. Assuming that the deviations are stationary, stochastic processes, crosstalk in practical cables can be calculated by means of methods used in modulation theory.

The model has been tested on a cable containing 4 starquads, and calculated values of near end and far end crosstalk is in accordance with measurements for all pair combinations in the cable. By means of the model it is possible to find optimum twist periods in practical cables.

1. INTRODUCTION

The Norwegian Telecommunication Administration has seen a need for using balanced pair cables in 3rd order PCM-systems and is developing new cables for this type of broadband use. A considerable crosstalk improvement is needed and in order to reach this aim a more realistic and accurate crosstalk model is needed. A better crosstalk model will also be important for use in system design.

The behaviour of crosstalk is quite random, thus a statistical model will be suitable. Previously a statistical model has been reported by Cravis and Crater [1], but this one does not relate crosstalk to geometrical parameters and is restricted to frequencies below 10 MHz. In order to improve cables we have found it important to look into cable geometry and extend the frequency range at least up to 30 MHz. This paper gives the theoretical development of a statistical model which is based upon the results of Cravis and Crater [1]. The model starts from statistical deviations from ideal geometry and calculates capacitance unbalances and far end and near end crosstalk at higher frequencies. Three

different contributions to far end crosstalk are considered; direct far end crosstalk, reflected near end crosstalk and double near end crosstalk via tertiary circuits. The model is verified for one specific type of cable.

2. COUPLING FUNCTIONS BETWEEN TRANSMISSION LINES

The number of independent transmission lines in a balanced pair cable is equal to the number of conductors. Usually only one half of the transmission lines are used for signal transmission, but phantom circuits as well as longitudinal circuits contribute to crosstalk. Assuming lossless conductors, homogeneous dielectric constant and TEM propagation of waves the coupling coefficient between two transmission lines is defined by W.Klein [2]:

$$k_{ij} = \frac{m_{ij}}{\sqrt{L_i L_j}} = \frac{K_{ij}}{\sqrt{K_{ii} K_{jj}}} \quad (1)$$

m_{ij} mutual inductance per unit length.
 L_i, L_j inductance of each line.
 K_{ij} elements in the inverse capacitance matrix.

The coupling functions are found by solving Laplace' equation for the cross section of the cable. We use a method given by H.Singer et. al. [3] which simulates the surface charge on each conductor by concentrated line charges inside each conductor.

The geometry of the cable is first assumed to be ideal. Deviations are taken into account in later chapters. We assume circular conductors, constant twist periods and constant distances between quads (pairs). In this case the variations of the coupling functions along the cable are given by Fourier series in the form:

$$k(x) = \sum_{i=1}^N c_i \sin(s_{Fi} x + \phi_{i0}) \quad (2)$$

The twist frequencies of each pair is defined by $s_i = 2\pi/p_i$ rad/m where p_i is the twist period. The frequencies s_{Fi} of each term in (2) are linear combinations of all twist frequencies in the cable.

For instance, the dominating terms in the coupling between pair 1 and pair 2 have the following frequencies:

$$s_{F1} = s_1 - s_2$$

$$s_{F2} = s_1 + s_2$$

$$\begin{aligned} s_{F3} &= s_1 + 3s_2 \\ s_{F4} &= 3s_1 + s_2 \\ s_{F5} &= 3s_1 + 3s_2 \end{aligned} \quad (3)$$

The coefficients c_i can be calculated by means of the Fast Fourier Transform.

3. REFLECTIONS WITHIN A PAIR DUE TO IMPEDANCE IRREGULARITIES

The characteristic impedance of a balanced pair will have small harmonic variations due to twisting of the pair. Assuming ideal geometry the impedance of a pair can be expressed as Fourier series in the same way as the coupling functions. The most significant term is the second harmonic of the twist frequency of the pair s_1 :

$$Z = Z_0(1 + c_2 \sin 2s_1 x) \quad (4)$$

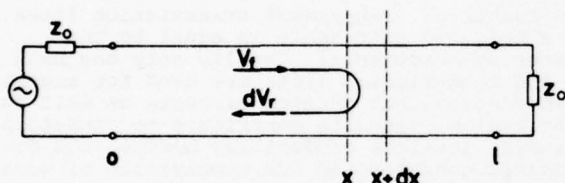


Fig. 1. Reflections due to impedance variations in a pair.

The voltage reflection from the impedance variations in a short piece of the pair in fig. 1 is given approximately by

$$\frac{dV_r}{V_f} = \frac{dZ}{2Z_0} \quad (5)$$

A differential reflection coefficient is defined by

$$\rho_d(x) = \frac{1}{V_f} \frac{dV_r}{dx} = c_2 s_1 \cos 2s_1 x \quad (6)$$

By integrating this coefficient the reflected wave may be estimated in a pair having small, continuous variations in characteristic impedance.

4. DEVIATIONS FROM IDEAL GEOMETRY

Works by Strakhov [4] and Holte [5] show that near end crosstalk attenuation is in the order of magnitude of 100 dB at 1 MHz in a cable having ideal geometry. In order to obtain a more realistic model, random deviations from ideal geometry have to be considered.

Our basic assumption is that the Fourier series expansion (2) of the coupling coefficients holds even if the geometrical parameters vary along the cable. This is strictly correct only for very slow variations of cable geometry, but it can be used as an approximation for the practical variations which have been considered.

Because of the variations in geometry the Fourier coefficients $c_i(x)$ and the fre-

quencies $s_{Fi}(x)$ will be functions along the cable. All types of deviations will produce either angle or amplitude modulation of each term in the Fourier series. Variations in distance between pairs give amplitude modulation of each term. Deviations from ideal twisting produce angle modulation of each term, and this effect is treated as phase modulation. One term in the Fourier series can be written

$$\kappa_i(x) = c(x) \sin(sx + \varphi(x)) \quad (7)$$

$\varphi(x)$ is the angle deviation from ideal twisting, and it is a linear combination of the angle deviations in each pair of the cable.

The quantities $\varphi(x)$ and $\varphi(x+\tau)$ in two adjacent positions in the cable will be strongly correlated because of the mechanical stiffness of the conductors. The sources of deviations in different parts of the cable are probably independent. The average twist frequency of a quad (pair) is produced within narrow limits by the cable machine. A mathematically convenient description which makes use of this limited information is obtained by assuming $\varphi(x)$ to be a stationary, zero mean, stochastic process having autocorrelation function:

$$R_\varphi(\tau) = \langle \varphi(x) \varphi(x+\tau) \rangle = \sigma_\varphi^2 \exp(-|\tau|/\tau_0) \quad (8)$$

If $\varphi(x)$ is small and $c(x)$ is constant, (7) can be expressed

$$\kappa_i(x) \approx c(\varphi(x) \cos sx + \sin sx) \quad (9)$$

The autocorrelation function of κ_i is:

$$\begin{aligned} R_1(x, y) &= \langle \kappa_i(x) \kappa_i(y) \rangle \\ &= c^2 R_\varphi(x-y) \cos sx \cos sy + c^2 \sin sx \sin sy \end{aligned} \quad (10)$$

The last term is purely deterministic and [4] and [5] show that this term contributes only negligibly to crosstalk.

The assumption that $\varphi(x)$ is small can be removed if $\varphi(x)$ is Gaussian. We have calculated exact expressions for $R_1(x, y)$ in this case, but the expressions are a bit complicated. If $\sigma_\varphi \ll 1$ the following formula is a sufficiently good approximation:

$$R_1'(x, y) = c^2 R_\varphi(x-y) \exp(-\sigma_\varphi^2) \cos sx \cos sy \quad (11)$$

The result from our simple approach above is only changed by a constant factor $\exp(-\sigma_\varphi^2)$.

The magnitudes of the Fourier coefficients $c(x)$ are functions of geometrical distances in the cross section of the cable. For instance, the distance between two pairs is denoted $d(x)$ and the deviation from nominal geometry is:

$$\Delta(x) = d(x) - d_0 \quad (12)$$

Different types of deviations will probably show similar statistical behaviour. Thus we assume $\Delta(x)$ to be a stationary stochastic process having autocorrelation function:

$$R_{\Delta}(\tau) = \sigma_{\Delta}^2 \exp(-|\tau|/\tau_0) \quad (13)$$

By means of linearization the autocorrelation function of κ_1 can in this case be expressed:

$$R_2(x, y) = \langle \kappa_1(x) \kappa_1(y) \rangle = D_{\Delta}^2 R_{\Delta}(x-y) \cos sx \cos sy$$

where

$$D_{\Delta} = \left[\frac{\partial C}{\partial d} \right]_{d=d_0} \quad (14)$$

The derivatives D_{Δ} are easily calculated by means of a small perturbation in the computer program which computes Fourier coefficients from ideal cable geometry.

Deviations from 90° angle between pairs in one starquad and unsymmetrical twisting axis in one pair can be treated in a manner similar to the approach described for variations in distance between pairs.

5. CAPACITANCE UNBALANCE

Capacitance unbalance between two pairs in a cable is given by

$$e_a = 4C_d \int_0^l \kappa(x) dx \quad (15)$$

C_d is the capacitance of each pair. Recalling the results from Chapter 4, we assume that $\kappa(x)$ has an autocorrelation function:

$$R(x, y) = \sigma^2 \exp(-|x-y|/\tau_0) \cos sx \cos sy \quad (16)$$

The mean value e_a^2 over an ensemble of different cables will be

$$\begin{aligned} \langle e_a^2 \rangle &= \langle 16C_d^2 \int_0^l \int_0^l \kappa(x) \kappa(y) dx dy \rangle = \\ 16C_d^2 \int_0^l \int_0^l R(x, y) dx dy &= \frac{16C_d^2 \sigma^2 l \tau_0}{1+s^2 \tau_0^2} \quad (17) \end{aligned}$$

If the Fourier series contain more than one significant term, the different terms are assumed to be statistically independent. In this case equation (17) turns into a sum.

Equation (17) gives the experienced \sqrt{l} relationship between capacitance unbalance and cable length. Usually the most critical frequency s is the difference twist frequency between the two pairs. The expression shows that it is important to keep the twist frequencies well separated.

6. NEAR END CROSSTALK

Near end crosstalk between two pairs for frequencies above 100 kHz is given approximately by Klein [2]:

$$N = j\beta \int_0^l \kappa(x) \exp(-2\gamma x) dx \quad (18)$$

Mean crosstalk power averaged over the same pairs in different cables is accordingly:

$$p(\omega) = \langle N^2 \rangle = \beta^2 \int_0^l \int_0^l R(x, y) \exp(-2\gamma x - 2\gamma^* y) dx dy \quad (19)$$

If $R(x, y)$ is given by (16), the integrals can easily be solved. The result is simplified by assuming $\alpha, \beta \ll s, 1/\tau_0$ and $l \gg 1/\alpha$ which will usually be satisfied in practical cables.

This leads to:

$$p(\omega) = \frac{\beta^2 \sigma^2 \tau_0}{4\alpha(1+\tau_0^2 s^2)} \quad (20)$$

This shows the experienced 15 dB/decade variation with frequency and it predicts correlation between capacitance unbalance and near end crosstalk at high frequencies.

7. FAR END CROSSTALK

In PCM systems one of the main problems is to reduce far end crosstalk, but the physical mechanisms which produce FEXT are yet not fully understood. Most earlier works consider only direct far end crosstalk. We have found that near end crosstalk increases 35 dB/decade of frequency, and thus it will be a dominating contribution to FEXT at higher frequencies. It will be quite important to control this effect in order to produce better balanced pair cables for broadband use.

For TEM-waves the electrical and magnetic coupling cancel exactly in the far end direction. In practical cables finite skin depth, nonhomogenous dielectric constant and twisting of pairs cause deviations from orthogonality between electrical and magnetic fields. A residual far end coupling function is assumed:

$$\kappa_F(x) = k_0 \kappa(x) \quad (21)$$

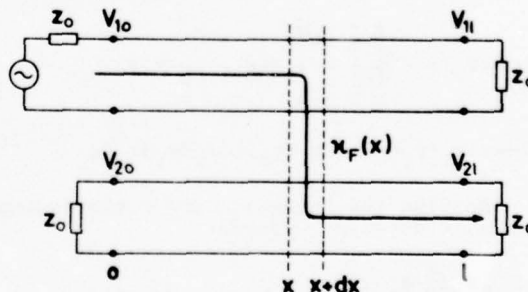


Fig. 2. Direct far end crosstalk.

Direct far end crosstalk is transmitted as indicated in fig. 2 and it is given by:

$$F_d = \frac{V_{2l}}{V_{1l}} = j\beta \int_0^l \kappa_F(x) dx \quad (22)$$

Using the coupling function given by (16), the mean direct far end crosstalk power in practical cables is

$$q_d(\omega) = F_d^2 = k_0^2 \beta^2 \int_0^l \int_0^l R(x, y) dx dy = \frac{k_0^2 \beta^2 \sigma^2 l \tau_0}{1+s^2 \tau_0^2} \quad (23)$$

If the constant k_0 is independent of frequency, this result shows the experienced 20 dB/decade variation with frequency and the 10 dB/decade variation with cable length.

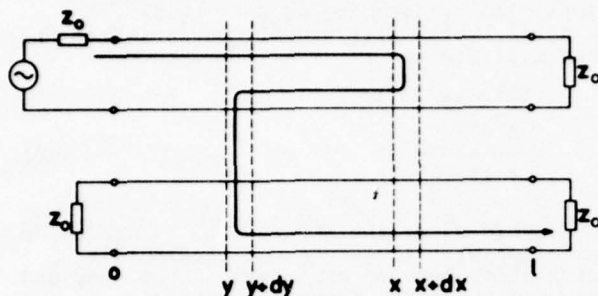


Fig. 3. Reflected near end crosstalk.

Reflected waves in one pair combined with near end coupling contribute to far end crosstalk as indicated in fig. 3. The differential reflection coefficient will according to chapters 3 and 4 have an autocorrelation function:

$$R_\rho(x, y) = \exp(-|x-y|/\tau_0) \cdot \cos s_2 x \cos s_2 y \quad (24)$$

s_2 is a twist frequency. Near end crosstalk coupling is given by (16).

The contribution to far end crosstalk is according to fig. 3:

$$F_r = j\beta \int_0^l \int_0^l \rho_d(x) \kappa(y) \exp(-2\gamma(x-y)) dx dy \quad (25)$$

If ρ_d and κ are uncorrelated the mean power is:

$$q_r(\omega) = \langle F_r^2 \rangle = \beta^2 \int_0^l \int_0^l \int_0^l \int_0^l R(x, y) R_\rho(x, y) \exp(-2\gamma(x_1 - y_1) - 2\gamma^*(x_2 - y_2)) dy_2 dy_1 dx_2 dx_1 \quad (26)$$

Solving the integrals under the assumptions $\alpha, \beta \ll s, l/\tau_0$ yields:

$$q_r(\omega) = \frac{\beta^2 \sigma_1^2 \sigma_2^2 \tau_0^2 l}{4\alpha(1+\tau_0^2 s^2)(1+\tau_0^2 s_2^2)} (1 - \frac{1-e^{-4\alpha l}}{4\alpha l}) \quad (27)$$

For long cables the last paranthesis approaches unity. The calculated expression is in accordance with the experienced 10 dB/decade variation with cable length for long cables. The frequency dependence is approximately 15 dB/decade.

Another contribution to far end crosstalk is double near end crosstalk via longitudinal circuits as shown in fig. 4.

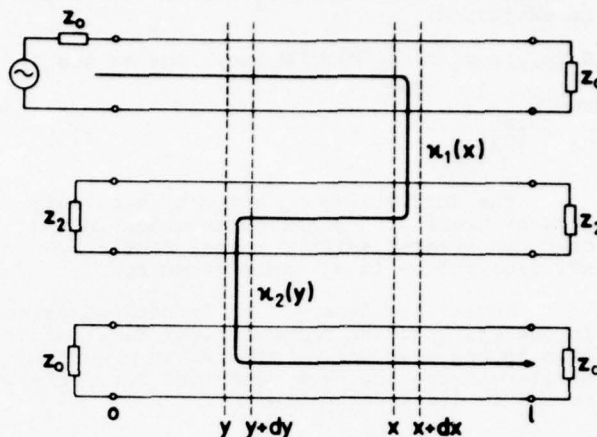


Fig. 4. Double near end crosstalk.

The most important term in the Fourier series expansion of coupling between a pair and a longitudinal circuit is usually the mean value term. According to Chapter 4 the coupling functions will have autocorrelation functions of the following type.

$$R_1(\tau) = \sigma_1^2 \exp(-|\tau|/\tau_0) \quad (28)$$

$$R_2(\tau) = \sigma_2^2 \exp(-|\tau|/\tau_0) \quad (29)$$

The far end crosstalk is accordingly:

$$F_n = \beta^2 \int_0^l \int_0^l \kappa_1(x) \kappa_2(y) \exp(-(\gamma + \gamma_2)(x-y)) dx dy \quad (30)$$

Mean power can be calculated in the same way as (27).

$$q_n(\omega) = \langle F_n^2 \rangle = \frac{2\beta^4 \sigma_1^2 \sigma_2^2 \tau_0^2 l}{\alpha + \alpha_2} (1 - \frac{1 - \exp(-2(\alpha + \alpha_2)l)}{2(\alpha + \alpha_2)l}) \quad (31)$$

$\gamma_2 = j\beta + \alpha_2$ is the propagation factor of the longitudinal circuit.

This effect increases 35 dB/decade with frequency.

Measurements and calculations show that double near end crosstalk is a dominating contribution to far end crosstalk above 10 MHz.

8. VERIFICATION OF THE MODEL

The stochastical parameters of the model can be found in different ways. One method is to extract them from mechanical or other direct measurements like Friesen [6].

We have adjusted the stochastical parameters by means of optimization in such a way that calculated capacitance unbalances fit with measurements both for unbalances between

pairs and between a pair and earth. The obtained solution is not unique but it shows one type of geometrical deviations that will produce the observed crosstalk. This method has been tested using a 0.9 mm, PE-isolated balanced pair cable containing 4 starquads. The cable is filled with petrol jelly, and it is shown in fig. 5;

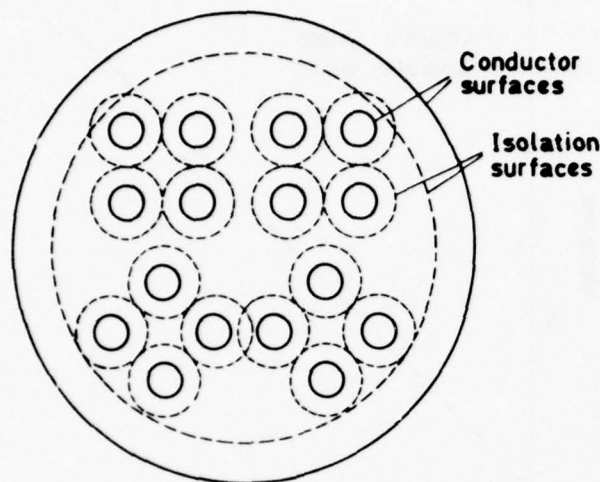


Fig. 5. Cross section of the cable.

The average capacitance unbalances observed in a large number of cables can be explained by the following deviations from ideal geometry:

- 1) The deviation from ideal twist angle (fig. 6a) has a mean square value $\sigma_\phi = 15^\circ$ for a twist period of $p=100$ mm. The correlation length τ_ϕ equals 140 mm. σ_ϕ is proportional to p in each quad.
- 2) The quads are moving tangentially in the cable as indicated in fig. 6b. This displacement has a mean square value $\sigma_\Delta = 9^\circ$ and a correlation length $\tau_\Delta = 140$ mm.

Factors 1 and 2 dominate the unbalance between pairs in different quads.

- 3) The angle between two pairs in one quad differs from 90° (fig. 6c) with a mean square value $\sigma_\alpha = 1.5^\circ$ and correlation length 140 mm. This is the main contribution to unbalance between pairs in the same quad.
- 4) Unsymmetrical position of the rotation axis in a pair is shown in fig. 6d. The displacement is assumed to be random having a mean square displacement $\sigma_{\Delta a} = 4\%$ of the distance between the conductors for twist period $p=100$ mm. $\sigma_{\Delta a}$ is proportional to p^2 within our observations. The correlation length is assumed $\tau_{\Delta a} = 1$ m. This gives the major contribution to the capacitance unbalance between a pair and earth.

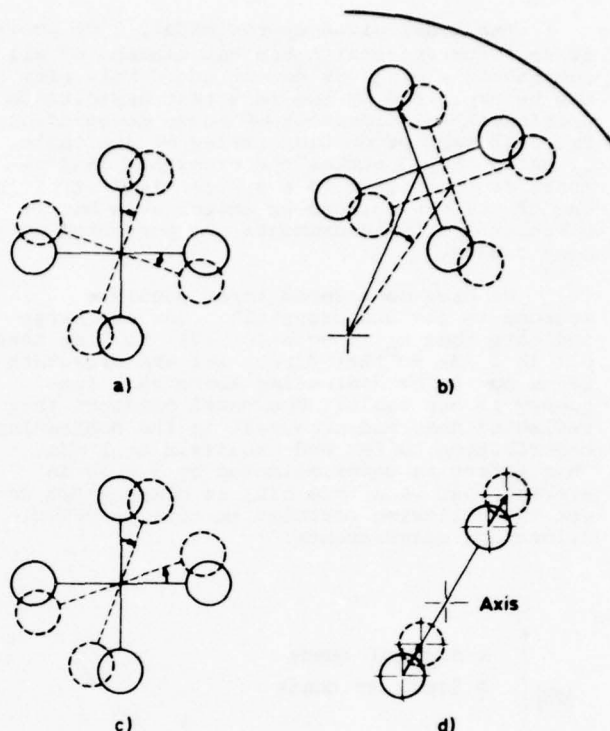


Fig. 6. Different types of deviations from ideal geometry.

Near end and far end crosstalk have been calculated by using the parameters estimated from capacitance unbalances. The near end crosstalk between pairs in different quads is averaged over 4 frequencies, 4 pair combinations and 3 different cables. It is the crosstalk power that is averaged and all measurements are referenced to 1 MHz.

Significant correlation is obtained between the model and the measurements as shown in fig. 7.

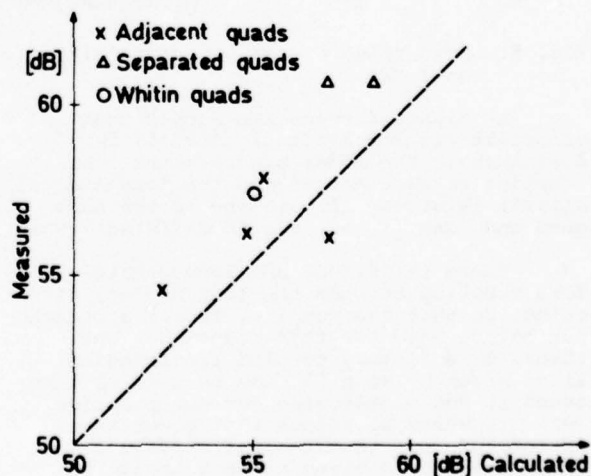


Fig. 7. Mean values of measured and calculated near end crosstalk at 1 MHz.

The model gives approximately 2 dB poorer near end crosstalk than calculated for all combinations of quads except one. This bias may be explained by the fact that capacitance unbalances and crosstalk have been measured on two different production series of the cable. By using only 3 cables the crosstalk measurements are sensitive to a systematical error in one of the cables, and we expect even better correlation if measurements are performed on many cables.

We have considered three possible sources to far end crosstalk. Our estimates indicate that k_o in equation (21) is less than 0.1 at 1 MHz so that direct far end crosstalk seems not to be dominating above this frequency in our cable. The model predicts that reflected near end crosstalk is the dominating contribution to far end crosstalk at 1 MHz. This effect is underestimated by 5.8 dB in average, but when this bias is compensated we get the following correlation between calculations and measurements:

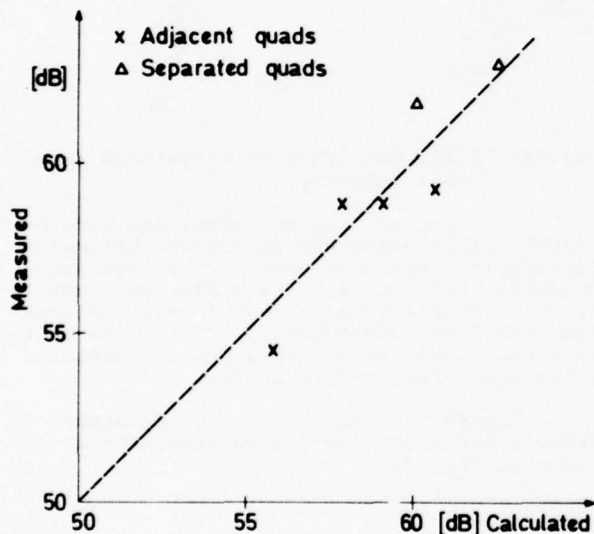


Fig. 8. Mean value of far end crosstalk at 1 MHz.

At higher frequencies double near end crosstalk via longitudinal circuits is dominating. The model predicts that the coupling between a pair and the longitudinal circuit is strong if both are in the same quad and weak if they are in different quads.

There is strong and approximately uniform coupling between the longitudinal circuits, so that the coupling factor approach can not be used for this coupling. The theory of uniformly coupled transmission lines given by Rice [7] may be used, but we found it too complicated for our practical work. Instead we assume that power transmitted into one longitudinal circuit almost immediately is divided on both transmission directions and all longitudinal circuits. From crosstalk measurements two empirical factors for coupling between longi-

tudinal circuits have been calculated:

$$k_n = -9.7 \text{ dB Adjacent quads}$$

$$k_d = -11.9 \text{ dB Separated quads}$$

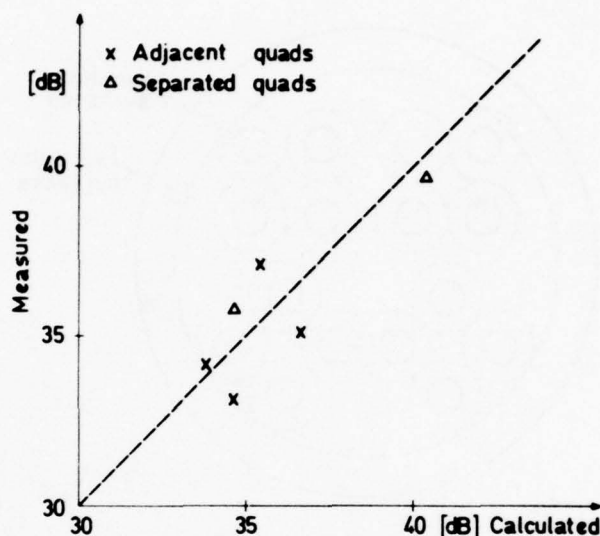


Fig. 9. Mean values of far end crosstalk at 12 MHz.

Fig. 9 shows relatively good correlation between the model and measurements at 12 MHz.

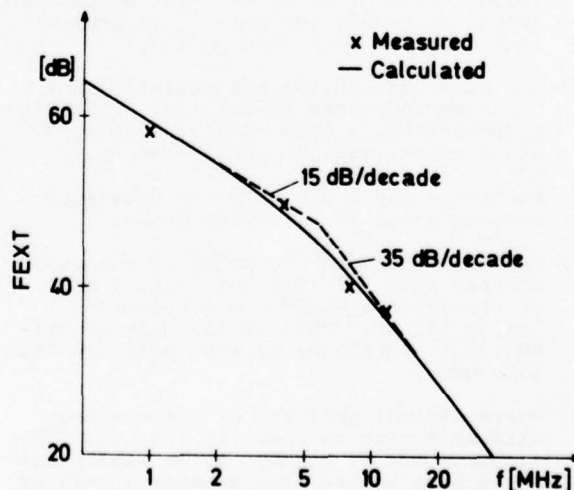


Fig. 10. Frequency variations of far end crosstalk.

The calculated average frequency dependence of far end crosstalk seems to coincide with our measurements as shown in fig. 10. The two contributions to far end crosstalk are approximately equal at 6 MHz.

9. OPTIMIZATION OF CROSSTALK PERFORMANCE

In our model all unavoidable production tolerances are taken into account by different empirical, statistical parameters. The average near end and far end crosstalk is a function of twist periods in the cable. Thus crosstalk performance can be optimized with respect to twist periods in one specific type of cable.

A 10 dB crosstalk improvement has been predicted for our type of cable by choosing shorter and essentially different twist periods. The improvement has not yet been verified.

10. CONCLUSION

We have verified a statistical cross-talk model which relates the observed cross-talk to deviations from ideal geometry in balanced pair cables. Only one type of cable has been used and the model predicts that far end crosstalk in this cable is dominated by reflected near end crosstalk in the range 1 - 6 MHz. At higher frequencies double near end crosstalk is dominating, and this contribution is found to increase 35 dB/decade of frequency.

The model shows that crosstalk depends strongly on the twist periods, and in principle it is possible to find optimum twist periods in a cable having experienced deviations from ideal geometry.

Another aspect of calculating the deviations from ideal geometry is to indicate whether significant crosstalk improvement can be obtained by narrowing production tolerances.

After some refinement of the model, it promises to be a helpful tool both in improving existing cable designs and for development of new balanced pair cables.

11. ACKNOWLEDGEMENT

The Norwegian Telecommunication Administration, Research department has been project client for this work. The author wishes to thank them for the permission to publish it.

12. REFERENCES

- [1] H.Cravis and T.V.Crater: Engineering of T1 Carrier System Repeatered Lines, Bell syst. tech.journ., Vol 42, March 1963, pp 431 - 486.
- [2] Wilhelm Klein: Die Theorie des Nebensprechens auf Leitungen. Springer Verlag, Berlin 1955.
- [3] H.Singer, H.Steinbigler, P.Weiss: A charge simulation method for the calculation of high voltage fields Paper T 74085-7, IEEE PES Winter Meeting, New York, Jan. 27, Febr. 1, 1974.
- [4] N.A.Strakhov: Crosstalk on multipair cable - Theoretical aspects National telecommunications Conf., Nov. 1973.

- [5] N.Holte: Calculation of crosstalk in balanced pair cables by means of a deterministic model. Report nr. STF44 F75178, Electronics Research Laboratory, Tr.heim, 1975 (in Norwegian).
- [6] H.W.Friesen: Relating the twist detection measurements of twisted pairs to their crosstalk performance. Int. Wire and Cable Symposium. Cherry Hill 1975.
- [7] S.O. Rice: Steady state solutions of transmission line equations, Bell syst. tech. journal, Vol 20, No 2, April 1941, pp 131, 178.



Nils Holte
Electronics Research
Laboratory
The University of
Trondheim
N-7034 Trondheim-NTH
Norway

Nils Holte received his M.Sc. in 1971 and his Dr.ing. degree in 1976 both from The University of Trondheim.

He has worked on different projects in filter design, digital transmission systems and cable design.

CUSTOMIZED GAS FEEDER PIPE
for
PRESSURIZING AND MONITORING TELEPHONE CABLE

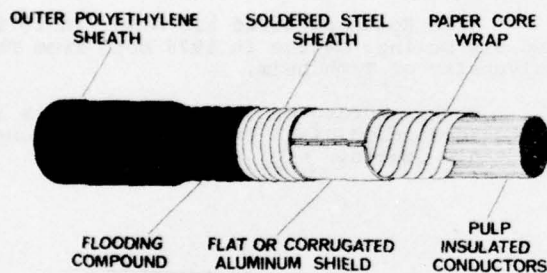
by

M. R. Dembiak and W. Purkert
Western Electric Company
Kearny, N. J.

Background

The most important engineering development in the past three decades in the area of cable sheath design has been the introduction of the multiple sheath to replace lead. Stalpeth, the multiple sheath for pulp insulated cable, is still essentially the same as originally developed while the Alpeth design for plastic insulation has had numerous modifications.

STALPETH DESIGN

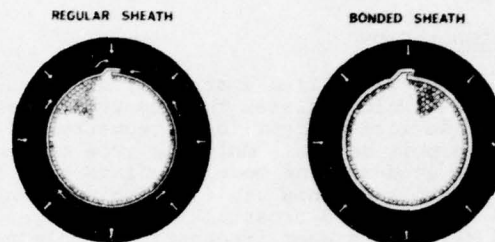


Innovations and changes solve some problems but invariably create or magnify others. One of the problems which accompanied the introduction of the multiple sheath was moisture permeation which eventually caused circuits to fail. The obvious solution was to pressurize the cables with dry air and while this presented no major problems for cables within a reasonable distance from the Central Office, the more distant runs could be so serviced only if a suitable system for conveying the air could be devised. The initial vehicle was polyethylene tubing similar to garden hose. Since this was not impervious to moisture, the water which permeated thru the polyethylene was being fed into the cable along with the dry air. This, therefore, was not an effective solution.

Moisture Diffusion

In the early 1960's a study was conducted by the Bell Telephone Laboratories on moisture diffusion through conventional cable sheath concluded that, in the aluminum polyethylene construction, the addition of bonding between the aluminum and polyethylene, leaving the overlap not bonded, reduced the moisture diffusion into the cable core by a factor of 18 to 180 depending on the diameter of the cable.

MOISTURE DIFFUSION



IMPROVEMENT BY BONDING JACKET TO SHIELD
X 18 TO X 180

IMPROVEMENT BY BONDING SHIELD OVERLAP
X 2000 TO X 30,000

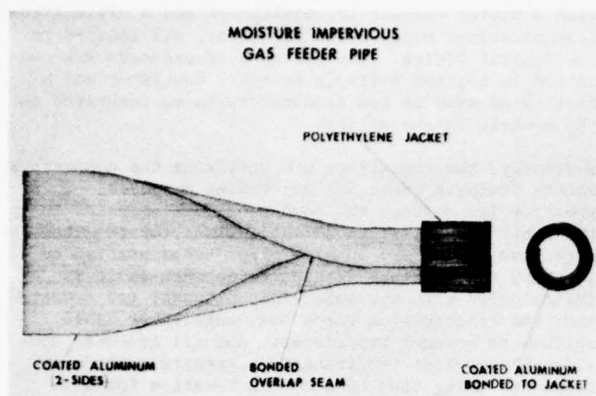
Bonding only the aluminum overlap so that the only path for moisture entry is through the adhesive layer in the overlap reduces moisture diffusion by a factor of 2,000 to 30,000 as the overlap varies from 1/4" to 1/2" length and the adhesive thickness from 4 to 1 mil.

It is apparent that the overlap bonding is decisive in providing a highly moisture impervious sheath. However, circumferential bonding is important in providing improved mechanical performance, corrosion protection for the aluminum and insurance against moisture if the polyethylene jacket should be punctured or failure of the overlap seal should occur.

Based on this study, the Bell Telephone Laboratories and Western Electric jointly applied this theory to develop the basic Gas Feeder Pipe to replace the plastic hose system.

Gas Feeder Pipe

The pipe, after several transitions, presently consists of 4-mil aluminum tape coated on both sides with a 2-mil thick adhesive copolymer. The coated tape is longitudinally formed into a tube having a 1/4" overlap seam, over which is extruded a 60-mil thick, low density, high molecular weight black polyethylene jacket. The heat transmitted during the extrusion operation bonds the aluminum overlap seam and the coated metallic tube to the outer jacket.



In order to maintain an adequate seal where joints are required during installation, special fittings were designed. This necessitated that the inside and outside dimensions of the pipe be held to close tolerances.

Furthermore, to insure bonding between the polyethylene and aluminum, the finished product must meet a circumferential pull test of 5.0 pounds average on a 0.5 inch wide strip. Also, each length is shipped under pressure (between 10-12 psi) to assure the customer that the pipe is not damaged in transit and the length is leak-proof as received. This design solved the initial need since it provided a moisture impervious pipe which runs alongside the placed cables in ducts, acting as the supply route for dry air from the Central Office to the cable at remote locations. It was used successfully for years and it is estimated that by the end of 1976, some 150 million feet will have been installed.

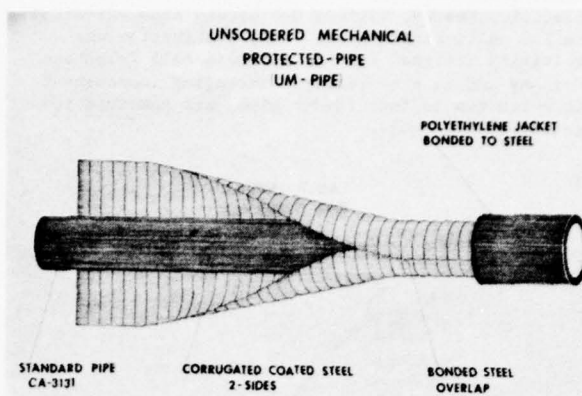
New Designs

As the technicians and field engineers become more and more familiar with this product and monitoring systems become more sophisticated, special installations, unique applications, improved hardware and field facilities required customizing.

To satisfy the telephone companies specific needs, the Western Electric Company developed three additional designs, namely - um-pipe, multi length pipe and pair pipe.

Um-Pipe

The abbreviation "um" is a sheath designation which provides unsoldered mechanical protection for pipe and cable. This protection consists of a 2-side coated steel tape, corrugated and applied longitudinally with an overlap, about the pipe core and finally another polyethylene jacket.



The design specifications are as follows:

1. Standard Gas Feeder Pipe Core (Described)
2. Coated Steel
 - a. 0.006" thick steel (tin, terne or black plate)
 - b. 0.002" thick adhesive copolymer
3. Polyethylene Jacket - 0.045" thick (nominal)
4. Finished outside diameter - 1.00"
5. Bonding specification - same as for coated aluminum mentioned previously.

The coated steel, unlike the aluminum, presented a problem in obtaining an adequate bond between the coating and the steel substrate. However, with the cooperation of the Lamcote Division of the Arvey Corp. in Jersey City, New Jersey, an adhesive agent was developed which met the bond characteristic required.

This um-pipe is primarily installed west of the Mississippi where gophers are prevalent and cables are placed directly into the ground. The steel in this design prevents rodents from chewing into the inner pipe, thereby eliminating gas leakage as experienced with conventional feeder pipe. Since this sheath is considered expendable - it is not pressurized and no special fittings are required.

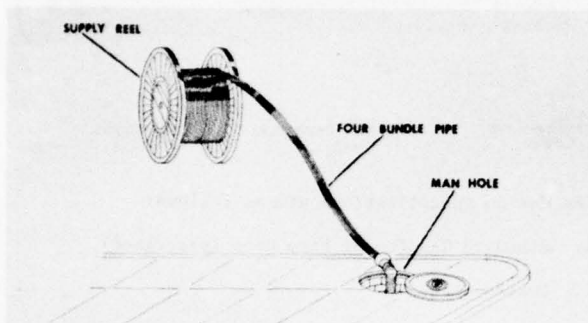
Multi-Length Pipe

As the telephone program expanded, the number of cables installed and the distance from the Central Office increased. The result was obvious in that the single pipe feed systems could not maintain the required air pressure at the end of the run. Accordingly, this necessitated placing several lengths into the same duct drawing the pipe through one length at a time. Obviously this becomes a very costly operation. To offset this problem, the crews in the field attempted to simultaneously place up to eight lengths of pipe, "paying" them off individual reels at the manhole location. This presented further problems such as:

- A. Positioning the reels at the particular site.
- B. Maintaining adequate tension and guiding.
- C. Obtaining exact lengths of individual pipe from stock.

After being informed of this situation, Western Electric, Kearny, devised its second pipe variation called multi-length pipe. This combination was initially designed for the Illinois Bell Telephone Company and is essentially a packaging improvement in which two to four feeder pipes are combined together on one reel.

**MULTI-LENGTH
GAS FEEDER PIPE**

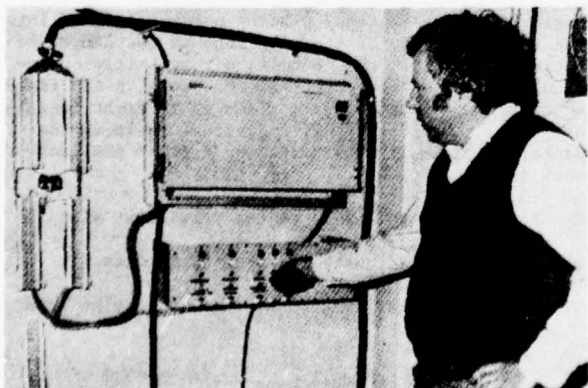


This combination of two to four permits the installer to place up to eight lengths simultaneously from a maximum of two reels. Also, about three or four times as much air pipe (up to 8,000 feet per day) can be placed in telephone cable ducts resulting in quicker, more efficient installation.

Therefore, to summarize - the pipe system method of cable pressurization is essentially an arrangement whereby cable pressures are reinforced at selected manholes along an underground cable route by manifolded the individual cables to a paralleling aluminum lined polyethylene pipe, which carries pressurized dry air from the air dryer in the Central Office. The resistance of the pipe is so low that the typical drop is only two to three PSIG at a distance of several miles from the Central Office. The relatively high pipe pressure and high available air flow through the pipe produces, in effect, a dry air source (just as at the Central Office) at each manifold location.

Monitoring System

Coupled with the air pressure system is a monitoring network which uses pressure transducers to send pressure readings back to the Central Office where an automatic monitoring device records and displays pressure data on schedule or on command. The recording devices set-off alarms for critical readings and generate a punched paper tape for time-shared analysis of pressure changes.



The system consists of a Sparton Southwest 5100 Series with a master console for monitoring and a dielectric communications Model 24000 Air Dryer, all located in the Central Office. The system's transducers are contained in Sparton Multiple Assembly Cannister which permits as many as ten transducers to be connected at the manhole in one splice.

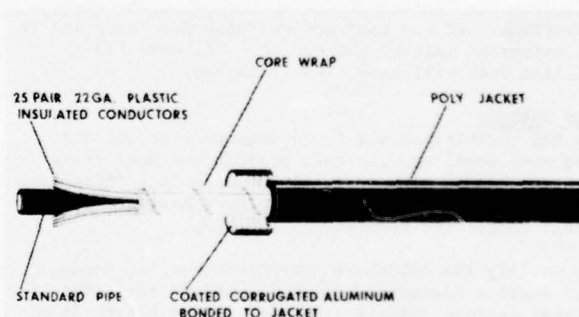
Currently, the installers are utilizing the conductors in the Stalpeth Cable for monitoring purposes. This practice (a) reduces the number of working pairs in the cable for telephone communication; (b) requires extensive inside and outside plant documentation to identify the pressure transducer network as it is intermingled with the subscriber network; (c) requires that the construction force open subscriber cable splices to connect transducers; and (d) involves considerable work at the frame to segregate transducer lines and bring them to a common location for connection to a house cable leading to the air dryer area.

Pair Pipe

A more direct approach was needed to separate the two systems. The answer to this was a new design air pipe developed at the Kearny Works with the assistance of Delaware's Diamond State Telephone Cable Engineers.

The new connectorized pipe (Western Electric Designation NCA-8000) dubbed "Pair Pipe" consists of a pipe core, plastic insulated conductors, plastic core wrap and an outer sheath of corrugated aluminum bonded to a black polyethylene jacket.

**CONDUCTORIZED GAS FEEDER PIPE
(PAIR - PIPE)**



The design criteria necessitated the following specifications:

1. Standard Pipe Core

2. Conductor Layer

- a. 25 Pr. - 24 Ga. plastic insulated conductors
- b. The twisted pairs to be applied and oscillated about the core, $360^\circ \pm 20^\circ$ over and back in 50 ± 20 feet in the same sequence as that of a similar pair size cable.

3. Core Wrap

The layer of conductors to be covered with a longitudinal serving of 0.003" thick polyethylene terephthalate (Mylar*) with a minimum 3/8" overlap. (*Trademark - DuPont Company)

4. Aluminum Layer

Over the core wrap a longitudinal wrap of two side coated (2 mil thick adhesive copolymer) aluminum

(0.006" thick) tape with a minimum of 1/2" overlap and electrically continuous in every length.

5. Finished Jacket

- a. The polyethylene jacket (0.075" thick) and aluminum tape be firmly and continuously bonded together for additional mechanical strength.
- b. The outside diameter not to exceed 1.30 inches

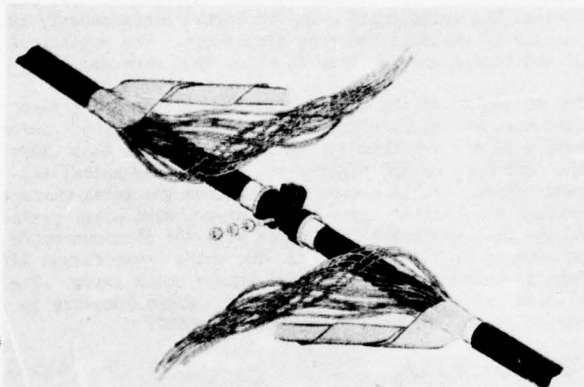
6. Electrical

All pairs are tested to guarantee no faults due to shorts, opens or crosses, plus a core to sheath breakdown test.

7. Pressure Test

Both the inner pipe core and the outer finished sheath must be hole free and maintain the required PSI average pressure.

The 25 pairs of conductors along with the inner air pipe will handle up to 50 transducers.



Splicing of this combination proved to be very simple - at splice locations, the amp-fit connectors have a central tube of metal that fits into the pair-pipe. The fittings outer tube covers the outside plastic pipe and finally a metal collar is crimped onto place over each end of the connector with the special reel provided by AMP.

Advantages of Pair Pipe

1. Plastic insulated pairs are fully color-coded to permit easy identification.
2. Eliminates the use of pairs, either working or dedicated, for monitoring gas pressure.
3. Saves the operating company the labor involved in opening working cables to get the pairs needed.
4. Avoids the troubles and record keeping which is necessary when cable pairs are used.
5. Keeps the air monitoring system which is an outside plant function distinct and separate from the Central Office switching system.

In conclusion, the data presented in this report shows the importance of keeping underground cables dry at all times and the progress made to update the monitoring and pressurizing systems in order to obtain this end result.

Acknowledgement

The authors are indebted to (1) Mr. G. H. Webster of the Bell Telephone Laboratories for his cable design assistance, (2) Mr. J. Paulich of the Arvey Corporation for his assistance in developing the steel coating application, (3) Messrs. H. E. Gowdy and J. Pelegrini, Western Electric Cable Consultants for their assistance in the introduction of Multi-Length and "Pair-Pipe" and (4) Messrs. J. F. Finnegan, T. B. Reece of the Diamond State Telephone Company and Howard Rudolph, Bell of Pennsylvania whose knowledge of field application was invaluable.



M. R. Dembiak is a Senior Development Engineer with 18 years of Western Electric experience in the wire and cable field. He attended Newark College of Engineering and has participated in numerous Cable Seminars and Symposia to which he has made significant contributions. He holds ten patents and has several pending.



W. Purkert has a Mechanical Engineering Degree from Stevens Institute and a Masters in Business Administration from N.Y.U. He is a licensed Professional Engineer in New Jersey and has been an Engineering Department Chief at Western Electric for 19 years, most of which has been in the development and manufacture of Exchange Area Cable.

ALUMINUM OXIDE INTEGRATED THIN FILM INSULATION FOR ALUMINUM WIRE AND STRIP CONDUCTORS

Henry Walker, Director of Research, Permaluster, Inc., Burbank, California

ABSTRACT

The reasons are well known why aluminum is used as a conductor in the electrical and electronic fields and why Al_2O_3 with a melting point of $2050^\circ C$. is used as an insulation. This concept is gaining recognition as one of the basic materials for various applications. Technical advancements in the anodic formation of the aluminum oxide lend their use for applications in electro-magnetic coils. Designers of such devices strive to achieve field producing coils with the highest rating per unit cost, size, weight and energy consumption. The improvement in design has come about mainly through the development of superior core materials and fabricating techniques. Conductors eliminating hot spots, thinner insulation with higher dielectric strength, lower dielectric losses, more compact components are the results of superior mechanical design also improving thermal dissipation. Lightweight coils are valuable in portable and airborne equipment, missile and space vehicle applications. Reduced component weight allows vital additional payload. Superior components can be achieved when aluminum conductor with thin insulation is used for rotating and other moving windings. Lower mass results in lower inertia, thus improving performance in a wide variety of equipment. Rotary equipment with low mass simplifies dynamic balancing as vibration from dynamic imbalance is reduced. Greater sensitivity and response in moving coil applications results from lower mass; this is characteristic in the design of electronic instruments, such as disk drive actuators and acoustical devices.

INSULATION CONDUCTORS

Compared to copper, aluminum with Al_2O_3 insulation operates cooler and will not oxidize. When operating in temperatures of above $100^\circ C$., copper will form an invisible film of cuprous oxide; above $200^\circ C$. cuprous and cupric oxide are formed readily on the surface, thus reducing the conductance as ultimately severe corrosion occurs and eventually the conductor is rendered useless. Even nickel coated copper is subject to a galvanic action of the two metals. In a high temperature operation, migration of atoms is created.

Performance of electrical components in high temperature is seriously handicapped due to the lack of suitable insulating materials as the components are subjected to severe physical stresses in environmental conditions. When failure occurs in organic insulations, the failure remains permanent owing to the electrical conductive carbon paths that are formed throughout the insulation as well as other endangering problems, such as lack of adhesion, oxidation, evaporation and aging.

Aging is accompanied by weight loss in organic material where shrinkage results in the resin portion causing it to lose its bond in the slot cells, thus creating failure. Variation of temperature or rotating speed causes mechanical abuses of the insulation. Thermal degeneration is faster close to the current-carrying conductors where the temperature is at a maximum; Therefore, the failure is induced at the hottest spot of the winding.

Aluminum conductor and Al_2O_3 insulation is free of galvanic action or oxidation. In case of a breakdown, the insulation does not create tracking of a permanent conductive path throughout the insulation. In fact, oxide from the air creates a new insulated oxide and could repair itself. Therefore, it is a good reason to consider the relation between operating temperature and insulation life. A component made with high temperature insulated material

will be more reliable and will protect itself and its payload from instant heat and pressure.

FORMATION

The oxide film is formed by an electro-chemical method which is a conversion process for thickening the natural occurring film several hundred times or more. This method is known as anodizing. Permaluster's patented process is similar to anodizing except:

- 1) It is performed in high speed to justify cost.
- 2) It eliminates mechanical contact to avoid racking spots.
- 3) It is controlled to eliminate crazing when bending.

Owing to the strict control methods employed in the processing, the oxide coating may be formed homogeneously in varying thicknesses and pore structures. The resistance of the formed alumina film is about 1800 ohms per cm^2 .

The mechanism of the anodic film formation and the fine structure of the film are not fully understood, but information is derived from the available evidence that under the influence of the electrolyte and the mechanical solvent action, aluminum ions migrate from the metal surface through the barrier layer to the oxygen rich upper portion of the film where the ions react with the aluminum oxide to form an anhydrous alumina. The oxide layer formed differs in character from the more porous outer layer. The alumina has an electrostatic charge and can function to absorb other inorganic or organic material.

PROPERTIES OF Al_2O_3

This step in the creation of aluminum oxide insulated film is an advancement in the technology of processing for applications in electro-magnetic coils. Thinner insulation with high dielectric strength, lower dielectric losses and more compact components are the results. The inorganic insulated film with its advantageous dielectric properties will withstand:

- 1) higher temperature
- 2) fungus, corona and contaminants
- 3) thermal or storage aging
- 4) oxidation

It will not outgas in high vacuum.

TABLE I—Thermal and electrical conductivities of aluminum and copper.

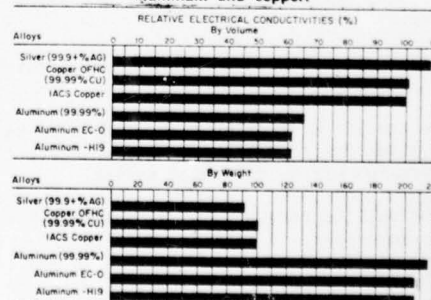


TABLE II—Properties of annealed aluminum and copper.

Property	Aluminum	Copper
Density (20°C)	2.7	8.9
Melting point	659°C (1218°F)	1083°C (1982°F)
Tensile strength (psi)	10-15 × 10 ³	30-34 × 10 ³
Assoc. elongation % (20°C)	30-45	38-50
Brinell hardness	15-25	39-40
Mod. of elasticity (psi)	10.3 × 10 ⁶	17.9 × 10 ⁶
Coef. linear expansion (per °C at 20°C)	24 × 10 ⁻⁶	16.5 × 10 ⁻⁶
Sp. heat (20°C) (cal/g. °C)	.214	.092
Thermal conductivity (cal/cm ² /sec/°C)	.5	.91
Sp. resistivity (20°C) (ohms/cm)	2.82 × 10 ⁻⁴	1.72 × 10 ⁻⁴
Temp. coef. resistivity (20°C)	4.1 × 10 ⁻³	3.9-4.2 × 10 ⁻³
Spectral emissivity % (at 0.660 microns)	18-28	17

* Mean Values

Lighter coils are made from aluminum, although the conductivity of EC grade is about 62% of that of copper, the weight factor of a comparable cross section is approximately 50% less than that of copper. See Figure 1. This means that a larger cross sectional area is required of aluminum wire to achieve comparable electrical resistance to copper. See Figure 2. With proper design of a compact nature, where losses are confined to small areas and where heat dissipates rapidly, small cross sectional wire with Al₂O₃ can be utilized.

ELECTRICAL PROPERTIES

- 1) Breakdown Voltage: The porous film of Al₂O₃ as produced on EC grade and high purity material without impregnation is approximately 30 to 40 volts per micron (0.00004"). The material composition affects the breakdown voltage which increases with the increasing purity of the metal. The film is homogeneous, uniformly thick without cracks, controlled to any thickness. The dielectric strength varies nearly in a linear fashion with the thickness as per Figure 3.

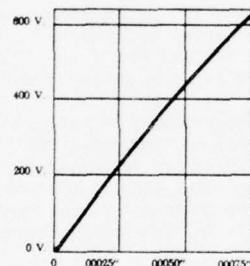


Fig. 1—Thickness of film vs. breakdown voltage (rms). The dielectric strength of the oxide film is approximately 35 to 40 volts rms per micron (0.00004").

- 2) Resistivity: The resistivity of the aluminum oxide varies with temperature and humidity. When the film is unsealed, it may vary 7×10^7 to 3×10^{12} ohms/cm. Under ideal conditions in a dry atmosphere, resistivity of 5×10^{12} ohm-cm was obtained at 20°C. after charging for 60 - 80 seconds.

TABLE IV—Properties of thin film Al₂O₃ Insulation.

Specific gravity (20°C)	4 (approx.)
Apparent average density (20°C)	2.5
Melting point	2050°C (3722°F)
Elongation (%)	10 (minimum)
Coef. of linear thermal expansion	8×10^{-6}
Refractive index	1.59
Reflectivity (%)	70
Emissivity (at 6 μ thickness)	≈ 50%
Specific resistivity (ohms/cm) (20°C)	10 ¹² (average)
Dielectric strength (volts rms/micron)	10 ⁴ (average)
Dielectric constant (20°C) (at 1 Mc/s)	35-40
Loss factor (tan delta) (20°C)	**8.5-9.5
	**0.0004

NOTES:

* Since aluminum oxide is hygroscopic and shows a considerable water absorption at relative humidities in excess of 90%, these figures relate to values obtained in air with relative humidity between 35% and 65%.

** These figures relate to values obtained in dry air.

- 3) Dielectric Constant: The dielectric constant (permittivity) of Al₂O₃ film lies between 8.5 and 9.5 when measured in dry air at one megacycle. Similarly

loss factor (tan delta) is 0.0004 under like conditions.

MECHANICAL PROPERTIES

- 1) Hardness: The film is ceramic in nature and will resist surface scratches and abrasion. The degree of hardness depends on the porosity and the depth of the oxide layer. Tests made on numerous samples of varying degrees of porosity by means of scratching the surface with a needle having a constant load of 130 grams showed that break through was achieved in the most porous sample after 16 strokes and the least porous sample after 48 strokes.
- 2) Flexibility: The film is highly flexible, unlike other forms of ceramic insulation, and retains the inherent qualities as long as the metallic base material is not subjected to undue strains. If the base material is over stretched or sharply bent, it exhibits cracking, then separation of the film may occur. A hard temper metal will not allow small diameter bending. In bare state, such wire will over stretch on the upper part of the bend, and the surface will be distorted at the lower bend. Owing to the firm bond between the aluminum substrate and the innermost layer of aluminum oxide, the insulated conductor can be made flexible, provided also that the temper of the conductor is such that it exhibits a good degree of ductility. Ductile wire and strip were wound around a mandrel having diameter four times the thickness of the conductor without flaking or cracking of the insulation.

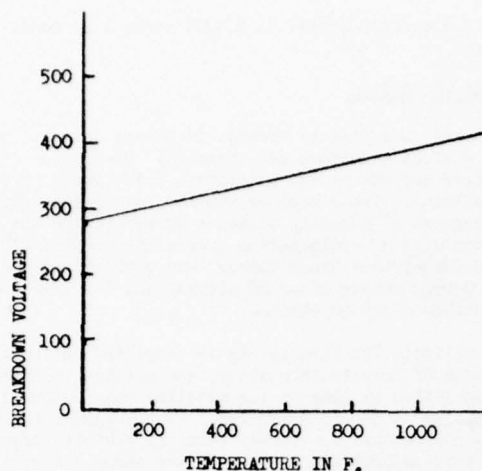
Fatigue: Tests have indicated that there is no fatigue loss due to the anodic film, even with a film thickness more than fifteen microns. This is owing to the flexibility of the film; there is no stress concentration between the metal and the film.

Strength: Tensile strength and elongation are not altered by the anodic film. With very thin material, allowance should be made for the thickness of the metal that is converted to oxide. There is no reduction in fatigue strength even at relatively high stresses. The alumina film has significant strength when detached from the metal.

Corona: As insulation is exposed to high voltage, the critical voltage is reached when visible or audible discharge occurs. This is the corona start voltage (CSV), and it is here that the ambient air becomes ionized and permits free flow of current. Most insulations exposed to this corona effect suffer erosion. It is also attacked by ozone produced from the oxygen of the atmosphere. Such chemical erosion within the body of the insulation is concentrated and results in a serious degradation of the quality of the insulation and causes premature failure of the system.

High Temperature: Heat is a very important factor in the use of a barrier type electrolyte, as it thickens the barrier layer for higher dielectric strength. Heating changes the electrical resistance and modifies the physical constance of the film; therefore, the pre-anodized aluminum heated up to 1000° F. leads to an increase in resistance and an apparent thickening of the barrier layer. It also influences the flexibility of the film. It will not blister or peel, although the thermal expansion of the film and the conductor is different.

Since the aluminum oxide melts at 3722° F. (2050° C.), the temperature maximum at which Permaluster insulated conductor may be safely employed is dictated by the melting point of the metallic conductor, which for aluminum is 1218° F. (659° C.). The insulation properties of the oxide film improves as the temperature in-



Annealed EC aluminum wire, Permaluster anodically processed of aluminum oxide Film thickness 8 microns (.0003")

creases as the moisture factor is eliminated. See Figure. It holds its dielectric properties whether it is operated at 50° C., 500° C. or -400° F. (cryogenic), thus making it suitable for Classes H and C insulation as well as exceeding Mil-Spec. for high temperature application.

It is insensitive to thermal shock. The insulated conductor can safely carry short term overload currents while in a high ambient temperature and can be subjected to sudden changes of temperature having a wide differential without deterioration.

Thermal conductivity of the Al_2O_3 is relatively close to the aluminum conductor as the film is minute. It has the ability to radiate heat rapidly in high temperature. A small coil with less weight and with high thermal conductivity will facilitate the transmission of heat. To achieve such a performance, the round wire has been replaced with flat wire or aluminum foil where all voids in the windings are filled.

Radiation: Inorganic Al_2O_3 film has an initial conductivity at zero dose rate of 10^{-12} (ohms/cm) $^{-1}$, the conductivity increases by order of the magnitude per each order of magnitude the dose rate increases; thus the dose rate of 10^5 roentgens/sec., the conductivity will have increased to 10^{-7} (ohms/cm) $^{-1}$. When materials are subjected to a short duration extreme intensity gamma pulse as encountered in nuclear explosion (where the intensity may reach to more than 10^7 roentgens/sec. in a fraction of a microsecond) the resistance of most organic insulations diminishes in value, while the inorganics including Al_2O_3 will recover rapidly after 10 to 100 microseconds.

Al_2O_3 is successfully applied in a radiation environment. A typical reaction environment of 8×10^{12} NV/cm 2 /sec. for neutrons and 6×10^{12} mev/cm 2 /sec. for gamma radiation, where the equivalent absorbed dose for each is approximately equal to 1×10^5 rads, has shown no deleterious effects.

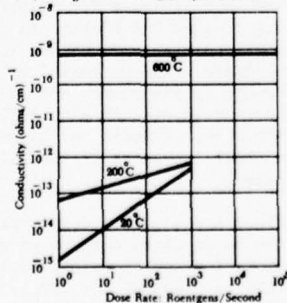
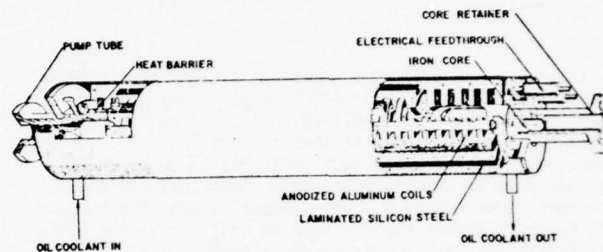


Fig. 2—Alumina (Al_2O_3) conductivity at various temperatures in gamma radiation.

Figure indicates alumina (Al_2O_3) conductivity at various temperatures in gamma radiation.

In a report by Idaho Nuclear Radiation and Argonne National Laboratories was described the design of an Annular Linear Induction Pump for the Mark II Loop, placing the most stringent requirements on the sodium pump. The four-pole version of the pump used 24 coils, and the five-pole version used 30 field coils. The field coils were designed to consist of flat ribbon wound pancake type coils of fully anodized EC aluminum. The Al_2O_3 insulated conductor was wound without interleaving and was successfully operated as the primary of a 60 cycle, one phase, 230 volts AC stepdown transformer at 425° C.

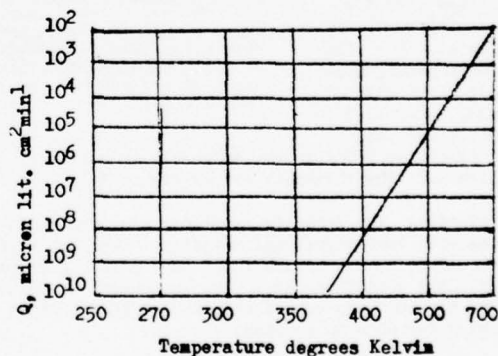


112-8624

Fig. 3. Annular Linear Induction Pump for Mark II Integral Sodium TREAT Loop

for over 500 hours without malfunction or failure (ANL-7369-Argonne National Laboratory), THE DEVELOPMENT OF PUMPS FOR USE IN FAST-REACTOR-SAFETY INTEGRAL-LOOP EXPERIMENTS by L. E. Robinson and R. D. Carlson.

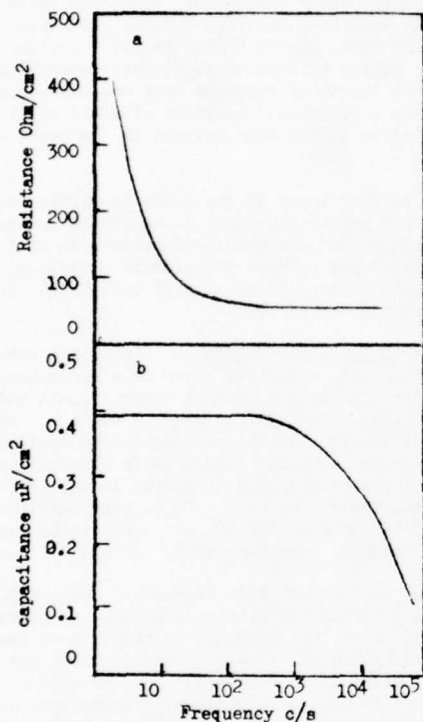
Low Temperature: Aluminum with oxide film excels in super cold environments; it is insensitive to abrupt changes at low temperatures, remains tough, ductile and strong. The high thermal conductivity of aluminum (the ability to transfer heat rapidly) makes it especially effective in high energy absorption.



Under pressure in liquid hydrogen

At sub-zero temperatures the tear resistance is as high or higher than that at room temperature. Aluminum has been used to stabilize super-conducting magnets and reacts only slightly in increases in magnetic field in resistivity or about 5 KG. In a typical room temperature, under zero stress, zero field resistivity of high purity aluminum is at 2.53×10^{-5} ohm/cm. Pure aluminum, oxidized with low strain was found to have low resistivity even in high magnetic field. In cryogenic applications at -450° F. in a magnetic field, such material operated easily at 120,000 gauss. The less strained aluminum retained its properties in high magnetic field. Its magnoresistance exhibited a predominately saturating behavior.

Frequency: Specific resistance of anhydrous and partially hydrated alumina is very high. The anodic film is approximately 5MQ/cm^2 per 1.5×10^{-3} cm film. There is no significant change over a wide frequency range. At frequencies above 1Kc/S , it is nearly constant. At 25Q/cm^2 changes will appear with varied film thicknesses. At frequencies below 10Kc/S , capacitance is nearly constant at 0.99uF/cm^2 . Figure shows some indication of fair representation of the impedance component of Permaluster tested base Al_2O_3 insulated material at room temperature.



Frequency dependence of balancing series (a) resistance (b) capacitance for annealed aluminum oxide film - Film thickness $1.5 \times 10^{-3}\text{cm}$.

Different values and properties can be obtained if the pores are sealed or impregnated.

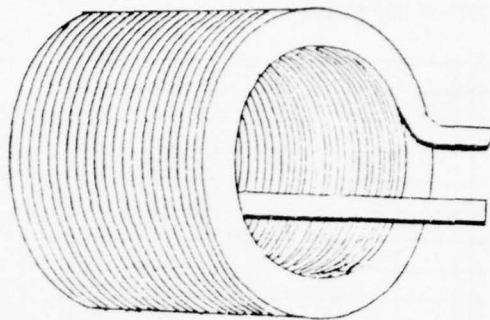
The impedance obtained in high frequency gives a more uniform response, as the mass of a moving system limits high frequency response of acoustic transducers.

By reducing the weight of the mass by more than 50%, frequency can be increased. The more density of the material, the faster the sound waves travel. For a given frequency, mass of the magnetic coil exhibits a major portion for the length of the wave to cycle. Lightweight aluminum rectangular wire, edge wound, with thin Al_2O_3 insulation, improved the design objective in obtaining the maximum power output per pound of weight and condensed unit for moving transducer coil and waveguides.

Steady state low frequency voltage would be distributed across a sheet winding in direct proportion to the turn impedance giving an essentially linear distribution of of such voltage across the turns.

The capacitance and inductance between adjacent or physically close turns and the capacitance to ground are uniform throughout a continuous sheet coil. Coils wound

from Al_2O_3 thin insulated strip have no interlayer capacitance, but only interturn capacitance; total capacitance of the coil is thus reduced.



Waveguide wound, for transmission of signals, using coil made of anodized aluminum rectangular wire, edge wound. Such coils are fast moving, lightweight, suitable for actuators, voice coils, servo system, shakers, etc.

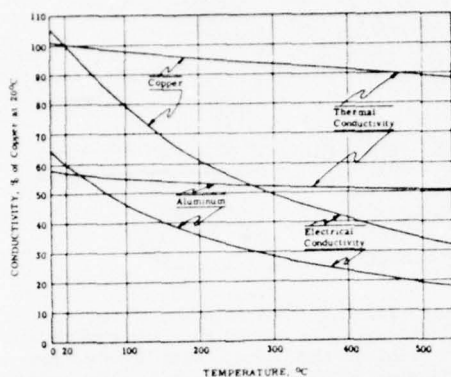
Vibration: An edge wound flat wire coil produced a flux density of 18 kilogauss in air gap (using 3 lbs. of Alnico 5 - 7 magnetic core) to provide a 6 lb. force for displacement and acceleration as shown in chart. The improved moving voice coil unit has an efficiency of 50% in the frequency range from 400 - 10,000 Hz. in a maximum acoustic output of 20 watts with high degree of reliability. Of course, higher frequency is no problem. The film is extremely tough and exhibits little deterioration under extensive mechanical vibration for extended periods of time. Coils wound with thin film insulated aluminum conductor have been successfully subjected to vibration tests both at room temperatures and elevated temperatures. Under 24 G vibration, applied at various frequencies between 50 cps and 5000 cps for one hour along each axis, no change in resistivity and only a slight change in inductance was recorded. During the test the current flowing through the coil was increased to raise the temperature to its limiting value and then reduced again.

High Vacuum: Aluminum oxide insulation may be used effectively in high vacuum. The film showed no effects under pressure below 10^{-12} Torr at 500°C . Other tests indicated that when Al_2O_3 was impregnated with carbon-free silicones, there was no evidence of any hydrocarbon residue when operated above 400°C . in extremely low pressure.

Design Consideration: Aluminum also has a high heat capacity with high capacitance for even voltage distribution. Aluminum strip or rectangular wire winding permits higher current density, due to each turn having lateral radiating edges exposed to the cooling medium, thus providing effective heat dissipation. This permits considerable design latitude in either reducing the cross section of the aluminum used or increasing the current rating for equivalent heat rise. Layer-to-layer temperatures are nearly uniform; hot spots inherent in conventional windings are virtually eliminated. The use of a thin high temperature dielectric film on flat material will require 1) less voltage per turn, 2) minimal amount of insulation, 3) minimal amount of thermal insulation. It renders greater volume in equal space and affords greater mechanical strength.

Consideration is given to life expectancy, reliability and normal stresses in performance. It is important to choose a dielectric with thermal stability when the rate of heat generation at some point will exceed the ability of the material to dissipate it. Heat is generated by

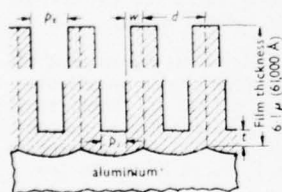
conduction current flow, principally ionic or by hysteresis under alternating stress. The heat generation rate is an increasing function of temperature in the electric field. An insulation with thermal stability should not be the limiting factor as it is the most important part of the component.



comparison of thermal and electrical conductivities of copper and aluminum at various temperatures.

The Oxide Film Structure: The Al_2O_3 insulated film can be varied in processing to meet different requirements. Permaluster produces such film that is flexible to allow winding in any form, including miniature coils and edge winding of rectangular wire under great stress. A film thickness sufficiently thick to insure good insulation and abrasion resistance can be produced.

Owing to the porosity of the oxide surface, the film exhibits hygroscopic properties, and its resistivity changes with relative humidity as well as with temperatures ranging from 10^8 Ohm/cm to 10^{14} Ohm/cm. If relative humidity is a factor, additional inorganics or organics can be impregnated into the pores of the film.



Structure of pores on anodic porous type film. Pore varies with operating conditions

Impregnated Films: Inorganic coatings have the advantage of resistance to environmental conditions, with no degradation by exposure to radiation. Al_2O_3 produced anodically is an integral part of the conductor. The inner layer of the oxide film is relatively compact and anhydrous, and on the surface is highly absorbent and ready to absorb either dissolved substances or molecules in state of colloidal dispersion. It is axiomatic that absorbing is a function of the porosity of the outer layer of the film. It is probable that oxy-type anions are a part of the pores that are capable of hydrogen bonding.

The conductivity of the outer layer provides the means of transporting anions hydroxyl ions from solvents or water toward the condensed layer, and hydrogen ions are easily bonded or fused with other substances. The transition frequency of protons in a hydrogen bond has been found to be of the order of infrared frequencies (10^{13} to 10^{14} per second). On this basis, the proton mobility in hydrogen bonded structures differs from the electron

mobility in metal itself by only 1 or 2 orders in magnitude. The pore diameter of the surface of the film is in the order of 10,50 millimeter microns, or their density is between 100 to 800 pores per square micron, sufficient to absorb other material. In some areas of applications, porous surface could have value, since it is chemically active surface. It acts as a good agent for mechanical bonding; other advantages include its retention of photo-litho emulsions, and it serves as a base for electroplating, printed circuitry and painting.

Pores can be impregnated with various materials, i. e., organics to inhibit water absorption, organo-ceramics for use in high temperatures. The Georgia Institute of Technology (WADC Tech. Report 58-13) sealed the film with Colloidal Silica in an electrophoresis deposition, also with a true liquid of ceramics that wet the inside pores by gelling a hydrolized solution of ethyl silicate so the particles of silica were trapped in the pores of the coating.

Actually, the barrier layer of the oxide is sufficiently protective for organo-ceramic filling of the pores. There is no danger that a carbon conductive path will pass the barrier layer in high temperature operation. In fact, even the organic material will operate at twice the temperature without effect.

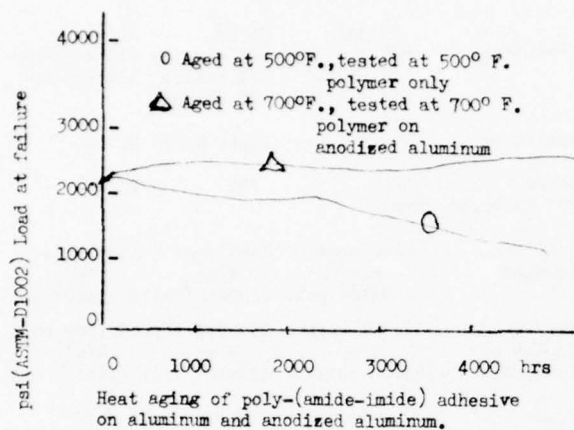
Impregnation With Inorganic Material: The anodic porous base coating with a barrier layer is a refractory, flexible film and can absorb or seal other organic and inorganic film with or without an organic vehicle. Another anodic or electrophoretic process can be applied for forming another composite film that is absorbed into the pores of the anodic base insulated layer. Barrier type electrolytes can be used. Tests performed showed that higher dielectric strength and flexibility were obtained after vacuum annealing at 450° to 500° C.

Oxide pores can be "sealed" with Tetraethyl orthosilicate, which is a refractory binder, a gelling agent for impregnation of porous material and is highly heat resistant. A hydrolized silicate gell heated to silica becomes a hard vitreous type material, a pure silica bonding agent which has the advantage of being insoluble in water; it is impervious to most acid and is excellent in high temperature. Hydrolization, using ethyl silicate solution, can be accomplished, as it penetrates completely into the porous Al_2O_3 to a complete hardness after heating.

A water solution of porcelain enamel or combinations of inorganic frits with or without resin combination, can be applied to create a strong bond with the oxide base. A strong intermolecular bond is responsible for the inertness of the base coating.

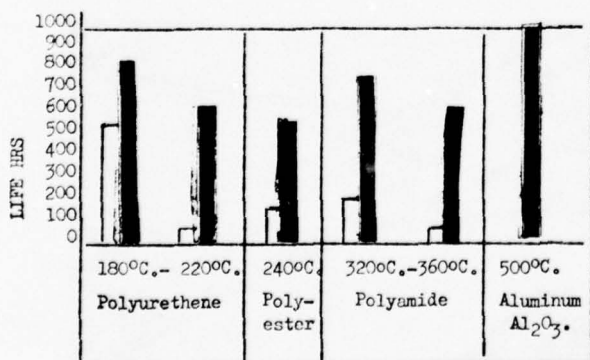
Organic Impregnation: A silicon-oxygen network interspersed with organic groups can be stabilized to a valuable film in conjunction with aluminum oxide. The solvent of the silicon mixture will oxidize and vaporize with other organic components, while the inorganic silica matrix remains and adheres to the Al_2O_3 . The pure silicon resins (crosslinked organopolysiloxanes) are almost unsurpassed for heat resistance. With aluminum oxide, the structure can withstand over 1400° F. without deterioration. A number of modified silicon resins have been used, such as silicon alkyds, or modifications with acrylics, epoxies or phenolics with a silicon content of about 25%. Such different varieties of resin combination can be formulated either by blending or co-polymerization to obtain heat resistance up to 1000° F. Such combinations are excellent in thermal shock resistance. Resin can be applied in pure form or can be combined with other resinous material. A mixture of resins put together to develop suitable properties that are compatible with the base Al_2O_3 can be achieved.

The choice of resin to be impregnated into the pores depends upon the application. The choice of an organic binder is made where little or no carbon residue remains after overheating; although, if some carbon does remain, it will have no effect, as the pores are protected by the refractory oxide film that has a melting point three times that of aluminum.



High temperature polymers offer versatility for use in electronic insulation and show stability in performance when impregnated into the Al_2O_3 "prime coat"; greater dependability has been achieved at high operating temperatures (about 850° F.).

Thermal aging of insulation in organic material is probably responsible for most failures found in the component. Thermal aging itself does not produce failures, but it renders insulation vulnerable to other factors, such as moisture penetration, brittleness, loss of thermal expansion before complete failure. Figure shows some experiments with organic film over Al_2O_3 .



Thermal aging of EC aluminum wire, anodically insulated and copper wire with various types of insulated films. Bars in grey indicate aluminum and oxide wire.

Such organic overcoat is produced in a cured or quasi-cured state. A coil can be formed and wound in any shape when a quasi-cured state is required. When heat-

ed, the turns bond together to form a solid structure. By employing this method, cores are eliminated; the coil becomes very strong and self supporting.

Less magnetic losses while decreasing the mass and improvement of thermal stability are the results of designing components using Al_2O_3 as a prime insulation or with impregnations. Two important factors are derived, weight reduction and greater reliability.

CONCLUSION

Most insulations are based on a thermal theory. Should a weak area in the organic insulation be heated more than other areas, and if the heat is not removed as rapidly as it is generated, the weak spot grows hotter and the resistance will lower. As the temperature continues to rise in operation, instability occurs; this will be followed by a breakdown in the weakest point of the insulation. This will not occur in Al_2O_3 insulation. In fact, the aluminum oxide insulation improves at temperatures above 220° F. The choice of insulation is often a decided factor that will govern the performance and reliability of the components. In applications where peak load is energized during low demand period, overall losses are always less in high temperature design. Examples are transformers, generators, solenoids, alternators, magnets, etc., whether for environmental or terrestrial operation.

The adaptation of aluminum conductor with Al_2O_3 insulation is the latest step in attaining improved operation through better balance in components to more efficient design through the reduction of mass, higher current flow, and consequently higher temperature operation.



HENRY D. WALKER
1844 North Keystone Street
Burbank, California 91504

Consultant Chemist

Originator of patented process, and founder of Permaluster, Inc.

CONTINUOUS CERAMIC FIBER REFRACTORY INSULATION

By
Karl A. Karst
Ceramic Fiber Project
3M Company
St. Paul, Minnesota 55101

ABSTRACT

Continuous filament ceramic fibers represent a major advancement in refractory fiber technology. These fibers are truly continuous fibers of metal oxides that can readily be converted into ceramic textiles which meet tough performance requirements in high temperature operating environments. The AB-312 fiber system can withstand temperatures up to 1400°C for extended periods and short term exposure to 1600°C.

Because the filaments are continuous and strong, ceramic textiles can be produced without the aid of other fibers or wire inserts. Fabrics, tapes, sleeveings, cordage, conveyor belts and thermocouple wire insulation are typical products.

These ceramic textiles offer strength, durability, efficiency and safety in useable forms. Additionally, the fibers have low elongation and shrinkage at operating temperatures, which allows a dimensionally stable product to be made. These novel fibers also offer good chemical resistance, low thermal conductivity, thermal shock resistance, low porosity and good electrical properties.

INTRODUCTION

Textile articles manufactured from continuous filament ceramic yarns have recently been made commercially available from the 3M Company. A unique combination of properties allows engineered textile products to be produced on conventional fiber handling equipment. The fibers themselves differ in properties from other commercially available inorganic fibers, such as fiber-glass and fused or leached silica. The 3M technology provides an entire family of fibers with varied properties to be manufactured.

PHYSICAL PROPERTIES

A variety of fiber compositions can be produced with the 3M ceramic fiber technology. Examples of these are alumina-boria-silica (AB-312), zirconia-silica (ZS-11) and alumina-silica-chromia (AC-02). The relative physical properties of these three systems are listed in Table 1.

Individual filaments of ceramic fibers are round, smooth, transparent and have a relatively low surface area. These properties may be altered by subsequent treatment. The transparent nature of these filaments can be seen in Figure 1, a magnified photograph of typical alumina-boria-silica filaments submerged in a refractive index oil.

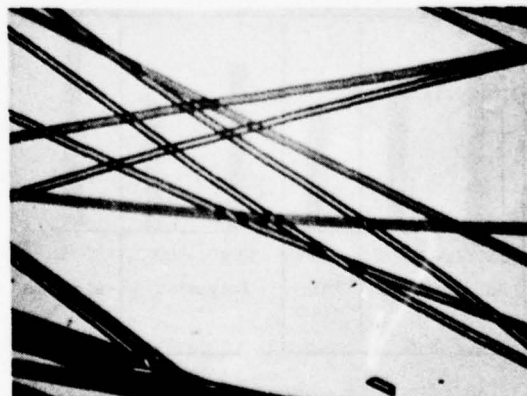
TABLE 1

TYPICAL PHYSICAL PROPERTIES OF CONTINUOUS CERAMIC FILAMENTS

	AB-312	AC-02	ZS-11
Composition	62% alumina 14% boria 24% silica	70% alumina 28% silica 2% chromia	67% zirconia 33% silica
Base Color	White	Light Green	White
Denier (390 Filament Yarn)	900	795	2060
Tensile Strength	1720 megga N/m ² (250x10 ³ psi)	1460 mega N/m ² (200x10 ³ psi)	1380 megga N/m ² (175x10 ³ psi)
Tensile Modulus of Elasticity	152,000 mega N/m ² (22x10 ⁶ psi)	159,000 mega N/m ² (23x10 ⁶ psi)	96,000 mega N/m ² (14x10 ⁶ psi)
Strand Strength (390 filament yarn)	2.3 kg (5.0 lb)	2.0 kg (4.5 lb)	2.0 kg (4.5 lb)
Filament Diameter	11μ (0.44 mil)	10μ (0.40 mil)	14μ (0.56 mil)
Density	2.50 gm/cc	2.80 gm/cc	3.70 gm/cc
Extended Use Temperature	1400°C (2550°F)	1425°C (2600°F)	1000°C (1830°F)
Short Term Use Temperature	1600°C (2900°F)	1650°C (3000°F)	-

FIGURE 1

MAGNIFIED VIEW OF AB-312 FILAMENTS



By the addition of small amounts of the proper metal oxides, a variety of colors can be imparted to the fibers. The color is internal and uniform throughout an individual filament and is retained during use at high temperature or in corrosive environments. This property not only can be decorative, but also is useful

for color coding, especially in thermocouple applications. Table 2 lists the resultant colors which can be obtained when various oxide additives are incorporated into the fiber system.

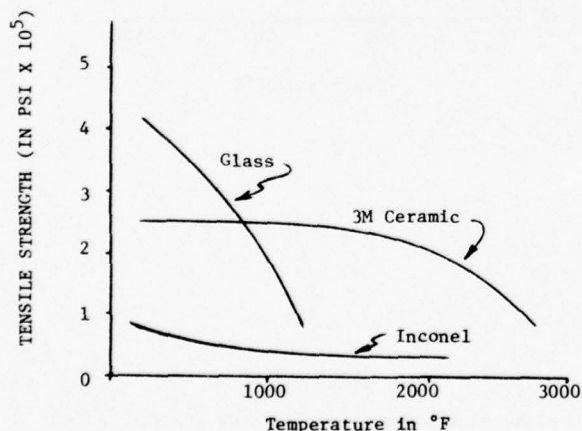
TABLE 2
COLORS OF CERAMIC FIBERS

Oxide Additive	General Color
Cr_2O_3	Green
Fe_2O_3	Yellow - Gold
CoO	Blue
NiO	Aqua
MnO	Brown

Still other unique properties can be generated by the addition of oxides and subsequent treatment. For example, if a small amount of iron oxide is added to the ZS-11 system and the fibers are heated in a hydrogen atmosphere, the reduced iron oxide or metallic iron will cause the fibers to become attracted to a magnetic field. This will be accompanied by a color change from gold to black.

Strength retention at elevated temperature is an important feature of the continuous filament ceramic yarns. Figure 2 shows a comparison of the AB-312 material with typical fiberglass and Inconel. Note the extended use temperature of the ceramic material.

FIGURE 2



For applications where low moisture or gas absorption is important, the 3M ceramic fibers perform satisfactorily.

The low surface area, generally less than $1.0 \text{ m}^2/\text{g}$, allows only 0.06% moisture absorption after long term exposures to air saturated with water at ambient temperature. This property can be very important in minimizing outgassing problems in certain applications.

CHEMICAL PROPERTIES

The oxide composition of the ceramic fibers allows them to withstand attack by virtually all common hydrocarbons and many acids and bases. To characterize this property, loss in filament tensile strength was measured after treatment at 90°C for eight hours in 12-18 molar chemical baths. The zirconia-silica filaments best withstood attack and would be superior for use in corrosive environments. Table 3 summarizes the results of these tests.

TABLE 3

PERCENT LOSS OF FILAMENT TENSILE STRENGTH AFTER CHEMICAL TREATMENT

Chemical	24% silica 62% alumina	2% chromia 70% alumina	67% zirconia 33% silica
	14% boria	28% silica	
HCl	decomp.	23	6
H_3PO_4	"	16	5
NH_4OH	"	11	3
NaOH	"	decomp.	33

The effects of various metals on a fabric woven from alumina-boria-silica yarns were determined at elevated temperature. Powdered metals were placed on the woven cloth and heated in air to 1100°C for one-half hour. Overall results are listed in Table 4.

TABLE 4

EFFECT OF METALS ON AB-312 FABRIC AT 1100°C

Metal	Effect at 1100°C
Aluminum, Boron,	No attack
Platinum, Cobalt,	" "
Chromium, Gold	" "
Iron, Nickel, Silicon	" "
Soft Solder	" "
Copper, Tin	Severe Attack

The metals which caused attack are extremely reactive at test temperature. Most common metals, however, have no effect on the AB-312 fiber system.

ELECTRICAL PROPERTIES

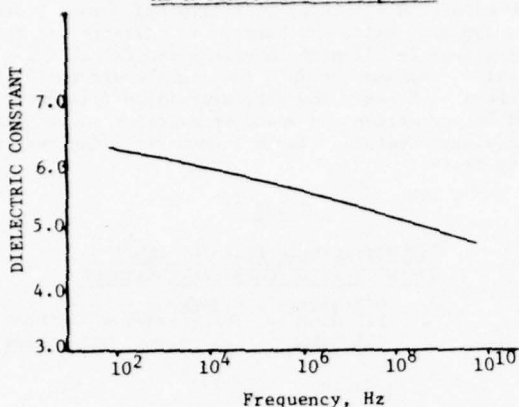
The dielectric constant for the 62% alumina-14% boria-24% silica system has been calculated over a frequency range of 10^2 to 10^{10} Hertz. Measurements of dielectric strength were made on unidirectional composites which contained 50 volume percent fibers and 50 volume percent resin matrix⁽¹⁾. Similar measurements were also made on the resin material by itself. Using the "rule of mixtures" expressed by equation 1, the dielectric constant was then calculated for fibers alone over a broad frequency range.

$$\ln E_c = (1-P) \ln E_m + P \ln E_f \quad (1)$$

Where E_c = composite dielectric constant
 E_m = matrix dielectric constant
 E_f = fiber dielectric constant
 P = fiber volume fraction

Figure 3 shows how the dielectric constant varies with frequency at ambient temperature.

FIGURE 3 - DIELECTRIC CONSTANT OF AB-312 FIBERS
AS A FUNCTION OF FREQUENCY



Loss tangent measurements were also made on the same composite samples and the resin alone over the same frequency range. These values are listed in Table 5.

TABLE 5
LOSS TANGENT AT VARIOUS FREQUENCIES

Frequency	Matrix	Loss Tangent Composite
10 ² cycles /sec.	0.014	0.010
10 ³	0.014	0.013
10 ⁴	0.016	0.018
10 ⁵	0.018	0.021
10 ⁶	0.041	0.018
10 ⁷	0.030	0.019
9.3x10 ⁹	0.033	0.020

The data shows that at 10² and 10³ cycles per second, the fibers plus the matrix have a lower loss tangent than the matrix resin alone. This indicates that at low frequencies, the loss tangent of the aligned fibers is less than that of the matrix material.

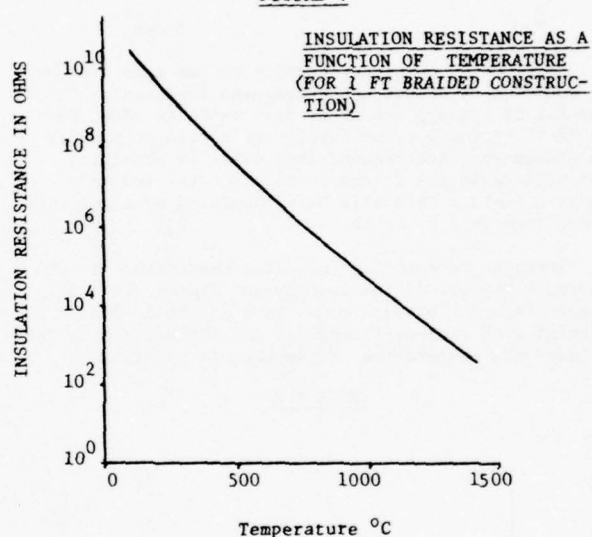
At the test frequencies shown, the loss tangent appears to rise from less than 0.010 to a maximum of about 0.025 at 10⁵ cycles per second. At higher frequencies (above 10⁶), the loss tangent of the fibers begins to drop. It is recognized that the loss tangent of the fibers will be a function of the particular filament configuration, so it is impossible to assign definite values to the loss tangent at any one frequency.

The insulation resistance of AB-312 braids on thermocouple wire was measured as temperature was increased from ambient to over 1400°C. The thermocouple wire composite was constructed by braiding AB-312 yarns around each of the two individual wires. Wall thickness was approximately 0.020 inches. Both braids were held together by a third overbraid, also composed of the AB-312 material. Eighteen inch samples were heated to above 800°C to remove organic contaminants. With one foot sections exposed to the test

temperature, the remainder of the wire extended through the oven wall and was connected to a test device. All wires were open ended. The insulation on one sample contained a fiberglass tracer yarn, but this did not appear to significantly affect the measured values of insulation resistance.

A typical curve of insulation resistance as a function of temperature is shown in Figure 4. The values of insulation resistance will change depending on wall thickness, length of thermocouple wire tested, and the braid construction, but these data are representative of common constructions.

FIGURE 4



APPLICATIONS

Continuous filament ceramic yarns are fabricated into a variety of textile products. Figure 5 shows some of these products including woven belting, braided sleeving, narrow fabrics, net fabrics and twisted/plied cordage.

FIGURE 5
CERAMIC TEXTILE PRODUCTS



Uses for these products are based on the unique combination of fiber properties mentioned previously, in particular, strength and temperature resistance.

Since the fibers remain flexible and experience minimal shrinkage after exposure to temperatures exceeding 1200°C, they have been found useful in insulating reusable thermocouple wires. Figure 6 shows a ceramic fiber covered chromel - alumel thermocouple.

FIGURE 6
THERMOCOUPLE WIRE INSULATED BY
CERAMIC FIBERS

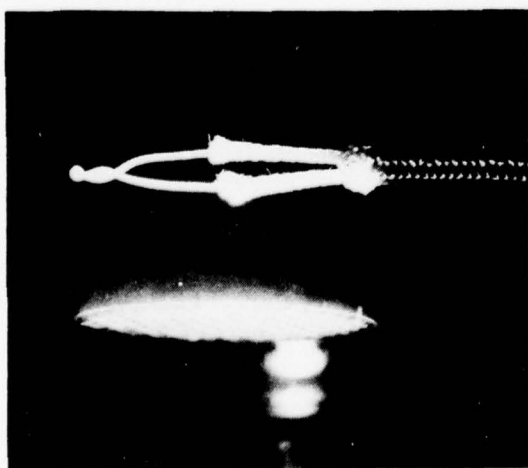
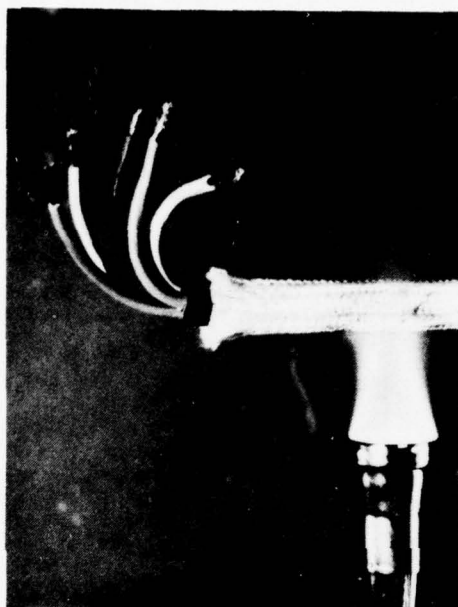


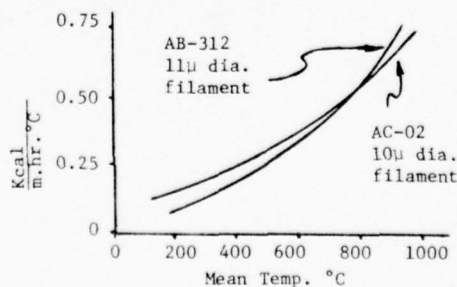
Figure 7 shows a braided cable insulation being exposed to a gas flame. In addition to its flame resistance, this insulation affords higher temperature capabilities than present in heretofore available materials.

FIGURE 7
CERAMIC FIBER CABLE INSULATION



Battings of these fibers exhibit good thermal resistance properties and can be used in insulating applications sometimes in conjunction with textile forms of the same fibers. Because the fibers are continuous, they can withstand mechanical vibrations better than the majority of competitive products. Figure 8 shows the thermal conductivities of two fiber systems.

FIGURE 8
COMPARATIVE THERMAL CONDUCTIVITIES*
(0.05 g/cc Density Batting)



* These curves were obtained by measuring temperature drops through bulk 3M Brand ceramic fibers in contact with other materials of known thermal conductivity. The test method was standardized using Fiberfrax[®] H (Carborundum Co.) and Saffil[®] Alumina Fiber (ICI America, Inc.) whose thermal conductivities are published.

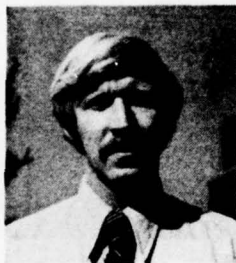
Because of the excellent temperature properties and the low surface area of the fibers, outgassing is minimized when batting and/or cloth are used in applications such as vacuum furnace linings.

High strength characteristics at elevated temperatures make the fiber useful for continuous, high-temperature conveyor belts, rope heaters, and heating element insulation. Perhaps most important, the unique combination of properties of these fibers will make them useful in many other applications.

Reference:

- (1) Dr. R. B. Pipes, Center for Composite Materials, University of Delaware, Newark, Delaware 19711

BIOGRAPHY:



Mr. Karst received his B.S. in 1968 and Masters in 1969 in Chemical Engineering from Cornell University, Ithaca, New York. Since graduation he has been employed by 3M Company, St. Paul, Minnesota and for the past five years has been involved with the development of continuous filament ceramic yarns.

LOW LOSS POLYETHYLENE FOR THE INSULATION OF SUBMARINE COAXIAL CABLE

by

H. Kishi, Y. Yamazaki, T. Nagasawa
H. Takashima, H. Fujita and I. Tsurutani
UBE Industries, Ltd.
Tokyo, Japan

SUMMARY

For the insulation material of submarine coaxial cable, very low dielectric loss as well as excellent mechanical strength and low level of contamination are required. It was necessary for the development of these polyethylenes to elucidate the relationship between molecular structures and dielectric properties and to establish the new production technique by the improvement of the polymerization and finishing process. Based on these technical development, UBEC1010 and UBEC2020 have been developed. In this paper, the developing process and characteristics of these polyethylenes are shown. Furthermore, an experimental grade of which dielectric loss was lower than that of UBEC2020 was produced. In the comparison of these materials, the image of insulation materials of submarine cable is reviewed.

In order to keep the excellent properties of material in the manufactured cable, sufficient considerations should be paid to the cable manufacturing conditions. The approaches to the optimum manufacturing conditions are shown.

INTRODUCTION

Two systems, that is, submarine cable systems and satellite systems are used for international telecommunication. The submarine cable systems, are superior in stability and secrecy of telecommunication. To meet the increasing demand of the communication, these systems have been mutually improved making up for their demerits. Various submarine cable systems have been developed and put to practical use such as previously developed SF system and the latest SG system of which top frequency is 6 and 30 MHz, respectively. The high operating frequency have been used in order to enlarge the transmission capacity to satisfy the increasing telecommunication demand. By use of the higher operating frequency, the attenuation of signal in the cable increases. In order to amplify the attenuated signal, repeaters are used. These repeaters are so expensive that it is required to decrease the number of repeaters for the cost saving of submarine cable systems. Therefore, low dielectric loss polyethylene must be used for the insulation material which is very effective on the attenuation of signal in the cable.

The repair of submarine cable at ocean bottom is so difficult that the long term reliability is required. For these reasons, the following severe properties and qualities are required for the high pressure polyethylene of the insulation of submarine cable.

- (1) Very low dielectric loss controlled in a narrow range
- (2) Extremely low level of contamination
- (3) Excellent processability of cable manufacturing and excellent mechanical and dielectric properties of the manufactured cable

The properties of the insulating polyethylene of submarine cable are recently reviewed by Matsuoka et al.¹⁾ Processability of cable manufacturing is discussed by Daane²⁾ from the viewpoint of a gripping force between the insulation and the innerconductor. The phenomena that water permeating into polyethylene on the cooling process of cable manufacturing increases the dielectric loss of polyethylene could not be disregarded. Some of the co-authors have already elucidated the optimum manufacturing condition by the simulation model of water permeating mechanism and cable manufacturing conditions.³⁾

In this paper, the properties required for the low loss insulation material of submarine cable are briefly described based on the development of SF and SG grades. The manufacturing conditions to avoid the dielectric loss increase and void formation are also described.

DIELECTRIC PROPERTIES

On the submarine cable system, repeaters are connected at constant intervals to amplify the attenuated signal. To decrease the number of expensive repeaters, it is desirable that the attenuation of signal in the cable is minimized. The relation between the attenuation and the dielectric properties of insulating polyethylene is shown by the following equation.¹⁾

$$\alpha = k_1 \sqrt{f} \left(\frac{1}{d\sqrt{\sigma_d}} + \frac{1}{D\sqrt{\sigma_D}} \right) \frac{\sqrt{\epsilon}}{\log_e D/d} + k_2 f \sqrt{\epsilon} \tan \delta$$

- where α : attenuation
 k_1, k_2 : constant
 f : frequency
 d, D : diameters of inner and outer conductors
 σ_d, σ_D : conductivities of inner and outer conductor
 ϵ : permittivity
 $\tan \delta$: dielectric loss

The first term in above equation is mainly the resistive loss in the conductor and the second term is the dielectric loss in the insulation. Because the constant of the second term is small than that of the first one, the contribution of the second term to the attenuation is small. However, in recent high frequency system, the second term is very important because the frequency is the first order. The

dielectric loss in the second term is the first order and, as described later, affected by many factors, so that it is necessary that the dielectric loss is kept to be low and in a narrow range.

Permittivity and dielectric loss of polyethylene which are effective on the attenuation of signal are described below.

Permittivity

Permittivity of polyethylene is, as shown in Fig. 1, proportional to density. Density presenting the types of polyethylene generally indicates the differences of molecular structure. But the density of polyethylene, even if the molecular structure is the same, is different as crystallinity changes by crystallization conditions or annealings. But as shown in Fig. 1, the permittivity is proportional to the density which depends on both molecular structure and whether or not specimens are annealed.

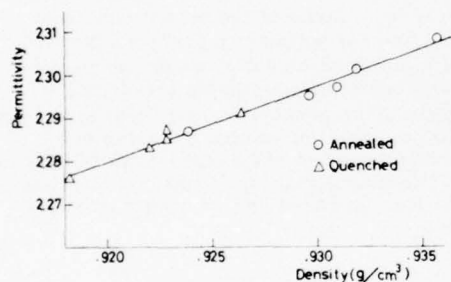


Fig. 1 Density vs. permittivity at 23°C, 1 MHz

Dielectric loss

Polyethylene is essentially an excellent insulation material and has low dielectric loss. As the key factor of the development of new systems, lower dielectric loss polyethylene has been required. In order to develop the polyethylene which satisfies the requirements, it is necessary to establish the following technical developments.

- (1) Establishment of a precise measuring method of the dielectric loss of polyethylene.
- (2) Elucidation of the relationship between the dielectric loss and the polymer structure.
- (3) Establishment of producing technique of polyethylene at aimed dielectric loss constantly.

Some precise measuring method of the dielectric loss for the insulating polyethylene of submarine cable were reported. (4), (5), (6) Authors have established a precise measuring method based on silicone displacement method using a Q meter, Yokogawa Hewlett Packard type 4342A. The silicone displacement method has various merits such as simple operation and good reproducibility. And it also enables to measure the permittivity precisely without the effect of air between specimen and electrode because the permittivities of silicone liquid and polyethylene are almost equal. The results by this

method is shown in Table 1.

Table 1 Results of dielectric loss measurement of UBEC2020 by our method at 23°C

Frequency (MHz)	Dielectric loss (10^{-6})	
	Average	Standard deviation
1	25.9	0.4
6	34.3	0.6
30	44.2	0.6

The dielectric loss of polyethylene is increased by chain branchings, unsaturations and impurities formed on the polymerization process and by anti-oxidant added to polymerized polyethylene.

In the radical polymerization process of ethylene, long and short chain branchings and unsaturations are formed besides the polymerized methylene unit. The long chain branching formed by intermolecular chain transfer reaction has almost the same length as main chain and its number is very few, so the increase of dielectric loss by long chain branching is negligible. The short chain branching is formed by intramolecular chain transfer, so called back-biting, reaction and copolymerization with α -olefin. They are mainly composed of methyl, ethyl and butyl branches. The unsaturations detected in high pressure polyethylene are end vinyl ($RCH=CH_2$), trans-vinylene ($RCH=CHR'$) and vinylidene ($RR'C=CH_2$). The number of end vinyl and trans-vinylene is generally less than that of vinylidene on high pressure polyethylene. As both the short chain branchings and vinylidene are formed from tertiary radicals, the number of vinylidene gives the same tendency as that of the short chain branchings.

Short chain branchings which are the most in number in polyethylene prevent the crystallization and decrease the crystallinity. So as shown in Fig. 2, density of polyethylene becomes high with the decrease of short chain branchings. Under certain polymerization condition where the short chain branchings decrease, the number of total unsaturations decrease simultaneously as shown in Fig. 2. Therefore, there is a large correlation between the density and the dielectric loss. The polyethylene with higher density has lower dielectric loss as shown in Fig. 3.

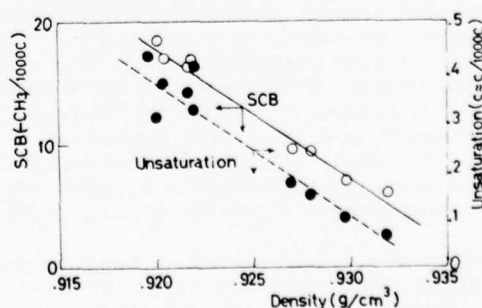


Fig. 2 Density vs. short chain branching and total unsaturation

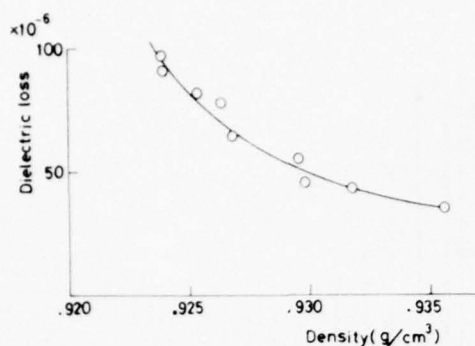


Fig. 3 Dielectric loss at 23°C, 30 MHz as a function of annealed density

Both the short chain branchings and the unsaturations are influenced by temperature and pressure of the polymerization reaction of ethylene. In order to control the dielectric loss at the aimed value and in a narrow range, it is necessary to control the short chain branchings and the unsaturations at constant value. From the industrial point of view, it is necessary to establish the optimum operating conditions and to control them to minimize the fluctuation. The reaction condition to produce the polyethylene with aimed dielectric loss could be easily established by the simulation model of polymerization of ethylene. The fluctuation of dielectric loss is mainly due to the fluctuation of reaction temperature. The fluctuation of reaction temperature could be minimized by the direct digital control system using a process computer.⁷⁾

As an initiator of high pressure ethylene polymerization, oxygen or organic peroxide is generally used. It is possible that the decomposed matter and the residue of initiator remain in the polyethylene as compounds which contain carbonyl and hydroxy or other chemical group. If air is mixed in molten polyethylene in the pelletizing extruder, carbonyl group is produced by oxidation. Even if the content of these polar group is extremely low, the dielectric loss of polyethylene increases because they have

large dipole moment. Therefore, it was necessary that the initiator consumption per unit polymer production was minimized, that the decomposed matter and residue were removed from the manufacturing process and that the penetration of air in pelletizing extruder was prevented.

In order to prevent the oxidative degradation in the cable manufacturing process and in practical use, antioxidant is added to the insulating polyethylene of submarine cable. Some antioxidant increases the dielectric loss of polyethylene. The dielectric loss of polyethylene which contains the various types of antioxidant for polyolefins is shown in Fig. 4. The performance of these antioxidant is shown in Table 2 as the oxidative induction period by DSC at 200°C. These results show that Ionox 330 scarcely increases the dielectric loss and has excellent anti-oxidative performance.

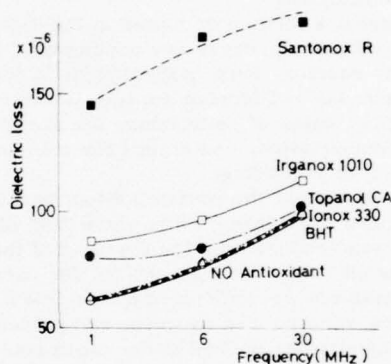


Fig. 4 Effect of antioxidant on dielectric loss at 23°C Concentration is 1000 ppm

Table 2 Oxidative induction period by DSC at 200°C Concentration is 500 ppm

	(min.)				
	BHT	Santonox R	Topanol CA	Ionox 330	Irganox 1010
	0	38	22	29	27

Table 3 Molecular structures and dielectric properties of the insulating polyethylene of submarine cable

	Unit	UBEC1010 (SF)	UBEC2020 (SG)	Experimental
Melt index	g/10 min	0.1	0.2	0.2
Density (annealed)	g/cm ³	0.923	0.931	0.935
Short chain branching	-CH ₃ /1000C	20	9	6
Unsaturation	C=C/1000C			
trans vinylene		0.08	0.03	0.01
end vinyl		0.04	0.03	0.03
vinylidene		0.25	0.04	0.03
Permittivity	—	2.285	2.299	2.306
Dielectric loss	10 ⁻⁶			
1 MHz		59	26	21
6 MHz		78	34	28
30 MHz		96	44	35

In order to produce the insulating polyethylene for submarine coaxial cable of which dielectric loss is very low and controlled in a extremely narrow range, above-mentioned various considerations are necessary. In Table 3, structures and dielectric properties of two insulating grades and an experimental product with lower dielectric loss are shown.

CONTAMINATION

Contamination in the insulation of submarine cable decreases the reliability of submarine cable system which is expected to operate for long time. It is possible that a large amount of contamination increases the dielectric loss of polyethylene. In order to reduce the contamination to extremely low level, some particular countermeasures had to be applied to production, transportation and packaging process of polyethylene.

Contaminations formed or mixed in the high pressure polyethylene process are decomposed polyethylene in the reactor, burnt polyethylene in the pelletizing extruder and foreign matters which come from the chilling water of pelletizing, the air of pneumatic transportation, containers for transportation and the air of packaging.

In order to prevent the contamination, the following countermeasures were taken. The same kind of polyethylene was produced for the cleaning of the process. The chilling water and the air for pneumatic transportation were filtrated by the fine filter. The containers were washed by water and polyethylene. Polyethylene was packed in the clean room circulated with the filtrated air. To improve the accuracy of the inspection of contamination, thin tape was extruded and then number and size of contamination of predetermined weight of the tape were measured by using multiplying glass. The inspection was performed in a clean room circulated with the filtrated air.

The typical distribution of contaminant in the polyethylene which was produced on the process taking the above-mentioned countermeasures is shown in Fig. 5. This result shows that some of very small contamination are detected but the level of it is extremely low. In Fig. 6, the cumulative volume of contamination of general purpose polyethylene manufactured without above countermeasures and the insulating polyethylene of submarine cable with countermeasures is shown. This result shows the volume of contaminant decreases approximately one-fortieth by these countermeasures.

In order to find the source of contamination, the contamination was analyzed by Raser Microprobe, type JLM-2 by Japan Electron Optics Laboratory. Particles in which inorganic elements could not be detected are assumed to be organic substances and they were about 80% in number. Inorganic elements were detected from particles of 20% and were Ca, Mg, Ni, Fe, Al, Cu, Si, etc. They are supposed to be the contaminants mainly from the producing instruments, the water and the air. The organic substances are supposed to be decomposed or burnt polyethylene in the reactor or in the pelletizing extruder.

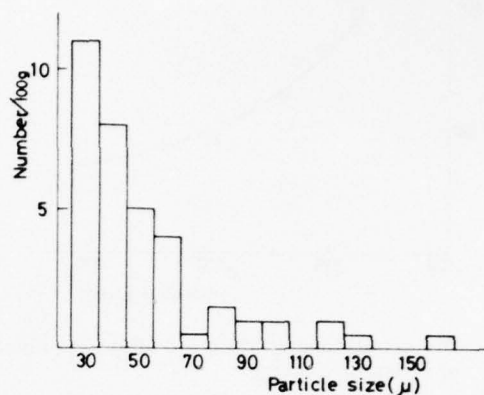


Fig. 5 Particle size of contaminant in tape of 100 g

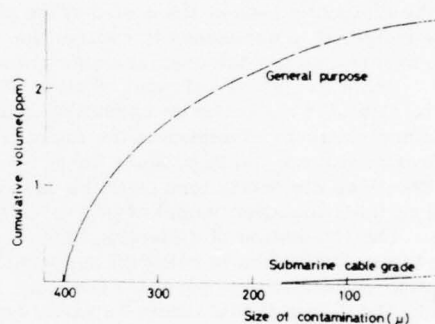


Fig. 6 Cumulative volume of contamination

PROCESSABILITY

The submarine coaxial cable is manufactured covering the innerconductor by extruded molten polyethylene. The extrudability of polyethylene is influenced by the melt viscosity at the extruding temperature and that of lower average molecular weight polyethylene is excellent because of lower melt viscosity. However, in order to satisfy the mechanical strength of the cable such as environmental stress crack resistance, relatively high melt viscosity, that is, high average molecular weight polyethylene, is used for the insulation of submarine cable.

It is well known from experience that the diameter of submarine cable is so large that voids are formed in polyethylene of the insulation if the molten cable is quenched. Therefore, the cable is cooled slowly in the multitroughs of water of which temperature is stepwisely decreasing. However, water permeates into the polyethylene on the cooling process because the cooling time is long and the cable is immersed in relatively high temperature troughs at the initial step. Polyethylene is essentially hydrophobic and the solubility of water is very small. Sometimes the dielectric loss of polyethylene increases by the permeating water as shown in Fig. 7. This result

shows the permeating water deteriorates the transmission performance of cable. Fig. 7 also shows that the increase of dielectric loss by water depends on the density of polyethylene. The increase of dielectric loss of higher density polyethylene is much more than that of lower density. Therefore, in the case of the cable of SF system using a relatively low density polyethylene, there was no problem of permeating water. On the other hand, in the case of SG cable, problems are sometimes caused by water. The diameter of SG cable is larger than SF cable to reduce the attenuation of signal. And the dielectric loss of polyethylene of SG system is reduced to a half of SF system and density becomes high to satisfy the dielectric loss. The larger cable with higher density polyethylene such as SG cable must be cooled more slowly to avoid void formation and to strengthen the gripping force. As the result of this cooling condition, much water permeates into the polyethylene. Furthermore, the dielectric loss increase of higher density polyethylene is sensitive to water, as shown in Fig. 7, so the dielectric loss increases to a large extent. As for the cooling conditions, slow cooling is desirable to avoid the void formation and to strengthen the gripping force. But quenching is desirable to prevent the increase of dielectric loss. On the cable manufacturing process, the cooling condition which satisfies these two conflicting conditions must be selected.

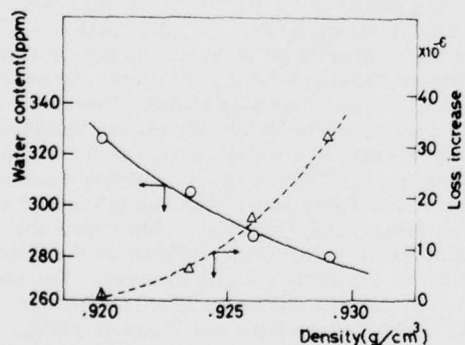


Fig. 7 Effect of water content on the increase of dielectric loss at 23°C, 30 MHz. Polyethylene is immersed in hot water and then measured.

Relationship between the manufacturing conditions and water content

The effect of manufacturing conditions on the water content and the dielectric loss was investigated by the model cables which were extruded and cooled stepwisely in multitroughs. The diameter of the insulation and the core of the model cables was 46 mm and 12 mm, respectively. The model cables were cooled by the conditions shown in Table 4. The water content of the cable was measured by Du Pont Moisture Analyzer type 26-321A. As shown in Fig. 8, the cable had a large distribution of water

content in the direction of the cable radius. The surface area of the cable had a large water content because the diffusion of water proceeds from the outer surface to the center. The distribution of water content is supposed to be different by the manufacturing conditions. In this paper, the water content of the cable is discussed by the average content.

Table 4 Water trough temperature and cooling time on model cable manufacturing

Trough number	1	2	3	4	5
Cooling time (min.)	15	10	10	25	50
Trough temperature (°C)	105	95	70	50	20
	100	90	70	50	20
	95	90	70	50	20
	90	80	70	50	20
	85	80	70	50	20
	80	80	70	50	20

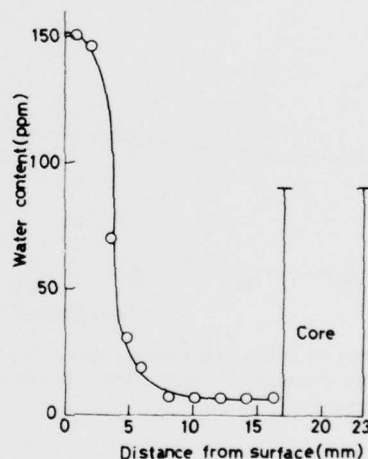


Fig. 8 Distribution of water content in the insulation of UBEC2020. Extrusion temperature is 185°C and first trough temperature is 95°C.

The main effective manufacturing conditions on the permeation and the diffusion of water into polyethylene are the cooling water temperature and the extrusion temperature. The effect of the cooling water temperature on the water content are shown in Fig. 9. This result shows that the water content increases with the first trough temperature and decreases with density of polyethylene at the same trough temperature. The effect of the extrusion temperature on the water content are shown in Fig. 10. The water content increased with the extrusion temperature but the effect is small in comparison with that of trough temperature.

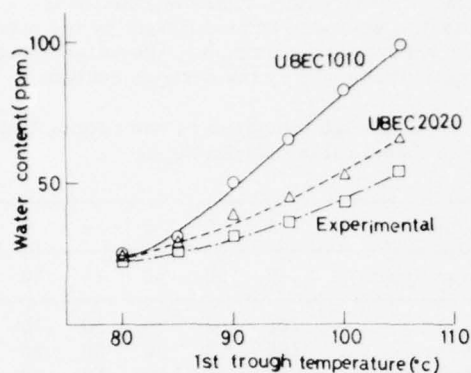


Fig. 9 Effect of cooling water temperature on average water content
Extrusion temperature is 185°C.

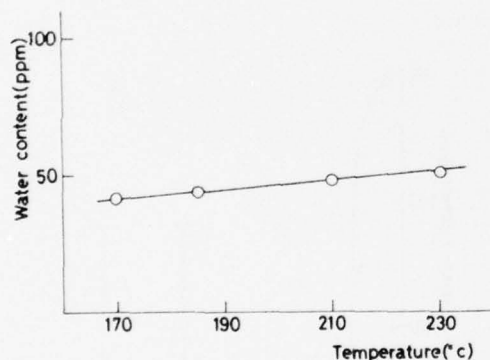


Fig. 10 Effect of extrusion temperature on average water content of UBEC2020. First trough temperature is 95°C.

The water content of the cable is influenced by many factors such as diffusion and solubility of water, the crystallization rate of polyethylene, etc. As water doesn't permeate in the polyethylene crystal, a large amount of water than expected is, as shown in Fig. 11, solubilized at the temperature where polyethylene is partially melt. And the solubility of water in molten polyethylene is, therefore, very high. The crystallization of the molten cable proceeds in the water troughs. From these facts, it is supposed that much water permeates into polyethylene while the cable is in the molten state before crystallization. The time until crystallization is determined mainly by the cooling water temperature. Therefore, water content of the manufactured cable is influenced by the trough temperature, in particular, the first trough temperature. These results show good coincidence with the calculated results by simulation model of water permeating mechanism.

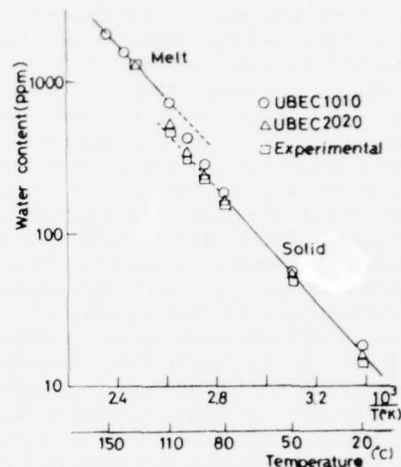


Fig. 11 Temperature dependency of saturated water content

From the viewpoint of polyethylene, the solubility of water in polyethylene, as shown in Fig. 7, has an intimate relation with the crystallinity (density) and water is more soluble in lower density polyethylene. The crystal of polymer begins to melt at the temperature lower than melting point. As water is soluble in amorphous region, the solubility of water is related to the partial melt of crystal. Therefore, as shown in Fig. 11, the solubility of water in lower density polyethylene is higher than that in higher density polyethylene in the range where polyethylene crystal partially melts. However, as shown in Fig. 9, at the relatively higher temperature of the first trough, the water content of the cable of lower density polyethylene is much higher than expected from the difference of the solubilities of higher and lower density polyethylene. This shows that the crystallization of polyethylene effects on the water permeation in the cable cooling process. The isothermal crystallization rate by DSC is shown in Fig. 12. Polyethylene film was fused at 130°C, then rapidly cooled to measuring temperature and kept at the temperature in DSC cell and then the time until exothermal peak was measured. From these results, in the case of the same first trough temperature, the lower density polyethylene begins to crystallize later than higher density one. So that the time of the molten state of lower density polyethylene is longer and the water content is higher than those of higher density polyethylene. Therefore, water content of the cable is influenced by both solubility of water and crystallization rate.

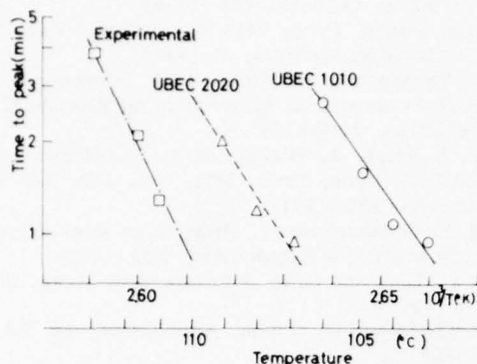


Fig. 12 Temperature dependency of isothermal crystallization by DSC

Relationship between water content and dielectric loss

To elucidate the relationship between the water content and the dielectric loss of polyethylene, the dielectric loss of remolded plaque of the model cable was measured at 30 MHz. The relationship between water content and dielectric loss is shown in Fig. 13. The dielectric loss increased linearly with the water content. On the same manufacturing condition, the water content of higher density polyethylene is less. But the dielectric loss increase at the same water content is larger than those of lower density polyethylene. Therefore, the cable manufacturing condition which minimizes the increase of dielectric loss by water should be emphasized for the higher density polyethylene. As shown in Fig. 13, higher extrusion temperature increased the dielectric loss to a large extent. From the result, lower extrusion temperature is recommendable because the increase of dielectric loss is low at the same water content. As described above, the increase of dielectric loss by remaining water is not simple and it is different with the types of polyethylene and manufacturing conditions.

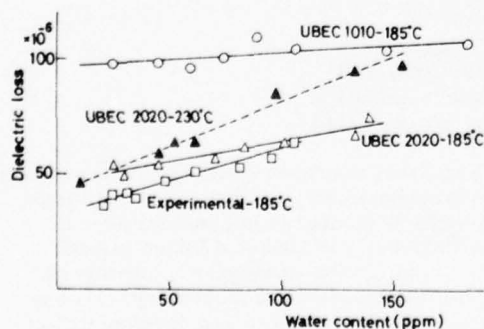


Fig. 13 Relationship between water content and dielectric loss at 23°C, 30 MHz of model cables

When the cable is cooled to room temperature, the water which permeates and diffuses into polyethylene at relatively high temperature in the cable manufacturing process remains more than the solubility of polyethylene at room temperature. As all of these remaining water cannot be soluble in the amorphous region, water is supposed to deposit in the polyethylene. The study of the shape of the remaining water has been already started.⁸⁾ The different shapes of the remaining water are supposed to give different effects on dielectric loss of polyethylene. The dielectric loss increase by two different water absorption methods is shown in Fig. 14. The dielectric loss increase by these two methods gives different tendency. The difference of the effect of remaining water suggests that the states of water in these two samples of polyethylene are different.

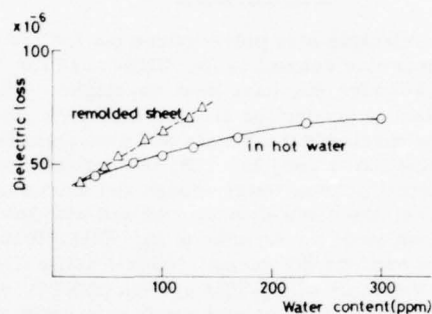


Fig. 14 Relationship between water content and dielectric loss at 23°C, 30 MHz by different absorption method

Void formation

For the optimum cable manufacturing condition, not only the water content but the gripping force or void formation should be considered. The void formed in the insulation of the model cable was observed. The relationship between void formation and the first trough temperature is shown in Fig. 15. The results of model cable may be slightly different from commercial cable manufacturing conditions. Therefore, the void formation influenced by the first trough temperature might be a little different. But the lowest temperature of the first trough to have void free cable is supposed to be between the void forming and void free temperature shown in Fig. 15. In fact, these temperature range shows the good coincidence to the result of the investigation of the optimum manufacturing condition by the simulation model.

Temperature(°C)	80	85	90	95
UBEC 1010				
UBEC 2020			Voidfree	
Experimental	Void			

Fig. 15 Relationship between void formation and first trough temperature. Extrusion temperature is 185°C

CONCLUSION

Low dielectric loss polyethylene for the insulation of submarine coaxial cable, UBEC1010 for SF and UBEC2020 for SG, have been developed. They are excellent in properties such as dielectric properties and mechanical strength and also their level of contamination is very low. By the optimum manufacturing conditions of lower trough and extrusion temperature, the cable without void and with low dielectric loss could be manufactured. UBEC1010 was supplied to produce the second Trans-Pacific Cable (TPC-2), the cable of CS-36M system of NTT, etc. UBEC2020 for SG system was supplied to produce the sixth Trans-Atlantic Telephone Cable (TAT-6).

REFERENCES

- (1) S. Matsuoka and L.D. Loan, *Plastics and Polymers*, October, 188 (1975)
- (2) J.H. Daane, *Proc. 24th International Wire and Cable Symposium*, 75 (1975)
- (3) K. Yamaguchi, H. Kishi and T. Nagasawa *IEEE International Symposium on Electrical Insulation*, 60 (1976)
- (4) W. Reddish, A. Bishop, K.A. Buckingham and P.J. Hyde, *Proc. IEE*, Vol. 118, No. 1, January, 255 (1971)
- (5) M.T. O'Shaughnessy, *Proc. 21st International Wire and Cable Symposium*, 320 (1972)
- (6) G.L. Link and G.E. Johnson, *Nat. Acad. Sci.*, 376 (1973)
- (7) S. Ohata and C. Okada, *Automation*, 15, 33 (1970)
- (8) H.E. Bair and G.E. Johnson, Private communication



Hidehiro Kishi
UBE Industries, Ltd.
8-1, Goi Migamikaigan
Ichihara, Chiba, Japan

Hidehiro Kishi is presently a manager of polybutadiene production department. He received a B.S. degree in applied chemistry from Kyushu University in 1959 and joined in UBE Industries, Ltd. in the same year. Initially he worked at Ube fertilizer plant. He had been engaged in the research and development of high pressure polyethylene and polypropylene since 1963 to 1976.



Yasuki Yamazaki
UBE Industries, Ltd.
8-1, Goi Minamikaigan
Ichihara, Chiba, Japan

Yasuki Yamazaki is presently an assistant manager of technical department, petrochemicals division. He received a B.S. degree in chemistry from Shizuoka University in 1963 and joined in UBE Industries, Ltd. in the same year. Initially he worked at plastics research laboratory. He has been engaged in the research and development of high pressure polyethylene and polypropylene since 1967.

Toshio Nagasawa
UBE Industries, Ltd.
3-10, Nakamiya Kitamachi
Hirakata, Osaka, Japan

Toshio Nagasawa is presently a chief researcher of the plastics research laboratory. He received a B.S. in 1962, a M.S. in 1964, and Ph. D in 1968 in Engineering from Kyoto University. From 1969 to 1971, he joined the polymer division of National Bureau of Standards in Washington DC. U. S. A., as a polymer physicist. He has been a member of the plastics research laboratory since 1971.



Hideaki Takashima
UBE Industries, Ltd.
8-1, Goi Minamikaigan
Ichihara, Chiba, Japan

Hideaki Takashima is presently a staff engineer of technical department, petrochemicals division. He received a B.S. degree in applied chemistry from Nagoya University in 1965. He joined UBE Industries in the same year, and has been engaged in research and development of high pressure polyethylene and polypropylene.

Hirokazu Fujita
UBE Industries, Ltd.
7-2, Kasumigaseki 3-chome
Chiyoda-ku, Tokyo, Japan

Hirokazu Fujita is presently a staff engineer of technical department, petrochemicals division. He received a B.S. degree in chemical engineering from Shizuoka University in 1967. He joined UBE Industries, Ltd. in the same year, and has been engaged in research and development of high pressure polyethylene and polypropylene.



Iwao Tsurutani
UBE Industries, Ltd.
8-1, Goi Minamikaigan
Ichihara, Chiba, Japan

Iwao Tsurutani is presently a staff engineer of technical department, petrochemicals division. He received a B.S. degree in petrochemistry from Kyoto University in 1971. He joined UBE Industries, Ltd. in the same year, and has been engaged in research and development of high pressure polyethylene.

ENERGY SAVINGS AND PRODUCT COST EFFICIENCY

THROUGH THERMOPLASTIC ELASTOMERS

by

William H. Korcz
Westhollow Research Center
Shell Development Company
Houston, Texas

Abstract

Processing cost and energy expenditure are evaluated in several specific end-use wire types where thermoplastic elastomers may compete directly with thermoset rubbers and thermoset plastics. Energy for fabrication is treated and compared in these examples, as is general cost applicable to each fabrication mode, considering insulating and jacketing materials utilized. A fundamental property of all material for wire and cable is cost contribution to the finished product, from conductor to printing ink. Insulation and jacketing materials meeting performance requirements for most applications are chosen largely on the basis of pound-volume cost. However, coupled to each thermally cured insulation or jacket material is a processing cost and energy expenditure, dependent upon each specific wire and cable type, CV equipment available and running rate. With the awareness of high energy cost, of projected higher cost and of a potentially energy short society, efficient processing and efficient processing energy utilization to produce acceptable wire and cable products become important planning and economic variables. BTU input is as much a cost in the final wire product as the price paid for basic materials requiring a cure. This BTU input is examined for three specific wire types.

Scope: Product Cost Efficiency through Thermoplastic Elastomers

Wire and cable costs, processing and materials, are economic matters. Treatments of comparative economics for wire and cable fabrication on a plastic extrusion line versus a CV line have been made in the past; the scope of those treatments have been complex and have attempted to be all encompassing. To be all encompassing, the generalizations and assumptions have been necessarily so broad (capital and labor estimates), and so limited (one specific wire type) that the bottom line economics is representative of

- a) no one wire and cable company/product
- b) all wire and cable companies/products

both at the same time. This absurdity results in an economic example of limited utility.

Why is this so? As each wire and cable businessman knows, his raw materials cost, his overhead, his labor, his capital amortization, his line maintenance, his plant space, his equipment utilization, his scrap rate, his product mix, his running rates are probably unique to his company, and virtually unknown in the sense he's not able to dissect the combination of numbers which represent one wire line, or the exact costs for one wire type. While comparisons of this nature are instructive, the result can be misleading. In the real world, one extrusion line, or product line isn't usually a separate entity; it is part of a whole

line of production equipment, and as such, is "lumped in" with the rest. Singling out a separate entity and showing its economics simply doesn't have meaning within this grouped overhead framework.

Most everyone is happy with the preceding assessment of the economic system as it prevails. Accepting this economic viewpoint does, however, have its combination of weaknesses and dangers because it says only that the roots of economic incentive to use thermoplastic elastomer as a substitute for CV cured rubber is difficult to quantify, universally, for all wire and cable people and all wire and cable types in a single, overall view. This does not weaken the total economic incentive to substitute thermoplastic elastomer for thermally cured rubber; it simply points out that the degree and extent of this incentive will vary from one wire and cable company to another. Intuitively, we know real overall economic advantages exist, in less labor, lower capital expenditure, and in faster production rates for TPE's. The important conclusion that is reached is that assessment of these advantages must be made on an individual basis, company by company, to seriously quantify the economic incentive, the product cost efficiency aspect and option, that is inherent in the concept of thermoplastic elastomer. Any attempt to "average" everyone and say it applies to all, is folly. It's as serious a mistake, however, to dismiss the entire overview without a realistic in-house look at the advantages offered in lower labor costs, lower capital expenditure for extrusion equipment and faster rates possible through thermoplastic elastomers.

These thoughts are summarized in Figure 1, with the notable exception of capital savings inherent in a plastic line versus a CV line. You'll notice there are no numbers attached to any of the relative processing costs, because they're your costs.

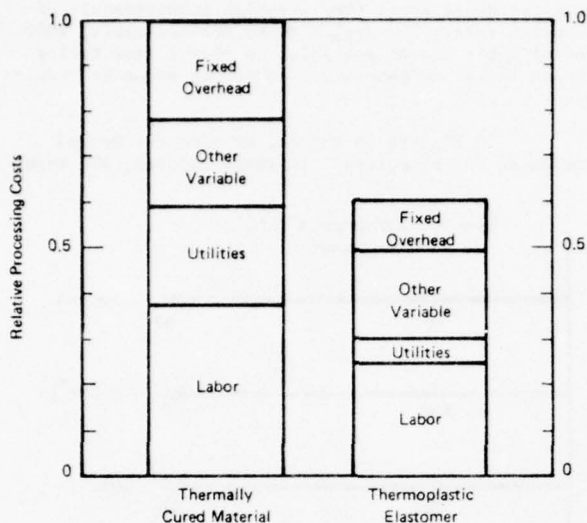


Figure 1. Overall Processing Economics

Labor costs are lower to process thermoplastic vs thermally cured rubber, either from a manpower assignment basis to keep the lines running, maintenance, or labor translated to a labor-dollars per thousand feet due to slower thermally cured rubber processing rates vs thermoplastic rubber. Fixed overhead is less for thermoplastic rubber; no capital expenditure for a steam generator, or steam tube is required. Does it apply to me? What are the savings? These are important questions, with unique answers for each wire and cable manufacturer addressing them, especially if he's under capacity or finding it necessary to expand production in certain product lines.

This is an extensive qualification of the economic scope, but necessary and realistic. Universally, real advantage exists to using TPE's. We're not capable of combining and quantifying the full economic scope of thermoplastic elastomers as they fit the wire and cable industry; however, we suggest each of you work through the exercise in-house and discover what the choice, and option, is worth.

Among all of these variables, there is one that is universally applicable: that small part of the energy and economic process concerned with the supply of BTU's necessary to make CV steam, and the amount of BTU's required to cure each pound of extrudate. It's a simple series of multiplications to get to dollars and cents from BTU's. This limited treatment represents the first step in viewing the whole economic picture, and is but a small contributor to the overall savings achievable through thermoplastic elastomers. Additional steps must follow if we wish to determine the full economic advantage outlined within the scope.

To make this treatment useful and relevant, we've selected flexible cords, automotive primary wiring, and welding cable for the basis of our comparison. We feel ELEXAR™ Rubber, a family of thermoplastic elastomers, offers an alternative in these specific wire types. ELEXAR grades are currently being used in these constructions, are submitted to U.L. for performance testing, or have demonstrated applicability in laboratory and field trials. These materials do not require a CV cure.

The Limited Scope: Direct Savings through Thermoplastic Elastomers

The energy treatment is made in a simple manner and can serve as a working model for anyone wishing to make comparisons for various wire types within his company. If you know the amount of fuel input to your steam generator, can time its cycling with a stopwatch, know the length of your CV tube, know your fuel type (gas, oil, coal), and know the running rate of the wire product, you're in business. There are, however, several other variables to consider, and we'll address those.

Premises

In attempting to quantify the number of BTU's necessary to cure rubber product, only two inputs are necessary; knowledge of running rates and a knowledge of steam generators.

I. Running Rates

The linear speed extrusion rate of thermally cured wire insulation is generally a function of residence time required to accomplish cure in the tube. This rate varies as a function of insulation thickness, wire construction, CV tube length and choice of curing chemicals. Generally, extruder output is not rate limiting. In order to calculate the number of BTU's used per pound of extrudate going down the tube, a knowledge of running rates is essential.

With this thought in mind, a questionnaire was mailed to about forty wire and cable companies. The questionnaire explained the purpose of this paper, and asked that running rates for welding cable (2/0), flexible cords (rubber) and automotive primary wire (XLPE) be supplied, along with extruder size and CV tube length. The answers varied from company to company, but not too greatly. Data revealed in these questionnaires form the basis for extrusion rates cited in this paper.

II. Steam Generators and CV Tubes

In gathering data for steam generators and CV tubes, we queried four manufacturers and several very helpful wire and cable companies. Much like any other group of experts in their field, they didn't reach a consensus, or find universal agreement. After all, each generator, each CV line had its own combination of efficiencies and leaks, and a single BTU number applying to everyone should be viewed with some suspicion. The variability of steam generator efficiency plays an important part in determining the input BTU's required to provide steam; it's no small matter to have a good idea of efficiency when making calculations. We've been conservative in our analysis, using an 80% efficiency in making input calculations in our natural gas fired steam generator example. If your boiler is old, your efficiency may be as low as 60%. An appropriate adjustment in BTU input would be necessary in these cases. I think the energy input we've developed in our examples is probably typical of what's found in the wire and cable industry for a 200 foot CV tube, and a 400 foot CV tube, with an efficient (80%+) steam generator.

As indicated earlier, it's a simple matter to calculate a BTU input number for your CV operation, and develop a number unique to your line; you'll easily discover how efficient your particular steam generator

is, and the exact input in BTU's required to keep your CV line at temperature and pressure.

Purpose: A BTU saved is a penny earned

How many BTU's per mile of completed cable do you spend? In the final analysis, is it justifiable, economically, to choose a material solely on a pound volume cost, or are processing considerations, rates and energy input, just as important? Suppose your corporate energy czar is doing an effective job, and says, let's cut our BTU consumption by 10% this year but maintain or improve output. Or he says, our natural gas allotment has been reduced 50%; make acceptable wire product and use less natural gas. Suppose you're running at full capacity and want to expand production without further capital expenditure. Thermoplastic elastomers offer some interesting possibilities for saving BTU's and expanding capacity at the same time.

The BTU Nomograph

Figure 2 represents one part of a simple nomograph we'll use to read directly the number of BTU's expended to make automotive primary wire (XLPE), welding cable (2/0) and flexible cords (rubber).

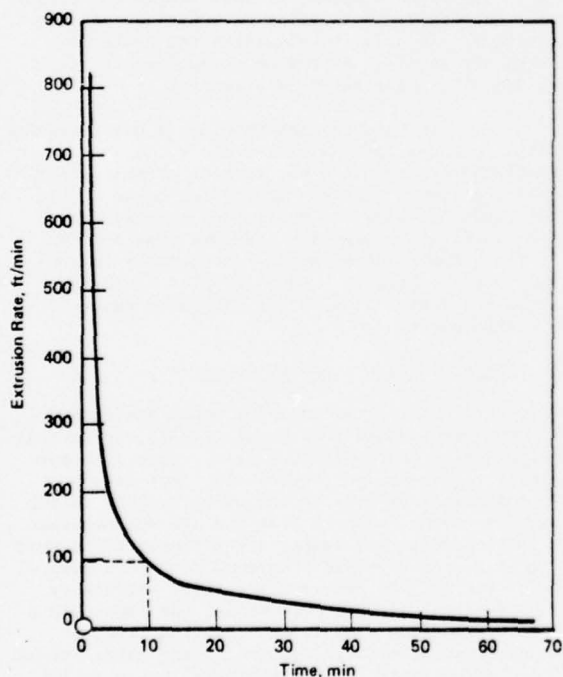
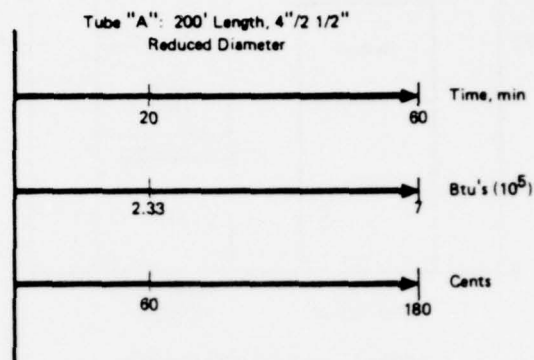


Figure 2. Production of 1000 ft of Cable

On the vertical axis in Figure 2 is running rate, feet per minute. On the horizontal axis is a minutes scale. The hyperbolic curve in the field of the graph represents the production of a 1000 foot length of cable. For example, if you're running at a rate of 100 feet per minute, it takes 10 minutes to produce 1000 feet of cable. Selecting any point on the running rate axis gives a coordinate for the real time necessary to produce 1000 feet of cable. This should not be confused with residence time in the tube to accomplish curing. The CV tube and steam generator do not care

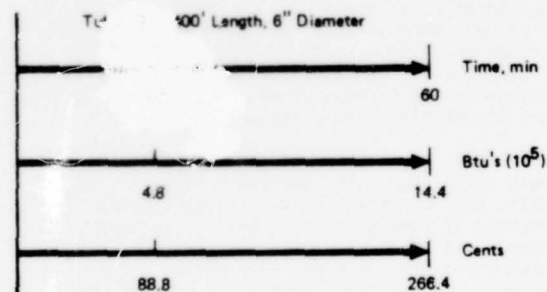
about residence time; they function independently of extrusion rate. The real time to produce cable, 1000 feet of cable in our analysis, is on the same timing line as the steam generator, producing steam by burning fuel.

In Figures 3A and 3B, we have the second portion of our nomograph. In these figures, BTU input



Basis: 5 gal of #2 Diesel Fuel Oil @ 36¢/gal.,
140,000 Btu/gal

Figure 3A. 250 psi Equilibrium Steam



Basis: 1000 lb of Steam/hr
Natural Gas Fired Generator

Figure 3B. 250 psi Equilibrium Steam

to a steam generator is related to a time line. For a period of 60 minutes, we find (at the right end point of the time line) the number of BTU's required to fire a steam generator just sufficiently to maintain the CV line with 250 psi steam, and cycling at equilibrium. This BTU input varies as a function of tube length and diameter, and heating fuel utilized.

The example used for the 200 foot CV tube, Figure 3A, is taken over a year's time production experience, and reflects actual measurements for a CV line and oil fired steam generator in place. Five gallons of #2 diesel fuel oil is consumed per hour. Armed with the BTU content of #2 diesel fuel oil (approximately 140,000 gross BTU/gallon), it's a simple matter to calculate the number of BTU's used to maintain equilibrium conditions in tube A.

Another expert source indicated 1000 lbs of steam per hour was required to maintain equilibrium conditions for a 400 foot, 6 inch diameter CV tube (Figure 3B). Using steam tables, and assuming an 80% efficient gas fired steam generator, this steam demand is translated into BTU input required to maintain equilibrium. This demand is easily translated into cubic feet of natural gas assuming 1000 BTU/cubic foot.

Using the current price of #2 diesel fuel oil (36¢/gallon, taxes not included), and the price of 1975 intrastate natural gas (185¢/mcf),¹⁾ BTU's may be converted directly to dollars and cents. This is done in Figures 3A and 3B. If your costs for oil and gas differ significantly from these, it is a simple matter to substitute your cost, and make appropriate calculations with your fuel prices.

If we combine Figures 2, 3A and 3B to produce Figure 4, we have a nomograph that has some utility and universal validity to calculate the BTU input required to make a cured rubber wire or cable product.

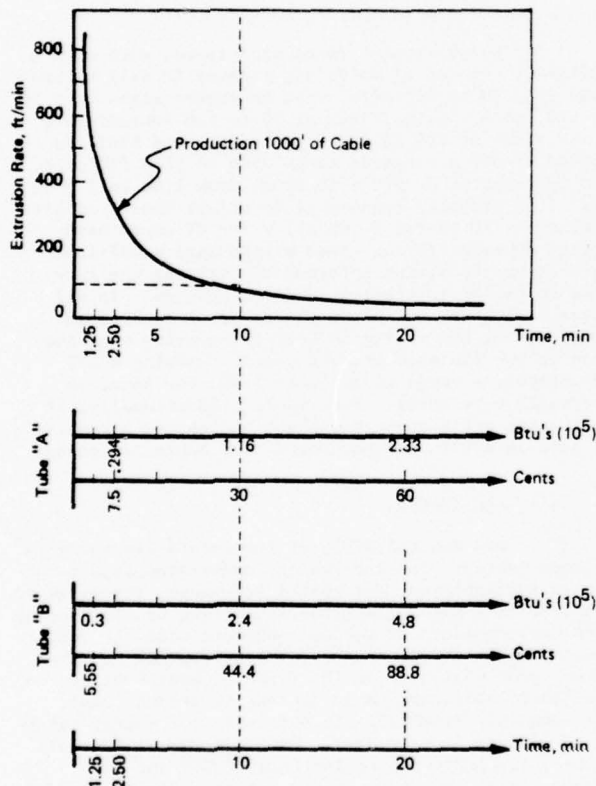


Figure 4. Btu Nomograph

For example, suppose we have a CV cured product we run at 100 feet/minute. To make 1000 feet of product requires 10 minutes; for the 10 minute period the steam generator produces 250 psi steam. Following the dotted 10 minute vertical time line in Figure 4, we find 1.16×10^5 BTU's were consumed at a cost of 30¢ for tube "A". For tube "B", 2.4×10^5 BTU's were consumed at a cost of 44.4¢. This is the energy fee paid to produce 1000 feet of cable in either tube A or B, respectively, extruding insulated wire at 100 feet/minute.

¹⁾ Source DRI '76 Energy outlook.

Specific Examples/Calculations

Based upon extrusion rates volunteered in the questionnaire, and our knowledge of BTU's to supply steam we can now make calculations using specific wire constructions as examples.

I. Automotive Primary Wire

Detailed examination:

Conductor: 16 AWG stranded
Wall: 32 mil
Insulation: XLPE
Sp. Gr.: 1.38
Insulation weight/M': 5.4 lbs

Case A: Tube "B", 800 feet/minute extrusion rate

From Figure 4, 1.25 minutes are required. Tracing the vertical time line at 1.25 minutes, we find 30,000 BTU's were necessary to make 1000 feet of cable, at a cost of 5.55¢.

Calculating BTU's per pound: $30,000 \text{ BTU's} / 5.4 \text{ lbs} = 5560 \text{ BTU's/lb}$.

Calculating cents per pound: $5.55¢ / 5.4 \text{ lbs} = 1.03¢/\text{lb}$.

Additional information: insulation residence time in tube is 0.5 minutes.

Case B: Tube "A", 400 feet/minute extrusion rate

From Figure 4, 2.5 minutes are required. Tracing the vertical time line at 2.5 minutes, we find 29,400 BTU's were necessary to make 1000 feet of cable, at a cost of 7.5¢.

Calculating BTU's per pound: $29,400 \text{ BTU's} / 5.4 \text{ lbs} = 5440 \text{ BTU's/lb}$.

Calculating cents per pound: $7.5¢ / 5.4 \text{ lbs} = 1.39¢/\text{lb}$.

Additional information: insulation residence time in CV tube is 0.5 minutes.

If insulation residence times of 1 minute in the CV tube is more typical to accomplish cure, then BTU's/lb and cents/lb numbers are doubled in both cases.

II. Welding Cable

Detailed examination:

Conductor: 2/0, stranded
Wall: 100 mil
Jacket: Polychloroprene
Sp. Gr.: 1.2
Insulation weight/M' = 82 lbs

Case A: Tube "B", 50 feet/minute extrusion rate

From Figure 4, 20 minutes are required. Tracing the 20 minute time line, 480,000 BTU's are required to make 1000 feet of cable, at a cost of 88.8¢.

BTU's per pound: 480,000 BTU's/82 lbs =
5850 BTU's/lb.

Cents per pound: 88.8¢/82 lbs = 1.08¢/lb.

Residence time: 8 minutes.

III. Flexible Cords

Detailed examination: SJ, 16/3

Singles

Conductor: 16 AWG, stranded
Wall: 30 mil
Insulation: SBR
Sp. Gr.: 1.25
Insulation weight/M' = 4.44 lbs.

Jacket

Conductor: 3 cabled singles + filler
Wall: 30 mil
Jacket: SBR
Sp. Gr.: 1.25
Jacket weight/M' = 16.3 lbs.

Case A: Tube "A"

This is a composite construction. We will consider an extrusion rate of 500 fpm for the singles, and 200 fpm for jacketing the cord.

Singles

2 minutes are required, representing 23,300 BTU, at a cost of 6¢ for each 1000 foot length of insulated single:

BTU's per pound: 23,300 BTU's/4.44 lbs. =
5250 BTU's/lb.

Cents per pound: 6¢/4.44 lbs. = 1.35¢/lb.

Jacket

5 minutes are required, representing 58,300 BTU's at a cost of 15¢ for 1000 feet of completed cord:

BTU's per pound: 58,300 BTU's/16.3 lbs. =
3580 BTU's/lb.

Cents per pound: 15¢/16.3 lbs. = .92¢/lb.

Treatment of only these wire types in our analyses should not be interpreted as the total scope of thermoplastic elastomers as suitable replacements for thermally cured insulations and jackets. We could have more completely included comparisons for vertical and horizontal flame retardant 125°C appliance wiring materials on smaller gauge wires. ELEXAR grades for these applications have been extruded, and have been submitted to U.L. for performance testing. Similarly, 125°C fixture wire submittals are being performance tested at U.L., with ELEXAR Rubber as the insulating material. Battery cable and trailer cable offer similar bases for comparison, but have not been treated within this paper.

Summary

I. The Present

Working with a few basic assumptions for extrusion rates, and several specific wire types, our calculations are summarized in Table I.

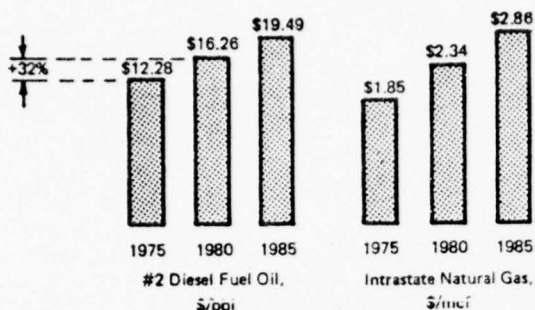
TABLE I

Wire Type	CV Tube	Extrusion Rate, ft/min	Residence Time, min	BTU's/ 1000 ft
APW (XLPE)	"B"	800	0.5	30,000
	"A"	400	0.5	29,400
Welding Cable	"B"	50	8.0	480,000
Flexible Cords, SJ				
Singles	"A"	500	0.4	23,330
Jacket	"A"	200	1.0	58,300

We've treated three wire types, each with a different insulating material, ranging in wall thickness from 30 to 100 mils, with conductor sizes from 16 to 2/0, with running rates of 50 to 800 feet/minute, on CV lines of 200 to 400 foot lengths and find the spread of BTU's expended to be 3580 to 5850 BTU's/lb, and the cost of CV BTU's to range from 1.0¢ to 1.50¢/lb. It's probably reasonable to adjust these figures upwards by 10 to 20% if we allow for CV steam used during non-equilibrium steam maintenance conditions, such as breaks/string up/blowdown, warming the tube, time to center insulation, and job changes. In all these instances, the steam generator is running and using BTU's, and making an energy intensive contribution to the finished product cost. Choosing a 15% adjustment, a range of 1.15¢ to 1.70¢ per pound to thermally cure appears reasonable. Additionally, if your rates are slower than those indicated, a penalty is paid in BTU's used per pound, and cents per pound.

II. The Future

Gas and oil BTU's of the future are going to be more costly. The uncertainty associated with natural gas availability, and restricted usage, forces us to consider each possibility for minimizing or eliminating this fuel choice. If you're concerned with the longer range energy outlook and energy conservation, as they affect your decisions on the types of equipment put on the floor, and energy contribution to product cost, then consider Figure 5. In the next four years, natural gas prices (intrastate), and No. 2 diesel fuel oil prices, are projected to increase by 26% and 32%, respectively. In 1985, prices for these fuels will be 55% to 59% higher than today's, respectively. These projections are those of Data Research Incorporated (June 1976) and are based upon current dollars. In Figure 6, we've applied these projected increases in energy costs to our cost-savings per pound analysis. In 1985, the range will be 1.8¢ to 2.70¢ per pound to thermally cure.



Source: Data Research Incorporation
Basis: All Prices Current Dollars

Figure 5. Predicted Trends in Fuel Prices

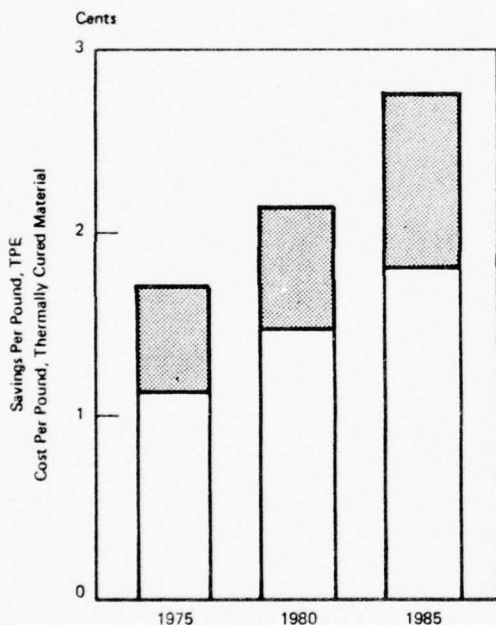


Figure 6. Savings/Cost Projections as a Function of Increasing Energy Costs

Conclusions

An overall energy savings perspective can be developed if we consider the energy intensive nature of one CV line. A 400 foot CV line making thermally cured product two shifts a day requires 40,000 gallons of fuel oil per year, with a steam generator operating at 80% efficiency. A 60% efficient generator will require more than 52,000 gallons! Add to that another energy expenditure for non-equilibrium steam usage conditions in warming a cold CV tube, or blowing down, and the total increases again. This magnitude of energy expenditure represents the direct saving possible through thermoplastic elastomer.

Extending this cost/savings concept, if additional extruder output is available, and the rate limiting CV tube is now out of the picture, then opportunities for faster extrusion rates are possible with thermoplastic elastomer. How do faster extrusion rates contribute to overall product cost efficiency? If the extrusion rate is doubled with thermoplastic elastomer, for every eight hour shift necessary to thermally cure a wire product, only four hours are now required to make equal production. The remaining four hours are available for additional production. This is added capacity at no additional capital expenditure. Secondly, the labor cost per 1000 feet of wire has been cut in half, assuming equal manpower allotment to either a CV or plastic line.

What is the magnitude of these savings? Our scope says there is no universally acceptable answer which will apply to all wire and cable companies. However, for the obvious exception, the case in which it is necessary for a wire and cable company to expand production capacity by adding more CV lines, a definite and real option is provided by thermoplastic elastomer: The option to put plastic extrusion equipment on the floor instead of CV equipment. This difference might be a \$100,000 capital expenditure savings.

Thus, a hierarchy of product cost efficiencies are established for thermoplastic elastomers, starting with energy savings:

- 1) BTU's/pound cost for thermally cured insulations and jackets = cents/pound savings for thermoplastic elastomers.
- 2) Cost efficiencies in labor and added capacity through faster extrusion and production rates for thermoplastic elastomer.
- 3) Cost efficiencies in capital expenditure provided by the option to choose a plastic extrusion line rather than a CV line to expand capacity.

The sum total will always include energy cost savings, projected to rise significantly in the next ten years. The magnitude of other cost efficiencies will vary for each wire and cable company, and will depend upon a realistic, in-house overall economic assessment to quantify the advantage found in the option provided by thermoplastic elastomers to replace thermally cured materials.

We'll close modestly: One million pounds of thermoplastic elastomer substituted for one million pounds of thermally cured material represents an energy saving of about 38,000 gallons of fuel oil. In a world of fuel allocations, rising fuel prices, and a necessity to conserve energy, thermoplastic elastomers make sense.

Acknowledgments

The author wishes to express a personal thanks to the many wire and cable people providing assistance in preparing this paper. Your candid response to the questionnaire was appreciated, considered and your confidentiality is preserved.



William H. Korcz
Shell Development Company
Westhollow Research Center
P. O. Box 1380
Houston, Texas 77001

Bill Korcz received a BS in Chemistry from Elmhurst College in 1975. Prior to joining Shell Development Company in March of 1976, he learned the wire and cable business for seven years at Belden Corporation, Technical Research Center. Work at Belden was focused on new materials research for wire and cable. Bill is a member of ASTM, D09.19, formerly D11.35, and is active in developing better flame tests for wire and cable. Bill also serves on the technical program committee, Electrical & Electronic Division of S.P.E. Activity with Shell Development Company, as a Senior Research Engineer, is split between technical service and various R&D programs in the development of ELEXARTM Rubbers for wire and cable applications.

CONTAMINANT TRACE GAS TESTING OF LEAD-STABILIZED POLYMERIC COMPOUNDS

J. P. Franey and T. E. Graedel
Bell Laboratories
Murray Hill, New Jersey 07974

Two alternative formulations of a PVC compound destined for use in telephone retractile cords have been tested for resistance to discoloration in corrosive environments. The test atmospheres included H_2S , NO_2 , and SO_2 gases in moist air, at concentrations 2-68 times those of severe field environments. Gas concentrations were continuously monitored throughout the tests. Samples formulated with a liquid Ba-Cd-Zn octoate stabilizer showed no significant color degradation. Samples stabilized with tribasic lead sulfate showed significant discoloration, the total color differences exceeding reasonable tolerances by factors of 2.6-5.9. The studies establish the color stability of the liquid stabilizer and imply that lead-stabilized polymers without further protective treatment are unsuitable for color-sensitive applications in severely contaminated field atmospheres.

Introduction

Polymer formulations that utilize lead compounds as stabilizers are widely used throughout the communications industry. These formulations generally demonstrate good process stability characteristics while also satisfying end-product performance criteria. The suitability of such formulations for applications demanding color stability has been uncertain, however, because of the possibility of color modification resulting from atmospheric contaminant interactions.

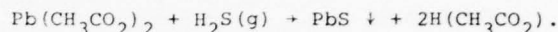
This paper reports the results of controlled exposures of polymers stabilized with leaded and unleaded compounds to a simulated atmosphere containing several corrosive gases. The techniques for generating and monitoring such test atmospheres were developed as part of this study, and are described below. The formulation of the polymers and the design of the exposure tests is discussed next. In the final section, the results are presented and conclusions drawn.

Generation and Monitoring of Mixed Gas Atmospheres

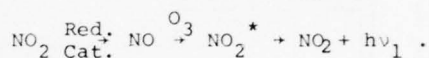
The experimental apparatus utilized in these tests is shown schematically in Figure 1. Within the environmental chamber the carrier atmosphere of 1:4 $O_2:N_2$ is generated from laboratory pressurized gas supplies, and maintained by a pressure switch feed mechanism designed to ensure a slight overpressure within the chamber. The desired relative humidity is achieved by controlled boiling of deionized water into the chamber. The corrosive trace gases are injected into the chamber through variable leak valves, followed by timed solenoids.

Concentration measurements of each of the trace gases are made continuously, utilizing techniques that are specific to

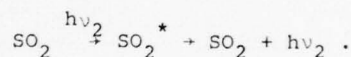
the gas in question. Hydrogen sulfide is detected by its reaction with lead acetate-impregnated filter tape:



The resulting lead sulfide precipitate is monitored by light transmission. Nitrogen dioxide is monitored by passing the air sample over a reducing catalyst, reacting the resultant nitric oxide with ozone, and monitoring the light intensity of the chemiluminescent reaction:



Sulfur dioxide is detected by pulsed fluorescence techniques:



The measured concentrations are recorded by strip chart and digital encoding techniques, and reduced and plotted by suitable computer codes.

The experimental apparatus shown on Figure 1 was designed to generate corrosive trace gases in concentrations of ~50-500 ppbv. These concentrations are readily detectable by the techniques described above, and provide a range of ~1-10 times typical atmospheric concentrations for NO_2 and SO_2 . The atmospheric concentrations of H_2S are not regularly measured and specification of typical values is thus uncertain. We discuss this point more fully below.

As gas samples are withdrawn from the chamber by the sampling instruments, corrosive and carrier gases are added at rates determined by the variable leak valve/solenoid control settings. Induction times of several days are found necessary to achieve stable concentrations of the trace gases. These effects have been determined to be consequences of adsorption onto solid surfaces and absorption into aqueous surface films. The sorption processes vary in magnitude with each of the trace gases used. Because of these effects, and because of the gas phase reactions that occur among certain trace species,¹ it appears impossible to accurately specify gas concentrations in laboratory environmental testing unless continuous measurement techniques are utilized.

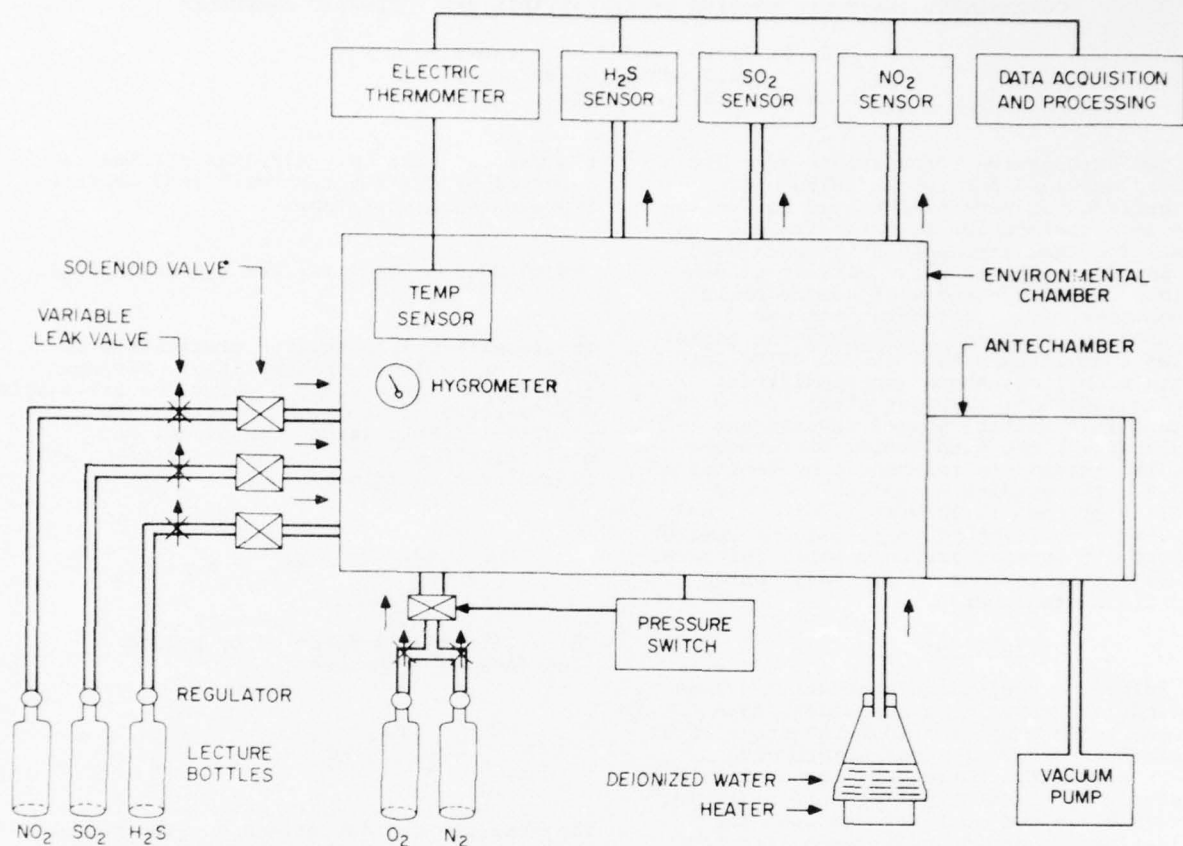
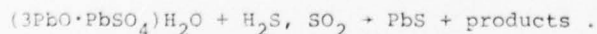


Figure 1. Schematic diagram of the experimental apparatus.

Polymer Formulations

The polymer formulations tested were alternates developed for possible use as telephone retractile cord jacket material. Because this application places the polymer in a great diversity of field environments, because it is readily visible to the user, and because the coil cord is color-matched to the telephone housing, color stability is a vital property.

The two test formulations utilize identical compositions of PVC resin, plasticizers, and fillers. They differ only in the stabilizer used, Type Pb PVC being stabilized with solid tribasic lead sulfate and Type BCZ PVC being stabilized with a liquid mixture containing barium-cadmium-zinc octoates and alkyl-aryl phosphites. The principal atmospheric degradation is expected to be the sulfiding of the tribasic lead sulfate to produce lead sulfide, a black metallic solid:



(The process here is presumably similar to that responsible for the darkening of lead-containing paints by H_2S .²)

The two polymer formulations were prepared in sheets of ~3 mm thickness, and 10x10 cm samples cut and labeled. The samples were colored an identical "moss green". The test sequence involved generation and stabilization of trace gas concentrations in the environmental chamber, insertion of samples of each of the polymer formulations, active monitoring of the chamber environment during exposure, and removal of the test samples for analysis. Control samples were maintained outside the chamber for comparison with the test samples.

Results and Discussion

Three pairs of samples were tested under a range of trace gas concentrations and exposure times. The test periods and average trace gas concentrations are indicated on Table I. The relative humidity was $90\% \pm 5\%$ throughout. Trace gas concentrations in the sub-ppm regime are difficult to control precisely; Figure 2 demonstrates their typical concentration behavior (in this case for the second of the exposure tests). These variations reemphasize the importance of continuous monitoring of test atmospheres during atmospheric exposure experiments.

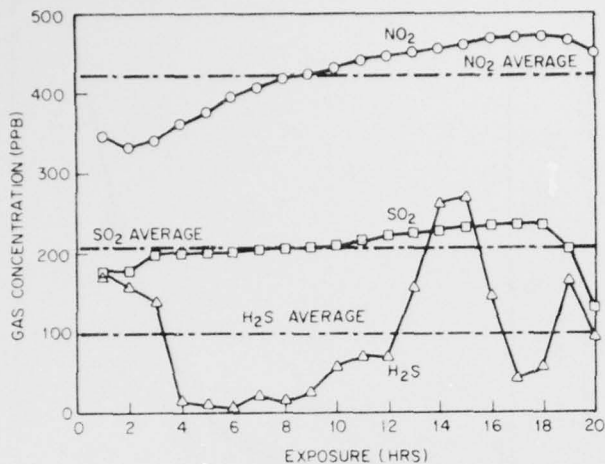


Figure 2. Measured concentrations of trace contaminant gases in the environmental chamber during Test 2.

The gas concentrations of Table I can be compared with atmospheric conditions by examining the distributions of air quality data measured by various governmental agencies at several hundred field locations throughout the United States.³ These distributions are shown on Figure 3 for NO₂ and on Figure 4 for SO₂. From the figures are derived and listed on Table I "atmospheric upper limit" (AUL) values. The values are exceeded by only about one percent of all field locations, and represent a reasonable "mean high water mark" for design and test purposes. H₂S is seldom measured at air quality monitoring sites and its AUL is based on much less data. The H₂S AUL is therefore considerably less well established than are those for NO₂ and SO₂.

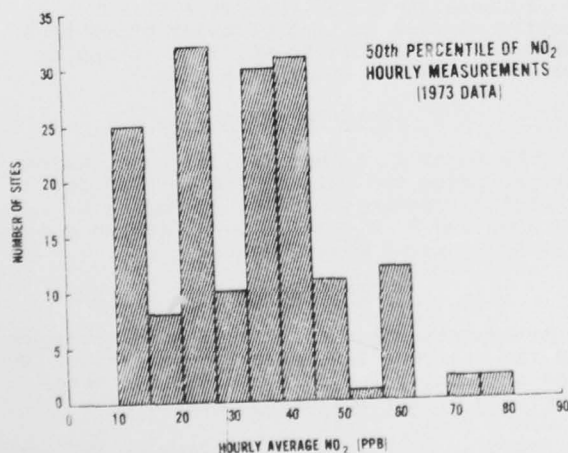


Figure 3. The distribution of 50th percentiles of NO₂ hourly measurements at air quality monitoring sites within the United States.³

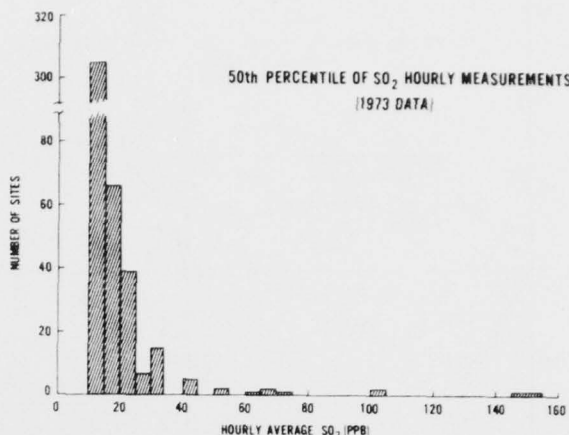


Figure 4. The distribution of 50th percentiles of SO₂ hourly measurements at air quality monitoring sites within the United States.³

The multiplication in gas phase concentrations of NO₂ and SO₂ over field conditions is small, ranging between about 2-6 for the three tests. For H₂S the factor is larger, with a range of ~10-68.

Visual degradation of the Type Pb PVC occurred on each of the three tests, as noted by comparison with the unexposed samples. No visual effects were seen on the Type BCZ PVC samples. To verify this result, the color changes were analyzed quantitatively on a Diano/Hardy visible light spectrophotometer configured for color measurements. The results of these measurements are given in Table II in FMC II^{4,5} color difference parameters. In this system, equal intervals in the total color parameter ΔE represent similar visual color intervals. The total color ΔE is defined by

$$\Delta E = \sqrt{\Delta L^2 + \Delta C_{rg}^2 + \Delta C_{yb}^2},$$

and the FMC II color parameters ΔL , ΔC_{rg} , ΔC_{yb} are related to the measured tristimulus values X, Y, Z by a transformation matrix. For convenience, a color hue and saturation plane is defined by parameters ΔC_{rg} and ΔC_{yb} ; movement in this plane is expressed in units of ΔC , where

$$\Delta C = \sqrt{\Delta C_{rg}^2 + \Delta C_{yb}^2}.$$

The color differences resulting from the exposure tests are placed in perspective on Figure 5, which shows the total color change (ΔE) vectors for the samples as plotted in the ΔL - ΔC plane. A trained color specialist can discern a total color change of $\Delta E \approx 1$ under perfect conditions. Any change in total color less than this is of no practical significance. Perception of color differences by the average person is generally less

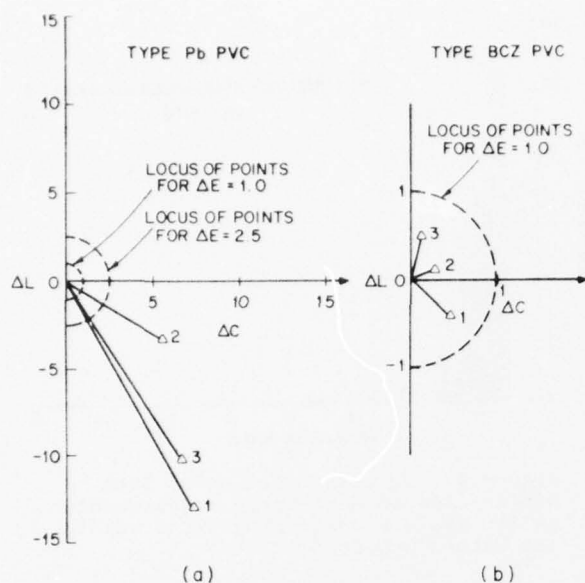


Figure 5. Total color changes ΔE for the test samples, plotted in the ΔL - ΔC plane. (a) Type Pb PVC samples; (b) Type BCZ PVC samples.

acute. The raw polymeric material for Bell System telephone housings is allowed a maximum color difference of $\Delta E = 2.5$. Since our test samples are for telephone cord use in proximity to the housings, a tolerance of $\Delta E \leq 2.5$ is conservative. The loci for $\Delta E = 1$ and $\Delta E = 2.5$ are plotted on Figure 5. It is apparent that the Type BCZ PVC samples showed negligible color differences. Those of the Type Pb PVC were substantial, exceeding the ΔE requirement by factors of 2.6-5.9. These color differences would readily be noticed by people without training in color matching.

A complete analysis of the physical and chemical processes involved in creating the observed color differences would require more extensive studies than are described here. Some insight may be gained, however, by examining the color difference parameters as a function of gas exposure. For the moss green polymer samples tested, the change in ΔC_{rg} is most meaningful.⁴ Since H_2S is the most likely active contaminant, we plot on Figure 6 the average H_2S concentration for each of the three tests as a function of ΔC_{rg} . The relationship is seen to be monotonic but nonlinear. This suggests that the color change process is limited by the reaction of diffusing species within the polymeric compound rather than by diffusion kinetics in the gas phase. This limitation is presumably a consequence of the rapid sulfiding of all available lead within reasonable sample diffusion depths.

Since the details of the chemical processes responsible for the color degradation have not been determined, we are unable to relate the exposures of Table I to actual field lifetimes. The acceleration

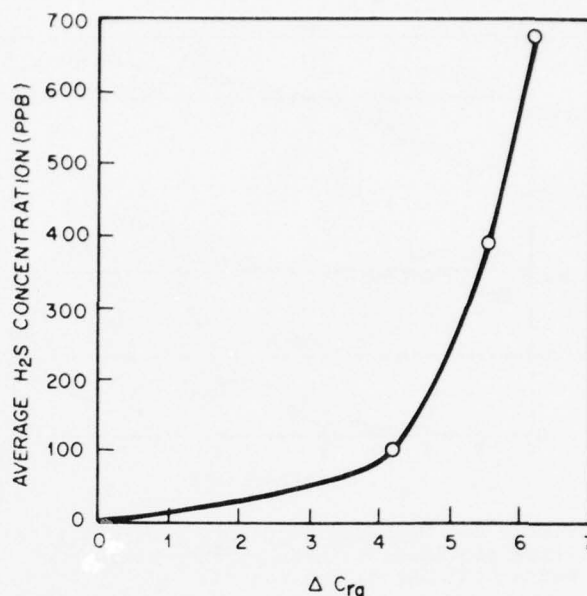


Figure 6. "Red-green" color change (plotted as the FMC II parameter ΔC_{rg}) for the Type Pb PVC samples as a function of average hydrogen sulfide concentration.

over AUL field conditions was not extreme, particularly in the case of the second test. That test involved less than one full day and concentration multipliers of ten or less, yet substantial color effects were still noted. It is clear that diffusion of sulfur gases into the polymer bulk, followed by subsequent sulfiding of the lead stabilizer, will produce readily detectable color changes in contaminated field environments. The Type BCZ PVC showed no significant color degradation. The results indicate that Type BCZ PVC is the more environmentally rugged of the two formulations, and that Type Pb PVC will require surface coating or other protective measures if it is to be utilized in applications requiring color stability.

Acknowledgements

We thank J. J. Mottine and P. C. Warren for providing the polymer samples and for helpful discussions, and D. J. Boyle, W. I. Congdon, and D. G. Wahl for performing and discussing color measurements.

References

1. Atmospheric chemical reactions are complex, and the relevant literature is extensive. A good starting point is P. Leighton, *Photochemistry of Air Pollution*, New York: Academic Press, 1961.
2. Wohlers, H. C., and M. Feldstein, Hydrogen sulfide darkening of exterior paint, *J. Air Poll. Contr. Assoc.*, 16, 19-22, 1966.
3. Graedel, T. E., and N. Schwartz, Atmospheric air quality specifications for materials design and test, submitted for publication, 1976.

4. Chickering, K. D., Perceptual significance of the differences between CIE tristimulus values, J. Opt. Soc. Am., 51, 986-990, 1969.
 5. Hemmendinger, H., Development of color difference formulas, J. Paint Technol., 42, 132-139, 1970.

TABLE I. MEASURED TRACE GAS CONCENTRATIONS DURING POLYMER EXPOSURE

Test	Test Period (hr)	NO ₂ *	SO ₂ *	H ₂ S*
1	28	345	121	675
2	20	423	207	99
3	54	392	148	390
Atmospheric upper limit	-	72	70	10

*Units are parts of trace gas per billion parts of air, v/v.

TABLE II. COLOR DIFFERENCE PARAMETERS

Sample	Test	ΔL	ΔC_{rg}	ΔC_{yb}	ΔC	ΔE
Type BCZ PVC	1	-0.4	0.2	-0.4	0.5	0.6
	2	0.1	0.2	-0.2	0.3	0.3
	3	0.5	0.3	0	0.1	0.6
Type Pb PVC	1	-12.9	6.2	3.8	7.3	14.8
	2	- 3.3	4.1	3.6	5.5	6.4
	3	-10.2	5.6	3.4	6.5	12.1



T. E. Graedel, Member of the Technical Staff



J. P. Franey, Technical Associate
 Environmental Chemistry Research Department
 Bell Telephone Laboratories, Murray Hill, New Jersey 07974

PROCESSING STABILITY OF SEVERAL POLYMERS

C. C. Swazey

Sandoz Colors & Chemicals

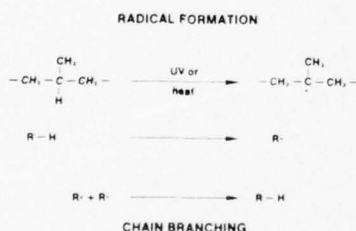
East Hanover, N. J.

INTRODUCTION

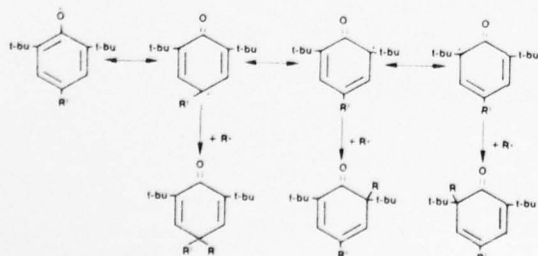
The trend in plastics fabrication, towards higher production output, has resulted in a continual increase in processing temperatures and shear stresses which has placed greater emphasis on the process stability of polymers. Also, the increased emphasis on the use of regrind, and recycling of plastic waste, demands the maintenance of polymer integrity through multiple processing stages. To endure such conditions without significant degradation, and consequent deterioration of physical properties, the polymer must be protected by improved processing stabilizers.

DEGRADATION OF POLYOLEFINS

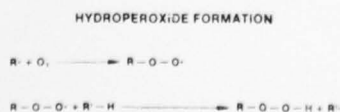
Polyolefins processed at high temperatures or subsequently exposed to UV-radiation in the presence of oxygen, free radical chain reactions take place leading to scission or crosslinking of the polymer chains and consequently to a deterioration of the polymer's physical properties.



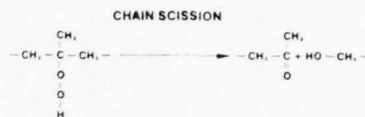
Once polymer radicals are formed they can be converted into neutral products by the use of antioxidants primarily the sterically hindered phenols. The antioxidant itself, transferred into a resonance-stabilized phenoxyl radical, does not further interfere with the radical chain except for addition of another polymer radical.



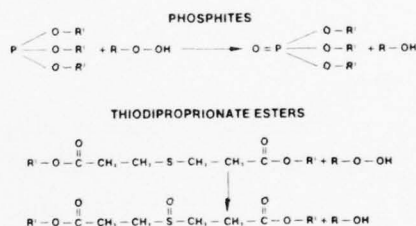
Polymer radicals R react readily with oxygen and in a following step with other polymer molecules to form hydroperoxides.



Due to their highly unstable configuration, hydroperoxides undergo disproportionation reactions which lead to a scission of the chain, noticeable in a drop of the polymer's melt viscosity.



Two main chemical classes of hydroperoxide-decomposers are thiodipropionates and organic phosphites; both groups convert hydroperoxides into inactive hydroxy groups, which do not promote further degradation.



LONGTERM STABILITY

The long-term stability of polyolefins is determined by an accelerated test, commonly known as the oven-test, where specimens are exposed to temperatures just below the crystalline melting-point of the polymer. Assuming no major differences in reaction mechanisms are found between room- and test-temperatures, this test simulates the performance of polyolefins in use over a long period of time.

Oven tests have shown, that sterically hindered phenols, particularly of higher molecular weight, increase the long-life stability of polyolefins substantially. It has also been found that thiodipropionate esters give synergistic effects when applied together with hindered phenols.

PROCESSING STABILITY

Unlike long term stability, processing stability has not been as specifically defined by the technical community. The processing of polyolefins involves the transformation of the polymer into a molten state by the application of temperatures higher than its crystalline melting point, and then pushing it through a dye or injecting it into a mold. Obviously, the oven test described above for the measurement of long term stability of polyolefins is unsuitable as an indicator of process stability as it does not simulate processing temperatures or shear

stresses. For this reason, the increase in Melt Flow Index with respect to multiple extrusions was taken as the measure of processing stability.

EXPERIMENTAL DESIGN

It was the intention of this work to study the influence of various compounds on the processing stability of several polymers.

For the investigation in polypropylene the following compounds were chosen:

RADICAL SCAVENGERS

AO-1 = Tetrakis [methylene 3, -(3',5'-di-tert-butyl-4'-hydroxyphenyl) propionate] methane

AO-2 = Octadecyl 3-(3',5'-di-tert-butyl-4'-hydroxyphenyl) propionate

BHT = 2,6-di-tert-butyl-p-cresol

HYDROPEROXIDE DECOMPOSERS

DLTDP = Dilaurylthiodipropionate

P-1 = Distearyl-pentaerythritol-diphosphite

P-2 = Tris (nonyl phenyl) phosphite

PEPO = Tetrakis [2,4-di-tert-butyl-phenyl] 4,4' biphenylenedi-phosphonite

TEST PROCEDURE

All processing stability tests were carried out by multiple extrusions on unstabilized polypropylene with a melt flow index of 2.2 (230°C/2,16 kg). Since polypropylene under the influence of oxygen at elevated temperatures undergoes degradation mainly by chain-scission, which is noted by a marked decrease in melt-viscosity, or by an increase in melt flow index (MFI), the measurement of MFI was chosen to determine the degree of polymer degradation. In order to reduce degradation during this measurement, and to increase the accuracy of the method, the MFI was taken at 190°C and 5 kg.

The multiple extrusions were performed on a small laboratory-extruder under the following conditions:

Screw diameter and length: 22 mm, 20 D

Screw compression : 1:3,5, short compression

Screw speed : 30 r.p.m.

Barrel temperatures : 240/240/240°C

Circular die with 7 mm in diameter, set at 210°C.

The extruded strand was cooled by an air-stream and cut into granules. The MFI of

the granules was measured after each passage.

PROCESSING STABILITY OF RADICAL SCAVENGERS

Diagram 1 shows the influence of radical-scavengers on processing stability, when applied at different concentrations.

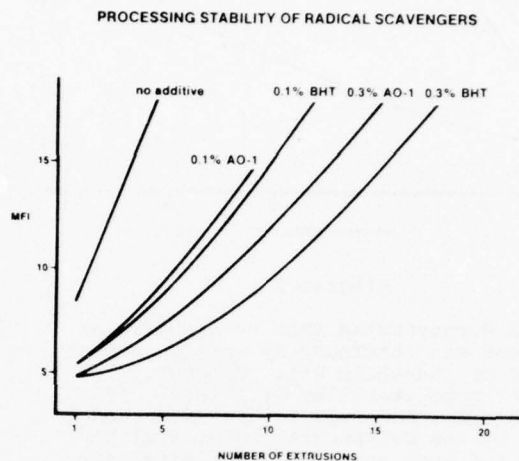


Diagram 1

Although there is no long-term stability to be obtained from BHT, its processing behavior and its low price have created an important and voluminous market for this product.

PROCESSING STABILITY OF HYDROPEROXIDE DECOMPOSERS

Hydroperoxide decomposers are often referred to as costabilizers because their effectiveness in the absence of radical scavengers is usually poor. Only few literature publications deal with processing stability of hydroperoxide decomposers like phosphites and thiodipropionates, but so far no information has been available on phosphonites. It was our intention to investigate one representative of the phosphonite class and compare it with other commercially established costabilizers.

Initial studies of all three chemical classes were tested at a concentration of 0.3% in the absence of radical scavengers.

PROCESSING STABILITY OF HYDROPEROXIDE DECOMPOSERS

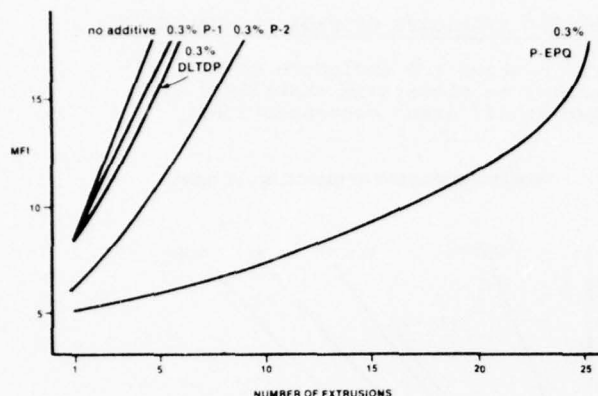


Diagram 2

Diagram 2 demonstrates that no significant improvement was obtained, by thiodipropionate DLTDP or phosphite P-1. Phosphite P-2 does offer some stability by itself. It was surprising, however, to find a marked increase by the phosphonite PEPQ, well beyond P-2 and even surpassing the effectiveness of radical scavengers like BHT and AO-1. Decreasing the concentration of PEPQ to 0.05% still led to better results than P-2 at 0.3%.

COMBINATION OF RADICAL SCAVENGERS WITH HYDROPEROXIDE DECOMPOSERS

Although the phosphonite PEPQ would provide maximum processing stability without the need of radical scavengers, phenolic-type antioxidants must be added to polypropylene in order to prolong its long-term stability. Depending upon the desired level of long-term protection and the quality of the chosen scavenger, the concentration of antioxidant usually lies between 0.05% and 0.2%.

COMBINATION OF RADICAL SCAVENGERS WITH HYDROPEROXIDE DECOMPOSERS

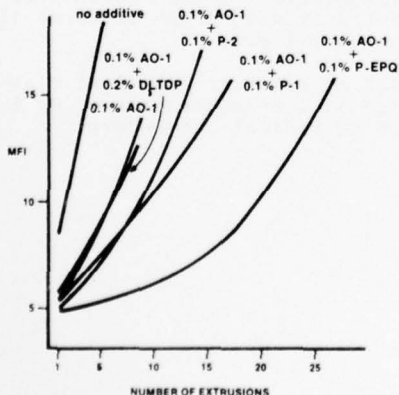


Diagram 3

From the results the following conclusions can be drawn:

- The thiodipropionate system (DLTDP) does not contribute to any improvement in processing stability, its advantage therefore lies only in long-term stability.
- The phosphites P-1 and P-2 synergize radical scavengers and increase their effectiveness significantly.
- The combination with the phosphonite PEPQ shows an enormous increase of processing stability well beyond that of the phosphites. It is evident, that this particular substance offers extremely high levels of protection, which can be further increased by higher amounts of PEPQ.

COMBINATION OF RADICAL SCAVENGERS

It is common practice to stabilize polypropylene by means of two radical scavengers, namely BHT and another sterically-hindered phenol of higher molecular weight.

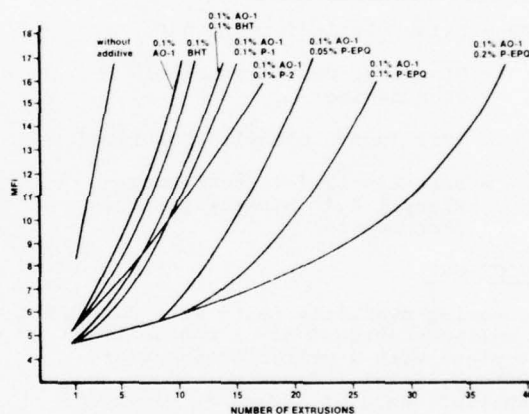


Diagram 4 - Processing stability of a combination of two radical scavengers

BHT exhibits only an additive effect on the primary antioxidant's efficiency. This indicates the possibility of substituting BHT with phosphites without loss in processing stability. An exchange of BHT by the phosphonite PEPQ leads to substantially higher stabilities. By substitution, both classes - phosphites and phosphonite PEPQ - avoid an adverse property of BHT, which has become a particular nuisance to some polypropylene manufacturers in the past year. BHT frequently causes discolorations either during processing or during storage of the polymer granules.

Diagram 5 demonstrates the color improvement when BHT is replaced by PEPQ.

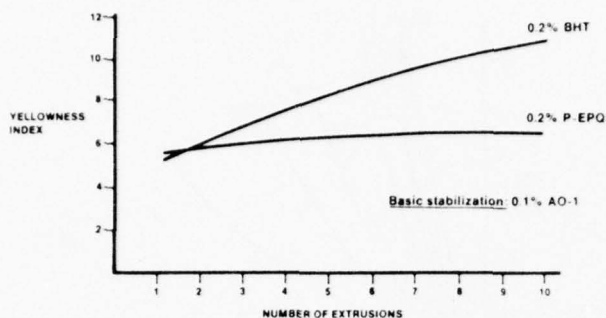


Diagram 5 - Change of color during processing

The color was determined by yellowness-index measurements (ASTM D-1925) on 1 mm thick sheets, which were compression-molded from the particular extrusion passages. BHT gives a pronounced discoloration with increasing number of extrusions, whereas the color change with PEPO is negligible.

INFLUENCE OF CALCIUM STEARATE ON PROCESSING STABILITY

Calcium stearate is usually added to polypropylene to deactivate acidic parts of the polymerization catalyst and also to act as a metal/polymer interface lubricant. Therefore it was of some importance to investigate the influence of calcium stearate on the processing stability of polypropylene.

Diagram 6 demonstrates that calcium stearate offers no improvement in the absence of stabilizers, however the stability increases remarkably when it is combined with radical scavengers like AO-1 or AO-1 + BHT.

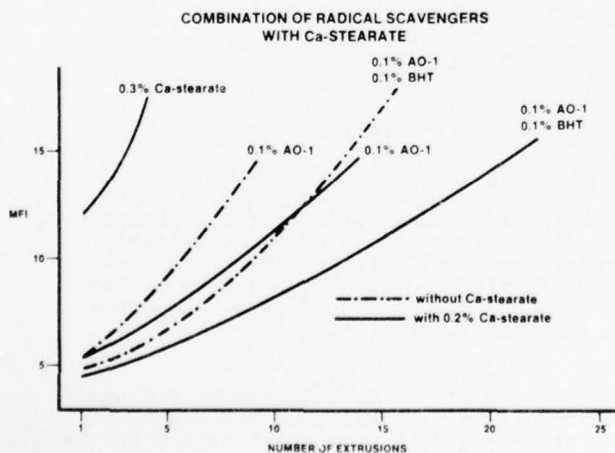


Diagram 6

If calcium stearate is added to combinations like AO-1/phosphite or AO-1/PEPO, it improves the effect of phosphite P-2 and phosphonite PEPO, but no stability increase was obtained with the system containing

phosphite P-1 (see diagram 7).

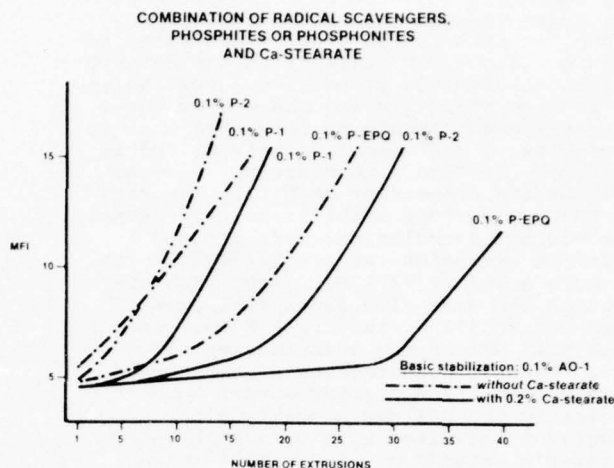


Diagram 7

The different behavior of phosphite P-1 and phosphite P-2 in the presence of calcium stearate might be explained by the distinct difference in hydrolytic stability of both substances. Hydrolysis-studies, carried out in water at 60°C, where the change in pH was followed over a period of hours, have shown a faster drop in pH for P-1 than for P-2. It could be speculated, that under the influence of calcium stearate P-1 hydrolyses to some extent during processing, whereby the positive influence of calcium stearate on processing stability might be somewhat offset by a decrease in concentration of active P-1. Phosphonite PEPO which is much more stable to hydrolysis leads to maximum processing stabilities and offers the best protection for the polymer.

HIGH DENSITY POLYETHYLENE

The performance of various stabilizers in high density polyethylene are compared in Diagram 8.

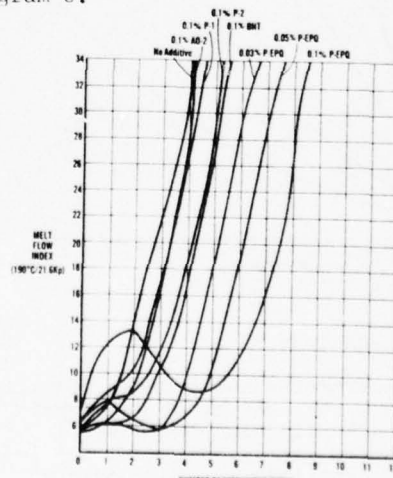


Diagram 8

When high density polyethylene (HDPE) is exposed to processing conditions, cross-linking and chain scission reactions compete for predominance. Above 450-470°F./230-240°C. chain scission usually dominates resulting in polymer degradation and deterioration of physical properties. Post polymerization cross-linking can modify the polyethylene molecule to the point that it resembles a thermosetting polymer and is extremely difficult to process. Diagram 8 shows the processing stability imparted to HDPE by various stabilizers used alone. The various formulations were exposed to multiple extrusions at 470°F./240°C. with a screw speed of 70 RPM. After each extrusion the Melt Flow Index (MFI) was measured at 374°F./190°C./21.6 Kp. The "nominal" MFI of the starting resin was 6.0. Careful measurements of nonexposed highly stabilized reactor powder however indicated the MFI was actually 9 or 10. Diagram 8 indicates that Sandostab P-EPQ initially retards polymer cross-linking as demonstrated by the increase in MFI with increased P-EPQ concentration. In subsequent extrusions the MFI decreases thereby preventing chain scission. As the Sandostab P-EPQ becomes depleted the MFI again begins to increase. Other tested stabilizers appeared to offer little protection from initial cross-linking and were quickly depleted allowing chain scission to proceed.

POLYCARBONATE

Diagram 9 demonstrates the relative process stability of various phosphorous stabilizers used alone in PC. Notice that increasing concentrations of stabilizers result in lower stability. 0.10% of Sandostab P-EPQ results in significantly less degradation than the conventional stabilizers.

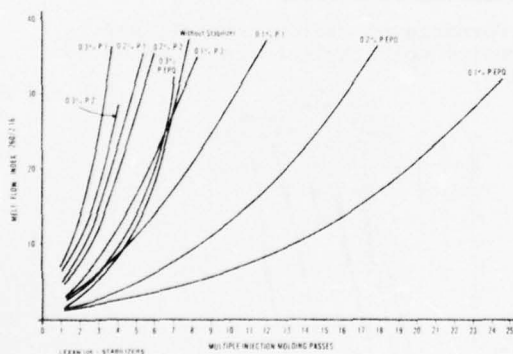


Diagram 9

Diagram 10 demonstrates the process stability provided by a combination of Sandostab P-EPQ and a sterically hindered phenol. While the phenolic antioxidant does not improve process stability, it is necessary for long term stability.

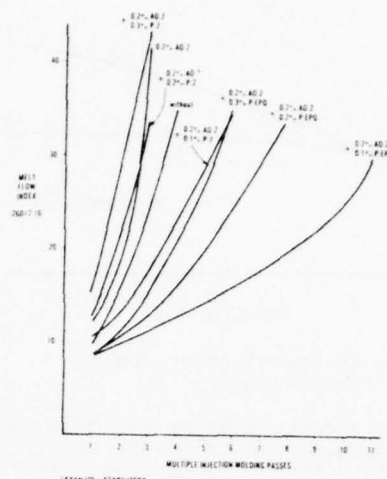


Diagram 10

As indicated in Table 1, improved processing stability results in the maintenance of physical properties over an increased number of processing steps. Table 1 presents the number of processing passes the polycarbonate received until the impact strength was deteriorated sufficiently to break the specimen.

	Number Of Passes, Until Samples Break	
	Manual Test	Break On Dynstat - apparatus
Without Stabilizers	4	5
0.2% AO-2	3	3
0.2% AO-2 + 0.1% PEPQ	12	13
0.2% AO-2 + 0.2% PEPQ	12	11-12
0.2% AO-2 + 0.3% PEPQ	8	7
0.2% AO-2 + 0.1% P-2	7	8
0.2% AO-2 + 0.2% P-2	5	4-5
0.2% AO-2 + 0.3% P-2	4	4

LEXAN 105 + STABILIZERS
INJECTION MOLDED 3MM SHEETS

Table 1

CONCLUSIONS

It has been demonstrated that the phosphonite class of compounds provide increased processing stability, and therefore prevention of polymer degradation and retention of physical properties compared to conventional stabilizers.

The efforts of Dr. F. Mitterhofer and Staff of Sandoz, Ltd., Basel, Switzerland in gathering the data upon which this paper is based, is gratefully acknowledged.

BIOGRAPHY

Chester C. Swasey received his Bachelor of Science (Chemistry) Degree from the City University of New York in 1965 and his Master of Business Administration Degree from Fairleigh Dickinson University in 1973.

From 1967 to 1971 he was employed at the St. Regis Paper Company in the Polymer Applications Dept. From 1971-1973, he was employed at the Dart Industries, Rexene Polymers--Product Planning Dept. Since 1973 he has been at the Sandoz Colors and Chemicals, where he is Product Manager of the Plastics Additives Department. He is a member of the Board of Directors of the Society of Plastics Engineers: Polyolefins and Thermoplastics Section.



RF LEAKAGE MEASUREMENTS DIRECTED TOWARD ACHIEVING ELECTROMAGNETIC COMPATIBILITY

Larry Rader
The Boeing Company
Wichita Division
Wichita, Kansas

Summary

In recent years it has become necessary to impose RF leakage limits on microwave transmission line components such as waveguide and coaxial cables in order to achieve electromagnetic compatibility in critical avionics systems. Various measurement techniques have been developed to assess the leakage character of these components. The use of a particular technique depends upon the type of component to be measured, the frequency range of interest, and the type of information desired, such as locating a point of leakage or determining the total leakage from a component. This paper discusses a leakage measurement technique developed at the Wichita Division of The Boeing Company for measuring the leakage from RF coaxial cables and connectors. The approach is applicable to qualification tests or production acceptance tests of coaxial cables and connectors having RF leakage requirements, and is presently called out in MIL-T-81490, Transmission Lines, Transverse Electromagnetic Mode, and in ASNAE 68-38A/1A, Coaxial Cables LT Type. The technique utilizes an adjustable TEM resonant cavity in which a test cable or mated test connector pair can be inserted. Power is applied through the test item and the energy leaked into the cavity is detected. A ratio of this power to the input power, corrected to account for the "Q" of the cavity, provides a measure of the energy leaked from the test item. A series of measurement cavities have been designed and built at Boeing covering the frequency range from 150 megahertz to 18 gigahertz. The detail design of the test cavities, the test equipment setup required to implement the use of the cavities, and measured data showing the level of leakage for a variety of standard cables are included.

Background

In 1971, the Wichita Division of The Boeing Company was awarded a contract N00-123-71-C-1056 from the U.S. Navy Missile Center, Point Mugu, California, to develop a method to evaluate RF leakage from coaxial transmission lines, to construct hardware and develop procedures to implement the method, and to conduct tests on representative types of coaxial assemblies. The goal of the test device was to provide an accurate, non-destructive method of measuring RF leakage from coaxial cable assemblies; i.e., to provide a method for evaluating a cable assembly for development, qualification, or production without causing physical or electrical change to the assembly. This contract resulted in establishment of a new RF leakage test method which has been incorporated in Military Specification MIL-T-81490(AS), "Transmission Lines, Transverse Electromagnetic Mode." Although the method has been in use since 1972, the details of the principles of operation and test hardware have not been published. This paper describes the principles of operation, design and operation details, and gives results of tests on several coaxial assemblies.

General

The principles of operation are described as follows. The technique utilizes an adjustable TEM resonant cavity depicted by Figure 1 that is formed by the test sample outer conductor and the inner surface of the test fixture. The ends of the cavity are terminated in sliding short circuits which are positioned at spacings of a multiple number of half wavelengths. Power is applied to the test item, and energy leaked into the cavity produces a resonant standing wave which is sampled by a probe and coupled to a detection system pre-calibrated in dB relative to the source at the input to the test sample. Referring to Figure 2, correction factors are derived for calculation of the RF leakage in dB per foot. The corrections are C_1 due to the cavity Q and C_2 to convert from total leakage to leakage per foot of the test sample contained within the cavity.

Detail Description

The operating principle of the test device is to produce a standing wave for the TEM mode which is in turn coupled to the detection probe. To implement this principle, sliding RF short circuits which are noncontacting with the cable assembly outer conductor (due to the presence of the cable jacket) and noncontacting with the test fixture (to prevent wear and a resultant inconsistent short) were designed and fabricated. The principle of the noncontacting sliding shorts is explained with the aid of Figure 3.

At the choke center design frequency, the path length

$$\beta_1 \ell_1 + \beta \ell_2 + \beta \ell_3 = \beta \ell_4 + \beta \ell_5 + \beta \ell_6 = \pi$$

The short circuit at the end of lengths ℓ_3 and ℓ_4 are thus transformed to a short circuit at the front face of the sliding short, which enhances the overall performance. The lengths ℓ_1 and ℓ_6 are not necessarily physically equal, and in our application are in fact unequal. This is necessary to achieve electrically equivalent lengths since the dielectric constants of the corresponding materials are unequal. The outer dielectric is teflon ($\epsilon \approx 2.1$) while the inner dielectric is that of the cable jacket (e.g. polyvinyl chloride $\epsilon \approx 3.0$, nomex $\epsilon_r \approx 3.0$). A photograph of the short circuits is presented as Figure 4.

A by-product of this test method is the enhancement of the available leakage signal due to the Q of the test cavity. The length in the cavity between the effective short-circuit of the noncontacting shorts is adjusted so that resonance occurs at the desired test frequency. At the resonant frequency the wave in the cavity is supported on a "per cycle" basis by the leakage from the test sample. At resonance the cavity Q is increased; i.e., the energy stored in the cavity which is detected by the cavity probe is increased. The result is that due to resonance the cavity energy level is increased and permits measurement of lower leakage levels relative to other measurement methods. The cavity Q is limited by the effectiveness of the shorts, losses in

the cavity such as the relatively lossy dielectrics of typical coaxial cable jackets, and mechanical obstructions of the natural resonance of the cavity such as bulkhead connector flanges.

In general, transmission lines are selected so that propagation is entirely restricted to the dominant mode. This case (TEM for coaxial lines) is considered in this discussion. However, the RF leakage in the test cavity can and will exist in both the dominant mode and several higher order modes at any frequency where wavelength is greater than the mean circumference of the cavity conductors. The higher order modes are typically TE₀₁, TE₁₁, TE₂₁, TM₀₁ and TM₁₁. The higher order modes all have one characteristic in common - their phase velocity in the cavity is higher than that of the TEM mode. This fact is useful in identifying and selecting only the TEM wave for measurement, and will be discussed during the test setup discussion.

In many applications it is desirable to know the leakage character of a cable at frequencies above its normal operating (TEM) range. For example, it is often necessary to determine cable RF leakage for harmonics of a transmitter. In this case where higher order modes can exist in the test sample RF leakage in the cavity may again exist in the TEM or higher order modes. These cavity modes can be isolated as before. However, measurement errors are introduced due to (a) conversion of TEM energy to higher order modes, which reduces the TEM power level incident to the section of cable being evaluated, (b) the mode conversion may occur in the test set-up transmission lines subsequent to calibration, resulting in measurement error, (c) higher order modes excited in the test section may not be representative of leakage from that sample during operation in its intended application due to bends, temperature effects on dimensions, etc. Thus, precaution should be exercised when conducting leakage tests at frequencies where the test sample can support higher order modes.

Test Setup and Performance

The test setup and performance which have been adopted by MIL-T-81490 are described and explained as follows. There are essentially three operations: (1) adjustment of the sliding shorts to achieve resonance of the cavity at the selected test frequency, (2) calibration, and (3) leakage measurement.

A photograph of the test setup is shown in Figure 5. The test setup and equipment list of Figure 6 and Table I are used for properly adjusting the positions of the sliding shorts for TEM resonance. A swept frequency input for the frequency band which includes the desired test frequency is provided at the test cavity detection probe and the sliding shorts are adjusted until TEM resonance occurs at the selected test frequency. The TEM resonance is unique from all other possible resonances, and can be identified by (1) for a given change in cavity length, a TEM resonance undergoes a greater frequency shift than TE or TM modes, and (2) it maintains a nearly constant amplitude for small changes in cavity length. Once the cavity length has been established, this length must be maintained until completion of the leakage test at that frequency. The cavity amplification factor due to resonance is computed from this setup. The resonant center frequency is recorded, as are the frequencies of the half power points on the resonance curve. During this step it is also necessary to determine the

length between the faces of the sliding shorts, i.e., the length of the test cable in the cavity. This is necessary to convert the total leakage to leakage per unit length.

Calibration is accomplished utilizing the test setup on Figure 7. The calibration levels can be made with a dynamic range of 60 dB. Experience indicates that the minimum oscillator power output is 20 milliwatts (+13 dBm) and the sensitivity of the network analyzer has a minimum value of -78 dBm. Thus a linear calibration from -30 to -90 dB can be assured. At frequencies below X-Band the network analyzer typically has a significantly greater sensitivity so that calibrations to -100 dB can be achieved. Greater values can be achieved if necessary by using a TWT having for example 10 watts output (+40 dBm). This assures calibrations to approximately -120 dB (+40 dBm output plus -78 dBm sensitivity). However, the operator must use precaution to assure that the higher power levels do not exceed the ratings of the test setup components, such as attenuators and couplers. The frequency range of the calibration can be the same as that selected for adjustment of the cavity, but in practice it is more convenient to calibrate for the entire bandwidth of the selected test cavity setup, and to use this calibration for measurement at several test frequencies. Once calibration is completed, the attenuators in the reference channel line must not be altered.

The leakage measurement is accomplished using the test setup of Figure 8 for the same frequency range as the calibration data. The measured leakage at the cavity resonant frequency is noted from the plot, and the leakage per unit length is calculated as shown on Figure 2. i.e.

$$\text{Leakage (dB per foot)} = \text{recorded value} \\ - 10 \log Q - 10 \log L_{(\text{ft})}$$

The test is then repeated for additional frequencies by repeating the cavity adjustment procedure for the new test frequency. The calibration remains valid if the swept frequency range and reference channel attenuation are not changed. Mated connector pairs can be measured using the procedure described above, with the measured value being corrected for the leakage attributable to the length of cable contained between the short circuits.

Typical data sheets are shown by Figures 9-11. Results of RF leakage measurements for selected coaxial cables are presented in Figure 12.

Other Applications

It is conceivable that this measurement concept could be utilized to determine RF leakage from flexible waveguide. The same basic principles are applicable, although the non-circular cross section must be considered with respect to the modes of propagation in the test cavity. Multiple cavities could be fabricated to allow testing at several waveguide flexed positions, for example straight; 30°, 60° and 90° E-plane bends; 30°, 60° and 90° H-plane bends; 30°, 60° and 90° twists; and at combinations of these bends/twists. It would represent an exciting challenge, and the obvious need indicates the desirability for pursuit of this idea.

Biography

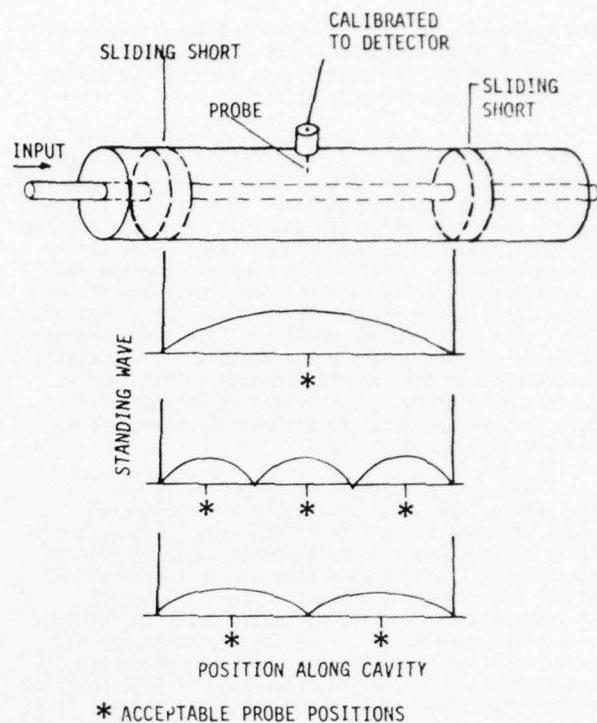


Mr. Larry D. Rader
Mail Stop K21-17
The Boeing Company
3801 South Oliver
Wichita, Kansas 67210

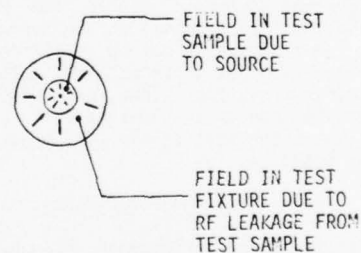
Mr. Rader graduated from Kansas State University with a BSEE degree in 1963. He was employed from 1963-1965 by the Weapons Systems Test Division of the U. S. Naval Air Test Center, Patuxent River, Maryland, where he was engaged in the test and evaluation of airborne antenna systems. He has been employed by The Boeing Company, Wichita, Kansas since August 1965 where he has been assigned to the Microwave Technology Staff which is engaged in DDT&E antenna systems, including antennas, radomes, transmission lines, and microwave filters. His assignments have included design, test and evaluation of antenna systems for CNI, ECM and data link systems for B-52 and EC-135 aircraft; antenna systems for the UTTAS helicopter being produced by the Boeing-Vertol Division; antenna systems studies for ECM systems for AWACS; and design studies for an SHF satellite communications radome for the E-4B AABNCP aircraft.

TABLE I
TEST EQUIPMENT LIST

ITEM	EQUIPMENT
1	Sweep Oscillator
2	Directional Coupler
3	Directional Coupler
4	Precision Attenuator
5	Directional Coupler
6	Frequency Counter
7	Precision Attenuator
8	Harmonic Frequency Converter (HP 8411A)
9	Network Analyzer (HP 8410B)
10	X-Y Recorder
11	Test Cavity (appropriate Boeing cavity and short circuits)
12	Detector
13	Oscilloscope
14	Termination

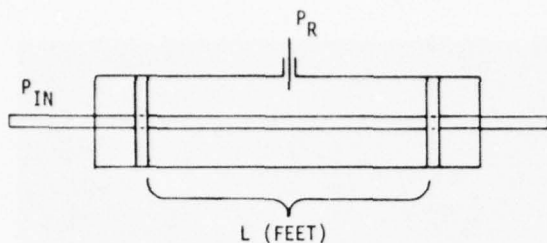


* ACCEPTABLE PROBE POSITIONS



FIELDS IN TEST FIXTURE DUE TO RF LEAKAGE FROM THE TEST SAMPLE

FIGURE 1



P_{IN} = power input to the test sample at the input to the test cavity, i.e. corrected for loss to the position of the input sliding short.

P_R = leakage power received at the cavity output.

P_L = total cable leakage from length L in the cavity.

P_U = cable leakage per unit length.

K = amplification at resonance due to cavity Q
 $(= \frac{f_0}{f_2 - f_1})$ where f_0 is the resonant frequency and f_2 and f_1 are the upper and lower frequencies at the half power points on the resonance curve).

$$P_R = K P_L = K (P_U \times L)$$

$$P_R = K \times L \times P_U$$

$$P_U = P_R / (K \times L)$$

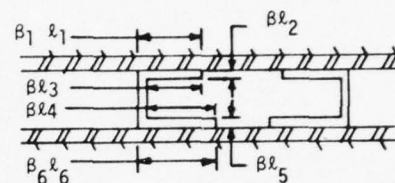
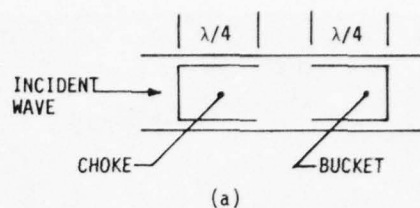
$$\frac{P_U}{P_{IN}} = \frac{P_R / (K \times L)}{P_{IN}}$$

$$10 \log \frac{P_U}{P_{IN}} = 10 \log \frac{P_R}{P_{IN}} - 10 \log K - 10 \log L$$

$$(\text{measured data}) - (C_1) - (C_2)$$

CORRECTION FACTORS FOR CALCULATION OF
 RF LEAKAGE POWER RATIO IN DB PER FOOT

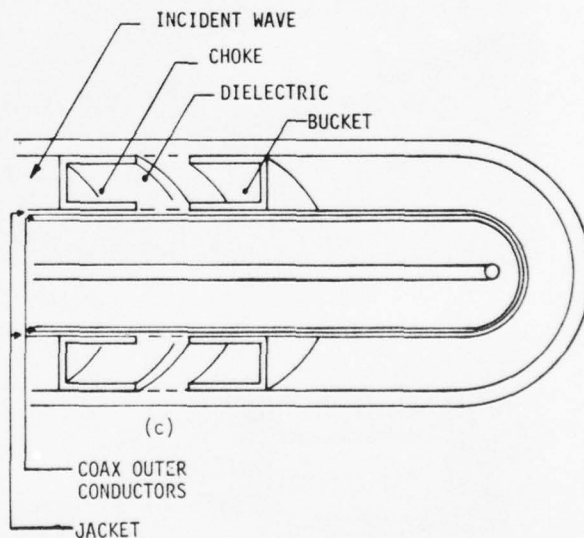
FIGURE 2



$$B_1 l_1 + B_2 l_2 + B_3 l_3 = \pi$$

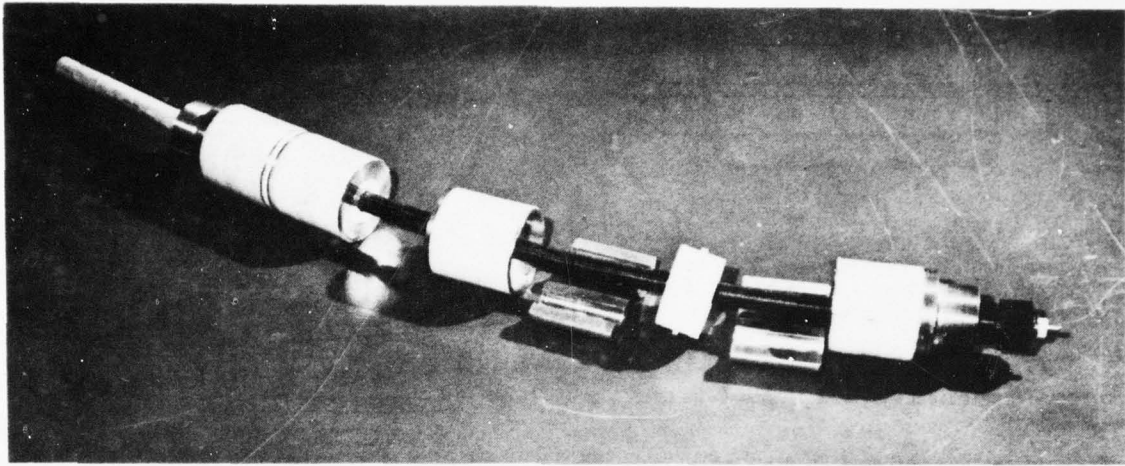
$$B_4 l_4 + B_5 l_5 + B_6 l_6 = \pi$$

(b)

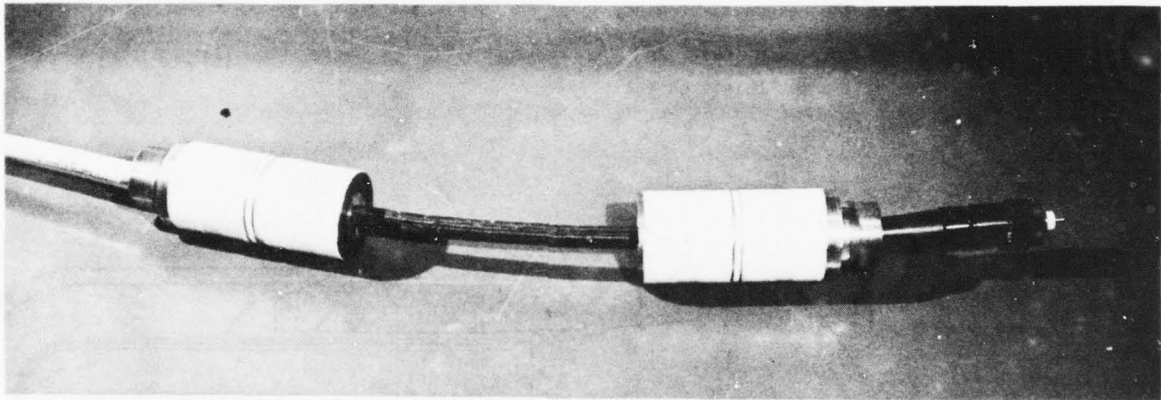


PRINCIPLES FOR NONCONTACTING SLIDING SHORTS

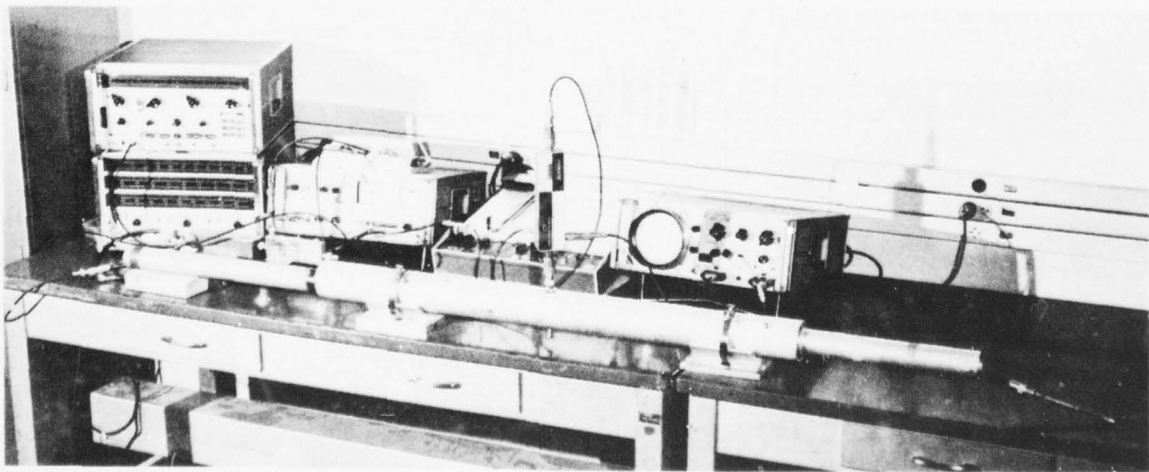
FIGURE 3



NONCONTACTING RF SHORTS
FIGURE 4a



NONCONTACTING RF SHORTS
FIGURE 4b



RF LEAKAGE TEST SETUP
FIGURE 5

AD-A032 801

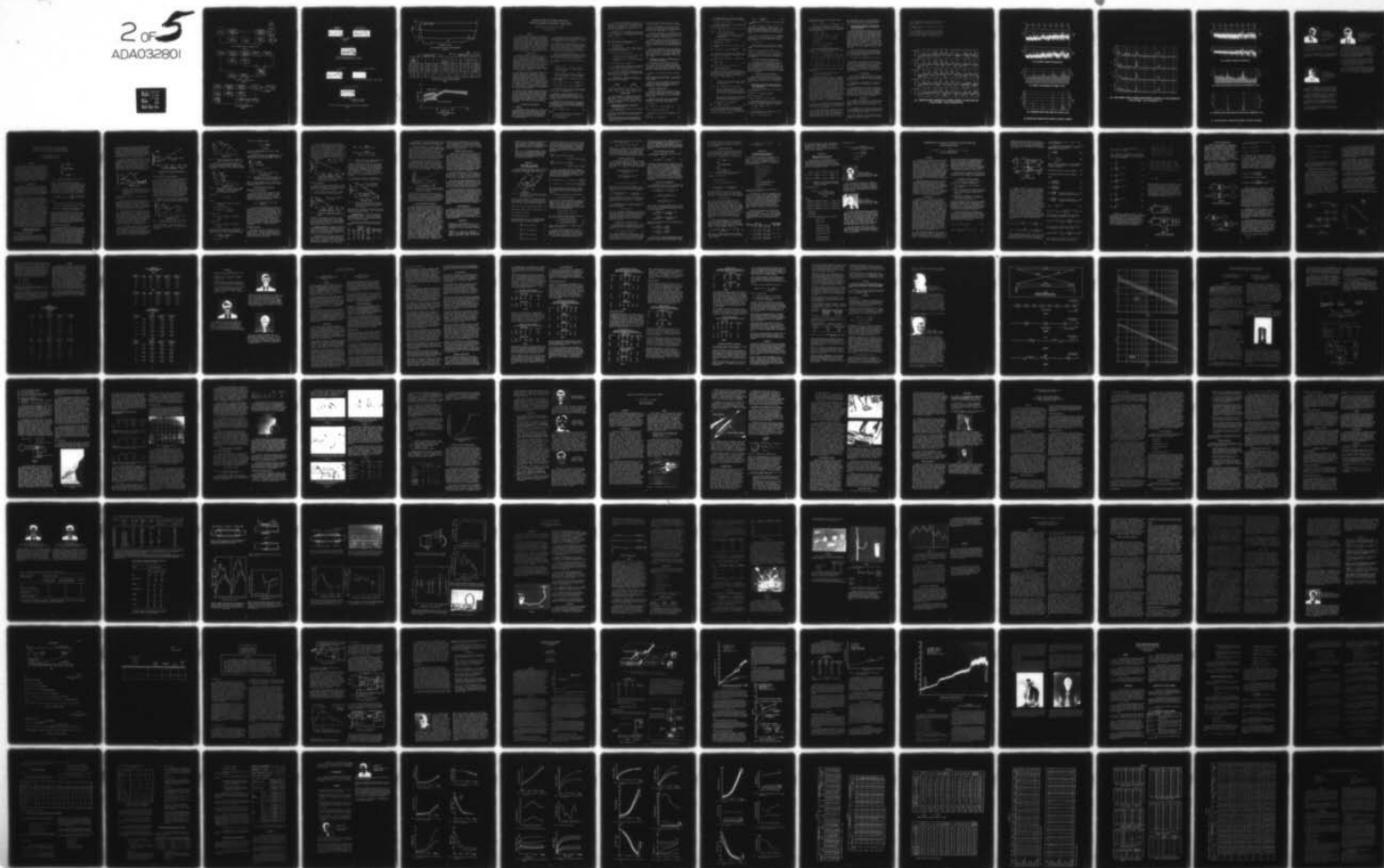
ARMY ELECTRONICS COMMAND FORT MONMOUTH N J
PROCEEDINGS OF INTERNATIONAL WIRE AND CABLE SYMPOSIUM (25TH) HE--ETC(U)
NOV 76

F/G 17/2

UNCLASSIFIED

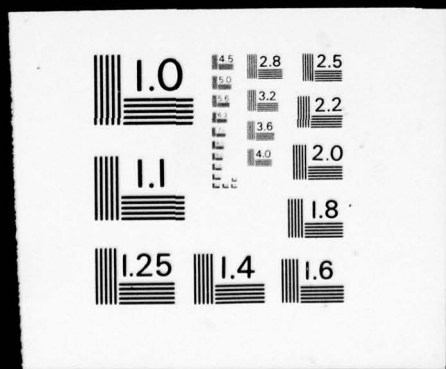
NL

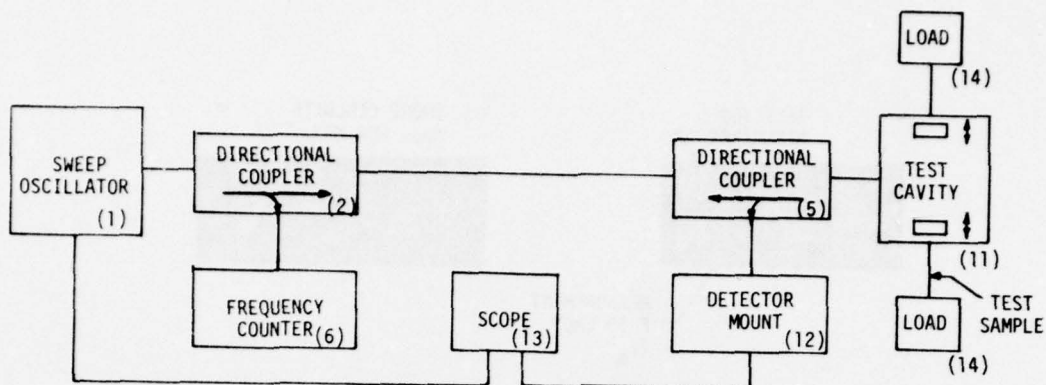
2 of 5
ADA032801



2 OF 5

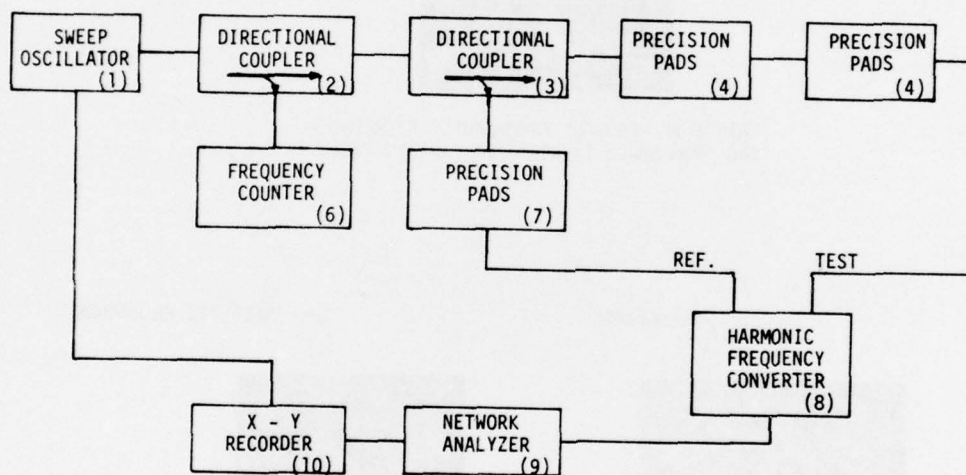
ADA032801





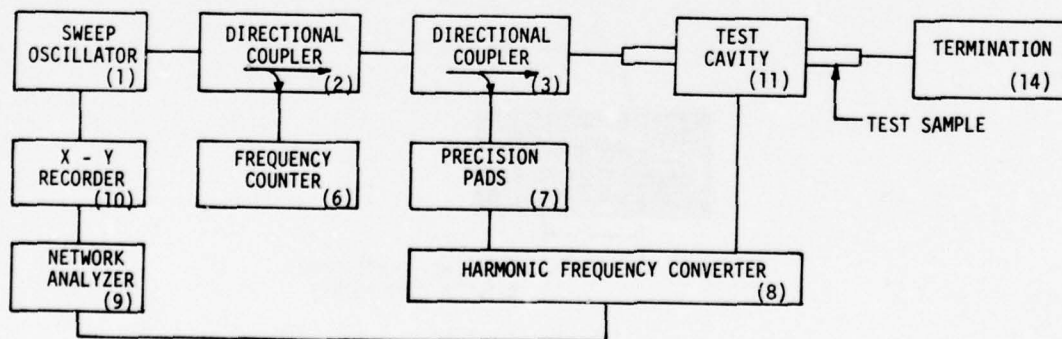
CAVITY ADJUSTMENT AND "Q" MEASUREMENT SETUP

FIGURE 6



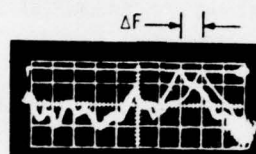
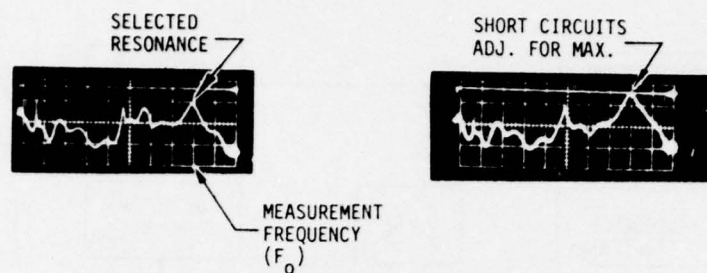
RF LEAKAGE CALIBRATION SETUP

FIGURE 7

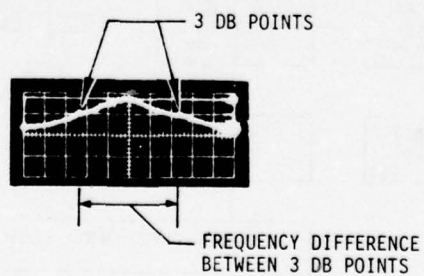
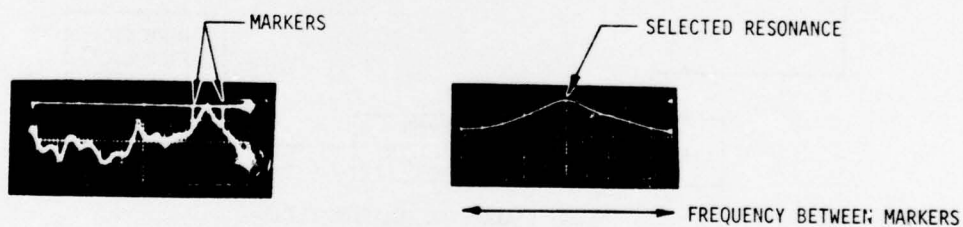


RF LEAKAGE MEASUREMENT SETUP

FIGURE 8

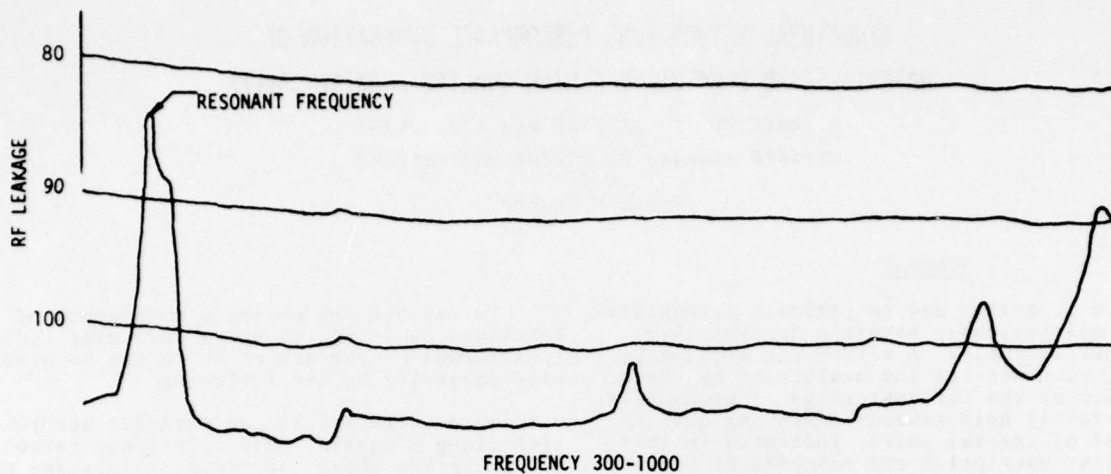


CHANGE OF RESONANT FREQUENCY (ΔF) RESULTING FROM SMALL INCREASE IN CAVITY LENGTH.



TYPICAL SCOPE DISPLAYS FOR CAVITY ADJUSTMENT AND Q MEASUREMENT

FIGURE 9

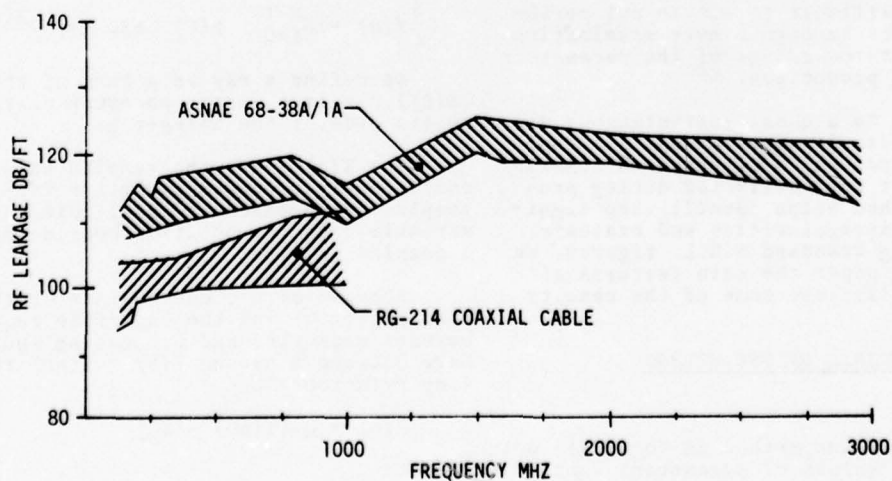


SWEPT FREQUENCY PLOT FOR RF LEAKAGE MEASUREMENT
FIGURE 10

DATE: _____
CABLE P/N: _____ LENGTH: _____
CONNECTOR TYPE: _____

l_0 CAVITY LENGTH		FREQUENCY IN MHZ				Q_0 $\left(\frac{f_0}{f_2-f_1}\right)$	$C_1 =$ $10 \log Q_0$ dB	L CHART dB	$C_2 =$ $10 \log(l_0)$ dB	$L_T =$ $L - C_1 - C_2$ dB
		f_1	f_0	f_2						
IN.	FT.									
W1	20	1.67	835	838.35	841.7	125.13	20.97	85	2.22	-108.19
W2	18.1	1.51	340	342.1	344.2	81.45	19.11	92	1.78	-112.89
W3	12.3	1.03	890	894.2	898.4	106.45	20.27	88	.11	-108.38
W4	18.0	1.5	339	341.4	343.8	71.13	18.52	83	1.8	-103.5

CALCULATION SHEET FOR RF LEAKAGE MEASUREMENT
FIGURE 11



RF LEAKAGE MEASUREMENT DATA
FIGURE 12

STRUCTURAL RETURN LOSS PERFORMANCE EVALUATION OF MATERIALS AND ELEMENTS FOR HIGH QUALITY COAXIAL CABLES

R. MATHIEU, Y. PELTIER and A.J. GHAZI

Société Anonyme de Télécommunications
(S.A.T.)
Paris - France

SUMMARY

S.R.L. spikes due to periodic irregularities could seriously handicap transmission over coaxial cables. A method for the detection of such defects and evaluation of their influence at the earliest stage of production can certainly help towards improving quality and cost of coaxial pairs. Indicated in this paper are description and examples of application of such a method, based on numerical processing performed on line. The positive results obtained are an encouragement for the use of the method as a current control tool.

1. - INTRODUCTION

Periodic impedance irregularities can severely affect the transmission characteristics of coaxial pairs. The corresponding S.R.L. requirements which are rather strict depend on the type of signals transmitted. For instance trunk CATV cables should have S.R.L. performance in the range of 26 to 32 dB ; for cables carrying high capacity analog FDM systems the limit is of the order of 40 dB ; while for cables supporting the more robust wideband digital systems the accepted limits may vary from 20 to 30 dB.

In order to optimize product quality and minimize rejects, it is highly desirable, from a manufacturing standpoint, to detect periodic irregularities as soon as they are produced, without awaiting final controls on the finished product. The threshold levels beyond which periodic defects may become nuisance are usually very small compared to those of random irregularities. It would therefore be indeed very difficult to single out periodic irregularities through a mere examination of the continuous recordings of the parameters monitored during production.

With a view to a quasi instantaneous detection of periodic irregularities, a method has been developed which is based on numerical processing of data collected during production. The method helps identify the significant periodic irregularities and evaluate the corresponding standard S.R.L. figures. We describe in this paper the main features of the method, and disclose some of the results obtained.

2. - PRINCIPLE OF THE METHOD

2.1. General

The object of the method is to single out through measured values of parameters continuously monitored during production, the periodicities due to material or manufacturing processes, and to estimate the resulting S.R.L. performances as they would appear on the completed cable.

To enhance the periodic components of the functions analyzed, we bring into play Fourier Transformation the use of which can be otherwise suggested by the following :

- to an arbitrarily shaped periodic deformation along a coaxial pair correspond harmonic S.R.L. spikes whose individual magnitudes conform to the decomposition of the original fluctuation into elementary sinusoidal ones. In particular a true sinusoidal deformation yields one and only one spike.

Since the frequency bandwidths of concern are limited, the transform is computed in its discrete form using a Fast Fourier Transform algorithm (FFT) to speed up calculation.

In the following we review some of the background :

Let :

- $\{X(n)\} = X(1), \dots, X(n), \dots, X(N)$
a sequence of real or complex numbers ;
 n is an integer.

- $\{\phi(\xi)\} = \phi(0), \dots, \phi(\xi), \dots, \phi(N-1)$
the Discrete Fourier Transform sequence (DFT) of the above ; ξ is an integer.

Then between the two sequences we have the relationships :

$$\begin{cases} \phi(\xi) = \frac{1}{N} \sum_{n=1}^N X(n) \cdot \exp(-j \frac{2\pi\xi(n-1)}{N}) \\ X(n) = \sum_{\xi=0}^{N-1} \phi(\xi) \cdot \exp(+j \frac{2\pi(n-1)\xi}{N}) \end{cases} \quad (1)$$

We define a ray as a term of the sequence $\{\phi(\xi)\}$. It is a vector moreover characterized by its order : the integer ξ .

The $X(n)$'s are the sampled values of a continuously recorded parameter $Y(z)$; the samples being taken at equal intervals D . The variable z is the position considered along a coaxial pair.

Because of the constraints of the measuring apparatus and the interface requirements between measuring and processing equipments we have between $X(n)$ and $Y(z) = Y(nD)$ the following relationship :

$$X(n) = q [Y(nD) - Y_0] \quad (2)$$

where :

- Y_0 is the nominal value of parameter Y ,
- D the sampling interval,
- q a scaling factor.

To do away with ambiguities relative to the values of the periods and resulting from sampling, the function $Y(z)$ is obtained from the physical parameter $M(z)$ through a filtering which eliminates all components with periods smaller than $h_0 = 2D$.

Therefore with a sampling interval D and the filtering, the investigation is extended up to a frequency F_0 corresponding to a wavelength λ_0 [Ref 1] :

$$\lambda_0 = 2 h_0 = 4 D \quad (3)$$

This could have also been derived from Shannon's theory of information.

2.2. System make-up

As shown on fig. 1, the system is made up of two main functional blocks : Data Collection and Data Processing.

- The collection of data includes :

- . Continuous recording of parameter $M(z)$
- . Filtering of $M(z)$ yielding $Y(z)$
- . Sampling of $Y(z)$ yielding the sequence $\{X(n)\}$.

- The processing steps comprise :

. Storage of the N values of the sequence $\{X(n)\}$ (to speed up calculation the number N is chosen as an integer power of 2).

. A Fourier Transform calculation from $\{X(n)\}$ to $\{\phi(\xi)\}$ using the Cooley-Tuckey algorithm, [Ref 2], followed by an estimation of the standard S.R.L. figure.

. An automatic display of the rays or the estimated S.R.L. values as a function of ray position or frequency.

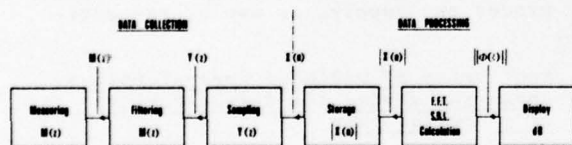


Fig. 1. FUNCTIONAL FLOW DIAGRAM

The principles of signal processing by sampling and Fourier Transformation are well known [Ref 2, 3, 4] and will not be dealt with here. Instead, we shall look more closely into the implications of analysis to the problem of concern.

2.3. Enhancement of periodic components through the D.F.T.

A ΔX amplitude fluctuation of the sequence $\{X(n)\}$ can yield :

- either one outstanding ray* with approximately a $\Delta X/2$ amplitude if the fluctuation is sinusoidal,

* (Only the $N/2$ first rays are significant since we are interested in magnitudes and $\{X(n)\}$ is real).

- or a multitude of rays (grass) with mean amplitude $\Delta X/\sqrt{N}$ if the fluctuation is random.

Thus the sharpness of discrimination of periodic from random irregularities depends essentially on the number N and can be characterized by the expression : $10 \log_{10} N$.

From what preceded it is evident that the better the "grass" performance the smaller is the number of samples required for discrimination, and the faster the computing time.

Therefore, given the average impedance regularity performance characteristic of a certain type of production, one can determine the number of samples N so as to distinguish clearly those rays resulting from periodic fluctuations.

The results obtained are not affected by the masking phenomenon of attenuation inherent to the standard S.R.L. measuring method. However since the yardstick is S.R.L. performance measured according to a standard method, the rays magnitudes are transformed to S.R.L. values in dB.

2.4. Estimation of S.R.L. - Determination of the number of samples

The N sampled values $\{X(n)\}$ collected over a cable section of length ND , theoretically carry all the information pertaining to the effect of the parameter monitored in the bandwidth investigated. One could then sample the whole length and compute the S.R.L. directly.

However this approach presents disadvantages :

- performances cannot be known - or estimated - before completion of the cable or one of its constituents,

- because of the larger number of operations and the more complex algorithm involved, the computation time is much greater than that required for shorter sections.

Periodic irregularities

Whenever significant, a periodic irregularity yields a ray proportional to the amplitude of the irregularity. It is then possible to derive the resulting S.R.L. for the whole cable length.

Suppose for instance that the parameter monitored is the linear capacitance which fluctuates sinusoidally with period h .

We have :

$$M(z) = C(z) = C_0 + \Delta C \sin(2\pi \frac{z}{h} + \theta_0) \quad (4)$$

$$X(n) = q \Delta C \sin(2\pi n \frac{D}{h} + \theta_0) \quad (5)$$

The order ξ_a of the corresponding ray is given by :

$$(N \frac{D}{h} - \frac{1}{2}) < \xi_a < (N \frac{D}{h} + \frac{1}{2}) \quad (6)$$

An approximation of the ray amplitude can be shown to be, within one dB, : [Ref 5]

$$|\phi(\xi_a)| = 0.43 q |\Delta C| \quad (7)$$

On the other hand the complex reflection coefficient is given by :

$$P(o, L) = j \frac{\pi}{\lambda} \frac{\Delta C}{C_0} \int_0^L \sin(2\pi \frac{z}{h} + \phi_0) e^{-2\gamma z} dz \quad (8)$$

where L is the cable length,

γ the propagation constant ; $\gamma = \alpha + j\beta$,

λ the wave-length at the frequency considered.

The maximum amplitude of $|P|$ is :

$$P_m = \frac{\pi}{8} |\frac{\Delta C}{C_0}| \frac{1}{\alpha h} (1 - e^{-2\alpha L}) \quad (9)$$

Elimination of ΔC and h in (6), (7) and (9) yields :

$$P_m = 0.91 \frac{1}{q C_0} |\phi(\xi_a)| \frac{\xi_a}{N} \frac{(1 - e^{-2\alpha L})}{D\alpha} \quad (10)$$

In the case considered q is expressed in volt/picofarad whereas the amplitude of the ray $|\phi(\xi_a)|$ is in volts.

The frequency affected F is implicitly given by :

$$\frac{F}{v(F)} = \frac{\xi_a}{2ND} \quad (11)$$

where $v(F)$ is the phase velocity at F .

Random irregularities

Here we make use of the known "grass" performance of a given production to determine the minimum required number of samples N ; the criterion being a sharp discrimination of periodic rays from random ones.

Let :

P_m a peak value of the reflection coefficient due to a periodic irregularity at frequency F ,

$|\phi(\xi_a)|$ the corresponding ray amplitude,

P_r the root mean square value of the reflection coefficient due to random fluctuations of the parameter considered in a small bandwidth centered on F .

ϕ_r the root mean square value of the rays magnitudes corresponding to the random fluctuations defined above.

We then have the relationship :

$$\frac{P_m}{P_r} = 1.6 \frac{|\phi(\xi_a)|}{\phi_r} (2\alpha ND)^{-1/2} \quad (12)$$

It can be shown [Ref 6] that periodic rays can be sharply discriminated against random ones when the ratio of amplitudes is 2 - i.e. when $|\phi(\xi)| = 2 \phi_r$; we then define a threshold of discrimination by :

$$P_{TD} = 3.2 \frac{P_r}{(2\alpha ND)^{1/2}} \quad (13)$$

Inspection of (13) leads to the following comments :

- P_{TD} can be written as : $P_{TD} = k P_r N^{-1/2}$; Which means that given a threshold level, the worse the grass performance the larger is the number of samples required to offset the effect of grass thus achieve proper discrimination.

- P_r is only the contribution of the parameter considered to the total grass amount $(|P|^2)^{1/2}$ as would be ascertained from S.R.L. measurements. Then

$$P_r < (|P|^2)^{1/2}$$

Account should be taken of this inequality when using data derived from S.R.L. recordings.

- since for the majority of coaxial pairs $(|P|^2)^{1/2}$ is proportionnal to $F^{1/4}$ and since α increases roughly as $F^{1/2}$ the threshold of discrimination is approximately independent of frequency.

S.R.L. due to random irregularities

It would be possible through a test on the rays amplitudes to separate the random rays and compute the corresponding S.R.L. in restricted bands by use of an appropriate formula. However, because of the lesser importance of random rays, and for speed sake, calculations for random rays were carried as though they were periodic.

3.- EXPLOITATION OF THE METHOD

The following two examples illustrate the potential of the method to detect sources of periodic irregularities and eventually modify processes, supply, or use of raw materials.

3.1. Monitoring of periodic irregularities appearing during the insulation process of a coaxial pair

The pairs considered have the following characteristics :

Attenuation : 24 dB/km at 100 MHz

Relative permittivity : 1.14

Average grass RMS : 55 dB at 100 MHz.

The parameter monitored is the linear capacitance. The bandwidth explored is 600 MHz ; therefore the sampling interval is taken as :

$$D < \frac{\lambda_{600}}{4} = \frac{0.47}{4} = 0.12 \text{ m}$$

$$D \sim 0.1 \text{ m}$$

The threshold of discrimination in dB is directly obtained from (13)

$$A_{TD} = -20 \log_{10} P_{TD} \text{ dB}$$

replacing symbols by corresponding values - where known - yields :

$$A_{TD} = -20 \log_{10} P_r + 10 \log_{10} N - 43 \text{ dB}$$

Following the comment of paragraph 2.4 we assume half the total grass contributed by the capacitance fluctuation of the insulated center conductor :

$$\text{i.e. } P_r^2 = \frac{|P|^2}{2}$$

$$\text{since } 10 \log_{10} (|P|^2) = -55 \text{ dB}$$

$$-20 \log_{10} P_r = 55 + 3 = 58 \text{ dB}$$

Therefore

$$\begin{aligned} A_{TD} &= 58 - 43 + 10 \log_{10} N \\ &= 15 + 10 \log_{10} N. \end{aligned}$$

The correspondence between number of samples N and resulting threshold levels A_{TD} is given in the following table.

N	$10 \log_{10} N$	$A_{TD} \text{ dB}$
$2^8 = 256$	24	39
$2^9 = 512$	27	42
$2^{10} = 1024$	30	45

For this type of pair, the S.R.L. requirements were :

38 dB in the lower frequency range

30 dB in the higher one.

So 256 samples could fulfill the analysis requisites. This small number of samples resulted in fast processing which was done on a desk calculator. The sampled sections were 26 m long (256 x 0.1). Since the speed of insulation was 10 m/min the data collection lasted about 3 min. The time of the processing being of the same order, we were able to obtain an information on the evolution of one or many rays every 5 or 6 min. An example of the indications obtained is shown on fig. 2 and 3. Fig. 2 displays the estimated S.R.L. on five different sections of the same coaxial pair 1000 m long. The 5 recordings exhibit a strong resemblance. We notice periodically spaced peaks above grass level ranging from 30 to 40 dB. Those peaks do correspond to various harmonics caused by a source we were able to identify.

Fig. 3 is a comparison between estimated and actually measured S.R.L. performances. It underlines the excellent correlation between the two sets of recordings.

The sequence of S.R.L. values corresponding to random rays can be considered as a sample from a random stationary sequence having no monotonic trends. The corresponding average energy loss should therefore be approximately $A_{TD} + 6 \text{ dB} = 39 + 6 = 45 \text{ dB}$.

This theoretical result is corroborated by the recording of fig. 3c where all random rays are attenuated by more than 40 dB.

3.2. Monitoring of periodic irregularities caused by imperfections of inner and outer conductors

Following the same procedure as that described for the control of insulation, we monitor here dimensional fluctuations instead of capacitance variations. The remark on discrimination of periodic from random irregularities through direct recording applies also here. In fact, suppose we had a $\pm 0.4 \mu\text{m}$ fluctuation on the thickness of the band making up the outer conductor. If it were sinusoidal with a 3 m period, the resulting S.R.L. would be around 40 dB ; If on the other hand the fluctuation were random and had a $\pm 4.0 \mu\text{m}$ amplitude, the S.R.L. would be of the order of 50 dB.

As an illustration to such an analysis we selected an example showing the possibility to detect spikes that could go unnoticed in a conventional control particularly when the level of grass is high.

The results are displayed on fig. 4 and 5.

On chart 4 we notice two types of outstanding rays. Large ones $\sim 0.7 \mu\text{m}$ and medium ones $\sim 0.3 \mu\text{m}$. On the measured S.R.L. (fig. 5a) the former do show up clearly whereas the latter are shadowed by the total grass. Consequently, we were able to take steps towards improving the intrinsic quality of the bands we used.

4. - CONCLUSION

In the preceding paragraphs we presented a method used to single out periodic irregularities on coaxial cables during the manufacturing process.

The set up is adaptable for a direct on-line monitoring of a parameter not readily accessible.

The method does not require cumbersome and lengthy operations for further processing such as punching cards or tapes, recordings, storage, etc... Such a real time numerical analysis while being presently a valuable monitoring tool could further similar developments of quality control assessments.

REFERENCES

- 1.- G. FUCHS.- Reflections in a coaxial cable due to impedance irregularities, The Proceedings of the Institution of Electrical Engineers, vol. 35, part IV, 1952, pp. 121 à 136.
- 2.- J.W. COOLEY and J.W. TUKEY.- An algorithm for the machine calculation of complex Fourier series, Mathematics of Computation, vol. 19, 1956, n° 90, pp. 297 à 301.
- 3.- J. MAX.- Méthodes et techniques de traitement du signal, et applications aux mesures physiques, Masson, Paris 1972.

4.- E.O. BRIGHAM.- The Fast Fourier Transform, Prentice-Hall, Inc. Englewood Cliffs; New Jersey, 1974.

5.- Internal report (Y. PELTIER, note technique SAT n° 2541).

6.- Y. PELTIER and G. FUCHS.- Relation entre l'affaiblissement de réflexion et la régularité des caractéristiques de transmission des paires coaxiales, Câbles et Transmission, n° 1, 26e année, Janvier 1972, pp. 71 à 85.

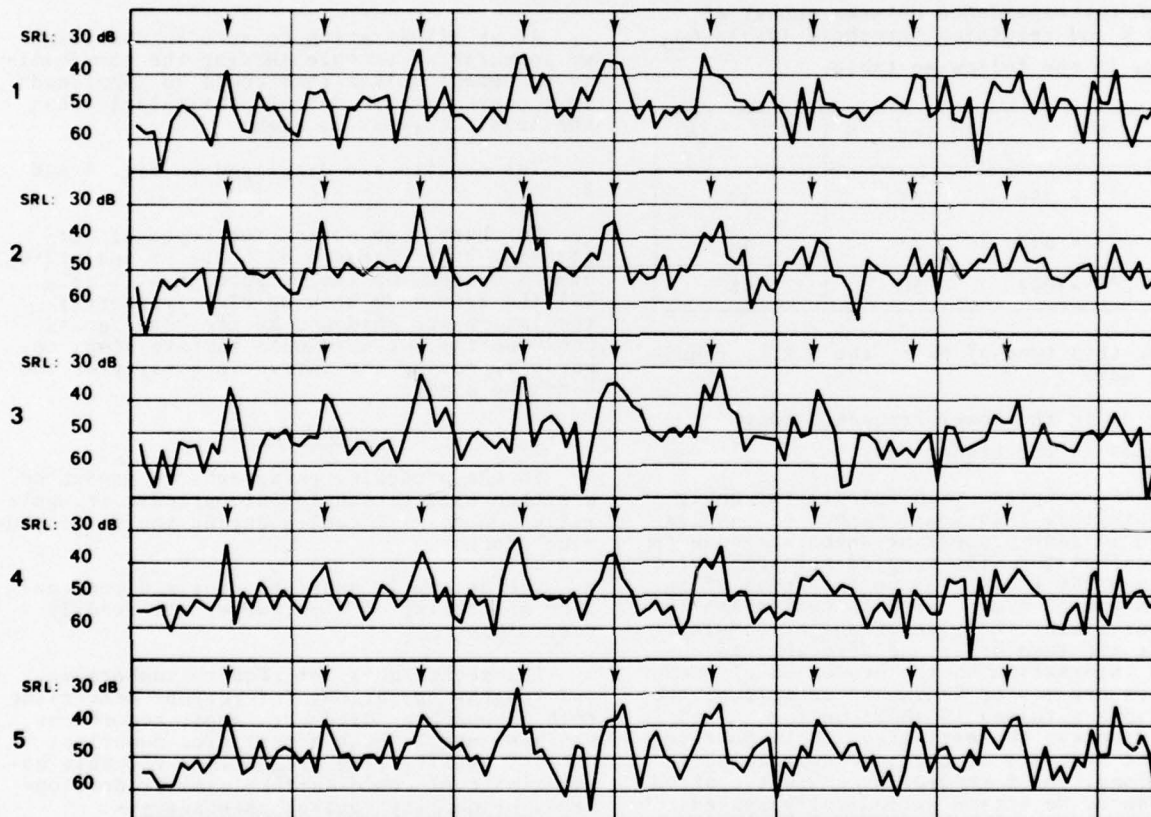


Fig.2 - INSULATION ANALYSIS - ESTIMATED SRL ON 5 DIFFERENT SECTIONS OF THE SAME COAXIAL PAIR
(x AXIS : RAY ORDER - y AXIS : RAY AMPLITUDE IN SRL)

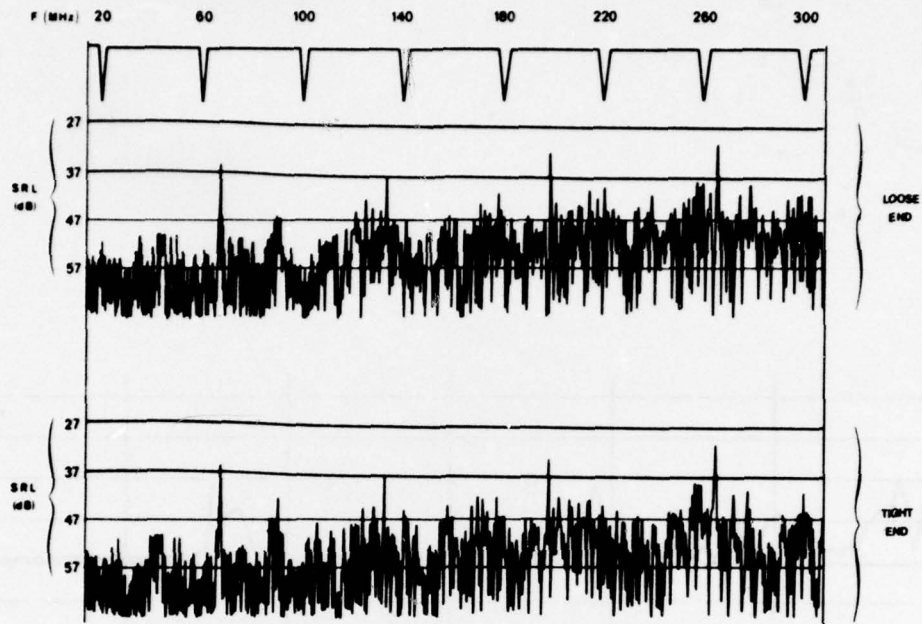


Fig.3a. SRL MEASURED ON COMPLETED PAIR FROM BOTH ENDS

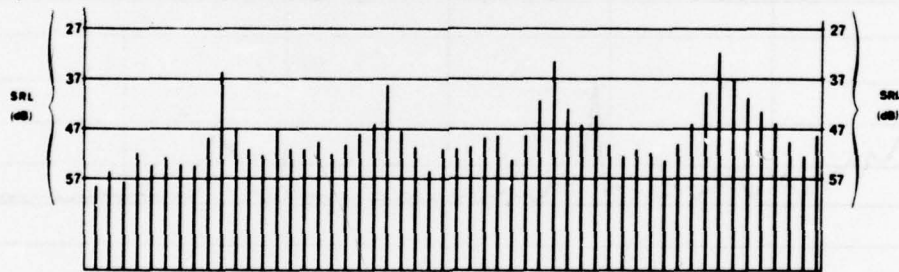


Fig.3b. ESTIMATED SRL VALUES AVERAGED OVER 5 SECTIONS (See Fig.2)

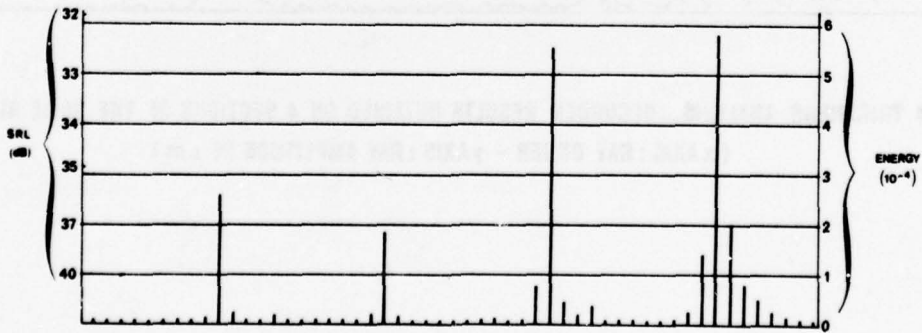


Fig.3c. CORRESPONDING ESTIMATED ENERGY AVERAGED OVER 5 SECTIONS (See Fig.2)

Fig.3. INSULATION ANALYSIS. COMPARISON BETWEEN MEASURED AND ESTIMATED SRL PERFORMANCE

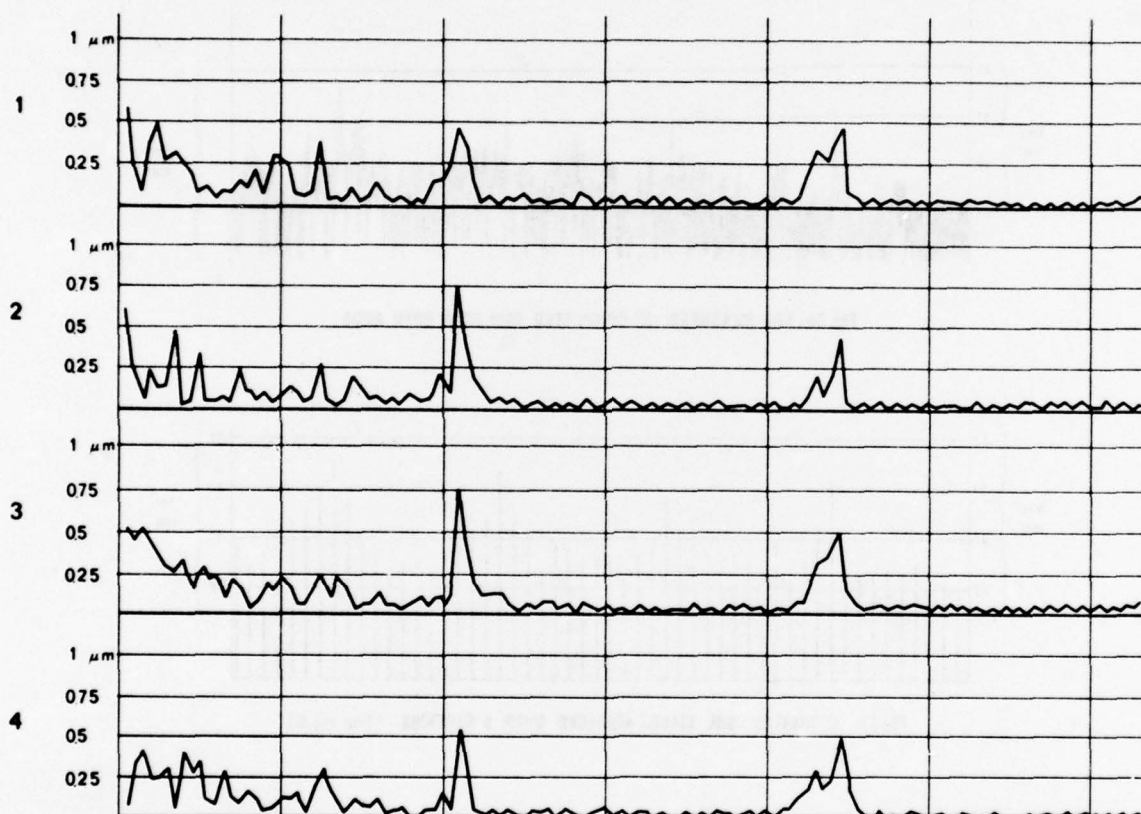


Fig.4. BAND THICKNESS ANALYSIS - RECORDED RESULTS OBTAINED ON 4 SECTIONS OF THE SAME ALUMINIUM BAND
(x AXIS : RAY ORDER - y AXIS : RAY AMPLITUDE IN μm)

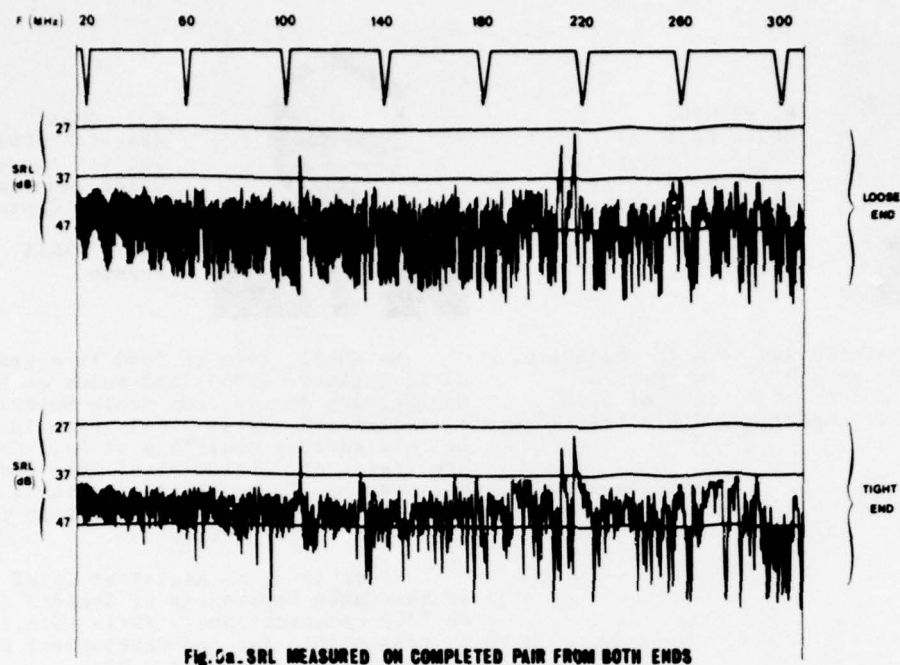


Fig. 5a. SRL MEASURED ON COMPLETED PAIR FROM BOTH ENDS

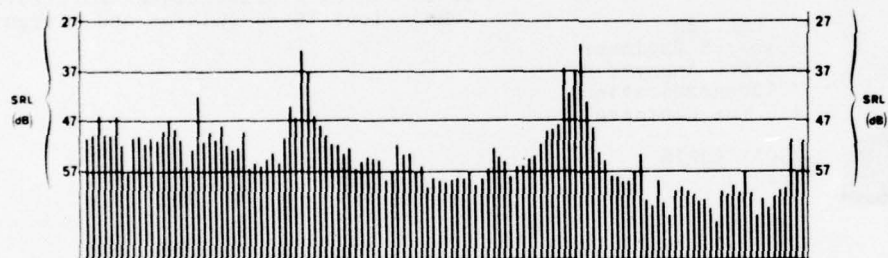


Fig. 5b. ESTIMATED SRL VALUES AVERAGED OVER 4 SECTIONS OF THE SAME ALUMINIUM BAND (See Fig. 4)

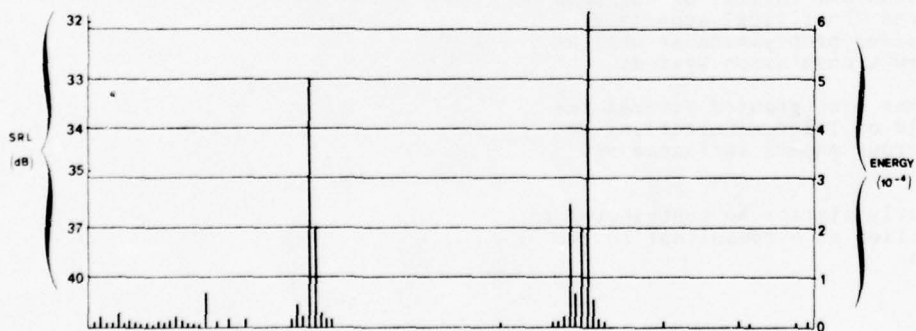


Fig. 5c. CORRESPONDING ESTIMATED ENERGY AVERAGED OVER 4 SECTIONS OF THE SAME ALUMINIUM BAND (See Fig. 4)

Fig. 5. BAND THICKNESS ANALYSIS - COMPARISON BETWEEN MEASURED AND ESTIMATED SRL PERFORMANCE



R. MATHIEU
Chief Engineer
Société Anonyme de
Télécommunications
41, rue Cantagrel

75013 PARIS
France

Mr Raymond MATHIEU was born in Couloutre, France in 1933. He is a Dipl. Engineer of Ecole Catholique d'Arts et Métiers of Lyon (1956) and of Ecole Supérieure d'Electricité of Paris (1958).

In 1958 he joined S.A.T. Cable Department. Mr Mathieu is responsible for Research and Development in the field of Communication Cables.



A.J. GHAZI
Assistant Chief Engineer
Société Anonyme de
Télécommunications
41, rue Cantagrel

75013 PARIS
France

Mr GHAZI, born in 1940 is a graduate Civil Engineer (1963) and holds an Electrical Engineering degree from Ecole Supérieure d'Electricité (Paris 1965). From 1966 to 1970 he held various positions at Bell Canada in the fields of Outside Plant Line and Radio Engineering. In the following three years he was with Bell Northern Research in the area of Outside Plant Protection.

Since 1973, as Assistant Chief Engineer in the Cable Department of Société Anonyme de Télécommunications - Paris (S.A.T.), he is responsible for the Development of high frequency communication media.

Mr Ghazi represents S.A.T. to C.C.I.T.T. (Comité Consultatif International Télégraphique et Téléphonique) COM V and COM VI as well as to I.E.C. (International Electrotechnical Commission) TC 46 (Cables and waveguides).



Y. PELTIER
Research Engineer
Société Anonyme de
Télécommunications
41, rue Cantagrel

75013 PARIS
France

Mr Yves PELTIER born in Nantes (France) in 1922, is a graduate from Ecole Nationale Supérieure des Télécommunications and holds a degree in Mathematics (Sorbonne University).

Since he joined SAT in 1947 he has been working on advanced theoretical aspects of free space and guided propagation as well as development of new transmission systems.

Mr Peltier has been granted several patents in the field of Telecommunication. He has authored numerous papers in France and abroad.

Since the early sixties he contributes to C.C.I.T.T. activities as a consultant to the French delegation.

EFFECT OF PAIR UNBALANCE ON CARRIER FREQUENCY

INSERTION LOSS AND CROSSTALK IN MULTIPAIR CABLE

by

A. F. Judy and J. J. Refi
Bell Laboratories
Norcross, Georgia 30071

Abstract

Insertion loss peaks and a special form of crosstalk have recently been observed in multipair cable. These phenomena arise because of the propagation of an undesired longitudinal signal on an unbalanced pair and can seriously limit the useful operating frequency of present cables. Empirical data together with analytic and heuristic models of the mechanism are presented. These reveal an inverse length-frequency relationship for the loss peaks and scaling rates of 12 dB per doubling of either frequency or length for far end crosstalk.

Introduction

Unbalance requirements for multipair telecommunications cable have traditionally been based on considerations of noise susceptibility in voice frequency trunks and subscriber loops. But as higher frequencies are used on twisted pairs, unbalance affects not only noise induction, but also signal propagation.

Signal propagation on twisted pairs occurs chiefly in two modes - balanced and longitudinal. The balanced mode is normally used for information transmittal while the longitudinal mode is generally considered undesirable (except when used for the D.C. powering of repeaters in simplex powering loops). To suppress the longitudinal signal, the conductors of a pair are normally excited with voltages that are equal and opposite. Perfectly balanced pairs propagate these voltages in the balanced mode, and the signals on each conductor maintain the same magnitude and opposite polarity at every point along the line. In reality, however, pairs are slightly unbalanced and the voltage on each conductor consists of two distinct components - a balanced mode signal and a longitudinal mode signal. It has recently been observed that this longitudinal signal gives rise to aberrations from the normal square root of frequency loss characteristic and also produces a special form of crosstalk.

Unbalance-Caused High Frequency Insertion Loss

Description of Phenomenon

Balanced transmission is the desired mode of propagation on twisted pairs, so pairs are most frequently excited with equal and opposite polarity voltages on each conductor as shown in Fig. 1. The difference

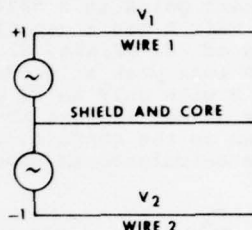


Fig. 1 - Normal excitation of pairs for balanced transmission.

between the voltages on each conductor, $V_1 - V_2$, is the signal normally detected. The equation for this signal is derived as Eq. 18 in Appendix A and can be used to express the insertion loss of an unbalanced pair. Evaluating this equation for a pair of length L and dividing it by the difference voltage at the source (2 volts from Fig. 1), the insertion loss of an unbalanced pair is given by

$$20 \log \left| \frac{V_1 - V_2}{2} \right| = -\alpha_b L - 20 \log \left| 1 + \frac{K_b K_\ell}{2 + K_b - K_\ell} \frac{[1 - e^{-(\gamma_\ell - \gamma_b)L}]}{2} \right|$$

where:

γ_b = near balanced propagation constant

γ_ℓ = near longitudinal propagation constant

K_b and K_ℓ = dimensionless constants proportional to unbalance

The $\alpha_b L$ term represents the customary balanced mode loss (in dB) which varies as the square root of frequency. The second term contributes additional loss due to pair unbalance and since it is dependent on the phase difference between the two modes, oscillates with frequency to produce loss peaks whenever the phase difference between the two modes is an odd multiple of π .

Relationship to Unbalance

Unbalance-caused high frequency loss was empirically observed in several jelly-filled T2-LOCAP cables. LOCAP is a low capacitance, low insertion loss multipair cable designed for use in the T2 Digital System.^{1,2} The cable uses 22 gauge copper conductors insulated with a dual expanded plastic³ and has a mutual capacitance of 46 nF/mile (39 nF/mile for the air core version). Because unbalance-caused degradations are functions of both frequency and cable length, and because T2 operates at twice the frequency (6.3 Mbaud/sec.) and at longer repeater spacings than

any other Bell System digital multipair cable system, unbalances in LOCAP are more likely to affect system performance than would unbalances in other cables and other systems. Additionally, capacitance unbalance to ground is generally higher in filled cables than in air core cables. For these reasons, filled LOCAP cables were extensively studied.

Figure 2 shows insertion loss plots for similar twist length pairs in a 5254' length of LOCAP cable. Pair A has a capacitance unbalance to ground of 282 pF/kft. (2.6%) and exhibits a 1.8 dB loss peak at 4 MHz. Contrastingly, Pair B with only an 83 pF/kft. unbalance has the normal \sqrt{f} loss shape. The dashed curve shown is the computed insertion loss of Pair A as calculated in Appendix B.

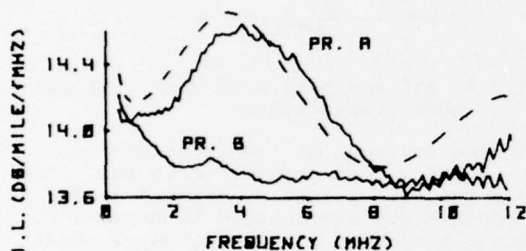


Fig. 2 - Insertion loss versus frequency for a highly unbalanced pair and a well-balanced pair. The dashed curve is the calculated loss for the unbalanced pair.

The calculated loss agrees well with the observed.

It should be noted here that not only capacitance unbalance to ground, but also unbalances in the other primary constants can generate longitudinal signals. However, capacitance unbalance is readily measurable and appears to be a major cause of the unbalance effects discussed in this paper.

In addition to the two pairs shown in Fig. 2, many others were examined for unbalance-caused excess loss. In most cases, the loss peaks occurred above 20 MHz. This enabled excess loss to be quantified by extracting an apparent dissipation factor over the 4 to 16 MHz frequency range. This dissipation factor is termed "apparent" because the phenomenon is not intrinsic to the cable's insulating or filling materials, but rather is related to pair unbalance.

A scatter plot of the apparent dissipation factor versus capacitance unbalance to ground is shown in Fig. 3 for 28 pairs. The logarithm of dissipation factor correlates highly ($\rho=0.89$) with capacitance unbalance - strongly suggesting that capacitance unbalance is the controlling mechanism.

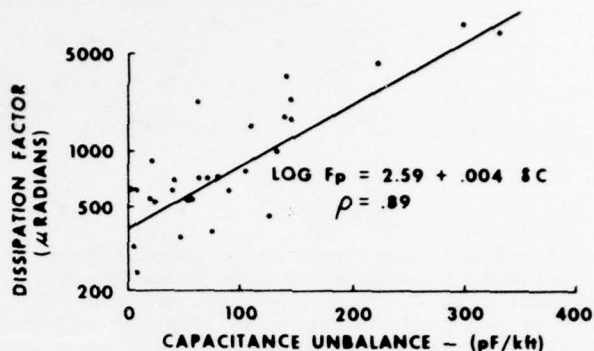


Fig. 3 - Apparent dissipation factor as a function of capacitance unbalance to ground.

Inverse Frequency-Length Behavior

As already discussed, the interaction of balanced and longitudinal modes produces loss peaks on the nominal \sqrt{f} loss shape. To a first approximation, these loss peaks occur whenever the phases of the balanced and longitudinal modes at the receive end differ by 180°. This occurs at a frequency inversely proportional to the difference in delays and cable length or $f=1/[2(\tau_R-\tau_D)L]$. This inverse frequency-length relationship was empirically demonstrated by measuring a specific pair in two individual cables and then splicing all the pairs in each cable together and rechecking the same pair in the spliced length.

Figure 4 shows the insertion loss of Pair 12 in Cable A. This pair has an unbalance of 190 pF/kft. and has 5 dB excess loss at 29 MHz

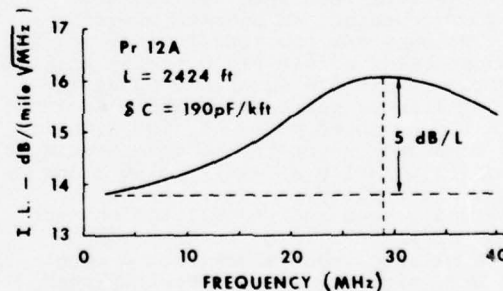


Fig. 4 - Insertion loss peak at 29 MHz in a highly unbalanced pair 2424' long.

in the 2424' length. Similarly, Pair 12 in the B cable (Fig. 5) has 7 dB excess loss at 22 MHz in a 2638' length. Its unbalance is 270 pF/kft.

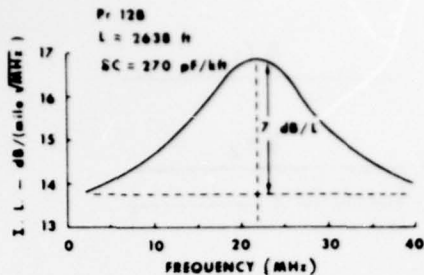


Fig. 5 - Insertion loss peak at 22 MHz in a highly unbalanced pair 2638' long.

When these two pairs were spliced together in an unbalance adding manner, the loss peak shifted to 12 MHz - about half the frequency of the peaks in the shorter lengths (Fig. 6).

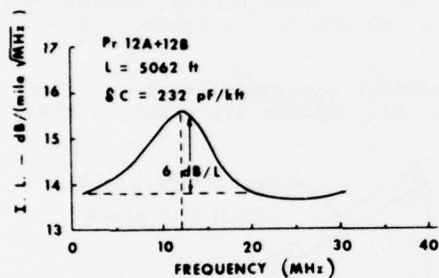


Fig. 6 - Insertion loss peak shifts to half the original frequency when length is doubled. Tip and ring are spliced unbalance adding.

As before:

$$f_i = \frac{A_i}{L_i}$$

where:

f_i = frequency of excess loss peak for Pair i

L_i = length of Pair i

$$A_i = \text{constant} = \frac{1}{2(\tau_{\ell i} - \tau_{bi})}$$

For Pair 12A,

$$A_i = A_{12A} = (29 \text{ MHz}) \times (2.424 \text{ kft.}) = 70.296$$

For Pair 12B,

$$A_j = A_{12B} = (22 \text{ MHz}) \times (2.639 \text{ kft.}) = 58.036$$

Since the two constants are not identical, an estimate of the grand A for the spliced length, $L = L_i + L_j$, is their weighted average:

$$A = \frac{A_{12A}L_{12A} + A_{12B}L_{12B}}{L_{12A} + L_{12B}}$$

$$A = 63.907$$

Then for the combined length

$$f = \frac{A}{L} = \frac{63.907}{5.062} = 12.6 \text{ MHz}$$

This is in good agreement with the 12 MHz observed in Fig. 6.

Reversing tip and ring conductors at the splice tends to cancel the unbalance and drastically alters the loss shape. The 6 dB

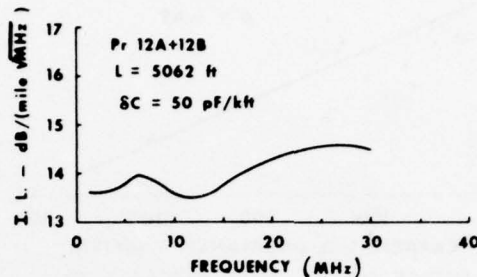


Fig. 7 - Insertion loss versus frequency for the pair in Fig. 6 when tip and ring are spliced to cancel unbalance.

peak at 12 MHz disappears, and a new smaller one is introduced that extends to even lower frequencies (Fig. 7).

Unbalance-Caused Crosstalk

Description of Phenomenon

As discussed earlier, unbalance causes two distinct voltages to propagate on each conductor of a pair. The sum of the total voltage on each conductor, $V_1 + V_2$, is frequently called the "longitudinal" signal and is given in Appendix A by Eq. 19.

$$V_1 + V_2 = \frac{K_b(2 - K_\ell)}{2 + K_b - K_\ell} \begin{pmatrix} -\gamma_\ell x & -\gamma_b x \\ e & -e \end{pmatrix}$$

For a perfectly balanced pair, $K_b = K_\ell = 0$, and $V_1 + V_2 = 0$. But for an unbalanced pair, this sum voltage has an associated current whose circuit is analogous to a coaxial tube. The two wires of the pair can be considered as the center conductor and all the other wires of the cable and its sheath constitute the outer conductor. At carrier frequencies, this "outer conductor" is primarily those pairs nearest the disturbing pair. Since these pairs carry portions of the longitudinal current, any unbalance in these pairs generates a difference signal - thereby producing crosstalk.

Near End Crosstalk

Near end crosstalk is overcome in T2 Systems through the use of separate go-and-return cables. Screened cables, however, are frequently used in other systems and their across screen near end crosstalk performance may impose system limitations.

Figure 8 shows a scatter plot of the across screen power sum near end crosstalk versus capacitance unbalance to ground for 28 pairs in a filled screened cable (14 pairs on each side of a bisecting screen). Although T2 does not use this type of cable, the measurements were made at T2's 3.15 MHz half-baud frequency. Correlation of near end crosstalk with capacitance unbalance is -0.69 , suggesting that unbalance-caused crosstalk contributes significantly to the total across screen crosstalk.

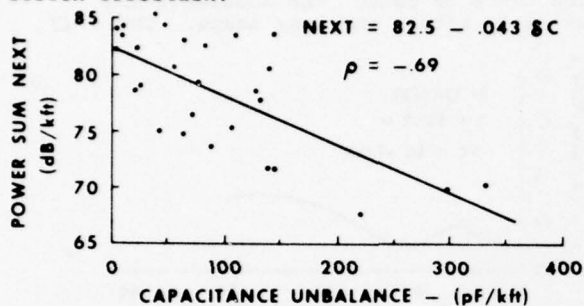


Fig. 8 - Across screen power sum near end crosstalk as a function of capacitance unbalance to ground.

Far End Crosstalk

T2 System repeater spacings are limited by thermal noise and far end crosstalk. Consequently, 3.15 MHz far end crosstalk performance is of considerable interest.

Figure 9 shows a scatter plot of power sum far end crosstalk versus capacitance

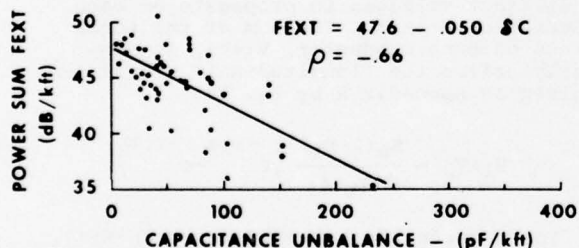


Fig. 9 - Power sum far end crosstalk as a function of capacitance unbalance to ground.

unbalance to ground for 50 pairs in a 5334' length of filled LOCAP cable. Correlation with capacitance unbalance is -0.66 , suggesting that unbalance-caused crosstalk contributes significantly to the far end crosstalk performance of these pairs.

Frequency Scaling - Frequency scaling of unbalance-caused far end crosstalk can be obtained from the following heuristic model. Although both impedance and admittance unbalances can be similarly argued, admittance unbalance will be treated here.

Consider Pair 1 in Fig. 10 to be a radiating transmitter whose signal strength is proportional to its total admittance unbalance, $\delta Y_1 L$. Similarly, Pair 2 is a receiving antenna whose sensitivity is proportional to its admittance unbalance, $\delta Y_2 L$. Then the

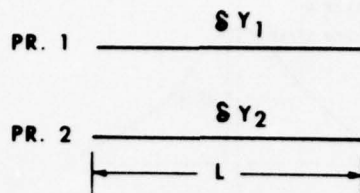


Fig. 10 - Model for far end crosstalk scaling between two unbalanced pairs.

crosstalk between these two pairs is proportional to the product of the two unbalances, $\delta Y_1 \delta Y_2 L^2$. Now $\delta Y = j\omega \delta C + \delta G$ and at carrier frequencies the conductance unbalance component is negligible. Consequently, δY is essentially dependent only on capacitance unbalance to ground (i.e., $\delta Y = j\omega \delta C$) and $XT \propto 20 \log (\omega^2 \delta C_1 \delta C_2 L^2)$. Consequently, crosstalk increases by 12 dB whenever frequency is doubled.

Two specific observed instances which demonstrate this scaling are shown in Fig. 11.

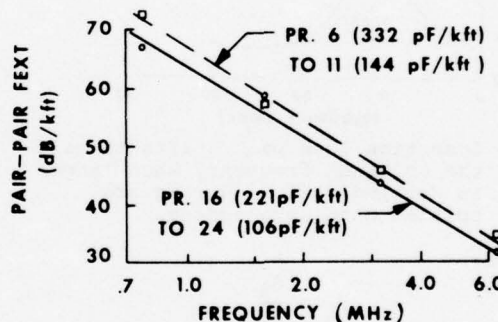


Fig. 11 - Two pair combinations illustrating the 12 dB per doubling of frequency scaling for unbalance-caused far end crosstalk.

Both these pair combinations exhibit frequency scalings near 12 dB/octave - twice that of the commonly assumed 6 dB rate.

Length Scaling - In the previous model it was argued that $XT \propto 20 \log (\omega^2 \delta C_1 \delta C_2 L^2)$. Consequently, length, L , which also appears as a squared term, will also increase crosstalk by 12 dB when doubled.

Two specific instances in which near 12 dB length scalings were observed are given below.

Cable No.	L(kft)	Capacitance Unbalance (pF/kft)		3.15 MHz FEXT (dB/L)	Degradation (dB) Meas. Predict	
		Pr.1	Pr.2			
A	5.3	125	-77	36.9	11.4	12.0
B	5.0	206	-93	36.5		
A+B	10.3	164	-85	25.3		
A	3.0	87	-253	41.1	11.3	12.1
B	2.3	122	-209	43.0		
A+B	5.3	102	-234	30.6		

Predicted and measured degradations agree extremely well. A sample calculation of the predicted degradation is given in Appendix C.

The above examples illustrate that far end crosstalk for individual pair combinations can scale at 12 dB per octave of length - four times the commonly assumed 3 dB rate. Power sum crosstalk, however, is the composite effect of many different kinds of crosstalk and so its length scaling is usually less than 12 dB/octave. Well-balanced pairs should scale at the standard 3 dB rate while highly unbalanced pairs should scale near 12 dB.

Length scaling for power sum far end crosstalk was empirically determined by measuring crosstalk at 3.15 MHz on a one-mile length of cable and then cutting the cable and remeasuring each half. Figure 12 shows a scatter plot of the length scaling as a function of capacitance unbalance. Correlation

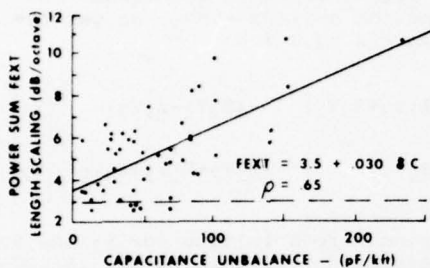


Fig. 12 - Power sum far end crosstalk length scaling as a function of capacitance unbalance to ground.

is 0.65 and the regression fit itself is intuitively satisfying in that the crosstalk-length scaling intercept is near the commonly assumed 3 dB. Length scaling for actual pairs is a strong function of their unbalance and average scaling for all 50 pairs is 5.3 dB/octave - 2.3 dB more than the 3 dB rule.

Carrier Frequency Unbalance

The previous data on unbalance-caused phenomena have been shown to correlate fairly well with capacitance unbalance to ground. It is clear, however, that capacitance unbalance is not the only form of unbalance. Since at voice frequencies $\gamma \approx \sqrt{j\omega RC}$, R and C essentially describe signal propagation. But at higher frequencies, inductance, L , becomes significant and $\gamma \approx \sqrt{(R + j\omega L)j\omega C}$. Consequently, while parameters which cause unbalance-phenomena at voice frequencies also cause phenomena at carrier frequencies, inductance unbalance also becomes significant. For example, an insulated conductor with a larger than nominal diameter over dielectric will not only have a lower capacitance to ground, but also a higher inductance. These unbalances tend to compensate each other and cause only a small aberration at carrier frequencies. On the other hand, if the change in ground capacitance is caused by a change in dielectric constant (such as through percent expansion of the insulation), then inductance unbalance will not occur. Consequently, the capacitive effect will not cancel and high frequency degradation could be substantial. Obviously, a

measure of all unbalances or "carrier frequency unbalance" would improve the correlations presented here. The fact that capacitance unbalance correlates as well as it does imputes it as being a major cause of high frequency unbalance effects.

Summary and Conclusions

Insertion loss peaks and a special form of crosstalk have recently been observed in multipair cable. The aberrations arise because normal excitation of an unbalanced pair with equal and opposite voltages causes not only a balanced signal but also an undesired longitudinal signal to propagate on the pair. When detected in the usual "balanced" fashion, these two signals interact with one another to produce loss peaks in the nominal square root of frequency loss characteristic. These peaks occur at frequencies inversely proportional to cable length and have magnitudes related to the degree of unbalance.

The longitudinal signal also causes a special form of crosstalk. Far end crosstalk can degrade at 12 dB per octave of frequency rather than at the normal 6 dB rate and at 12 dB per octave of length rather than at 3 dB.

The impact of these degradations on carrier systems performance depends on both the nature of the unbalance and on the particulars of the carrier system. High unbalance pairs in high frequency systems which use long repeater spacings are the most vulnerable.

Unless unbalances are improved, unbalance effects can seriously limit the application of present multipair cables. The problem is particularly acute with filled cable because its capacitance unbalance is generally higher than for air core. This is understandable since filling a cable exacerbates the capacitance unbalances which are already present. But nevertheless, the recent experiences with unbalance phenomena discourage any relaxation of unbalance requirements for carrier system cables.

Acknowledgements

Mr. W. G. Nutt of Bell Laboratories proposed the frequency and length scaling model for crosstalk and has offered many insights into unbalance phenomena. Mr. W. T. Anderson also of Bell Laboratories has done much work on unbalanced lines and has contributed through his comments and internal Bell Laboratories documents.

References

1. Setzer, D. E. and Windeler, A. S., "A Low Capacitance Cable for the T2 Digital Transmission Line," Proc. 19th International Wire and Cable Symposium, December 2, 1970.
2. Durham, R. L., Nutt, W. G. and Refi, J. J., "LOCAP: A Low Capacitance Cable for a High-Capacity System," Bell Laboratories Record, July/August, 1974.

3. Mitchell, D. M., "Material Savings by Design in Exchange and Trunk Telephone Cable, Part I: Waterproof Cable with Dual Insulation," Proc. 23rd International Wire and Cable Symposium, December 4, 1974.
4. Marx, K. D., "Propagation Modes, Equivalent Circuits, and Characteristic Terminations for Multiconductor Transmission Lines with Inhomogeneous Dielectrics," I.E.E.E. Trans. Microwave Theory Tech., pp. 450-457, July 1973.

Appendix A

Transmission Line Model Of an Unbalanced Pair

A differential length of a pair of wires adjacent to a shield or cable core can be represented by the model shown in Fig. A-1.

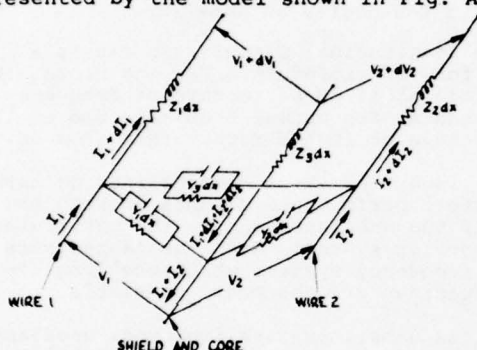


Fig. A-1 - Transmission line model of a pair adjacent to a shield or other wires in a cable core.

Each Z_i is composed of a resistive and inductive component and each Y_i a conductive and capacitive one. The voltage and current relations for this structure can be written as:

$$-dV_1 = (Z_1 dx)(I_1 + dI_1) + (Z_3 dx)(I_1 + dI_1 + I_2 + dI_2) \quad (1)$$

$$-dV_2 = (Z_2 dx)(I_2 + dI_2) + (Z_3 dx)(I_1 + dI_1 + I_2 + dI_2) \quad (2)$$

$$-dI_1 = V_1 Y_1 dx + (V_1 - V_2) Y_3 dx$$

$$-dI_2 = V_2 Y_2 dx + (V_2 - V_1) Y_3 dx$$

As dx approaches zero, it can be shown that the dI 's in Eqs. (1) and (2) become vanishingly small and the equations become

$$-\frac{dV_1}{dx} = (Z_1 + Z_3) I_1 + (Z_3) I_2 \quad (3)$$

$$-\frac{dV_2}{dx} = (Z_3) I_1 + (Z_2 + Z_3) I_2 \quad (4)$$

$$-\frac{dI_1}{dx} = (Y_1 + Y_3) V_1 - (Y_3) V_2 \quad (5)$$

$$-\frac{dI_2}{dx} = -(Y_3) V_1 + (Y_2 + Y_3) V_2 \quad (6)$$

If we assume that none of the Z 's or Y 's are functions of length (i.e., we have a uniform line), the voltage equations (3) and (4) can be differentiated with respect to x and Eqs. (5) and (6) can be substituted to eliminate the I 's. This reduces the four first order differential equations to two second order equations:

$$\begin{aligned} -\frac{d^2 V_1}{dx^2} = & [(Z_1 + Z_3)(Y_1 + Y_3) - Z_3 Y_3] V_1 \\ & + [(Z_1 + Z_3) Y_3 - (Y_2 + Y_3) Z_3] V_2 \\ -\frac{d^2 V_2}{dx^2} = & [(Z_2 + Z_3) Y_3 - (Y_1 + Y_3) Z_3] V_1 \\ & - [(Z_2 + Z_3)(Y_2 + Y_3) - Z_2 Y_3] V_2 \end{aligned} \quad (7)$$

This is solved by the usual method of hypothesizing the solution to be of the form $V_1 = v_1 e^{-\gamma x}$ and $V_2 = v_2 e^{-\gamma x}$ and finding the values of γ that yield acceptable solutions. So substituting for $d^2 V_i / dx^2 = \gamma^2 V_i$, we get the following matrix equation:

$$\begin{bmatrix} \gamma^2 - (Z_1 Y_1 + Z_1 Y_3 + Z_3 Y_1) & -(Z_3 Y_2 - Z_1 Y_3) \\ -(Z_3 Y_1 - Z_2 Y_3) & \gamma^2 - (Z_2 Y_2 + Z_2 Y_3 + Z_3 Y_2) \end{bmatrix} \begin{bmatrix} V_1 \\ V_2 \end{bmatrix} = \begin{bmatrix} 0 \\ 0 \end{bmatrix}$$

This yields nonzero solutions for V_1 and V_2 when the determinant of this matrix is zero. So γ can be found by solving the quadratic equation:

$$\begin{aligned} & [\gamma^2 - (Z_1 Y_1 + Z_1 Y_3 + Z_3 Y_1)] [\gamma^2 - (Z_2 Y_2 + Z_2 Y_3 + Z_3 Y_2)] \\ & = (Z_3 Y_1 - Z_2 Y_3) (Z_3 Y_2 - Z_1 Y_3) \end{aligned} \quad (8)$$

The solution is straightforward though complicated since all the Z 's and Y 's are complex numbers. But since it is readily solvable by computer we will not expand it further. Rather, we will approximate its solution for a slightly unbalanced transmission line by making the following assumptions:

$$Z_1 = Z; Z_2 = Z + \delta Z; |\delta Z| \ll |Z|$$

$$Y_1 = Y + \delta Y; Y_2 = Y; |\delta Y| \ll |Y|$$

Eq. (7) can then be approximately solved to give the following four solutions:

$$\gamma_b = \pm \sqrt{(Z_2 + \delta Z)(Y_3 + Y/2) + Z \delta Y/2} \quad (9)$$

$$\gamma_l = \pm \sqrt{(Z_3 + Z/2)(2Y + \delta Y) + \delta Z Y/2} \quad (10)$$

Here we have neglected all crossproducts and powers of δZ and δY .

It will be shown later that γ_b can be associated with the propagation constant of a balanced pair that has been excited with a balanced signal. Likewise, γ_l will be shown to be the longitudinal signal that can exist on a pair with an additional return path.

The general solution of the voltage on Wire 1 can now be written:

$$V_1 = Ae^{-\gamma_b x} + Be^{-\gamma_\ell x} + Ce^{\gamma_b x} + De^{\gamma_\ell x} \quad (11)$$

where A, B, C, D are constants determined by the boundary conditions (i.e., how the line is excited and terminated). The A and B terms with the negative exponent represent waves traveling in the positive direction. The C and D terms represent negative traveling waves.

Infinite Length Line

To keep the equations simple, we can assume an infinite length line. Then, in order to have finite voltages at all points, C and D must equal zero. Proceeding with this assumption, Eq. (7) is used to find the voltage on Wire 2:

$$V_2 = \frac{(Z_1 Y_1 + Z_1 Y_3 + Z_3 Y_1 - \gamma_b^2)}{Z_1 Y_3 - Z_3 Y_2} Ae^{-\gamma_b x} + \frac{(Z_1 Y_1 + Z_1 Y_3 + Z_3 Y_1 - \gamma_\ell^2)}{Z_1 Y_3 - Z_3 Y_2} Be^{-\gamma_\ell x} \quad (12)$$

or

$$V_2 = -(1+K_b)Ae^{-\gamma_b x} + (1-K_\ell)Be^{-\gamma_\ell x} \quad (13)$$

where K_b and K_ℓ are defined from Eq. (12). Once again, we can assume a slightly unbalanced line and derive the following approximations:

$$K_b \approx \frac{\delta Z(Y+2Y_3) - (Z+2Z_3)\delta Y}{2(ZY_3 - Z_3Y)}; \quad K_\ell \approx \frac{Z\delta Y - \delta ZY}{2(ZY_3 - Z_3Y)} \quad (14)$$

Note that K_b and K_ℓ are directly proportional to the unbalances in Z and Y. So as δZ and δY approach zero, K_b and K_ℓ will approach zero.

The denominator of K_b and K_ℓ is the difference of two terms. It can be approximately shown that:

$$2(ZY_3 - Z_3Y) \approx \gamma_b^2 - \gamma_\ell^2$$

So if the two modes' propagation constants are close to each other, the denominator will become small and K_b and K_ℓ can become large even though the unbalances are small. When this occurs the voltage on Wire 2 becomes very different from V_1 and unusual transmission effects will occur.

Difference or Balanced Signal

The usual mode of operation of a pair is to send and receive a balanced signal. That is, one deals with the difference between V_1 and V_2 :

$$V_1 - V_2 = (2+K_b)Ae^{-\gamma_b x} + K_\ell Be^{-\gamma_\ell x} \quad (15)$$

If the pair is perfectly balanced (i.e., $\delta Y = \delta Z = 0$), then $K_b = K_\ell = 0$ and the difference signal is just $2Ae^{-\gamma_b x}$. That is, even if both modes are excited and A and B are nonzero, the difference between the voltages will be deter-

mined only by the γ_b term, providing the pair is perfectly symmetrical. Otherwise, the voltage difference is given by Eq. (15). In this case, the voltage difference has two components or modes that interfere and reinforce, and the "balanced" signal is no longer truly balanced.

Sum or Longitudinal Signal

We can also talk about the sum or longitudinal signal. This is

$$V_1 + V_2 = -K_b Ae^{-\gamma_b x} + (2-K_\ell)Be^{-\gamma_\ell x} \quad (16)$$

If $K_b = K_\ell = 0$, this sum signal is $2Be^{-\gamma_\ell x}$. This is at times called the longitudinal signal on a pair because the current is traveling in the same direction on both conductors and is returning entirely on the shield or other conductors. As long as the pair is perfectly symmetrical, the signal will be determined entirely by the γ_ℓ term so γ_ℓ is frequently called the longitudinal propagation constant and $e^{-\gamma_\ell x}$ the longitudinal mode. This terminology is accurate only if K_b and K_ℓ are zero. Otherwise, the sum signal actually consists of both modes.

Currents and Impedances

Substituting Eq. (11) for V_1 and Eq. (13) for V_2 into Eqs. (5) and (6), we calculate the currents for an infinite line to be:

$$I_1 = \frac{Y_1 + (2+K_b)Y_3}{\gamma_b} Ae^{-\gamma_b x} + \frac{Y_1 + K_\ell Y_3}{\gamma_\ell} Be^{-\gamma_\ell x}$$

$$I_2 = -\frac{(1+K_b)Y_2 + (2+K_b)Y_3}{\gamma_b} Ae^{-\gamma_b x} + \frac{(1-K_b)Y_2 - (K_\ell)Y_3}{\gamma_\ell} Be^{-\gamma_\ell x}$$

where K_b and K_ℓ can be found from Eq. (12) for any line or can be approximated from Eq. (14). For a perfectly balanced line, $K_b = K_\ell = 0$, and it is easily shown that

$$I_1 = 2\sqrt{\frac{Y_3 + Y/2}{2Z}} Ae^{-\gamma_b x} + \frac{1}{2}\sqrt{\frac{2Y}{Z_3 + Z/2}} Be^{-\gamma_\ell x}$$

$$I_2 = -2\sqrt{\frac{Y_3 + Y/2}{2Z}} Ae^{-\gamma_b x} + \frac{1}{2}\sqrt{\frac{2Y}{Z_3 + Z/2}} Be^{-\gamma_\ell x}$$

From this we can define the two characteristic impedances to be:

$$Z_{0b} = \frac{V_1 - V_2}{(I_1 - I_2)/2} = \sqrt{\frac{2Z}{Y_3 + Y/2}}$$

$$Z_{0\ell} = \frac{(V_1 + V_2)/2}{I_1 + I_2} = \sqrt{\frac{Z_3 + Z/2}{2Y}}$$

When $K_b \neq 0$ or $K_\ell \neq 0$ these impedances can no longer be so simply defined since the sum and difference signals contain both modes. Rather

an impedance matrix must be used to relate V_1 and V_2 to I_1 and I_2 .⁴ In this case, Z_{0b} and $Z_{0\ell}$ as defined above no longer have any intrinsic meaning.

Boundary Conditions

To see how A and B are determined by the boundary conditions, assume that the infinite line is excited by connecting a perfect voltage source to the beginning of the line (Fig. A-2). Therefore, at $x=0$, we must have

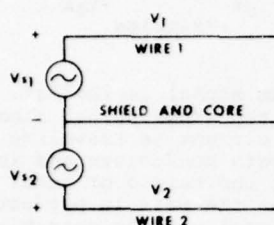


Fig. A-2 - Boundary conditions at the source on an infinitely long pair.

from Eqs. (11) and (13)

$$V_1(x=0) = V_{s1} = A + B$$

$$V_2(x=0) = V_{s2} = -(1+K_b)A + (1-K_\ell)B$$

So

$$A = \frac{V_{s1}(1-K_\ell) - V_{s2}}{2+K_b-K_\ell}; \quad B = \frac{V_{s1}(1+K_b) + V_{s2}}{2+K_b-K_\ell} \quad (17)$$

This implies that if one has an unbalanced line and desires to excite only the γ_b mode, then Eq. (17) can be used to find the type of excitation that would set $B=0$. This requires

$$V_{s2} = -V_{s1}(1+K_b)$$

So, if $K_b=0$, the two voltages need to be equal in magnitude and opposite in sign. This is the normal condition for exciting a balanced pair. However, if $K_b \neq 0$, since K_b is a complex number, the two generator voltages will be unequal in magnitude and with a phase difference other than 180° . But, even though this excitation will generate only one mode, there will still be both a net difference signal (Eq. (15)) and a sum signal (Eq. (16)). This cannot be avoided if the line is unbalanced since it is impossible to set Eq. (16) equal to zero over a wide frequency range.

Since unbalanced pairs are usually excited in a balanced manner, let us continue and calculate the transmission response for $V_{s1}=+1$ and $V_{s2}=-1$ volts. A and B are found from Eq. (17) and the difference or "balanced" signal is found from Eq. (15) to be

$$V_1 - V_2 = e^{-\gamma_b x} \left[2 - \frac{K_b K_\ell}{2+K_b-K_\ell} \left(1 - e^{-(\gamma_\ell - \gamma_b)x} \right) \right] \quad (18)$$

Similarly, by substituting A and B from Eq. (12) into Eq. (16), the sum or "longitudinal" signal becomes

$$V_1 + V_2 = \frac{K_b(2-K_\ell)}{2+K_b-K_\ell} \begin{pmatrix} e^{-\gamma_\ell x} & -e^{-\gamma_b x} \end{pmatrix} \quad (19)$$

Appendix B

Computed Insertion Loss of 282 pF/kft Unbalanced Pair

The insertion loss of the LOCAP pair in Fig. 2 having a capacitance unbalance of 282 pF/kft. (2.6%) was calculated using the formulas developed in Appendix A. The various wire parameters used are as follows (all units are per mile):

$$Y_1 = j\omega C_1 = j\omega (57.02 \text{ nF})$$

$$Y_2 = j\omega C_2 = j\omega (58.51 \text{ nF})$$

$$Y_3 = j\omega C_3 = j\omega (16.81 \text{ nF})$$

$$C_1 - C_2 = 282 \text{ pF/kft}$$

$$L_1 = L_2 = 610 \text{ } \mu\text{H}$$

$$L_3 = 190 \text{ } \mu\text{H}$$

$$R_1 = R_2 = 250 \sqrt{\text{Freq. (MHz)}} \text{ ohms}$$

$$R_3 = 90 \sqrt{\text{Freq. (MHz)}} \text{ ohms}$$

$$Z_i = R_i + j\omega L_i$$

Here we have neglected the small effect of conductance on the Y's.

The values for the above parameters were derived as follows: the C's were measured at 1 kHz using a capacitance bridge; the balanced R_1 and L_1 were derived from the nominal attenuation and phase of LOCAP; the lack of any R or L unbalance was determined from open and short circuit impedance measurements on the two conductors of the pair; R_3 and L_3 were estimated from the attenuation and delay of the longitudinal signal as well as being selected to locate the loss dip at 4 MHz.

When these parameters are substituted into the exact Eqs. (8), (12) and (18), the following values for γ_b , γ_ℓ , K_b , K_ℓ and transmission deviation are derived. (The approximate equations, (9), (10) and (14), are not sufficiently accurate for unbalances this large.)

Freq. (MHz)	Mode	Gamma		K		Transmission Dev.	
		(nep)	(rad)			(dB)	(Deg)
1	b	1.54	j 46.85	-.612	-j.049	-.2	4.4
	l	1.63	j 47.63	-.736	-j.122		
4	b	3.07	j187.3	-.617	-j.025	-1.9	1.8
	l	3.27	j190.4	-.756	-j.063		
8	b	4.35	j374.6	-.618	-j.018	-0.2	-.4
	l	4.62	j380.8	-.759	-j.045		
12	b	5.32	j561.9	-.618	-j.014	-1.8	1.6
	l	5.66	j571.2	-.760	-j.037		

As this table and Fig. 2 show, the attenuation deviation peaks whenever the difference between the two modes' phases is an odd multiple of π . Also apparent is the fact that K_b and K_l are mainly real and vary only slightly with frequency.

Appendix C

Sample Calculation of FEXT Degradation with Length

The predicted crosstalk degradation is calculated by taking the product of the capacitance unbalance for each pair in the long length and dividing this by the weighted average of the unbalance product for the two pairs in each shorter length.

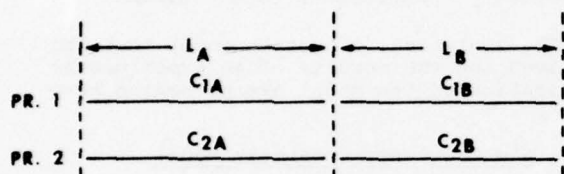


Fig. C-1 - Model for calculating unbalance-caused far end crosstalk degradation with length.

FEXT degradation =

$$20 \log \frac{|C_1 C_2|}{\frac{|C_{1A} C_{2A}| L_A + |C_{1B} C_{2B}| L_B}{L_A + L_B}}$$

Where:

C_{1A} = total unbalance of Pair 1 in length L_A

C_{1B} = total unbalance of Pair 1 in length L_B

C_{2A} = total unbalance of Pair 2 in length L_A

C_{2B} = total unbalance of Pair 2 in length L_B

$$C_1 = C_{1A} + C_{1B}$$

$$C_2 = C_{2A} + C_{2B}$$

For the first example given in the text:

$$L_A = 5.3 \text{ kft}$$

$$L_B = 5.0 \text{ kft}$$

$$C_{1A} = 125(5.3) = 662$$

$$C_{1B} = 206(5.0) = 1030$$

$$C_{2A} = -77(5.3) = -408$$

$$C_{2B} = -93(5.0) = -465$$

$$C_1 = 662 + 1030 = 1692$$

$$C_2 = -408 - 465 = -873$$

FEXT degradation =

$$\begin{aligned} & 20 \log \frac{|1692(-873)|}{|662(-408)|5.3 + |1030(-465)|5.0} \\ & \quad \quad \quad 5.3 + 5.0 \\ & = 20 \log \frac{1,477,116}{371,381} \\ & = 20 \log 3.98 \\ & = 12.0 \text{ dB} \end{aligned}$$



Arthur F. Judy
Bell Laboratories
2000 Northeast Expressway
Norcross, Georgia 30071

Mr. Judy received his B.S.E.E. Degree from the University of Maryland in 1967, and his M.S.E.E. from the University of Michigan in 1968. Since then, he has been a Member of Technical Staff at Bell Laboratories working on the theory and measurements of coaxial and multipair cable.



James J. Refi
Bell Laboratories
2000 Northeast Expressway
Norcross, Georgia 30071

Mr. Refi began work with Bell Laboratories in 1966 at the Baltimore Laboratory as a Member of Technical Staff. His early assignments dealt with land coaxial cable and with techniques for controlling crosstalk in multipair cable. More recently, Mr. Refi has worked on the development of filled and larger pair sizes of T2-LOCAP cable at the Atlanta Laboratory. He has contributed to the knowledge of structural return loss and unbalance phenomena in multipair cable.

Mr. Refi received the B.S.E.E. from Villanova University in 1966 and the M.S.E.E. from the Polytechnic Institute of Brooklyn in 1968. He is a member of I.E.E.E., Tau Beta Pi and Eta Kappa Nu.

CHARACTERIZATION OF CROSSTALK IN TWISTED PAIR TELEPHONE CABLES WITH NONMATCHED TERMINATIONS

by

J. C. Isaacs, Jr., T. F. McIntosh and T. D. Nantz
Bell Laboratories
Norcross, Georgia 30071

Abstract

A mathematical model is presented which predicts pair-to-pair crosstalk in twisted pair telephone cables for any set of non-matched, but balanced, terminating impedances. This model can be used to greatly reduce the number of measurements required to characterize crosstalk performance in the low frequency range down to voice frequencies. Using four nonmatched crosstalk measurements for a given pair combination, along with the propagation constants and characteristic impedances of both the disturbing and disturbed pairs, the model predicts crosstalk at a given frequency for any matched or nonmatched terminations.

Extensive measurements show good agreement between measured and model-predicted crosstalk values to frequencies as low as 10 KHz. Differences between the measurements and predictions are typically less than half a dB for a wide range of terminating conditions. These results show that it is possible to utilize the model to characterize crosstalk at low frequencies for any terminating conditions with a relatively small basic set of nonmatched measurements.

Introduction

Crosstalk is a significant source of interference which can limit the rate of information transmission in multipair cable systems. Previous characterizations of crosstalk in multipair cables have been based on measurements made principally in the frequency range from 100 KHz to 10 MHz, with the terminations reasonably well matched to the impedances of the pairs. Crosstalk data below 100 KHz has been sparse and of limited usefulness because the characteristic impedance of the cable pair changes rapidly with frequency in this range. Thus it is impossible to approximately match the pairs with fixed terminations except over a relatively narrow bandwidth. For the nonmatched conditions, voltage reflections at the terminations can significantly affect measured crosstalk, particularly as the attenuation drops with decreasing frequency. Crosstalk loss measurements made for one set of terminating conditions can differ by 10 dB or more from those at the same frequency for a different set of terminations.

The increasing number of new services on multipair cable which operate in the frequency range below 100 KHz has emphasized the need for crosstalk characterization in this range. Since crosstalk at low frequencies is

strongly affected by the terminating conditions of the pairs, a prohibitively large amount of crosstalk data measured under various terminating conditions would be required for adequate characterization. A theoretical model for crosstalk prediction which accounts for the effects of nonmatched terminations was needed to keep the number of necessary measurements to a minimum.

The analytical crosstalk model that was developed and the results of an experimental verification of the model are presented herein.

Low Frequency Crosstalk Model

The low frequency crosstalk model is based on the following assumptions:

- (1) The crosstalking circuits comprise a linear system.
- (2) "Weak" coupling exists between the pairs, i.e., the effects of the disturbed circuit on the disturbing circuit can be neglected.
- (3) Single mode propagation is present on both pairs. (This paper is confined to balanced mode propagation.)

The first assumption implies that the superposition principle holds. The weak coupling assumption allows for a straightforward analysis of the voltage and current on the disturbing pair. The third assumption greatly simplifies the derivation of the model formulas and reinforces assumption 2.

Since weak coupling is assumed, the voltage and current on the disturbing pair can be analyzed independently of the voltage and current on the disturbed pair. Using elementary transmission line analysis¹, the voltage and current at point x on the disturbing pair are of the form:

$$V_1(x) = A_1 e^{-\Gamma_1 x} + A_2 e^{\Gamma_1 x} \quad (1a)$$

$$I_1(x) = \frac{1}{Z_{01}} [A_1 e^{-\Gamma_1 x} - A_2 e^{\Gamma_1 x}] \quad (1b)$$

where A_1 and A_2 are complex coefficients determined from the terminating conditions of the disturbing line, Γ_1 is the propagation constant for the disturbing line, and Z_{01} is the characteristic impedance of the disturbing line.

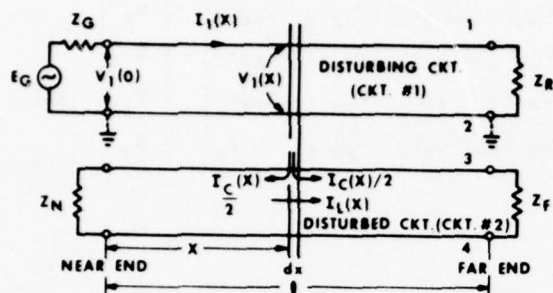


FIGURE 1
CROSSTALK CIRCUIT MODEL

Figure 1 shows the circuit diagram for the crosstalk model. Currents and voltages are induced in the disturbed circuit through capacitive and inductive couplings (See Reference 2). At a given point x along the disturbing line the currents and voltages given by Equation (1) represent steady state values. These voltages and currents can be considered as resulting from a summation of steady state component values caused by reflections from the disturbing pair terminations. Similarly, the voltages and currents on the disturbed pair can be considered as a sum of steady state components resulting from termination reflections. Since the disturbed circuit does not affect the disturbing circuit, and the principle of superposition applies, the summation process in the disturbed circuit can be analyzed using the voltages and currents represented by Equation (1). The initial steady state current on the disturbed line at point x can be resolved into a near-end and far-end component (See Figure 1).

$$I_N(x) = V_1(x) j\omega \frac{C_c(x)}{2} - I_1(x) j\omega \frac{L_c(x)}{2Z_{02}} \quad (2a)$$

$$I_F(x) = - \left\{ V_1(x) j\omega \frac{C_c(x)}{2} + I_1(x) j\omega \frac{L_c(x)}{2Z_{02}} \right\} \quad (2b)$$

where the subscripts N and F refer to the near end and far-end, respectively. $C_c(x)$ and $L_c(x)$ are the capacitive and inductive coupling components at point x . Z_{02} is the character-

istic impedance of circuit 2, and ω is the radian frequency.

If the near-end crosstalk, $N(\omega)$, and the equal level far-end crosstalk, $F(\omega)$, are defined as (See Figure 1)

$$N(\omega) \triangleq \frac{V_2(0)}{V_1(0)} \quad (3a)$$

and

$$F(\omega) \triangleq \frac{V_2(l)}{V_1(0)e^{-\Gamma_1 l}} \quad (3b)$$

then a reflection analysis of the disturbed circuit, using Equation (2), yields the following formulas:

$$N(\omega) = K_N [C_{N1}N_A(\omega) + C_{N2}F_{12}(\omega) + C_{N3}F_{21}(\omega) + C_{N4}N_B(\omega)] \quad (4a)$$

$$F(\omega) = K_F [C_{F1}N_A(\omega) + C_{F2}F_{12}(\omega) + C_{F3}F_{21}(\omega) + C_{F4}N_B(\omega)] \quad (4b)$$

where:

$$K_N \triangleq \frac{Z_N(1+k'_N)}{(A_1+A_2)K_{NF}} \quad (5a)$$

$$K_F \triangleq \frac{Z_F(1+k'_F)}{(A_1+A_2)K_{NF}} \quad (5b)$$

$$k'_N \triangleq \frac{Z_{02}-Z_N}{Z_{02}+Z_N} = \text{current reflection coefficient for the near-end.} \quad (5c)$$

$$k'_F \triangleq \frac{Z_{02}-Z_F}{Z_{02}+Z_F} = \text{current reflection coefficient for the far-end.} \quad (5d)$$

$$K_{NF} = 1 - k'_N k'_F e^{-2\Gamma_2 l} \quad (5e)$$

$$N_A \triangleq j\omega \int_0^l \frac{1}{2} \left[Z_{02}C_c(x) + \frac{L_c(x)}{Z_{01}} \right] e^{-(\Gamma_1+\Gamma_2)x} dx \quad (5f)$$

= $N(\omega)$ (circuit 1 to circuit 2) with terminating impedances matched to the lines.

$$F_{12} \triangleq j\omega e^{(\Gamma_1-\Gamma_2)l} \int_0^l \frac{1}{2} \left[Z_{02}C_c(x) - \frac{L_c(x)}{Z_{01}} \right] e^{-(\Gamma_1-\Gamma_2)x} dx \quad (5g)$$

= $F(\omega)$ (circuit 1 to circuit 2) with terminating impedances matched to the lines

$$F_{21} \triangleq j\omega e^{(\Gamma_2-\Gamma_1)l} \int_0^l \frac{1}{2} \left[Z_{01}C_c(x) - \frac{L_c(x)}{Z_{02}} \right] e^{-(\Gamma_2-\Gamma_1)x} dx \quad (5h)$$

= $F(\omega)$ (circuit 2 to circuit 1) with terminating impedances matched to the lines.

$$N_B \Delta j \omega \int_0^l \frac{1}{2} \left[Z_{02} C_c(x) + \frac{L_c(x)}{Z_{01}} \right] e^{-(\Gamma_1 + \Gamma_2)(l-x)} dx \quad (5i)$$

=N(ω) (circuit 1 to circuit 2) with terminating impedances matched to the lines, and measured at the opposite end of the cable from which N_A was measured.

$$C_{N1} = \frac{A_1}{Z_{02}} \quad (5j)$$

$$C_{N2} = \frac{-k'_F A_1}{Z_{02}} e^{-(\Gamma_1 + \Gamma_2)l} \quad (5k)$$

$$C_{N3} = \frac{A_2}{Z_{01}} e^{(\Gamma_1 - \Gamma_2)l} \quad (5l)$$

$$C_{N4} = \frac{-k'_F A_2}{Z_{02}} e^{(\Gamma_1 - \Gamma_2)l} \quad (5m)$$

$$C_{F1} = \frac{-k'_N A_1}{Z_{02}} e^{(\Gamma_1 - \Gamma_2)l} \quad (5n)$$

$$C_{F2} = \frac{A_1}{Z_{02}} \quad (5o)$$

$$C_{F3} = \frac{-k'_N A_2}{Z_{01}} e^{-2(\Gamma_2 - \Gamma_1)l} \quad (5p)$$

$$C_{F4} = \frac{A_2 e^{2\Gamma_1 l}}{Z_{02}} \quad (5q)$$

Equation (4) indicates that $N(\omega)$ and $F(\omega)$ can be calculated for any set of balanced terminating conditions if the matched coefficients N_A , F_{12} , F_{21} , and N_B are known. These coefficients can be obtained by measuring $N(\omega)$ and/or $F(\omega)$ under four sets of terminating conditions. Using two near-end and two far-end measurements, Equation (4) can be expressed in matrix notation as:

$$\begin{bmatrix} (N(\omega))_1 \\ (N(\omega))_2 \\ (F(\omega))_1 \\ (F(\omega))_2 \end{bmatrix} = \begin{bmatrix} K_N & 0 & 0 & 0 \\ 0 & K_N & 0 & 0 \\ 0 & 0 & K_F & 0 \\ 0 & 0 & 0 & K_F \end{bmatrix}$$

$$\times \begin{bmatrix} (C_{N1})_1 & (C_{N2})_1 & (C_{N3})_1 & (C_{N4})_1 \\ (C_{N1})_2 & (C_{N2})_2 & (C_{N3})_2 & (C_{N4})_2 \\ (C_{F1})_1 & (C_{F2})_1 & (C_{F3})_1 & (C_{F4})_1 \\ (C_{F1})_2 & (C_{F2})_2 & (C_{F3})_2 & (C_{F4})_2 \end{bmatrix} \begin{bmatrix} N_A \\ F_{12} \\ F_{21} \\ N_B \end{bmatrix} \quad (6a)$$

or

$$\underline{X}_U = K \underline{C} \underline{X}_M \quad (6b)$$

The subscripts 1 and 2 on the terms in parenthesis indicate measured or calculated quantities for terminating conditions 1 and 2. The matrix Equation (6b) can be solved for \underline{X}_M to obtain the matched crosstalk coefficients. These coefficients can then be used in Equation (4) to calculate $N(\omega)$ and $F(\omega)$ for any set of balanced terminations, given the propagation constants and the characteristic impedances of the two pairs.

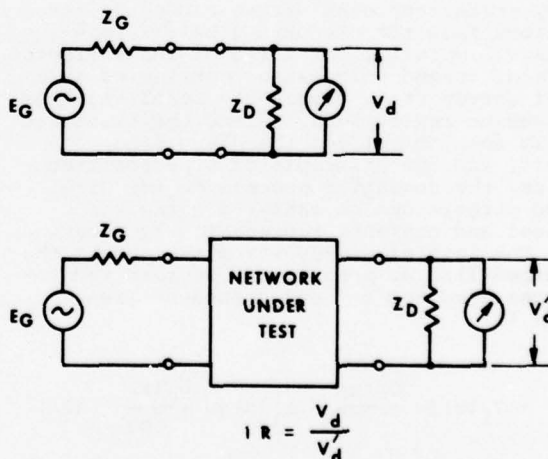


FIGURE 2

INSERTION RATIO MEASUREMENT

Crosstalk Measurements

Crosstalk measurements are performed utilizing a Computer-Operated Transmission Measuring Set (COTMS)³. COTMS employs a standard/unknown comparison technique to measure insertion loss and phase in the 50 Hz to 1 GHz range. Loss levels up to 150 dB can be measured over a frequency band of 10 KHz to 10 MHz with a repeatability of 0.1 dB. A repeatability of 1.0 degrees for phase is attainable at the 150 dB level. Below 100 dB, the repeatability of loss and phase for the full frequency range is improved to 0.05 dB and 0.1 degrees³.

The crosstalk of a cable pair can be expressed in terms of the insertion loss and phase which COTMS measures. Referring to Figure 2, the insertion ratio (IR) is defined as the ratio of the voltage at the detector prior to the insertion of the network (V_d) to the voltage at the detector after insertion of the network (V'_d). Insertion loss is equal to $20 \log_{10} |IR|$ and insertion phase is the angle of IR.

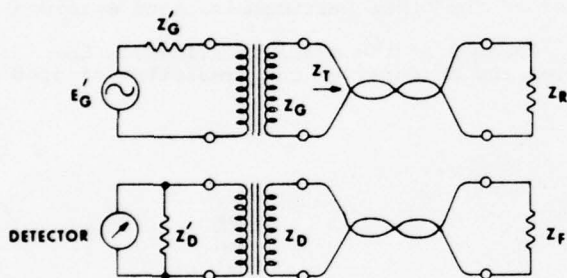


FIGURE 3

NEAR-END CROSSTALK MEASUREMENT

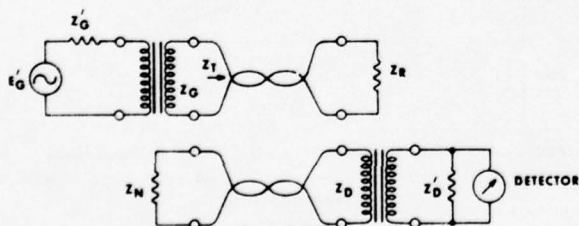


FIGURE 4

FAR-END CROSSTALK MEASUREMENT

The near-end and far-end crosstalk losses are defined by

$$N(\omega)_{dB} = -20 \log_{10} |N(\omega)| \quad (8a)$$

$$F(\omega)_{dB} = -20 \log_{10} |F(\omega)|, \quad (8b)$$

where $N(\omega)$ and $F(\omega)$ are given by Equation (3). Equation (8) expresses crosstalk loss as a positive number. Crosstalk phase is the angle of either $N(\omega)$ or $F(\omega)$. Figures 3 and 4 show the COTMS circuit configurations for insertion ratio measurements from which near-end and far-end crosstalk losses and phases are derived. Z_R , Z_N and Z_F are selectable resistive terminations. In terms of the measured insertion loss and the terminating conditions, the near-end crosstalk becomes

$$N(\omega)_{dB} = IL_{dB} - 20 \log_{10} \left| \frac{(Z_G + Z_T)Z_D}{(Z_G + Z_D)Z_T} \right| \quad (9)$$

For equal level far-end crosstalk,

$$F(\omega)_{dB} = IL_{dB} - 20 \log_{10} \left| \frac{(Z_G + Z_T)Z_D}{(Z_G + Z_D)Z_T} \right| + 20 \log \left| e^{-\Gamma_1 l} \right| \quad (10)$$

When the generator, detector, and resistive terminations are matched to the characteristic impedance of the pairs, the near-end crosstalk loss $N(\omega)_{dB}$ in Equation 9 is equal to the measured crosstalk insertion loss. For this same matched case, $F(\omega)_{dB}$ reduces to the measured crosstalk insertion loss minus the transmission insertion loss of the disturbing pair, measured between the same matched generator and detector. If the generator and/or the detector and/or the terminating resistors are not matched, as will generally be the case in the low frequency range, the crosstalk of interest must be computed from Equations 9 or 10.

In addition to the crosstalk insertion loss measurements, the propagation constant (Γ) and characteristic impedance (Z_0) for each pair must be obtained at each measurement frequency. These parameters are obtained from transmission insertion loss measurements utilizing previously published techniques⁴.

The measurements of pair-to-pair near-end and far-end crosstalk loss and phase, along with the transmission properties of the individual pairs, provide the inputs required to solve Equation (6) for the matched crosstalk coefficients (N_A , F_{12} , F_{21} , N_B). Four crosstalk measurements with known terminating conditions are required. After extensive testing, the following four conditions were selected (Refer to Figures 3 and 4):

1. Near-end crosstalk measured with

$$Z_R = Z_F = \infty$$

2. Near-end crosstalk measured with

$$Z_R = Z_F = 0$$

3. Far-end crosstalk measured with

$$Z_R = Z_N = \infty$$

4. Far-end crosstalk measured with

$$Z_R = Z_N = 0$$

The actual measurements to verify the crosstalk model were all made on a 2000-foot length of standard production 25-pair, 26-gauge air core PIC cable.

Computations and Model Verification

The measurement data for the 25-pair, 26-gauge cable were transferred to a general purpose computer for processing and analysis. Computer programs have been implemented to accomplish the basic data flow shown in Figure 5. The dashed vertical line divides the COTMS measurements and processing from the general purpose processing. Crosstalk measurements for selected mismatched conditions are used as input to Equation (6) to evaluate the matched crosstalk coefficients. These coefficients in turn are used to compute pair-to-pair crosstalk for other termination conditions. Comparisons can be made on a pair-to-pair or statistical basis. The transmission properties are measured separately and become input parameters to the programs.

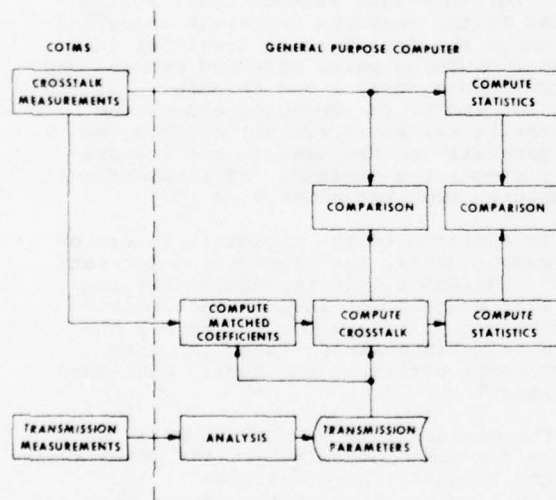


FIGURE 5
SIMPLIFIED DATA FLOW CHART

The model verification program divided naturally into two phases. Phase A involved performing measurements and predictions for a small set of pair combinations for a range of frequencies and for a variety of termination mismatch conditions. Phase B examined a large set of pair combinations for a range of frequencies and for a single set of mismatched terminations.

Table I shows a sample comparison at 100 KHz from Phase A, utilizing pair number 03 for the disturbing circuit and pair number 04 for the disturbed circuit. No significant change in accuracy was observed for an extensive variety of terminating conditions. Two other pair combinations were examined for selected sets of non-matched terminations with similar results.

The two near-end and two far-end measurements used to obtain the matched crosstalk coefficients are included in Table I.

One test of the validity of the model is to examine the maximum differences between measurements and predictions for all termination conditions tested. This worst-case comparison is shown in Table II for four frequencies for pair combination 03/04. The apparent improving model performance with increasing frequency was not consistently observed for other pair combinations examined.

Phase B of the model verification involved the measurement and prediction of cross-

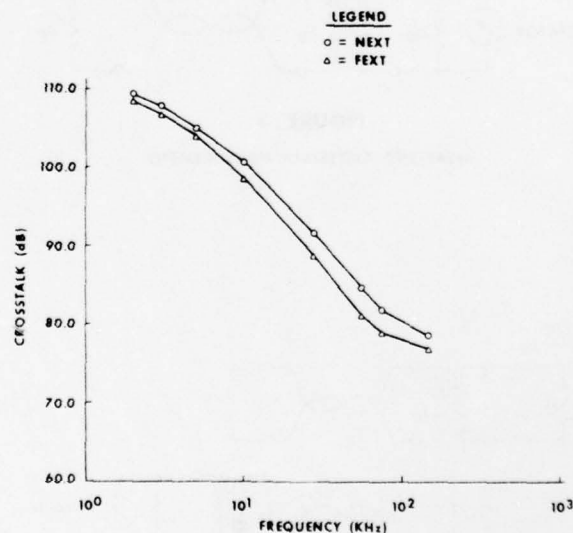


FIGURE 6
AVERAGE CROSSTALK

talk for a large set of the 300 possible pair combinations of the 25 pair cable. This phase tests the model under a variety of pair separations, twist length configurations, and capacitance unbalance conditions. Two near-end and two far-end measurements were made for each pair combination, utilizing the open and short circuit conditions required for evaluating the matched coefficients. Measurements were also made for the following additional set of nonmatched terminations:

$$Z_G = 600 \text{ ohms}$$

$$Z_R = 900 \text{ ohms}$$

$$Z_N = Z_F = 135 \text{ ohms.}$$

Figure 6 shows the average near-end and far-end crosstalk loss versus frequency for this termination condition.

Table III compares the statistics of the measured and predicted near-end and far-end crosstalk for five frequencies. The difference between the mean measured and predicted crosstalk is less than approximately 0.5 dB, and this difference exhibits no apparent trend with frequency.

Summary

A mathematical crosstalk model has been described which can greatly reduce the number of measurements required to characterize the crosstalk performance of twisted pair cable with nonmatched terminations. The model is particularly useful for the low frequency range down to voice frequencies. Extensive model verification testing has been performed using a 25-pair, 26-gauge PIC cable for a range of terminations, frequencies, and pair combinations. The model typically predicts near-end and far-end pair-to-pair crosstalk to within 0.5 dB of measured values for termination conditions between zero and infinite ohms, for frequencies between 10 KHz and 150 KHz, and for the pair configurations, twist schemes and capacitance unbalances characteristic of standard production cables.

Future work will expand the model verification to other gauge and pair size cables, and to lower frequencies, and will examine crosstalk length scaling laws for nonmatched terminations.

TABLE I
PAIR-TO-PAIR CROSSTALK
PAIRS 03/04
100 KHz

NEXT				
Z_R (Ohms)	Z_F (Ohms)	Measured (dB)	Predicted (dB)	Difference (dB)
∞	∞	86.13	86.13	-
0	0	75.26	75.26	-
100	∞	83.86	83.88	0.02
100	0	78.13	77.91	-0.22
100	100	80.30	80.18	-0.12
∞	100	83.98	83.91	-0.07
0	100	77.86	77.95	0.09
FEXT				
Z_R (Ohms)	Z_N (Ohms)	Measured (dB)	Predicted (dB)	Difference (dB)
∞	∞	83.48	83.48	-
0	0	69.85	69.85	-
100	∞	75.89	75.93	0.04
100	0	72.93	72.72	-0.21
100	100	74.33	74.29	-0.04
∞	100	81.44	81.33	-0.11
0	100	70.84	71.01	0.17

TABLE II
PAIR-TO-PAIR CROSSTALK
PAIRS 03/04

NEXT					
Frequency (kHz)	Z_R (Ohms)	Z_F (Ohms)	Measured (dB)	Predicted (dB)	Difference (dB)
10	0	600	107.65	106.32	-1.33
50	0	600	89.41	89.85	0.44
100	600	0	81.17	80.92	-0.25
150	100	100	75.55	75.66	0.11

FEXT					
Frequency (kHz)	Z_R (Ohms)	Z_N (Ohms)	Measured (dB)	Predicted (dB)	Difference (dB)
10	0	∞	97.83	96.81	-1.02
50	100	∞	78.84	79.25	0.41
100	∞	0	78.79	78.45	-0.34
150	600	∞	86.57	87.02	0.45

TABLE III
AVERAGE CROSSTALK

NEXT				
Frequency (kHz)		Measured (dB)	Predicted (dB)	Difference (dB)
10	Mean	100.67	100.46	-0.21
	σ	6.60	6.55	-0.05
28	Mean	91.79	91.40	-0.39
	σ	6.50	6.77	0.27
56	Mean	84.73	84.38	-0.35
	σ	6.12	6.19	0.07
76	Mean	81.94	81.59	-0.35
	σ	6.37	6.69	0.32
150	Mean	78.69	78.40	-0.29
	σ	7.02	6.90	-0.12

FEXT				
Frequency (kHz)		Measured (dB)	Predicted (dB)	Difference (dB)
10	Mean	98.70	98.39	-0.31
	σ	6.65	7.26	0.61
28	Mean	88.88	88.37	-0.51
	σ	7.12	7.88	0.76
56	Mean	81.21	80.80	-0.41
	σ	6.60	7.50	0.90
76	Mean	79.09	78.66	-0.43
	σ	6.71	6.76	0.05
150	Mean	76.95	76.64	-0.31
	σ	6.82	6.84	0.02

REFERENCES

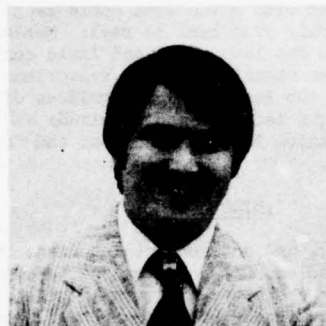
1. Johnson, W.C., "Transmission Lines and Networks," McGraw Hill, 1950.
2. Campbell, G. A., "Dr. G. A. Campbell's Memorandum of 1907 and 1912," BSTJ, October, 1935.
3. Anderson, R.E., "Computer Controlled Cable Measurements," 21st International Wire and Cable Symposium, December, 1972.
4. J. Kreutzberg and T. D. Nantz, "Precision Insertion Loss Measurements and Data Analysis on Multipair Cable," 24th International Wire and Cable Symposium, November, 1975.



Thomas F. McIntosh graduated with a BSEE from North Carolina State University in 1959, and received his MSEE from Duke University in 1961. He has been employed by Bell Laboratories since 1959. He is currently a Member of the Technical Staff in the Transmission Media Laboratory. Tom has worked on computer modeling of electrical performance and costs of multipair cables.



J. C. Isaacs, Jr., received his BEE, MEE, and PhD degrees from the University of Virginia. He joined Bell Laboratories in 1970. Since that time he has engaged in studies of crosstalk in multipair cable. Jim is currently employed by Honeywell, Inc., Marine Systems Division, Seattle, Washington.



T. D. Nantz received the BSEE from the University of Pennsylvania in 1968, and the MSEE from Northeastern University in 1972. He is currently a Member of Technical Staff at Bell Laboratories engaged in measurement of transmission and crosstalk properties of multipair cable.

EFFECTS OF CABLE UNBALANCES ON POWER INDUCED CIRCUIT NOISE

by

Myron L. Brewer
Rural Electrification Administration
Washington, D. C.

and

Howard P. Price
Central Telephone Company
Chicago, Illinois

SUMMARY

The telephone industry, in establishing cable specification parameters, appears to have overlooked the effects of cable unbalances on power induced circuit noise under field operating conditions. Until recently, for example, capacitance unbalance objectives were specified to shield. Actual operating conditions indicate that objectives for capacitance unbalance to ground are more realistic.

While there have been some internal studies completed with various organizations, there is little recently-published data on this important subject. Such studies as there are have usually been based on mathematical models which assume uniformity of the various factors contributing to circuit noise over the entire length of the cable selected (i.e., uniform capacitance unbalance to ground, resistance unbalance, and power exposure).

These factors are all variables under field conditions with capacitance and resistance unbalances varying from pair to pair within the same cable length as well as in the same pair from reel to reel. Measurement of circuit noise in the laboratory and field confirm that the circuit noise magnitude at the subscriber location is dependent on the location and magnitude of cable unbalances and the location and magnitude of the power exposure in relation to the subscriber and central office location.

INTRODUCTION

Economic, energy, and environmental considerations have created problems not only for the telephone industry but for the power industry as well. Maximum utilization of available power sources is essential to meet increasing demands while at the same time staying within economic and environmental restrictions. The overall effect of accomplishing these complex and often conflicting goals can be an increasingly hostile environment for the operation of voice frequency telephone circuits in multipair cable.

In many areas of the country, the magnitude of power influence (noise-to-ground) is increasing. This makes it more difficult to maintain quiet voice frequency circuits. It is sometimes difficult, if not impossible, for a power company to effectively reduce the magnitude of power influence to an acceptable level.

For example, let's consider an overhead three-phase power line from which a single-phase tap must be extended. Many government jurisdictions today require that all new utility wire extensions be placed underground. When the single-phase extension is buried, it will effectively appear like a capacitor across that phase of the three-phase system at the point of connection, and it can magnify undesirable harmonics which may be induced in an adjoining telephone system. There will usually be an increase in power influence in the area of the three-phase line. Due to the close relationship of the buried conductors to ground, there is no practical treatment available which may be applied to the buried tap to offset this effect.

Heretofore, communications circuits with a balance of 60 dB (decibels) and greater would usually provide quiet subscriber service meeting telephone industry objectives of 20 dBrnc (decibels reference noise - C-message weighted), 26 dBrnc for long rural circuits. This was partially due to the fact that the magnitude of the majority of power influence levels were in the 70 to 80 dBrnc range.

With the rise in power influence levels in some areas today, values of power influence in the range of 90 dBrnc and above are not uncommon. Thus, to meet noise objectives in such areas, an operating telephone circuit must have a balance of 70 dB or greater. A brief discussion of circuit balance, as derived from noise measurements, is included in Appendix A.

INDUCTIVE INTERFERENCE

Principles of the induction of longitudinal voltages on communication conductors from paralleling power lines have long been established and understood, so they will not be further discussed in this paper. The overall manner of the conversion of these longitudinal voltages to circuit voltages (noise metallic) due to unbalances, is also generally understood.

Circuit noise due to series (resistance) unbalance is a function of the longitudinal current flowing in the two conductors of the cable pair. If the cable pair is open circuited at both ends with no connection to ground, there can be only a slight conversion from longitudinal to circuit noise due to series unbalances. Conversely, circuit noise resulting from shunt (capacitance) unbalance is a function of the longitudinal voltage on the two conductors of the circuit.

Subscriber Loops

Subscriber loops have a high longitudinal impedance to ground at the subscriber location and a low longitudinal impedance to ground at the central office. Highest impedance to ground at the subscriber location will occur where bridged ringing is used. Where ringing is divided, the impedance to ground will be lower but will still be significantly higher than that at the office location.

Distribution of voltage to ground along a subscriber loop ranges from a minimum value at the central office to a maximum value at the subscriber location. Thus, a shunt unbalance in the cable nearest the subscriber location will result in higher longitudinal to circuit noise conversion than will occur when cable with the same shunt unbalance value is located near the central office. Magnitude of voltage to ground at the office location is the voltage drop across the relay winding.

Subscriber loop longitudinal noise current is inverse to noise voltage to ground; minimum at the subscriber location and maximum at the central office. Series unbalance in cable located near the office will produce higher longitudinal to circuit noise conversion than will occur with the same unbalance value in cable near the subscriber location. The relationship of longitudinal voltage and current distribution along subscriber

loops is shown in Figure 1.

This discussion will not include a detailed description of longitudinal to circuit noise conversions in physical trunk circuits. When such conversions in subscriber loops are understood there should be little problem in considering trunk circuits. Generally trunk circuits have a low longitudinal impedance to ground at both ends and thus circuit noise resulting from series unbalance in cable located near either end of the trunk route will be highest. Effects of shunt unbalances will be greatest in cable located near the center of the trunk route where voltage to ground will be highest.

Circuit Unbalances

Studies have been made to analyze the contribution of resistance and capacitance unbalances to circuit noise in multipair communications cables. Unfortunately many of these studies were completed for internal use within the company or system for which they were prepared and therefore are not available for general information. As a result, there has been little recent information published on this important subject. The most notable recent work has been the Bell Laboratories; "Inductive Interference Engineering Guide." 1

These studies have usually been based on mathematical models and assume uniformity of various factors over the entire length of the cable studies, i.e., uniform capacitance unbalance to ground, uniform resistance unbalance, uniform power exposure. Such ideal conditions do not exist with cable in the field.

Other studies have divided the cable in segments of perhaps ten kilofeet and analyzed the effects of average unbalance in shorter segment models. While this does provide additional information, there is some question whether true field conditions are being simulated. For example, three such segments would be used for a thirty kilofeet subscriber loop. Assuming one ten kilofeet length with high shunt unbalance, there would be three magnitudes of longitudinal to circuit noise conversion depending on its location in relation to the subscriber. It is still difficult to develop realistic limits for cable specifications which minimize noise problems.

Subscriber loops are usually made up of more than one cable size between the central office and subscriber location. Long rural loops may be made up of several sizes. Where long lengths of the same size cable are required, there may be several reels involved. This results in varying values of unbalance, series and shunt, throughout the length of a subscriber loop. Larger pair count cables are usually provided in shorter reel lengths than small pair count cables.

Splicing two reels together will often mate offsetting unbalances and effectively reduce overall circuit noise. This occurs most frequently near office locations where there are more frequent splices due to the shorter reel lengths.

Splicing can also match two unbalances which add rather than offset, thus increasing noise levels. A short reel may contain pairs with severe unbalance but due to the length will not contribute significantly to noise levels in the overall finished circuit.

Smaller pair count cables are normally provided with long lengths on a single reel. Along rural subscriber loops a long run of a single size small pair count cable is quite likely. The location of such long lengths of small pair count cable is always near the subscriber location. Capacitance unbalance to ground

in these cables can result in severe noise problems even when the magnitude of unbalance is below the maximum averages usually published in existing specifications.

FIELD EXPERIENCE

During a noise investigation it was determined that individual cable unbalances were within the specification limits and power influence was not excessive. The only solution was to analyze the noisy pairs individually and do any work necessary to improve the overall balance.

The first circuit was 24-gauge, 58,233 feet long with 12 load points. Power influence was 80 dBrnc and circuit noise 27 dBrnc for a balance of 53 dB. A resistance unbalance of approximately 12 ohms was found between load points 2 and 4. The tip and ring conductors were reversed at load point 3. Power influence at the subscriber location was still 80 dBrnc and circuit noise was now 17 dBrnc for a balance of 63 dB.

A second circuit 18,561 feet long was next investigated. Power influence at the subscriber location was 82 dBrnc and circuit noise 21 dBrnc for a balance of 61 dB. The 9000 feet of 12-24 cable adjacent to the subscriber location had a capacitance to ground unbalance of 175pF/kf, below the 200pF/kf maximum average currently specified by REA. After reversal of the tip and ring conductors at the midpoint of the unbalance power influence was 81 dBrnc and circuit noise was 10 dBrnc for a balance of 71 dB.

A 29,227 foot circuit was also investigated. Power influence at the subscriber location was 79 dBrnc and circuit noise 28 dBrnc for a balance of 51 dB. There was 6,669 feet of cable adjacent to the subscriber location with a capacitance unbalance to ground of 600pF/kf. The tip and ring conductors were reversed at a point 4,500 feet from the subscriber location. Power influence was now 79 dBrnc and circuit noise 12 dBrnc for a balance of 67 dB.

A circuit 51,285 feet in length was found with a power influence of 80 dBrnc and a circuit noise of 26 dBrnc for a balance of 54 dB. Unbalances ranged from 800pF/kf between load points 5 and 6 to 65pF/kf between load points 7 and 9. Three tip and ring reversals were made between the fourth load point and the ninth load point. After completion of the reversals, the power influence was 80 dBrnc at the subscriber location and circuit noise 14 dBrnc for a balance of 66 dB. A reduction in circuit noise of 7 dB was achieved with the reversal of the tip and ring conductors at load point 8 in the cable with only 65pF/kf unbalance.

Analysis of the improvements in noise performance accomplished by tip and ring reversals to offset unbalances in adjacent cable sections indicated best results were obtained with capacitance unbalance when it was located near the subscriber location. This was especially notable with the 51,285 foot circuit when it was determined the greatest reduction in circuit noise was obtained in the cable with the lowest capacitance unbalance to ground.

LABORATORY INVESTIGATION

A laboratory study was undertaken to investigate further the effects of unbalance location on circuit noise. An artificial line 69 kilofeet in length of 24 H-88 cable was used. The artificial line was of three part design with capacitance to ground and was composed of one 12 kilofeet section at the office end followed by three 18 kilofeet sections with 3 kilofeet

of non-loaded cable at the subscriber end. Noise was placed longitudinally on the line through the ports consisting of balanced three winding transformers. One transformer was used in each of the 18 kilofeet sections.

Capacitance unbalance to ground was then placed on this line with a capacitor decade and the resulting circuit noise measured at the subscriber end of the line. Unbalances were located at the office end, 12 kilofeet, 30 kilofeet, 48 kilofeet and at the subscriber end. The line before introducing unbalances, had 80 dBrnc of power influence and 18.5 dBrnc of circuit noise for a balance of 61.5 dB. Capacitance unbalance to ground simulating 6000 feet of cable with 150pF and 800pF/kilofeet were used. Results of these tests are shown in Table 1.

6000 Feet of Cable Unbalance
Circuit Noise Measured @ Subscriber Location

150pF/kilofeet.					
	C.O.	12kf	30kf	48kf	Subscriber
PI	80	80	80	80	80
CN	18.5	18.7	20	21	24
Bal.	61.5	61.3	60	59	56

800pF/kilofeet.					
	C.O.	12kf	30kf	48kf	Subscriber
PI	80	80	80	80	80
CN	18.9	22	24.5	28	34
Bal.	61.1	58	55.5	52	46

TABLE 1

A second set of unbalances were used simulating 12 kilofeet of cable with 150pF and 800pF/kilofeet. It is acknowledged that continuous reel lengths of 12 kilofeet are most likely to occur in small pair count cables located near the subscriber. Closer to the office cables will be in larger pair count sizes and thus are supplied in shorter lengths per reel. Results of these tests are shown in Table 2.

12000 Feet of Cable Unbalance
Circuit Noise Measured @ Subscriber Location

150pF/kilofeet.					
	C.O.	12kf	30kf	48kf	Subscriber
PI	80	80	80	80	80
CN	18.5	19.5	21	23	27.5
Bal.	61.5	60.5	59	57	52.5

800pF/kilofeet.					
	C.O.	12kf	30kf	48kf	Subscriber
PI	80	80	80	80	80
CN	19.5	26	28.5	32.5	39
Bal.	60.5	54	51.5	47.5	41

TABLE 2

Recorded results of these tests further indicate that the greatest conversion from longitudinal to circuit noise due to capacitance unbalance occurs when the unbalance is located near the subscriber. The cable size and distance between the subscriber and central office do not appear to have a bearing on this.

In rural companies it often occurs on the longer cable routes in smaller pair count cables. Where the area is more urban it can also occur in larger pair count cables along shorter cable routes. The magnitude of power influence, of course, usually determines whether or not the unbalance will be detected due to a noise problem.

FIELD INVESTIGATION

Since it could not be determined that the method used for imposing longitudinal noise on the artificial lines was having the same effect as the induced noise on cable pairs in the field, it was decided to continue the investigation in the field. Individual parameters of each loading section were measured in addition to noise measurements at the subscriber location.

Abbotsburg, North Carolina

The first cable studied was in Abbotsburg, North Carolina. It was approximately 51 kilofeet in length (Figure 2) and unbalances were introduced at approximately 7, 16, 25, 34, and 43 kilofeet. The cable was 24 D-66 and composed of 900, 600, 400, 300, 150, 100, 50 and 18 pair sizes. Pairs 2 and 3 were used for the tests and the results are shown in Table 3. Values of 150pF and 800pF/kilofeet for 4500 and 9000 foot lengths of cable were used. Before testing power influence was 73 dBrnc and circuit noise -1 dBrnc on pair 2 and 4.5 dBrnc on pair 3 for balance of 74 and 68.5 dB respectively.

Abbotsburg, North Carolina
4500 Feet of Simulated Cable Unbalance
Circuit Noise Measured @ Subscriber Location

Pair 2 150pF/kilofeet.					
Unbal. @	7kf	16kf	25kf	34kf	43kf
PI	73	73	73	73	73
CN	-5	4	3	6	8
Bal.	78	69	70	67	65

Pair 3 150pF/kilofeet.					
PI	73	73	73	73	73
CN	4	-2	3	6	8
Bal.	69	75	70	67	65

Pair 2 800pF/kilofeet.					
PI	73	73	73	73	73
CN	-5	3	12	16	19
Bal.	78	70	61	57	54

Pair 3 800pF/kilofeet.					
PI	73	73	73	73	73
CN	4	4	5	14	17
Bal.	69	69	68	59	56

TABLE 3

The same measurements were then repeated introducing unbalances to simulate 12 kilofeet of cable with 150pF and 800pF/kilofeet unbalance. Results of these tests are shown in Table 4.

Study of these test results show patterns similar to those originally found during noise investigations in the field and laboratory investigations. The unusual drop in circuit noise found on Pair 3 when faults were introduced at the 16 kilofeet point was due to a high capacitance unbalance on the other conductor immediately adjacent to that location. This was being balanced out by the unbalance being added during the tests.

Abbottsburg, North Carolina
9000 Feet of Simulated Cable Unbalance
Circuit Noise Measured @ Subscriber Location

<u>Pair 2</u> <u>150pF/kiloft.</u>					
Unbal. @	7kf	16kf	25kf	34kf	43kf
PI	73	73	73	73	73
CN	-5	3	6	10	12
Bal.	78	70	67	63	61

<u>Pair 3</u> <u>450pF/kiloft.</u>					
PI	73	73	73	73	73
CN	4	-1	1	7	11
Bal.	69	74	72	67	62

<u>Pair 2</u> <u>800pF/kiloft.</u>					
PI	73	73	73	73	73
CN	-1	7	17	21	24
Bal.	74	66	56	52	49

<u>Pair 3</u> <u>800pF/kiloft.</u>					
PI	73	73	73	73	73
CN	5	9	13	20	23
Bal.	68	64	60	53	50

TABLE 4

Olivia, North Carolina

The next tests were made at Olivia, North Carolina on a 41,250 foot 22 D-66 cable. The circuit was made up of approximately 20,250 feet of 200 pair, 13,500 feet of 150 pair and 7,500 feet of 18 pair cable (Figure 3). Faults were introduced at points approximately 7, 16, 25, and 33 kilofeet and at the subscriber location. Values simulating 150pF/ and 800pF/kilofoot for 4500 and 9000 lengths of cable were used. Recorded results of these tests are shown in Table 5. Power influence before the tests was 90 dBrnc and circuit noise 8 dBrnc for a balance of 82 dB.

Olivia, North Carolina
4500 Feet of Simulated Cable Unbalance
Circuit Noise Measured @ Subscribers Location

<u>150pF/kiloft.</u>					
Unbal. @	7kf	16kf	25kf	33kf	Subscriber
PI	90	90	90	90	90
CN	5	8	9	16	25.5
Bal.	85	82	81	74	64.5

<u>800pF/kiloft.</u>					
PI	90	90	90	90	90
CN	5	6	11	18	31
Bal.	81	81	73	65	52

<u>9,000 Ft. of Simulated Cable Unbalance</u> <u>150pF/kiloft.</u>					
PI	90	90	90	90	90
CN	5	6	11	18	31
Bal.	85	84	79	72	59

<u>800pF/kiloft.</u>					
PI	90	90	90	90	90
CN	18	18	24	30	44
Bal.	72	72	66	60	46

TABLE 5

Again the data shows the high circuit noise which occurs when the capacitance unbalance is located near the subscriber. The effects diminish rapidly as the unbalance is located at greater distances from the subscriber location. This example is more striking due to the high value of power influence. To meet noise objectives of 20 dBrnc a cable balance of 70 dB is necessary.

Manito, Illinois

The last work in the field was two series of tests on the same cable pair in Manito, Illinois. The first series was with the pair approximately 24,000 feet in length. The cable had approximately 3.8 kilofeet of 400-22, 15.8 kilofeet of 300-22 with the balance 101-22 (Figure 4) and was H-88 loaded. Unbalances were introduced at the office, 12 kilofeet and the end of the cable where all measurements were made. Since actual power influence from power lines in this area was below 65 dBrnc a noise generator was placed in the center tap of the terminating box at the central office and the output adjusted to provide 81 dBrnc power influence so measurements could be completed. Before starting tests the power influence was 81 dBrnc and circuit noise 18.5 dBrnc for a balance of 62.5 dB. Results of these tests are shown in Table 6.

Manito, Illinois
6000 Feet of Simulated Cable Unbalance
Circuit Noise Measured @ Subscriber Location

<u>166.7pF/kiloft.</u>			
Unbal. @	C.O.	12kf	Subscriber
PI	81.0	81.0	81.0
CN	22.5	27.5	29.0
Bal.	58.5	53.5	52.0

<u>833.3pF/kiloft.</u>			
PI	81.0	81.0	81.0
CN	35.5	39.0	41.0
	45.5	42.0	40.0

TABLE 6

The same characteristic increase in circuit noise is obvious as the unbalance is located closer to the subscriber location. The increase with an unbalance at the office seems high. However, this is likely to occur should the source of the power influence be located near the office.

The second in this series of tests utilized the same cable pair. Approximately 10,000 feet of 100-22 cable (Figure 5) was added to the subscriber end. Unbalances were added at 12 kilofeet, 24 kilofeet and the subscriber location. Results of these tests are shown in Table 7. Power influence before tests was 80 dBrnc and circuit noise 13 dBrnc for a balance of 67 dB.

The same patterns appear but here the resulting changes are smaller than in the first series of tests. This seems to indicate again that the results are valid for a situation where the power influence source is close to the office. The location and length of the power influence has a strong bearing on the magnitude of circuit noise when an unbalance is located near the middle of the cable.

Manito, Illinois
6000 Feet of Simulated Cable Unbalance
Circuit Noise Measured at Subscriber Location

<u>166.7pF/kiloft.</u>			
Unbal. @	<u>12kf</u>	<u>24kf</u>	<u>Subscriber</u>
PI	80.0	80.0	80.0
CN	<u>20.5</u>	<u>21.5</u>	<u>23.5</u>
Bal.	59.5	58.5	56.5

<u>833.3pF/kiloft.</u>			
PI	80.0	80.0	80.0
CN	<u>30.8</u>	<u>34.5</u>	<u>36.7</u>
Bal.	49.2	45.5	43.3

TABLE 7

The effects of resistance unbalance were explored at the two locations in North Carolina, but the results were shaded by the location of the power influence source. Basic influence was from the 540 Hz harmonic and at both sites was located near the subscriber end of the cable. At the Abbottsburg test site the power line analysis found significant influence only in the last 2000 feet of cable at the subscriber end. At Olivia it was only in the last 8000 feet of cable. This resulted in a stable current along the cable to the office rather than an increasing current as is normally expected.

Thus the effects of resistance unbalance tests are not conclusive. The results of tests with resistance unbalances in the same cable as in Table 5 are shown in Table 8. Power influence before tests was 90 dBm and circuit noise 8 dBm for a balance of 82 dB.

Olivia, North Carolina
Circuit Noise Measured @ Subscribers Location

<u>1 Ohm Unbal.</u>					
	<u>7kf</u>	<u>16kf</u>	<u>25kf</u>	<u>33kf</u>	<u>Subscriber</u>
PI	90	90	90	90	90
CN	<u>10</u>	<u>11</u>	<u>13</u>	<u>13</u>	<u>8</u>
Bal.	80	79	77	77	82

<u>8 Ohm Unbal.</u>					
PI	90	90	90	90	90
CN	<u>17</u>	<u>17</u>	<u>18</u>	<u>18</u>	<u>8</u>
Bal.	73	73	72	72	82

TABLE 8

NEW METHOD OF MEASURING UNBALANCES

The conventional method of measuring cable unbalances requires several pieces of test equipment.

Resistance unbalance is measured with a Wheatstone Bridge. This entails a varley measurement which with some equipment can be read only to the nearest ohm. More accuracy can be obtained by measuring the resistance of each conductor separately using the cable shield as a return path. Then the capacitance unbalance bridge is measured with a capacitance unbalance bridge.

In addition to the bridge, an oscillator and null detector are required. Many companies do not have the manpower capability or equipment to perform these measurements.

IEEE has published a Standard, P455-1975,² describing a method for measurement of longitudinal balance. A test set designed to utilize this method provides the magnitude of series and shunt balance (conversion from longitudinal signal to metallic signal) of various component parts of the telephone system.

Since the major component of series unbalance in a length of telephone cable is resistance and that of shunt unbalance is capacitance, the possibility of using this test for determining cable balance was considered.

The design of the set is based on the formula:

$$\text{Balance in dB} = \frac{X_1 + X_2 + \frac{X_1 X_2}{R} + R}{X_1 - X_2}$$

Where for testing cable:

- X_1 = Longitudinal impedance of tip conductor
- X_2 = Longitudinal impedance of ring conductor
- R = Internal test set impedance

For series balance, X_1 and X_2 are the conductor resistances. For shunt balances they are the capacitance reactance of each conductor to ground. Computations were made for various resistance and capacitance unbalances which were plotted on graphs. Two of these are included as Graph 1 and 2 for series and shunt unbalances, respectively for 4500 and 6000 foot sections of cable.

During these noise investigations both conventional and longitudinal measurements were made on loading section lengths of cable. Precise values of capacitance and resistance unbalance could be obtained from the charts based on series and shunt longitudinal balance measurements.

There are some definite advantages when using the longitudinal balance method. Only one test set is required with one connection to tip, ring and shield at the measuring end. The conventional method requires two test sets with more complex test setups and each must be connected independently at the measuring end.

At the far end the same procedure is required for both methods, tip and ring shorted and connected to the cable shield for series (resistance unbalance) and open circuited for shunt (capacitance unbalance) measurements.

CONCLUSION

This paper has presented data showing the relationship between cable unbalances (series and shunt) and power induced circuit noise under field operating conditions. The data affirms that all elements contributing to circuit noise are variable and thus, attempts to compute such effects generally fall short of actual performance. Location, length and magnitude of both power influence and communications cable unbalances vary from route to route.

Pair size of the cable does not appear to have a bearing on circuit noise. When exposed to power influence, unbalanced pairs will have circuit noise whether in large or small pair count cable. Due to manufacturing problems the specification requirements for capacitance unbalance are not as restrictive for cables smaller than 12-pair.

In a rural environment, capacitance unbalance in small pair count cable installed near the subscriber location will most often be a major factor to circuit noise. Capacitance unbalance in large pair count cables will be a major factor to noise when located near the subscriber in urban areas.

Capacitance unbalances below the maximum average values shown in existing cable specifications will produce unacceptable circuit noise in the presence of medium power influence when the unbalanced cable is close to the subscriber location. When the sole source of power influence is short and located near the subscriber, circuit noise will drop rapidly as the location of a single cable capacitance unbalance is moved from the subscriber end toward the office.

This drop in circuit noise will not occur as rapidly if the power influence is distributed along the total length or near the middle of the cable route. When the capacitance unbalance is moved toward the office the drop in circuit noise will be much smaller when the sole source of power influence is located near the office.

The REA Specification For Filled Telephone Cables, PE-39, contains the following requirements for pair-to-ground capacitance unbalance and conductor resistance unbalance:

"The pair-to-ground capacitance unbalance as measured on the completed cable shall not exceed the following values when tested at a frequency of 1000 ± 100 Hz and a temperature of $23^\circ \pm 3^\circ\text{C}$:"

Number of Cable Pairs	Capacitance Unbalance to Ground	
	pF/kf (pF/km)	pF/kf (pF/km)
	Indiv. Max.	Max. Average
6	800 (2625)	
12 or more	800 (2625)	200 (656)

"The difference in dc resistance between the two conductors of a pair in the completed cable shall not exceed the following:"

Resistance Unbalance - Maximum for any Reel		
Gauge	Average	Individual Pair
19 & 22	1.5%	4.0%
24	1.5%	5.0%
26	2.0%	5.0%

Where: % Res. Unbal. = $\frac{(\text{Max. Res.} - \text{Min. Res.})}{\text{Min. Res.}} \times 100$

Cables having capacitance and resistance unbalance values near specified maximum averages will result in unacceptable balance in subscriber loop plant. In many areas the magnitude of power influence is at the point where it is difficult to maintain quiet voice frequency circuits.

There is no indication that improvement will occur in the future. We believe that existing cable specifications are not tight enough to provide the quiet circuits the telephone user has a right to expect, regardless of his location.

Even though it may be impractical to reduce average unbalance requirements immediately effort should be directed toward improving the state of the art in cable production. Results from this investigation indicate there is a need for communication cable with better balance.

Testing of individual cable circuits one by one to isolate areas of unbalance in noise problems can be time consuming and expensive. Many small companies do not have the manpower capability or equipment to undertake such a project.

Data presented herein is an introduction to a long range investigation with the ultimate goal of realistic unbalance objectives for cable specifications. More locations should be studies for effects of both series and shunt unbalances.

REFERENCES

1. "Inductive Interference Engineering Guide," Bell Laboratories, Electromagnetic Interference Department, Loop Transmission Division, Preliminary Issue, March 1974.
2. "Standard Test Procedure for Measuring Longitudinal Balance of Telephone Equipment Operating in the Voice Band," IEEE Standard 455-1976.

APPENDIX A

Circuit Balance

Circuit balance is a measure of the susceptibility of a telephone circuit. Susceptibility may be expressed as the relationship between the longitudinal noise (common mode) and the metallic noise that will result from a given longitudinal influence.

A common method of determining the balance of various components and devices is by application of a balanced longitudinal voltage to the terminals of the component or device being tested. Resulting metallic voltages are then measured and the balance determined as follows:

$$\text{Component Bal.} = 20 \log \frac{V_L}{V_m}$$

Where: V_L = Longitudinal Voltage

V_m = Metallic Voltage

Determination of overall circuit balance is similar to the method for individual components but some new factors must be considered. Location, length and magnitude of inductive exposure along the length of the circuit; location, length, magnitude and polarity of various unbalances (series and shunt); dc voltage levels; and the frequencies of induced voltage all contribute to the overall circuit balance.

Longitudinal voltage induced on the tip and ring conductors of a telephone circuit is balanced and may be utilized for test purposes like the balanced longitudinal voltage applied in the longitudinal balance test circuit. Unbalances in the circuit will result in some of this induced longitudinal voltage being converted to metallic voltage. Magnitudes of these two voltages measured as noise may be used to determine overall circuit balance. Values of noise-to-ground (power influence) and noise metallic (circuit noise) are obtained from measurements at the subscriber location. Overall circuit balance may now be determined as follows:

$$\text{Circuit Balance (dB)} = N_g - N_m$$

The resulting circuit balance is a measure of the ability of the circuit to prevent longitudinal to metallic conversion of voltages and currents. Levels and frequency of inductive interference are subject to changes depending on load demand along the power

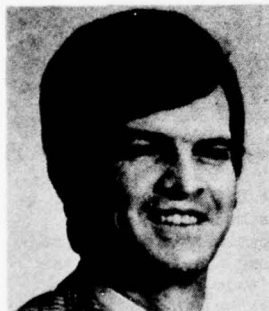
circuit. In general, the circuit balance is indicative of conditions only at the time the measurement was made.



Myron L. Brewer
Rural Electrification
Administration
Washington, D. C. 20250

Myron L. Brewer was born in Lincoln, Nebraska on June 24, 1922. He joined General Telephone Company of California in 1947 and held several positions in their engineering department. In 1960 he joined the United States Military Mission to Greece as a consulting engineer for outside plant design and voice frequency transmission. Since 1968 he has been with the Rural Electrification Administration, Washington, D.C. as a Communication Specialist. He is assigned to the Transmission Branch of the Telephone Operations and Standards Division where his primary duties are development of standards and specifications related to voice frequency transmission and inductive coordination.

Mr. Brewer is a member of the Institute of Electrical and Electronics Engineers.



Howard P. Price
Central Telephone Company
Chicago, Illinois 60637

Howard P. Price was born in Lebanon, Tennessee on June 19, 1936. He received the BS in Electrical Engineering from Tennessee Technological University, Cookeville, Tennessee in 1959. From 1960 thru 1967 he was employed by the Telephone Standards Division of the Rural Electrification Administration, Washington, D. C., as a Voice Frequency Transmission Engineer where his primary duties were the development of standards and specifications for voice frequency transmission and inductive coordination. In January 1968 he joined the Anaconda Company's research and development center in Sycamore, Illinois where he was supervisor of the electrical laboratory, conducted field evaluations relating to customer complaints on transmission and noise, and also conducted customer seminars. Since October 1971 he has been the Transmission and Protection Engineer on the Telephone Operations Staff of the Central Telephone Company in Chicago, Illinois where his primary duties are the development of standards, practices and specifications with respect to transmission, protection and inductive coordination.

Mr. Price is a member of the Institute of Electrical and Electronics Engineers.

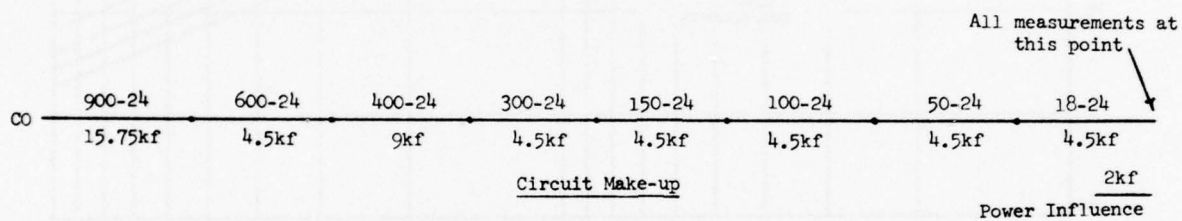
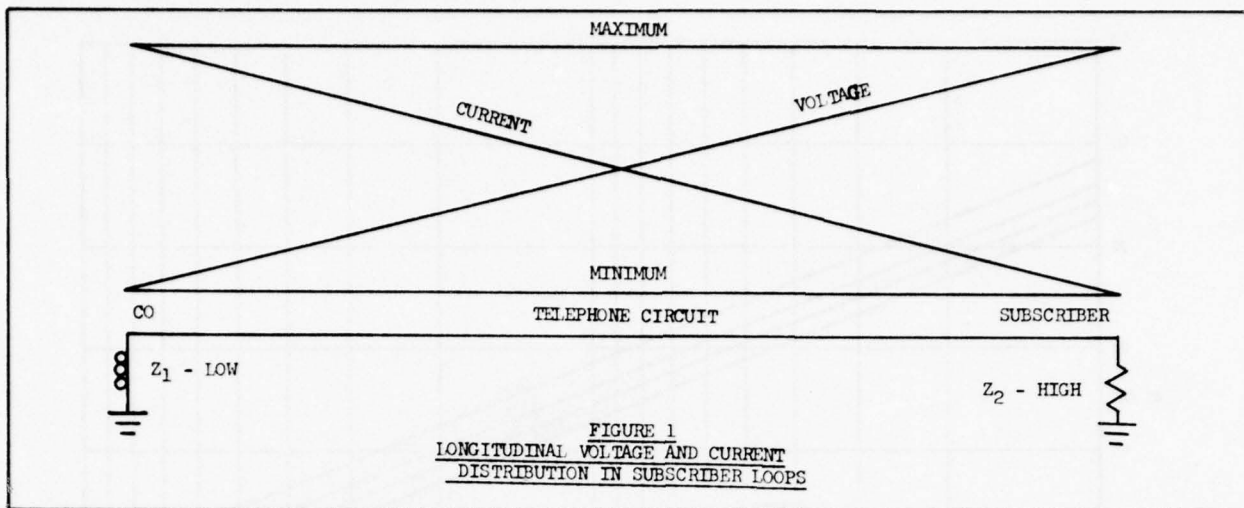


FIGURE 2

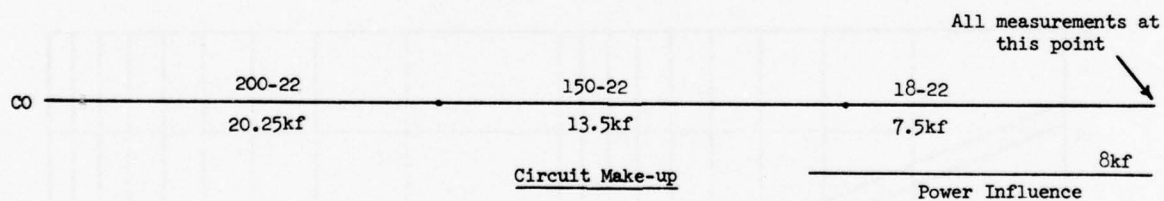


FIGURE 3

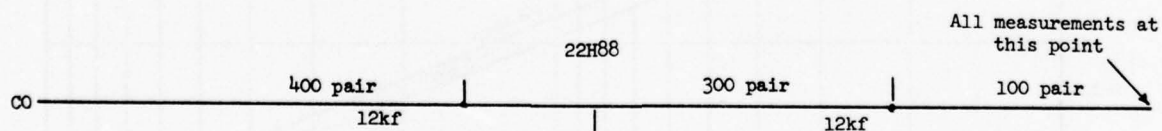


FIGURE 4

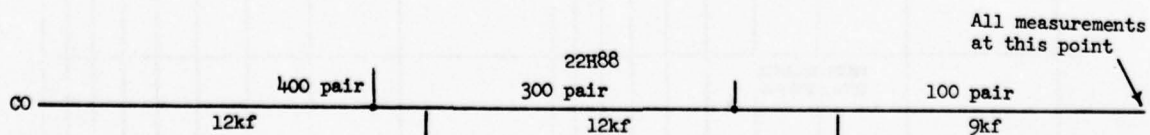
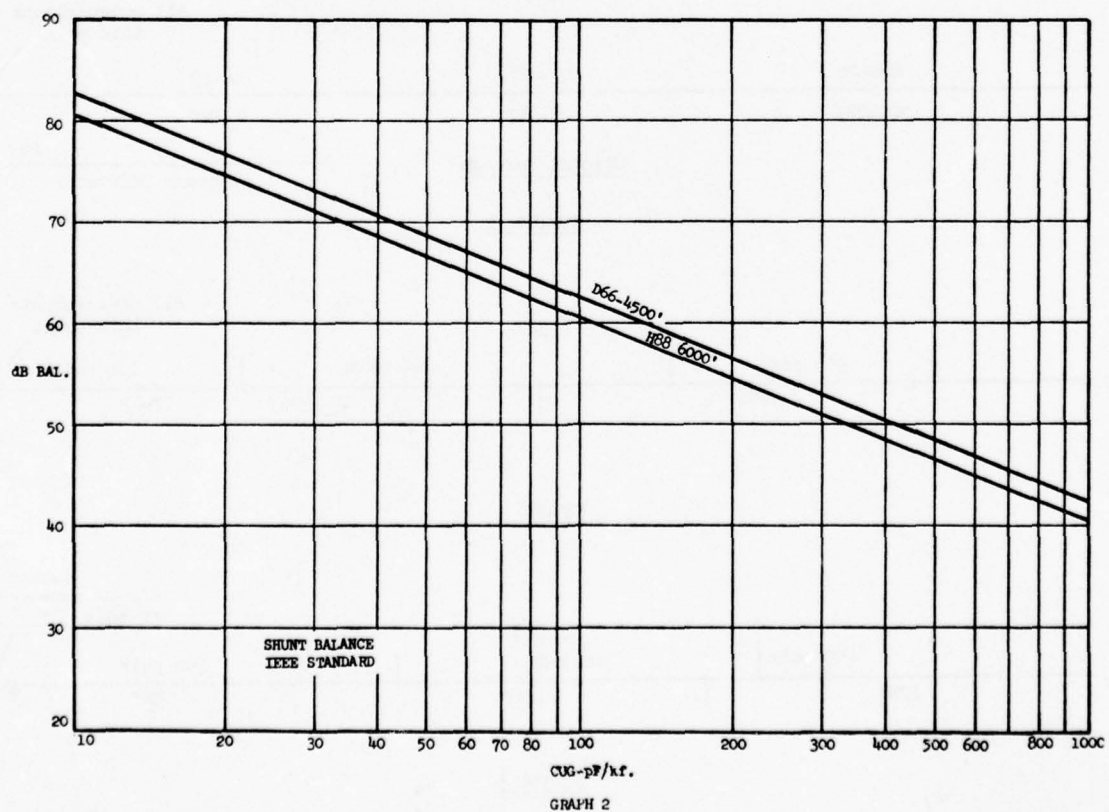
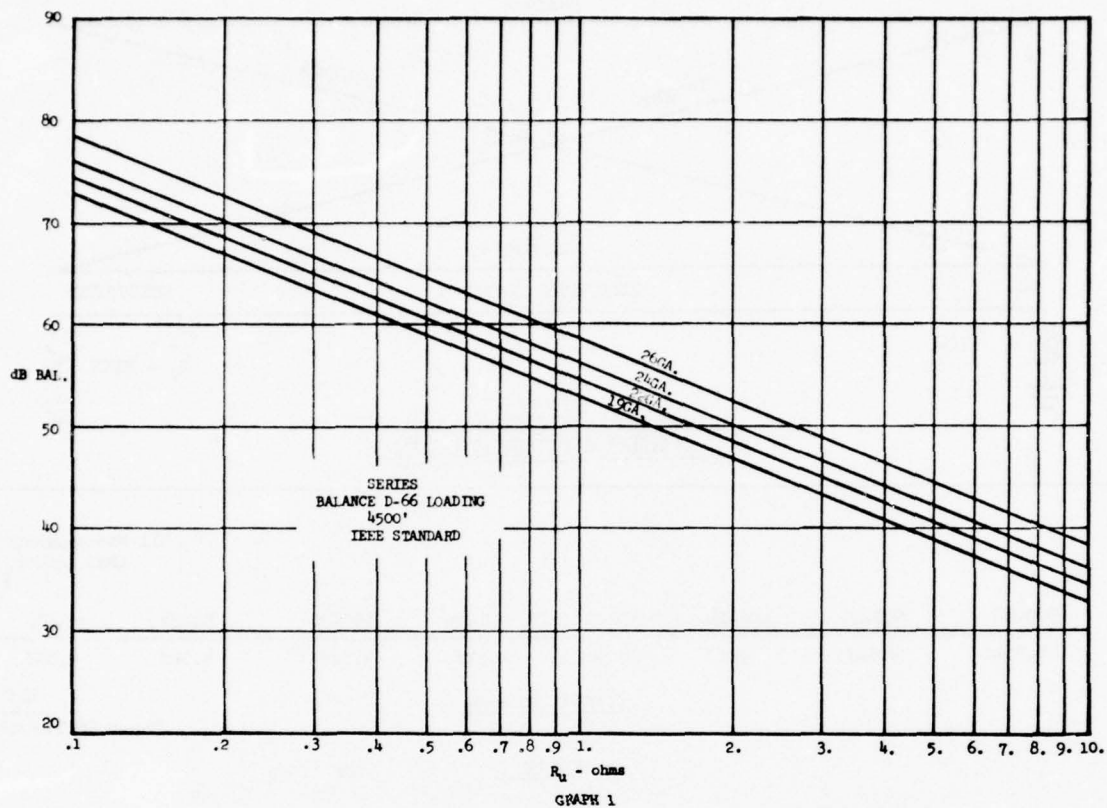


FIGURE 5



RODENT BITING PRESSURE AND CHEWING ACTION AND
THEIR EFFECTS ON WIRE AND CABLE SHEATH

by

N. J. Cogelia
Bell Telephone Laboratories
Norcross, Georgia

G. K. LaVoie & J. F. Glahn
U. S. Dept. of Interior
Wildlife Research Center
Denver, Colorado

Abstract

The biting force of the Gray Squirrel (*Sciurus carolinensis*), Plains Pocket Gopher (*Geomys bursarius*) and Norway Rat (*Rattus norvegicus*) was measured and their biting pressures calculated from the contact area of their incisors. Representative biting pressure of the squirrel was 22,000 psi, the gopher 18,000 psi, and the rat 7,000 psi.

It was found that the rodent gnawing action consisted of very rapid bites up to six per second with an average of 1.5 bites per second. The biting activity among the three species of rodents differed such that in a seven day cage exposure test a specimen could have a total of 90,000, 45,000 and 18,000 bites inflicted by the gopher, squirrel and rat, respectively.

Two modes of wire and cable sheath failure resulting from rodent gnawing action are proposed. In the case of soft materials such as flexible vinyl plastic, polyethylene, aluminum, lead, and annealed copper, the failure is by cutting wear. In the case of relatively hard materials such as steel and copper alloy, ultimate failure is by deformation wear. A toughness index criteria, related to material hardness, breaking strength, and strain, is established as an aid in selecting rodent resistant sheath material.

Introduction

The service life of buried and aerial communication or power distribution wire and cable is often limited by gnawing rodents, particularly pocket gophers, squirrels and sometimes rats. During the past thirty years numerous studies were made of the rodent resistance of a great variety of plastic, ferrous, and non-ferrous wire and cable sheaths.^{1,2,3,4} The studies were primarily aimed at determining the susceptibility of materials to rodent damage and the relationship of thickness, size and shape. These studies greatly assisted the selection of improved sheaths. However, none of the past studies focused on the influence of rodent biting pressure and gnawing frequency nor failure mode. A study of rodent biting pressure and chewing action was undertaken in the belief that it would contribute to the understanding of the sheath failure mechanism and lead to more reliable designs. Furthermore, we believed that such a study would lead to a more rapid means of screening candidate sheath materials.

A detailed description of the incisor cutting surface area and hardness, biting force instrumentation, and biting force and

pressure of the plains pocket gopher, gray squirrel, and norway rat is presented. Evidence is offered and it is argued that the failure mode of thermoplastic jacket, aluminum, lead and annealed copper sheath is via cutting wear. It is primarily related to incisor/material hardness and frictional force. The failure mode of copper alloys, tin plated steel, and stainless steel is via deformation wear and is primarily related to sheath toughness and gnawing frequency. Mechanical properties of shield/armor necessary to the survival of rodent attack are relative hardness and toughness. A critical toughness index number is proposed.

Materials and Methods

Incisor Surface Area and Hardness

The cutting edge of the rodent incisor is not uniform as in the case of a knife or chisel edge, but irregularly serrated. The irregularity is apparent in the gopher incisors shown in Figure 1. The incisors of squirrels



Fig. 1. Lower incisors of the plains pocket gopher (*Geomys bursarius*) showing irregularity of biting surface area.

and rats are similar in size and irregularity. In order to obtain a realistic, but conservative estimate of this surface area, all points of the incisors were considered to be contacting a hard surface with the animal's head in the normal position. Various methods of measuring this area were tried, such as ink prints similar to fingerprints; however, none, with the exception of the one described below, were acceptable.

Biting surface area prints were made by pressing the upper and lower gopher incisors

into a piece of .005" thick thermoplastic film taped to a standard microscope slide. A similar procedure was used with rats and squirrels. Slides were then projected at 45X and the outline of the impression traced (Figure 2).

Calculation of the surface area was determined using a planimeter and converting the readings to square inches. Incisor hardness was measured with a Shore D Durometer while the incisor lay on its side within a tight fitting cavity cut into a piece of hard wood.⁵ The estimated biting surface areas and hardness for each species are listed in Table 1.

Except in a few instances, the biting surface area of the lower incisors of all three species was less than the upper incisors. The greater mobility of the lower jaw resulting from its flexible muscular attachment to the skull probably accounts for the difference in surface area.

Construction of Gnathodynameter

The Gnathodynameter ("biteometer") consists of a variable resistance force transducer, bite-bar, power supply and associated circuitry which converts the changing resistance to a changing voltage that drives a strip chart recorder. A schematic is shown in Figure 3. A description of the components is as follows:

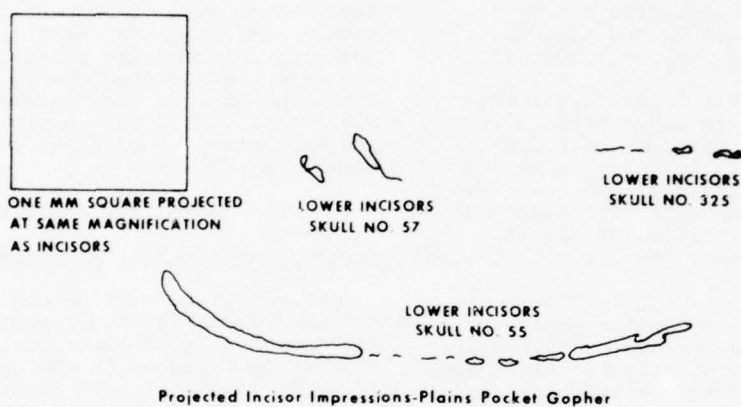
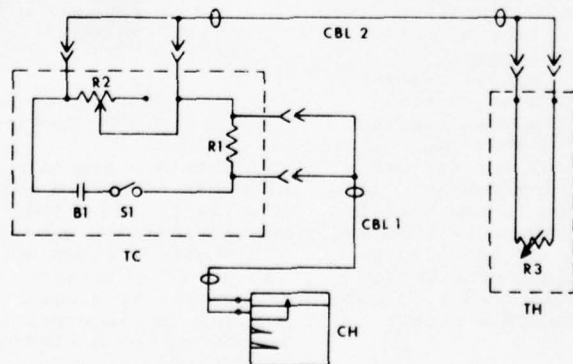


FIGURE 2

TABLE 1

Maximum Biting Surface Areas and Incisor Hardness of Three Species of Rodents

Species	n	Mean Maximum Incisor Surface Area (in ²)		Shore D Hardness
		Upper	Lower	
Plains Pocket Gopher (Geomys Bursarius)	15	0.00015	0.00005	95
Norway Rat (Rattus Norvegicus)	18	0.00041	0.00013	95
Gray Squirrel (Sciurus Carolinensis)	16	0.00019	0.00013	95



Gnathodynameter and Associated Circuitry

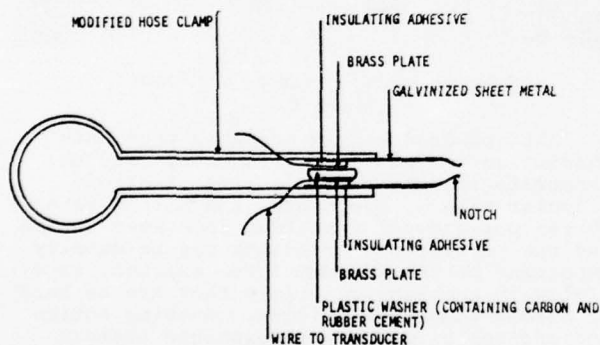
FIGURE 3

R_1 = 0.25 ohm resistor (1% Tol.)
 R_2 = 0-500 ohm potentiometer
 B_1 = 1.5 volt dry cell
 R_3 = Variable resistance force transducer
 CBL_1 and CBL_2 = Shielded twisted pair

CH = Strip Chart Recorder
 TH = Transducer Holder (bite-bar)
 TC = Transducer Controller housed in aluminum mini-box
 S1 = Single pole, single throw mini-switch

The heart of the "biteometer" is the variable resistance force transducer (R_3). The transducer's resistance decreases with increasing force and is a component of a simple voltage divider circuit. It is shunted by the variable resistance (R_2) which provides a means of zero-setting the transducer under no-load conditions. The transducer action results in 1 to 16 millivolts across (R_1) for the range of rodent biting forces.

A commercial transducer was tried first, but was abandoned when its variable resistance material prematurely age-hardened. New transducers were constructed by the authors employing a mixture of rubber cement with finely powdered activated charcoal.⁷ The ratio of charcoal to rubber cement was varied until a transducer of the desired sensitivity was achieved. When a greater amount of charcoal was added to the cement, the sensitivity to pressure increased. The transducer was mounted within a bite-bar which provided the rodent a means of activating the transducer (Figure 4).



Bite-Bar
FIGURE 4

During the course of the experiment, several transducers were calibrated and used in obtaining the data presented. The unit was adjusted to 1 mV output with no pressure on the transducer. Then, 100 gram weights were added to the bite-bar via 1/8" diameter rod. This procedure was repeated ten times for each weight category and the means and range plotted for each category. Transducers were discarded if the ranges for any two weight categories overlapped. Transducers were calibrated on the day of their intended use since their response to pressure changed from day to day due to drying of the rubber cement. It was found that the transducer yielded an immediate response upon application of pressure; however, the response slowly increased if the

pressure remained on the transducer. This property did not significantly affect the measured forces since all species exerted force on the bite-bar only momentarily with each bite.

The Gnathodynameter described here is a functional instrument with which biting forces can be determined with a reasonable degree of accuracy. However, it should be noted that several physical variables which influence biting force are inherent in the design of the instrument. First, the thickness of the bite-bar has a direct bearing on the amount of force that can be applied. Biting forces are dependent on the vertical separation of teeth, and when the mouth is open widely, total muscular force cannot be applied. (This is a decided advantage of larger size cables.) The thickness of the bite-bar was approximately 3/16 inch and the total mouth opening of the test animals was approximately one inch. This probably influenced the biting force, but not to a significant degree. In fact, studies have shown that the greatest degree of damage inflicted by rodents have been on wire structures with diameters between 0.20" and 0.50".

Second, the position of the incisors on the bite-bar possibly accounts for some of the variations between animals of the same species. During calibration, it was found that a point 1/16 inch from the tip and along the centerline of the bite-bar was the most responsive area. When biting the bar, some animals may not have bitten this area even though numerous attacks were elicited from each test animal.

Rodent Biting

During biting force measurements, gophers were placed in an open-front cage (Figure 5). One of the front feet of the gopher was grasped lightly with forceps which were in close



Gopher Biting the Bite-Bar
FIGURE 5

proximity to the bite-bar. The gopher striking at the source of irritation readily bit the bite-bar. This procedure was repeated with each of the eighteen gophers. Biting force varied during this time and the highest trace recorded for each gopher was considered its maximum capable force. A similar procedure was used to measure the biting force of eighteen Norway rats and sixteen gray squirrels. However, the rats were placed in a restrainer which covered the entire body except the head, and squirrels were hand-held using a mink handler's glove.

Summary of Maximum Biting Forces and Pressures

TABLE 2

Gray Squirrel Maximum Biting Force			
Body Weight (lbs.)	Biting Force (lbs.)	Biting Pressure (lbs./in. ²)*	Ratio Biting Force to Body Weight
\bar{x} =	1.32	2.89	22,245
σ =	0.17	0.35	2,679
Max. =	1.61	3.30	25,385
Min. =	1.02	2.29	17,615
Range =	.59	1.01	7,770

*Based on mean maximum biting surface area of 0.00013 in.² for lower incisors.

Plains Pocket Gopher Maximum Biting Force			
\bar{x} =	0.42	0.92	18,300
σ =	0.08	0.13	2,525
Max. =	0.60	1.20	24,000
Min. =	0.30	0.71	14,200
Range =	0.30	.49	9,800

*Based on mean maximum biting surface area of 0.00005 in.² for lower incisors.

Norway Rat Maximum Biting Force			
\bar{x} =	0.66	0.95	7,115
σ =	0.20	0.26	1,955
Max. =	1.01	1.56	11,642
Min. =	0.40	0.67	5,000
Range =	0.61	0.89	6,642

*Based on mean maximum biting surface area of 0.00013 in.² for lower incisors.

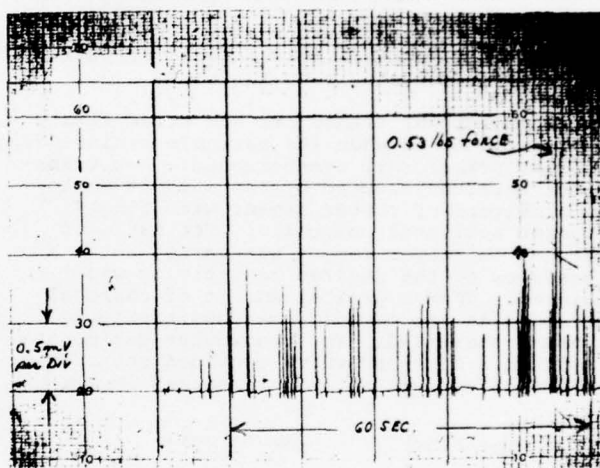
The squirrel produced the greatest biting pressure (22,000 lbs./in.²) followed by the gopher (18,000 lbs./in.²) and the rat (7,000 lbs./in.²). Also, the biting force of the squirrel (3 lbs.) was about three times greater than that of the gopher or rat. However, the surface area of the squirrel's lower incisors was almost twice as great as the gopher's and this appreciably decreased their biting pressure. The mean biting force to body weight ratio was identical for the squirrel and gopher and about 50 percent greater than that of the rat.

The pressure exerted by any of the three species on wire and cable sheaths (metal shield/armor and plastic jacket) under field conditions could be several times greater than that reported here. It would depend upon the

angle of the animal's head as it relates to the amount of incisor surface area contacting the sheath. For example, the area of five contact points of lower incisors total .00005 in.²; however, the gopher could exert 0.93 pounds force using only one of the points. Therefore, the biting pressures reported herein are considered to be conservative values.

Gnawing Action

During the course of this experiment, it was observed that the gnawing action of the rodents seldom approached the maximum forces reported here. Usually the gnawing action consisted of very rapid bites, up to six per second, the magnitude of which was one-half or less of the maximum force (Figure 6).



Gopher Biting Frequency and Force
FIGURE 6

It appeared highly probable that this gnawing action was more frequently used to penetrate sheaths than a series of strong singular bites. Therefore, the biting rate (bites per second) resulting in a wear action and the persistence of attack may be equally important as the maximum force exerted, especially in damaging materials that are as hard or harder than the incisors. Gnawing action and incisor hardness were examined against sheath penetration evidence to establish the principle mode of mechanical failure.

Discussion

As described in the preceeding paragraph, the gnawing action of the rodents consisted of very rapid bites at a maximum rate of six per second and an average rate of 1.5 per second. If each rodent did nothing but gnaw continuously at the average rate, then 900,000 bites could be inflicted on any wire or cable specimen during the "standard" seven day cage test. (During this test, ten specimens are exposed for seven consecutive days to each of ten individually caged rodents. The rodent has access to the horizontally mounted specimen through a 2 inch x 2 inch opening in the front of the cage. Wire or cable designs are judged rodent resistant if at least 80 percent of the test specimens are not penetrated through the armor/shield.)

Our laboratory observations and measurements indicate that the gopher is actively gnawing approximately 10 percent of the time (90,000 bites), the squirrel 5 percent of the time (45,000 bites) and the rat 2 percent of the time (18,000 bites). Based on the above duty cycles and past experience, the seven day criterion is a reasonable one for gopher tests. However, it should be extended to 14 days for squirrel tests and 35 days for rat tests for comparable biting activity.

An examination of rodent sheath damage was made in order to associate the damage or failure mode with biting pressure, biting frequency and incisor hardness. Those sheath materials that were completely penetrated and rendered discontinuous yielded small chips of sheath, plastic and metal, which were dislodged by the rodent. These materials were rated as failures by cutting wear. The ratio of incisor/material hardness and frictional force are associated with this type wear.

Those sheath materials that either resisted penetration or exhibited penetration without the evidence of residue chips were rated damaged or failures by deformation wear. Gnawing frequency and material toughness, the latter characterized as the product of ultimate tensile strength of the material by the strain at fracture, are associated with this type wear.

In the following paragraphs, whenever rodent damage is mentioned, it refers to either gopher or squirrel damage to small size (0.2 inch to 0.4 inch diameter) buried wire structures. The degree of damage caused by gophers and squirrels is similar. Since rats are not a major cause of damage to communication wire and cable, no specimens were exposed to them. We would expect similar types of damage from the rat. The rat biting data may be of use to those concerned with protecting foodstuffs.

Proposed Sheath Failure Modes

Failure by Cutting Wear

During cutting wear, a hard particle or rough edge cuts a chip from the wearing surface. The rough edge in our case is the rodent's incisors. If a chip is cut, then very high rates of wear will result. For this type wear to occur, the cutting agent must have a hardness greater than 1.2 times the material being cut and must have a cutting angle with the wearing surface which is greater than θ_C .⁸ The angle θ_C is defined as follows:^{9,10}

$$\tan(\theta_C - 90^\circ) \approx \frac{1 - \mu^2}{2\mu}$$

where θ_C = critical angle for cutting
 μ = friction coefficient.

A tabulation of these conditions for aluminum, annealed copper, lead, polyethylene and poly (vinyl chloride) sheath materials is contained in Table 3.

TABLE 3

Incisor/Substrate Interface	μ_k	θ_C	Shore D Hardness (Substrate)	Ratio Incisor/Substrate Hardness
Gopher/flexible PVC	0.77	104.8*	32	2.97
Gopher/L.D. polyethylene	0.64	114.8	45	2.11
Gopher/lead	0.68	111.6	70	1.35
Gopher/annealed copper	0.34	142.4	79	1.20
Gopher/aluminum(soft)	0.48	128.7	80	1.19

The hardness ratios of annealed copper and aluminum are borderline with respect to the critical value of 1.2, but experimental error can account for the required margin. Figure 7 shows the gopher incisors are capable of assuming the position of a cutting tool with the required range of critical angles.

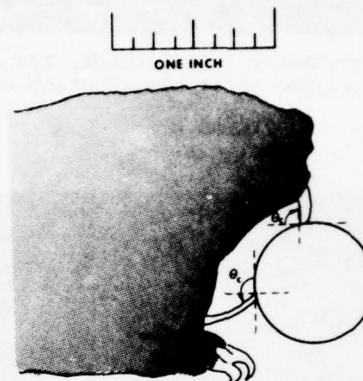


FIGURE 7

Kinetic coefficient of friction (μ_k) between the incisors and substrates was measured in accordance with ASTM D 1894-63 Standard Method of Test for Coefficient of Friction of Plastic Film except for the following change. Three rodent incisors were mounted in tripod fashion on a separate rubber pad and placed beneath the sled. The weight of the rectangular sled was 200.5 grams and the weight of gopher incisors plus rubber pad was 12.7 grams.

The Shore D Durometer Hardness Tester per ASTM Standard D 2240 was selected because its 30° spherocone indenter with 0.004 inch radius simulated the sharp rodent incisors better than other type hardness testers.

It has been well known that the relatively soft metals and plastics listed in Table 3 are susceptible to rodent penetration, but a failure mode was not previously assigned. A cutting wear mode is now proposed.

Failure by Deformation Wear

The relatively hard metal sheaths, such as tin plated steel, austenitic and ferritic steels, and certain copper alloys, have Shore D hardness values ranging from 90 to 95 and incisor/metal hardness ratios ranging from 1.00 to 1.05. These ratios are well below the 1.2 level required for cutting wear.

Examination of these metal surfaces after seven day gopher exposure tests revealed the presence of wear tracks. Examples of wear tracks of varying degrees on several of the above metals are shown in Figures 8-11.



CDA 220 Bronze Armor (.005" thick, 1/4 hard)
On 1-Pair 19 AWG Rural Distribution Wire

FIGURE 8



Type 430 Stainless Steel Armor (.0025" thick,
annealed) on 1-Pair 19 AWG Rural
Distribution Wire

FIGURE 11



CDA 220 Bronze Armor (.005" thick, 1/4 hard)
On 1-Pair 19 AWG Rural Distribution Wire

FIGURE 9



Type 304 Stainless Steel Armor (.003" thick,
annealed) On 1-Pair AWG Rural
Distribution Wire

FIGURE 10

This physical evidence suggests damage by deformation wear. "Deformation wear consists of the continual plastic working of a surface until cracks form, grow, coalesce, and a wear particle is produced."⁸ Under conditions where stresses are high, wear tracks are produced and particles are dislodged from the edge of the wear track. Although no direct correlation has been established for metals, specialists in the field of wear agree that high toughness is necessary to resist deformation wear. It will be shown that such is the case for rodent gnawing action on certain metals.

A metal sheath material that has consistently resisted gopher and squirrel penetration in the laboratory and in service (in the absence of corrosion damage) is .006" thick Terneplate (tin plated steel). Its hardness, tensile strength, elongation, and toughness index number are compared to other armor/shield materials in Table 4.

TABLE 4

Shield Material	Shore D Hardness	Tensile Strength (P.S.I.)	ϵ (in/in)	Toughness Index (T)
CDA 220:				
Bronze - 1/2 hard	---	52,000	0.11	5,720
- 1/4 hard	94	45,000	0.25	11,250
CDA 195 Precipitation Temper Copper Alloy	---	80,000	0.15	12,000
Terneplate	94-95	54,000	0.26	14,040
CDA 220 Bronze - "1/4 hard"	93-94	48,600	0.34	16,525
Stainless Steel Type 430	95	80,000	0.26	20,800
Stainless Steel Type 304	95	112,000	0.29	32,480

One of several methods of evaluating toughness is to calculate the toughness index number (T).¹¹ It is obtained by multiplying ultimate tensile strength of the material by the strain at fracture ($T = U.T.S. \times \epsilon$). Toughness is expressed as the amount of energy absorbed per unit volume of material, normally in pound-force-inches per cubic inch.

It can be seen from Table 4 that, in general, the various steel materials have superior toughness as compared to the copper alloys. However, one lot of copper alloy yielded a toughness index somewhat greater than that of tin plated steel. The data was taken on shield materials after processing into completed wire to allow for work hardening effects, particularly in the case of Type 304 Stainless Steel.

If the toughness index is a reliable indicator of the resistance to deformation wear caused by rodents, then there must be a correlation between increasing toughness and improving performance in the cage tests. A comparison of relative performance is shown in Table 5. In order to emphasize the effects of shield thickness and minimize the effects of width, the toughness index was modified as follows:

$$T_1 = T(w \times t)$$

$$T_1 = U.T.S. \times \epsilon (w \times t)$$

$$T_1 = B.S. \times \epsilon$$

where

$w = 0.200"$, an arbitrarily small width equal to that of two gopher incisors.
 t = metal sheath thickness, inches.
 U.T.S. = Ultimate tensile strength (psi)
 B.S. = Breaking strength, (lbs.)
 ϵ = strain, (in./in.)
 T_1 = Modified toughness index

Shield width per se, short of enclosing the underlying core, does not contribute to rodent resistance, but is a necessary component of toughness - hence, the selection of a constant arbitrarily small width.

TABLE 5
One or Two Pair Buried Distribution or Service

Shield Material	Thickness (inch)	Wire With Helically Applied Shield			Cage Test Percent Surviving ¹⁴
		Breaking Strength (lbs)	ϵ (in/in)	T_1	
CDA 220 Bronze					
1/2 hard	.005	52	.11	5.7	10
1/4 hard	.005	45	.25	11.2	37
CDA 195 Precipitation Temper Copper Alloy	.005	80	.15	12.0	20
Stainless Steel Type 430 Annealed	.003	48	.26	12.5	30
CDA 220 Bronze "1/4 hard"	.005	48.6	.34	16.5	80
Stainless Steel Type 430 Annealed	.004	64	.26	16.6	90
Template, Annealed	.006	64.8	.26	16.8	100
Stainless Steel Type 304 Annealed	.003	67.2	.29	19.5	100
Stainless Steel Type 304 Annealed	.005	112	.29	32.5	100

The relationship between T_1 and percent surviving specimens is more easily determined from Figure 12. A correlation of improving performance with increasing toughness is apparent. The cut-off point of minimum acceptable performance is quite sharp at $T_1 = 16.5$.

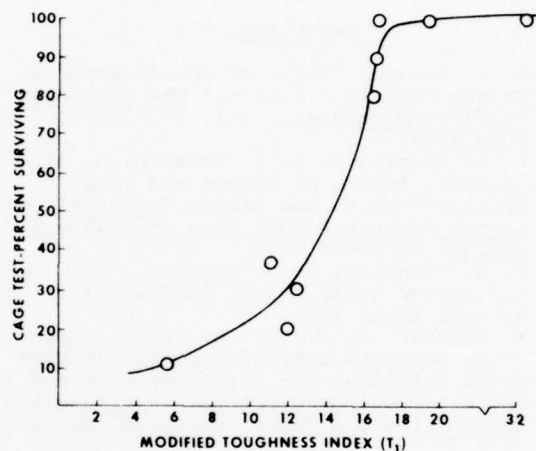


FIGURE 12

Conclusions and Recommendations

Two modes of sheath failure resulting from rodent gnawing action have been proposed. First, relatively soft materials such as flexible vinyl plastic, polyethylene, aluminum, lead and annealed copper fail by cutting wear. Small chips of these materials are dislodged by the rodent's incisors. The key factors are an incisor/substrate hardness ratio greater than 1.2 and an incisor cutting angle with the wearing surface which is greater than θ_c . The angle θ_c is a function of the coefficient of friction between the interacting surfaces. Presently, there is no practical economical way to impart rodent resistance to these soft materials short of physical isolation.

Second, the relatively hard materials such as stainless steel, tin plated steel, and certain copper alloys ultimately fail by deformation wear. It involves the continual plastic working of a surface until cracks form, grow, and a wear particle is produced. The key factor is material toughness which is expressed as the product of ultimate tensile strength and strain at fracture. A modified toughness index, the product of breaking strength and strain at fracture, is used to further evaluate material thickness effects.

The following guidelines are recommended for selecting rodent resistant armor/shield material for wire or cable. Select a material which will yield a Shore D Hardness of ≈ 94 and a toughness index equal to or greater than

14,000, preferably after processing into completed product. Adjust the thickness (keeping width constant at 0.200 inch) such that the modified toughness index will be equal to or greater than 16.5.

While these guidelines will provide acceptable rodent resistance with reference to the seven day cage tests, a higher index and greater margin of safety may be desirable for special situations. Depending upon the metal selected, adjustments to thickness may be required to compensate for corrosion wear and the need for low d.c. resistance to minimize the effects of inductive interference and lightning surge currents.

References

1. W. E. Howard, "Tests of Pocket Gophers Gnawing Electric Cables," The Journal of Wildlife Management, Vol. 17, No. 3, July 1953.
2. B. F. Lizell, J. S. L. Roos, G. R. Bjorck, "Rodent Attack on Rubber and Plastic Insulated Wires and Cables," Proceedings of the Seventh Annual Wire and Cable Symposium, December 1958.
3. R. A. Connolly, N. J. Cogelia, "The Gopher and Buried Cable," Bell Laboratories Record, April 1970.
4. R. Baboian, J. R. Hartley, E. D. Hyman, "High Strength Corrosion Resistant Clad Metal Shielding for Telephone Wire and Cable," Proceedings of the 23rd International Wire and Cable Symposium, December 1974.
5. N. J. Cogelia, "Durometer Hardness of Various Wire and Cable Armoring and Jacketing Materials," unpublished Bell Laboratories document, February 1968.
6. N. J. Cogelia, "A Device for Measuring Rodent Biting Force," unpublished Bell Laboratories document, May 1969.
7. J. F. Glahn, G. K. LaVoie, "Estimated Biting Pressures of the Plains Pocket Gopher (*Geomys bursarius*), The Norway Rat (*Rattus norvegicus*) and The Gray Squirrel (*Sciurus carolinensis*)," unpublished Bell Laboratories Document prepared under contract to the Wildlife Research Center, Denver, Colo.
8. M. B. Peterson, Maj-Britt K. Gabel, Martin J. Devine, "Understanding Wear," ASTM Standardization News, September 1974.
9. A. J. Sedriks, T. O. Mulhearn, "Mechanics Of Cutting and Rubbing in Simulated Abrasive Processes," Wear, Vol. 6 (1963), pp. 457-466.
10. A. J. Sedriks, T. O. Mulhearn, "The Effect Of Work-Hardening on the Mechanics of Cutting in Simulated Abrasive Processes," Wear, Vol. 7 (1964), pp. 451-459.
11. J. E. Shigley, Mechanical Engineering Design, 2nd Edition, McGraw-Hill Book Company, pp. 192-193.
12. R. A. Connolly, N. J. Cogelia, R. E. Landstrom, G. K. LaVoie, "Gopher and Squirrel Wire and Cable Cage Test Results," 1967-1975, unpublished Bell Laboratories documents.



Nicholas Cogelia
Bell Laboratories
Norcross, Georgia

Nicholas Cogelia has been with Bell Laboratories since 1956. His work involves the design and development of aerial, buried and station wire and cable. He received a B.S. Degree from Loyola College of Baltimore and has two patents related to aerial and station wire.



Keith LaVoie
Denver Wildlife
Research Center
Denver, Colorado

Keith LaVoie is a Wildlife Biologist with the U. S. Fish and Wildlife Service, Denver Wildlife Research Center. Keith was born in Denver, Colorado June 25, 1934. He is a graduate of the University of Colorado. He served as a medical technician with the U. S. Army in Leipzig, Germany for three years. He started his career with the Service in 1957 as a laboratory technician. Keith has worked primarily with rodent problems in agriculture and industry, and spent two years studying rodent damage to rice at the Rodent Research Center in the Philippines. Keith is the Project Leader of the Industrial Rodents Project at Denver. He is married and has two children.



James Glahn
Denver Wildlife
Research Center
Denver, Colorado

Jim Glahn is a Wildlife Biologist with the U. S. Fish and Wildlife Service, Denver Wildlife Research Center. Jim was born in Blue Island, Illinois October 29, 1945. Undergraduate studies were completed at Cornell University and graduate studies at Colorado State University. He served with the U.S. Army in Munich, Germany for two years as a medical laboratory specialist. He began his professional career with the Service in September 1972. He is currently the Project Leader at the Fresno Field Station dealing with rodent problems in agriculture. Jim is married and has two children.

CONNECTORIZED EXCHANGE CABLE SPLICING (CONECS)

by

D. R. Frey and A. G. Hardee

Bell Laboratories
Norcross, Georgia

ABSTRACT

CONNECTORIZED EXCHANGE CABLE SPLICING, CONECS, a new Bell System development by AT&T, Bell Labs, and Western Electric utilizing the 710 Connector makes it practical to connectorize reels of cable for fast, simple plugging together in the field. A complete, tested and field evaluated package of documentation and hardware is now being used to introduce CONECS for buried and aerial applications. A package for underground applications will be introduced early in 1977.

INTRODUCTION

Historically, telephone cable splicing has been very labor intensive and craft oriented. For more than eighty years the standard wire splice, for all but special trunk circuits, was the unsoldered twisted joint. The splices were enclosed in lead sleeves sealed by skillfully wiping with melted lead solder. During the last fifteen years many changes have been introduced in cable splicing. Practically all connections today are made with solderless insulation piercing connectors, many installed with high production machines. Various types of splice cases made from materials ranging from aluminum and cast iron to plastic have replaced most of the lead sleeves. These changes significantly improved productivity and helped to meet the large demands for new types and amounts of service during the past two decades. Even so, cable splicing remains more labor intensive than most other parts of the outside plant.

Connectorized cable prepared in a factory, shipped to the field, installed in place, and plugged together has been an old idea of Bell Labs development engineers and others. However, conventional pin-and-jack connectors long used by the military and for some commercial applications were unsuitable because of cost and the difficulty in rearranging circuits. This was recognized early and several proposals emerged for modular designs of sub-multiples of the cable in the late fifties and early sixties. These were keyed to the emerging color coded PIC cable, but could also be used on pulp cable. Serious development was deferred until recently in favor of developing more urgently needed field splicing methods which are required even with connectorized cable.

CONECS

After extensive field experiments starting in 1974, in May of this year the Bell System began a phased introduction of a new system for efficiently constructing high quality outside plant, called CONECS, for CONNECTORIZED EXCHANGE CABLE SPLICING. The newly developed system makes it practical to pre-connectorize and pretest reels of standard multipair cable in a factory or remote location for fast, simple plugging together in the field. CONECS is the result of a joint effort of AT&T, Bell Labs, and Western Electric to develop a complete, tested and field evaluated system package including:

- Documentation for implementation
- Training packages for users and manufacturing
- Hardware to do the job

At the heart of CONECS is the Western Electric manufactured, Bell System standard, 710 modular Connector System,^{1,2} which is now in use throughout the system for conventional field splicing of multipair cables. The basic element of CONECS is the plug-in bridge feature of the 710 Connector system. Typically, at a CONECS splice location, one of the cables is preterminated in connector (or female) modules and the other cable end is preterminated in bridge (or male) modules. These are quickly plugged together with the aid of a hand tool. The concept is illustrated in Figure 1.

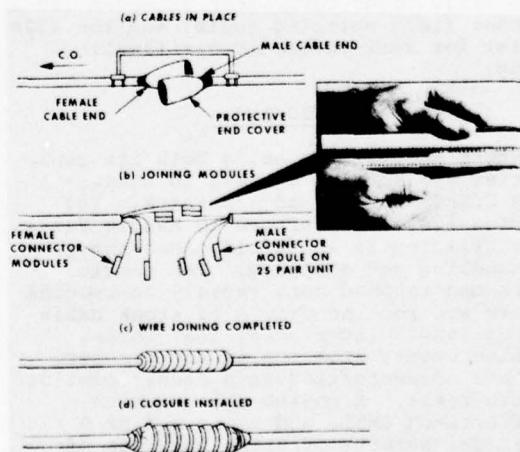


Figure 1. Sequence of CONECS Splicing

CONECS splices are fully compatible with 710 field splicing and are easy to rearrange. In color coded cable the plug-in bridge can be transferred from one cable count to another by simply unplugging and replugging together. Branch cables can be added to the top of the connector module of a CONECS splice in the field by using a hand tool.

At dedicated straight splices where quick disengagement and reassembly are not required, one of the cable ends can be pre-terminated in indexed-wire-holders and the mating end preterminated in connector modules as shown in Figure 2.

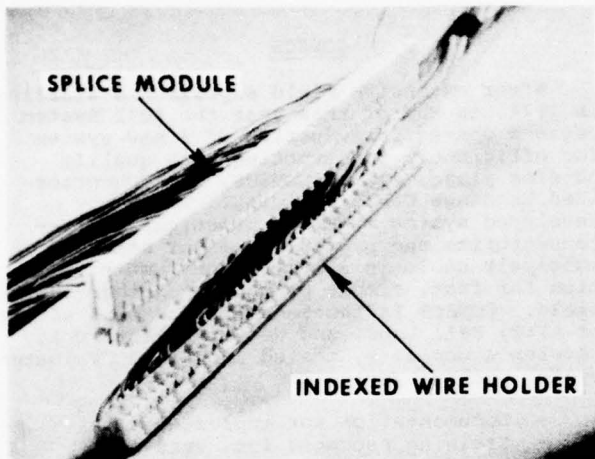


Figure 2.

The indexed-wire-holder securely retains the cable conductor ends in alignment and mates with the connector module to form a 25 pair splice in the same manner as the conventional index strip in a field splice. Branch cables could still be added to these splices without circuit interruptions, by terminating the branch cable in plug-in bridge modules.

Another option which is useful in certain critical field locations is the half-CONECS splice. One cable end is preterminated in connector modules and the other is left blank and connected to the preterminated end in the field using compatible standard 710 Connector field splicing tools, and the 152A Test Set for semi-automatic verification testing.

MANUFACTURING

Western Electric is using both its cable factories and service centers to connectorize CONECS cables and apparatus. The factories are best equipped to handle large orders efficiently and avoid unnecessary reel handling and shipping. The service centers can respond more rapidly to special requests and routine orders of stock cable and apparatus. Interfaces, load coils, apparatus cases, stub cables and pressure plugs are connectorized in a manner similar to cable reels. A coding system which specifies each cable end using a 4 or 5 digit code, permits offering hundreds of splice and closure combinations for full flexibility in outside plant design.

CONECS cable leaves the factory or service center fully tested and ready for installation. In addition to being connectorized, the sheath ends are prepared for the closure specified. Compound is thoroughly cleaned from waterproof cable ends, which eliminates the need for field cleaning and improves the quality of encapsulated splices. The cable is placed on specially constructed reels which have space allocated for storage of the connectorized ends.

ENGINEERING AND CONSTRUCTION WITH CONECS

CONECS is technically and economically feasible for most splices of every large cable installation. Long runs of trunk and feeder cables are prime candidates for CONECS, but backbone distribution cable in a serving area is also a likely candidate. Any size cable can be connectorized, but it is economically more favorable at this time for cables of 200 pairs and larger.

Standard methods can be used for placing aerial, buried, or underground CONECS cables, but restrictions apply to certain methods and situations. For example, only one end can be connectorized if the stationary reel method is used to place aerial cables, or if the cable is placed in the underground. As shown in Figure 3, cables can be pulled both directions from one manhole which permits CONECS splices in alternate holes.

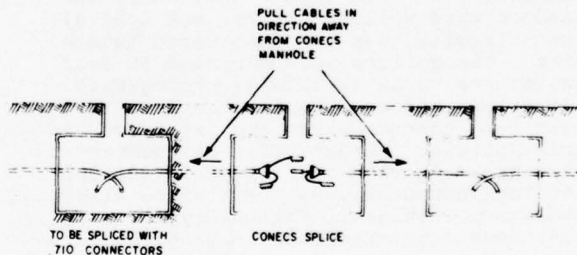


Figure 3. Underground CONECS Splice

A point worth emphasizing is that not every splice of a cable installation need be connectorized nor should CONECS be avoided just because the location of a few splices is critical. Good job planning will purposely include several field splices for length adjustments and for verification testing through the completed CONECS splices. Often cable placing can emanate in both directions from a critical splice location or these locations can be used for the field splices.

Only three inexpensive special tools are required for CONECS. These are:

- A simple toggle type plier hand tool for seating the bridge module or indexed wire-holder into a connector module.
- An alignment bar that properly spaces the cable ends during aerial or buried placing. It is adjustable for use on top of the ground or at the final grade level in a buried splice pit. A bar can be removed after the cable is secured in place and used

on other splices.

The last tool is a split feed tube to guide cable into underground ducts. This is required because the splice bundle is too large to pass through the opening of a standard feed tube.

The CONECS concept and hardware are simple, but planning and coordination between engineering and construction forces are essential to insure that at installation everything will fit together smoothly. A complete package of information and training aids has been prepared. The package includes "How to--" manuals with audio/visual aids and a course leader's guide. Separate segments are directed to management and craft personnel. Operating company trainers are being taught by Bell Labs and Western Electric during the introductory period and the material will be included in standard training courses as information sources.

A key difference between CONECS and standard construction is the joint planning by engineering and construction which is done prior to ordering the cable. It is necessary for the plant engineer and construction supervisor to determine placing methods and directions, specify the location of splices, splice configuration, type of closure, and direction that branch, load, or apparatus stubs will enter a splice if part of new construction. In standard construction these decisions are often left to the construction crews or contractors. Consequently, more engineering involvement with the construction phase is needed for CONECS, but this has benefits. Construction is of better quality, less costly, and more standardized. Revisions and deviations are essentially eliminated. In the case of underground plant the additional planning for CONECS yields better control and utilization of ducts and manhole space which are often critical facilities. The training emphasizes the use of a simple schematic of the route which provides a means of accounting for all of the details accurately and quickly.

ADVANTAGES OF CONECS

Including the Western Electric charges for CONECS, more engineering involvement, and slightly more complicated placing, CONECS installation costs are comparable to field splicing. But, higher productivity, higher quality and fringe benefits provide overall savings. Plugging together modules is much faster, less tiring, and less sensitive to craft experience than conventional splicing. For example a 600 pair buried splice, shown in Figures 4 and 5, that may take six hours to complete conventionally can be completed in less than 1 1/2 hours with CONECS with little skill required. A 2700 pair underground splice that may take three shifts or more to complete conventionally can be completed by one splicer in 1/2 shift. The tedious job of handling hundreds of pairs of conductors is reduced to plugging together a few modules. The cables are fully tested and in the case of waterproof cable, completely cleaned. The precleaned ends eliminate an unpopular field operation and



Figure 5. Closeup of Hand Tool

improves the encapsulation of buried splices and housekeeping in pedestals. Connectorized ends are inherently cleared of crosses and shorts, which facilitates verification testing at field splices. This is extremely valuable for underground CONECS where at least every other splice is a field splice. Opening of adjacent holes for clearing cable ends is eliminated.

The faster splicing reduces costs with a leverage greater than the direct cost of the splicer's time. Construction intervals can be shortened resulting in substantial reduction in the period capital investment is in a nonearning status, which reduces carrying charges. Nonproductive time of manhole guards and costs of guarding open splice pits is also reduced.

CONECS is especially valuable for busy streets with restricted work hours. Splices and site restoral can be completed faster reducing periods of traffic disruption and public inconvenience. Coordination with placing crews is simplified since CONECS splicing can easily keep pace with placing. Duplicate (lost) time associated with temporary splice closures and return trips to complete splices is essentially eliminated.

STATUS AND FUTURE

All aspects--training, engineering,

placing, splicing and manufacturing, for aerial and buried PIC cable applications were thoroughly tested and refined in field trials in two Bell System operating companies before introducing CONECS to other companies. The trials were very successful; more than 120 reels of cable were installed in five sites of aerial and buried plant. Cables were plowed and trenched in the buried trials and the splices were placed in both buried closures and pedestals. Over 800 reels of cable were placed by one operating company following the trials using the training material furnished for the trials. The trials confirmed the practicality of the CONECS system and demonstrated that attention to detail is essential to realize the full benefits of CONECS.

A carefully planned and timed introduction in three Bell System operating companies, Southwestern Bell, South Central Bell, and Northwestern Bell, began in May of this year and was soon expanded to four other companies, Bell of Pa., Southern, Mountain Bell and Pacific Northwest Bell. By the end of this year, aerial and buried PIC CONECS will be available to all Bell operating companies. Western Electric has timed their manufacturing capability to coincide with the introductory program.

The development of underground CONECS is trailing the aerial and buried applications by about six months. Underground field trials began in November, 1975. These trials are proceeding very smoothly; they have benefitted substantially from the experience with buried and aerial applications. Implementation and training documentation packages will be ready for introduction of underground CONECS in several operating companies early in 1977.

In the initial form CONECS is very attractive in many applications and has been accepted enthusiastically by the operating companies (Ref. 3). As it matures, cost reductions from continued imaginative manufacturing engineering will make CONECS even more attractive in the future.

ACKNOWLEDGEMENTS

CONECS is the result of a joint effort of the Engineering and Customer Services Organization of AT&T, The Cable Splicing Department of Bell Labs, and the Western Electric, Loop Transmission Apparatus and Cable Product Engineering Control Centers. Many in all three companies contributed to the work reported. Further, we are indebted to the operating company staffs and the Western Electric Service Distribution Center at Nashville, Tennessee who helped with the field trials which were invaluable to the development. It is difficult to acknowledge specific individuals in a development like this without unintentionally omitting some very deserving person, but we feel it is necessary to give special acknowledgment for the efforts of the Western Electric, Loop Transmission Apparatus, Product Engineering Control Center.

REFERENCES

- ¹ R. W. Henn, 1973 Proceedings of 22nd Intl. Wire and Cable Symposium, pp. 195-200, "Systematic Encapsulated Cable Splicing Connector for Aluminum and Copper Wire."
- ² D. R. Frey and D. C. Borden, 1976 Proceedings of 2nd Intl. Symposium on Subscriber Loops and Systems, pp. 68-117, "A System of Wire Joining with Connection Verification."
- ³ J. Johnson, August 9, 1976, Telephony, pp. 74-76 "Putting CONECS to the Test."



Dean R. Frey is a Member of the Technical Staff at Bell Laboratories in Norcross, Georgia and supervises the Wire Joining Development Group of the Cable Splicing Department. For the last 10 years he has been active in developing splicing apparatus and hardware for the Bell System. Prior to this he was involved with the development of hardware for underwater systems. Mr. Frey received a BSME degree from the Pennsylvania State University and a MME degree from New York University.



A. G. Hardee is a Member of the Cable Joining Department of Bell Laboratories. He received his Ph.D. from the University of Florida in 1968. He served as a member of the faculty of the University of Florida, and later Colorado State University. He joined Bell Laboratories in 1972 where he has been involved in the development of splicing systems.

SPlicing METHOD USING HEAT-SHRINKABLE TUBES FOR SUBMARINE LOCAL CABLES

Yoshinori Kubota and Shinzo Yamakawa
Electrical Communication Laboratories
Nippon Telegraph and Telephone Public Corporation
Tokai, Ibaraki 319-11, Japan

ABSTRACT

A new splice enclosure has been developed for multipair shallow-sea cables, which are jelly-filled and have an aluminum-laminated polyethylene sheath. This splice enclosure uses an aluminum-laminated polyethylene sleeve as the splice case to retain the hydrogen sulfide-proof integrity equivalent to that of the cable. The sleeve is jointed to the cable by a fusion method using heat-shrinkable tubing of irradiated polyethylene and thermoplastic adhesives consisting essentially of ethylene-ethyl acrylate copolymer and low-density polyethylene. To improve the bonding reliability of the joint, a temperature-indicating pigment, the color of which changes reversibly at about 130°C, is incorporated into the adhesive. The design considerations, the adhesive development, the bonding reliability of the joint, the sulfide and mechanical resistances of the enclosure are discussed.

INTRODUCTION

As one of the local (short-distance) communication cables to connect a number of islands of Japan, polyethylene-insulated, polyethylene-sheathed multipair submarine cables (called the PE-P submarine cable) have been used since 1956. Since the cable sheath has no barrier to corrosive gas permeation, however, the cable often had the insulation failures due to the hydrogen sulfide trees.² In addition, it is unfilled cable having poor waterproofness. To solve these problems, NTT has developed a new multipair shallow-sea cable in cooperation with the Ocean Cable Co. Ltd.¹ This cable is filled with a polybutene compound and has an aluminum-laminated polyethylene sheath; hence the name¹ is Jelly-Filled Laminated Aluminum Polyethylene sheathed submarine cable (called the JF-LAP submarine cable).

These shallow-sea cables, although installed initially without cable splice, require a splicing method for repairing cable failures. A welding technique using an electrical heating wire has been used for enclosing the PE-P submarine cable splices. However, the enclosure uses a PE sleeve as the splice case, which has no barrier to corrosive gas permeation. In addition, the welding operation demands a critical heating control for satisfactory welds. The introduction of the new sulfide- and water-proof cable requires the development of a more reliable splice enclosure than that used in the old-type PE-P submarine cable. This paper presents a new method of enclosing the multipair shallow-sea cable splices, whose method uses heat-shrinkable tubing of irradiated PE and thermoplastic adhesives.

DESIGN CONSIDERATIONS

Requirements

The splice enclosure for the shallow-sea cables must (1) have the sulfide- and water-proof integrity equivalent to that of the cable, (2) withstand the water pressure up to 20 kg/cm² corresponding to 200 m of sea depth, (3) be strong enough to withstand the tensile and bending loads and the kinks developing when cables are laid or recovered. Furthermore, the enclosure requires

(4) short installation time, (5) no special tool or equipment, (6) no high degree of skill, (7) minimum number of parts for a given enclosure size, and (8) minimum range of part sizes to accommodate all the cable sizes.

Sleeve and Encapsulant

The enclosure is designed to have the sulfide- and water-proof integrity equivalent to that of the JF-LAP submarine cable. According to this primary design objective, an aluminum-laminated PE sleeve was used as the splice case and was filled with the same compound as that used in the cable. The sleeve has the same laminate structure as the cable sheath and is manufactured in the same way as the cable; accordingly, it is referred to as the LAP sleeve. The LAP sleeve has two holes for injecting the encapsulant.

Sleeve-Cable Jointing

In the splice enclosure for the PE-P submarine cable (Figure 1), the PE sleeve having no metal barrier is jointed to the cable by a welding technique with an electrical heating wire consisting of copper wires embedded between PE sheets. This jointing method (referred to as heating wire method), which is similar to those^{3,4} in land cables, requires a very careful heating control to weld reliably the sheath without its thermal deterioration and distortion. In addition to the correct interface temperature, the welding operation requires a correct pressure, i.e., a tight contact between the surfaces to be welded. A neoprene tape is used for this purpose. However, the pressure-applying method cannot be applied to the LAP sleeve (for the JF-LAP submarine cable), which is too rigid to the radial pressure of the rubber tape. In fact, the jointing of the sleeve and the cable by the heating wire method resulted in faulty welds.

An answer to solving this problem is to weld or melt bond the cable sheath to the outer surface, but not to the inner surface, of the LAP sleeve. As one of such jointing methods, we chose a melt-bonding or fusion method using heat-shrinkable tubing as the pressure-applying material and thermoplastic adhesive as the binder of tube, sheath, and sleeve (referred to as heat-shrinkable tubing method). The principle is shown in Figure 2, where propane or gasoline torches are used as the heating tool. In the design, it is desired that the tube-adhesive and adhesive-sheath bonds have a high bond strength and environmental resistance similar to those of PE-PE weld. The desire led us to a choice of material combination: irradiated low-density PE as the tubing material and ethylene copolymers or PE produced by the high pressure method as the adhesive polymer. Although heat-shrinkable tapes of irradiated PE can be used in place of the tubing, the shrink forces and the workmanship of application are inferior to those of the tubing. According to the requirement that the joint must have the tensile strength equivalent to that of the cable sheath or the LAP sleeve, the minimum thicknesses of the tube and the adhesive layer were decided to be 1.6 mm and 1.0 mm, respectively.

Heating Control and Adhesive

The welding of land cable sheaths, the PE of which contains carbon black, requires the minimum temperature of 140°C ³ and the optimum temperature of $180\text{--}200^{\circ}\text{C}$ ^{3,4} at the welding interface. The welding of the submarine cable sheaths, the PE of which contains no carbon black, requires the interface temperatures similar to those in land cables.

In the heat-shrinkable tubing method (Figure 2), achieving such a high interface temperature requires heating with a strong flame torch for at least 3 min; the requirement of such a strong heating is a consequence of large temperature gradient (decreasing toward the inside) of the heating portion. However, the direct heating of the tube raised the surface temperature to more than 450°C and thus caused the thermal degradation of the tube PE containing no carbon black. In some cases, it resulted in the development of small surface cracks or crazing and the subsequent failure of the tube, whose failure occurs at the temperature of which the shrink force exceeds the breaking stress of tubing. According to the induction time data⁵ in autooxidation of stabilized low-density PE, it is recommended that the surface temperature of the tube does not exceed 250°C for 5-min heating. To prevent the overheating, accordingly, the tube surface was protected from direct flame by wrapping it with heat-shrinkable films or tapes such as irradiated PE films. Figure 3 shows the temperature increase curves at the each interface of the jointing assembly (Figure 2), which was strongly heated with a propane torch by two different operators (A and B). Apparently, the tube surface is effectively protected from overheating with the wrapped film (0.2 mm thick), and the interface temperature (T_1) between the film and the tube is maintained at about 250°C even when it is heated with strong flame torchs.

The interface temperature (T_3) between the sheath and the adhesive is of prime importance for achieving a high integrity joint by the heat-shrinkable tubing method. When low-density PE is used as the adhesive, the reliable welding of the interface requires relatively high interface temperatures (more than 140°C) and thus a critical heating control; in one case the interface temperature reaches 170°C (Figure 3B) and in other case it does not exceed 140°C (Figure 3A) for 5-min heating. A further stronger or longer heating might eventually result in the thermal distortion of the sheath and the sleeve and in burning of the tape and the tube. If the sheath PE is strongly bonded with a thermoplastic or hot-melt adhesive at lower temperatures than the welding temperature of PE, such an adhesive will relieve the critical heating control problem and improve the operation reliability of bonding. As a result of extensive investigations on a number of PE and ethylene copolymers, we developed a thermoplastic adhesive consisting essentially of ethylene-ethyl acrylate copolymer and low-density PE, which has a high bondability to PE even at bonding temperatures near the melting point of PE (see below). In this case, raising T_3 to 130°C ensure the integrity bond of the interface. As the T_3 indicator, a heat-sensitive pigment was used, whose color changes reversibly from yellow to orange at about 130°C . The reversibility permitted the pigment to be incorporated into the adhesive.

The shrink force of the tubing, consisting of irradiated low-density PE, begins to develop at about the melting point, increases abruptly at $110\text{--}130^{\circ}\text{C}$, and then reaches a constant value at about 140°C (Figure 4). The temperature inside the tube (T_2) always exceeds 140°C at the temperatures $T_3 \geq 130^{\circ}\text{C}$ (Figure 3).

Sulfide Capture

Although the use of the LAP sleeve decreased significantly the amount of sulfide penetrating through the enclosure, two additional paths of sulfide penetration was found: (1) the injection and vent holes in the LAP sleeve, (2) the gap and PE layers between the sheath and sleeve aluminums. To prevent the sulfide penetration through these paths, there are three possible ways: (A) to wrap the splice with adhesive aluminum tapes to make the penetration paths longer, (B) to incorporate sulfide scavengers into the encapsulant, (C) to seal the holes and the lap joints (between the sheath and the sleeve) with the adhesive copolymer containing sulfide scavengers, which is applied on the inner side of the adhesive with no scavenger (Figure 5). Table 1 summarizes the effects of these three methods on the sulfide prevention, where two copper strips ($0.2 \times 5 \times 230$ mm) were placed on the splice to detect sulfide penetration. The enclosure (Figure 5) was immersed in a sulfide aqueous solution of 1000 ppm at 30°C , under the same condition as which the JF-LAP submarine cables have no corrosion of the copper conductor. A lead acetate powder was used as a model scavenger dispersive with the encapsulant (method B), and a copper powder was used as a model scavenger dispersive with the adhesive copolymer (method C). It can be seen from Table 1 that method C is the best way to prevent the sulfide penetration. The adhesive copolymer with sulfide scavenger is referred to as the sulfide capture sealant.

PARTS AND MATERIALS

Figure 5 shows the enclosure developed for the JF-LAP submarine cable splices. The parts used are illustrated in Figure 6. They include:

1. LAP sleeve
2. Encapsulant
3. Heat-shrinkable tubing
4. Heat-shrinkable tape
5. Adhesive
6. Sulfide capture sealant.

The LAP sleeve is accompanied with two aluminum screws for sealing the injection and vent holes in the sleeve. The heat-shrinkable tubing is made of an irradiated low-density PE containing antioxidants and no carbon black. In field, a long piece (about 2 m) of the tubing is cut off to proper lengths for sleeve-cable jointing, injection holes sealing, and enclosure protection. The heat-shrinkable tape, which is made of an irradiated low-density PE film, is used for both the protection of the tube surface from direct flame and temporary fixing of wrapped adhesive tapes (see below). The adhesive consists of ethylene-ethyl acrylate copolymer, low-density PE, heat-sensitive pigment, and antioxidant. The adhesive sheet has a groove (on the inner side) serving as a guide line of air removal and as a temperature indicator at the interface. The sulfide capture sealant, which is provided as a sheet, consists of ethylene-ethyl acrylate copolymer, low-density PE, sulfide scavenger, and a combination of stabilizers.

PROCEDURE OF ENCLOSING

The following is a detailed description of the procedure of enclosing the JF-LAP submarine cable splices:

1. The LAP sleeve and the five tubes are inserted on the cable prior to splicing.

2. After the splice is completed, the sheath and sleeve surfaces to be bonded are wiped with a cotton cloth impregnated with petroleum benzin.
3. The sulfide capture sealant sheet is wrapped on the lap portion. Overlapping the sealant sheet, the adhesive sheet is wrapped over both the sleeve and the sheath and temporarily fixed with the heat-shrinkable tape.
4. The heat-shrinkable tubes are moved onto the wrapped adhesive tapes and pre-heated only to shrink them. On the shrunk tubes, the heat-shrinkable tape is herically wrapped and then heated with a strong propane torch until the color of the heat-sensitive pigment in the adhesive changes from yellow to orange and until the grooves on the inner surface of the adhesive tape melt away (the heating time is 4--5 min).
5. After the jointed part is cooled, molten polybutene compound is injected into the LAP sleeve through one of two holes in the sleeve.
6. After the holes are closed with the aluminum screws and after the neighborhoods are cleaned with petroleum benzin, they are sealed with the sulfide capture sealant, the adhesive, and the tube in the same way as that described above.
7. The application of a long piece of the tubing for the enclosure protection completes the enclosure.

The total time taken to enclose the splice is about 50 min. This time is 20 min shorter than that in the heating wire method.

ADHESIVE DEVELOPMENT

The design considerations in development of the adhesive follow those in the splice enclosure discussed above. The adhesive must have:

1. a high melt bondability to sheath PE at lower bonding temperatures than the welding temperature of the PE, and the bond must have a high strength and durability similar to those of the PE-PE welding at the field conditions,
2. also a high melt bondability to the heat-shrinkable tubing of irradiated PE,
3. a high cohesive strength and environmental resistance similar to those of the PE since it must also function as a gap-filling adhesive (or sealant) or must be applied in the state of a thick layer.

Before the enclosure development program began, studies were carried out on the hot-melt adhesive bonding of PE with the ethylene copolymers and on the methods of jointing land cables and PE sleeve.^{6,7} Accordingly, the objective of the adhesive development was to find a thermoplastic adhesive copolymer applicable to the splice enclosures in land cables as well as those in the submarine cables. This design feature extends the maximum design service temperature from 30 to 60°C and the PE to be bonded from no-carbon PE to black PE. As a candidate meeting these requirements, we noted ethylene copolymers produced by high pressure method, having high cohesive strength. Conventional hot-melt adhesive compounds, which consist essentially of ethylene copolymers, waxes, and tackifiers, cannot be used as the adhesive because of their low cohesive strength and the resultant low bond strength (especially at relatively high ambient temperatures). The

following is a short summary of aforementioned studies.

Table 2 summarizes hot-melt adhesive bondability of the various ethylene copolymers to a low-density PE (melt index 0.3 g/10 min, density 0.922 g/cm³). When the three types of ethylene copolymers are compared at similar comonomer content, it is apparent that the increasing order of peel strength of the joints bonded at 140°C is as follows: EEA > EVA > EAA. When low-density PE itself is used as a thermoplastic adhesive for the PE adherend, the welding does not occur at the bonding temperatures near the melting point (110°C); this is due to insufficient mobility of the polymer molecules to flow and interdiffuse at the temperatures. On the other hand, the use of ethylene-ethyl acrylate (EEA) copolymers as the adhesive yields high peel strengths even at bonding temperatures of 110°C, which is near the melting point of PE and about 20°C higher than those of the copolymers. This increased melt-bondability at 110°C by the introduction of the comonomer units, concurrent with the increase in polarity, arises from the lowered melting point.

When low-density PE is melt blended into the EEA copolymers, the peel strength at 70°C of joints bonded at 140°C with the polymer blends passes through a maximum at the PE content of about 10 wt % and the decreases with PE content (Figure 7). The peel strength at 60°C gave a similar result. Furthermore, the polymer blend of EEA-1/PE-1 = 9/1 showed a higher peel strength (at 23°C) at low bonding temperature (110°C) than does EEA-1 (Figure 8).

According to these results, a polymer blend of EEA copolymer and low-density PE was used as the adhesive material. The incorporation of heat-sensitive pigments, stabilizers, and sulfide scavengers into the adhesive copolymer resulted in little decrease in peel strength. The application of the adhesive copolymer to the sleeve-cable jointing decreased the optimum interface temperature from 180--200°C (of PE-PE welding) to 130--140°C, and improved significantly the operation reliability of the jointing.

OPERATION RELIABILITY OF BONDING

In the sleeve-cable jointing operation, the operation reliability of sheath-adhesive bonding is of prime importance to obtain a high integrity enclosure. The bond integrity was evaluated by a peel test along the cable circumference as shown in Figure 9, where the jointed portion was cut off (to a width of 1 cm) normal to the length of cable, and the sheath-adhesive interface was separated by a tensile test machine at a crosshead speed of 10 cm/min. Figure 10 shows typical autographic load curves of peeling of the bonds prepared by the heat-shrinkable tubing method (A) and by the heating wire method (B). From the curves, the maximum, the average, and the minimum peeling loads were determined.

Cleaning of Sheath Surface

To clean up the sheath surface, it was wiped with a cotton cloth impregnated with organic solvents. Table 3 summarizes the effects of solvent wiping on the resultant adhesive bond strength, where the sheath surface was contaminated with the polybutene compound in advance of wiping. It can be seen that the use of aliphatic and aromatic hydrocarbon solvents is effective in removing the encapsulant, although the use of acetone and ethanol is ineffective. Also these solvents were effective in removing grease and oil. According to these results, contaminated sheath surfaces were cleaned with petroleum benzin, one of these solvents, to ensure satisfactory bonding.

Effects of Climate Conditions

The operation reliability of jointing was examined in the range of -20 to 40°C of ambient temperature and in the range of 0 to 5 m/sec of wind. The heating time was 4--5 min. In case of 5 m/sec of wind, the heating operation with flame torchs was impossible. In case of 3 m/sec, the minimum peel strength was 5--11 kg/cm, whereas the average peel strength was 15--22 kg/cm. In the other cases, the jointing operation resulted in minimum peel strength of at least 15 kg/cm, and in average peel strength of at least 19 kg/cm without exceptions.

Differences among Splicers

Differences in bond strength among operators were examined by nine different laboratory persons. Further, a field trial was done by four different splicers. Both tests indicated that the operation reliability of bonding was excellent; the average peel strengths exceed 16 kg/cm without exceptions. The heating time, which was judged by the color change of the pigment and the disappearance of the grooves on the inner surface of adhesive, was in the range of 3.7--9.6 min (about 5 min in average). On the other hand, the heating wire method gave faulty welds in some cases (Figure 10).

DURABILITY OF BOND

The bonding mechanism of PE and ethylene copolymers has been discussed.⁶ Although whether the bond strength is due to interfacial Van der Waals forces or interdiffusion of polymer molecules through the interface is still in question, we believe that the resultant strong bond strength includes the contribution of the latter. In this case, the bond is expected to withstand field environments as well as PE-PE welds. The cut-off specimen (1 cm width, see Figure 9) was immersed in various aqueous solutions including sea water at 60°C for 21 months, and then the peel strength was measured at 23°C. The average peel strength showed no significant change (Figure 11).

PERFORMANCE OF ENCLOSURE

Sulfide Resistance

No sulfide corrosion was observed in the copper conductors and the copper strips placed on the splice, when the enclosures were immersed for 1 year in hot waters (containing hydrogen sulfide of about 30 ppm) at the Beppu hot-spring. Furthermore, the immersion test in a sulfide aqueous solution of 1000 ppm at 30°C showed no sulfide attack except the neighborhood of the injection holes in the sleeve (Table 1).

Water Pressure Resistance

The JF-LAP submarine cables are usually installed in shallow seas of less than 100 m. Without water penetration, the enclosures were placed for 6 months under the water pressure of 20 kg/cm² corresponding to 200 m of sea depth.

Mechanical and Gas-Tight Tests

The enclosures are required to have the tensile load resistance equivalent to that of the cable sheath. A tensile test, which was carried out at 50 mm/min of crosshead speed, showed no failure of the jointed portions but of the cable sheath. A kink test, as shown in Figure 12, were also done by the same tensile test machine at 15 mm/min of crosshead speed. The test showed some cracks in the laminated aluminum of cable and sleeve at about 500 kg load and some breaks in the cable sheath near the joint at about 600 kg load. On

the other hand, no failure was observed in the jointed portions.

Moreover, various mechanical and gas-tight tests, performed usually for the enclosures in land cables, showed no gas leak and mechanical failure in the enclosure. In these tests, the enclosures were not filled with the encapsulant but pressurized to 1 kg/cm². These tests include a heat-cycling test (-10 to 50°C) under 40 kg load, a bending test to a diameter of 12D (D = 3.6 cm, D is the diameter of cable) under 20 kg static load, a repeated bending test to a diameter of 50 cm, and a vibration test (-10 and 40°C) at 600 rpm of frequency to 1×10^6 cycles.

SUMMARY

The newly developed method of jointing sleeve to cable provides a high integrity splice enclosure for multipair shallow-sea cables. This jointing method, heat-shrinkable tubing method, has much higher operation reliability of melt bonding and demands lower degree of skill and shorter installation time for splicers than do welding methods using electrical heating wires. The enclosure withstands the shallow-sea environments and the tensile and bending loads which develop during laying and recovering. Currently, the enclosure system is undergoing field introduction.

ACKNOWLEDGMENT

Many people within NTT have contributed to developing the splice enclosure system, but special thanks are due to N. Niimura, M. Tozuka, H. Yamashita, S. Uruno, K. Nakamura, F. Yamamoto, and the staff engineers of the Engineering Bureau, NTT. Also, the authors are indebted to the Ocean Cable Co. Ltd. for the sulfide resistance tests and to the Sumitomo Electric Co. Ltd. for supplying the parts and the materials.

REFERENCES

1. K. Suzuki and R. Sawada, Proc. 23rd Int. Wire and Cable Symp., 1974, p 91.
2. T. Fukuda, T. Hisatsune, H. Nagai, and M. Hasebe, Proc. 21st Int. Wire and Cable Symp., 1972, p 75.
3. H. Ishikawa and K. Nagata, 14th Int. Wire and Cable Symp., Atlantic City, N. J. (December, 1965).
4. W. Buchholz, Siemens Review, 33, 25 (1966); H. E. Martin, 16th Int. Wire and Cable Symp., Atlantic City, N. J. (December, 1967); D. F. Gill, Proc. 24th Int. Wire and Cable Symp., 1975 p 99.
5. J. B. Howard and H. M. Gilroy, Polym. Eng. Sci., 15, 268 (1975).
6. S. Yamakawa, Polym. Eng. Sci., 16, 411 (1976).
7. S. Yamakawa and F. Yamamoto, ECL Tech. J., 24, 1525 (1975).



Yoshonori Kubota
Electrical Communication Laboratories
Nippon Telegraph and Telephone Public Corporation
Tokai, Ibaraki 319-11, Japan



Shinzo Yamakawa
Electrical Communication Laboratories
Nippon Telegraph and Telephone Public Corporation
Tokai, Ibaraki 319-11, Japan

Y. Kubota received a B.S. in Electrical Engineering from Yamaguchi University in 1964. Since joining Electrical Communication Laboratories in 1964, he has involved in studies on durability of encapsulant for electronic parts and in development of cable splice enclosures. He is a member of the Institute of Electronics and Communication Engineers of Japan and of the Society of Polymer Science, Japan. He is currently Assistant Chief of Cable Facility Section, Outside Plant Development Division.

S. Yamakawa received a B.S. in Applied Chemistry from the University of Kanazawa in 1962 and a M.S. in Polymer Chemistry from Kyoto University in 1966. He joined Electrical Communication Laboratories in 1966 and has been involved in studies on the radiation modification and adhesive properties of polyolefins. He is a member of the Society of Polymer Science, Japan. He is currently Assistant Chief of Radioisotope and Radiation Section, Component and Material Development Division.

Table 1. Prevention of Hydrogen Sulfide Penetrating through Enclosures.

Prevention of hydrogen sulfide penetration	Hydrogen sulfide attack ^a		
	Cu strip on the side of injection holes	Cu strip on the opposite side of injection holes	Cu conductor
None	×	△	×
A. The splice is wrapped with adhesive aluminum tape	△	△	△
B. Lead acetate is incorporated into encapsulant	×	○	×
C. Cu powder is incorporated into adhesive copolymer	△	○	○

^a The enclosures were immersed in a hydrogen sulfide aqueous solution of 1000 ppm at 30°C for 112 days. (○) no change, (△) slightly blackened, (×) completely blackened.

Table 2. Hot-Melt Adhesive Bonding of Polyethylene with Ethylene Copolymers.

Adhesive ^a	Comonomer ^b content	Melt index ASTM D1238	Density ASTM D1505	Melting point	Average T-peel strength at 23°C, kg/25 mm ^d	
					Bonded at 110°C	Bonded at 140°C
	wt % (mol %)	g/10 min	g/cm ³	°C		
PE-1	-	0.25	0.919	106-107	0.2	35 ^e
PE-2	-	7.0	0.922	-	-	35 ^e
PE-3	-	20	0.914	-	0.6	38 ^e
EVA-1	8 (2.8)	2	0.93	93	3.5	39 ^e
EVA-2	14 (5.1)	3.3	0.93	87	6.0	16.5
EVA-3	19 (7.1)	2.5	0.94	80	2.6	8.0
EVA-4	19 (7.1)	150	0.94	77	-	12.3
EVA-5	28 (11.2)	6	0.95	-	-	1.7
EVA-6	28 (11.2)	150	0.95	-	-	3.0
EEA-1	15 (4.7)	1.5	0.930	87-89	25.0	45 ^e
EEA-2	18 (5.8)	6	0.931	87	15.0	45 ^e
EEA-3	19 (6.2)	2.2	0.933	83-85	24.0	45 ^e
EAA-1	6-7 (2.4-2.8)	10	0.935	96	-	10.7
EAA-2	6-7 (2.4-2.8)	10	-	97	-	13.0
EAA-3	20 (8.9)	50	0.96	95	-	0.5

^a The ethylene-vinyl acetate copolymers (EVA) were supplied by Mitsui Polychemical Co. Ltd., and the ethylene-ethyl acrylate copolymers (EEA) and the ethylene-acrylic acid copolymers (EAA) by Union Carbide Corp.

^b Determined by infrared spectroscopy and titration.

^c Determined from the peaks of endothermic curves of the differential scanning calorimeter.

^d A T-peel specimen, consisting of PE (2 mm) — adhesive (0.5 mm) — PE (2 mm), was prepared by heating for 5 min with a hot press at 110°C or 140°C, and the T-peel strength was measured according to ASTM D1876-61T.

^e Adherend failure.

Table 3. Effects of Solvent Cleaning of Contaminated Cable Surface on Adhesive Bond Strength.^a

Solvent	Peel strength, kg/cm		
	Maximum	Average	Minimum
None	5.0	2.5	2.0
	4.5	2.5	2.5
Ethyl alcohol	19	6.0	2.0
	14	6.0	2.0
	11	4.0	2.0
Acetone	25	21	11
	24	18	13
	24	19	7.0
Petroleum benzin	22	21	18
	23	21	16
	25	22	18
toluene	25	22	19
	26	25	24
	26	25	24
decalin	24	22	19
	23	21	20
	24	21	19
Tetralin	24	22	22
	24	22	20
	27	25	22

^a The cable sheath was contaminated with a polybutene compound in advance of solvent cleaning.

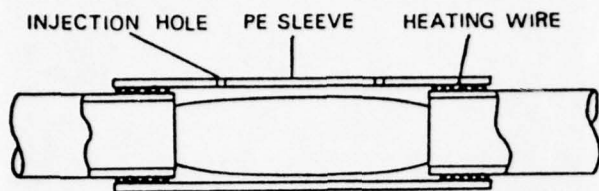


Figure 1. Splice enclosure for the PE-P submarine cable, which uses a welding technique using an electrical heating wire for sleeve-cable jointing.

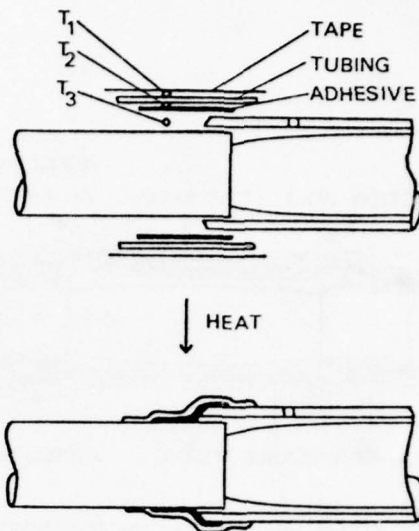


Figure 2. Heat-shrinkable tubing method for sleeve-cable jointing.

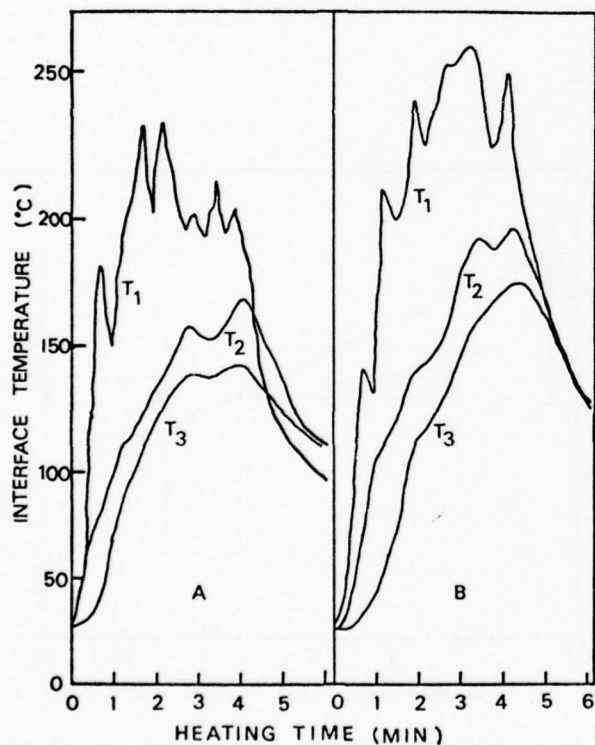


Figure 3. Temperature increases at the interfaces of jointing assembly (Figure 2), which was heated with a propane torch by two different operators (A and B). The thicknesses of tape, tube, and adhesive were 0.2, 1.6, and 1.0 mm, respectively.

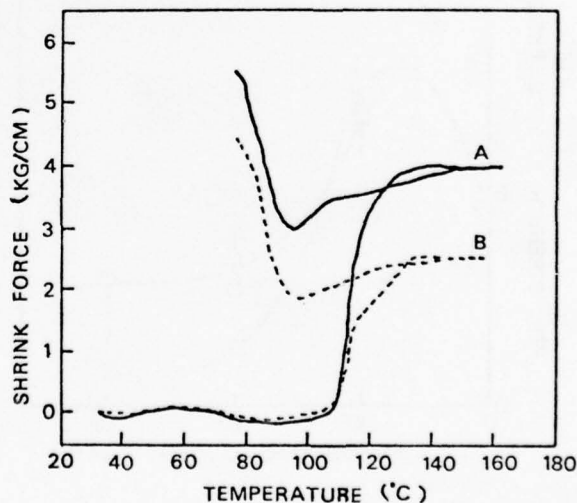


Figure 4. A typical change in shrink force of tubing with increasing and decreasing temperature. Two tubings (1.6 mm thick), which consist of an irradiated low-density PE and have different shrink forces (A, B), were heated at 2--3°C/min of heating rate in a circulating oven.

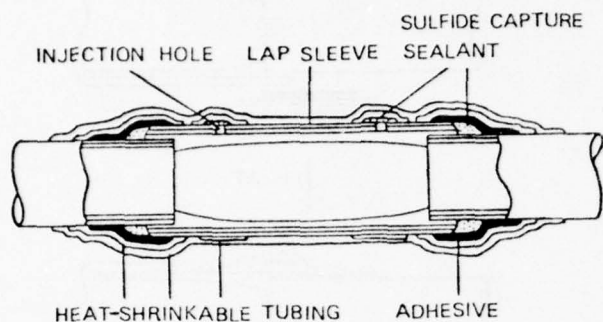


Figure 5. Splice enclosure for the JF-LAP submarine cable, which uses heat-shrinkable tubing and thermoplastic adhesive copolymer for sleeve-cable jointing.

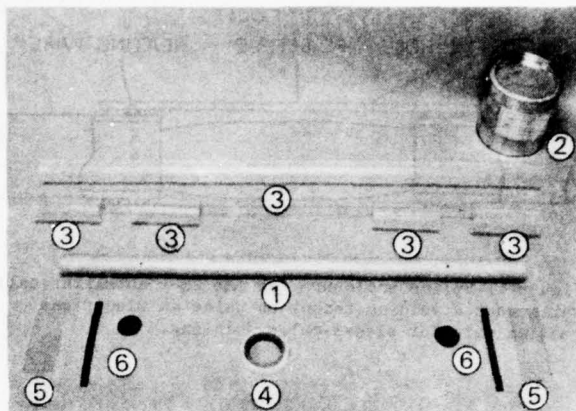


Figure 6. Parts and materials for enclosing the JF-LAP submarine cable splices: (1) LAP sleeve, (2) encapsulant, (3) heat-shrinkable tubing, (4) heat-shrinkable tape, (5) adhesive, (6) sulfide capture sealant.

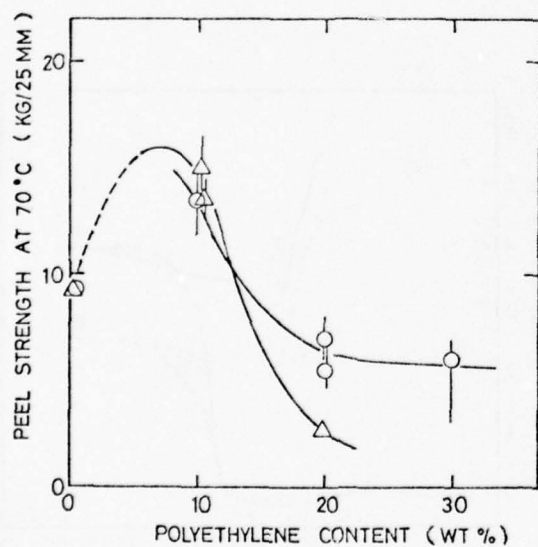


Figure 7. Effects of blended polyethylene content on peel strength at 70°C of joints bonded at 140°C for 5 min with ethyl acrylate copolymer (EEA-1) - polyethylene polymer blends: (○) PE-1, (△) PE-2.

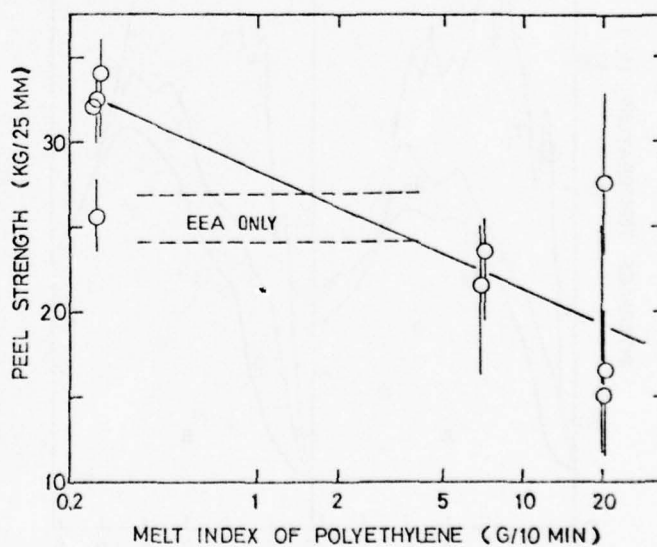


Figure 8. Effects of melt index of blended polyethylene on Peel strength at 23°C of joints bonded with polymer blend (EEA-1/PE = 9/1) at 110°C for 5 min.

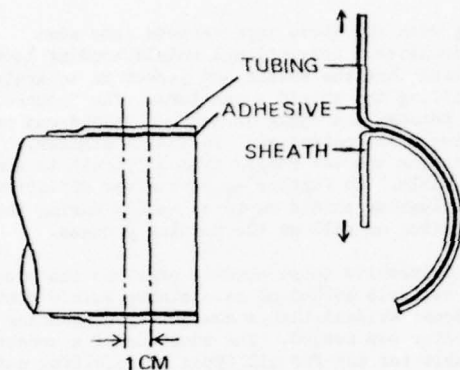


Figure 9. Peel test for evaluating the bonding reliability of cable sheath--adhesive interface.

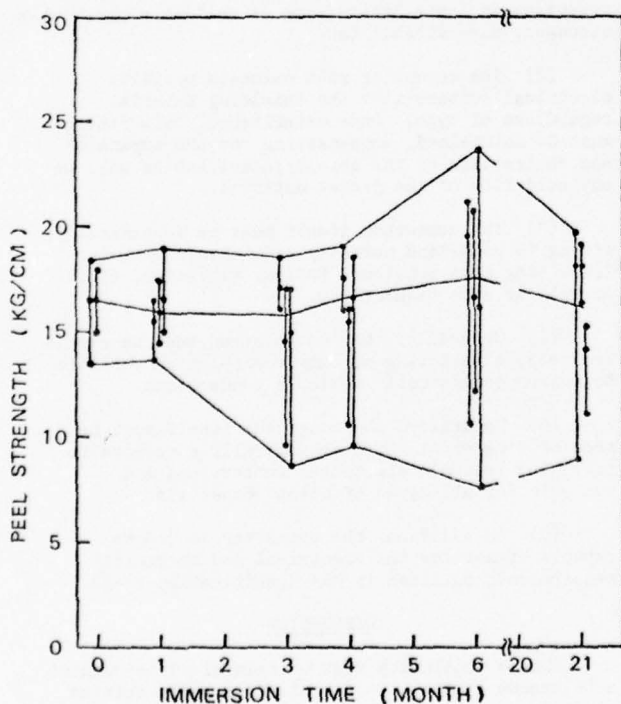
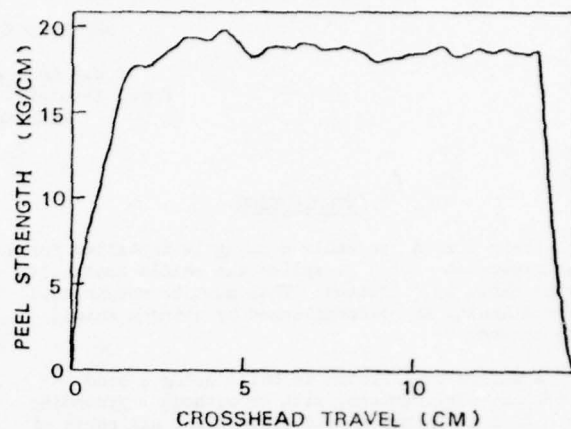
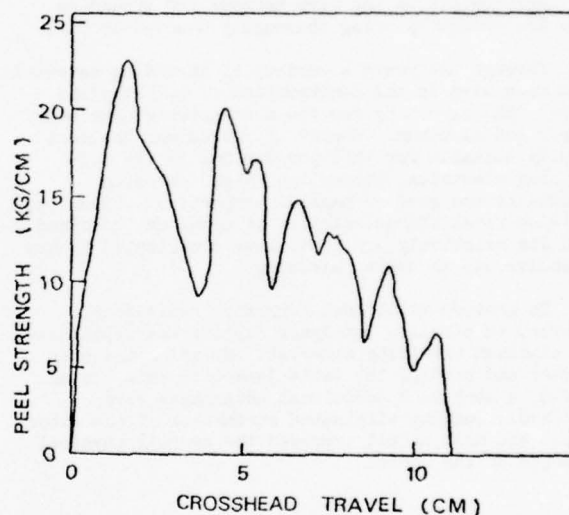


Figure 11. Peel strength vs. immersion time. The cut-off specimen (Figure 9) was immersed in a sodium chloride aqueous solution of 7.2 % at 60°C, and the peel strength at 23°C was measured.



A. HEAT-SHRINKABLE TUBING METHOD



B. HEATING WIRE METHOD

Figure 10. Typical autographic load curves of peeling of bonds prepared by the heat-shrinkable tubing method (A) and of welds prepared by the heating wire method (B)

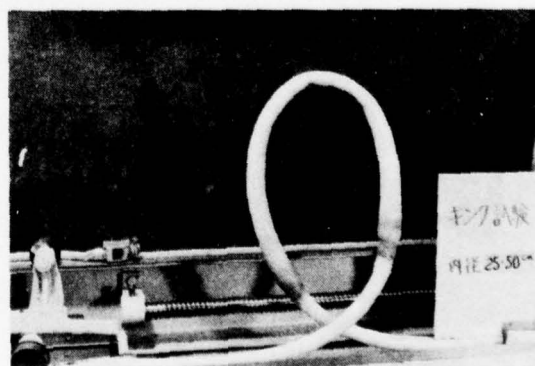


Figure 12. Kink test of enclosure.

SHIELD BONDING CONNECTORS

Louis Ance and H. M. Hutson
Rural Electrification Administration
Washington, D. C.

INTRODUCTION

Every time a new cable housing is installed for a subscriber connection or splice the shield continuity of the cable is disrupted. This must be reconnected. The continuity is re-established by using a shield bond system.

A shield bond system is built using a bond connector, wire harness, with or without a grounding lug. To restore the shield connection, all parts of the system must be installed properly. This paper deals mainly with the bond connectors. Considerations for improvements on the wire harness and grounding lugs are presently being thoroughly studied by REA.

Through the years a variety of shielding materials have been used in the construction of polyethylene jacket cables, but by far the most notable have been copper and aluminum. Copper of course was the most ideally suitable for this purpose due to its outstanding electrical properties, high corrosion resistance and good mechanical properties. Likewise, the electrical characteristics of aluminum, combined with its relatively low cost, have contributed to its extensive use in cable shielding.

To provide additional corrosion resistance, however, an ethylene copolymer coating was applied to the aluminum shielding material. By going one step farther and bonding the cable jacket to this coated shield, a number of additional advantages were realized. Bonding eliminated shrinkback of the outer jacket and most of all improved the overall physical strength of the cable.

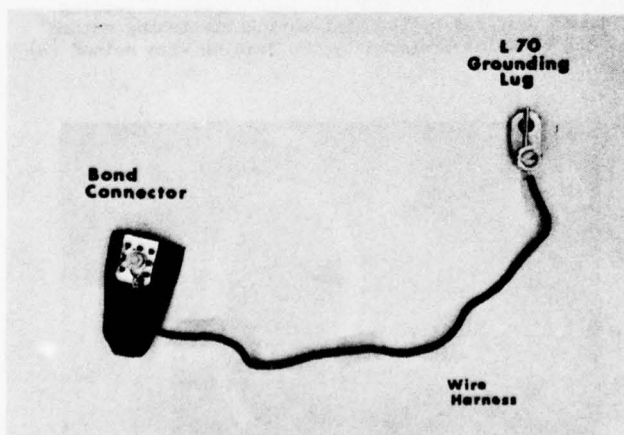


FIGURE 1

Along with all these improvements came some difficulties. Conventional shield bonding techniques required that the shield and jacket be separated before installing the shield connectors. The "controlled" bond between the cable jacket and shield was very difficult to control and, in most instances, separating the two ranged from difficult to almost impossible. To further aggravate the situation, the soft aluminum shield ruptured easily during the separating as well as the bonding process.

To resolve these bonding problems and provide a more reliable method of maintaining shield continuity, it became evident that a new universal bonding connector was needed. The adoption of a connector suitable for use for all types of shielding material would ensure proper application of the product. It would also reduce initial construction cost as well as the maintenance cost.

Suggested design parameters and desirable features which could possibly be incorporated into the design of a new connector included the following:

(1) Connector should be installed directly over the shield and jacket regardless of shield type to avoid the need to separate the shield from the cable jacket. This feature would result in a substantial reduction in installation time as well as a physically stronger, more durable tab.

(2) The connector must maintain positive electrical contact with the shielding material regardless of type. Once established, this contact must be maintained, compensating for the expansion and contraction of the shield/jacket tab as well as any cold flow of the jacket material.

(3) The connector itself must be mechanically strong to withstand normally encountered stresses (resulting from tensional forces, vibration, etc.) as well as some mishandling.

(4) Generally, the installation must be simple and easy, eliminating as many variables as possible to insure consistently reliable connections.

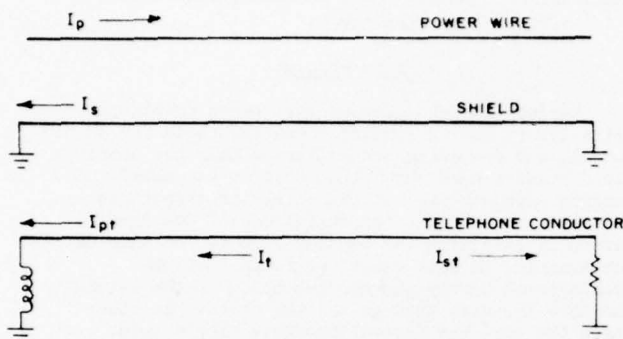
(5) Naturally, the connector itself must be made of a material which is generally conducive to providing reliable electrical connections and suitable for all types of shield materials.

(6) In addition, the connector should be capable of meeting the electrical and mechanical requirements outlined in REA Specification PE-33.

DISCUSSION

Shield continuity must be maintained throughout a telephone system. Good continuous cable shields are necessary to minimize problems with power induced noise, lightning and electrical system fault currents. One purpose of the shield is to

effectively reduce the magnitude of harmonic frequencies of the fundamental power frequency that appear in the voice frequency band and are induced longitudinally on the cable conductors. A simple illustration of the effect of shielding is shown in Figure 2.



EFFECT OF SHIELDING

FIGURE 2

Unbalance currents (I_p) in the power system induce voltage in both the shield and conductors of a communication cable. The conductor has a low impedance to ground at the office through the relay windings and a higher impedance at the subscriber location. A longitudinal current (I_{pt}) will thus flow on the conductor. When the shield is grounded at both ends a current (I_s) will flow through the low shield resistance and a magnetic field will be set up around the shield. Due to its close proximity to the cable conductors a voltage will be induced in the conductors in opposition to that induced by the power line. Its magnitude will depend on shield resistance, shield bond resistance and the ground resistance. This voltage produces a current (I_{st}) on the conductor. The residual current (I_t) still flowing on the conductor will be the difference between the current (I_{pt}) and (I_{st}). In practice perfect shielding will seldom occur but the reductions achieved by adequate shields and shield continuity result in noise levels that are satisfactory for most situations.

Cable shielding for lightning induced currents operate in the same way as noise currents except that the magnitude of currents is much higher and the function of the shield is to minimize dielectric voltage differences between cable conductors and the shield rather than noise voltages.

Reduction in voltages from these sources not only protects the cable conductors from failures but assists in protection of equipment such as carrier repeaters connected to the cable circuits.

Shield grounds are obtained at the subscriber's premises by tying into the multi-grounded neutral of the power system. These are the best grounds obtainable. On the average there are about four subscribers per mile. With such subscriber density, under normal circumstances it is not necessary to use auxiliary grounds at the pedestal.

A good bond connection to the shield means no contact resistance between the shield and the connector. While in practice it is impossible to obtain such a connection, there are connectors on the market which have very low contact resistance when installed properly. (Values in the order of 10^{-4} ohms or below).

When the contact resistance of the connection increases, there is a large amount of heat produced when large currents pass through the connector. One source of the large currents a shield conducts is due to lightning induced voltages. The voltages which are large in amplitude and of short duration induce large currents on a cable shield and can cause dielectric failures in the cable. If the shield bond connector has a high contact resistance, the high current can cause a hot spot and burn open the shield at this point. Likewise power system fault currents can induce high voltages with resulting large currents on cable shields. These tend to be of longer duration than lightning surges so that hot spots from high resistance shield bond contacts can be a problem under these circumstances.

Any design of shield bond connectors that meet all of the requirements outlined above, require proper installation to be effective. Experience has indicated that there is a great deal of misapplication of bond connectors in the field.

Improperly installed bonding connectors are not an isolated problem related to one or two telephone companies. This is a universal problem throughout the country.

Laboratory Data

REA Specification PE-33, "Cable Shield Bonding Connectors" requires the following tests which a bonding connector must pass before it is considered acceptable by REA:

1. Initial Vibration
2. Temperature Cycling
3. Heat Aging
4. Current Cycling
5. Hydrogen Sulfide Exposure
6. Final Vibration
7. Fault Current

Of the above tests the most significant are the Temperature Cycling and Heat Aging.

Temperature Cycling

The environmental cycle is:

Temperature Cycle (°C)	Cycle Hours	Number of Cycles
-40° to 60° to -40°	4	50

Measurements of the millivolt drop across the bonding connectors were made at the beginning of the first cycle and at the completion of the 50th cycle. The measurements were made while a 3 ampere direct current was passing through the

bonding connector. It is realized that noise current shielding requires far lower currents than the 3 amperes, i.e., 100 Ma. Revisions in REA Specification PE-33 are being considered which will involve more testing at lower current levels.

Five different sets of bonding connectors were put through the test using cables with a coated aluminum shield. The table below gives the average of each set. Each bonding connector set has four samples. Only two connector types were stable enough to pass this test. (A change of less than 1 millivolt is considered acceptable).

Bonding* Connector	Preaging Millivolts	Postcycling Millivolts	Change Millivolts
A	2.77	35.20	32.43
B	2.21	52.73	50.52
C	1.90	2.00	0.10
D	2.03	7.92	5.94
E	6.84	7.20	0.36

*1" cable diameter

Bonding connector "E" was then placed in the Temperature Cycle test using coated aluminum, copper and coated aluminum plus steel shielded cable.**

**Consists of two independent shields - 8 mil coated six mils terne plated steel.

Shield* Type	Preaging Millivolts	Postcycling Millivolts	Change Millivolts
.005" copper	2.23	2.24	0.21
.008" coated aluminum	2.38		0.17
coated alum.-steel	10.39	10.55	0.16

*1.125" cable diameter

Even though all samples passed, there is a significantly higher magnitude of voltage when coated aluminum-steel shields are used. This indicates a poorer contact but it is still stable with only 0.16 millivolt change.

Heat Aging

Bonding connector "E" was then put through the Heat Aging test under the following conditions:

Aging Temperature	Duration (Hours)
65°C	24

The voltage drop across the bonding connector with a constant of 3 amperes direct current was measured before and after the cycle.

The bonding connector passed when used with the shield types investigated and again the millivolt magnitude of the connection coated aluminum-steel was about five times the copper or coated aluminum.

Shield* Type	Preaging Millivolts	Post Aging Millivolts	Change Millivolts
.005" copper	2.43	2.46	0.03
.008" coated aluminum	2.55	2.56	0.01
coated alum.- steel	10.55	10.55	0.0

*1.125" cable diameter

Field Problems

During the past year we have heard considerable criticism regarding bonding connectors both for shield bonding and grounding connections within the housings. Field studies have shown that most of the shield bonding problems are not caused by the connectors themselves but by the improvisations of the craftsman in attaching the bonding wire to the shields. For example, in some cases, we found that the craftsman merely punched two holes in the shield and wove the wire through the two holes. In other cases the wire was forced through a single hole, bent back on itself and crimped as a fishhook on both copper and aluminum shields. Still in another case standard connectors were installed improperly not following manufacturer's recommendations resulting in poor joints. In our field study we found approximately 23 methods of incorrectly attaching the bonding wire to the shields.

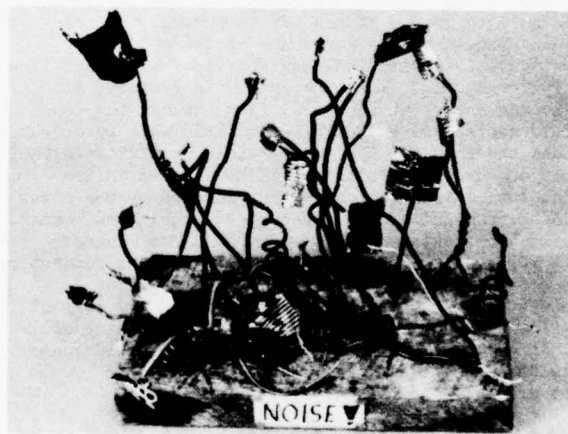


FIGURE 3

Field Data

A field trial to measure the stability of existing bonding connectors was arranged at a telephone company. The trial was initiated by taking a route that had noisy circuits and had a history of lightning outages. To insure that properly installed bonds were made, all bonding connectors were made by the same telephone company splicer under the supervision of the authors. Before removal, the old bonding connectors were measured

and photographs taken of any unusual appearances. A typical example is shown in Figure 4.

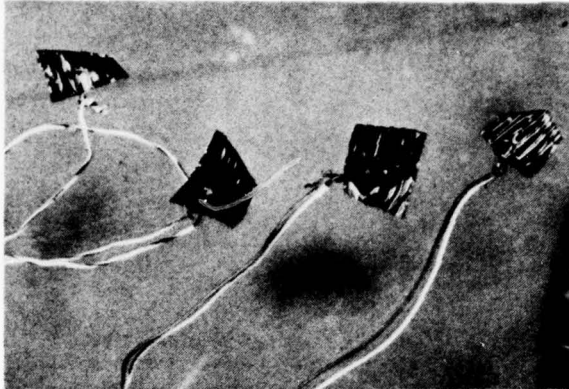


FIGURE 4

After new bonds were installed, measurements were made. The bonding connections were remeasured after six months.

Average Millivolt Drop

	<u>Cable</u>	<u>Wire</u>
Pre-field trial	1.46	1.66
Initial	0.36	0.54
6 months	0.46	0.69

The pre-field trial data shows a lack of good bonding when compared with the newly installed connectors. After the six month period the connectors remained stable electrically.

The field trial data is separated for cables and wires to show that good bonds can be obtained on 2 and 3 pair wire using standard bonding connectors.

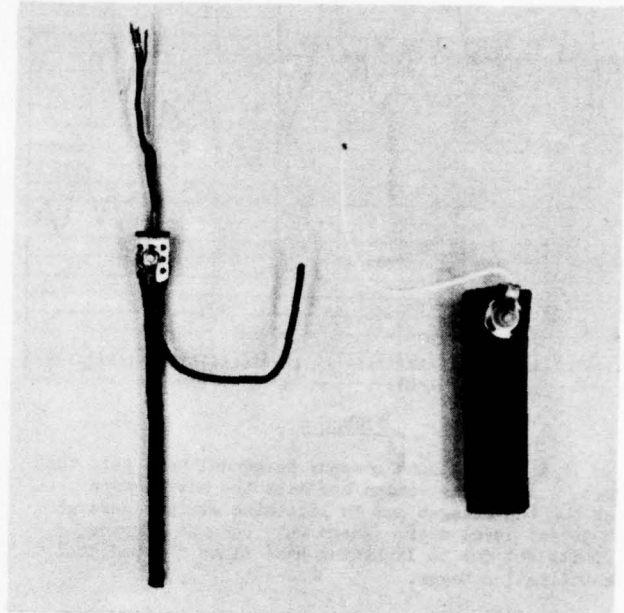


FIGURE 5

Noise measurements on this route have shown a marked improvement.

	<u>Pre Installation of New Bonds</u>	<u>Post Installation of Good Bonds</u>	<u>Typical Readings Indicating Good Shielding</u>
Circuit Noise (dB)	33	14	20
Power Influence (dB)	94	81	90

Since the field trial has begun there have been no subscriber complaints or lightning outages.

Overall data from the telco has shown a trouble index reduction from 8.5 per 100 subscribers to 7.0 for the same period this year. The telephone company began an overall rehabilitation of all pedestals in the fall of 1975 and since that time there has been a steady decrease in the trouble index.

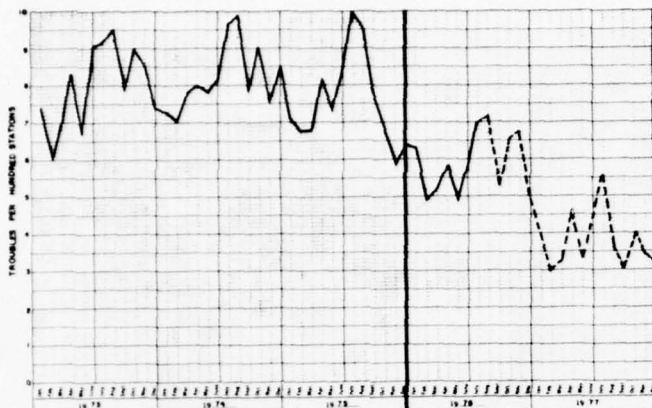


FIGURE 6

In fact telephone company personnel have said that the 1976 lightning season has been the most severe ever but the outages due to lightning strikes were at the lowest level ever. There have been no carrier circuits out due to lightning hits since the pedestal rehabilitation began.

Economics

In 1975 it cost the telephone company \$970 K for labor maintenance during the first seven months of the year. In early fall a rehabilitation of pedestals was initiated and the subscriber trouble index began to drop. In the first seven months of 1976 it cost \$730 K in labor maintenance resulting in a savings of nearly \$240 K over the prior year. Assuming a decreasing trouble index leveling at the target objective of 4.0 by the end of 1977 would result in a net saving of over \$2.4 million in the next five years. It is clear that rehabilitation programs to ensure that cable shield bonding are properly installed as well as other potential plant problems is a good investment to lower operating costs.

Conclusions & Recommendations

As the results of our field study indicate, we believe that the average craftsperson has no idea of the importance of proper bonding of cable shields. It also appears from our field evaluation of many sample bonding connectors that they have no concept of what is considered an acceptable shield connection. We therefore recommend that an extensive educational program be initiated to acquaint the craftsperson with fundamentals of making proper shield connections and determining the adequacy of the connections through test methods.

We also recommend that each telephone company test their bonding system and rehabilitate the entire bonding system if necessary. We believe the expense of rehabilitating the bonding system will more than pay for itself in the long run.

Maintenance required for service restoral is costly not only from a labor standpoint, but causes poor customer relations. Preventive maintenance creates good will with customers by improving service and because it is a planned maintenance, it eliminates excess labor costs for overtime payments and emergency crews.

BIOGRAPHY

Louis Ance is on the staff of the Outside Plant Branch of REA's Telephone Operations and Standards Division. Previously he was a manager of Product Engineering, System Equipment Plant, Superior Cable and Equipment Division, Hickory, North Carolina. Most of his work has been in the field of outside plant application and designing and is the holder of 6 patents in Telephony.

Harry M. Hutson graduated from Johns Hopkins University with a B.S.E.E. degree in 1970 and attended Georgia Tech in 1971 and 1972. He is presently an Outside Plant Engineer with the Rural Electrification Administration. He was previously associated with Bell Telephone Laboratories, Atlanta, Georgia.

ENVIRONMENTAL EFFECT OF TELEPHONE FACILITIES

Malcolm N. Evans
Southern New England Telephone
New Haven, Connecticut

Summary

Telecommunications facilities, in particular telephone facilities, have been with us now for about one hundred years. The most prevalent form of these facilities is pairs of wire. Through the years steel then copper have been the most popular conductors. Recently some aluminum has been used, but it has not been a popular alternative for a variety of reasons. These conductors have been strung between poles, placed in underground conduits or buried directly in the ground both as individual pairs of conductors or bundled into cables. The networks that have evolved allow for a physical metallic connection between any two telephone customers in the world. Indications for the future are that the network will continue to expand as newer and wider service offerings are developed. In keeping with most conveniences enjoyed by modern man, little concern has been shown in the past with regard to the impact of providing these telecommunications facilities on the environment. This paper will attempt to point out some of the possible effects and suggest directions which should tend to reduce the detrimental impact and insure the continued availability of high quality communications to the individual citizen.

Visual Pollution

The most obvious and immediate environmental effect is the one we see, feel or hear. Telecommunications facilities, described in the 1969 National Environmental Policy Act as "Underground cable or waveguide routes, and aerial transmission lines, for Long Distance Telecommunication, . . .", affect what we see. The Federal Communications Commission has effectively limited the impact considerations to possible visual pollution by referencing "--- the visual or aesthetic impact of (communications facilities) as their primary environmental affect. In most cases indeed, if aesthetics were not a factor, we doubt very much that routine environmental input and processing would be justified." This may be a short sighted statement and will be treated as such in a later section of this paper. For the moment the aesthetic impact will be considered.

We must first accept the fact that wire communications are a part of our way of life. With today's technology the only economical way to provide large percentages of the population with telephone service is to provide an electrical path from a local switching center to each customer. The earliest telephone systems utilized a pair of wires along a street onto which were bridged several individual customer's lines. As a result the connection from customer to switching center was a shared facility and provided party lines. The wires to provide this service were almost entirely

run along lines of poles, also utilized to provide electric service.

As the requests for telephone service grew, and party lines became more and more unusable, additional wires were run along the same poles. This quickly led to unsightly and unservicable conditions. The introduction of covered copper wire permitted the use of telephone cables as opposed to open wire. Large scale introduction of cables generally occurred in conjunction with the introduction of rotary dial telephone service. Utility poles that formerly contained several cross-arms with many wires now had a single cable connected directly to the pole. The reduction in visual pollution was not the goal of this evolution but a result of a more efficient system.

We have concentrated on telephone facilities on poles or aerial cable. Telephone cable has also been placed underground in conduit. Due to the high cost of this type of construction it has been traditionally used only in high density areas. That is, areas where large numbers of facilities are required. Generally speaking, business centers and heavily populated residential locations. The result of underground construction is aesthetically pleasing - nothing is observed but an occasional manhole cover. Once again, however, the reduced visual pollution is a result of construction that took place for reasons other than reduction of unsightliness. One should not get the impression that the telephone industry reduces visual pollution by accident. More recent trends, particularly in new suburban housing developments, show a willingness on the part of telephone companies to absorb some degree of economic penalty in order to place new cables underground. This can be accomplished in residential areas when subsequent cables will not be required by burying the telephone cable directly in the ground. In this type of construction the conduit is not placed and the cost is reduced.

Increasing use of electronic devices also has consequences in visual pollution. Recent innovations, which will be discussed in more detail in a later section, reduce the need to place additional cable sheaths by allowing existing cable pairs to provide more customer connections. While reducing the unsightly additions to aerial cable runs, electronic devices require housings for the equipment somewhere near the customer's location. Although these housings are being reduced in size through technological advances in electronics, they are of a size that can be considered visually detrimental. The solution has been to camouflage the housings either by screening with shrubbery, fencing or even simple painting.

The factor that most often results in visual pollution is the cost of constructing "out of sight" facilities. Since the telephone company is responsible for funding the construction of distribution facilities, and this funding ultimately comes from the customer, tight budgetary constraints are maintained on construction expenditures. Since it is so very difficult to assign dollar value to aesthetics it is little wonder that reduction of visual pollution more often becomes a result of meeting other requirements rather than the cause for higher cost facilities.

Impact on Natural Resources

Poles

Standing across the United States today there are perhaps 100 million wood poles supporting telephone and electric service wires and cables. These poles are supplied to the telephone industry ready to be placed into service. This makes the industry highly reliant on the pole suppliers to maintain adequate forest areas for harvesting the trees to be used as poles. This large scale use of a natural resource has prompted much conservation effort by the wood industry.

Wooden poles, exposed to the elements and in constant contact with the ground, are all subject to rot and insect attack. This potential destruction is held at bay through the techniques of wood preservation. Very simply stated, wood preservation involved impregnating dried lumber with hop preservatives under pressure. This procedure enables a pole to remain in use for periods averaging thirty years. This generally exceeds the length of time required for a new tree to grow. Integrating these preservation techniques along with good forestry techniques has led to the present situation in which more trees are being grown than removed. As a result, wood utility poles, which represent about one quarter of the treated wood market, are in good supply at low cost. The installed cost of a utility pole ranges between one hundred and two hundred dollars. If the pole is in joint use by two or more utilities this cost is distributed accordingly. Since each pole can support about one hundred and fifty sheath feet of cable the cost of this aerial cable construction is hard to beat.

This, of course, leads us back to the first topic covered in this paper - Visual Pollution. To minimize visual pollution a structure capable of supporting communications facilities must compete economically with poles and aerial construction. To get telephone cables out of sight they are placed in the ground. Under ideal conditions the cost of 150 feet of trench may be about double the cost of a single pole. Reduced maintenance and extended life of the cable once it is in the ground tend to reduce the recurring costs, however, it is seldom more economic to bury the cable. The cost problem is often aggravated by roadway or development contractors' time schedules that ignore the needs of the utilities. Rather than coordinating construction efforts the telephone utilities are left to construct their facilities over, under and around the other facilities. Again the re-

sulting decision is between cost and visual pollution - a real versus an aesthetic value.

Copper

While visual pollution is an intangible effect on our environment, viewed differently by various individuals, some effects of building and maintaining a telephone network are measurable and irreversible. Use of natural resources that are not regenerated has to be controlled by responsible users. The telephone industry uses the world's copper resources at a very high rate. Copper provides the most satisfactory medium over which telephone messages can be transmitted. The worldwide telephone networks are probably the largest users of the dwindling copper reserves. It has been estimated that the Bell System alone uses one ninth of the world's copper production annually. Projections made in the early 1970's by the Club of Rome in "Limits of Growth" indicate that the world's copper resources may be exhausted as soon as 1991 (see figure 1). While this may be a pessimistic view, nonetheless copper is a limited resource that is being rapidly used up.

Southern New England Telephone serves approximately 1.3 million customers in a primarily suburban environment. The exchange cable we placed in 1974 equated to 2,655 tons of copper. Reviewing the placements we found that about 94% of the growth requirements were served by slightly more than 1,400 tons of copper. This means that almost half of our copper usage serves only 6% of our facilities requirement. (See figure 2). We have no reason to believe that this was an unusual year, nor do we feel that our usage differs greatly from that of other operating companies in a similar environment.

Recent developments in the field of electronics have the potential of greatly affecting the existing telephone networks. Riding on the shirtrails of the computer and aerospace technologies, "Loop Electronics" include devices that can increase the resistance design limit or reduce the number of wire pairs required to provide facilities to the customers. These devices are referred to as range extenders and pair gain devices respectively. Projected cost trends indicate that the cost of electronic devices will be coming down, while the material and labor costs associated with placing cable will continue to rise. Increased use of electronics in the local network will result in greatly reduced need for copper. A proposed design change that may be economical before the 1980's would utilize electronic devices and only fine gauge cable to serve the entire local network (See figure 3). If adopted, this design could reduce the copper use by as much as 75%. Environmental considerations are a prime factor in the attempt to start implementation of this plan.

Underground Construction

This paper repeatedly refers to underground or buried cable as the solution to the problem of visual pollution. Perhaps this is so, but then again perhaps this just ignores one problem and aggravates another. Space in public rights of way is very limited. In

urban areas where heavy business or residential occupation is occurring, construction of underground facilities is extremely difficult almost to the point of being impossible. The increased difficulties are reflected in the costs associated with constructing underground conduit. It is possible for costs of conduit to run in excess of \$1,000 per duct for the same 150 feet the \$200 pole supported.

Many telephone companies have adopted policies limiting the number of cable sheaths on a pole line. Usually this limit is three to five sheaths. Beyond that point, regardless of the cost the conduit must be constructed. The subsequent engineering is concerned with minimizing the cost of the construction. This presents a tremendous challenge to find space for a conduit structure that may measure three feet square in cross section, plus occasional manholes measuring at least 10' x 5' x 7'.

Once again the salvation to these problems may be in the wider application of electronic systems that minimize the need for providing additional numbers of cable pairs. In cases where conduit does not exist, the aerial cable pairs can be used to support pair gain systems that may eliminate the need for additional cable and as a result eliminate the need for conduit. In areas where conduit does exist electronics can be applied to allow the use of finer wire. This in turn permits many more pairs of wire to be placed in each underground duct, making them more efficient. Additional electronic applications using pair gain systems would eliminate or defer the need to construct additional underground structure when all existing ducts are filled with cables.

Planning Techniques

Planning for the provision of telephone facilities is somewhat unique. Since a cable pair is required for each individual service and facilities are expected to be available when a new customer requests service, telephone cable is sized on the basis of projected growth. A statement such as that may lead some people to think that telephone companies invest large sums of capital on the basis of guesses. This, of course, is not quite so. Growth projections are based on careful evaluation of zoning, population movements, economic trends, as well as observations from realtors, developers, bankers and much more. The growth projections that have been developed have been highly accurate on a town by town basis, however, as the area becomes smaller the possibility for error becomes greater. For this reason telephone planners have separated the local exchange network into two parts. First is the distribution portions, the cable which extends down the side streets to provide a link from a customer to the feeder cable. The feeder cable generally runs from the switching center along major routes to serve entire sections of a town or city. The distribution cable is fairly short in length, therefore it is economic to place cable made up of enough pairs to serve the ultimate number of customers. These cable pairs are not necessarily connected to feeder cable pairs. Since the feeder cable is common to many distribution cables its size can be deter-

mined from the growth projections for that particular area. As facilities are required in a specific distribution cable those pairs can be connected to the feeder pairs, and subsequently, to the switching center. As a community develops the placing and connecting of cable pairs increases in complexity. Many schemes have been applied, with varying degrees of success, for the best combination of flexibility and cost. The most satisfactory planning has evolved around the physical separation of feeder and distribution cables, together with economic analysis based on growth projections for the timing and sizing of feeder cables.

Plans are developed for the continued development of local networks based on present cable design and then amended for the economic application of electronics. The economic selection is then designed for the most aesthetic, buildable plan that is feasible. Hopefully, the network is designed to be adaptable to new innovations in exchange network facilities.

Future Trends

Telephone service in the United States today reaches more than 90% of the households. The expansion of the telephone network that was seen in the past has, for all practical purposes, passed its peak. Present day construction of local network facilities are more often for modernization or extensions into newly developed areas. There is much more concern with the appearance of the facilities. Many proposals have been put forward for evaluation with the intention of reducing harm to our environment.

One such proposal points up many of the considerations that must be allowed for in dealing with reducing environmental effects of utilities. Utility corridors have been proposed to bring together in a common right of way such things as electrical transmission lines, railroad, interstate highway, long haul telephone, pipeline and other overland utility routes. The first problem that arises with such a proposal is waste to some utilities. Rail lines and highways have maximum grade limitations which often force circuitous routing. Aerial wires and overland pipelines are not restricted and increased costs would result if these utilities were constructed to conform to the transportation corridors. Another consideration is the size of such a corridor. Due to the high level of electrical inductance created by high voltages in the transmission and rail lines interference is caused when telephone cables are run parallel for any appreciable distance.

High voltage induction also causes acceleration in the corrosion of underground pipelines in areas adjacent to the transmission lines. To minimize these inductive effects proper spacing of each of the utilities is a must. The width of the resulting corridor is almost 800 feet (see figure 4) which might be feasible through the great plains, but would rest heavy on environmentalist if it were proposed through woodlands. To attempt such a corridor through populated areas along the east coast would be beyond reality. It appears

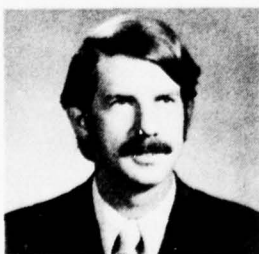
that each utility in its own way must work to improve its own environmental effects. The telephone industry is doing this with increased use of electronics which minimizes the need for additional aerial cable as well as reducing the amount of copper required in the cable that is placed. More telephone facilities are being placed underground even when the economics of such construction is marginal or involves minor penalties to the telephone company. As the technology evolves more and more services through the telephone network the considerations of environmental effects will play an ever more important role.

Conclusion

The environmental effects of telephone facilities have been previously defined as aesthetic only. While this is probably the most obvious effect, there are indications that more concern should be shown with regards to the use up of natural resources.

The technological evolution of the telephone network has resulted in reduction of visual pollution. While it has not been a primary concern in the past, the appearance of local facilities is gaining in importance as a consideration. The state of the art today as well as the indications for the future indicate increasing use of electronics and decreasing demands for copper by the industry. It is conceivable that in twenty years local telephone facilities may be provided with no copper cable whatever. The future network is envisioned with fiber optic feeder facilities and microwave radio links distributing to the customers premises.

The future environmental considerations will center around the placing of cabinets in the neighborhood environment. Camouflaging seems to be a temporary solution, but is the most satisfactory solution to date. There is a general trend toward more underground telephone cable. This is very often occurring on a replacement basis when aerial cables are removed and new cable is placed in the ground. However, the high cost of this type of operation precludes large scale operations to eliminate above ground cables.



Malcolm N. Evans
Southern New England Tel.
227 Church Street, Rm.1317
New Haven Conn. 06506

Mr. Evans came to Southern New England Telephone in 1969 as an Outside Plant Engineer. Four years later he moved to corporate long range planning for local exchange facilities. He currently has these responsibilities with the title of Senior Engineer - Long Range Plans. Mr. Evans holds an A.A.S. degree in Electro - Mechanical Engineering and a B.S. in Civil Engineering.

By its very nature the telephone, and the network that links the telephones to one another, reaches into virtually every household. Limiting the effects to visual impact equally shared by all the users is the most reasonable approach to expect. The minimization of this impact then follows based on response and willingness of the users to bear the burden of expense involved in reducing any visual pollution.

References

1. Evans, M. N., "Loop Electornics, What Do Telcos Gain", Telephone Engineer and Management, Wheaton, Illinois, May 15, 1975
2. Meadows, D.H., Meadows, D. L., Jorgen, R., Behrens, W.W., The Limits to Growth, Universe, New York, 1972
3. Navich, J., and Swartwood, D., "The (real) Development of Subscriber Loop Design," Telephone Engineer and Management, Wheaton, Illinois, December 15, 1972
4. Pearlston, C. B., "EMC in Utility Corridors", Conference Record, National Telecommunications Conference, Volume 1, December, 1975
5. Roche, J. N., Wood Preservation - The Important Factor in Conservation, American Wood Preservers Association, 1965
6. Simokat, F. L., "FDM Subscriber Carrier: Expansion of Electronics in Telephone Plant Technology", Conference Record, IEEE INTERCON 75, New York, April, 1975
7. TELECOMMUNICATIONS TRANSMISSION ENGINEERING, Volume 3 - Networks and Services, American Telephone and Telegraph Company, Winston-Salem, North Carolina, 1975
8. Whitehead, J. R., "The Impact of Telecommunications on the Evolution of Society", public address presented in Ottawa, Canada, May, 1974

Figure 1

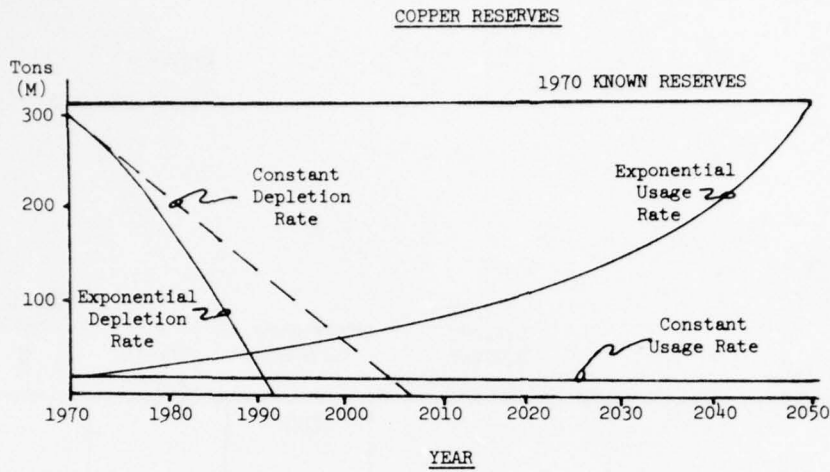


Figure 2

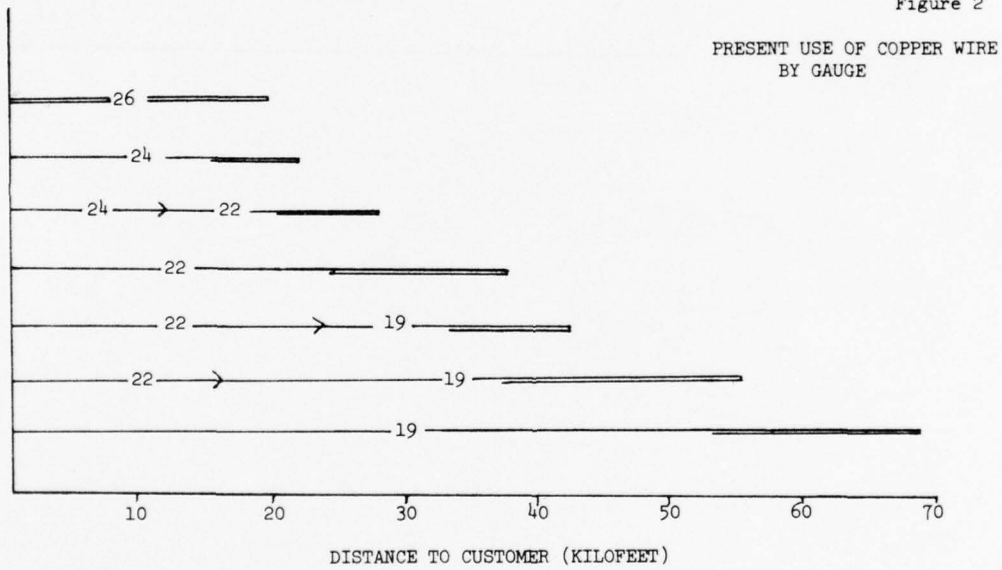


Figure 3

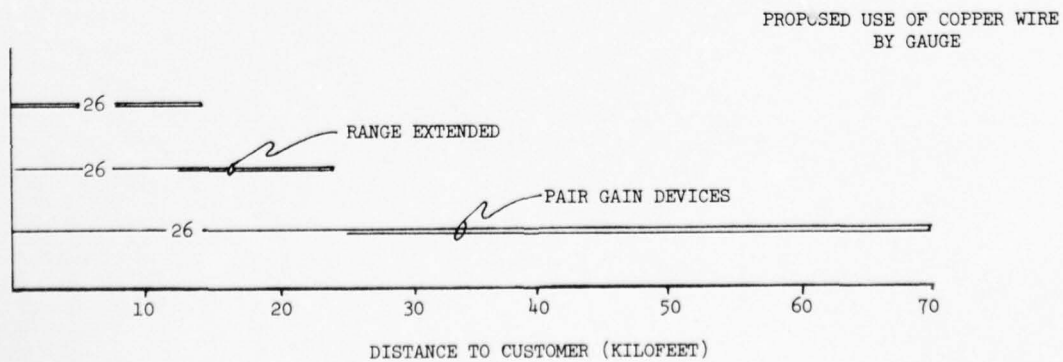
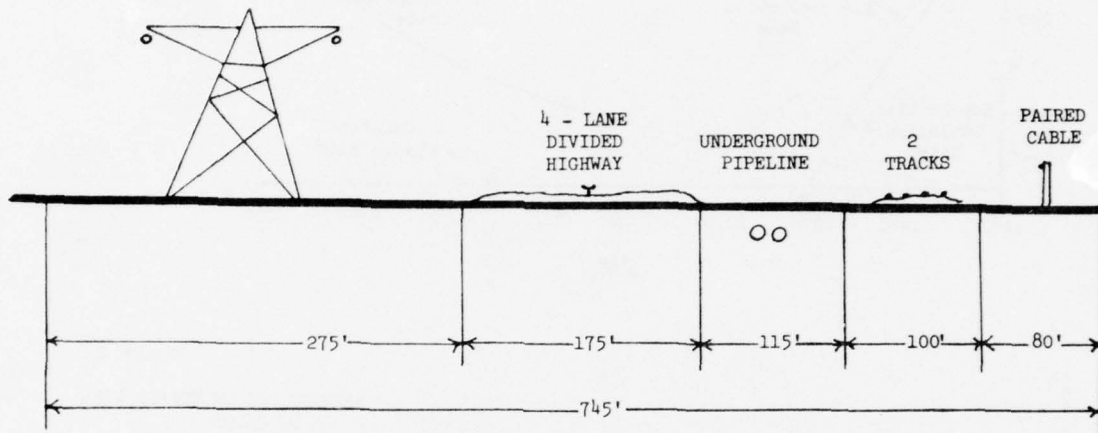


Figure 4
UTILITY CORRIDOR



THE CABLE ENTRY SYSTEM

Dr. Jose E. Godts
Martin Marietta Aerospace
Orlando Division
Post Office Box 5837
Orlando, Florida 32805

SUMMARY

The hardening of electronic systems, connected to long lines, against transient electromagnetic environments (EMP and lightning) is a highlight of today's technology. The cable-induced and conducted transient stresses are imposing strong demands on the input/output electronics, particularly with recent IC designs. Since line equipment is also subjected to operational transients, the author combines the impact of the environmental and operational stresses to design interface protections of low-cost and low-insertion impact. The most current cable designs are used to exemplify the design. Current transient capabilities are stated quantitatively.

INTRODUCTION

Transient electromagnetic environments impose heavy stresses on current electronic systems. These stresses are produced when the environment is coupled through the equipment shelter, rack and black box wall, directly in the circuits, or, more commonly and more severely, through the cabling connected to the electronic system. It is these heavy currents coupled in the cable that usually are the cause of cable damage and/or electronic circuitry damage. This paper describes the approaches used successfully by the author to protect the electronic circuits connected to long cables from the EMP (nuclear burst induced electromagnetic pulse) and the lightning stresses.

Since the cable configurations used in communication systems are realistically represented by the two types, i.e., coaxial cables and multipair cables, it is expected that the design principles exemplified will be of direct application to the reader. We remind the reader that final testing of his configurations under simulated stresses is a must since present electronic systems offer unthought-of paths of entry which are sometimes the source of extraordinary system weakness, e.g., transformer capacitance, semiconductor capacitance, and protection lead inductances.

THE ENVIRONMENTS

Military and civilian systems rely on high wire density or high data density cables to transfer the ever increasing communication traffic volume. The loss of the terminal circuit functions, or of the cable, has severe repercussions on the operations controlled, managed, or monitored by these communication lines. Moreover, the temporary loss of

transmission can delay the encrypted or coded messages much longer than it takes to switch to alternate links because of synchronization or algorithm requirements.

Hence, the importance of maintaining continuity of the communication functions has spurred tight requirements on the hardening against EMP and lightning stresses of the related components and subsystems. The recently released (March 1976) FCC Rules, Part 68, impose important lightning hardening requirements on civilian communication systems. Similar requirements for EMP are now enforced on all military cable communication systems under classified specification requirements defined according to war scenarios determined by operation analysis processes. The lightning hardening of military systems is not as clear for ground systems due to the lack of threat definition. A contractor has attempted to link the probability of hit that would be excessive for the system to the system lifetime based on existing (Reference 3) statistical lightning parameters. This trend should define the lightning cable threat and be a base for standard threat definition. Operational transients due to switching, connecting, and ringing are also imposed on the communication systems. These transients are defined in standards for civilian (FCC, Part 68) (Reference 4) and military systems (MIL-STD-188-100) (Reference 5).

The philosophy of hardening discussed in this paper is based on the assumption that all the input/output subsystems must be hardened against the operational transients as required in the procurement specifications and defined in the FCC or MIL standards. The hardening against lightning and EMP consists then of providing the cable interfaces with the system of devices that bring the lightning and EMP transients stresses below the stress levels of the operational transients (Figure 1.)

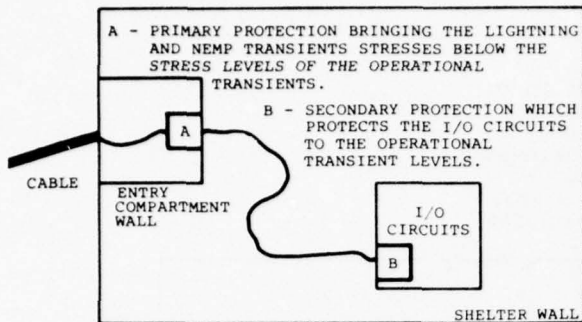


Figure 1. Philosophy of Protection

THE COUPLING OF COMMUNICATION LINES TO TRANSIENT ENVIRONMENTS

In military and civilian applications two types of cables are prevalent: the multi-pair type (WM 130 - 26 pairs cable) and the multicore type (CX 11230 - shielded twin-ax cable). When the cables are long enough (longer than 500 feet), the distribution of the transients between the elements of the cable are not dependent on the terminal impedances and each wire contributes to the transient stress transfer. Cable coupling stresses are explained and calculated in References 1 and 5 for EMP and in References 2 and 6 for lightning.*

For typical ground systems consisting of communication shelters and long communication cables, the stresses can be enveloped by the time history of Figure 2. The actual time history varies according to the authors but the maximum amplitudes are well characterized by the typical values given in the figure.

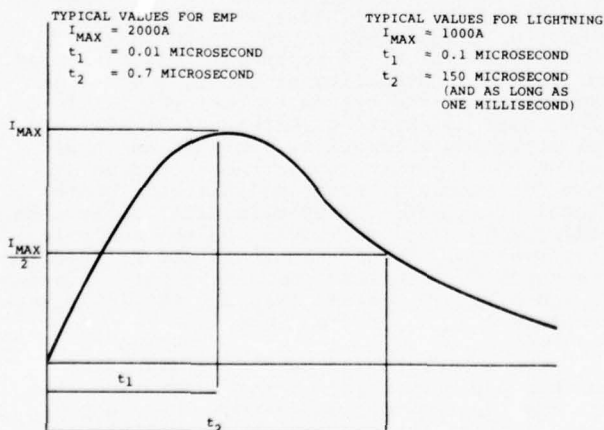


Figure 2. EMP and Lightning Induced Current in Communication Cables

THE PROTECTION

In cables provided with several shields, the bulk of the current passes in the shields and grounding of those shields at the entry panel bypasses a large amount of the coupled energy to the ground. This limits the stresses of the protective circuits. Typical of this condition is the circuits connected to the military CX 11230 cables.

Figure 3 shows schematically the cable in the grounded shelter. The cable length from the entry compartment to the circuit must be long enough so that the cable impedance is the dominant factor in the impedance loading of the entry compartment output. This helps to avoid short term resonances (particularly in the rise time of the pulse) which could amplify the peak voltage of the stress. Generally, lengths of 20 feet are sufficient. In the example illustrated in Figure 3 the input is provided with an EMI filter**.

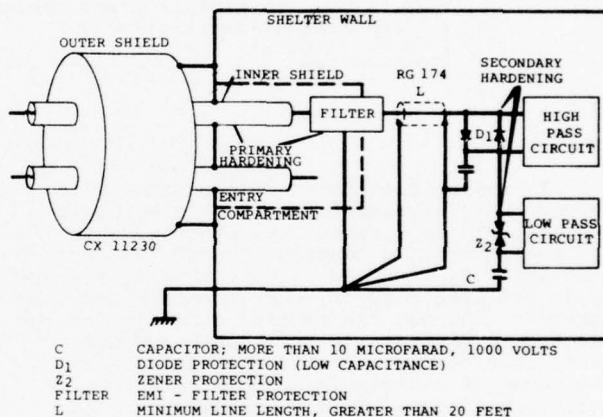


Figure 3. CX 11230 Interface Circuit Protection

For multipair cables the primary hardening is illustrated in Figure 4 and consists of balanced lightning arrestors of low capacitance (less than 2 pF to ground per side) and of EMI filters.

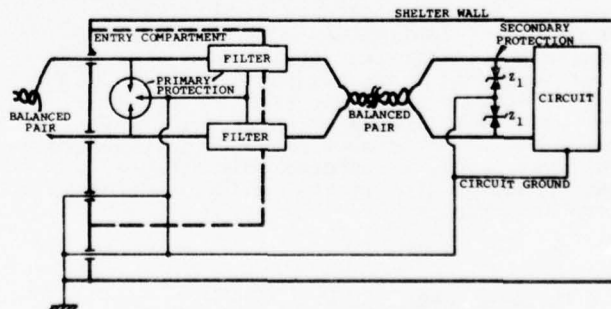


Figure 4. Multiple Pair Interface Protection

**Note that the shield of RG 174 is grounded at both ends inside the shelter where field environments are very small. This grounding is unavoidable because the terminal circuits are grounded through the power supplies and the filter is grounded at the entry panel.

*Also consult corporations listed in Appendix to Chapter 7 of Reference 1.

The ground path is of importance, and since very heavy current could be carried, it is essential that the ground conductors do not radiate in the shielded shelter area or induce large differences in potential in the circuit ground returns. Hence, the ground conductor shall be short, avoiding bends and shall be of proper current carrying cross section (No. 6 minimum, but it is not unusual to use No. 2/0 for such application). The lightning arrestors and the filters must be designed to limit the vestigial transients in the in-shelter run of the balanced pairs below the levels of operational transients specified in FCC Part 68 or MIL-STD-188-100 or any other circuit interface standard chosen to design the secondary protection.

CONCLUSIONS

The paper identified a philosophy of protection against typical transient cable conducted threats for current communication cables. The protection scheme takes advantage of existing operational standards imposed on on-line equipment and specifying the transient hardening levels of their line interface. This process offers the double advantage of compatibility with the latest equipment or, by retrofit, bringing the existing system to hardness levels compatible with present standards and gives a front end protection against the hard threats with minimum impedance insertion losses. The two step protection defined yields maximum protection at minimum cost using readily available parts. High cost is avoided by complementary protection (field induced and operational).

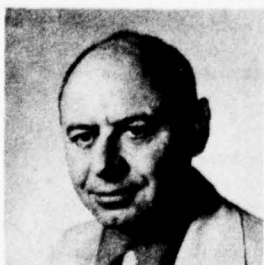
The protections described have been tested and shown to be effective to levels where cable

destruction occurs from excess current without damage to the terminating circuits.

For the future, the fiber optic interconnections will offer field induced protection while the subsystems may still be subjected to operational transients generated by adjacent subsystems.

REFERENCES

1. EMP Engineering and Design Principles, Bell Telephone Laboratories, Whippany, New Jersey, (1975).
2. Bodet, David W., "Electronic Surge Protection Equipment Characterization of Lightning Surges in Telecommunication Plant," Joslyn Electronic Systems, Goleta, CA, (1972).
3. Cianos, N. and Pierce, E. T., "A Ground-Lightning Environment for Engineering Usage," SRI, Menlo Park, CA, (1972).
4. FCC Rules Part 68. Consolidated copy provided by Electronic Industries Association, Washington, D. C.
5. MIL-STD-188-100, 15 Nov 1972, Military Standard. Common long haul and tactical communication system technical standards (particularly paragraph 4.3.1.3.3.9).
6. TCCF (Tactical Communication Center Facility). Several documents of limited distribution. List and details available from Electronic Systems Division, Air Force Systems Command, USAF, HAWK AFB, Redford, Mass.



DR. JOSE E. GODTS

as AN/WSC-2 (XN-1) (V) Shipboard Communication Sets and AN/TSQ 85 Video Technical Control Center. Dr. Godts participated in the design and implementation of the Orlando Division's Long Wire Antenna Simulator and has performed several original studies related to pulsed electromagnetic fields and their effects on equipment. Prior to joining Martin Marietta, Dr.

Dr. Godts is presently a staff member of the System Design Department. In this function, he coordinates the EMP efforts of the department and participates in the technical effort of marketing the EMP capability of the Orlando Division. Dr. Godts was responsible for the EMP hardening of several systems such

as AN/WSC-2 (XN-1) (V) Shipboard Communication Sets and AN/TSQ 85 Video Technical Control Center. Dr. Godts participated in the design and implementation of the Orlando Division's Long Wire Antenna Simulator and has performed several original studies related to pulsed electromagnetic fields and their effects on equipment. Prior to joining Martin Marietta, Dr. Godts was with Westinghouse Electric Corporation, where he was in charge of the development of mathematical methods to study nuclear reactor control. This responsibility also covered the new methods of analog simulation, and he was one of the pioneers in using analog simulators in multispace problems, including nonlinear control analysis. Dr. Godts is a former senior lecturer at the Carnegie-Mellon Institute of Technology and associate professor at the Brussels University (Belgium). He received Masters of Science from the Brussels University (Belgium) in Mechanical, Electrical, and Aeronautical Engineering and a Masters of Science and Doctorate in Nuclear Sciences from the Carnegie-Mellon Institute of Technology. He is the author of numerous papers in the fields of mathematics, nuclear reactor control, analog computers, and nuclear weapons effects and has more than 10 patent disclosures and 20 technical reports to his credit.

INFERRING DUCT-RUN GEOMETRY FROM CABLE-TENSION DATA: A CASE HISTORY

by

A. L. Hale
Bell Laboratories
Whippany, New Jersey

and

M. R. Santana
Bell Laboratories
Norcross, Georgia

SUMMARY

The placing characteristics of a small, experimental optical cable were established by tests at Bell Laboratories in Chester. Tensions measured in subsequent pulls at the Atlanta Laboratory were unexpectedly high and showed large sudden increases not consistent with the presumed geometry of the duct run. Since no direct means short of excavation was available to establish the true configuration, the existence of vertical-plane S bends adjacent to the manholes was postulated. The tension data were fitted using nonlinear least-squares procedures, and the assumed geometry was adjusted to improve the fit. The friction coefficients for the final fit agreed well with the Chester results and with other measurements performed at Atlanta. Elevations measured at the exposed ends of the ducts were consistent with the adjusted geometry. A satisfactory interpretation of all the data, based on substantial departures from nominal duct-run geometry, was thus achieved. Although this technique is not recommended for general use in the field, it was critical in this application because of the importance of the cable placing characteristics in studies of potential system applications.

Introduction

A critical aspect of system application studies for a small experimental fiber-optic (FO) cable¹ is the length of the cable that can be pulled into a typical underground duct run without excessive tension. Cable tension depends mainly on the configuration of the duct run and the friction coefficient between the cable and the duct wall. Much effort has gone into the experimental determination of the cable friction coefficient from laboratory tests² and from measurements of winch-line tension made during trial installations in duct runs of known configuration³.

Figure 1 shows test results for the friction coefficient between the high-density polyethylene (HDPE) cable jacket and the duct material plotted against average sliding speed. In the tests² performed at the Murray Hill Laboratory, the normal and frictional forces were measured directly. Each of the two left-hand points in Figure 1 is the average of three measurements. In the installation tests³ conducted at the Chester Laboratory, tension at the winch was recorded continuously as the cable was pulled into the duct. Least-squares values of the friction coefficients of both the cable and winch line with the duct wall were fitted to the complete record (see Appendix). The right-hand point in Figure 1 represents the results of 8 pulls.

In the installation tests, comparatively short lengths (less than 500 ft) of cable were pulled into a duct run containing many bends. Subsequent tests involving duct runs more representative of field installations were planned for the underground duct facility at the Atlanta Laboratory.

Atlanta Duct Facility and Cable Pulling Arrangements

Figure 2 shows the general features and layout of the Atlanta duct system. Figure 3 is a dimensioned sketch of the system. Origin-

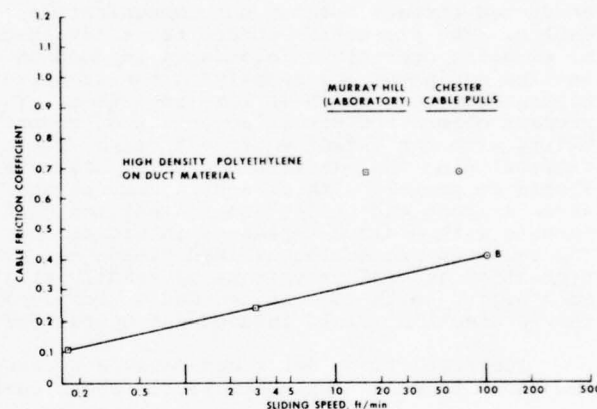


Figure 1. Cable Friction Coefficient Versus Sliding Speed

ally, it was assumed that the ducts were straight over their entire length. The cable-pulling results reported herein and some investigative work performed as a consequence of these results demonstrated that the original assumption of straight ducts was incorrect.

Figure 4 is a layout of the cable-pulling, load measuring, and recording apparatus used at Atlanta. A multigroove dual-sheave capstan provides the power to pull the winch line and cable through the duct system.⁴ The maximum rated pulling load for the capstan in continuous duty is 250 pounds at pulling speeds up to 100 ft/min. Speed control by the use of the tachometer feedback mode of operation and linear speed indication are also provided.⁵ The load-measuring equipment consists of a calibrated yoke and load-cell assembly through which the winch line is passed.³ A load-cell analog readout and stripchart recorder complete the measurement system.

Preliminary Results

A series of preliminary placing experiments with FO cable were performed at Atlanta to check out techniques and equipment. Initial results indicated an excessively high winch-line coefficient of friction. The winch line used in this experiment was a 3/16-inch nylon-coated wire rope. The high friction coefficient is due to the nylon coating. As a result of the above observations, an uncoated 1/16-inch 7x7 wire rope was used in subsequent FO cable-placing experiments.

Summary of Cable-Placing Experiments at Atlanta

Table I summarizes the series of experiments performed at Atlanta. For the last two entries in this table, an intermediate capstan drive was used to insure survival of all transmitting optical fibers after the pull into the duct.⁴

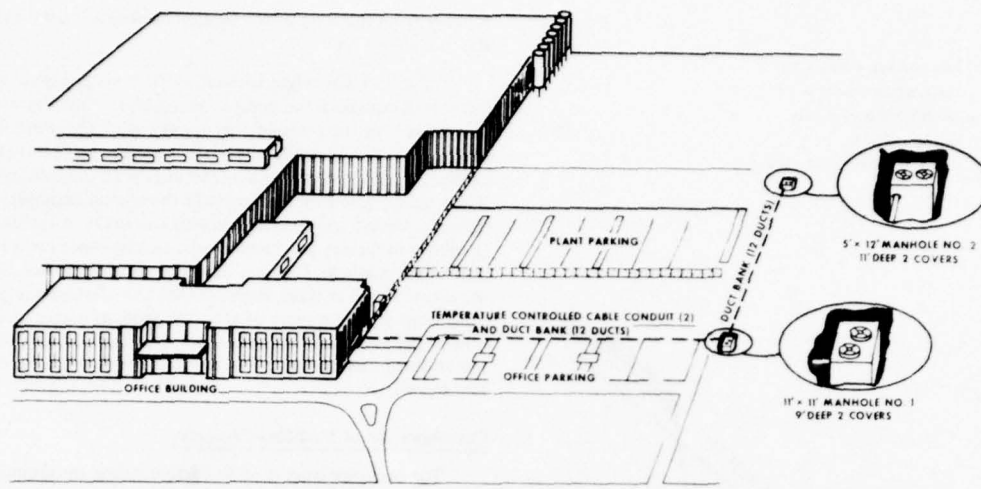


Figure 2. BTL (Atlanta) Underground Cable Conduit and Duct Facility

TABLE I
SUMMARY OF TESTS

Pull No.	Cable Weight (lb/ft)	Sliding Speed (ft/min)	Tail Load (lb)	Number of Replicate Pulls
1	0.051	10	4	1
2	0.051	30	4	1
3	0.051	10	4	1
4,5	0.051	10	1.8	2
6	0.063	10	4	1
7	0.063	10	3	1

- NOTES: 1. A 1/16-inch 7x7 uncoated wire rope (weight ≈ 0.0073 lb/ft) was used as a winch line for all of the above pulls.
2. Cable outside diameter ≈ 0.5 in.
3. All pulls were made without lubrication.

Resolution of Tension Anomalies

Typical Tension Record

When the tension records obtained from pulls of the FO cable through the Atlanta duct run were compared with the theoretical best-

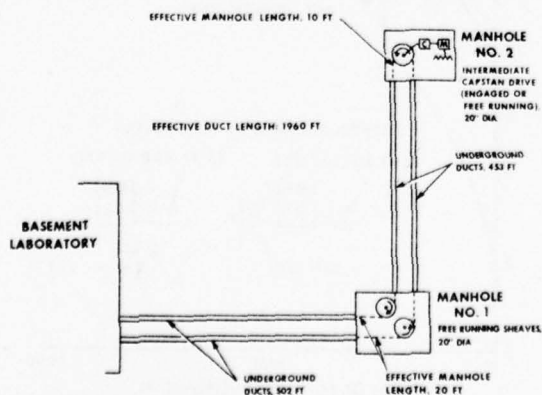


Figure 3. Atlanta Duct System

fit tension and with the prediction from the Chester tests,³ troublesome discrepancies were apparent. If the Atlanta results were correct, serious doubts were raised about the anticipated ability to place kilometer cable lengths in actual duct runs. Figure 5 illustrates the discrepancies observed on the fourth pull listed in Table I. Tension at the winch is recorded against the length of cable in the duct. Line A shows the best-fit theoretical tension consistent with the assumed geometry of the duct run (ducts straight and level). The fitted friction coefficients are $f_c = 1.13$ for the cable and $f_w = 0.22$ for the winch line. In contrast, line B shows tension predicted from the applicable Chester tests (mean friction coefficients $f_c = 0.41$ and $f_w = 0.47$).

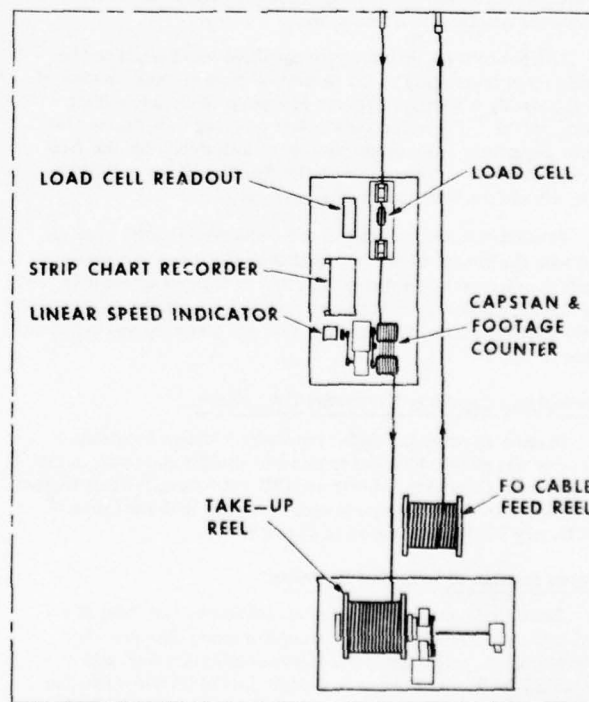


Figure 4. Cable Pulling and Load Measuring Apparatus

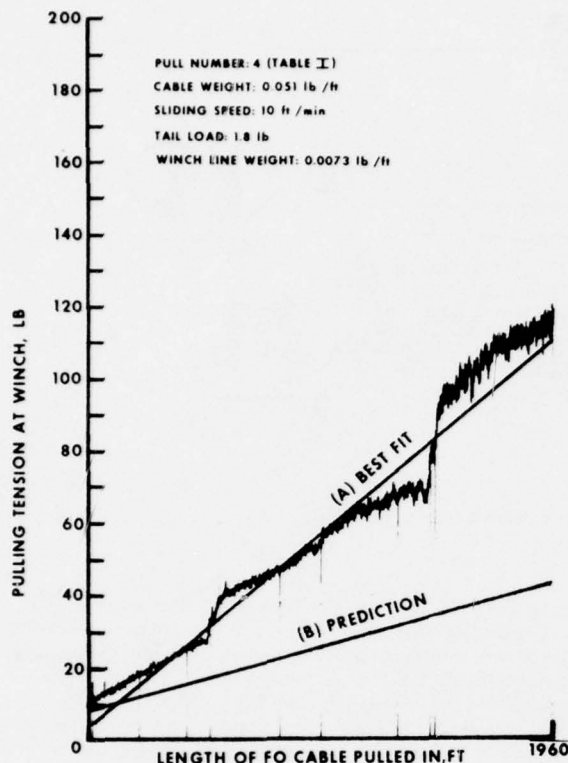


Figure 5. Typical Tension Record

The best-fit cable friction coefficient (1.13) is far outside the 95-percent confidence interval from the Chester tests (0.41 ± 0.13). In addition, the quality of the fit is very poor. The sudden increases in tension as the cable end passes the first manhole in both directions are not present in the fitted curve. These sudden increases were noted on all pulls into the Atlanta duct run.

Absence of these features from the fitted curve could not be attributed to inadequacy of the theoretical tension model in view of the supposedly featureless duct run geometry, the steady pulling speed, and the uniform duct, winch line, and cable conditions. Only minor departures from uniformity were introduced by the free-running sheaves. No reasonable model based on these conditions could predict the large sudden changes seen.

Tension excursions similar to those observed are often associated with the passage of the cable end through a bend in a duct run. Bends in otherwise straight runs are often introduced adjacent to manholes in order to effect changes in elevation or in the arrangement of the duct formation. The assumed duct run geometry was therefore suspect.

Development Capability Laboratory (DCL) Tests

In order to verify the earlier results for a known geometry, a FO cable was pulled at various speeds into straight inner duct in the Development Capability Laboratory (DCL) at Atlanta.⁶ Cable friction coefficients for the various pulls were consistent with the Chester³ and Murray Hill² results shown in Figure 1.

Reconsideration of Duct Run Geometry

Since no direct means short of excavation was available to establish the true configuration of the underground duct run, the geometry of the suspected bends was postulated. On each side of Manhole 1, an S bend tangent to straight duct at the outer end and normal to the manhole wall at the inner end was assumed. The arc length of each S bend was estimated from the duration of the excursion on the pulling record. The total angle of bend was estimated

roughly from the ratio of the tensions before and after the tension rise.

Cable and winch-line friction coefficients giving the best non-linear least-squares fit of computed to actual winch tension were then determined for the postulated geometry using the computer program described in the Appendix. The fitted tension was plotted and the assumed duct geometry adjusted to improve the qualitative agreement. Slight bends were added adjacent to the second manhole. After re-fitting, a second and final adjustment was made. A radius of 12 ft (available in factory-produced plastic bends) was chosen for the bends at the first manhole. Figure 6 shows the final fit of the computed to the actual winch tension, together with the corresponding computed cable tension. The quality of the fit is good, as judged against a collection of similar plots from field-trial⁷ and Chester pulls. The details of the assumed vertical-plane S bends in the revised duct geometry are also shown.

Corroboration of Modified Geometry

The occupied duct is 63 in. farther below the ground surface at the building than it is at Manhole 1. The corresponding computed difference based on the modified geometry is 55 in. For the run between the first and second manholes, the agreement between measured and computed depths was also good. These comparisons make the modified geometry still more plausible. Additional evidence includes earlier unsuccessful attempts to place conventional cable in one of the ducts in the run, when a pull from the building to the first manhole could not be completed.

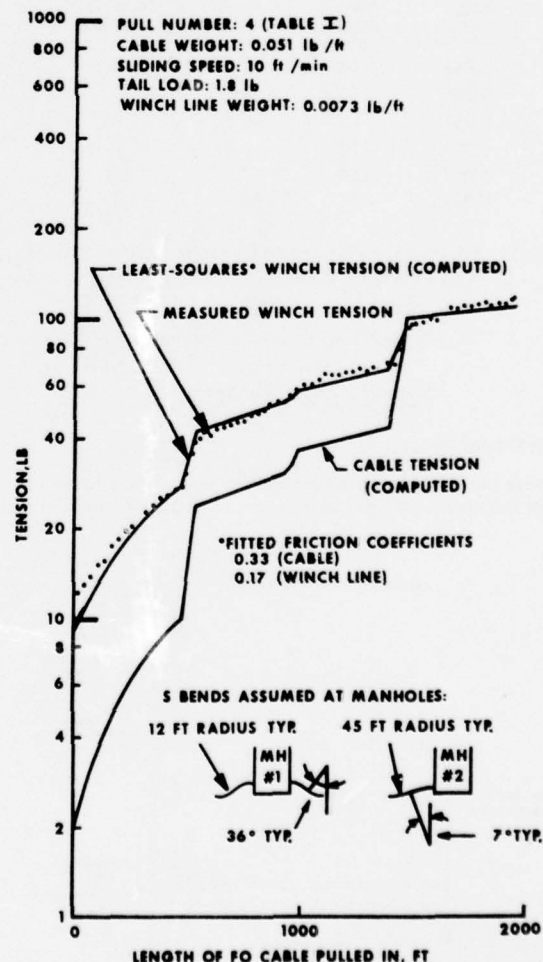


Figure 6. Data Fit for Modified Duct Run Geometry

Results And Observations

Table II lists the best-fit friction coefficients based on the modified duct-run geometry for the pulls listed in Table I. The standard deviation of the values for the cable is about 1/3 of that for the Chester results. Figure 7 repeats the data of Figure 1 and adds the Atlanta data from the DCL (diamonds) and the modified underground run (open triangles). For comparison, the solid triangle shows the value based on the unmodified duct-run geometry.

TABLE II
RESULTS OF TESTS

Pull No.	Cable Weight (lb/ft)	Sliding Speed (ft/min)	Friction Coefficients	
			Cable	Winch Line
1	0.051	10	0.38	0.19
2	0.051	30	0.34	0.22
3	0.051	10	0.34	0.18
4	0.051	10	0.33	0.17
5	0.051	10	0.33	0.18
6	0.063	10	0.38	0.20
7	0.063	10	0.34	0.23
Mean	For Pulls at		0.35	0.19
Standard Deviation	10 ft/min		0.024	0.021

Figure 8 reproduces the tension record for the one pull at 30 ft/min. The tension fluctuations about the mean are substantially larger than those in Figure 5. The fluctuations for the first two pulls at 10 ft/min, however, are also considerably larger than those in Figure 5. Thus the noise reduction should probably be attributed to refinement of the pulling arrangement as well as to the speed reduction.

For pulls 4 through 7 of Table I, slack cable was payed off the reel onto the floor, and the tail load was due entirely to the friction of the slack cable sliding on the floor. Tail load was estimated from the extent of the suspension from the duct entrance to the floor. The flexural stiffness of the cable had a marked effect on the shape of the suspension. There were obvious variations in sliding speed of the cable entering the duct, although speed of the pulling capstan was always steady. Eliminating the drag of the reel and the effect of its speed variations may have been responsible for much of the reduction in winch-tension fluctuations.

Discussion

Implications of Revision in Duct-Run Geometry

The revision necessary to produce good-agreement between experimental and computed tension was simple and plausible. The success of the revision in reconciling theory and experiment and the agreement of the friction-coefficient results with data from other sources restores confidence in the feasibility of placing FO cable in kilometer lengths in suitably selected duct runs. The episode emphasizes, however, that the selection must be based on accurate geometric information.

It also suggests that available information may frequently be inaccurate. Conduit drawings that represent ducts by straight lines between manholes should not be accepted at face value. Even when the records appear realistic, there is a need to verify their accuracy prior to any attempt to place a valuable high-capacity cable.

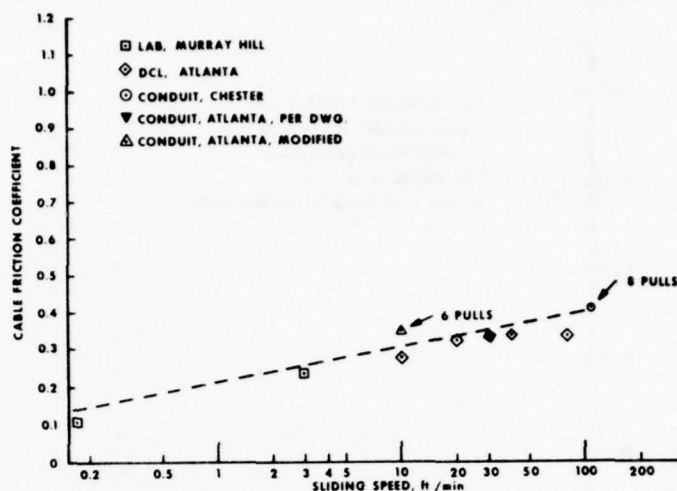


Figure 7. Cable Friction Coefficient Versus Sliding Speed (Atlantic Data Included)

The successful inference of the Atlanta configuration from tension data might suggest use of the procedure as a general tool for verifying duct-run geometry in the field. Such use is not recommended. The indirectness of the procedure makes it vulnerable both to violations of the assumptions underlying the tension model (see Appendix) and to the inherently noisy nature of frictional phenomena. In the Atlanta episode, the critical nature of the application and the continued experimental use to which the duct run would be put made the undertaking essential, and the uniform experimental conditions made it feasible.

A more direct means of verifying duct-run geometry, but one not yet available, would be use of a measuring device to record duct curvature as a function of distance. Information about orientation of the plane of curvature is not needed for adequate accuracy of pulling-tension predictions. Such a record would constitute the primary geometric description for purposes of tension estimation.

Summary and Conclusions

Tensions and friction coefficients have been determined for a series of pulls of FO cable into the Atlanta underground duct facility. To obtain satisfactory agreement of computed and measured tension, it was necessary to infer, from the tension data, a suitable correction to the duct-run geometry described by the conduit drawings. The addition of vertical-plane S bends adjacent to both manholes produced good agreement. The resulting cable friction coefficients also agree well with those from other tests at Chester and Atlanta. Kilometer-length pulls into selected ducts without the assistance of an intermediate capstan drive remain feasible. The tests have shown that the intermediate capstan drive is effective in reducing the maximum tension during cable placement, thus making additional continuous 1-km pulls practical. A need exists, however, for a means of establishing the true geometry of duct runs in the field.

Acknowledgements

The authors wish to express their appreciation to Messrs. G. F. Edwards, R. A. Kempf, E. D. Knab, W. P. Maxey, and S. C. Shores for their valuable assistance in the planning and performance of the experiments described in this paper, as well as to D. L. Pope for reviewing earlier versions of the manuscript.

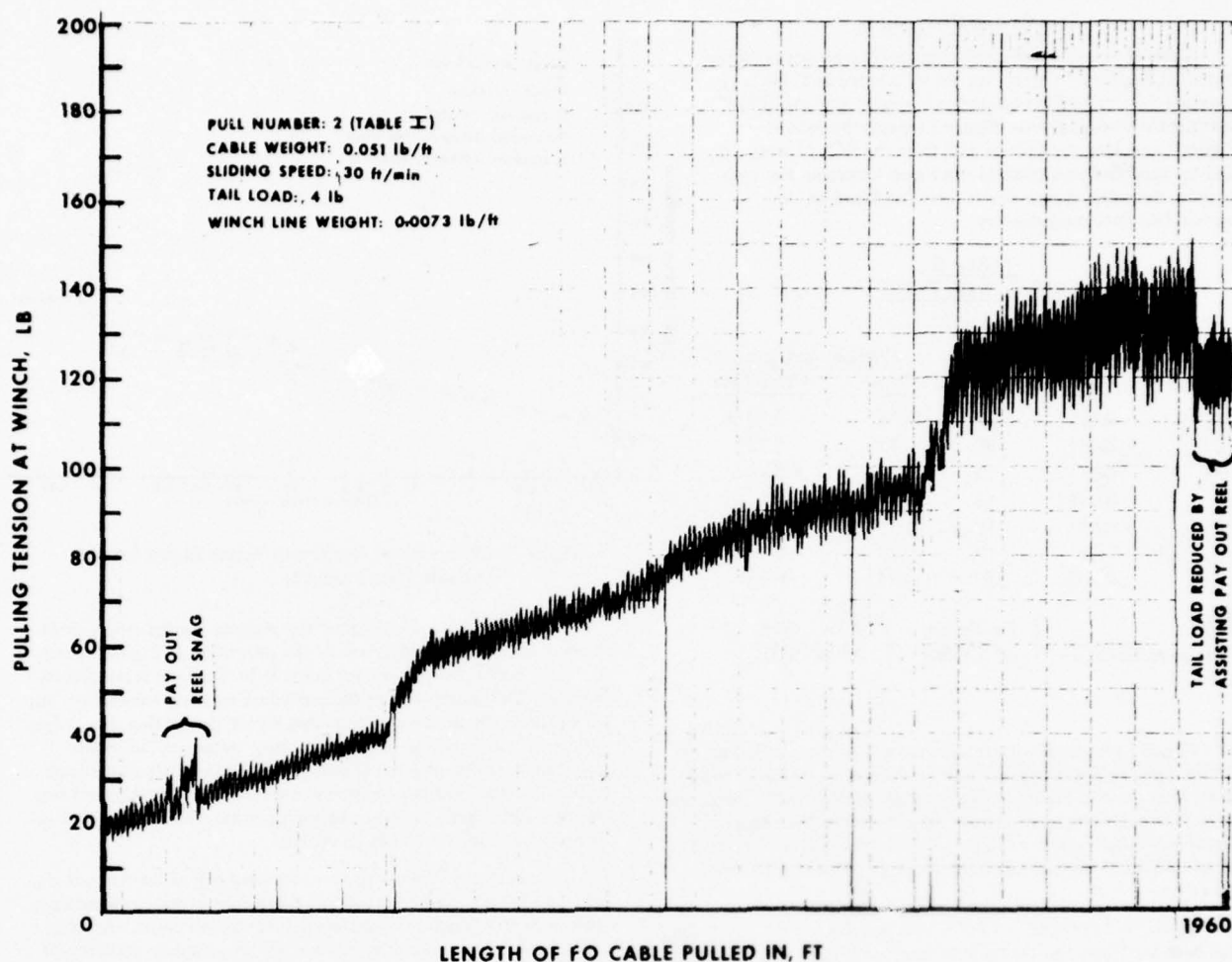


Figure 8. Tension Record for Pull at 30 ft/min

REFERENCES

1. M. I. Schwartz, R. A. Kempf, and W. B. Gardner, "Design and Characterization of an Exploratory Fiber Optic Cable", Second European Conference on Optical Fibre Communication, Paris, September 27-30, 1976.
2. T. T. Wang, unpublished work.
3. K. P. Wells, unpublished work.
4. E. D. Knab, unpublished work.
5. W. P. Maxey, unpublished work.
6. S. C. Shores, unpublished work.
7. J. Donegan and A. L. Hale, unpublished work.
8. Buller, F. H., "Pulling Tension During Cable Installations in Ducts or Pipes", General Electric Review, v. 52, No. 8, August, 1949, pp. 21-23.
9. Rifenburg, R. C., "Pipe-Line Design of Pipe-Type Feeders", Trans. AIEE, December, 1953, pp. 1275-1288.

APPENDIX TENSION COMPUTATION AND ANALYSIS

Tension Model

The tension at any point in the duct run is established by a step-by-step procedure starting with the back tension (tail load) in the cable as it enters the duct. The duct run is considered composed of three basic types of segments (straight segment, either horizontal or inclined, constant-radius bend in a horizontal plane, and constant-radius bend in a vertical plane). Beginning with the first segment into which the cable is fed, the tension at the pulling end of each segment is calculated from that at the feed end. Between the duct entrance and the leading end of the cable, the properties used are those of the cable; from that point to the duct exit, the winch-line properties are used.

The necessary equations are well known^{8,9} and will not be repeated here. They are equilibrium equations and so must be interpreted as applying to some tension near the middle of the range of any dynamic fluctuations that may actually occur. The flexural stiffness of the cable is also neglected, but it may be significant if tension is low enough so that the cable does not follow the duct wall. In addition, the friction coefficient between the duct wall and the cable or winch line within each segment is treated as constant and independent of location and time. Finally, the duct cross section is circular or at least has no corners into which the cable can tend to wedge under tension in a bend.

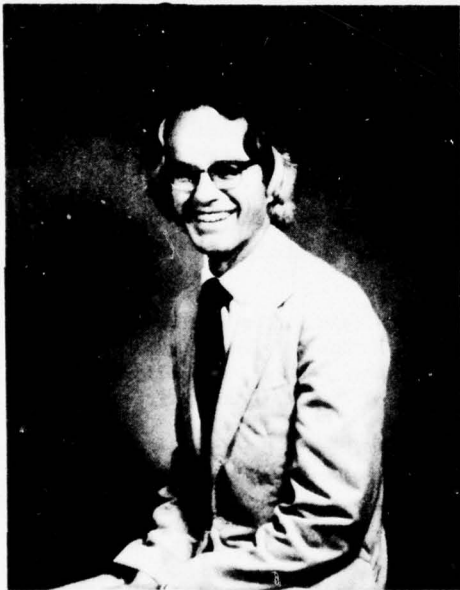
The tension expressions for both types of bends depend on the ratio T_0/wr , where T_0 is the tension at entry into the bend, w is the weight of the cable (or winch line) per unit length, and r is the bend radius. When T_0/wr is large, the tension T at exit from the bend approximates the "capstan" value $T_0 e^{f\beta}$, where f is the appropriate friction coefficient and β is the angle of bend in radians. The exponential tension buildup in bends is the major cause of high pulling tension. Correspondingly, accurate knowledge of the angle and location of each bend in a duct run is essential for satisfactory prediction of tension.

Computer Program

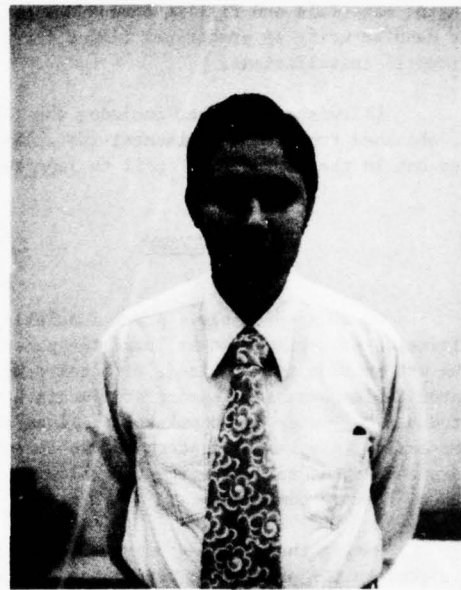
When tail load is constant, the tension at any point in a duct run is constant once the cable end has passed that point. The tension distribution in the cable just before the conclusion of a pull is therefore calculated readily in one computational pass through any duct run. A programmable pocket calculator is an adequate tool for the purpose. To determine winch-line tension at the winch as a function of length of cable in the duct, however, it is necessary to make one pass along the winch line for each location of the cable end.

A time-sharing computer program has been written for this job. It obtains a description of the duct-run geometry from a file designated by the user. Using cable and winch-line properties and friction coefficients entered from the terminal, it optionally prints or plots tension at the cable end and at the winch for successive locations of the cable end.

The program is also used for the analysis of experimental tension records. In this application data points extracted from the record at uniform intervals are stored on a file and are read by the program at the user's command. For one or more pairs of assumed friction coefficients, the program computes and prints the mean-square difference between measured and predicted winch tension, together with the partial derivatives of that mean square with respect to the friction coefficients. Using these results, the analyst searches interactively for the friction coefficients minimizing the mean-square error. Measured and predicted tensions can then be plotted by the program as in Figure 6.



Albert L. Hale received his B.S., M.S., and PhD degrees in Mechanical Engineering from the University of California, Berkeley, in 1947, 1949, and 1956, respectively. He has been at Bell Telephone Laboratories since 1956, first in Submarine Cable Systems Development and most recently in Loop Plant Installation.



Manual R. Santana received his B.S. degree in Electrical Engineering in 1970 from the University of Hartford and his M.S. degree in Electrical Engineering in 1971 from Georgia Institute of Technology. Since 1970, he has worked on cable design and development in the Bell Telephone Laboratories Loop Transmission Division. He is a member of the I.E.E.E.

FILLED CABLE FOR AERIAL INSTALLATION
by Luis M. Molleda and Enrique Used
Compañía Telefónica Nacional de España
Research and Study Center
Madrid - Spain

SUMMARY

This paper examines the present problems of cables installed aially in Spain, the main climatological conditions (temperature, humidity, rain, wind, snow, etc.) and the tests leading up to the design of a new type of filled cable for aerial use.

Here are also shown the analysis carried out on different filling compounds available in the market and laboratory test on several combinations of insulating materials and filling compounds, which led to the manufacturing of prototypes cables for first experimental installations.

Likewise, the paper includes the first results, obtained from the experimental installations carried out in the period from April to June 1976.

INTRODUCTION

When water enters a paper insulated cable the situation is serious but at least the paper swells and the wet section is localized. With polyethylene insulated cable when water enters no immediate failure is noted but the water can completely fill an aerial span of cable. This was of concern to the telephone companies and means to stop water from flowing in this type of cable were considered.

During the last few years and as a result of this concern the main Cable Development Centers, both manufacturers and telephone companies have presented at the IWCS a great number of papers on water-proof and moisturetight cables, using petroleum jelly filling compounds.

The efficiency of the studies presented on this matter is clearly demonstrated by the fact that most telephone companies have adopted this technique.

In the last few years, trying to get a combination which under real operating conditions guarantees a suitable cable performance (stability of physical and electrical characteristics) and a mean life similar to that of cables manufactured with air core, an important evolution has been observed, mainly in insulating materials and filling compounds.

In the beginning, low and medium density solid PE were used, with low drop point petroleum jellies, now the trend has evolved towards the use of high density solid and ellular PE with high drop point petroleum jellies.

High density cellular PE is being adopted almost in a general way⁽¹⁾; nevertheless, in the presence of certain extreme temperature conditions combined with mechanical stresses (wind, rain, snow, etc.) their possibilities must be carefully studied and compared with those of solid HDPE.

In Spain, studies in this field begin in 1973. In this first stage it was demonstrated that due to the climatological conditions of Spain, it was not advisable to use the products then available in the market. It was decided, for this reason, to make studies directed at obtaining a prototype suitable for its use on aerial lines. In order to know accurately the working conditions in our country it was decided to carry out a study on its climatology for analyzing, in a second stage, the possibilities of insulating and filling materials under these conditions.

CONSTITUTION OF C.T.N.E.'s NETWORK

Spain is the second most mountainous country in Europe and its topography shows many and high mountains. Besides, its solid rock subsoil is only 30 or 50 cm. below the surface.

Taking these factors into account, buried installation of cables shows serious technical and economical problems. This is the reason for which aerial installations are used almost exclusively in C.-T.N.E.

Table 1 shows the present constitution of C.T.N.E.'s network.

TABLE 1. CONSTITUTION OF C.T.N.E.'s NETWORK

INSTALLATION TYPE	CABLE TYPE
Buried	Coaxial cables (2.6/9.5 mm., 1.2/4.4 mm.).
In Ducts	Coaxial cables, trunk cables and feeder cables (> 400 pairs).
On walls	Local distribution cables (< 400 pairs).
Aerial Line	Local distribution cables and toll cables (< 400 pairs).

There are two types of cables for aerial installations:

- a) Paired and quaded cables with paper insulation and lead sheath (not manufactured since 1974), and
- b) Paired cables with solid PE insulation and composite sheath type Alpeth, Stalpeth, FPA, etc.

Nowadays, 70 % of toll cables are installed on aerial lines.

Coaxial cables are the only ones directly buried, since the systems supported by them require a high degree of reliability. Yet, trench digging is an extremely expensive operation.

The present trends in aerial cable installation are directed towards the use of self-supporting (Figure 8) cables with FPA sheath.

PROBLEMS OF AERIAL CABLES IN SPAIN

The general performance of aerial cables deteriorate, compared to buried cables, due to the following factors:

- Variation of transmission characteristics due to the wide change of service temperature.
- High number of failures.

Resistance is affected considerably by changes in temperature. Inductance is affected slightly and temperature has only an insignificant effect on conductance and mutual capacitance.

As can be seen in Table 4 (Appendix I) and Figs. 1 to 4 this R and L variation modifies, in turn, the secondary parameters (Z_0 , α , β and V_p); such a modification is, however, insignificant and does not seriously degrade the cable quality.

The number of failures in aerial cables is larger than for buried installations, due to:

- Sheath breaks
- Joint breaks
- Ageing of materials.

Sheath and joint breaks result in water entrance into the cable core. This problem gets considerably worse in Spain due to its extreme climatological conditions (sun, rain, wind, snow, frost, etc.).

The most common causes of these breaks are:

- Atmospheric storms with lightning discharges on cables or supports.
- Vibrations due to wind stress.
- Vibrations due to road proximity.
- Sudden changes of temperature and humidity.
- Abrasion (Trees, walls, etc.).
- Holes due to hunters.
- Workmen other than C.T.N.E.
- Damage due to insect attack.

Water coming in through these cracks, flows along the cable and causes considerable damage, (as has already been established by various authors⁽²⁾), to the transmission characteristics of cables. Table 5 (Appendix II) and Figs. 5 to 8, show the variation observed in a 0.9 mm. gauge 26 pair sample cable, having its core filled up of water. In these Figures can be seen that the resistance and inductance are not affected by water.

Mutual capacitance increases 2.3 times more or less, its value. This is an expected value, since the cable behaves as a coaxial with its inner conductor of copper and the outer formed by a film of water on the insulation. In this case, the measured capacitance should be:

$$C = \frac{1}{2} \frac{24.1275 \cdot \epsilon}{\log 10 \frac{D}{d}} = 121.3 \text{ nF/Km.}$$

which agrees with the one measured and exposed in Table 5.

On the other hand, water considerably increases the dissipation factor, for which the conductance is given by the expression:

$$G = \omega C \cdot \tan \delta$$

and will be doubly increased when increasing C and $\tan \delta$.

As far as secondary parameters are concerned (attenuation, impedance, phase shift and propagation velocity) all of them are seriously affected by water entrance. Figures 5 to 8.

Water damages, likewise, the insulating materials and sheath, which considerably decreases the life. When water entrance is accompanied by high temperatures, cable insulation resistance considerably decreases resulting, even, in out-of-service breakdowns.

In C.T.N.E.'s toll network the failure rate for aerial cables is very high; according to the data corresponding to 1974 and 1975, approximately, 16 failures per 100 Km. each year, that can be detailed as follows:

- 60 % are due to sheath breaks.
- 30 % due to joint breaks.
- 5 % due to conductor breaks.
- 5 % due to another's causes.

For reducing the number of failures and to improve the operation of aerial cables, some solutions have been studied according to the world trends in this field.

SOLUTIONS STUDIED

Once the main factor (water entrance) affecting the behaviour of aerial installations was determined, studies were started in order to get suitable solutions.

World trend in this field is well defined; at the beginning, the use of mechanically stronger sheaths was proposed. This solution, apart from extremely increasing the cable price, did not solve the problem, and was only used as an intermediate step. Nowadays, the design has almost exclusively been directed to the manufacturing of cables filled with a waterproof material, that prevents water entrance through the sheath and its diffusion along the cable core.

This solution has been adopted by most countries, that are trying to find an ideal compound that could be applied to all cables, without modifying their characteristics. Many papers and articles on this subject have been discussed at previous IWCS meetings.

Due to this concern there are now in the market many filling compounds that are being used in every country according to their needs.

After analyzing many of these products we find that most of them have been oriented to be used in buried cables or in countries whose climatological changes are not very severe. Accordingly, the number of products able to be used on aerial installations is very limited and, in general, a careful choice both of the filling compound and of the insulating material will be needed, in order to keep the electrical characteristics stable.

CLIMATOLOGICAL CONDITIONS

At the time of selecting materials and before carrying out the compatibility test between them,

it is necessary to know the real operating conditions to which they have to be submitted. To this purpose, a statistical study has been performed on the following climatological phenomena:

- Max. and min. temperatures
- Mean temperatures
- Total rainfall and number of rainy days per year
- Number of storm days per year
- Max. wind speed

Figs. 9 & 10 and Tables 6 to 9 (Appendix III) show these data and give, the different regional variations for each month of the year.

Data referring to temperature have been taken in national meteorological observatories by means of meteorological housings, placed in the shade at a height of 1.5 m.

According to the experiments performed, temperature in areas directly exposed to the sun (aerial cables), there was a difference of about +10°C from the temperatures recorded in the meteorological housing.

On the other hand and according to that expressed by other authors⁽³⁾, cable core generally reaches a temperature higher than air temperature by 10°C to 15°C. The core can be at a temperature of 20 to 25°C above the max. temperature given by Meteorological Observatories.

In this way and according to the graph shown in Fig. 9 it can be established that cable cores will reach max. temperatures of about 70 to 75°C.

It can also be observed that in some areas min. temperatures differ from max. ones of about 20 to 30°C, and cables are submitted to ageing cycles with high temperature differences that seriously affect the mean life of filled cables.

There are also some areas where max. temperatures in summer and min. ones in winter occur, for which cracking danger of materials increases.

Graphics show, likewise, that in various regions the periods with max. temperatures agree with high rainfalls and storms which considerably impairs the operating conditions of the cables.

According to these data, it can be established that the limiting operating conditions of cables will be:

- Max. Temperature 75°C
- Min. Temperature -20°C
- Max. gust of wind 156 Km/h.
- Max. number storm days 15 per station

Therefore, both material compatibility and operating cable tests should be done taking these factors into account.

MATERIALS USED IN TESTS

INSULATION

Having in mind the european trend in this field, only the PE in its three varieties has been

used for insulation:

- Low density polyethylene (LDPE)
- Medium density polyethylene (MDPE)
- High density polyethylene (HDPE)

With these three PE types in solid and cellular state test have been performed.

Table 2 shows the main characteristics of the PE used.

PE - TYPE PROPERTIES AT R.T.	A SOL. LDPE	B SOL. MDPE	C SOL. MDPE	D SOL. HDPE	E CEL. LDPE	F CEL. MDPE	G CEL. HDPE
Density g/cm ³	0.91	0.921	0.93	0.945	(*)	(*)	(*)
Melt. Index g/10 min.	0.21	0.22	0.23	0.3	0.3	0.3	0.3
Dielectric Constant. 1 MHz	2.26	2.20	2.30	2.32	2.26	2.30	2.30
Tensile Strength Kg/cm ²	160	146	145	218	125	125	150
Elongation %	610	580	590	720	150	150	150

(*) Depending on the foaming grade.

TABLE 2. PROPERTIES OF THE PE MATERIALS USED FOR THE INSULATIONS

To obtain this Table of characteristics, the following ASTM standards have been taken into account:

- Tensile strength and elongation D-638
- Melt Index D - 1238
- Dielectric Constant D-1531
- Volume Resistivity D-257

These polyethylenes and filling compounds incorporate the same antioxidants and copper deactivators.

FILLING COMPOUND

Filling compounds used are petroleum jellies electrically pure distilled from raw petroleum and are composed of a microcrystalline wax mixture and mineral oils.

In order not to impair the transmission characteristics of cables, they should have, low permittivity and loss tangent at audiofrequencies. They should also show a good compatibility with the insu-

lation polymer so as not to impair its dielectric and mechanical characteristics. Likewise, they should have good physical properties so that they do not become extremely hard at low temperatures or extremely fluid at the high temperatures to which it will be submitted during cable operation.

After analyzing some european and spanish filling compounds, the three types shown in Table 3, according to their main characteristics, were selected.

To obtain these characteristics, the following ASTM standards have been taken into account:

- Drop point D-127
- Flash point D-92
- Viscosity D-88
- Dielectric Constant D-150
- Volume Resistivity D-150

TABLE 3. PROPERTIES OF THE MATERIALS USED FOR FILLING COMPOUNDS.

PJ - TYPE PROPERTIES	L	M	N
Drop Point °C	97	85	96
Flash Point °C	307	296	256
Viscosity sus	114	108	100
Penetration m.m. at 25°C	4'8	7	4'7
Dielectric Constant, a 1 MHz	2'46	2'49	2'37
Volume Resistivity at 23°C	$1.4 \cdot 10^{15}$	$1.8 \cdot 10^{15}$	$1.3 \cdot 10^{15}$

FILLING AND INSULATION COMPATIBILITY

In order to get a cable with suitable physical and electrical characteristics and, at the same time, stable during cable life, a full compatibility is needed between filling material and insulating polymer as well as a minimum interaction between them.

Usually, when filling and insulating PE are in contact, the insulation absorbs a certain amount of filling compound and progressively deteriorates.

This phenomenon has been widely studied by various authors and all agree in advising a good and careful choice of them for mitigating this effect.

For choosing the products suitable to our climatological conditions the following compatibility tests, with different filling and insulation types have been performed:

- Tensile strength and elongation

- 1) Before and after air stove ageing at 85°C and 100°C.
- 2) After immersion in a filling compound at RT, 50°C, 70°C and 80°C for 2 days, 2 weeks and 3 months.

- Thermal shock

It takes place at 100 and 120°C after immersion of the samples in a filling compound 2 days, 2 weeks and 3 months at RT, 50, 70 and 85°C. This phenomenon can be observed when crackings occurs.

- Weight change

On 25 cm. samples of each conductor insulation after immersion in a filling compound 2 days, 2 weeks and 3 months. They are weighed before and after being submerged.

- Diameter change

On 25 cm. samples of each insulation, measuring the diameter before and after immersion in a filling compound 2 days, 2 weeks and 3 months.

- Wrap test

It takes place by submitting the samples to an immersion period, for later exposure, during 90 days, to temperatures of 70, 80 and 85°C.

The results are shown in Tables 10 to 17 (Appendix IV) and Figs. 11 to 14.

According to them, the following conclusions can be made:

- HDPE is, at first, more suitable for being used at high temperatures than LDPE and MDPE, since it presents a lower filling absorption.

- As far as the filling compounds analyzed are concerned, the most suitable is type L, since it shows a higher drop point and lower interaction with PE used.

According to these results, PE type "D" and "G" and filling compound type "L" have been selected for carrying out prototypes.

PROTOTYPES MANUFACTURED AND TESTS PERFORMED

According to the materials selected in Laboratory, two prototypes were selected with the following characteristics:

CABLE	GAUGE	NºOF PAIRS	INSULATION	FILLING	SHEATH
1	0.91 19 AWG	25	HDPE Solid	L	FPA
2	0.91 19 AWG	25	HDPE Cellular	L	FPA

Test performed were:

- Transmission parameters (1st and 2nd) at temperatures of -20°C, 0°C, 40°C, 60°C and 80°C.
- Waterproofness.

- Insulation resistance.
- Dielectric strength.

The results are shown in Figs. 15 to 23 and in Table 18 (Appendix V).

In primary parameters two phenomena can be observed:

- temperature affects them the same as dry cables, R and G change, and C remaining almost constant.
- with increasing frequency, R and G change, but their change percentage is less than in dry cables.

Referring to secondary parameters, it can be seen that HF attenuation improves, mainly due to a lower variation of R and G, as noted in the previous paragraph.

Capacitance unbalances between pairs and ground increase in filled cables; this phenomenon will be widely studied to try to reduce it.

Fig. 23 shows the insulation resistance variation versus temperature. An important change can be observed between -20°C and $+60^{\circ}\text{C}$. Yet, the variation below and above these limits is insignificant.

PE with antioxidants and copper deactivators has a volumetric resistivity of 4×10^{15} ohm-cm at 50°C decreasing lightly when temperature increases. Filling compounds have a volumetric resistivity value lower than 2×10^{13} ohm-cm., which indicates that these compounds are the main cause of the low insulating resistance experienced in filled telephone cables when temperature increases.

This phenomenon will be actively studied.

Waterproofness tests, with a complete cable have been performed and all meet the specifications.

FIELD TRIALS IN A REAL INSTALLATION

Both cable prototypes, have been installed in four routes belonging to areas where climatological conditions are very extreme in order to verify the characteristics found in the laboratory. To this purpose, a long-term test plan has been prepared.

The results of the first tests performed with max. temperatures of 25°C are shown in the following Table:

FIELD TRIAL - MEASUREMENTS			
RESISTANCE D.C. ohm/Km.		54.56	
MUTUAL CAPACITANCE 800 Hz, nF/Km.		53	
GROUND CAPACITANCE UNBALANCE 800 Hz pF/550 m.		315	
IMPEDANCE (Z_0) ohm.	800 Hz	460	
	150 KHz	112	
	1 MHz	104	
ATTENUATION dB/Km.	800 Hz	0.73	
	150 KHz	4.1	
	1 MHz	10.6	
FEXT dB/1,830 m.	Center	150 KHz	81
		1 MHz	67
	First Layer	150 KHz	87
		1 MHz	78
	Second Layer	150 KHz	76
		1 MHz	73
NEXT dB	Center	150 KHz	81
		1 MHz	70
	First Layer	150 KHz	76
		1 MHz	65
	Second Layer	150 KHz	72
		1 MHz	57
	Center to first layer	150 KHz	83
		1 MHz	73
	First to Second Layer	150 KHz	78
		1 MHz	66

The results obtained fully agree with those expected according to laboratory measurements.

CONCLUSIONS

What has been described in this paper demonstrates that although the use of filled cables on aerial lines is feasible in practice, even under extreme operating conditions, it will be necessary to carry out a careful choice of insulating and filling materials to ensure a good cable mean life.

High density PE solid and cellular insulations show the best compatibility levels with filling products. From these products those with high drop point are, undoubtedly, the most reliable.

Having, however, in mind the high capacitance unbalances and low insulation resistance that have been found in their operation above 60°C it will be necessary to study them wider and pursue the development, both of materials and manufacturing process, overall, when cables have to be used with high frequency systems.

According to the operating results obtained from now on, it is intended to continue the development in order to get a cable fully useful to be installed on our aerial lines.

ACKNOWLEDGEMENTS

We wish to acknowledge and thank the Managing and Laboratory Personnel of Cables de Comunicaciones S.A. for their help in carrying out the laboratory tests.

REFERENCES

1. Twenty-Third IWCS. Cellular Insulation as an Answer to material conservation, E.D. Metcalf.
2. Transmission Properties of Polyethylene Insulated Telephone Cables at Voice and Carrier Frequencies G.S. Eager, Jr. L. Jachimowicz, I. Kolodny and D.E. Robinson.
3. Twenty-Fourth IWCS. The Properties of Cellular Polyethylene Insulated Filled Communication Cable and its Increasing Use. S.M. Beach, K.R. Bullock and D.F. Cretney.
4. Twentieth IWCS. Long Term Stability of Polyethylene Insulated Fully-Filled Telephone Distribution Cables. S. Verne, R.T. Puckowski and A.A. Pinching.
5. Twenty-Fourth IWCS. Change of Cosstalk Properties in Correlation to the Interaction of Polyethylene/Petroleum-Jelly. H.J. Anderka, H.G. Dagefördl and H.A. Mayer.



Luis M. Molleda
C.T.N.E.
Avda. José Antonio, 28
MADRID - SPAIN

Luis M. Molleda is presently Head of the Outside Plant Group in the Research and Study Center of the National Telephone Company of Spain (C.T.N.E.).

Born in 1941 in Vitoria, Spain, he was graduated as an Industrial Engineer in 1969. After graduation, he began to work at the National Telephone Company of Spain in the Projects Engineering Department and has been working since 1970 in the Outside Plant Group of the Research and Study Center especially in Communications cable design.



Enrique Used
C.T.N.E.
Avda. José Antonio, 28
MADRID - SPAIN

Enrique Used is presently Manager of the Research and Study Center of C.T.N.E.

Born in 1941 in Zaragoza, Spain, graduated as a Telecommunication Engineer in the E.T.S.I.T. of Madrid, in 1966.

On this date he began to work in C.T.N.E., first as a Chief of the Maspalomas Satellite Earth Station (Gran Canaria, Spain), later as a Section Chief of the International Department and Subdirector of the Technical Secretary. In 1974 he was promoted to his present position of Manager of the Research and Study Center.

He is a member of the IEEE and of the Managing Board of this Institute in Spain.

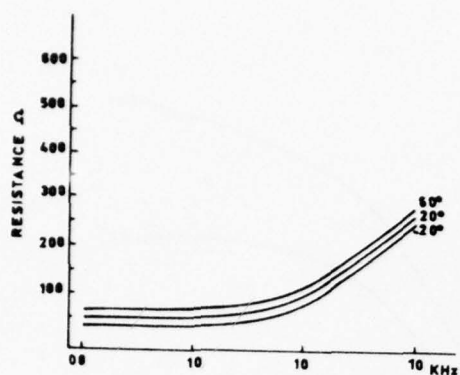


FIG. 1. Resistance/frequency at -20° , 20° and 60°C for 19 AWG cable.

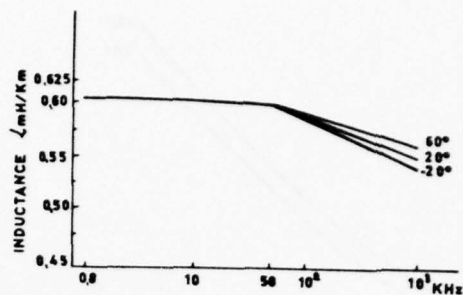


FIG. 2. Inductance/frequency at -20° , 20° and 60°C for 19 AWG cable.

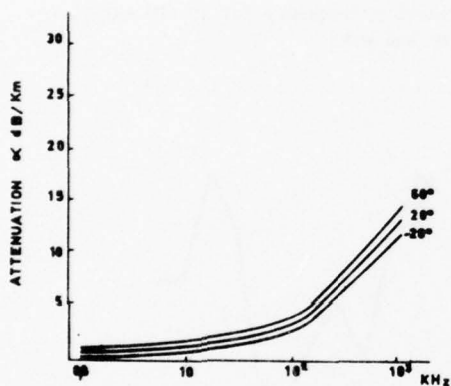


FIG. 3. Attenuation/frequency at -20° , 20° and 60°C for 19 AWG cable.

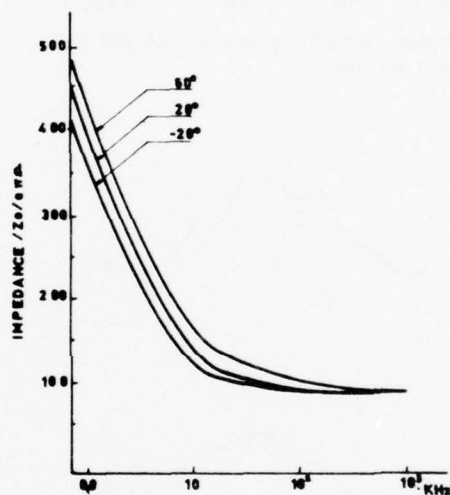


FIG. 4. Impedance/frequency at -20° , 20° and 60°C for 19 AWG cable.

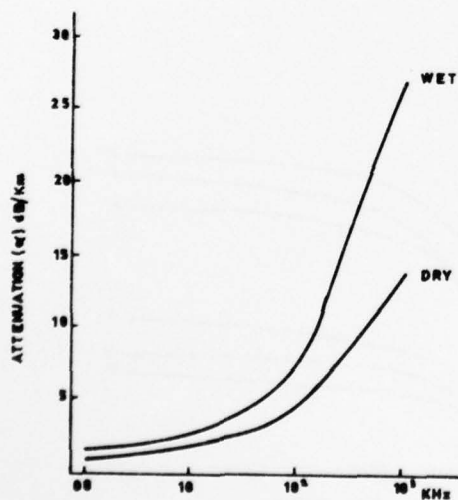


FIG. 5. Attenuation/frequency for 19 AWG cable, dry and wet.

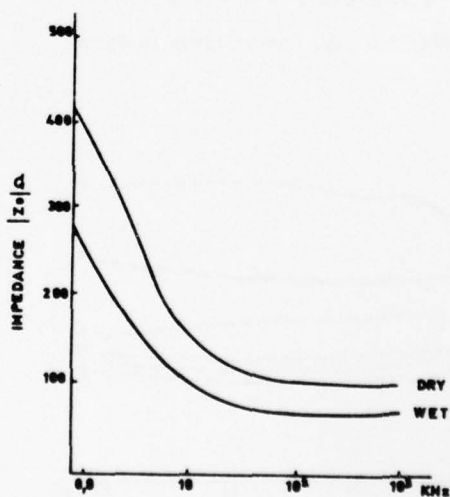


FIG. 6. Impedance/frequency for 19 AWG cable, dry and wet.

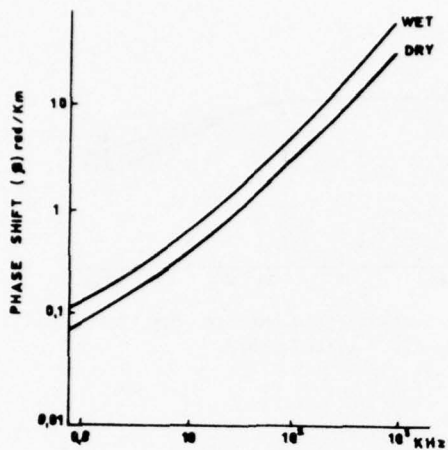


FIG. 7. Phase shift/frequency for 19 AWG cable, dry and wet.

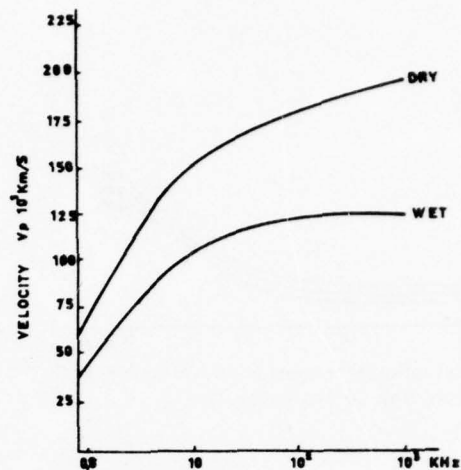


FIG. 8. Velocity/frequency for 19 AWG cable, dry and wet.

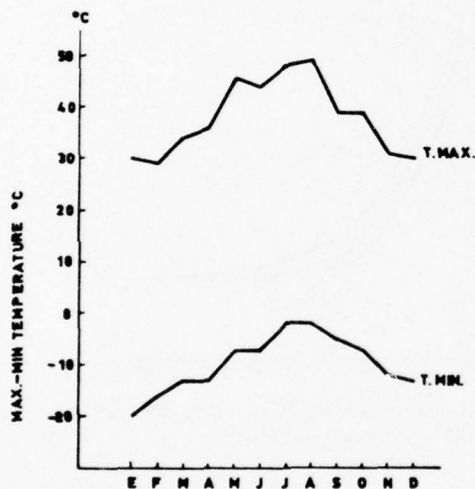


FIG. 9. Máx. and Min. temperatures in Spain.

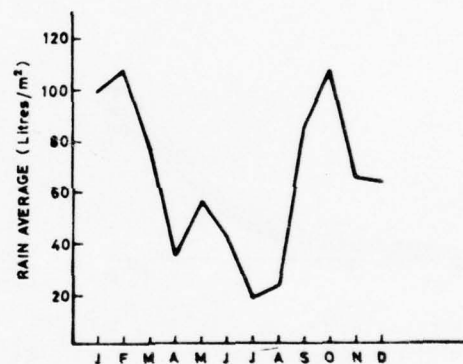


FIG. 10. Rain average in Spain.

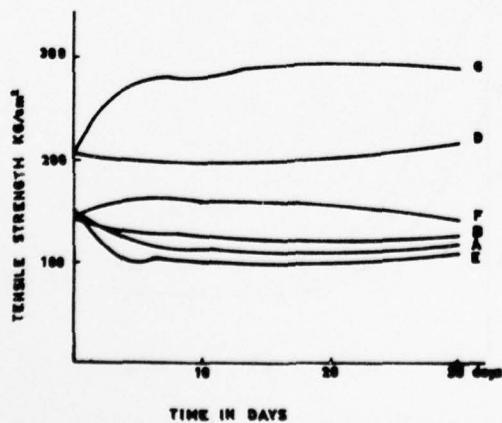


FIG. 11. Tensile Strength of PE's into L filling compound.

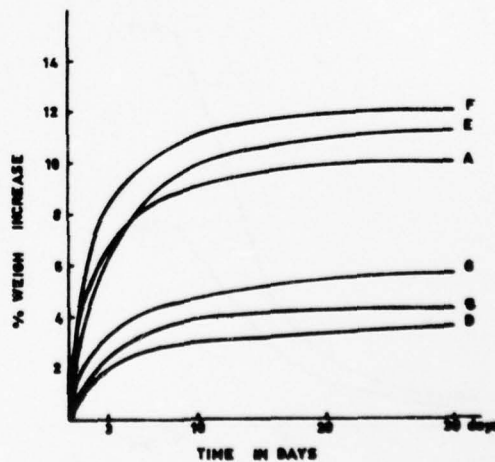


FIG. 12. Absorption of compound L by different PE's.

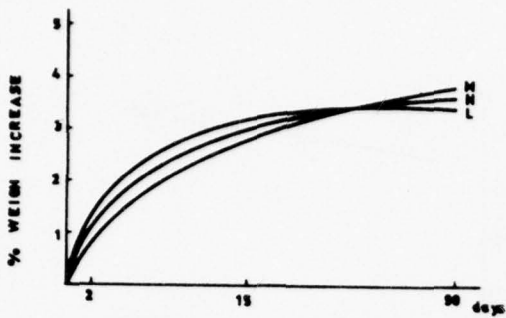


FIG. 13. Absorption of different compounds by PE, "D".

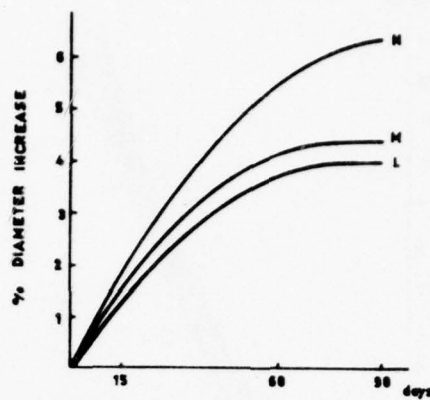


FIG. 14. Absorption of different compounds by PE, "D".

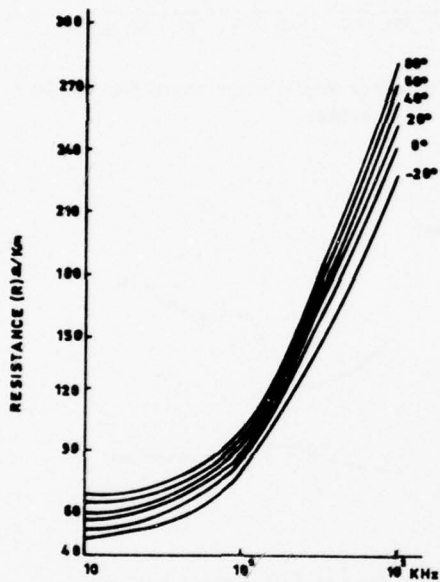


FIG. 15. Resistance/frequency for 19 AWG filled cable.

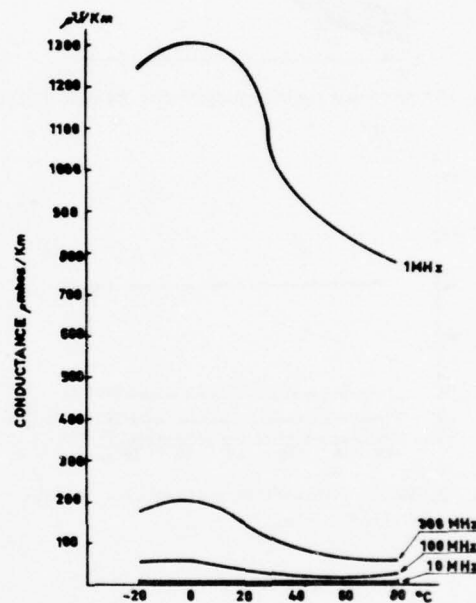


FIG. 16. Conductance/temperature for 19 AWG filled cable.

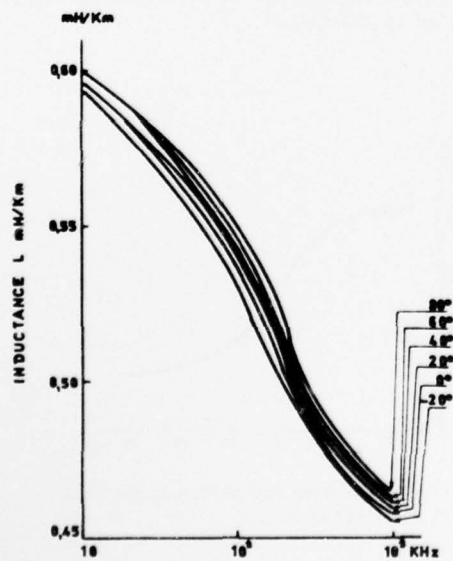


FIG. 17. Inductance/frequency for 19 AWG filled cable.

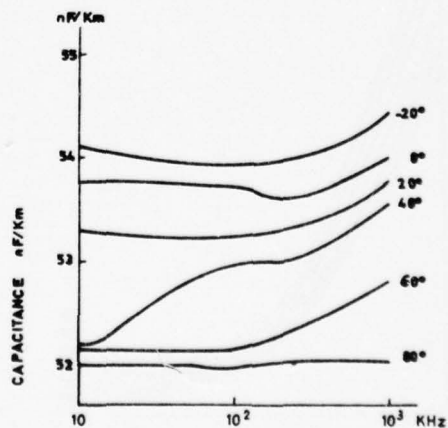


FIG. 18. Capacitance/frequency for 19 AWG filled cable.

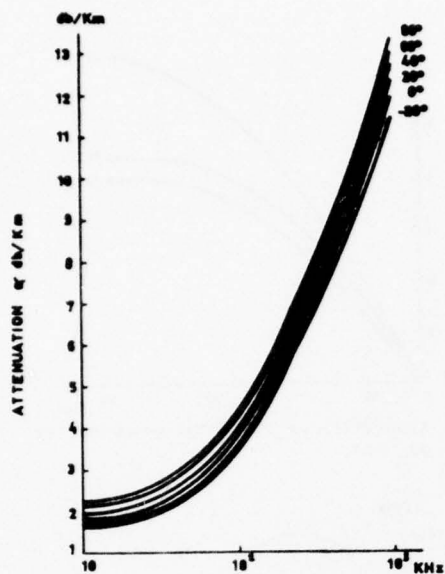


FIG. 19. Attenuation/frequency for 19 AWG filled cable.

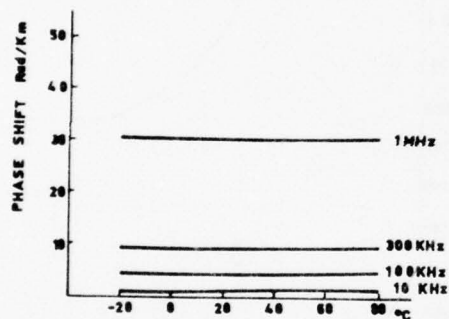


FIG. 20. Phase change/temperature for 19 AWG filled cable.

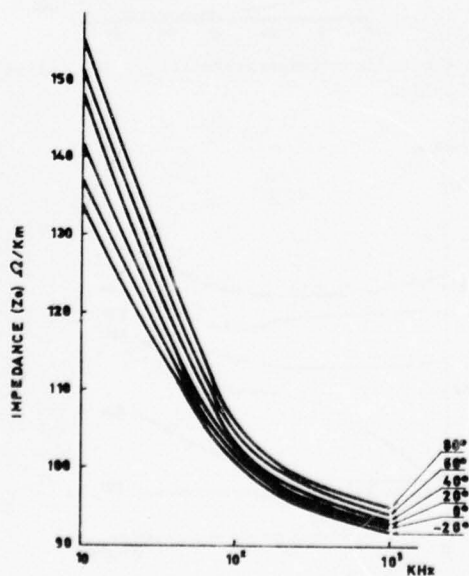


FIG. 21. Impedance/temperature for 19 AWG filled cable

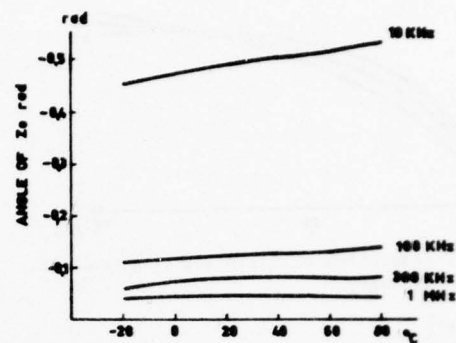


FIG. 22. Impedance angle/temperature for 19 AWG filled cable.

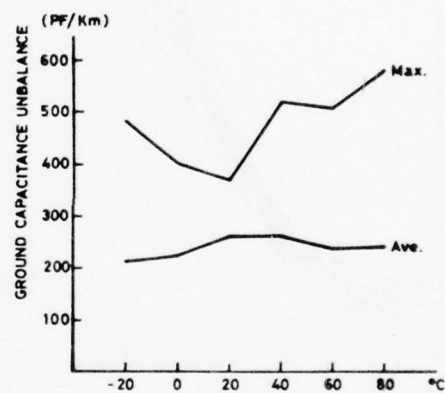


FIG. 23. GROUND capacitance unbalance/temperature for 19 AWG filled cable.

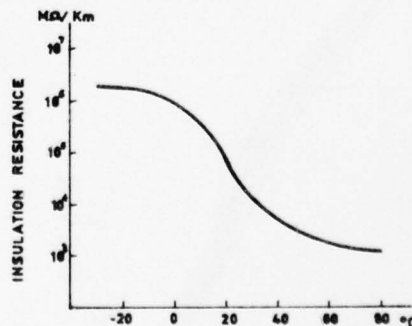


FIG. 24. Insulation Resistance/temperature for 19 AWG filled cable.

APPENDIX I

FREQUENCY KHz	PRIMARY PARAMETERS						SECONDARY PARAMETERS									
	R Ohm/Km.		L mH / Km		G umhos/Km		C nF / Km		Zo ohms.		Zo rad. (-)		ATTENUATION db / Km		PHASE SHIFT rad / Km	
	1	2	1	2	1	2	1	2	1	2	1	2	1	2	1	2
0.8	54.2	54.2	0.602	0.6	0.028	23.4	52	119	456	300	0.757	0.738	0.71	1.09	0.086	0.13
4	56	56	0.602	0.6	0.157	34.6	52	118	209	138	0.651	0.646	1.44	2.30	0.217	0.33
10	55.9	56.3	0.602	0.599	0.441	52.5	52	118	144	95	0.487	0.487	1.91	2.93	0.415	0.62
50	71.7	68.7	0.597	0.595	3.43	254.2	52	117	111	73	0.183	0.173	2.86	4.84	1.78	2.66
100	89.5	88.3	0.587	0.563	9.47	700.1	52	118	108	70	0.118	0.117	3.64	5.73	3.49	5.16
150	103.9	105	0.570	0.551	18.62	1968	52	119	106	69	0.095	0.092	4.30	7.27	5.16	7.67
772	234.3	211.5	0.521	0.521	458	39000	52	119	100	66	0.044	0.082	10.62	25.12	25.27	38.29
1000	268.8	-	0.512	-	638	-	52	52	99.4	-	0.037	-	12.8	-	33.23	-

Table 4. Parameters of 19 AW 6 PIC. 1, DRY, 2 WET

APPENDIX II

FREQUENCY KHz	TEMPERATURE 0°C	PRIMARY PARAMETERS					SECONDARY PARAMETERS				
		R Ohm/Km	L mH / Km	G umhos/Km	C nF/Km	Zo		Zo rad. (-)	ATTENUATION db/Km	PHASE SHIFT rad/Km	
						Ohm.					
0.8	- 20	46.11	0.602	0.028	52	52	420.4	0.752	0.65	0.08	
	20	54.20	0.602	0.028	52	52	455.7	0.757	0.71	0.086	
	60	62.72	0.602	0.028	52	52	490.1	0.761	0.77	0.093	
10	- 20	47.86	0.602	0.441	52	52	136.6	0.450	1.69	0.402	
	20	56.83	0.602	0.441	52	52	143.7	0.467	1.91	0.415	
	60	64.71	0.602	0.441	52	52	151.5	0.520	2.14	0.429	
100	- 20	77.93	0.590	9.475	52	52	106.8	0.105	3.19	3.470	
	20	89.44	0.596	9.475	52	52	107.8	0.119	3.64	3.496	
	60	92.89	0.590	9.475	52	52	108.2	0.122	3.76	3.509	
300	- 20	134.86	0.539	49.980	52	52	102.3	0.065	5.76	10.008	
	20	150.86	0.544	49.980	52	52	102.9	0.072	6.41	10.059	
	60	160.04	0.549	49.980	52	52	103.4	0.076	6.77	10.10	
1,000	- 20	240.16	0.508	638	52	52	99	0.033	11.59	33.9	
	20	268.84	0.512	638	52	52	99.4	0.037	12.81	33.22	
	60	284	0.518	638	52	52	100	0.039	13.41	33.42	

Table 5. Parameters of 19 AW 6 PIC. at - 20°, 20° and 60°C.

APPENDIX III

AREAS	NORTE Y N.W.	DUERO	TAJO	GUADIANA	GUADAL- QUIVIR	SUR	SEGURA	LEVANTE	EBRO	PIRINEO ORIENTAL	TOTAL
JANUARY	72	12	1	47	37	7	3	2	5	0	186
FEBRUARY	68	68	37	82	100	47	23	54	62	26	567
MARCH	245	110	86	317	139	40	86	114	421	92	1660
APRIL	376	1292	345	567	186	43	50	79	409	34	3381
MAY	533	2116	679	732	291	40	489	831	1434	164	7309
JUNE	639	3269	838	892	495	68	514	864	1292	229	9098
JULY	440	775	53	40	33	9	53	171	910	261	2745
AUGUST	876	3474	759	525	225	23	256	1074	2325	705	10242
SEPTEMBER	62	179	96	27	138	36	222	269	1025	282	2336
OCTOBER	299	57	29	20	104	73	116	38	34	90	860
NOVEMBER	63	9	29	91	22	1	2	1	45	29	292
DECEMBER	5	0	3	5	0	6	0	0	0	0	19
ALL YEAR	3678	11361	2955	3345	1770	391	1814	3497	7962	1912	38685
0	294	768	292	410	176	74	164	294	505	132	3109
S/O	12.5	14.8	10.1	8.2	10.1	5.3	11.1	11.9	15.8	14.5	12.4

0 - STATION S - STORM

TABLE 8. Storms in different regions of Spain.

AREAS	NORTE Y N.W.	DUERO	TAJO	GUADIANA	GUADAL- QUIVIR	SUR	SEGURA	LEVANTE	EBRO	PIRINEO ORIENTAL
JANUARY	120	85	88	76	111	95	89	94	94	130
FEBRUARY	156	110	85	94	138	72	58	133	104	135
MARCH	116	95	83	66	87	95	66	109	86	136
APRIL	104	79	77	76	102	97	86	103	100	122
MAY	116	83	63	72	94	83	54	82	79	101
JUNE	74	79	61	59	78	74	58	72	97	75
JULY	101	72	65	61	85	61	43	79	83	94
AUGUST	105	77	76	52	87	56	47	90	78	106
SEPTEMBER	76	88	58	74	74	85	55	110	76	99
OCTOBER	108	95	122	83	76	81	58	90	80	143
NOVEMBER	118	83	76	72	89	113	72	93	91	153
DECEMBER	128	81	65	80	101	111	62	90	65	140

TABLE 9. Max gust of wind in Km/hour.

APPENDIX III

AREAS	JAN.		FEB.		MAR.		APR.		MAY.		JUN.		JUL.		AUG.		SET.		OCT.		NOV.		DEC.	
	Máx.	Mín.	Máx.	Mín.	Máx.	Mín.	Máx.	Mín.	Máx.	Mín.	Máx.	Mín.	Máx.	Mín.	Máx.	Mín.	Máx.	Mín.	Máx.	Mín.	Máx.	Mín.	Máx.	Mín.
Norte y N.O.	25	-15	22	-9	26	-11	30	-8	33	-7	34	-3	41	2	39	0	35	-3	29	-4	29	-7	29	-11
Duero	15	-20	23	-10	27	-13	32	-10	40	-8	40	-7	42	-2	44	-2	36	-5	30	-7	24	-11	23	-12
Tajo	24	-20	28	-10	32	-11	36	-10	43	-5	44	-3	45	0	49	-1	39	-5	33	-6	27	-12	22	-12
Guediana	22	-12	23	-7	30	-7	36	-8	41	-2	44	1	46	4	44	6	39	1	36	-3	29	-5	27	-7
Guadaluquivir	22	-11	25	-6	35	-5	36	-5	44	-3	41	2	48	6	44	6	39	1	39	-4	31	-5	24	-7
Sur	24	-10	28	-10	29	-7	34	-7	41	-5	43	5	47	9	41	9	36	3	39	0	31	-2	29	-5
Segura	24	-15	28	-9	29	-4	35	-5	40	-2	42	2	48	5	41	3	37	-1	32	-3	30	-5	24	-8
Levante	20	-13	25	-8	28	-7	33	-8	41	-4	41	-1	41	2	37	2	34	-2	32	-4	28	-8	24	-10
Ebro	21	-18	23	-16	33	-13	37	-13	46	-7	43	-4	42	-1	41	-2	35	-3	36	-8	29	-12	22	-13
Pirineo	24	-17	23	-9	26	-5	30	-11	33	-3	34	2	39	2	36	4	30	-1	29	-3	26	-7	22	-6
ALL COUNTRY	30	-20	29	-16	35	-13	36	-13	46	-8	44	-7	48	-2	49	-2	39	-5	39	-8	31	-12	30	-13

TABLE 6. Máx. and Mín. temperature in the main areas of SPAIN.

AREAS	JAN.		FEB.		MAR.		APR.		MAY.		JUN.		JUL.		AUG.		SEPT.		OCT.		NOV.		DEC.	
	Máx.	Mín.	Máx.	Mín.	Máx.	Mín.	Máx.	Mín.	Máx.	Mín.	Máx.	Mín.	Máx.	Mín.	Máx.	Mín.	Máx.	Mín.	Máx.	Mín.	Máx.	Mín.	Máx.	Mín.
Norte	206	199	199	199	112	112	137	137	193	193	85	85	31	31	71	71	68	68	95	95	81	81	98	98
Noroeste	198	258	258	258	153	153	73	73	87	87	37	37	12	12	27	27	63	63	157	157	132	132	145	145
Duero	91	117	117	117	54	54	26	26	47	47	41	41	23	23	15	15	70	70	100	100	47	47	72	72
Tajo	117	158	158	158	84	84	22	22	28	28	26	26	16	16	4	4	99	99	147	147	68	68	86	86
Guediana	99	97	97	97	78	78	22	22	26	26	12	12	5	5	4	4	64	64	120	120	53	53	64	64
Guadaluquivir	108	111	111	111	106	106	26	26	37	37	12	12	4	4	2	2	52	52	129	129	48	48	70	70
Sur	87	56	56	56	101	101	23	23	35	35	20	20	1	1	1	1	56	56	130	130	93	93	44	44
Segura	24	18	18	18	54	54	30	30	43	43	32	32	7	7	13	13	73	73	127	127	106	106	5	5
Levante	47	37	37	37	54	54	25	25	47	47	33	33	20	20	42	42	123	123	92	92	101	101	26	26
Ebro	70	69	69	69	49	49	34	34	72	72	85	85	35	35	50	50	125	125	56	56	48	48	38	38
Pirineo	97	75	75	75	72	72	73	73	125	125	127	127	66	66	78	78	145	145	70	70	42	42	41	41
ALL COUNTRY	99	108	108	108	77	77	36	36	57	57	43	43	19	19	24	24	86	86	108	108	66	66	64	64

TABLE 7. Rain Average in litres/m²

APPENDIX IV

PE - TYPE	2 DAYS	15 DAYS	90 DAYS
A	92	97	66
B	99	99	76
C	92	76	73
D	99	91	89
E	96	87	83
F	94	81	93
G	97	124	106

Table 10. Effect of time on the Tensile Strength after immersion in L type compound

PE - TYPE	2 DAYS	15 DAYS	90 DAYS
A	89	85	21
B	96	88	85
C	94	89	29
D	102	107	97
E	85	18	17
F	74	24	18
G	99	97	117

Table 11. Effect of time on the Elongation after immersion in L type compound

PE - TYPE	70°C	80°C	85°C
A	Fail	Fail	Fail
B	Pass	Fail	Fail
C	Pass	Pass	Fail
D	Pass	Pass	Pass
E	Fail	Fail	Fail
F	Pass	Fail	Fail
G	Pass	Pass	Pass

Table 12. Effect of temperature on performance in Wrap test after 7 days immersion and subsequent exposure for 90 days.

PE - TYPE	2 DAYS	15 DAYS	120 DAYS
A	Fail	-	-
B	Fail	-	-
C	Fail	-	-
D	Pass	Pass	Pass
E	Pass	Fail	-
F	Fail	-	-
G	Pass	Pass	Pass

Table 13. Thermal Shock after immersion in L type compound at 85°C

PJ - TYPE	WEIGHT INCREASE	DIAMETER INCREASE %
L	3.6	4
M	3.8	4.4
N	3.5	4.6

Table 16. Weight and diameter increase after immersion in L type compound for 90 days.

PE - TYPE T°C	2 DAYS %	15 DAYS %	90 DAYS %
A 85	96	98	95
A 100	92	89	83
B 85	93	97	98
B 100	99	91	71
C 85	103	100	98
C 100	77	73	69
D 85	100	74	87
D 100	83	72	69
E 85	93	95	93
E 100	83	84	78
F 85	93	99	83
F 100	96	82	84
G 85	113	122	124
G 100	126	127	130

Table 14. Effect of time on the Tensile Strength after aging at 85° and 100°C.

PE - TYPE T°C	2 DAYS	15 DAYS	90 DAYS
A 85	98	75	25
A 100	96	69	18
B 85	93	92	93
B 100	96	102	104
C 85	98	92	94
C 100	97	67	22
D 85	100	100	110
D 100	100	114	110
E 85	95	101	97
E 100	85	87	10
F 85	81	89	91
F 100	98	60	12
G 85	98	85	109
G 100	100	79	78

Table 15. Effect of time on the Elongation after aging at 85 and 100°C.

PE - TYPE	WEIGHT INCREASE %	DIAMETER INCREASE %
A	10	8.5
B	5.2	6
C	4.2	4.4
D	3.6	4
E	11.2	7.7
F	12	6
G	5.7	4

Table 17. Weight and diameter increase after immersion in L Type compound for 90 days.

APPENDIX V

TABLE 18. PARAMETERS OF 19 AWG FILLED CABLES. 1: SOLID HOPE. 2: CELLULAR HOPE.

FREQUENCY	PRIMARY PARAMETERS										SECONDARY PARAMETERS									
	T ° C		R		L		G		C		IMPEDANCE			ANGLE		ATTENUATION		PHASE SHIFT		
			Ohm/Km		mH/Km		unhos/Km		nF/Km		Ohm			rad.		db/Km				
	1	2	1	2	1	2	1	2	1	2	1	2	1	2	1	2	1	2		
10 KHz	-20	48.3	48	0.59	0.68	5.21	3.55	54.1	53.5	134	138.4	-0.46	-0.42	1.7	1.6	0.40	0.42			
	0	52.1	52.1	0.60	0.68	3.34	3.57	53.8	52.2	137.8	146.4	-0.47	-0.42	1.8	1.7	0.41	0.44			
	+20	56.8	56.4	0.60	0.68	1.85	1.53	53.3	51.9	142.5	147.4	-0.49	-0.46	2	1.9	0.42	0.43			
	+40	60.8	60.5	0.60	0.69	0.75	1.58	52.2	51.8	148.4	149.4	-0.51	-0.47	2	2	0.42	0.44			
	+60	65	64.5	0.60	0.69	2.28	0.41	52.1	51	151.4	155.8	-0.52	-0.49	2.1	2	0.43	0.44			
	+80	68.9	68.5	0.60	0.69	0.15	0.17	52	49.7	155.1	161.2	-0.53	-0.50	2.2	2.1	0.44	0.44			
100 KHz	-20	79.6	75.4	0.53	0.63	55.3	18	53.9	52.4	100.6	110.4	-0.12	-0.09	3.5	3	3.39	3.62			
	0	83.3	79.3	0.54	0.63	55.6	43	53.7	52.1	101.4	111.1	-0.12	-0.10	3.6	3.1	3.40	3.61			
	+20	87.7	83.6	0.54	0.64	34.1	34	53.3	51.9	102.4	112	-0.13	-0.10	3.8	3.3	3.40	3.63			
	+40	92.3	87.3	0.54	0.64	17.7	12	53	51.6	103.1	112.5	-0.13	-0.11	3.9	3.4	3.40	3.62			
	+60	94.9	90.8	0.55	0.64	17.2	7.2	52.1	51	104.3	113.7	-0.13	-0.11	4.0	3.5	3.39	3.62			
	+80	99.1	94.4	0.56	0.66	24.7	4.7	52	49.7	104.9	115.7	-0.14	-0.11	4.2	3.6	3.39	3.59			
300 KHz	-20	130.2	123	0.49	0.59	176.8	52.4	54	52.4	95.7	106.3	-0.07	-0.06	6	5.1	9.71	10.48			
	0	136.9	129	0.49	0.59	203.4	121.5	53.6	52.1	96.4	107.2	-0.07	-0.06	6.3	5.3	9.72	10.51			
	+20	142.7	135	0.49	0.60	151.9	147.7	53.3	51.9	97.1	107.6	-0.07	-0.06	6.5	5.5	9.73	10.51			
	+40	149.2	140.7	0.50	0.60	89.7	77.2	53.1	51.7	97.6	108.2	-0.08	-0.06	6.7	5.7	9.73	10.52			
	+60	154.5	145.8	0.50	0.60	64.8	46.2	52.3	51.1	98.7	108.8	-0.08	-0.06	6.8	5.8	9.67	10.48			
	+80	161.9	150.8	0.51	0.61	59.6	30.5	52	49.8	99.3	110.9	-0.08	-0.07	7.1	5.9	9.71	10.39			
1 MHz	-20	231.7	219.9	0.46	0.56	1230.7	710.4	54.5	53	91.9	102.6	-0.04	-0.03	11.4	9.6	31.41	34.15			
	0	243.2	230.4	0.46	0.56	1305	1054.9	54.1	52.6	92.6	103.3	-0.04	-0.03	11.9	10.2	31.40	34.13			
	+20	253.4	239.9	0.46	0.56	1267.1	1148.5	53.8	52.6	93	103.4	-0.04	-0.03	12.4	10.6	31.41	34.15			
	+40	264.5	249.6	0.47	0.56	950.8	1161.9	53.6	52.6	93.4	103.5	-0.04	-0.03	12.7	10.9	31.40	34.20			
	+60	273.1	258.7	0.47	0.57	850.7	784.2	52.8	51	94.3	106.3	-0.05	-0.03	12.9	11.4	31.24	33.9			
	+80	282.6	291.7	0.47	0.59	773.8	273.8	52.5	47.3	94.8	111.9	-0.05	-0.04	13.2	11.3	31.21	33.2			

EXTENDED FIELD TRIALS ON CONDUCTIVE
PLASTIC SHEATHED TELECOMMUNICATION CABLE IN A TRUNK NETWORK

P. Calzolari
M. Barbaro Forleo

Industrie Pirelli S.p.A.
Milan, Italy

G. Cosimi
E. Fucini

S.I.P. - Società Italiana Per
l'Esercizio Telefonico p.A.,
Rome, Italy

Summary

In Summer 1973 a 13 km experimental link was carried out between Vigevano and Mortara (Northern Italy near Milan) employing a lead sheathed 0.7/2.9 coaxial cable with outer PVC conductive covering. The purpose of the experimental link was to evaluate the characteristics and the behaviour versus time of the new type of covering, by means of field and laboratory tests.

The characteristics of the experimental link, the results of the measurements and the conclusions so far reached on the future utilisation of the new material are illustrated in the present Paper.

1. Introduction

The sheaths for buried telephone cables have always developed in close association with the technology of both metallic and plastic materials. Tight metal sheaths protected with suitable covering are still recognized to be the most reliable.¹

Any reference to protection in this Paper will apply to this type only.

The life of the materials used for cables protection is difficult to forecast, as it is directly associated with the economic life of the telephone cables, generally in the range of tens of years. During this time the cable and particularly its protection may be subjected to several kinds of trouble:

- mechanical stresses
- rodent and insect attack
- corrosion
- electric induction
- lightning discharges

The experience gathered in Italy during the last ten years on manufacture, installation and service of buried cables, both local and trunk, has confirmed the convenience of using metallic sheaths, either lead or aluminium alloy, the latter mainly for trunk cables covered with plastic insulating material (PVC or PE) and possibly provided with steel tape armour.

Particularly with reference to trunk cables, some of the types of protection are considered (see table 1). As known, metallic sheaths when protected by a plastic insulating covering have to be earthed at suitably spaced points in order to ensure the necessary level of protection against induction and lightning.

An improvement to the cable protection is given by the armour which increases the screening effect. A greater advantage is obtained when the armour is covered by a textile fibre protection instead of a covering of plastic insulating material. Treated jute, for instance, can practically give a continuous earthing for the armour itself, but not for the underlying metallic sheath.

The requirements of the protection from 1) corrosion and 2) induction and lightning may be in opposition; in fact, while on one hand it would be necessary to have isolation from environmental attacks, on the other hand the metallic sheath would require to be as near as possible to the earth potential. This problem could be solved eventually by using a newly developed material i.e. a plastic covering having the following characteristics:

- good electric conductivity
- possibility of preventing electrochemical contact between metallic sheath to be protected and external environment
- characteristics of use similar to those of current compounds now widely experimented with.
- constant behaviour of properties versus time.

We can see that a compound having all these characteristics is not easy to obtain, this is demonstrated by the fact that actual installations, although experimental, are small in number. Studies in this direction have been promoted also by CCITT following a request formulated by many Countries². The V and VI Commission have been invited to investigate a new problem concerning: "Coordinated protection schemes for telecommunication cables" (question Z/VI; re CCITT AP VI No 70E).

For many years³ the problem has been faced in several Countries and investigations are also in progress in Italy with the aim of obtaining through accurate laboratory and field tests some practical results that will give real application in the field of trunk cables in a reasonably short time.

2. Organisation of the experimental work

Reason for selecting PVC

Conductive compounds are readily available on the market, as they are generally used as inner and outer screen for M.V. power cables with extruded insulation. The utilisation of these materials as protective covering on telephone cables is relatively recent. Among the various products, polyethylene and elastomer-

AD-A032 801

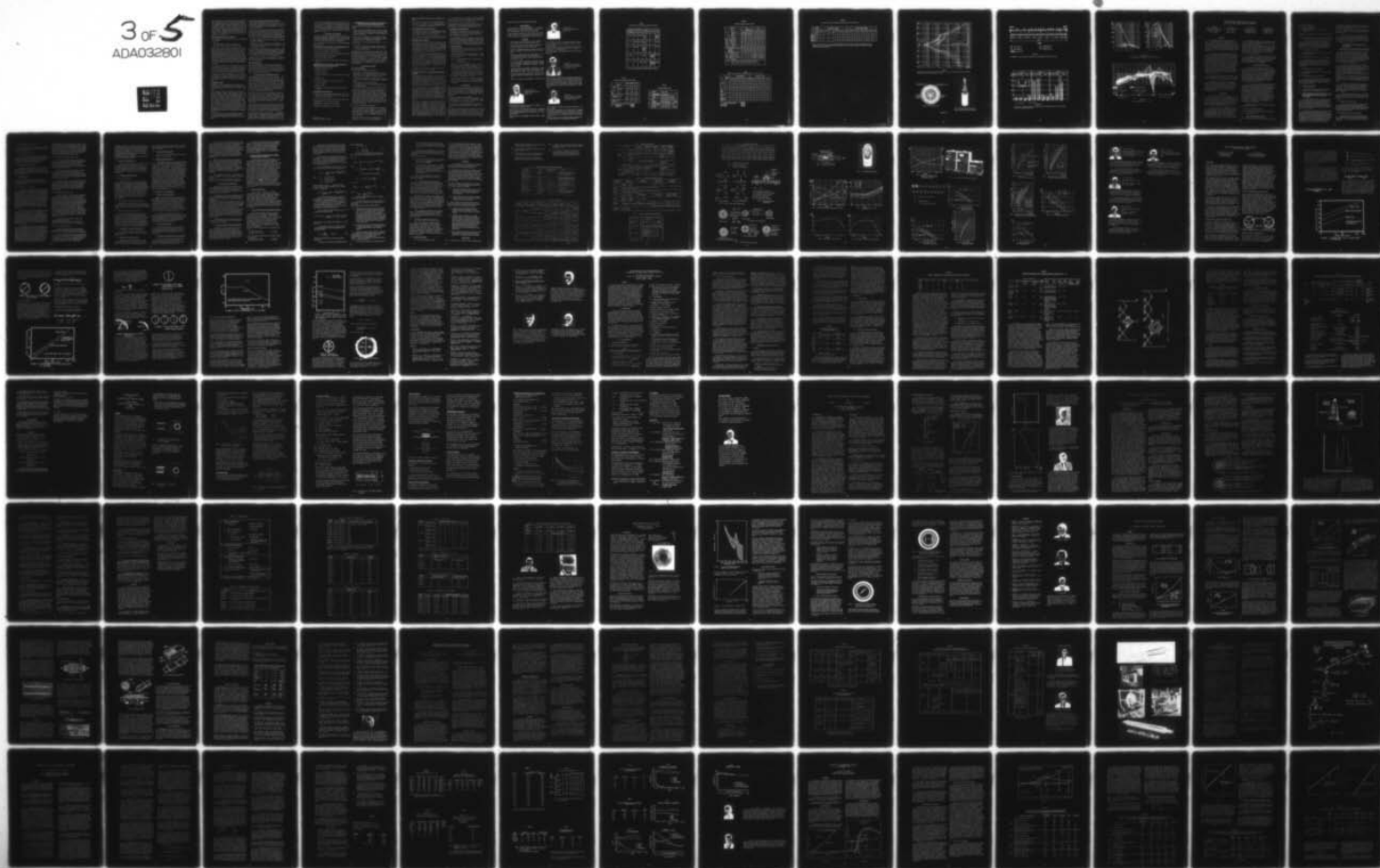
ARMY ELECTRONICS COMMAND FORT MONMOUTH N J
PROCEEDINGS OF INTERNATIONAL WIRE AND CABLE SYMPOSIUM (25TH) HE--ETC(U)
NOV 76

F/G 17/2

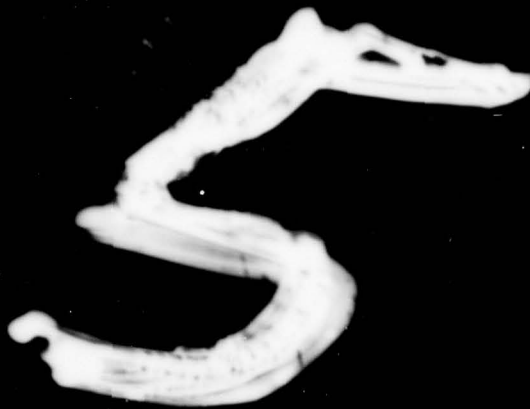
UNCLASSIFIED

NL

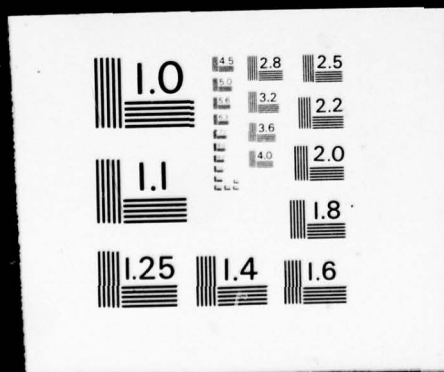
3 of 5
ADA032801



3 OF



ADA032801



mer
has
the
ed
rac
tiv
the
als
tru
van

Bas

The
is

-
-
-

A 2.
amo
rac
wou
the
whi
cul
pou
res
on
1 of

The
re
scri
tion
cati

In
ed
tive
bon
pour

Pole

Pole
this
iour
lati

Fig.
for
G5-7
tain
the
tion
of t
the
the
1.5
poun
ble
cont
slow

The
of t
in p
trod

meric compounds are largely employed; little attention has been devoted so far to PVC. For this experiment, the investigations were initially directed to PVC based compounds, since different formulations having characteristics similar to normal PVC compounds are relatively easy to obtain. Also the economical aspect of the relatively simple compounding technology possible also with small equipment, and the possibility of extruding with standard PVC extruders are additional advantages to be considered.

Basic characteristics of the compound

The formulation of the compound used for the experiment is as follows:

- 50% PVC
- 26% plasticizers, fillers and stabilizers
- 24% finely dispersed conductive carbon black

A 24% level of carbon black is considered the optimum amount as regards both compounding and electrical characteristics. As a matter of fact, smaller amounts would cause the volume resistivity to rapidly exceed the maximum admissible values (approx $10^6 \text{ ohm} \cdot \text{cm}$), whilst larger amounts would involve compounding difficulties. The value of volume resistivity in this compound allows the metallic sheath to reach a transverse resistance of approximately the same value as obtained on the jute protected cable laid in a trench (approx $1 \text{ ohm} \cdot \text{km}$).

The choice was directed to a compound that could ensure characteristics as similar as possible to those prescribed by the Specification in force (SIP Specifications 1035 and similar, for instance, German Specification VDE 0209 and English Specification BS-6745).

In Table 2 some typical characteristics of the selected compound (A) are given in comparison with a conductive compound of different formulation and higher carbon black content (B) and a traditional insulating compound (C).

Polarization tests⁴

Polarisation tests were preliminarily carried out on this compound to investigate its electrochemical behaviour in the presence of corrosion due to current circulation.

Fig. 1 shows the anodic and cathodic curves obtained for this compound through a potentiostatic method (ASTM G5-71) in aerated and non aerated water solutions containing the ions that are most frequently present in the soil. The curves obtained for the different solutions have a similar shape. A notable characteristic of the compound is the high potential needed to allow the circulation of very weak current densities, with the consequence there is a wide potential range (above 1.5 V), around the equilibrium value at which the compound is in a state of possible passivation: the possible degradation of carbon inside the compound, but in contact with the electrolyte, takes place at extremely slow rates.

The problem concerning the electrochemical behaviour of this compound is very complex. A further study is in progress to investigate the reactions at the electrode.

Manufacture of compound and conductive covering

The manufacturing technology is rather simple, but the mixing times are longer than usual; moreover it is necessary to eliminate the risk of atmospheric pollution by the carbon black.

The PVC conductive covering was applied by a conventional extruder, as currently used for microcoaxial cables. Extrusion conditions are practically the same as for normal compounds which is one aim of our investigation. The risk of other insulating compounds being contaminated by the conductive compound can be easily avoided by:

- ensuring a separate flow path for conductive compound and normal compound.
- carrying out careful cleaning of the machine by extruding normal PVC at the end of the conductive compound extrusion stage.

Normal acceptance tests carried out on samples of covering taken from the cable were satisfactory both longitudinally and transversally (tensile strength and elongation at break before and after ageing, hot deformation, cold flexibility, impact tests and flammability).

A specification for tests on finished cable is being finalized on the basis of the tests indicated in Table 5 and 6 described later.

Choice of the cable

The cable employed in the experimental installation, that will be described, is a type commonly used in the Italian trunk network, namely, a 12 pair 0.7/2.9 mm coaxial cable with 0.6 mm PE insulated service quads anti monial lead alloy sheath specifically provided with an outer conductive covering (Fig. 2)

3. Description of the experimental link

The experimental microcoaxial cable is the final part of the Milano-Mortara link and connects Vigevano and Mortara exchanges. The total length of the experimental link is 13 km, 3 km of which in the terminal local areas are in duct; the remaining portion is laid in a trench along the main road at a 0.7 m depth inside a concrete trough. Another trunk cable, lead and PVC sheathed, and in some sections a lead sheathed local cable with steel tape and jute protected armour are installed as well in the same trough along the entire route.

The cable installation is running parallel to the Mortara-Vigevano D.C. railway at a maximum distance of 1 km and crosses the railway near Vigevano. The railway electricity substation is located in Mortara. Moreover there are crossings with a gas and an oil pipeline, whose structures are cathodically protected by two unidirectional drains.

In the local area of Mortara and Vigevano the ducts (concrete and partly PVC) which accommodate the coaxial cable contain many other lead sheathed local telephone cables. The cables when nearing the Mortara exchange have cathodic protection provided by two unidirectional drains.

To ensure a full control of the cable protection, the lead sheath, running continuously from one terminal to the other, is connected to the earthing network of the terminal exchange of Vigevano and Mortara. Due to the conductivity of the covering, the lead has not been pro

vided with any intermediate earth connections. The housing of the four PCM repeaters (8 Mbit/s PCM systems, to be increased in the near future to 34 Mbit/s) situated between Mortara and Vigevano are earthed independently of the cable sheath merely with the purpose of ensuring a control of the conductive covering. The cable is pressurized at 0.7 bar.

4. Choice of the controls

In order to evaluate the behaviour of the conductive covering, both field and laboratory tests were carried out at various intervals, scheduled so that possible variations during the cable life could be identified.

For this purpose the following main characteristics have been evaluated:

Characteristics to be evaluated on the installed cable

- a) DC specific transverse resistance (*)
- b) AC specific transverse resistance (*)
- c) specific transverse resistance at lightning current
- d) impedance/frequency characteristic
- e) lightning current dispersion
- f) electrical influence of stray currents and geological cells

Characteristics to be evaluated in the laboratory on samples taken from the installed cable

- Chemical and physical tests
 - g) specific weight
 - h) water absorption
 - i) plasticizer amount in the outer layer of the covering
- Mechanical tests
 - l) tensile strength and elongation at break
 - m) cold flexibility
- Electrical tests
 - n) surface and volume resistivity before and after bending

Environmental characteristics

- o) analyses of soil samples taken from along the cable route and of water samples taken from particular points of the cable route.

The above test were scheduled as follows (see table 3):

- measurements on original cable samples
- measurements 6 months after installation
- subsequent measurements every 12 months.

(*) per unit length of cable

5. Arrangement of the test devices for carrying out field measurements and taking the samples

The test device were arranged as illustrated in fig. 3 namely:

- installation of measurement points in the most significant sites along the cable route, where other structures or particular environmental and installation conditions are present;
- installation of insulating joints, normally shunted at the cable ends (exchanges or repeaters) and when changing the type of laying (duct-trench);
- identification of three particular points (F, H, K) as follows:

H = buried in trench with low stray current density
F = buried in trench with high stray current density
K = in duct (In Mortara).

Cable lengths of 50 and 100 m were sectionalized with insulating joints, normally shunted, in order to check the behaviour of the installed cable in comparison with the cable samples: two 20 m cable lengths laid at positions corresponding to H - F - K. One of these samples is constantly connected to the cable so as to simulate the actual conditions. Laboratory tests were carried out on cable sections subsequently taken from the six cable samples.

6. Measurements results

6.1 Field measurements

- a) D.C. specific transversal resistance

The results of the measurements carried out on field cable samples and on cable lengths of 100 m maximum arranged near such samples, are given in fig. 4.

For a better interpretation of the results obtained it has to be noted that the voltage/current characteristic

- is dependent on the applied voltage
- has a tendency to form a linear curve versus voltages higher than 5 V
- is partly dependent on the voltage variation rate.

From the analysis of the results, the resistivity of the conductive covering of the buried cable, shows steady values between 200-400 $\Omega \cdot m$, independent of the stray currents density, whereas values ranging between 500 and 2000 $\Omega \cdot m$ are found for the covering of the cable in duct. The higher value found for the covering in duct may be due to the fact that in this case the cable is in contact with the surrounding only along a narrow longitudinal surface of the conductive covering.

- b) A.C. specific transversal resistance

The A.C. measurements were carried out simultaneously with the D.C. ones at a frequency of 75 Hz according to the method normally adopted for evaluating the earth resistance. The A.C. results, also given in fig. 4, appear to be in good agreement with those obtained with D.C.

The method used for the A.C. measurements is to be preferred as it is easier and more reliable.

c) Specific transversal resistance to lightning currents

The correlation between voltage and pulse current measured on two samples of buried cable was found to be linear. The specific transverse resistance showed an approximate value of 300 ohm · m.

d) Impedance-frequency characteristics

The impedance was measured on some samples of buried cable by means of special equipment ensuring a frequency range between 50 Hz and 1.6 MHz.

The correlation between impedance and frequency is linear, the specific resistance being approx 200 ohm · m

e) Lightning current leakage

The condition of a direct strike was simulated on the cable lead sheath by means of a lightning surge generator. In this situation the shape of the longitudinal current wave along the sheath and the corresponding transversal voltage to earth were measured from the current entry to one cable-end, the situation being symmetrical at the other cable-end.

The results of these measurements are given in fig. 5. It can be observed that the lightning current is subjected to distortion and to considerable attenuation all along the cable: at 500 m distance from the source, the current is reduced by 20 times and the voltage to earth by 200 times. This result is due to the fact that the cable protected by the conductive covering is buried in ground having a resistivity of approx 150 - 200 ohm · m.

Different values of ground resistivity would cause the results to be somewhat changed.

f) Electrical influence of stray currents and geological cells.

The potential to earth (referred to the Cu/CuSO₄ non polarizable electrode) and the longitudinal current of the lead sheath are examined. Since the cable is mainly affected by the electric field of the Vigeva no-Mortara D.C. railway, its electrical behaviour may rapidly change during 24 hours as a function of the stray current intensity and the different siting.

Fig. 6 shows the results of the measurements carried out in two different periods as scheduled in Table 3. The maximum scatter of the results obtained for both potential and current at each measurement point has been indicated. The results obtained from the two test cycles are very similar thus proving that practically no variation has occurred in the electric field or the conductive covering during a period of one year.

The analysis of the electrical conditions shows that the conductive covering is nearly always and everywhere at such potentials as to reveal a passivation of the carbon contained in the compound. The severest condition is observed in F position; the electrical situation of the cable samples has also been evaluated and five of them, i.e. the total number except for the sample connected to the main cable at F, show an electrochemical behaviour which is similar to that of main cable whereas sample 6 (in F position)

is in a worse situation as indicated by the measurements; an entry current of approx 17 μ A/cm² has been measured at some intervals during a 24 hours period.

The importance of the laboratory test results is to be emphasized for this particular cable sample for which the electrical situation was particularly severe.

g) Environmental characteristics

The results of the analysis of the water taken from three manholes (one near K position) and from the soil adjacent to the four buried cable samples in F and H are reported in Table 4.

The soil composition in the different route positions is sufficiently uniform and comparable to the average values of the soil generally present in Italy; the soil resistivity, on the contrary, is very low thus involving the risk of possible environmental attacks.

6.2. Laboratory tests

Laboratory tests have been carried out on samples taken from the cable field sample after 6 and 18 months after laying.

The measurements carried out are described under paragraph 4 (items g to n) and reported in Table 5 and 6, namely:

Table 5: Physical-chemical (g-h-i) and mechanical (l-m) tests

Table 6: Electrical tests (n)

The results of the measurements carried out on the cable samples after 18 months' operation do not differ from the original ones, thus showing that no significant decay has occurred in the sheath.

In particular no significant indication of decay or surface alteration was observed even on the samples taken from F position which were subjected to the severest electrochemical stresses.

New results are expected to be obtained from the future experience that will be directed to systematic tests on samples taken from the field cable every 12 months.

7. Conclusion

Final conclusions cannot be drawn from the present experience but the results are so encouraging that we may expect that on one hand the experimental investigations will be further extended and on the other hand the first actual application of the conductive covering will be achieved.

The following program is under study:

- to extend the use of PVC conductive coverings, as an outer protection on the armour, to trunk cable lengths of the order of 50 to 100 km per year.
- To install other experimental lead sheathed cables with outer conductive PVC covering in links of 10 to 20 km.

This more extensive experimental program will facilitate the gathering of new results to be added to the ones that are still being provided by the first trial link. Both technical and economical aspects of the industrial production could be optimized in view of the expected

wider utilization of this conductive compound.

Acknowledgments

The authors wish to thank the management of Industrie Pirelli and S.I.P. for the opportunity to perform this work and permission to publish the present Paper.

A very important contribution to this work was provided by SINTI - Milan in the installation of the trial link and by CSELT - Turin in carrying out the field tests.

References

1. CCITT Booklet on the jointing of plastic-sheathed cables. Editing group of study group VI 1975.
2. CCITT Libellés des nouvelles questions proposées à l'étude. Document AP VI No 72 Juillet 1976.
3. Electrical conduction mechanism in carbon filled polymers. E.O. Forster - Transaction Paper No 70 TP552 PWR.
Electrical characteristics and requirements of extruded semiconducting shields in power cables. G. Bahder and F.G. Garcia - IEEE Transaction Paper No 70 TP 553 - PWR
A review of resistive compounds for primary URD cables. R.C. Mildner - IEEE Special Technical Conference on Underground Distribution: Conference Record New York 1969.
Corrosion studies on shielding materials for underground telephone cables. Part 1. Development of test methodology. T.S. Choo - Cherry Hill Symposium 1975
4. Atlas of electrochemical equilibria in aqueous solutions. M. Pourbaix - Pergamon press 1966 pag. 449-457.
Leçon en corrosion electrochimique. - Cebeclor 1975



M. Barbaro Forleo
Industrie Pirelli S.p.A.
Milan, Italy

Born in 1941. He received his degree in Chemistry at the University of Pavia in 1966.

In 1967 he joined the Research Laboratories of Industrie Pirelli S.p.A. where he has been involved in research into insulating materials for magnet wires and cables applications.

Since 1975 he has been Manager of Special Cables laboratory.



P. Calzolari
Industrie Pirelli S.p.A.
Milan, Italy

Born in Bologna in 1931, he graduated from the University of Bologna with a B.S. degree in Electrical Engineering in 1955.
He joined Industrie Pirelli in 1956 and he has been associated with the manufacture and then the design of telephone cables since that time.
He is now manager of the Telecommunication Cable Design Department.



G. Cosimi
S.I.P. - Società Italiana
per l'Esercizio Telefonico
p.A., Rome - Italy

Born in Turin in 1938, Electrical Engineering graduate, he joined CSELT (Institute for Telecommunication research Turin) in 1965 interested in local network design problems. Since 1970 he has worked in SIP (Italian Telephone Operating Company) engaged in planning development and installation of trunk cables and associated equipments.



E. Fucini
S.I.P. - Società Italiana
per l'Esercizio Telefonico
p.A., Rome - Italy

Born in 1936. He received his Chemical engineering degree in 1962.

Since 1963 he has worked in SIP (Turin) Italian telephone Operating Company where he is involved in research arising from the use of the trunk network cables and he is a specialist in the cathodic protection of telephone routes.

He is now manager of the Electrochemical Laboratory for the study and inquiry into materials behaviour.

TABLE No 1

Protection efficiency of different types of sheath used in trunk cables.

No	Degree of protection against			Type of sheath	Type of covering	Armour Protection	Earth connection
	Electrochemical corrosion	lightning	induction				
1	Inadequate	Adequate	Inadequate	Plain lead alloy she	—	—	Not necessary for cable protection
2	Good	Inadequate	Inadequate	Lead alloy	PE	—	Necessary
3	Good	Adequate	Good	Al (purity greater than 99,9%)	PE	—	Necessary
4	Very good	Good	Good	As above	PE	Steel tape armour and outer treated jute covering	Necessary
5	Good	Good	Very good	As above	PE	Steel tape armour and outer treated jute covering.	Not necessary

** The use of plain lead alloy sheath with or without armoring is now unusual.

TABLE No 2

Comparison between normal compounds and conductive compounds

PVC COMPOUND			Conductive A	Conductive B	Normal C
Compound sheet	Density (g/cm ³)		1,32	1,39	1,43
	Original	TB kg/cm ²	1,450	1,410	1,650
		SB %	238	77	311
		T ₆ °C	-17,0	-10,0	-10,8
		T ₇ °C	-29,2	-31,3	-15,2
	After ageing 5 days at 100°C	TB kg/cm ²	1,420	1,110	1,660
		SB %	211	50	251
		T ₆ °C	-16,2	-6,8	-7,6
		T ₇ °C	-28,3	-10,2	-13,2
Cable	Volume resistivity	ohm cm	1360	1100	1,1x10 ¹¹

TB and SB: tensile strength and elongation at break (ASTM D638)
 T₆: brittleness (ASTM D746)
 T₇: cold flexibility (ASTM D1043)
 Rv: volume resistivity (ASTM D257)

TABLE No 3

Schedule of operations on cable

1973	MAY/JULY	Cable laying
	OCTOBER/DECEMBER	Cable splicing
1974	FEBRUARY	Repeater housing installation
	APRIL	Cable samples (20 m each) laying
	NOVEMBER	Cable samples taken - 1st phase
1975	NOVEMBER/DECEMBER	Field measurements - 2nd phase
	NOVEMBER	Cable samples taken - 2nd phase

TABLE No 4

Chemical and physical analysis of ground

Material			Water			Ground			
Position			K	manhole		P(1)	P(2)	H(1)	H(2)
				A	B				
WATER OR WATER EXTRACT	Chemical characteristics (mg/l)	Ammonia	<0,05	<0,05	<0,05	1,6	0,4	1,8	1,7
		Nitrite	<0,05	<0,05	<0,05	1	0,3	2,3	0,5
		Nitrate	2,6	2,3	0,4	0,4	0,05	0,8	0,05
		Chloride	16,8	24,8	78	18,1	13,3	10,6	13,3
		Sulphate	92	92	14	13	15	21	17
		Sulphite	<1	<1	<1	<1	<1	<1	<1
		Alkalinity	273	185	113	23	20	70	44
	Physical-chemical characteristics	Specific gravity g/cm ³	1,002	1,002	1,002	1,002	1,001	1,001	1,001
		pH	6,80	6,90	7,06	7,26	7,61	7,58	7,21
		Resistivity ohm m	15	20	24	52	80	39	15
GROUND	Characteristics %	Water content	-	-	-	27,43	24,17	15,01	13,91
		Max water content	-	-	-	44,32	31,34	43,48	33,10
		Carbonate	-	-	-	0	0	0	0

NOTE: 1) sample taken near cable sample connected to main cable
2) sample taken near cable sample non connected to main cable

TABLE No5

Mechanical, physical and chemical tests on conductive covering after 6 and 18 months service

TESTS	Values of the original samples	SAMPLES AFTER 6 MONTHS						SAMPLES AFTER 18 MONTHS					
		Connected to main cable			Not connected to main cable			Connected to main cable			Not connected to main cable		
		R	P	K	R	P	K	R	P	K	R	P	K
TS kg/mm ²	1,310	1,300	1,290	1,310	1,310	1,290	1,310	1,320	1,310	1,330	1,330	1,310	1,290
EB %	168	161	171	173	168	157	152	204	184	206	184	188	207
TF °C	-27,7	-27,5	-27,3	-26,3	-26,7	-27,6	-27,8	-26,6	-27,7	-27,1	-25,2	-27,3	-26,9
Specific gravity g/cm ³	1,301	1,319	1,307	1,318	1,315	1,291	1,315	1,290	1,290	1,292	1,268	1,307	1,288
Water permeability mg/cm ²	2,49	2,200	2,570	2,980	2,500	2,830	2,900	2,372	3,300	3,795	2,620	2,850	2,810
Extractable substances (plast.) %	26,4	26,1	26,3	25,0	25,8	26,2	25,8	25,6	26,3	25,9	25,0	25,8	25,8

TS and EB: tensile strength and elongation at break (ASTM D538)
TF : cold flexibility temperature (ASTM D1043)
Specific gravity (ASTM D792)
Water permeability (ASTM D570)
Plastic content (ASTM D2124)

TABLE No 6

Electrical tests on the conductive covering after 6 and 18 service months

Measurements	Values of the original sample	SAMPLES AFTER 6 MONTHS						SAMPLES AFTER 18 MONTHS					
		Connected to main cable			Not connected to main cable			Connected to main cable			Not connected to main cable		
		H	P	K	H	P	K	H	P	K	H	P	K
surface resistivity ($\Omega \cdot \text{cm}$)	665	695	-	-	367	305	450	162	5400	800	110	210	520
volume resistivity ($\Omega \cdot \text{cm}$)	1360	1700	-	-	1360	2050	1550	2900	6800	13600	1870	4600	5100

The tests have been carried out according to ASTM D257 method, except for the test voltage (12 V instead of 500 V DC). Comparable results have been obtained from the same tests carried out after bending the sample on a mandrel with diameter 15 times the cable outer diameter.

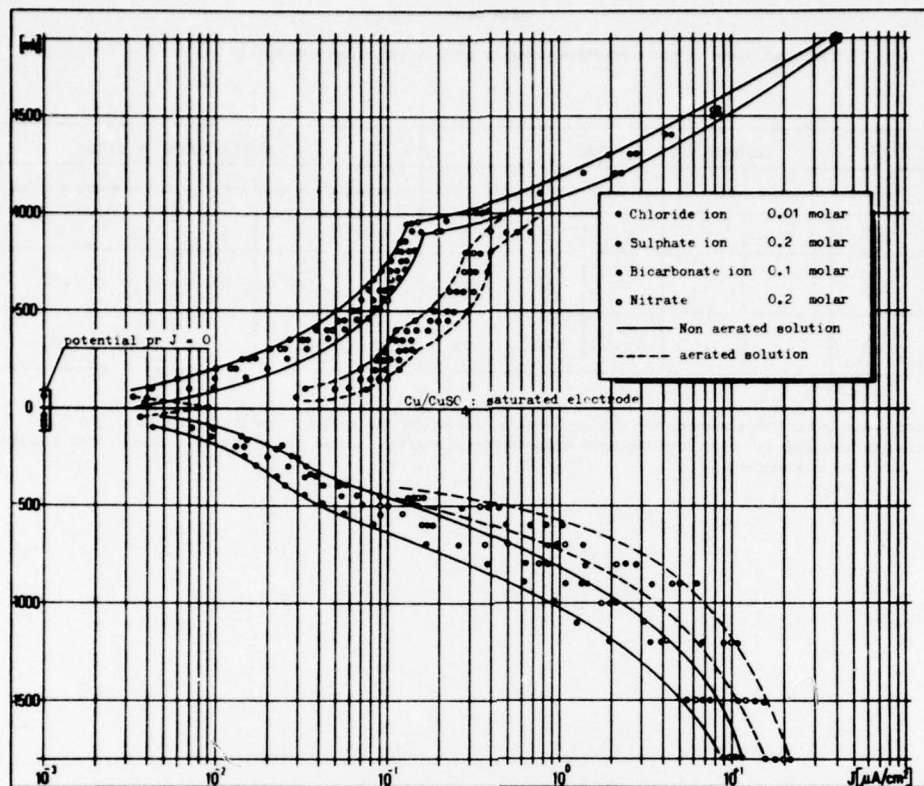
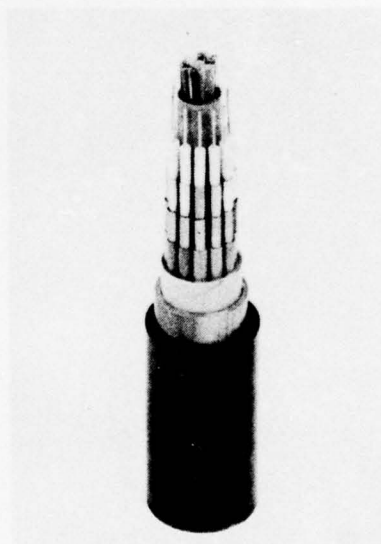
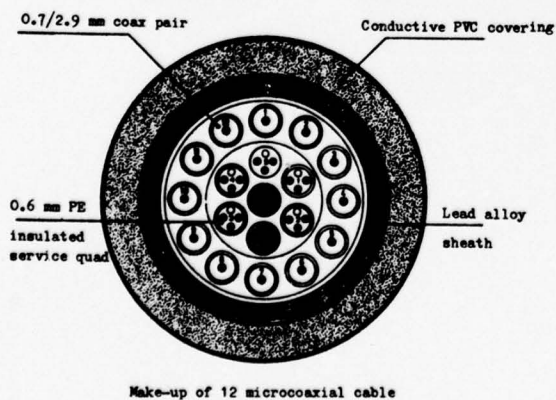


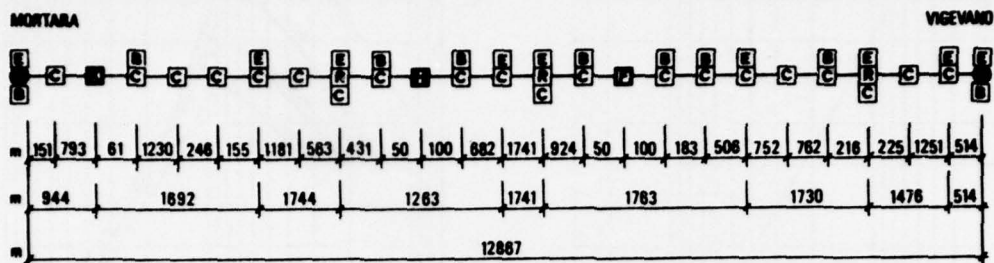
FIGURE No 1

Anodic and cathodic curves obtained for conductive compound in aerated and non aerated water solution containing the ions that are most frequently present in the soil.



12 microcoaxial cable, lead alloy sheath and conductive PVC covering

FIGURE No 2



LEGEND

- INSULATING JOINT
- EARTH CONNECTION
- CABLE SAMPLES
- MEASUREMENT POINT
- REPEATER POSITION

FIGURE No 3

Arrangement of the test devices for carrying out field measurements and taking the samples

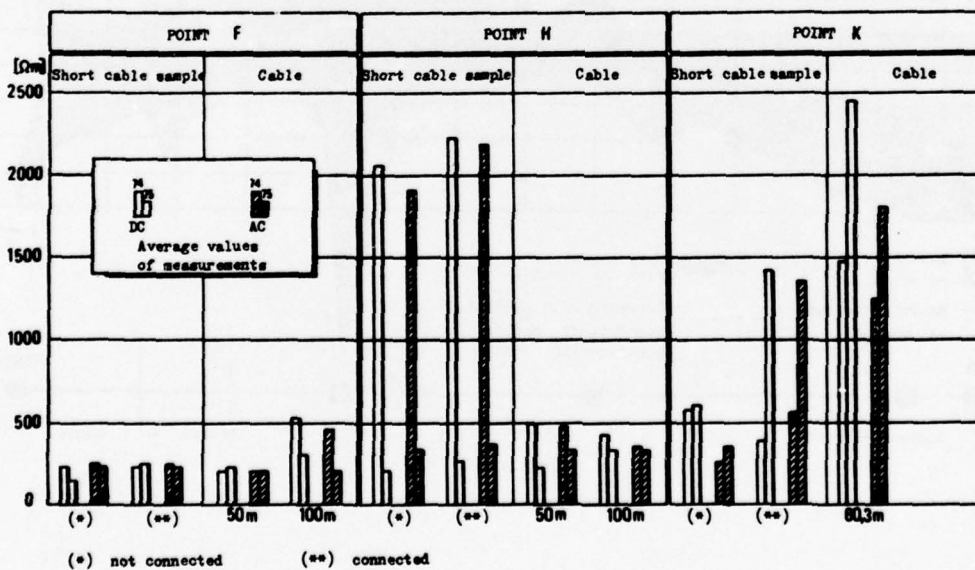
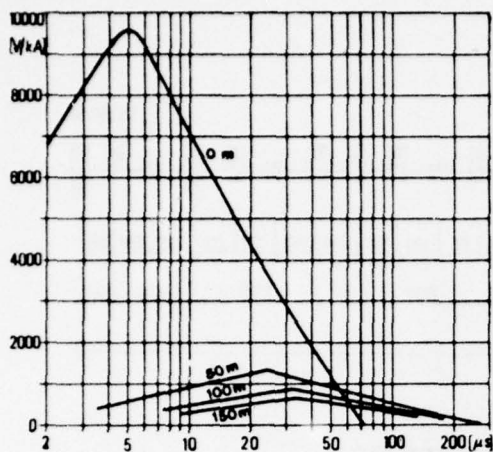
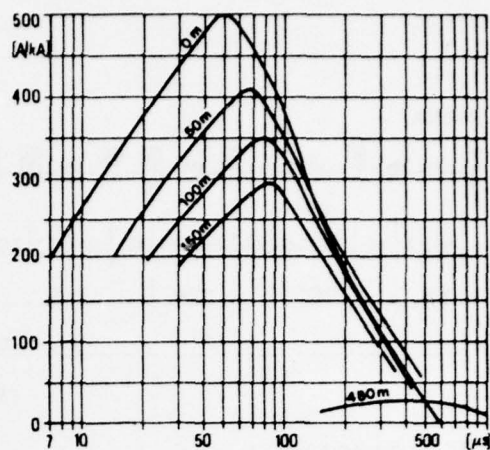


FIGURE No 4

Average values for specific transverse resistance of the short cable sample and of the cable, measured in D.C. or A.C. during 1974 and 1975.



A) Voltage between lead sheath and earth



B) Current in the lead sheath

FIGURE No 5
The propagation of lighting voltages and currents over
the lead sheath versus the distances from the direct strike point

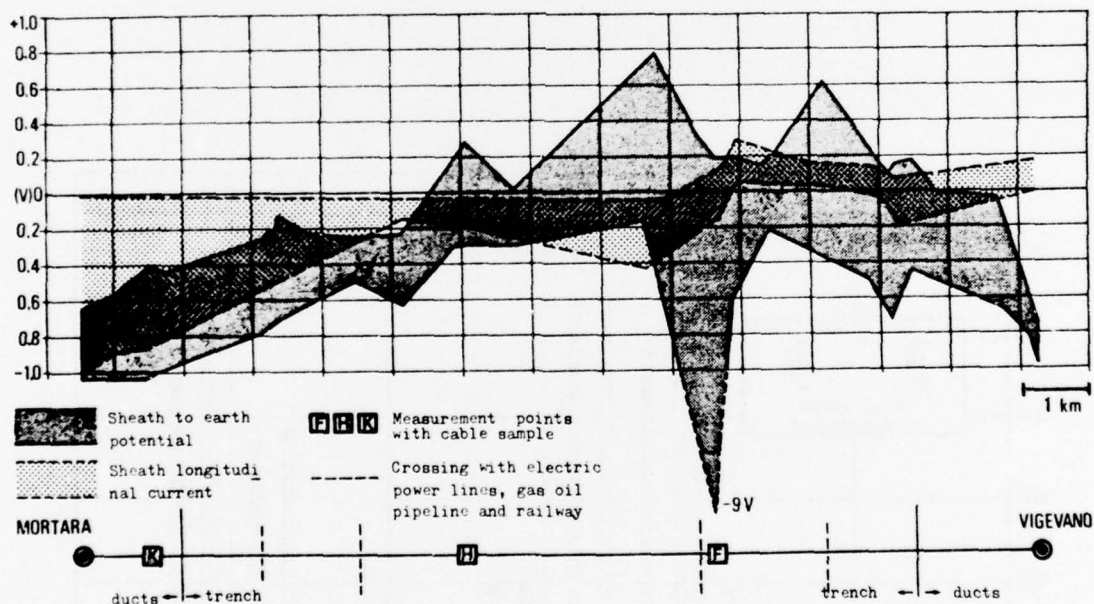


FIGURE No 6
Electrical situation of the cable

VARIOUS KINDS OF NEW PAIR TYPE CABLES FOR LOCAL BROADBAND NETWORK SYSTEMS

K. Oshima
Nippon Telegraph and
Telephone Public Corp.
Tokyo, Japan

J. Niwa
The Furukawa Electric
Co., Ltd.
Tokyo, Japan

S. Hiramatsu
Sumitomo Electric
Industries, Ltd.
Yokohama, Japan

T. Maruoka
The Fujikura Cable
Works, Ltd.
Tokyo, Japan

Summary

This paper describes local broadband networks, various kinds of new broadband pair type cables, their electrical and mechanical characteristics and cable commercial test measurement results. It is concluded that a direct distribution system using baseband transmission system with broadband pair type cables is a desirable broadband network for the near future.

The largest size broadband pair type cable which can be installed in NTT's standard conduits contains 320 pairs. Each conductor is insulated by 0.45 mm thick foamed polyethylene (50 % blowing degree) and conductor diameter is 0.65 mm. Unit shielded cable structure is adopted so as to reduce near-end crosstalk. Every pair in a unit is twisted at a different pitch to decrease far-end crosstalk. Cable loss at 4 MHz is 20 dB/km. Furthermore, various new types of cables, such as broadband termination cable, broadband gas pressure plug cable and pair-shielded stub cable (for ITV repeater use) have also been developed and have attained superior performance.

NTT has conducted commercial tests, using these broadband pair type cables, since the end of 1975, for adoption in the new ITV Service in Tokyo.

In addition, measurements of lengthwise additive features for high frequency crosstalk in a long haul route show that average crosstalk value in power, increases with the power sum rule and crosstalk distribution functions conform with the log-normal distribution or the two-dimensional normal distribution.

1. Introduction

In Japan, the demand for broadband communication services, such as video-telephone, ITV (Industrial Television) and super high speed data and facsimile telecommunication, has increased year by year. According to long-range estimates, the number of video-telephone subscribers will amount to about 300,000 within the next 15 years.

In using existing local telephone networks for those new services, various new problems arise regarding high frequency transmission characteristics of conventional local telephone cables and network constitution. Thus, essentially new approaches were taken into account with regards to local network and, recently, new pair type cables

for local broadband communication networks, which excel in economy and transmission characteristics, were successfully developed. After several field tests conducted since 1970, NTT has succeeded in improving electrical characteristics of these cables and developing new broadband pair type cables for commercial use. Since the end of 1975, ITV service commercial tests using these cables have been conducted.

This paper describes the constitution of local broadband networks, various kinds of new broadband pair type cables, a summary of commercial tests using these cables and the lengthwise additive features of FXT (far-end crosstalk).

2. Local Broadband Networks

The demand for broadband communication services, that is, video-telephone, ITV and super-high speed data and facsimile telecommunication has increased year by year. These services will effect a great change in transmission, exchange and local distribution systems. Many types of local distribution networks are considered according to the quantity and quality of requested services, their demand distributions and climatical and social circumstances where they occur.

It is necessary to establish local distribution networks to satisfy essential network properties, readiness to meet demands, good service quality and economical considerations. It may be possible to supply broadband communication services using existing telephone networks when such demand is small. However, as the demand increases, it evidently becomes difficult to use the existing telephone networks because of many restrictions, such as crosstalk, pair selection and increased number of repeaters. Therefore, it is necessary to construct local broadband networks besides the existing telephone networks.

Essential factors to study on local broadband networks are as follow:

- (1) Basic network configurations
- (2) Local distribution and transmission systems
- (3) Transmission media

2.1 Basic Network Configurations

Basic network configurations are classified as follow:

- (1) Star configuration
- (2) Branch configuration
- (3) Loop configuration
- (4) Complex combinations of the above three configurations

General view of these four configurations are shown in Fig. 1.

2.2 Local Distribution and Transmission Systems

Local distribution systems are classified into direct distribution systems and distribution systems with line concentrators. Transmission systems are classified into baseband transmission system and multiplexing transmission system.

(1) Direct Distribution System

This system connects each subscriber directly to the telephone office.

(2) Distribution System with Line Concentrators

In this system, line concentrators are installed between subscribers and the office, which concentrates several subscriber's calls into one multiplexed channel and so shares one channel among them.

(3) Baseband Transmission System

This system transmits voice or video signal without modulation.

(4) Multiplexing Transmission System

In this system, multiplexers are installed between each subscriber and the office and transmits multiplexed signals by frequency division or time division modulation.

2.3 Transmission Media

Transmission media, as shown in Table 1, can be applied in local broadband networks.

2.4 Local Broadband Distribution Network Constitution and Broadband Pair Type Cable Development

As mentioned previously, various types of network constitutions could be considered possible by combining these three constitution factors. However, considering the properties of each factor, proper combinations are limited to some extent. As a result, local distribution networks include only those listed on Table 2.

It is difficult to find the most effective local broadband distribution network among them. The applicable network for the near future, configuration S₁ in Table 2, the baseband transmission system using pair type cable, is promising from economical considerations and ease of installation and cable splicing work. It is out of the question for local broadband distribution networks, using a line

concentrating-multiplexing transmission system with optical fiber cables, etc. to be ideal if economy is to be satisfied in the future.

However, configuration S₁ is the most effective as a temporary network for interim use before reaching the future goal.

In view of the above mentioned stand points, NTT has started developmental research on new broadband pair type cables for broadband communication services since 1970. Details of these cables are reported in the following.

3. Various Kinds of New Broadband Pair Type Cables

3.1 Broadband Pair Type Cable System Constitution

The broadband transmission cable for baseband transmission of broadband signals, such as TV signals, requires a superior electrical performance as well as easy construction and maintenance work similar to that of conventional telephone cables. For this reason, it is necessary to use cables with the most suitable structure and performance in accordance with their application.

The broadband pair type cables are mainly used as junction cables between offices. The broadband pair type cable system requires good gas pressure plug airtightness and easy termination work in the cable lead-in parts to the offices. However, it has proved difficult to construct a reliable pressure plug for broadband pair type cable in the field. Results are that it is desirable to manufacture short-length cables with reliable gas pressure plug in the factory and splice them to the broadband termination cables.

Furthermore, stub cables are required to connect a manhole repeater with the broadband pair type cable. In the telephone office, broadband switchboard cables are also required, to connect main distribution frame (MDF) with intermediate station repeaters.

For the reasons described above, the broadband pair type cable system has been made up with cables having the structure and performance shown in Fig. 2.

(1) Broadband Pair Type Cable

Main broadband transmission line is made up of this cable, which contains both broadband pairs and voice pairs. The broadband pairs possess excellent electrical performance (attenuation and crosstalk characteristics).

(2) Broadband Gas Pressure Plug Cable

This cable is used as a gas pressure plug for broadband pair type cables in a telephone office cable vault. It has good airtightness and is easily installed.

(3) Broadband Termination Cable

This cable is used for terminating broadband pairs between MDF and cable vaults, and is easily installed and terminated.

(4) Pair-shielded Stub Cable

This cable is used to connect repeaters in a manhole with broadband pair type cables. Stub cable structure has superior crosstalk characteristics in the wiring in the housing and has superior air-tightness in the gas pressure plug part.

(5) Broadband Switchboard Cable

This cable is used for the office wiring of the broadband pairs between MDF and intermediate station repeaters. It has superior electrical performance (very small deviation in attenuation and crosstalk characteristics).

3.2 Cable Structure

This section describes cable structures including the development study. Structures of various cables which are in practical use are shown in Table 3 and Fig. 3.

(1) Broadband Pair Type Cable

It was most important to take many factors into consideration in determining the broadband pair type cable structure. These factors include costs of repeaters, cable installation and underground plant construction. A study was conducted to determine the most suitable cable attenuation and pair and unit structure for minimum cost broadband transmission lines. As a result, it has been found that the most suitable cable attenuation is 20 dB/km at 4 MHz. Pair structure has been adopted in which 0.45 mm thick foamed polyethylene (PEF) insulation (50 % blowing) is coated on a 0.65 mm diameter copper conductor.

Furthermore, to avoid pair selection restriction due to crosstalk, which is a weak point of existing local telephone cables, small pair unit structure has been adopted. Crosstalk among units can be avoided by wrapping a lapped double layer of thin laminated aluminum polyethylene (LAP) tape (0.025 to 0.030 mm thick aluminum) on each unit. Transmissions in the same unit are performed only in the same direction, so that restrictions due to NEXT can be avoided.

The number of pairs in the unit determines the maximum number of pairs accommodated in the cable and the FXT in the unit. From economical efficiency considerations, it is desirable to accommodate as many pairs as possible in a fixed diameter cable, too many pairs in one unit could yield an adverse FXT combination. For these reasons, the number of pairs in one unit is fixed at 20 pairs. Moreover, in order to reduce the FXT in one unit, twisting pitches in all pairs are different. As the result of these studies it has been possible to

transmit 4 MHz signals without pair selection. The pair number in the unit is identified by the tracer pair and the unit number is identified by the color of tape wrapped around the unit. In addition to the broadband pair, there are also as many or more voice pairs as there are broadband pairs for power-feeding, talking and manhole repeater supervision. (Fig. 4 is a picture of the broadband pair type cable)

(2) Broadband Gas Pressure Plug Cable

Since the broadband gas pressure plug part is larger in diameter than an ordinary cable part and cannot be passed through conduits, this cable is carried directly to the cable vault. Moreover, considering easy installation work, the length of this cable has been fixed at 7.5 m.

Solid PE insulation is adopted for complete air-tightness of the gas pressure plug part. Conductor diameter is 0.5 mm to maintain the same impedance as the broadband pair type cable. Transmission loss does not cause a major problem because the cable length is short.

The cable structure is the same as that of the broadband pair type cable, except for the insulation. The gas pressure plug part is filled with compound, as shown in Fig. 5, after peeling the cable sheath off and replacing LAP tape on the unit with porous metallic tape to prevent crosstalk characteristics deterioration.

(3) Broadband Termination Cable

Considering easy installation and terminating work and, splices between various kinds of broadband pair type cable pairs, the number of pairs is determined as 80 and 100 pairs. Conventional termination cables are used for the voice pair terminations. Solid PE insulation is adopted for the mechanical and thermal requirements in the installation and termination work, instead of PVC insulation which is inferior in electrical characteristics. Conductor diameter is 0.5 mm to keep the same impedance as the broadband pair type cable. The external diameter of the insulated conductor is almost the same as that of 0.65 mm PEF insulated conductor. Transmission loss does not cause a major problem, because cable length is very short.

Unit structure is the same as that of the broadband pair type cables. The sheath structure is fire-proof PVC sheath, because it is used in intra-office line installations.

(4) Pair-shielded Stub Cable

The stub cable consists of shielded-pairs transmitting the broadband signals and interstitial pairs used for power-feeding, supervision and talking.

In order to meet the severe crosstalk standards and prevent deterioration in crosstalk characteristics in wiring parts in the housing, shielding is applied to every pair by metallic braiding. Additional unit shielding is applied to the units by LAP tape.

Conductor diameter is 0.5 mm and PEF insulation is adopted for the cable conductor insulation, taking into account the effect of the metallic braiding on characteristic impedance. Furthermore, surface treatment is performed on the conductor insulation for easy gas pressure plug formation, resulting in good adhesiveness to compound. The sheath is the same LEPETH structure (Lead + PE) as conventional stub cables.

3.3 Electrical Characteristics

The electrical specifications of various kinds of new pair type cables are shown in Table 4. Various transmission characteristics of the broadband pair type cables are mainly described below. Various crosstalk characteristics, such as FXT lengthwise additive features are described in detail in Section 6.

3.3.1 Broadband Pair Type Cable

(1) Secondary Constants

Frequency characteristics of secondary constants are shown in Fig. 6. The characteristic impedance at high frequencies converges to about 140 ohms. The attenuation constant approximately follows \sqrt{f} characteristics at high frequencies and is about 20 dB/km at 4 MHz. This value is lower by around 30 % than the attenuation constant of 0.65 mm toll PEF cables, which have been used in NTT as toll transmission lines, owing to making the characteristic impedance higher. (The characteristic impedance of 0.65 mm toll PEF cables is about 120 ohms.)

(2) Insertion Loss Frequency Characteristics

With input and output impedances of 140 ohms, insertion loss frequency characteristic measurement results, taking line length as a parameter, are shown in Fig. 7.

(3) Near-end Crosstalk Characteristics

FXT measurement results are described in Section 6. The near end crosstalk attenuation between units is more than 115 dB/250 m at 4 MHz on the average, and its standard deviation is 4 to 5 dB. The worst value is 95 dB/250 m. However, this never causes any problem in the transmission performance. Frequency characteristics are shown in Fig. 8. Characteristics remain approximately flat up to 10 MHz, due to the shielding tape effect.

3.3.2 Broadband Gas Pressure Plug Cable

The important characteristic here is the NXT between units. Frequency characteristics are shown in Fig. 9.

3.3.3 Broadband Termination Cable

Impedance frequency characteristics and attenuation constants are shown in Fig. 10. The worst value of the far-end crosstalk attenuation in

the unit is 50 dB/200 m at 4 MHz. That of the near-end crosstalk attenuation between units is 115 dB/200 m at 4 MHz.

3.3.4 Pair-shielded Stub Cable

The worst value of NXT between units is 120 dB/8 m at 4 MHz.

3.4 Mechanical Characteristics

LAP sheath is used in the broadband pair type cables. This LAP sheath has been adopted in NTT as local CCP cable and multi-pair PEF-LAP junction cable sheath. It has superior moisture-proof and mechanical characteristics. The gas pressure plug mechanical performances of broadband gas pressure plug cable have been studied closely. To investigate the performance deterioration of the gas pressure plug part due to a change in atmospheric temperature, a heat cycle test, ranging from 70°C to -20°C, has been performed at 100 cycles, without performance deterioration. To simulate slight repeated vibration on the gas pressure plug part, ± 10 mm amplitude vibration and 600 cpm has been continuously applied. Results show that the part withstands more than 1 million vibrations. Furthermore, the part is designed to withstand a tension of 500 kg, taking into consideration abnormal tension, such as cable creeping phenomenon.

3.5 Splicing and Jointing Method

3.5.1 Splicing of Broadband Pairs

Both manual twisting and connector splicing method can be considered as pertinent broadband pair splicing methods. The advantage of the former is that the splice is small. On the other hand, its disadvantage is that the contact resistance may increase or tensile strength may decrease over a long time. For this reason, intermittent disconnections may sometimes occur because of vibration in the splicing part. This results in an increase in bit error rate or synchronization failure.

The connectors adopted here have been developed aiming at splicing work man-power saving and achieving high quality multi-pair telephone cable conductor splicing in NTT. Furthermore, extra splicing conductor length is shortened to prevent crosstalk performance deterioration.

3.5.2 Sheath Jointing Method

An auxiliary lead sleeve roller-squeezing method is used in NTT as a sheath jointing method on gas pressurized LAP sheathed cable. This method is adopted to the broadband pair type cable sheath joint.

4. Automatic Crosstalk Measuring Apparatus

It is necessary to measure the FXT, NXT, insertion loss and characteristic impedance to guarantee transmission characteristics after the installation of broadband pair type cables.

In case of far-end crosstalk attenuation within a unit, which amounts to a total of 190 combinations, much measuring time is necessary when using conventional apparatus and manual measuring method. Furthermore, the crosstalk measurement in high frequency range reduces measurement reliability and makes it difficult to get the same measurement results repeatedly on account of a very low signal level. A reliable automatic crosstalk measuring apparatus has been developed to overcome these difficulties.

Signal oscillating unit and level measuring unit of this equipment has 20 measuring channels. Each of 20 pairs in a unit can be connected to these channels through connectors. The measuring channel combination can be selected automatically. Measurement results are displayed in 7 digits and printed out on paper at the same time. A paper tape punch can be attached for data processing by computer.

This apparatus is small in size and light in weight. Therefore it can be easily used in a manhole and so on. The main features of this apparatus are shown in Table 5. Fig. 11 is a picture of the apparatus.

5. Commercial Test Summary

Based on the results of several field tests, new broadband pair type cables have become feasible due to their superior electrical and mechanical characteristics. They have been in commercial use in Tokyo since the end of 1975.

These cables are used as transmission media for Metropolitan Police Department Traffic Control System, in which a 4MHz-ITV transmission system is adopted. Broadband pair type cable line length is about 20 km out of 60 km total line length and the rest are existing local telephone cables. In this test, these broadband pair type cables are used mainly for junction cables between offices where there is heavy traffic. Through this test, technical research has been under way on installation, splicing, electrical characteristics and maintenance of these broadband pair type cables. The results of this commercial test will clarify many problems in application to local broadband networks.

The following section briefly describes the results of FXT measurement, which is especially important for these cables.

6. Far-end Crosstalk Measurement Results

Broadband pair type cables have excellent near-end crosstalk characteristics which are sufficiently good to preclude any significant factors from limiting repeater gain. Some theories have dealt with the additive far-end crosstalk features of long distance transmission lines. However, few of these theories are found to be proved by far-end crosstalk measurement results.

Therefore, measurement of such crosstalk is essential to determine the maximum transmission length. It is interesting, from a theoretical viewpoint, to observe how the crosstalk distribution function pattern and average value vary as the transmission length increases. The following sections discuss additive far-end crosstalk feature measurement results.

6.1 Distribution Function Pattern and Crosstalk Lengthwise Additive Features

Crosstalk derives from electromagnetic and electrostatic couplings in cables and repeaters. This crosstalk is most annoying in cables. Lack of uniformity in cable pairs appearing at various points, which is attributable to the production process, is considered to be a cause of such crosstalk. This is why crosstalk in cables shows a certain distribution function pattern, for instance, the log-normal distribution or the two-dimensional normal distribution. Where a transmission line extends over a long distance, the crosstalk distribution pattern, the average value and the standard deviation value have been studied from various theoretical aspects, but few reports have been published on the crosstalk measurement, itself. This report discusses the results of various experiments that have been performed, mainly to determine the additive features of FXT in broadband pair type cables on commercial test routes.

6.1.1 Measurement Routes

Fig. 12 shows an outline of crosstalk measurement routes. Capital letters in the figure represent intermediate station repeaters, while the small letters indicate repeaters installed in manholes. Measurement was conducted of all pair combinations within a unit, which amounted to a total of 190. Cable lines between telephone exchanges A, B and C were connected in due order at A and C to provide additional transmission line return sections so that the total length of line to be measured could be extended.

6.1.2 Crosstalk Distribution and Additive Features

The additive features of far-end crosstalk attenuation can be reasonably represented by the average value of such crosstalk. Fig. 13 and 14 show the lengths of transmission lines in the abscissa axis and the average value of far-end crosstalk attenuation at 4 MHz in the ordinate axis. As illustrated in these figures, the average value becomes aggravated in accordance with $-A \log L$, whose coefficient A varies depending on the combinations of crosstalks.

In case of all pair combinations of crosstalk within a unit :

Average value in dB	A = 14.46
Average value in power	A = 11.72

In case of all pair combinations of crosstalk between adjacent pairs :

Average value in dB	A = 12.22
Average value in power	A = 10.62

The average crosstalk attenuation in power varies approximately in accordance with the power sum of $-10 \log L$. This does not exactly represent the power sum rule, because some of the coupling distribution characteristics in the cable and of the coupling characteristics at the joints would deviate from the rule.

The distribution of crosstalk attenuation is discussed in the following paragraphs. As mentioned in Section 6.1, the log-normal distribution and the two-dimensional normal distribution are the two conceivable patterns of crosstalk distribution appearing in transmission lines.

Here, the probability density function of log-normal distribution can be given in the following:

$$f(x) = \frac{1}{\sqrt{2\pi}\sigma x} \exp\left\{-\frac{(\ln x - \ln x_0)^2}{2\sigma^2}\right\} \quad (1)$$

where x = crosstalk value
 σ = standard deviation
 x_0 = average value

The distribution function, formula (2) below, can be represented as a straight line on a normal probability graph paper.

$$F(x) = \int_0^x \frac{1}{\sqrt{2\pi}\sigma z} \exp\left\{-\frac{(\ln z - \ln x_0)^2}{2\sigma^2}\right\} dz \quad (2)$$

The two-dimensional normal distribution is discussed below. Considering that crosstalk is attributable to unbalanced admittance, $\dot{Y} = \xi + j\eta$, between the inducing circuit and the induced circuit, the distribution of (ξ, η) usually forms a two-dimensional normal distribution with covariance 0 and average value $(0, 0)$, according to measurement results obtained by NTT.

Thus, probability density function $p(\xi, \eta)$ is expressed in the following:

$$p(\xi, \eta) = p(\dot{Y}) = \frac{1}{2\pi\sigma_\xi\sigma_\eta} \exp\left\{-\frac{1}{2}\left(\frac{\xi^2}{\sigma_\xi^2} + \frac{\eta^2}{\sigma_\eta^2}\right)\right\} \quad (3)$$

where σ_ξ and σ_η represent the standard ξ and η deviation.

The relation between \dot{Y} and the far-end crosstalk attenuation x can be expressed in the following formula:

$$x = \ln \frac{8}{Z_0 |\dot{Y}|} \quad (\text{Neper}) \quad (4)$$

where Z_0 represents the circuit characteristic impedance.

Formular (3) can also be expressed by the

following parameter:

$$\sigma^2 = \sigma_\xi^2 + \sigma_\eta^2 \quad (5)$$

$$b = \frac{\sigma_\xi^2 - \sigma_\eta^2}{\sigma_\xi^2 + \sigma_\eta^2}$$

Formulas (6) through (8) below show distribution functions of x , where parameter $b=0$ or $b=1$.

For $b=0$

$$P_0(x) = \int_{-\infty}^x p_0(x) dx = \exp\left\{-e^{-2(x-\bar{x}_e)}\right\} \quad (6)$$

where

$$\bar{x} = \int_{-\infty}^{\infty} x p_0(x) dx = \frac{1}{2} \left(A + \ln \frac{32}{\sigma^2 Z_0^2} \right) \quad (7)$$

$A = 0.577215$ (Euler's constant)

$$x_e = \bar{x} - \frac{1}{2} A = \frac{1}{2} \ln \frac{32}{\sigma^2 Z_0^2}$$

For $b=1$

$$P_1(x) = 1 - \Phi\left\{\frac{1}{\sqrt{2}} e^{-(x-x_e)}\right\} \quad (8)$$

where

$$\Phi(t) = \frac{2}{\sqrt{\pi}} \int_0^t e^{-u^2} du$$

It should be noted that x and x_e in the above formulas are in Neper.

The distribution functions of $P_0(x)$ and $P_1(x)$ are shown in Fig. 15 with $x - x_e$ as the abscissa axis in dB.

These functions can be described as follow:

- Since $\sigma_\xi = 0$ for $P_1(x)$, there is no portion of crosstalk that is induced from the real part of \dot{Y} , it is only induced from the imaginary part. It is considered to be a crosstalk distribution as is seen where the phase of the crosstalk signal deviates by 90° or -90° from the original signal only due to electromagnetic coupling or electrostatic coupling. The phase cannot be varied at random by an amplifier or any other device.
- For $P_0(x)$, $\sigma_\xi = \sigma_\eta$, this is considered to be a crosstalk distribution as is seen where the crosstalk signal phase can be changed at random.

Based on the above-mentioned basic patterns of distribution and measurement results, the distribution patterns in a cable length or in a long transmission line are discussed below.

Fig. 16 shows two examples of crosstalk distribution in a 250 m long cable:

- all pair combinations of crosstalk within

a unit (amounting to 190 combinations per unit); and (b) the combinations of crosstalk between adjacent pairs (25 combinations per unit).

The category (a) combination can be used for cable crosstalk characteristics estimation, while category (b) can be used for that of the worst crosstalk value.

Fig. 16 also indicates:

- (a) In the case of all combinations of crosstalks within a unit, crosstalk distribution is in log-normal distribution.
- (b) In the case of all combinations of crosstalks between adjacent pairs, which have certain specific characteristics, the comparatively worse part of crosstalk distributions conforms with the two-dimensional normal distribution at $b=1$.

Fig. 17 and 18 illustrate the changes in distribution patterns in accordance with transmission line length.

Fig. 17 shows the distribution pattern variation in case of all pair combinations within a unit. Each of these curves can be considered as a rectilinear form that shows a log-normal distribution. It should be noted, however, that the inclination of these straight lines increases (i.e. their standard deviation decreases) as the transmission line becomes longer, and that the crosstalk tends to converge around a certain average value.

Meanwhile, Fig. 18 describes changes in the distribution patterns in the case of combinations of crosstalks between adjacent pairs. Curve ① in this figure, where $L=1.5$ km, represents the distribution pattern of $P_1(x)$ which is approximately the same as in the case of a cable length. On the other hand, curve ⑤, where the transmission line extends over a fairly long distance, assumes rather the distribution pattern of $P_0(x)$.

This is probably attributable to the random shift in crosstalk phase which has been caused by numerous amplifiers being inserted at various intermediate points along the transmission line, as mentioned above.

6.1.3 Crosstalk Frequency Characteristics

Table 6 describes the relation between transmission line length and crosstalk frequency characteristics, while Fig. 19 shows frequency characteristics of average values. These data indicate that the frequency characteristic remains at $20 \log f$ or 6 dB/octave, regardless of changes in transmission line length, and that the standard deviation has a tendency to become slightly larger as frequency increases.

6.1.4 Multiple Crosstalk

Fig. 20 shows multiple crosstalk

attenuation measurement results obtained from a 3.1 km long transmission line. It has been found that the average value of the multiple crosstalks in power adds up in accordance with approximate $-10 \log n$ (where n : number of systems). However, no experiment for specific evaluation purposes has so far been reported to determine the relation between additive features of multiple crosstalks at such single frequency and those at actual signals particularly of a color television. This is a problem which must be studied in the future.

7. Conclusion

This paper mainly describes the new broadband pair type cable and its commercial tests. Conclusions may be outlined as follows:

- (1) Broadband local networks can possibly assume many different forms, depending on the demand distribution and density, distribution systems, transmission systems and media, and types of services. As a type of network for the near future, however, it is desirable to adopt a direct distribution system using baseband transmission system with broadband pair type cables.
- (2) Various kinds of broadband pair type cables, required for composing broadband local networks, have been successfully developed.
 - (a) The broadband pair type cable has sufficient capability to transmit 4 MHz signals at as low attenuation as 20 dB/km without any pair selection.
 - (b) Various other kinds of broadband pair type cables have also shown excellent electrical and mechanical characteristics.
- (3) The commercial test has brought about the following achievements regarding the measurement of FXT, which are of particular importance:
 - (a) A new automatic crosstalk measuring apparatus has been developed, which is capable of providing substantial man-power savings.
 - (b) Through intensive studies on crosstalk additive features, it has been found that the average crosstalk attenuation value adds approximately in line with the power sum rule. It has been also proved that, although the distribution patterns of crosstalk vary, depending on kinds of combinations, such patterns conform with the log-normal distribution or the two-dimensional normal distribution.
 - (c) The crosstalk frequency characteristics have been proved to conform with 6 dB/octave, regardless of the transmission line length.

References

- ① J. Takizawa, K. Oshima, "Cable Connector and

Automatic Splicing Machine for Communication Cable Conductor", JTR Vol. 17-3

② H. Takashima, "A New Broad Band Pair Type Cable", JTR Vol. 14-3

③ H. Fukutomi, K. Tochigi, "Broadband Subscriber Cables and Network Constitution"

Paper proposed to the First International Symposium on Subscriber Loops and Service

④ I. Nassel, "Some Properties of Power Sums of Truncated Normal Random Variables", BSTJ, November, 1967

⑤ L. F. Fenton, "The Sum of Log-Normal Probability Distributions in Scatter Transmission Systems", IRE Transactions on Communication Systems, March, 1960

Table - 1. Various Transmission Media for Broadband Local Networks

Transmission Media	Cable Loss	Largest Size Cable in 75mm Conduit	Remarks
Conventional Local Telephone Cable (0.5mm Paper-insulated cable)	58 dB/km at 4MHz	1800 pairs	Good Space Occupancy Factor Inferior Electrical Characteristics in High Frequency Range
0.65mm Broadband Pair Type Cable	20 dB/km at 4MHz	320 pairs	For Broadband Transmission Use Excellent Electrical Characteristics in High Frequency Range
1.2/4.4 Coaxial Cable	54 dB/km at 100 MHz	80 Coaxial-pairs	For Multiplexing Transmission Use in High Frequency Range, especially now for Toll Multiplexing Transmission Line Use
2.6/9.5 Coaxial Cable	23 dB/km at 100MHz	18 Coaxial-pairs	
4.4/17 Local Coaxial Cable	27.5 dB/km at 288MHz	Single pair	Low Loss Cable for CATV Use
Optical Fiber Cable (Clad-Type Fiber)	several dB/km at 0.8 μ m optical wave length	A few hundred cores	For Optical Communication Use Two Types of Clad-Type Fiber and Convergent-Type Fiber

Table - 2. Local Distribution Network Classification

Network Configuration		Distribution System	Transmission System		Transmission Medium	Demand Distribution	Demand Density	Application Area	Service
			Feeder Line	Distribution Line					
S ₁	Star	Direct-Distribution	Baseband Transmission		Balanced pair cable	Dispersion	High Low	Large city Small city Country	Telephony Broadband service
S ₂			Multiplexing Transmission		Balanced pair cable	Concentration	Low	Small city Country	Telephony
S ₃					Coaxial cable Optical fiber	Dispersion	High	Large city business d. * shopping d.	
B	Branch	Direct-Distribution	Multiplexing Transmission		Coaxial cable	Concentration	High	Large city residential d. factory d.	Broadband service
					Optical fiber	Dispersion	High	Large city business d. shopping d.	
L	Loop	Direct-Distribution	Multiplexing Transmission		Coaxial cable Optical fiber	Dispersion	Low	Large city residential d. factory d. Small city	Broadband service
C ₁	Complex	Distribution with line concentrators (LC)	Multiplexing Transmission	Multiplexing Transmission	Coaxial cable Optical fiber	Dispersion	High	Large city residential d. factory d.	Broadband service
C ₂				Baseband Transmission	Balanced pair cable Coaxial cable Optical fibers	Concentration	Low	Small city Country	Telephony
C ₃			Baseband Transmission		Balanced pair cable	Concentration	Low	Small city Country	
						Dispersion	High	Large city	

* : district

Table - 3. Broadband Cable Structures

Items			Broadband Pair Type Cable	Broadband Gas Pressure Plug Cable	Broadband Termination Cable	Pair-Shielded Stub Cable	Broadband Switchboard Cable	
Broad-band Pair	Pair	Conductor	0.65mm Copper	0.5mm Copper	0.5mm Copper	0.5mm Copper	0.5mm Tinned Copper	
		Insulation	0.45mm PEF	0.5mm PE	0.5mm PE	0.5mm PE	0.5mm PE	
		Shielding	-	-	-	Copper Braiding	-	
	Unit	Number of Pairs	20			10	-	
		Shielding	Lap Shielding Tape (2 thicknesses)			Lap Shielding Tape (1 thickness)	-	
	Number of Pairs in Cable		260	260	80, 100	40	10	
Voice Pair	Quad	Conductor	0.5mm Copper	0.5mm Copper	-	0.5mm Copper	-	
		Insulation	0.12mm PEF	0.15mm PE		0.3mm PE		
	Number of Pairs in Unit		100	100		6 and 8		
	Number of Pairs in Cable		300	300		26		
Sheath			LAP	LAP	PVC	LEPETH	PVC	

Table - 4. Broadband Cable Electrical Characteristics

Electrical Characteristics	Broadband Pair Type Cable		Broadband Termination Cable	Broadband Gas Pressure Plug Cable	Pair-Shielded Stub Cable	
Conductor	Nominal Maximum	52.5 Ω /km 56.5 Ω /km	Maximum 93.5 Ω /km			
Insulation Resistance	More than 10 kM Ω -km after 1 minute charge of 100 to 500 volts in direct current between each conductor and ground					
Dielectric Strength	No breakdown after 1 minute charge of 500 volts in direct current or 350 volts in alternate current between each conductor and ground					
Capacitance	Nominal Maximum	33 nF/km 35 nF/km	Average Less than 40 nF/km	Average Less than 500 pF/7.5m	Maximum 41 nF/km Minimum 25 nF/km	
Attenuation at 4MHz	Nominal Maximum Minimum	20 dB/km 22 dB/km 18.5 dB/km	Less than 30 dB/km	-	-	
Crosstalk Attenuation at 4MHz	FXT Average Worst	More than 61 dB/250m More than 41 dB/250m	FXT Average Worst	More than 62 dB/250m More than 42 dB/250m	FXT Worst NXT Worst	More than 45 dB/7.5m More than 64 dB/5.5m More than 90 dB/7.5m More than 104 dB/5.5m
Characteristic Impedance	138 Ω at 4MHz 140 Ω at 1MHz		-	-	-	

Table - 5. Automatic Crosstalk Measuring Apparatus Features

Frequency Range	4 MHz (1 KHz to 30 MHz in use of optional attachment)
Measuring Level at 4MHz	FXT and Cable Loss : 0 to -80 dBm NXT : 0 to -120 dBm
Measuring Speed	About 7 minutes for 190 combinations (FXT) About 14 minutes for 400 combinations (NXT)
Size and Weight	Oscillating Unit 282 x 445 x 285 mm, less than 23 kg Level Measuring Unit 282 x 445 x 285 mm, less than 25 kg Control Unit 282 x 245 x 285 mm, less than 16 kg
Measuring Channel	20

Table - 6. Lengthwise FXT Additive Features.

Frequency	Measured line length								
	6.1 Km			12.3 Km			34.1 Km		
	me	m	σ	me	m	σ	me	m	σ
200 KHz	75.6 dB	80.0 dB	6.27 dB	69.7 dB	75.4 dB	6.04 dB	64.2 dB	68.3 dB	6.04 dB
500	67.9	73.7	7.63	63.8	68.9	6.96	56.1	62.0	7.27
1000	61.8	67.7	7.71	57.7	62.5	6.99	52.2	56.5	6.88
4000	46.8	52.8	7.55	43.5	48.7	6.88	39.3	43.1	6.42

me : Average power FXT attenuation value
m : Average FXT attenuation value
σ : FXT attenuation standard deviation

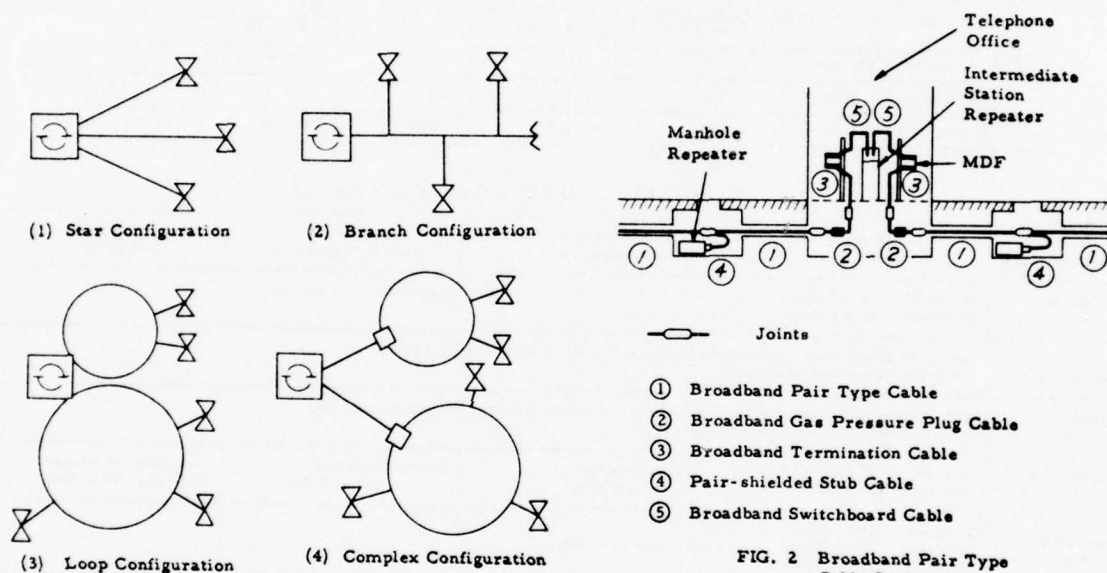
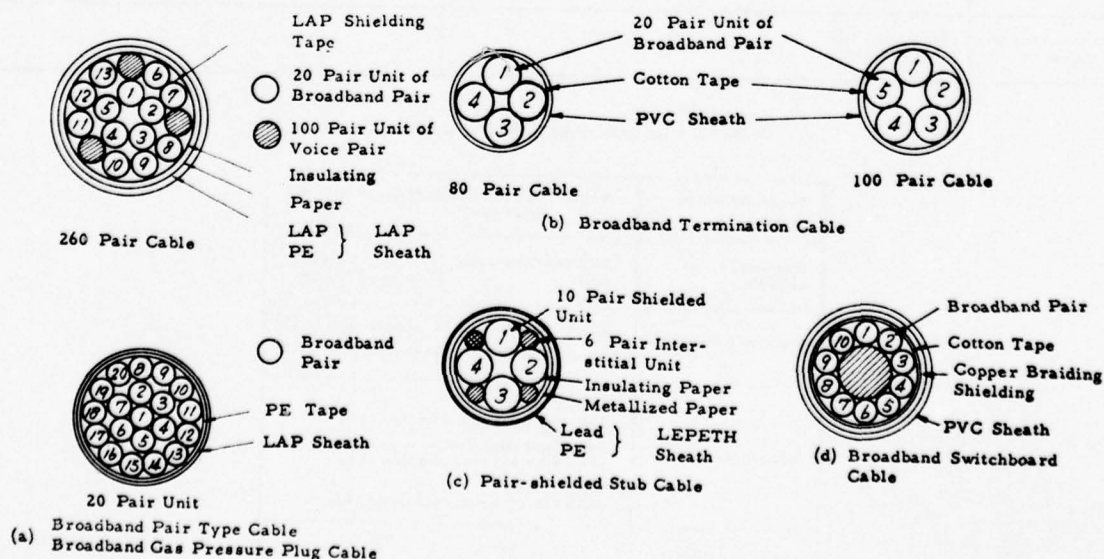


FIG. 1 General Views of Basic Configurations



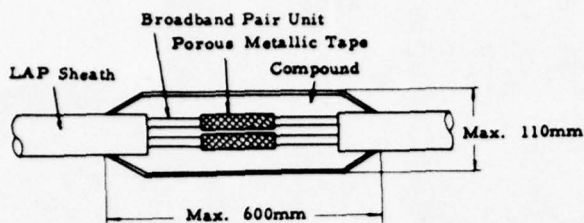


FIG. 5 Gas Pressure Plug Part



FIG. 4 Broadband Pair Type Cable

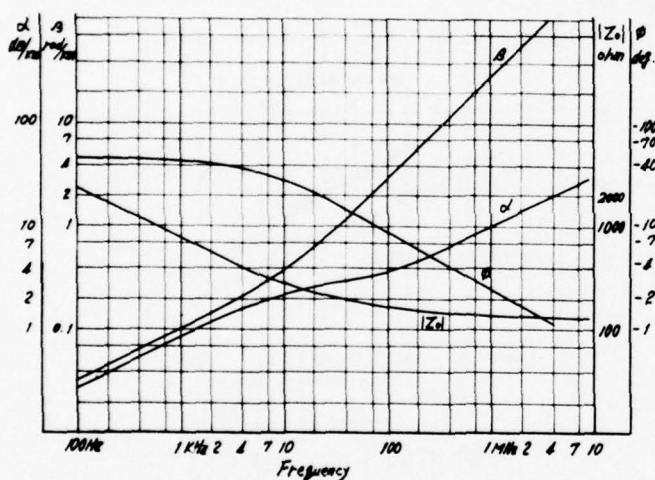


FIG. 6 Broadband Pair Type Cable Secondary Constants

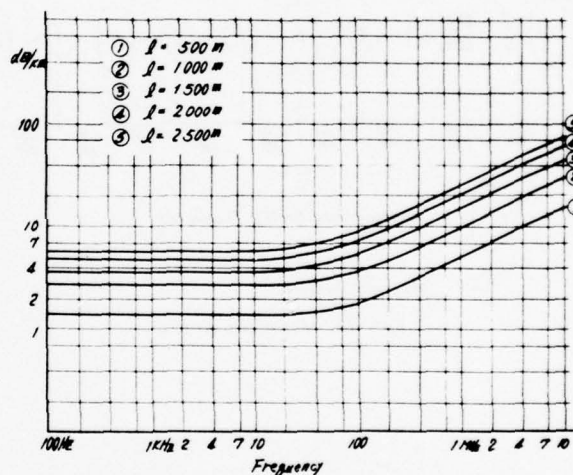


FIG. 7 Broadband Pair Type Cable Insertion Loss

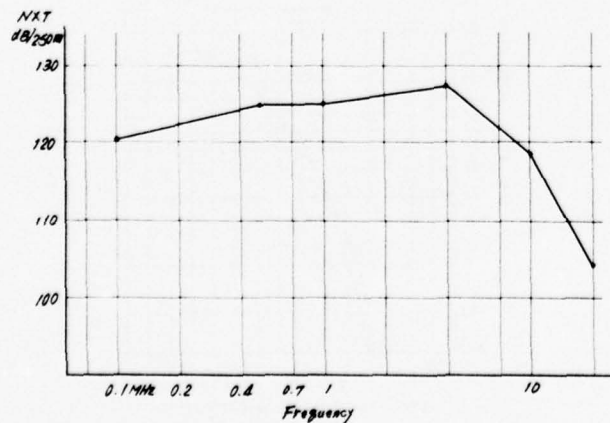


FIG. 8 Broadband Pair Type Cable NXT

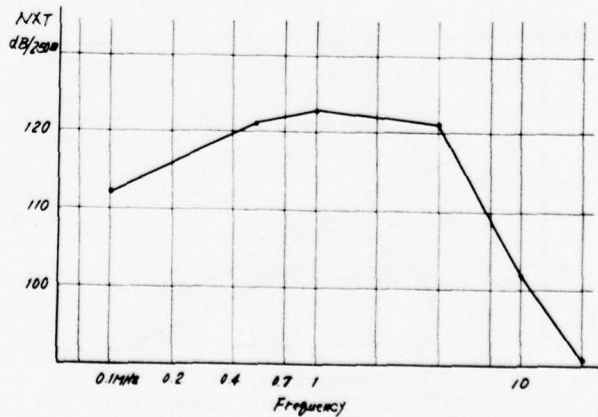
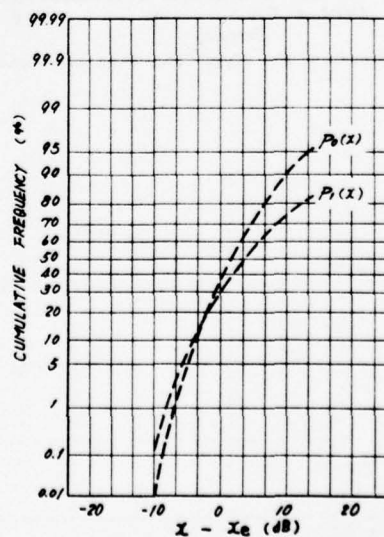
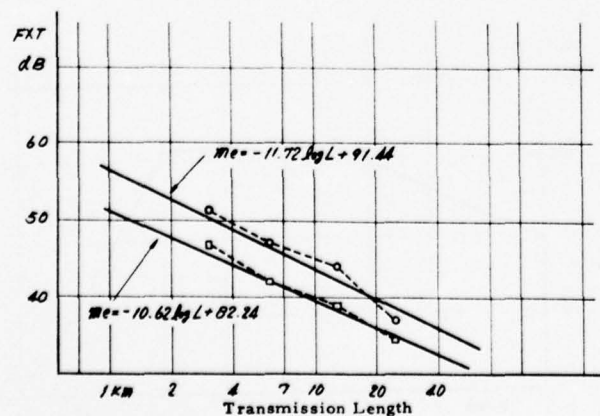
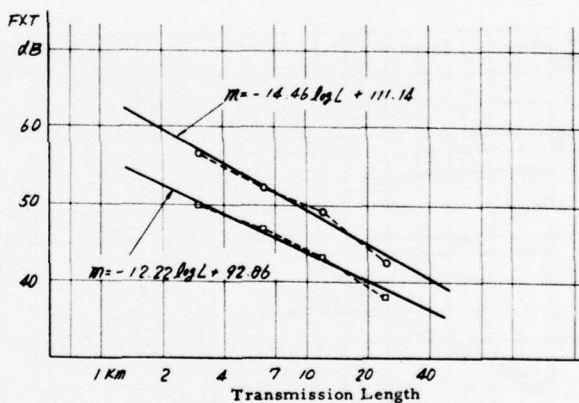
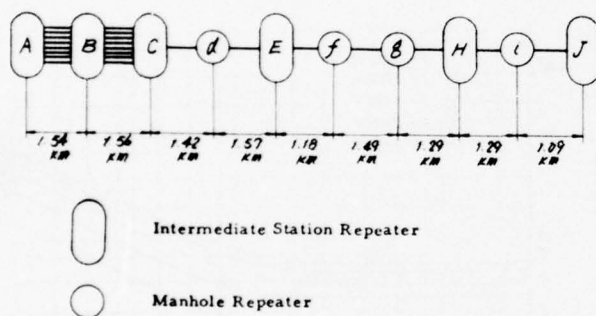
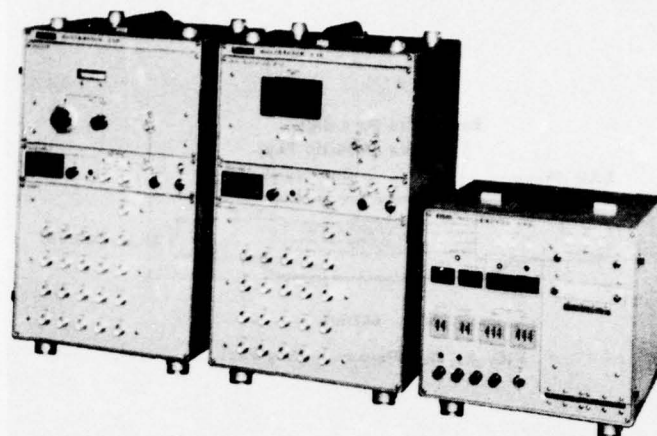
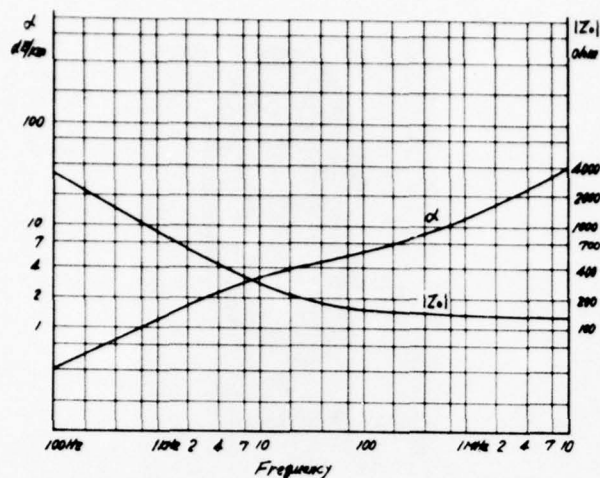


FIG. 9 Broadband Gas Pressure Plug Cable NXT



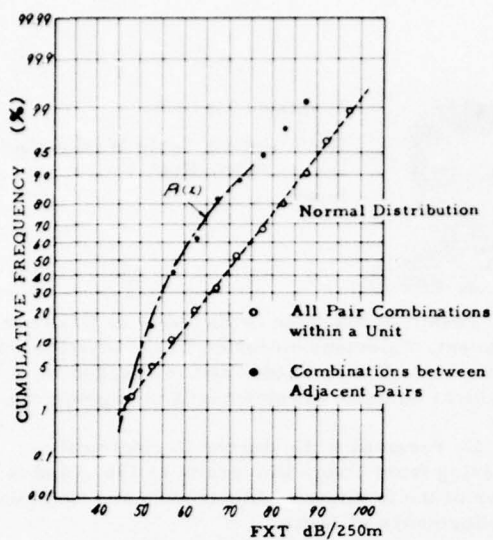


FIG. 16 250m Long
Broadband Pair Type Cable FXT

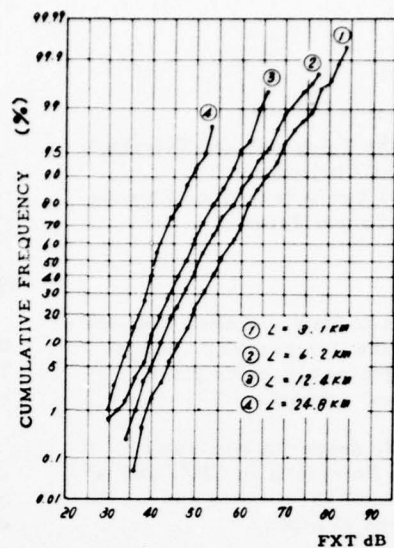


FIG. 17 FXT Distribution Pattern Changes
(All Pair Combinations within a Unit)

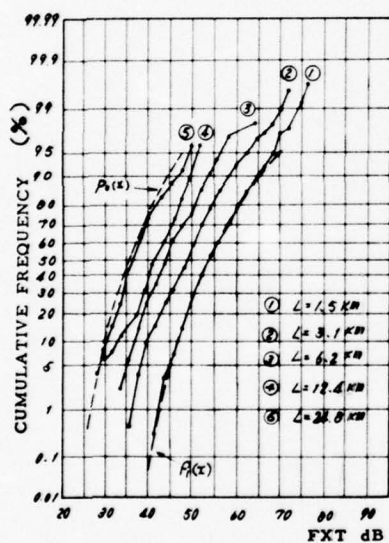


FIG. 18 FXT Distribution Pattern Changes
(Combinations between Adjacent Pairs)

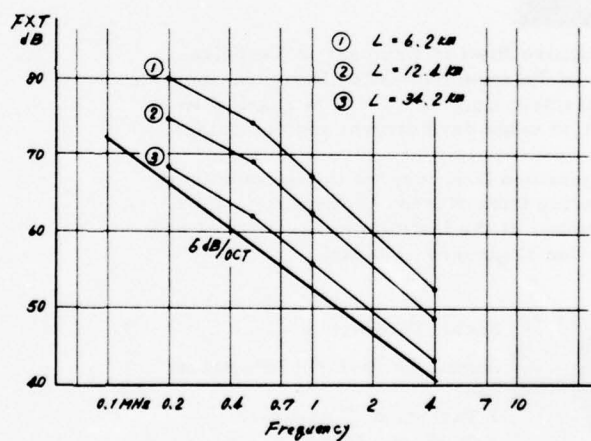


FIG. 19 FXT Frequency Characteristics

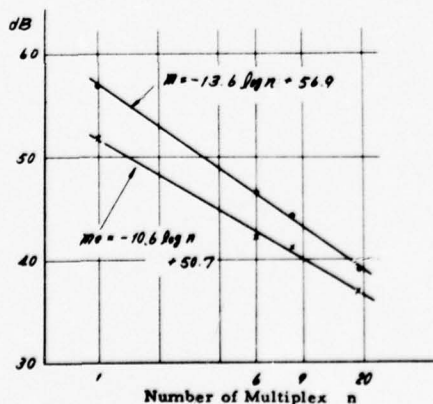


FIG. 20 Multiple FXT



Kazuyuki Oshima
Nippon Telegraph and Telephone
Public Corporation
1-1-6 Uchisaiwai-Cho, Chiyoda-
Ku, Tokyo, Japan

Kazuyuki Oshima is Staff Engineer, Outside Plant Division Engineering Bureau, NTT, and is now in charge of development of outside plant, especially broadband local network.

He received B. E. degree in electronic engineering from Tokyo University in 1964, and is a member of the Institute of Electronics and Communication Engineers of Japan.



Jun'ichiro Niwa
The Furukawa Electric Co.,
Ltd.
2-6-1, Marunouchi, Chiyoda-
Ku, Tokyo, Japan

Jun'ichiro Niwa is Engineer in Technical Department of Telecommunication Division, the Furukawa Electric Co., Ltd., and is engaged in communication cable development and designing.

He received B. E. degree in telecommunication engineering from Waseda University in 1969, and is a member of the Institute of Electronics and Communication Engineers of Japan.



Sachio Hiramatsu
Sumitomo Electric Industries,
Ltd.
1 Taya-Cho, Totsuka-Ku,
Yokohama, Japan

Sachio Hiramatsu is Engineer in Communication Engineering Section of Communication Division, Sumitomo Electric Industries, Ltd., and is engaged in communication cable development and designing.

He received B. E. degree in electronic engineering from Kyoto University in 1965, and is a member of the Institute of Electronics and Communication Engineers of Japan.



Toshikuni Maruoka
The Fujikura Cable Works, Ltd.
1-5-1, Kiba, Koto-Ku, Tokyo,
Japan

Toshikuni Maruoka is Engineer in Engineering Department, Telecommunication Cable Division, the Fujikura Cable Works, Ltd., and is engaged in communication cable development and engineering.

He received B. E. degree in electrical engineering from Tokyo University in 1967, and is a member of the Institute of Electronics and Communication Engineers of Japan.

NEAR END CROSSTALK PROPERTIES OF COMPARTMENTALIZED PCM CARRIER SYSTEM CABLES

A. P. Gabriel and J. Peveler
General Cable Corporation
Research Center
Union, New Jersey

J. J. Woods
General Cable Corporation
Communication Products Operation
Colonia, New Jersey

INTRODUCTION

The 24 channel, pulse code modulated (PCM) carrier system, commercially introduced in the early '60's⁽¹⁾ fast became a viable component of exchange and toll connecting telephone service. During 1974 a new generation digital system providing 48 channels over two cable pairs was inaugurated⁽²⁾. This system offered twice the information capacity but, with twice the bandwidth required, compounded noise shielding and crosstalk control problems.

Early installations of the 24 channel system used both single and dual cable approaches. The former system had the carrier pairs for alternate directions of transmission separated by voice frequency units. Generally speaking, the two cable system, using one cable for each direction of transmission, was both economically and functionally acceptable, since most PCM systems of the time serviced areas of relatively high population density. Entry of these systems into much less settled areas proved to be a prime mover in the development of the internally shielded, partitioned or screened cable⁽³⁾, which permitted utilization of all pairs in single cable operation, dedicated to PCM transmission.

The internally screened cable, which for so many years had serviced the needs of the 24 channel system, became a highly desirous transmission link in the 48 channel system as well. Because of the higher bit rate, however, increased crosstalk susceptibility and shielding degradation became of vital concern.

It is the intent of this paper to provide a discussion of screened cable crosstalk behavior, at both the 24 and 48 channel equivalent frequencies, as a function of cable pair count, at 100 percent cable fill. Some acumen is offered as to the mechanisms of screened cable operation, with particular attention paid to the analysis of longitudinal seams in the partition. Basic methods of screen fault detection and location are also discussed.

SHIELD FUNCTIONS OVER SINGLE CABLE ROUTES

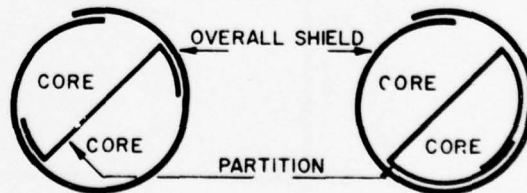
For two-way transmission, confined to a single internally screened cable, the purpose of the shields is two-fold. They must prevent external source interference from entering the cable information circuits, and likewise must inhibit transmitted signals on the cable pairs from crosstalking into other circuits. In general, the overall shield does perform its function, but its interaction with the internal shield becomes a factor in internal crosstalk control.

The most significant couplings involved in single sheath, bi-direction transmission cable, over PCM routes, are those of near-end crosstalk (NEXT) between pairs in opposite directions of transmission. Cross-talk is, of course, frequency dependent; its prominence

substantially magnified by the introduction of 48 channel carrier systems. Procedures to reduce such internal pair couplings have been known for many years. For example, suppression of NEXT may be achieved through judicious selection of pair lays or the individual shielding of pairs or pair groups. Optimum pair lay schemes have been employed by cable manufacturers for some time, but do not provide adequate crosstalk separation for PCM operation in a single cable sheath. Shielded pairs or units which do provide adequate separation are considered to be prohibitively costly and may lead to manufacturing difficulties. The introduction of an internal metallic partition provides favorable results with reduced economic and manufacturing problems. Of course, one must recognize that two cable routing schemes are possible, but such implementations can bring other problems into being; the foremost being installation economics.

TYPES OF INTERNAL SCREENS FOR PCM CABLES

For all intents and purposes, there are only two distinct types of internal screen, or partition. One variety bisects the cable core such that the resultant cross-section possesses geometric symmetry about the partition axis. This concept is exemplified by commercially available "T"⁽³⁾ or "Z"⁽⁴⁾ screened cables, which do indeed suffice for intramodal signal isolation when employed in 24 channel PCM systems. The technological successor to this form of shielding is the closed partition internal screen. One of the earliest commercially available constructions, employing this type of shielding, was the "D"⁽⁵⁾ screened cable. Core-half isolation is generally enhanced by an electromagnetic barrier which completely encloses one half the cable core. Figure 1 conceptualizes both of these models.



(a) Open Screen Model (b) Closed Screen Model
FIGURE 1: General Classification of Internal Screen Designs.

MERITS OF THE BASIC SCREEN DESIGNS

Papers have been published^(3,4,5), and patents have been issued^(6,7) extolling the merits of the various screen designs. For the system designer, dealing with single cable routings, there is one question. Will the completed cable perform as required?

To investigate the performance of cable partitioning with respect to transmission, it becomes imperative to know which PCM system will be used. Will it be a 24 channel system operating at 1.544-Mb/s or a 48 channel system at 3.152-Mb/s or yet another PCM system, with another bit rate? Since the preponderance of PCM systems operating on paired facilities range between 24 and 48 channels, the discussion will be confined to these limits, with Nyquist frequencies of 772 KHz and 1.576 MHz, respectively.

The 24 Channel System

Basic to an understanding of the 24 channel PCM system is a knowledge of the engineering rules set down by Cravis and Crater⁽¹⁾. This referenced paper methodically illustrates that the PCM system design must be guided by the error rate which the system is capable of tolerating. For the 24 channel system the maximum error rate between end terminals was determined to be 10^{-6} for satisfactory transmission. By utilizing the error rate as a focal point, an equation was developed placing boundary maxima on both the mean section loss (L) and the number of permissible systems (n) in the form:

$$\bar{L} + 10 \log_{10} \left(\frac{n}{25} \right) = m - \sigma - 40 \quad \dots(1)$$

Where:

\bar{L} = mean repeater section loss, dB.

m = mean NEXT coupling loss at 772 KHz, dB.

σ = standard deviation of the NEXT coupling losses at 772 KHz, dB

and n = number of carrier systems used in the cable.

If the balance of this equation is maintained for each section length, the error rate objective will be met. By simple manipulation, this equation may be described in terms of (m- σ):

$$(m-\sigma)_{24} = 65.5 + 10 \log_{10} (n) \quad \dots(2)$$

based on a maximum section loss of 33.5 dB at maximum expected temperatures, less 1.5 dB for pair-to-pair manufacturing variations and a 6 dB reduction for "margin". (Margin may be defined as a figure of merit which is allocated in order to compensate for unknown system degradations. It insures that the error rate objective will be met for most situations.) Graphing (m- σ) of equation (2) as a function of cable pair count, yields a curve which represents the minimum acceptable level of cable performance for the 24 channel PCM system. This is illustrated in Figure 2.

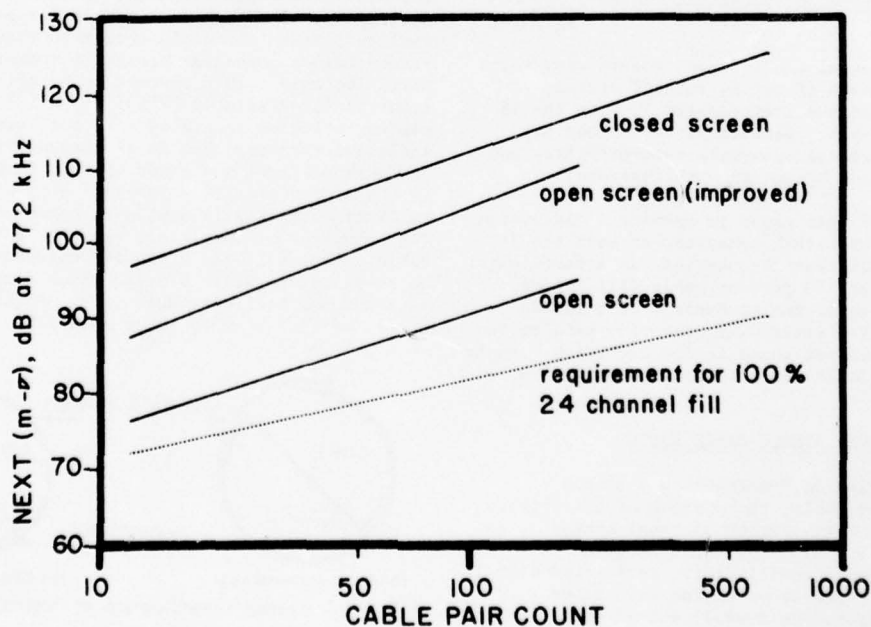


FIGURE 2: AVERAGE NEXT (m- σ) vs. PAIR COUNT at 772 kHz.

By adding the performance curves of the two previously described screened cable models to Figure 2, their merits may be compared for employment in the 1.544 Mb/s system. For added interest, the characteristics(8) of an improved open screen design have also been plotted. Figure 3 illustrates the geometry of the two open screen designs.



FIGURE 3: Cross Sections of Open Screen Designs of Two Tab Lengths.

The 48 Channel System

The emergence of the 48 channel PCM system changed the engineering rules for section design. Since NEXT is still the limiting factor in single cable operation, engineering rules for 48 channel systems have been formulated(9,10,11) based on NEXT requirements. These rules have as their foundation the earlier works of Nasell(12) and Marlow(13), on the properties of truncated normal random variable power sums, and it is not surprising that there is close agreement. For the sake of consistency and ease of computation, the method by Bradley(10), as employed in the General Telephone and Electronics Practices(14) for 48 channel systems, is used for this analysis.

The equation used for repeater section NEXT loss requirements, based on 100 percent pair utilization, at maximum repeater spacings and maximum operating temperature is noted to be:

$$(m-r)_{48} = 81.6 + (10 + \frac{\sigma}{2}) \log_{10}(n) \quad \dots(3)$$

where the crosstalk is measured at or corrected to 1.576 MHz.

As with the 24 channel system, a graph of $(m-r)$ was constructed with respect to cable pair count, which determines the minimum acceptable level of $(m-r)$ at 1.576 MHz and is shown in Figure 4. The performance curves of the open and closed screen designs are also plotted. The early version of the open screened cable is not shown, since it clearly will not meet system requirements.

Analysis of Figure 4 shows that the basic closed type of partition offers an advantage to the system design. It may be employed in either of the two PCM systems under consideration, at maximum repeater spacings and 100 percent cable fill.

ELECTROMAGNETIC FIELDS AND THE PARTITION

At frequencies such that skin depth is less than shield thickness, from Terman's formula(12),

$$\text{Skin Depth} = 1.9815 \sqrt{\rho / f} \text{ mils} \quad \dots(4)$$

Where ρ = resistivity, μ ohm cm
and f = frequency, MHz,

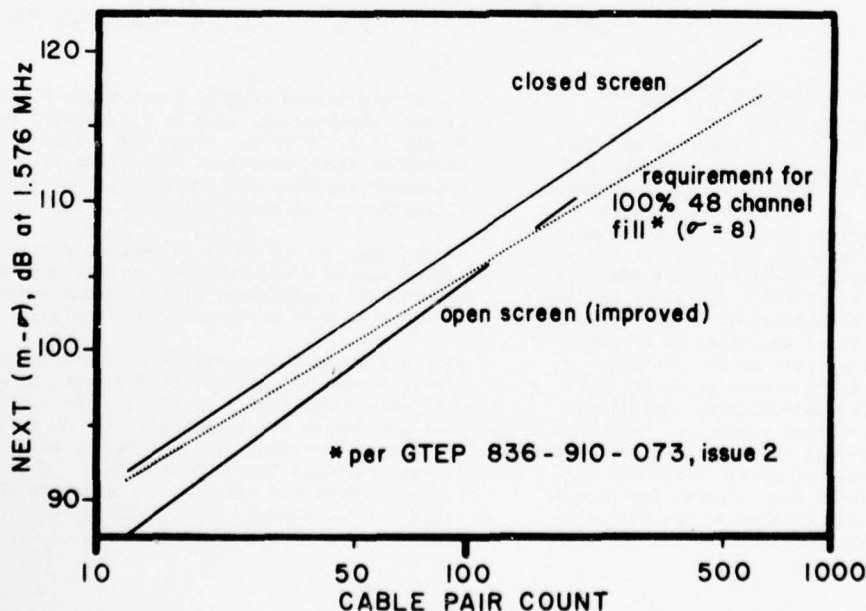


FIGURE 4: AVERAGE NEXT $(m-r)$ vs. PAIR COUNT at 1.576 MHz.

it can be shown that the screen provides shielding which is dictated by the surface transfer impedance. The 0.004" aluminum screens used in most partitioned cable applications falls into this category. At PCM frequencies most of the interfering current is confined to the screen surface nearest the disturbing circuit, and the voltage drop along the far surface is less than the drop along the near surface. The surface transfer impedance is defined⁽¹⁶⁾ as

$$Z_{\alpha\beta} = \frac{V_{\alpha}}{I_{\beta}} \quad \dots(5)$$

where α and β represent the far and near surfaces, respectively.

For homogeneous tubes the surface transfer impedance decreases with frequency, yielding improved shielding efficiency. For shields with longitudinal seams, current leakages through the seams predominate at frequencies between 1 and 10 MHz and raise the effective surface transfer impedance. This phenomenon has been examined^(16,17,18) and although methods of measuring flux leakage or theoretical calculations of its magnitude have been presented, they are complex, and beyond the scope of this paper. The ideal PCM screen would be a homogenous metallic cylinder, but in reality overlapping is a commonly employed technique for screening applications.

In the open screen model the premise is to interface the screen and overall shield to mitigate intra-compartmental coupling. In general, however, the screen-to-overall shield interface consists of a multiplicity of components as depicted in Figure 5(a).

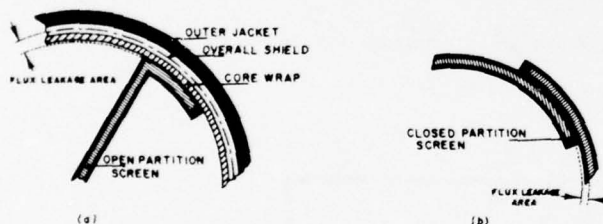


FIGURE 5: Magnified View of Partition Overlap Area.

Because of the large amount of dielectric material encountered between the two metallic members, a substantial path for flux leakage exists. A degree of crosstalk reduction may be achieved through slight geometric variations in the screen design. Quite simply, any extension of the open partition end tabs tends to mitigate the effects of NEXT. A recent paper by Okamoto, et al⁽⁴⁾ describes in detail the effect of tab length extensions up to a point where the open screen model converges to a double compartmented closed partition array. This is illustrated in Figure 6. A review of these findings indicates the difficulty in achieving additional NEXT isolation with increased coverage. Extension of the tabs does not reduce the interface gap between the metallic components, but merely lengthens the intracompartamental path of the interfering signals. Outer shield corrugations further debase intra-compartmental crosstalk suppression.



FIGURE 6: Convergence of the Open Screen Model to a Closed Screen Array.

Changes in the closed screen design are limited in extent. Only the position of the screen overlap may be controlled. A review of Figure 7 clearly demonstrates that 7(a) is the preferred overlap position because it provides greater separation between the screen leakage point and the other compartment. Locations depicted in 7(b) or 7(c) place the overlap in closer proximity to the alternate core-half. In any event, the interfacing gap between the ends of the metallic tape can only be equal to twice the thickness of the screen dielectric as shown in Figure 5(b). In this case, overall shield corrugation effects upon the screening agent are insignificant and gapping is minimal. In addition, intracompartamental couplings, via the overall shield, are reduced by the closed partition.

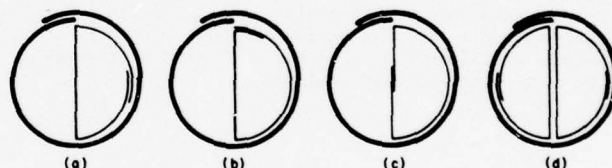


FIGURE 7: Overlap Placement in the Closed Screen Partition.

The closed screen partition may be doubled to form two closed compartments, such as illustrated in Figure 7(d). However, since the closed shield partition shown in Figure 7(a) provides adequate crosstalk suppression, the addition of a second closed screen is not justified at this time.

If the open screen model is made to approximate the closed screen design through extreme end tab extensions, performance of the screen would possibly approach that of a closed screen design.

Figure 8 shows the crosstalk characteristics of a closed screen 52 pair No. 22 AWG cable in the frequency range of 0.1 to 10 MHz. It can be seen that the curves are relatively flat up to about the 24 channel operating frequency where the seam leakage currents become predominant. This causes a slope of about 4.5 dB/octave, similar to the slope noted for unscreened unit couplings⁽¹⁹⁾.

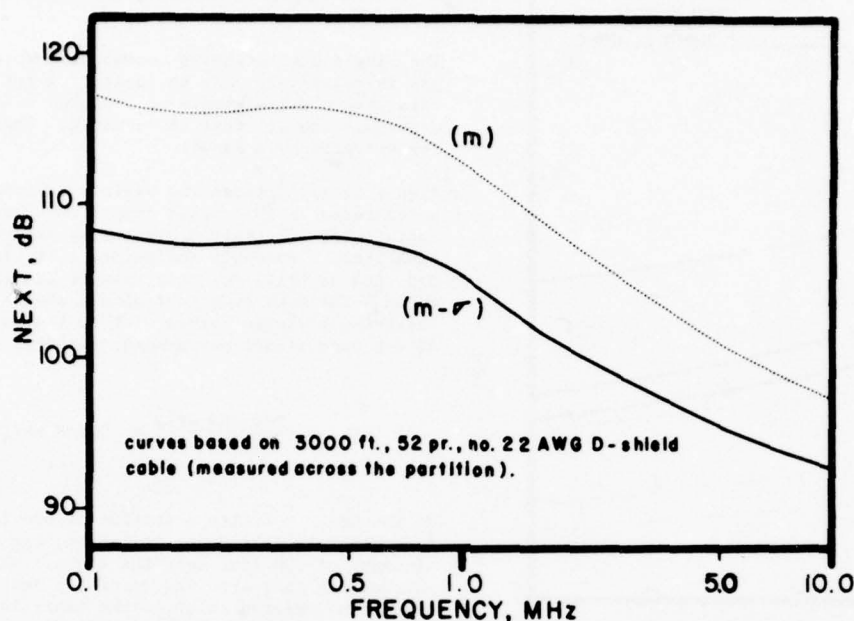


FIGURE 8: NEXT vs. FREQUENCY, 0.1 to 10.0 MHz

THE INFLUENCE OF SCREEN DISCONTINUITIES

Except for the presence of the partitioning screen, internally shielded cables are similar to other telephone cables; subject to the same problems during manufacture and field installation. Discontinuities in the screening circuit do, however, have an effect upon cable crosstalk performance. Most critical are circumferential gaps in the partitioning member so that the pairs serving opposite directions of transmission are unscreened for a portion of the cable length.

In the manufacturing process discontinuities can be caused by excessive tensions during the application of the tape, which may open a tape splice or cause a circumferential break in the metallic portion of the screen. This may also occur during installation.

In its simplest form a circumferential discontinuity will have a virtually zero length gap, which will result in insignificant crosstalk degradation. When a finite length of the partitioning screen is missing, substantial reduction of crosstalk shielding will occur.

An important cause of poor NEXT crosstalk performance in installed systems can be the failure to carry the screening through splice points throughout the route. It is not necessary to establish dc continuity, but the shielding must be physically continuous to afford maximum crosstalk separation.

The extent of NEXT degradation with screen faulting is dependant upon two factors. The first is the physical location of the fault within the repeater section, and the second is the length of the screen discontinuity. When faulting occurs in close proximity to the line repeater, the worst case condition results,

since at this point the interfering signal is at a maximum. Gaps occurring further downstream are subject to both forward and reverse line attenuation, thereby diminishing the effect.

Crosstalk degradation with respect to gap length has been the subject of laboratory work⁽²⁰⁾. Induction through the gap has been seen to be approximately proportional to the length of the gap. In addition, work completed on both open and closed screen cable models has indicated that the latter design is more seriously affected by the presence of such gaps. This is not an unexpected phenomena since the closed screen cable represents what may be termed a higher performance type of cable. Figure 9 clearly demonstrates the validity of this claim for various cables of both designs.

The effects of screen faults make it obvious that the cable manufacturer must insure that shipped cable lengths are free from such defects. In addition, outside plant personnel must take adequate precautions to maintain the integrity of the screening.

DETECTION OF PARTITION FAULTS

There are a few techniques which readily lend themselves to the determination of internal shield faults. A very simple approach is the measurement of the "through", or direct, capacitance, which yields rapid and accurate results. The "through" capacitance as used in this context, refers to the capacitance existing between the two core halves, with the intervening screen grounded. This is illustrated in Figure 10. The technique requires that the pairs in each core half be short circuited together, so that each group appears as a single conductor of a balanced pair. The partition, an intervening barrier, is brought to a reliable ground, along with the overall shield at the measuring end.

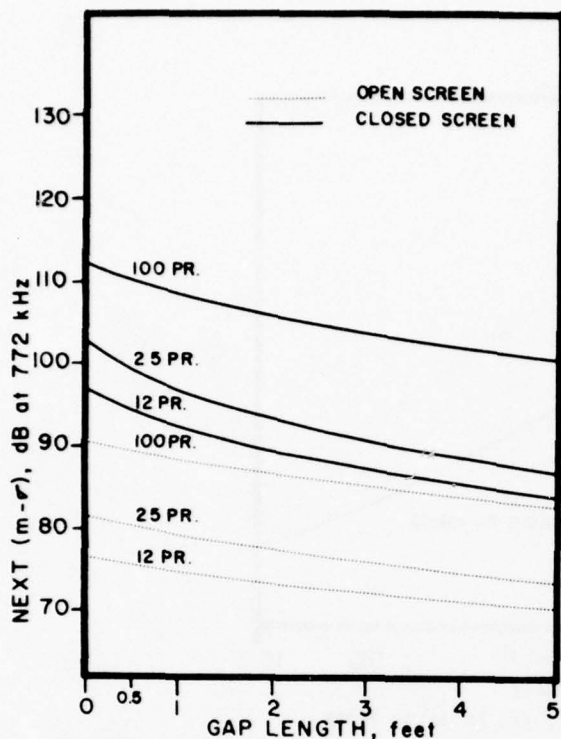


FIGURE 9: NEXT (m-φ) vs. GAP LENGTH. Curves based on being located at repeater output (worst case condition).

Generally speaking, if the screen is continuous, the capacitance existing between the two core halves will be zero since the interjacent screen is an electrostatic barrier. Realistically, some electrical leakage does occur, due to non-perfect shielding, but a 1 nF or less "through" capacitance level, when measured at one kilohertz on a reel length of cable is acceptably small enough to insure relative freedom from screen gaps. Cables which do house screen voids will exhibit far greater levels of direct capacitance; the discrete value dependant upon the length of the gap. If the capacitance value exceeds the 1 nF benchmark, it must be determined whether the problem is a simple break or a discontinuity of finite gap length.

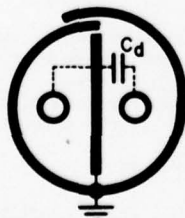


FIGURE 10: The Concept of "Through" or Direct Capacitance.

If the initial measurement of direct capacitance is greater than 1 nF, the next step is to ground each screen end to the overall shield. If the value of capacitance returns to the realm of 1 nF or less, then a screen break with virtual zero gap length is the problem. Such occurrence does not degrade crosstalk performance and, therefore, corrective measures need not be implemented. If, however, the

capacitance value does not change, or does not fall below the benchmark, a single partition discontinuity of finite length is present, or there are multiple screen breaks.

The single discontinuity accompanied by a discrete gap is relatively easy to locate. A few simple capacitance measurements accompanied by a ratioing procedure are all that is required. This is best demonstrated by example.

Figure 11 illustrates the various capacitances encountered in the closed compartment partitioned cable, with arbitrary designations assigned the capacitors. Possible indicators of faulting include C₁₂, C₁₃ or C₁₄. For this example C₁₃ was measured on an 1,186 foot length of single sheath cable employing a closed screen with no faults. The first direct capacitance measurement yielded:

$$C_{13} = \frac{294.480 \text{ nF}}{1186 \text{ ft.}} = 0.248 \text{ nF/ft.}$$

To introduce a fault, a section of partitioning approximately six inches in length, was removed at a distance of 200 feet into the cable. The sheath surrounding this area was carefully restored to the state that existed prior to the fault introduction. A screen ground was applied to the short end, with the other end of the partition left in an ungrounded state. C₁₃ was again measured with the following results:

$$C_{13}' = 49.010 \text{ nF}$$

By simple ratioing the fault was located at:

$$\frac{49.010 \text{ nF/"x" ft.}}{0.248 \text{ nF/ft.}} = 197.6 \text{ ft.}$$

from the outside end.

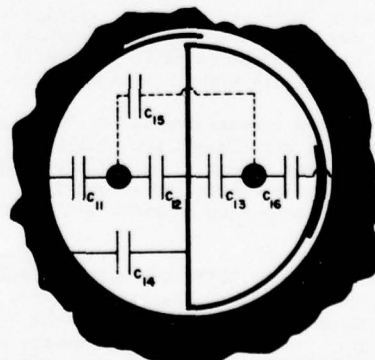


FIGURE 11: Partial Capacitances in the Closed Screened Cable.

Extensive laboratory work has shown this method to yield results accurate to within one percent; the error being attributed to cable dimensional (capacitance) non-uniformity.

The fault locating technique is noted as a general procedure, since several cable parameters seriously influence the final results. For example, although most direct capacitance measurements may be correctly performed at a one kilohertz generator frequency, a certain percentage will necessitate a generator frequency downshift to compensate for propagation effects. Such errors are themselves attributable to a multiplicity of factors; the most notable being conductor gauge size, cable length and pair count. The foregoing procedure lends itself well to plant inspection techniques and all cables should be tested prior to shipment to insure screen integrity. In the field, screen discontinuities will manifest themselves by causing excessive error rates in many span lines simultaneously. After localization of the faulty repeater section, and if subsequent visual inspection of the repeater points reveals no screen irregularities, then fault locating procedures should be attempted.

Since the cable pairs are not readily accessible for shorting, the factory test procedure for fault locating is not a practical method. The capacitance between the outer shield and screen can be measured using simple capacitance bridges in the unbalanced mode. The same ratiometric technique can then be used to determine the location of shield faults, provided that C₁₄ is known for an unfaulted cable of the same design. The use of a pulse echo method is not recommended due to the very low impedance path existing between the overall shield and screen, which lowers the sensitivity of these instruments.

SUMMARY

This paper has discussed the near end crosstalk characteristics of internally screened telephone cables used for PCM transmission. Various shield designs have been discussed in conjunction with crosstalk requirements for 24 and 48 channel PCM systems. Shielding principles were reviewed with regard to the performance of the different shield configurations. Finally, the effect of screen discontinuities was shown and fault locating procedures recommended.

ACKNOWLEDGEMENTS

We wish to acknowledge the help of a number of people at General Cable who read the manuscript and made many valuable suggestions. These especially include I. Kolodny, J. A. Olszewski and H. Lubars. In particular, we wish to express deep gratitude to H. Simon for the help we received in our discussions on shielding phenomena and his analysis and excellent translation of the work by Kaden. We also express our appreciation to M. Kermod and D. Tunnell for the preparation of the manuscript.

REFERENCES

- Cravis, H., and Crater, T. V., "Engineering of T1 Carrier System Repeatered Lines". Bell System Technical Journal, 42: 431-86, March 1963.
- Lombardi, J. A., Maurer, R. E., and Michaud, W. P., "The T1C System". International Conference on Communications, 11th, San Francisco, 1975. Conference Record, pp. 39-1 - 39-9. Institute of Electrical and Electronics Engineers, New York 1975.
- Roberts, W. L., and Wilkenloh, F. N., "Multipair Cable Shielding for PCM Transmission". International Wire and Cable Symposium, 19th, Proceedings, pp. 175-81, Atlantic City 1970.
- Okamoto, K., Noda, H., and Onishi, M., "High Frequency Crosstalk Performance of Z-Type Shielded Cable", International Conference on Communications, 8th, Philadelphia, 1972. Conference Record, pp. 19-13 - 19-18, Institute of Electrical and Electronics Engineers, New York 1972.
- Jachimowicz, L., Olszewski, J. A., and Kolodny, I., "Transmission Properties of Filled Thermoplastic Insulated and Jacketed Telephone Cables at Voice and Carrier Frequencies". International Conference on Communications, 8th, Philadelphia, 1972. Conference Record, pp. 19-7 - 19-12, Institute of Electrical and Electronics Engineers, New York 1972.
- U. S. Patent 3,603,340. "D" Internal Shield in Telephone Cables. L. Jachimowicz and J. A. Olszewski to General Cable Corporation, April 9, 1974.
- U. S. Patent 3,622,683. Telephone Cable with Improved Crosstalk Properties. W. L. Roberts and F. N. Wilkenloh to Superior Continental Corporation, November 23, 1971.
- Superior Continental Corporation. Superior Cable Division. "New Extended Coverage T-Screen Cable". (Advertisement) Telephone Engineer and Management, 79: p. 141, October 1, 1975.
- Fitzsimmons, J. P., and Maybach, W. J., "Engineering T1C Carrier Systems", International Conference on Communications, 11th, San Francisco 1975. Conference Record, pp. 39-5 - 39-9, Institute of Electrical and Electronics Engineers, New York 1975.
- Bradley, S. D., "Crosstalk Considerations for a 48 Channel PCM Repeatered Line", Institute of Electrical and Electronics Engineers, Transactions on Communications, COM-23: 772-31, July 1975.
- Murphy, B. R. N., "Crosstalk Loss Requirements for PCM Transmission", Institute of Electrical and Electronics Engineers, Transactions on Communications, COM-24: 88-97, January 1976.
- Nasell, I., "Some Properties of Power Sums of Truncated Normal Random Variables", Bell System Technical Journal, 46: 2081-89, November 1967.
- Marlow, N. A., "A Normal Limit Theorem for Power Sums of Independent Random Variables", Bell System Technical Journal, 46: 2081-89, November 1967.
- GTE-Lenkurt, "48 Channel Repeatered Line Equipment Transmission Engineering Considerations", GTE Practices, Engineering - Plant Series. Section 836-910-073. Issue 2, February 1976.
- Buckingham, R. P., and Gooding, F. H., "The Efficiency of Non-Magnetic Shields on Control and Communications Cable", Institute of Electrical and Electronics Engineers, Transactions on Power Apparatus and Systems, PAS-89: 1091-9, July/August 1970.

16. Griffith, D. E., "Surface Transfer Impedance on Cable Shields Having a Longitudinal Seam", National Electronics Conference, Proceedings, 26: 952-7, 1970.
17. Schelkunoff, S. A., Electromagnetic Waves, Princeton, New Jersey, Van Nostrand, 1943.
18. Kaden, H., Wirbelströme und Schirmung in der Nachrichtentechnik, 2nd Edition, pp. 333-4, Berlin, Springer, 1959.
19. Eager, G. S., Jachimowicz, L., Kolodny, I., and Robinson, D. E., "Transmission Properties of Polyethylene Insulated Telephone Cables at Voice and Carrier Frequencies", American Institute of Electrical Engineers, Transactions, 78 (Pt. I): 618-39, November 1959.
20. Woods, J. J., and Olszewski, J. A., "Effects of Discontinuity or Gap in Internal Shielding on NEXT Characteristics of T1 Cables", General Cable Corporation, Research and Development Center, Research Report 15042, (Internal Report), August 23, 1971.



ANTHONY P. GABRIEL received a B.S. degree in Engineering Science from Richmond College, the City University of New York, in 1972. He has been employed by the General Cable Research Center since 1967. In his present position, as Research Product Manager, Communications Cable, he is responsible for the development and analysis of carrier telephone cables and outside plant wire products. Prior to his employment with the Research Center, he was affiliated with both Western Electric and the Bell Telephone System.



JOHN J. WOODS received a B.S. degree in Engineering Science from Richmond College, the City University of New York, in 1972. He is currently a Senior Applications Engineer at the Communication Products Operation Headquarters, with responsibilities for the application of balanced pair telephone cables in the communications industry. Prior to this he was a member of the corporate Research Center, from 1964 to 1974. Before joining General Cable he was affiliated with the Phelps-Dodge Copper Products Corporation, Habirshaw Division.



JOHN PEVELER, currently a candidate for a B.S. degree in Engineering Science from Richmond College, the City University of New York, has been employed by the General Cable Research Center since 1968. He is currently involved in the measurement and analysis of multipair telephone and coaxial cables.

THE DEVELOPMENT OF SUPER HIGH TEMPERATURE WIRE
AND CONNECTORS FOR GENERAL PURPOSE AEROSPACE APPLICATIONS

F.D. Bayles and M.A. Dudley
Canada Wire & Cable Technology Development Department
Noranda Research Centre
Montreal, Quebec, Canada

SUMMARY

This paper describes the approach taken to design and develop a family of electrical wires and connectors for general purpose aerospace applications in service environments of 650°C and higher. An assessment was made of the operating restrictions dictated by the Statement of Work, and this was related to other contract approaches and commercially available high temperature wire to determine their inadequacies and to establish the logic of the experimental approach chosen. Details are given of the development of the subcomponent materials, the assembly into the preferred design and the performance of the prototype. In conclusion, the present status of the program is outlined, and consideration is given to compatible connector development and other potential end use applications for the unique combination of performance properties inherent in this wire design.

1. INTRODUCTION

In 1972 the Technology Development Department began development, on behalf of the U.S. Air Force Aero Propulsion Laboratory and the Canadian Defence Research Board, of a family of electrical wires and connectors for general purpose aerospace applications requiring both long term continuous and cyclic resistance over a temperature range of from -65°F to 1250°F and pressure corresponding to altitudes from sea level to 110,000 feet, for 1000 hours under rated power of 600 volts rms.

The program was divided into two sections, with Phase I, detailed in this report, having the objective of determining the materials and assemblies suitable for performance under the design criteria and Phase II having the objective of optimization of the prototype units and proving the commercial feasibility of volume production. The development of suitable connector systems was subcontracted to the ITT Cannon Electric Canada Company Ltd. with overall coordination being provided by Canada Wire & Cable Limited.

2. DESIGN APPROACH

2.1 Performance Requirements

Table I details the performance requirements specified in the program Statement of Work.

TABLE I

PERFORMANCE REQUIREMENTS OF PROTOTYPE ASSEMBLIES

2.1.1 Environment

- a) Operating temperature range: -65°F to 1250°F
- b) Operating pressure range: sea level to 110,000 feet
- c) Humidity tolerance: 0 to 100%
- d) Vibration resistance: 20 g, 10 to 2,000 cps
- e) Physical shock resistance: 50 g, 11 ± 1 milliseconds

- f) Design life at maximum temperature: 1,000 hrs
- g) Flight profile test: 200 cycles consisting of consecutively 2 hours at 77°F/50% R.H., 1 hour at 77°F/100% R.H., 1 hour under rated power at either -65°F or 1250°F (performed concurrently on parallel samples) and 1 hour at 77°F/50% R.H. Total 5 hours per cycle.

2.1.2 Wire Assembly

- a) To contain a suitably stable conductor in 12 through 22 AWG inclusively
- b) Maximum continuous potential rating at temperature: 600 volts rms
- c) Resistivity: $< 6 \times 10^{-6}$ ohm-cm
- d) Tensile strength: 35,000 psi
- e) Insulation resistance: >1 megohm at 1250°F
- f) Susceptibility to blocking at 1250°F
- g) Dielectric strength: 1200 volts to ground under all conditions
- h) Flexibility: No deterioration of performance after winding on a mandrel of $\frac{1}{20}$ times the finished wire diameter
- j) Shrinkage: $\frac{1}{2}$ 0.06 inches
- k) Thermal shock resistance
- l) Abrasion resistance
- m) Susceptibility to sublimation under all conditions
- n) Flex fatigue life

2.1.3 Connector

- a) Contact spacing and configuration to permit steady state working voltage of 600 volts, 400 Hz
- b) Insulation resistance contact/contact and contact/shell at 1250°F: 2000 megohms
- c) Specify contact resistance at temperature and ageing
- d) Specify contact retention performance
- e) Specify contact and shell design
- f) Specify ozone, salt spray and organic liquids resistance
- g) Specify corona resistance
- h) Interfacial sealing to moisture-proof quality

As can be seen from the Table, there were a number of potentially incompatible performance requirements which were judged to influence and limit the choice of wire and connector design. Among these were (a) excellent conductivity while retaining oxidation resistance and tensile strength, (b) an insulation package which would retain a high level of dielectric strength while exhibiting good flexibility under extremely severe

thermal cycling and (c) a requirement for minimal smoking, fuming and blocking under all conditions.

2.2 Potential Wire Configurations

The next step in the program was to undertake a thorough information review, considering (a) theoretical articles discussing potential conductors and insulations useful in the service temperatures, (b) published reports of research and development by other workers, (c) patents issued for high temperature resistant wire and cable, and (d) commercially available wire and cable recommended for ~1250°F service.

The majority of the theoretical articles proposed the use of conductors having a thermally and oxidatively stable outer layer, with a primary dielectric made up of high temperature resistant ceramics, refractories or glasses. Organic polymers would be tolerated but only at minimum loadings which would evolve very low levels of smoke or degradation products on exposure to the operating temperature. The primary dielectric could be in the form of cloth, braid, tape or coating.

Considering the published reports of research by other workers, three general design configurations were favored: (a) composite wires, (b) coated wires, and (c) packed sheathed wires. The conductors used in the composite wires, with three exceptions, were nickel clad copper; the exceptions were nickel clad silver, silver clad Inconel and rhodium, the latter being used in a wire designed for service at 2000°F. The insulation was generally ceramic braid or tape, asbestos or mica/glass tape with outer protective layers of ceramic braid and optional sheath or knit armouring. The coated wires used conductors of copper, clad copper, nickel clad silver or rhodium with insulation of ceramic frits applied from slurry or electrocoating suspensions. The packed sheathed wires employed either copper or rhodium conductor with magnesium oxide as the primary dielectric. Nickel alloy was the preferred sheath.

Patented designs for high temperature resistant wire generally followed both the configurations and materials described above. Potential service temperature ratings ranged from 600 to 2000°F. The wires, however, were all found deficient in many of the other performance requirements, i.e. shock resistance, flexibility, susceptibility to fuming, etc.

After scanning the literature describing commercial high temperature resistant wires which were alleged to perform in the range of 900 to 1500°F, thirteen samples were obtained and evaluated. All of the wires, with the exception of one packed, sheathed design, were of composite construction, using nickel clad or plated copper conductor overlaid usually with multiple inner layers of braided glass or ceramic with further dielectric strength supplied by layers of asbestos or polymer impregnated mica tapes, and an outer layer of braid impregnated with silicone polymer or ceramic slurry.

All the wires were subjected to a short test cycle (see Appendix A) which approximated two cycles of the Flight Profile. The samples were rated for moisture absorption, weight change, initial and retained dielectric breakdown value and retention of mechanical integrity.

Susceptibility to moisture absorption after firing varied from 0.03% on the packed sheathed design to 13% on a thermocouple wire overbraided with refractory silica yarn. Weight losses varied from 0.4 to ~55%,

depending on polymer binder loading. Dielectric breakdown strength, initially excellent at an average of 4 KV, deteriorated significantly to <1 KV. The mechanical properties of all the composite wires after firing was relatively poor, with significant oxidative damage to the conductor, and severe loss of integrity in the dielectric layers. As would be expected, those wires which employed silicone polymer as an impregnant were highly flammable and showed copious fuming. Only the packed, sheathed configuration would be tentatively acceptable within the limits of the initial screening.

Upon completion of the survey, four potential design approaches were postulated and assessed for their potential for success within the restrictions of the Statement of Work.

(a) Sheathed, Gas-Filled Wire: This configuration would require sophisticated connection and pressurization subassemblies with the added complication of maintaining a hermetic seal and the need to flush and repressurize after repair. The wire would be inherently stiff, heavy, and have a high space factor and would be extremely expensive. This approach was rejected.

(b) Sheathed, Dense Dielectric Packed Wire: This configuration, commonly known as MI cable, has excellent dielectric and thermal stability, however, it tends to be extremely hygroscopic, and is difficult to fabricate and terminate. It is inherently stiff, heavy and has a poor space factor. No significant advance in technology could be foreseen using such an approach; the concept was rejected.

(c) Coated Wires: Extensive studies have been made of wire coated with a continuous dielectric sheath, using ceramic or glass frits applied as slurries. The major drawback to this technique is that it results in a wire which, before firing, has a "green" or fragile uncured surface and which, after firing, is covered in a glassy matrix. As these dielectrics have very limited flexibility and vibration resistance, the concept was rejected.

(d) Composite Wires: The composite insulation approach was finally chosen as the most practical way to design a wire which would meet the program performance requirements, as it offered a starting point based on previously disclosed approaches, and a high potential for significant technological advances. Furthermore, the need for a general purpose wire would be best served by a composite construction which would potentially use a high proportion of commercially available materials.

3. SUBCOMPONENT MATERIALS EVALUATION

3.1 Conductor

Since the program objective was for a general purpose high temperature wire, it was decided that the finished wire should preferably incorporate a commercially available conductor having suitable tensile strength, electrical properties and thermal stability.

A thorough literature review of potential materials was completed, resulting in the selection of the following conductor combinations for intensive study:

- (a) Nickel or nickel alloy clad copper
- (b) Nickel clad, diffusion barrier overcoated copper
- (c) Stainless steel clad copper
- (d) Nickel or nickel alloy clad silver
- (e) Dispersion strengthened copper

Selected manufacturers were canvassed to obtain samples for heat stability testing. Material (c) was only available with a 66% cross section area sheath and was rejected as having poor electrical characteristics; no sample of dispersion strengthened copper could be obtained. Short lengths of the remaining candidates were heat aged for 1000 hours at 1250°F, samples being removed at set times during exposure for subsequent mounting, etching, and metallographic examination.

Considering each of the conductor configurations, nickel clad silver after 1000 hours showed no diffusion zone between core and sheath, although there was a slow continuous development of surface oxide which spalled on removal from the furnace. Significant grain growth occurred in both the core and cladding.

Nickel alloy clad silver showed no surface oxide growth or interfacial diffusion after 1000 hours. Significant grain growth had occurred in the silver, but the sheath remained grain-free.

Nickel clad copper exhibited substantial diffusion between the cladding and core after 1000 hours. There was slight surface oxidation. Both the clad and core had substantial grain growth, although the wire remained flexible and the sheath adherent.

Nickel alloy clad copper showed no evidence of surface oxidation, although there was evidence of copper diffusion into the cladding which resulted in microcracking. There was no noticeable grain growth in the sheath but massive grain development in the core.

The nickel clad, diffusion barrier coated copper failed within 500 hours due to catastrophic failure at the core sheath interface.

The nickel clad copper, nickel clad silver and nickel alloy clad silver candidates were selected for further examination. Electrical resistivities and tensile strengths were determined on both the unaged and fully aged samples. The results are shown in Table II.

TABLE II

PERFORMANCE CHARACTERISTICS OF
CANDIDATE CONDUCTORS

Conductor	Wire Diam. (cm)	Resistivity		Change		Tensile Strength Change	
			(microhm-cm)	%		(psi)	%
Nickel clad silver	0.0635	A	1.97			35,300	
		B	1.90	-3.4		24,000	-32.0
Nickel alloy clad silver	0.102	A	2.39			45,700	
		B	2.41	+0.83		42,300	-7.4
Nickel clad copper	0.206	A	2.25			38,800	
		B	2.59	+15.0		32,400	-16.5

A: Sample, as received
B: After 1000 hours at 1250°F

Based on these evaluations, the nickel alloy clad silver was chosen as the preferred candidate conductor. A survey of selected commercial wire manufacturers failed to find a source of this wire; a contract was finally let to the Reuter Stokes Company Ltd. of

Cambridge, Ontario, Canada, who have expertise in drawing nickel alloy tube for nuclear applications. Five prototype Inconel 600 oversheathed fine silver wires of nominal 12 AWG were received for evaluation of both production techniques and the effect on performance of varying the core/clad ratio from the first candidate wire (75/25 cross section area ratio) to a 50/50 ratio. Based on further determinations of thermal stability, electrical resistivity and tensile strength, a design having a 60% cross section area fine silver core and a 40% cross section area Inconel 600 sheath was selected as the best compromise, and a further prototype was obtained for evaluation. This sample showed the same exceptional level of thermal stability, ambient electrical resistivities of $\sim 2.7 \times 10^{-6}$ ohm-cm and ambient tensile strengths before and after ageing of $\sim 57,000$ psi. Prototype 18 AWG and 22 AWG wire to the same configuration also was well within specification requirements. The design was established as the prime candidate conductor for the remainder of the development program.

3.2 Dielectric

3.2.1 Introduction

As was described in Section 2, a number of commercial wires were obtained and evaluated for their potential usefulness at 1250°F. None performed sufficiently well to warrant extensive testing. Physical deterioration of the insulation was marked usually by embrittlement or complete disintegration. As the majority of the assemblies were heavily impregnated with silicone polymers, there was heavy exudation of silica fume. Weight losses after thermal exposure were generally high, with marked susceptibility to moisture absorption.

It was concluded that the wires had no potential for cyclic performance requirements but that a few were possibly valuable for a single exposure situation. The general method of assembly did, however, reinforce the basic decision to pursue a composite layered dielectric approach, which gave excellent initial flexibility, high dielectric strength to volume ratio, and the use of a significant proportion of commercially available components.

3.3.2 Candidate Dielectric Selection

A general literature review was made to determine which materials would be suitable for use as one or all of the dielectrics in the wire design, considering the following restrictions: (a) thermal stability significantly in excess of 1250°F, (b) insignificant weight change, relatively non-absorptive and have little tendency to smoke or exude, (c) available in an easily handleable form and in thin section, (d) a high dielectric strength to thickness ratio, and (e) stable in the cyclic environment specified in the Statement of Work.

Combining this review with the materials disclosed in other contract approaches, the following candidate materials were selected for further study: asbestos, alumina, silica, alumina-silica, stabilized zirconia, boron nitride borosilicate glass, mica, beryllia and silicon nitride. Table III correlates the potential candidate dielectric materials with the forms in which they are commercially available. The review also suggested that for ease of application the most logical forms would be yarns, cords, wools or sheets. It was decided to eliminate all other candidate forms; wools were also rejected due to their inherent fragility, difficulty of application and low dielectric strength per unit thickness.

TABLE III

FORMS OF COMMERCIALY AVAILABLE CANDIDATE DIELECTRIC INSULATIONS

Material Form	Asbestos	Alumina	Silica	Alumina/ Silica	Zirconia	Boron Nitride	Glass	Mica	Beryllia	Si ₃ N ₄
Yarn			X	X		X	X			
Cord	X		X	X		X	X			
Cloth			X	X	X	X	X			
Sheet	X	X		X	X	X	X	X		
Wool	X		X	X	X	X	X			
Solid	X	X	X	X	X	X	X	X	X	X

Considering the remaining materials, asbestos was rejected due to its lack of product uniformity, low dielectric strength and its susceptibility to weight and phase changes in the range of the program service temperature. Alumina was only found available in board and was also found to need significant and impractical densification to achieve optimum performance properties. Silica and alumina-silica are excellent high temperature thermal and electrical insulations which, when appropriately stabilized, have a continuous service ceiling well in excess of 1250°F. Being available in yarn and cord, these products were retained as potential secondary dielectrics. Zirconia was rejected as it was only available in stiff board. Boron nitride was found to be sensitive to humidity which affected its dielectric strength, and to require densification for optimum performance. Mixed glasses were rejected as in general they are susceptible to deteriorative phase changes in the range of the program service temperature. Highly specialized mixed glasses, such as "S" and "Z" grades, were briefly considered but were not available in useful yarn or cord diameters. Beryllia and silicon nitride were immediately rejected as they were only available as solids. The remaining candidate material, mica, has an excellent combination of thermal stability and high dielectric strength versus thickness ratio. Further, as a reconstituted fine particle size paper, it also has excellent flexibility. However, in this latter form, mechanical strength is weak and is a direct function of moisture content, thus necessitating the addition of binders to achieve optimum performance. Mica was retained as a potential candidate primary dielectric.

Screening tests were performed on a large number of potential candidate yarns and cords fabricated from silica and silica-alumina, as well as on various commercial types of reconstituted mica paper. Selected examples are listed in Table IV, and serve to show the general trend of performance. As described in Appendix A, moisture absorption, weight change, mechanical handling characteristics, tensile strength and dielectric strength were all evaluated in an effort to rate the material's performance.

Of the yarns and cords tested, refractory silicas and the chromia stabilized silicas offered the best overall combination of initial and retained performance and were chosen as candidates for secondary dielectrics or protective braids in the prototype wire design.

Of all the materials evaluated as potential primary dielectrics, mica was considered to offer the best combination of dielectric strength and potential mechanical properties coupled with being available in thin enough section to result in an assembly with a potentially good space factor. In particular, mica paper of nominal 0.002 inch thickness made from very small flake was particularly satisfactory and was

selected as the preferred candidate primary dielectric. However, in its raw state, this product had poor tear strength, was susceptible to creasing, and disintegrated in high humidity.

Various commercial impregnated mica papers and backed, impregnated mica papers were obtained and examined and, while they had significantly improved initial mechanical and electrical performance characteristics, they exhibited high weight losses, poor mechanical strength, heavy smoking and fume evolution and poor retained dielectric strength after exposure to 1250°F.

From these results it was concluded that a new impregnation approach for mica paper was needed that would overcome these deficiencies. Three approaches were considered:

- Impregnation with easily pyrolyzed organic polymers.
- Impregnation with inorganic salts.
- Impregnation with inorganic polymers.

Impregnation with organic polymers was quickly rejected as it was realized that, although the polymer bound mica sheet would have significantly superior initial handling characteristics, exposure to 1250°F would result in generation of smoke and carbonization and the mica paper would ultimately revert to its initial raw and fragile state within the wire. Some effort was expended in attempting to reduce the susceptibility of silicone polymers to evolve copious silica fume on pyrolysis, to no avail.

Much time was spent in attempting to develop binders based on in-situ formation of oxides of selected metals from salts impregnated into mica papers. Among the materials evaluated were alkyl silicates, poly(silicic acids) and acid esters, titanium esters and poly(titanates), zirconium salts and organo zirconium esters, boron salts both alone and in admixture with phosphates, chromium phosphinate polymers and inorganic polymers of alkyl tin oxides.

These experiments can be summarized very briefly. The majority of the salts and adducts were difficult to incorporate as they were generally prepared in aqueous solution and damaged the integrity of the mica paper during impregnation.

The inorganic salts generally caused increased moisture absorption, higher weight losses and only marginal improvements in initial tensile strength and mechanical handling properties. After exposure to 1250°F, the composites had very poor handling characteristics, significant loss of tensile strength and poor retained dielectric strength.

TABLE IV
PERFORMANCE CHARACTERISTICS OF SELECTED CANDIDATE DIELECTRIC MATERIALS

Material	Form Tested	Moisture Absorption		Weight Change (%)	Handling Properties		Tensile Strength		Dielectric Strength	
		Before Exposure to 1250°F (%)	After Exposure to 1250°F (%)		Before 1250°F	After 1250°F	Before 1250°F (lb)	After 1250°F (lb)	Before 1250°F (volts/mil thick)	After 1250°F (volts/mil thick)
Refractory silica	Yarn/cord	5-12	5-8	1.5-3.0 loss	Good flexibility & abrasion resistance		5-10	5-10	-	-
Refractory silica chromia doped	Yarn/cord	1.5-4	0.5-5	1.5 loss	Good flexibility & abrasion resistance		5-15	5-15	-	-
Fused quartz	Yarn	0.5	0.05	0.1 loss	Good flexibility & abrasion resistance. Significant deterioration on thermal exposure		5-10	5-10	-	-
Alumina/silica	Yarn	3.0	0.05	20.0 loss	Good flexibility & abrasion resistance. Significant deterioration on thermal exposure.		2.5-5.0	2.5-5.0	-	-
Reconstituted mica	Paper	0.1	0.1	0.1 loss	Excellent flexibility, poor abrasion & tear strength		1.5-2.0	1.5-2.0	1.5-2.0	1.5-2.0
Alumina/silica	Paper	0.5-1.0	0.5-1.0	4-7 loss	Excellent flexibility, poor abrasion & tear strength		1.5-2.0		1.5	1.0

Upon completion of the various series of experiments which studied different approaches to impregnating the candidate mica primary dielectric, it was concluded that, although the studies had revealed some interesting combinations of materials, none were suitable for use as a flexible, high temperature resistant dielectric. Concurrently, although commercial silicone impregnated mica papers and tapes had excellent initial properties, their postfired characteristics showed significant deterioration coupled with fuming and exudation during initial high temperature exposure. It was felt that if an organometallic polymer similar to a silicone resin could be identified, having good initial performance properties, while retaining a significant measure of these without fuming or exudation, this material, in combination with mica paper, would probably result in a satisfactory primary dielectric. Accordingly a literature review was made to gain familiarity with the chemistry and to act as a guide to further evaluation.

Within the past twenty years there has been a concerted effort to develop practical "inorganic polymers" with the general target being thermal stability and resistance to oxidation and hydrolysis. One approach has been to develop homochain inorganic polymers which show comparable performance to organic equivalents; however, the internal bond strength of organic polymers is so significantly superior to their inorganic analogs that little success has been reported. Efforts to develop heterochain polymers have met with more success, however, the bonds in these polymers, while in many cases stronger than organic analogs, are equilibrium dependent rather than kinetically influ-

enced. Thus the susceptibility for molecular rearrangement is high and this type of deterioration is frequently more objectionable than oxidative charring.

Among the most popular elements incorporated into inorganic polymers are boron, oxygen, and phosphorus and nitrogen. In many instances silicon-oxygen linkages are an integral part of the polymer backbone which tends to yield materials similar to the silicone resins. If a proportion of the silicon is in turn substituted by another element, yielding polymetallaxanosiloxanes, some measure of improved thermal stability is achieved.

One approach to this has been the subject of intensive research for the last 10-15 years under sponsorship by various U.S. Government agencies, and has led to the development of thermally and chemically stable polymers containing boron as an essential element. The chemistry of these polymers is both complex and sophisticated; the extensive literature on the subject has been admirably compiled by the National Technical Information Service under the title Polycarboranes (NTIS/PS-75/554). For the purposes of this paper it is sufficient to say that a poly(carborane) is basically a silicone polymer in which has been introduced a highly stable and protective cage composed of either 5 or 10 boron atoms (Figure 1). The net effect of this substitution is a significant increase in thermal stability with a concurrent reduction in smoke and fume evolution. Poly(carborane siloxanes) have found some use in stationary phases for gas chromatography and experiments have shown them to be useful as coatings and gasketing up to 1000°F.

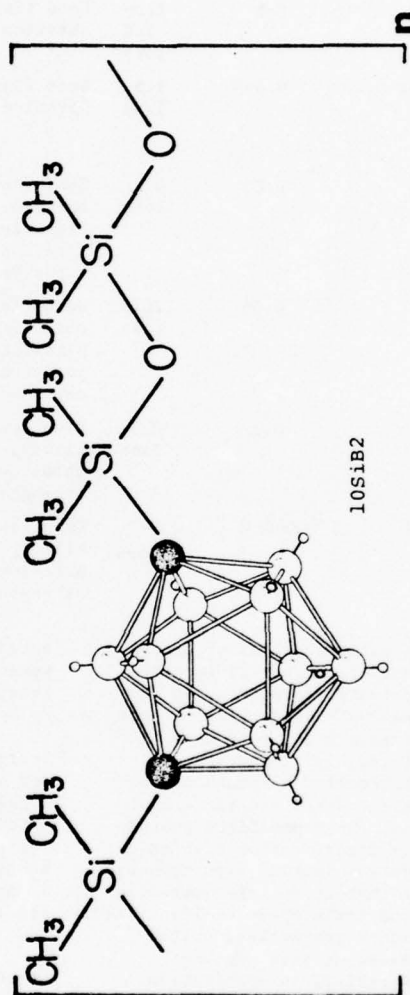
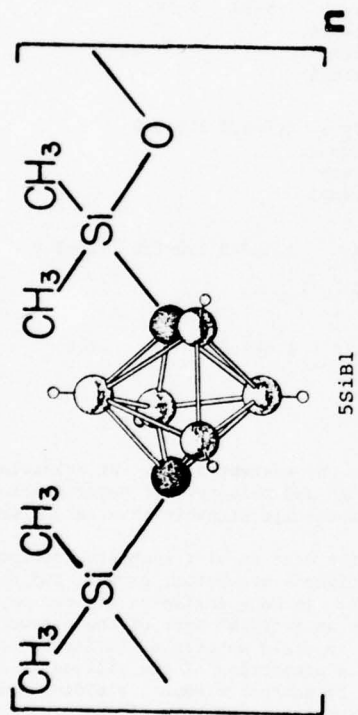


Figure Representative carborane-siloxane polymer structure

As an initial evaluation of these most promising of the organometallic polymers, samples were procured and characterized by differential scanning calorimetry and thermogravimetric analysis. Representative results are shown in Table V. It can be seen that there is a significant improvement in resistance to oxidative degradation. These polymers offer the further advantage of being soluble in common aromatic solvents, thus allowing easy incorporation into an absorptive substrate such as mica paper.

TABLE V

THERMAL ANALYSIS OF SELECTED POLY(CARBORANES)
(Temperature 25 to 600°C)

Material	Onset of Weight Loss in Air °C	Total Weight Loss %
10 boron containing	250-300	5-15
5 boron containing	150-250	~10
Poly(siloxane) control	125-175	25-75

Using a development sample of a decaborane siloxane polymer solubilized in xylene as impregnant, a brief series of experiments was undertaken using 0.002 inch thick mica paper to determine if the use of these materials had any merit. Completely unexpectedly, the initial samples showed an outstanding combination of performance properties, most of which showed significantly less property degradation after exposure to 1250°F. As can be seen in Table VI, a representative number of poly(carborane siloxane) impregnated mica tapes have, at substantially lower loadings of polymer, a combination of performance properties which make them highly attractive for use as the primary dielectric. It should also be mentioned that these tapes have no supportive backing, whereas the control has unidirectional glass filament, and that there is no detectable smoke or fume given off by these materials during pyrolysis.

Following this initial success, considerable effort was expended to optimize polymer loadings and cure schedules to achieve a tape which was successfully used as the primary dielectric in the first prototype high temperature resistant wire. It is believed that this poly(carborane) impregnated mica tape represents the first in a whole new family of novel high temperature stable mica insulation.

3.3 Armour

After due consideration of other reported approaches to wire armouring, a tubular knitted mesh outer sheath was chosen, for optimum flexibility with abrasion resistance. This was especially important in light of the fact that it was intended to overlay the multiple layers of poly(carborane) impregnated mica tape with an outer braid of refractory yarn. Oxidation resistance was achieved by using a 24 AWG Inconel 600 wire.

Although braided sheathing was not completely rejected, to achieve a metallic braid armour which would be both flexible, light in weight and non-abrasive to the layers below would necessitate braiding at a low percentage coverage; this would run the risk of displacement on flexing or vibration resulting in gaps

in the armour. Failure of any of the strands in the braid would tend to weaken the whole braid in that plane as the wire worked free, whereas a break in the knit at any spot would cause minimal damage as a knit structure failure tends not to propagate.

Evaluation of both the 24 AWG knit wire and a lighter 36 AWG wire showed minimal oxidative degradation over 1000 hours at 1250°F, with no significant loss of tensile strength or flexibility. Thus the Inconel knit was considered satisfactory for use as the prototype overarmour.

4. PROTOTYPE WIRE ASSEMBLY

Twenty-five feet of 12 AWG Inconel 600 sheathed fine silver wire was overbraided with a single layer of refractory silica yarn on a Wardwell braider, giving a pick count of ~25 per inch. This in turn was overlaid with four layers of poly(carborane) impregnated, unbacked, 0.002 inch thick mica paper applied as a 0.25 inch wide tape, helically butt wound with a 25% advance. This in turn was overlaid with a second braid of refractory silica yarn at a pick of ~16 per inch. The armour was then knitted in place using 24 AWG Inconel 600 wire.

5. PROTOTYPE WIRE PERFORMANCE

Table VII compares the performance of the prototype wire with the requirements detailed in the Statement of Work. It can clearly be seen that this wire design meets or exceeds virtually all of the specifications.

6. CONNECTOR DEVELOPMENT, PHASE I

As mentioned at the beginning of the paper, the connector design and development was subcontracted. The Phase I effort on behalf of this subcomponent was limited to the choice and evaluation of materials for the connector and establishment of a prototype design for fabrication in Phase II. This program was successfully completed.

7. PROGRAM STATUS 1976

The mandate for Phase II was to optimize the prototype units and prove the commercial feasibility of volume production. This has largely been achieved.

A complete family of conductors from 12 AWG through 22 AWG inclusively has been fabricated in long lengths (>100 continuous feet) and certified.

Braiding of both the inner and outer refractory yarn layers has been optimized and proven for long lengths on commercial equipment.

A refractory yarn having significantly improved performance to the preferred Phase I material has been identified and successfully substituted.

The primary dielectric poly(carborane) impregnated mica tape has been optimized in bench studies; pilot trials are scheduled shortly.

The overarmouring has been optimized as to wire diameter and loop size; long lengths of armour have been successfully knitted.

Four conductor cable has been fabricated and successfully tested.

TABLE VI
COMPARATIVE PERFORMANCE OF SELECTED POLY(CARBORANE) IMPREGNATED MICA TAPES

Sample	Impregnant Load % w/w	Moisture Gain %			Mechanical Handling		Tensile Strength (psi)		Dielectric Strength Kv/mil thick		Comments
		Before	After	Weight Change	Initial	Retained	Initial	Retained	Initial	Retained	
		Exposure to 1250°F									
A	3.0	~0	0.48	-0.7	Excellent	Very good to excellent	7,000	12,400	2.25	2.00	No flaming, no fuming
B	5.5	0.1	0.45	-0.5	Excellent	Very good to excellent	7,500	9,600	2.21	2.21	No flaming, no fuming
C	15.2	0.4	0.50	+0.2	Excellent	Very good	15,100	11,800	2.05	2.10	No flaming, no fuming
Control poly (siloxane) commercial 0.002" tape	~23	0.16	1.8	-14.5	Excellent	Poor	27,000	820	>2.6	1.0	Heavy smoke, flame & silica fume

TABLE VII
PERFORMANCE OF PROTOTYPE WIRE

Test	Specification	Prototype	
Conductor resistivity (microhm-cm)	<6	12 AWG	2.72
		22 AWG	2.76
Tensile strength (psi)	35,000	12 AWG	58,900
		22 AWG	54,000
Insulation resistance (megohms/ft)	>1 @ 1250°F		1.3
Dielectric strength (KV/AC)	1.2 under all conditions		2.0 - >5.0
Mandrel flex	D20X wire diameter		Passed
Thermal shock resistance	MIL STD 202D		Passed
Vibration resistance	10-2000 cps 20G		Passed
Mechanical shock resistance	50 G 11 ±1 millisecond		Passed
Abrasion resistance	-	Failed at 30 inches of garnet tape	
Flame resistance	Fed. STD 228, #5211		Passed
Life cycle	As specified Statement of Work	Passed >10 cycles. Full cycle planned Phase II.	
Flex & flex fatigue	20X wire diameter		Planned Phase II
Blocking	-		None
Shrinkage	0.06 inches		None
Sublimation	Specify under all conditions		Minimal

Prototype connectors have been fabricated and successfully certified, using the design and materials information developed in Phase I.

The connectors have been found fully compatible with the wire conductor and insulation package. Successful termination of insulated wire to the connector has been demonstrated.

Full certification testing is underway and shows every indication of success.

Although this program was intended to develop an aerospace wire and connector system, it has become obvious from continued experimentation that there are many other potential end use applications which could benefit from the unique combination of performance properties inherent in this design. It has been found, for example, that the wire is fully capable of carrying in excess of 2 KV for over 8 hours in an 1800°F environment and after cooling and flexing over a mandrel of 10-20X continuing to carry the voltage for a further extended period of time.

The components have been established as completely stable for an extended period of time in high radiation areas.

Even under very severe direct flame conditions the cable does not propagate and releases minimal levels of fume.

These experiments suggest immediately applications in nuclear facilities, rapid transit systems, shipboard wiring, commercial aircraft, chemical plants, institutional and high rise wiring and emergency control and lighting systems among others. An ongoing program has been mounted to explore these possibilities.

Full details of the Phase I program have been published and are available from the U.S. National Technical Information Service under the code AD N74-786890/4GA.

ACKNOWLEDGEMENTS

We extend our thanks to the Air Force Aero Propulsion Laboratory, Wright Patterson Air Force Base, and to Canada Wire & Cable Limited for permission to publish this paper. We also wish to thank our associates who contributed to the development of the system.

APPENDIX A

SHORT TERM TEST CYCLE FOR MATERIALS EVALUATION

1. All samples handled in platinum crucibles.
2. Record weight of crucible (W1).
3. Bring to constant weight at 200°C, record (W2).
4. Expose to 100% R.H./77°F for 1 hour, record (W3).
5. Expose to 1250°F in air for 55 minutes, cool for 5 minutes; expose to 1250°F for 60 minutes; cool to room temperature, record (W4).
6. Expose to 100% R.H./77°F/or 1 hour, record (W5).

% moisture gain before exposure to 1250°F

$$\frac{W3 - W2}{W2 - W1} \times 100$$

% moisture gain after exposure to 1250°F

$$\frac{W5 - W4}{W4 - W1} \times 100$$

% weight change after exposure to 1250°F

$$\frac{W4 - W2}{W2 - W1} \times 100$$

In all instances where another characteristic, i.e. handling, is reported "after 1250°F exposure", it is performed on the sample after this test cycle.

F.D. Bayles (Speaker)
Canada Wire & Cable Technology Development Department
Noranda Research Centre
240 Hymus Boulevard
Pointe Claire, Quebec, Canada

A graduate of Sir George Williams University, Montreal, Mr. Bayles has had extensive experience in the organic coatings field. He joined the Noranda Research Centre in 1971 where he has specialized in the application of polymer technology to wire and cable development. Mr. Bayles is a Group Leader in the Technology Development Department.

M.A. Dudley

Dr. Dudley gained a Ph.D. from the National College of Rubber Technology, London, England in 1967. After experience in the plastics industry, he joined Noranda Research Centre in 1970 as Department Head of the Technology Development Department. Dr. Dudley is presently Manager of Technology for Canada Wire & Cable Limited.

ALUMINIUM WAVEGUIDE
WITH
ALUMINIUM OXIDE DIELECTRIC LINING

Friedrich Krahn
Felten & Guillaume Carlswerk AG
Cologne
West Germany

SUMMARY

In an optimum millimetric waveguide system dielectric lined waveguides with a certain percentage of helix waveguides are used. To avoid peeling of the dielectric layer a new waveguide has been developed. It consists of an aluminium tube of 70 mm diameter lined with aluminium oxide and fitted with precision flanges.

The tube production steps are extrusion, drawing and straightening. The geometrical tolerances of the tubes, in particular, the critical axis deviation, are sufficiently small. The dielectric oxide layer is produced by "hard coating", an electrochemical process. This layer has excellent mechanical and satisfactory electrical properties. The tube length is 5 m.

The waveguide has excellent mechanical properties, e.g., bending radii < 60 m are possible without permanent deformation.

Theoretical calculations and electrical measurements show that this waveguide has an attenuation < 1.5 dB/km in the frequency range between 35 and 110 GHz.

INTRODUCTION

A millimetric waveguide suitable for long distance transmission consists of a round conducting tube, the inner diameter of which is usually between 50 and 70 mm. The waveguide is operated in the low-loss TE_{01} mode in a frequency range between 30 and 110 GHz. The attenuation of the waveguide increases

by conversion of the TE_{01} mode into undesired modes. To reduce this conversion two kinds of waveguides are used:-

- a dielectric lined waveguide consisting of a tube, the inside of which is highly conductive (Cu or Al) and coated with a dielectric layer

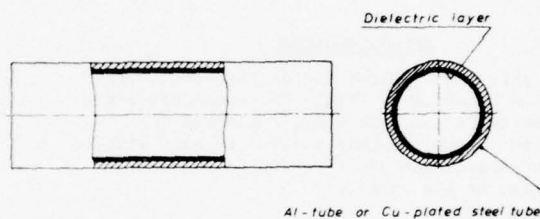


Fig. 1 Construction of a dielectric lined waveguide

- a helix waveguide consisting of a tube made by a helically wound copper wire surrounded by a dielectric shield. A cladding is provided for mechanical purposes.

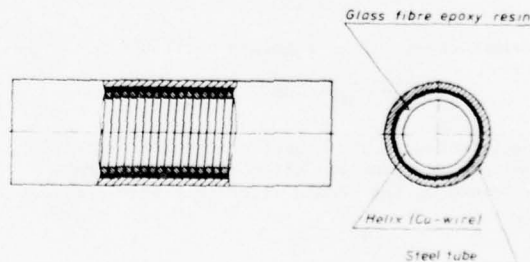


Fig. 2 Construction of a helix waveguide

The electrical attenuation of a waveguide is caused by:-

- the finite conductivity of the inside of the tube
- the dielectric lining
- the geometrical imperfections of the tube, especially the inner axis curvatures
- the misalignment of the tube couplings.

The typical TE_{01} attenuation as a function of the frequency is shown in Fig. 3.

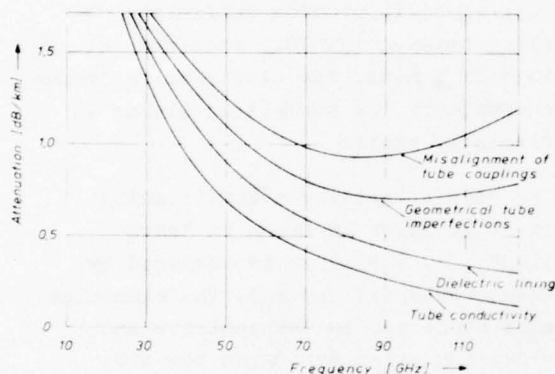


Fig. 3 Typical TE_{01} attenuation in a millimetric waveguide

An optimum waveguide line is a hybrid system consisting of dielectric coated waveguides with a certain percentage of helix waveguides. A capacity up to 500 000 voice circuits and a repeater spacing up to 50 km can be reached.

In a conventional dielectric lined waveguide peeling of the lining and thus a reduction in the service life may occur. To avoid this effect a new waveguide has been developed.

TUBE PRODUCTION

As tube material a malleable AlMgSi alloy was chosen (aluminium with small additions of magnesium and silicon).

The first production step is extrusion: from an aluminium block a preformed tube is pressed with an inner diameter and wall thickness somewhat larger than the corresponding dimensions of the finished tube. Nevertheless, the preformed tube must have a uniform wall thickness and diameter.

This preformed tube is drawn in two steps, so that a tube is obtained with the final dimensions:

inner diameter 70 mm
wall thickness 4 mm.

This tube has a uniform wall thickness. Although cross-section fluctuations (diameter deviation, ellipticity, 3rd order deviations) are sufficiently low, the required straightness is not obtained.

With a straightening machine the following problems had to be solved:-

- how to obtain the required straightness
- how to keep the periodical tube-diameter deviations caused by the straightening rolls sufficiently small.

The best type proved to be a 6-roll straightening machine (1). The machine was built specially for the production of waveguide tubes. The profile of the straightening rolls was exactly adapted to the 78 mm outer tube diameter. A mean effective bending radius > 3000 m and periodic deviations $< 1 \mu$ m (peak to peak) were obtained with this machine.

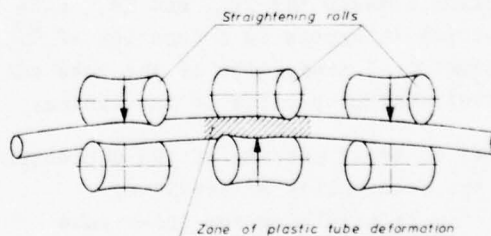


Fig. 4 Principle of a 6-roll straightening machine

DIELECTRIC LINING

In unlined round waveguides the phase constants of the TE_{01} mode and the undesired TM_{11} mode are equal. A complete conversion between these modes thus occurs and long distance transmission is possible.

The TE_{01} and TM_{11} modes are decoupled by a dielectric layer inside the tube.

$$\frac{\Delta\beta}{\beta} = A \cdot \frac{\epsilon_R - 1}{\epsilon_R} \cdot d^{(2)} \quad (d \ll \alpha)$$

β = Phase constant of the TE_{01} mode, $\beta = \frac{2\pi}{\lambda}$
 $\Delta\beta$ = Difference of phase constants between TE_{01} and TM_{11} mode

A = Constant factor

ϵ_R = Relative dielectric constant of the layer

d = Layer thickness

α = Inner radius of the tube

The dielectric layer causes losses of the TE_{01} mode

- inherent losses in the layer

$$\Delta\alpha_1 = B \cdot \epsilon_R \cdot \tan \delta \cdot f^2 \cdot d^3 \quad (d \ll \alpha, f \ll f_c)$$

$\Delta\alpha_1$ = Additional loss

B = Constant factor

$\tan \delta$ = Loss factor of the layer

f = Frequency of the TE_{01} mode

f_c = Cut-off frequency of the TE_{01} mode

- losses due to the influence of the layer on the electric field

$$\Delta\alpha_2 = C \cdot (\epsilon_R - 1) \cdot f^2 \cdot d^2 \quad (2)$$

$\Delta\alpha_2$ = Additional loss

C = Constant factor

Because of these losses the layer must not be too thick. To provide sufficient decoupling between the TE_{01} and TM_{11} mode the optimum thickness is a function of the geometrical properties of the tube and the electrical properties of the lining.

In order to avoid peeling of the dielectric layer the possibility of providing the lining by oxidizing the inner tube surface was studied.

The mechanical properties of the oxide layer are excellent. The hardness is greater than that of steel, the melting point higher than 1000°C and peeling of the layer practically impossible.

The electrical properties of the oxide layer are satisfactory. The loss factor ($\tan \delta$) was measured as $3 \cdot 10^{-2}$ for waveguide frequencies. This value is high compared with other dielectric materials, i.e., polyethylene ($\tan \delta \approx 2 \cdot 10^{-4}$), but as the dielectric constant is as high as 8 the layer thickness may be $< 100 \mu\text{m}$ and the lining still provide sufficient decoupling between the TE_{01} mode and the undesired TM_{11} mode. The electrical attenuation caused by the dielectric lining is sufficiently small.

The process of getting a sufficiently thick oxide layer is known as "hard coating" (3). The layer is obtained by an electrochemical process. The aluminium tube is connected to the positive and an aluminium cylinder inside the tube to the negative pole of a current source. A refrigerated electrolyte is pumped through the tube.

The uniform thickness of the layer ($\pm 2 \mu\text{m}$) was obtained by preliminary treatment of the inner tube surface, exact centering of the internal cylinder and pumping the electrolyte at sufficiently high speed through the tube.

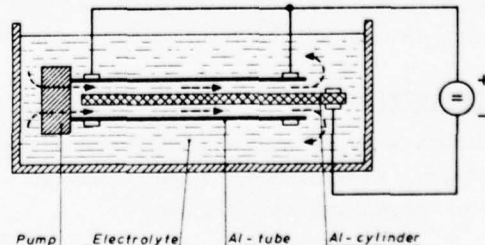


Fig. 5 Principle of the hard coating process

TUBE COUPLINGS

The average tube length is 5 m. To avoid mode conversion by periodical geometric distortion the tube length in a waveguide line will be statistically between 4.80 and 5.20 m.

The tubes are coupled by "unit flanges" developed by the German Post Office Research Centre (Fernmeldetechnisches Zentralamt) together with several German companies. They consist of precision screw collar rings screwed on the tube ends and bonded with an adhesive. The couplings are adjusted by a centering ring and fixed by screws.

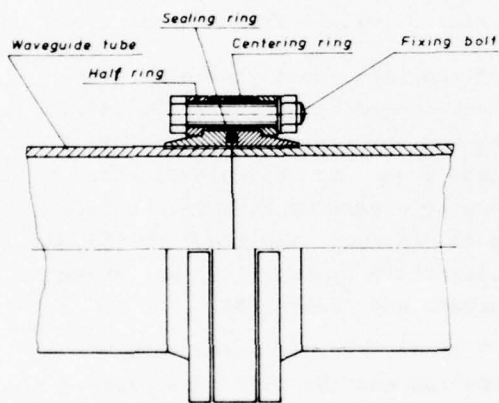


Fig. 6 Unit flange waveguide coupling

MECHANICAL MEASURING EQUIPMENT

Three kinds of tube properties were measured:-

- cross-section fluctuations
- straightness deviations
- lining thickness fluctuations.

All the measuring probes operate continuously. They are pulled at a constant speed through the tube by an electric motor.

CROSS-SECTION FLUCTUATIONS

A mechanical scanning probe was used. The relevant movement of two opposed feelers scanning the diameter is trans-

mitted to an inductive displacement pick-up which gives an electrical signal proportional to the distance of the feelers. The amplified signal is recorded. Diameter deviations of about $0.2 \mu\text{m}$ can be detected. Ellipticity and deviations of higher order are measured by rotating the tube along the axis.

STRAIGHTNESS DEVIATIONS

The mechanical scanning probe consists of two connected sliding carriages. The angle between the longitudinal axes of the carriages indicates the curvature of the tube axis. The change in angle is transmitted to an inductive displacement pick-up. The electrical pick-up signal is amplified and recorded.

The precision of the straightness measuring equipment allows the detection of bending radii between 15 and 50 000 m. During one measurement run curvatures corresponding to radii even larger than 50 000 m can be detected.

This equipment also allows the measurement of the angular and axis misalignments between the tube couplings.

LINING THICKNESS

The measuring method is as follows:- A high frequency current is passed through a coil which has a distance from the layer defined by a mechanical scanning sapphire feeler. The magnetic field of the coil causes eddy currents in the aluminium and the amount of electrical energy extracted by eddy currents indicates the lining thickness.

The reproducibility of the measurements is $\pm 2 \mu\text{m}$. Thickness variations even $< 1 \mu\text{m}$ will be recorded during one measuring run.

MECHANICAL PROPERTIES OF THE WAVEGUIDES

- GEOMETRICAL TOLERANCES DUE TO MANUFACTURING PROCESS

The tolerances are summarized in the following table:

Diameter

Differences from tube to tube $\pm 20 \mu\text{m}$

Mean effective diameter deviation in each tube $< 5 \mu\text{m}$

Ellipticity

Systematical ellipticity

($d_{\text{max}} - d_{\text{min}}$) $< 30 \mu\text{m}$

Mean effective elliptic variation $< 5 \mu\text{m}$

Higher order cross section deviations $< 3 \mu\text{m}$

Straightness

Mean effective bending radius $> 3000 \text{ m}$

Couplings

Mean effective radial misalignment $< 50 \mu\text{m}$

Mean effective angular misalignment $< 1.5'$

Lining

Thickness $60 \mu\text{m}$

Thickness deviation $\pm 2 \mu\text{m}$

- GEOMETRICAL TOLERANCES DUE TO FORCED CURVATURES

As a practical waveguide line will contain bends with radii down to 100 m there will be a tube deformation caused by external forces. The influence of these forces on the tube was investigated:

- the elliptic diameter caused by forced curvatures
- the range of tube elasticity
- the range of coupling elasticity.

Results

- The ellipticity caused by forced curvatures is shown in the following table

R [m]	200	100	75	50	30	25	20
$\Delta_2 [\mu\text{m}]$	1	1	1	2.5	10	14	20

R : bending radius of forced curvatures

Δ_2 : contraction of minor tube axis [μm]

The ellipticity makes only a negligible contribution to the total attenuation.

- The tubes may be bent down to radii $< 30 \text{ m}$ without permanent deformation.
- The couplings may be bent down to radii of 50 m without permanent angular misalignment.

The results show that the waveguide tubes may be installed in practice in waveguide routes ($r_{\text{min}} \geq 100 \text{ m}$) without any deformation problems.

ELECTRICAL ATTENUATION CALCULATIONS

The calculation of the TE_{01} -attenuation due to random axis curvatures are based on studies carried out by Kettler (4) regarding the power density spectrum of the axial curvature frequencies.

The attenuation due to the other geometrical imperfections, the dielectric lining and the finite conductivity of the tube itself are calculated with a computer programme by Garlich (5), based on his own investigations (6), on investigations by Unger (7) and those by Janssen and Odemar (8).

Fig. 7 shows the calculated total attenuation and the different parts.

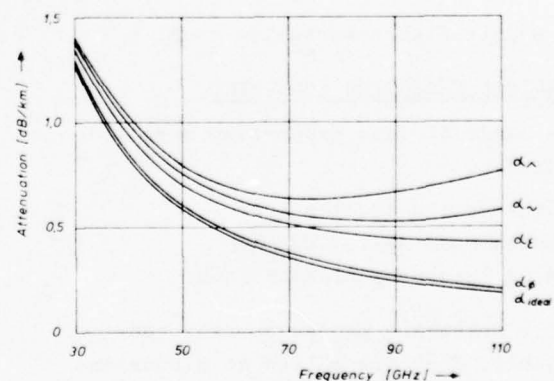


Fig. 7 Calculated TE_{01} -attenuation of the aluminium waveguide with aluminium oxide dielectric lining

- α_{ideal} = attenuation due to the finite conductivity of the tube
 α_{ϕ} = attenuation due to diameter deviations
 α_{ϵ} = attenuation due to the dielectric layer
 α_{\sim} = attenuation due to axis deviations
 α_{\wedge} = attenuation due to angular misalignment at couplings

Inner diameter : 70 mm

Thickness of dielectric lining : 67 mm

The attenuation is caused mainly by:-

- theoretical losses
- losses by the dielectric lining
- angular misalignment on couplings
- straightness deviations.

A difference between the calculated and measured attenuation may occur, as the property of the transition zone between the aluminium oxide lining and the pure aluminium is not known in sufficient detail. (Although it should be known from the loss-factor measurements.) This zone may cause a slight increasing of the attenuation.

Nevertheless, the total TE_{01} -attenuation should be far below 1.5 dB/km up to 110 GHz.

ELECTRICAL ATTENUATION MEASUREMENTS

The measurements have been carried out by the German Post Office Research Centre. The attenuation is determined by a shuttle pulse method.

The measurements which have been made up to now show an attenuation < 1.2 dB/km between 35 and 70 GHz^{*}). In this range theoretical and experimental values are nearly the same so that it may be assumed that the attenuation will keep this low value up to a frequency of 110 GHz.

^{*}) It may be possible to report the results at the conference for higher frequencies too.

CONCLUSION

An aluminium waveguide with an aluminium-oxide dielectric lining has been developed. As the electrical attenuation is below 1.5 dB/km between 35 and 110 GHz the mechanical properties are good. A peeling of the dielectric lining is practically impossible and the production costs are estimated to be not higher than for other dielectric lined waveguides so that the aluminium waveguide seems to be a well suited element for a millimetric waveguide system.

REFERENCES

- (1) A.N. Brown, "Selection of Cross Roll Straightening Machines for Rounds and Tubes" Iron & Steel International, August 1973
- (2) H.G.Unger, "Circular Electric Wave Transmission in a Dielectric Coated Waveguide" Bell Syst. Techn. Journ. 37, (1958), p. 1599 - 1647
- (3) H. Benninghof, "Fortschritte der Anodisieretechnik; Galvanotechnik 63, (1972)2, p. 169 - 174
- (4) G. Kettler, "Spektralanalyse regelloser Achskrümmungen in Hohlkabelrohren ... ", FTZ 452 TBr 28, December 1975
- (5) G. Garlichs, "Private Communication"
- (6) G. Garlichs, "Phasenkonstanten und Schwebungswellenlängen der Eigenwellen im dielektrisch beschichteten Rundhohlleiter", FTZ 333 TBr 24, November 1973
- (7) H.G.Unger, "Lined Waveguide", Bell Syst. Techn. Journ. 41, (1962), p. 745 - 768
- (8) W.Janssen and N.Odemar "Toleranzen bei Hohlleitern der Weitverkehrstechnik" Frequenz 26(1972)9, p. 258 - 265

ACKNOWLEDGEMENT

The author wishes to thank the German Post Office Research Centre, especially Mr. Richter, for the attenuation measurements and Mr. Garlichs and Mr. Kettler for the computer programmes to calculate the attenuation. Also his colleague Mr. Brumann for carrying out the mechanical measurements and his assistance in evaluating the computer data.

This research work was sponsored by the Minister of Research and Technology of the West German Government.



Friedrich Krahn graduated from the University of Münster in 1970 with a Dr. rer. nat. in Physics. He then joined Felten & Guillaume Carlswerk AG and was first engaged in the field of innovation and diversification. In 1973 he was appointed head of the department for the development of millimetric waveguides and optical communication cables.

Testing of Tensile Strength of Optical Fiber Waveguides

by

C. K. Kao

M. Maklad

T. Reed

ITT ELECTRO-OPTICAL PRODUCTS DIVISION
P. O. Box 7065
Roanoke, Virginia 24019

Introduction

The tensile strength of an optical fiber waveguide is an important parameter for cable design. It determines both the stress levels permitted along the fibers during cabling and during service. In general, strong fibers require less exacting cabling machinery design and allows more flexible choice of strength reinforcing material for making up a cable to meet specific strength requirements.

The tensile strength of an optical fiber waveguide is governed by the existence of a stress concentration along the fiber, such that fracture stress is reached at that point. Current evidences suggest that surface flaws are principally responsible for the development of high stress concentrations and that failure of a uniformly stressed fiber in tension occurs at the deepest surface flaw. Furthermore, in the presence of moisture or other polar vapors, the flaws over the fiber surface would enlarge under a stress level well below that of the fracture stress. This effect is known as fatigue or stress corrosion. The stress level, above which crack propagation takes place, is called the fatigue limit. Thus, if the service stress is higher than the fatigue limit it could lead to premature failure.

The measurement of fiber strength is complicated by the statistical variation of fiber strength along the length of a fiber. If sufficient data can be gathered such that the statistics of the large but rare flaws are characterized then extrapolation of statistical values of fiber tensile strength of one test gauge length to that of another gauge may be defined with known confidence limits. Otherwise, extrapolation is at best fortuitous. On the other hand, if the nature of the rare flaws are known, then more suitable testing techniques may be evolved. What is desired is to have test procedures which enable reliable long length strength to be predicted, while the procedures should be simple and should not destroy more fiber than necessary. The simplest method is to perform tensile test on short gauge length samples and process the results by assuming a Weibull distribution. The long length strength can be obtained by extrapolation. However, this method proves to be inadequate. This paper discusses these inadequacies and indicates by way of experimental evidences how an improved testing procedure could be developed.

Discussion

If the fibers are made by a consistent process, then the statistics of flaws is well defined. If there are more than one way for the flaws to be formed in that process, then the flaw distribution may be multimodal and the Weibull probability plot may assume an "S" shape. This situation was commonly found in many fibers. In that case the statistics of the rare large flaws are extremely important to be determined accurately, otherwise extrapolation for long length strength may lead to gross inaccuracies. If the flaws are caused by a single mechanism, then a linear Weibull plot results. In that case the extrapolation accuracy should improve even if the end values are not well defined.

The above argument leads to the following test procedure. From short gauge length tests the Weibull probability plot is constructed for a particular fiber, using

$$F = 1 - \exp [-(\sigma/\sigma_0)^m (L/L_0)(t/t_0)^r]$$

From the plot the Weibull parameter m is determined. In the case of a "S" shaped plot the determination of a valid m is in question.

Extrapolation of long length (L_2) strength from short length test results at a particular failure probability is given by

$$(\sigma_1/\sigma_2)^m (L_1/L_2) = 1$$

This can be substantiated by using a proof test at a stress equal to the expected stress where a given probability of failure will occur. For experimental purposes the proof stress chosen may be for a 50% probability of failure so that by testing a few lengths of long samples the extrapolation validity may be verified.

If m is not well defined then the choice of proof stress becomes difficult. In such cases proof tests must be carried out at different stress levels in order to determine the rare flaw distribution.

In the proof test it is necessary to take into consideration the stress corrosion effects. If the proof stress is applied over a considerable time the fiber strength will decrease. The permissible duration can be inferred from static fatigue failure data.

Sample Preparation and Test

The samples tested were prepared by drawing fibers of long lengths on a vertical tower using H_2-O_2 flames. The fibers were subsequently coated on-line with protective claddings to reduce the possibility of mechanical abrasion of the fiber surface.

The tensile strength on short gauge length was obtained by the following technique. A long sample was divided into the number of specimens to be tested of specific gauge length. A specimen was then mounted on the tensile tester (figure 1)

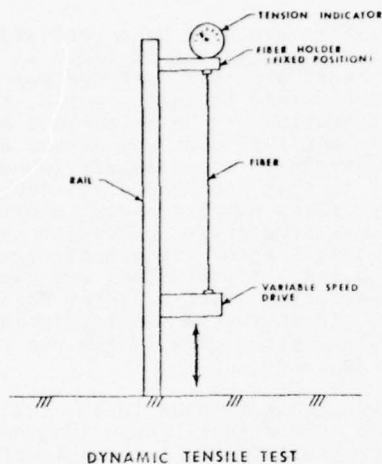


Figure 1

by looping one end around a large diameter spool ($d = 6''$) which was attached to a tensile gauge (0-200 lbs). The other end was threaded around another spool of the same diameter which was attached to a lever which was used to apply the load. The end of the fiber was then wrapped again around the first spool and attached. The load was applied instantaneously or at a known rate and the fracture load values read from the tension gauge.

The test for long gauge length tensile strength was as follows. The long length sample was held on a spool and reeled off between two large rollers as in figure 2.

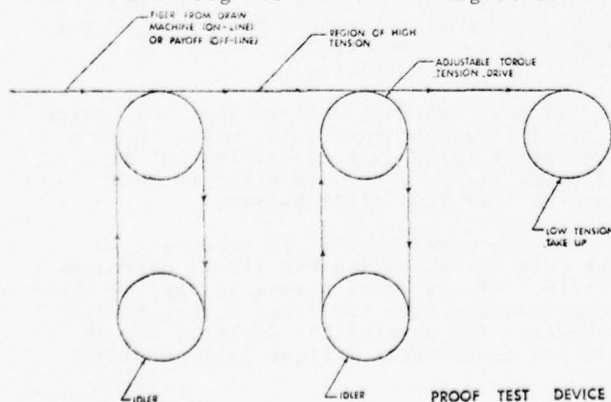


Figure 2

A tension gauge was used to measure the stress developed between the two rollers by a controlled slip clutch on the drive wheel. In this manner, the entire length of the sample can be tested.

Static fatigue tests were performed on short gauge length samples by applying a fixed load to the fibers which were mounted as in the short length tensile test. Times to failure were recorded.

Experimental Evidences

A typical Weibull plot for a short length gauge test of a fiber sample (A) made without special precautions is as shown in figure 3. This also shows an experimental

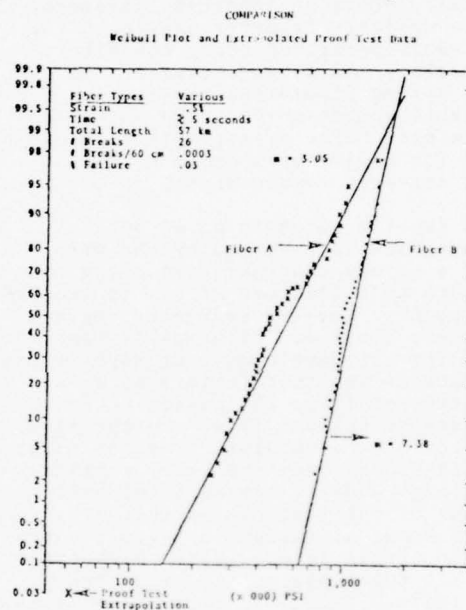


Figure 3

plot of long length strength test extrapolated to short gauge length. This clearly illustrates that, should the extrapolation be reversed, the predicted long length strength will be too optimistic.

A typical Weibull plot for a short length gauge test of a fiber sample made with special precautions is as shown in figure 4. It can be seen that the m value is greatly improved and that the Weibull plot is linear. Proof test at 200 kpsi showed no failure.

Static fatigue tests showed the time-to-failure for the same fiber (illustrated in figure 5) at different stresses. The m value was calculated from figure 5 and was found to be 26. If the fiber is subjected to a proof test load of about 1.9 times the service load for a duration of 10 seconds, the expected service life can be calculated.

$$T_2 = 10 \text{ sec} \left(\frac{1.9}{1} \right)^{26} = 2046 \text{ days}$$

At the proof test stress the fiber therefore

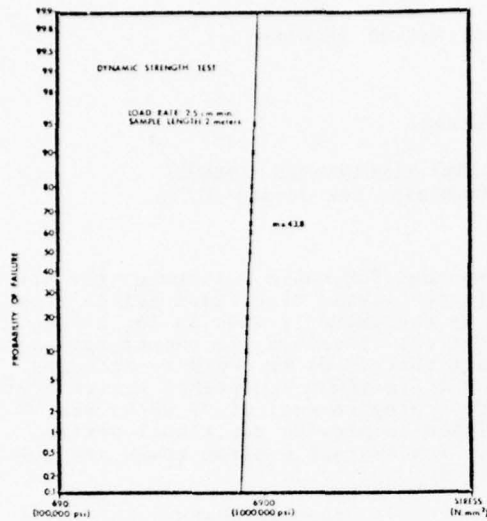


Figure 4

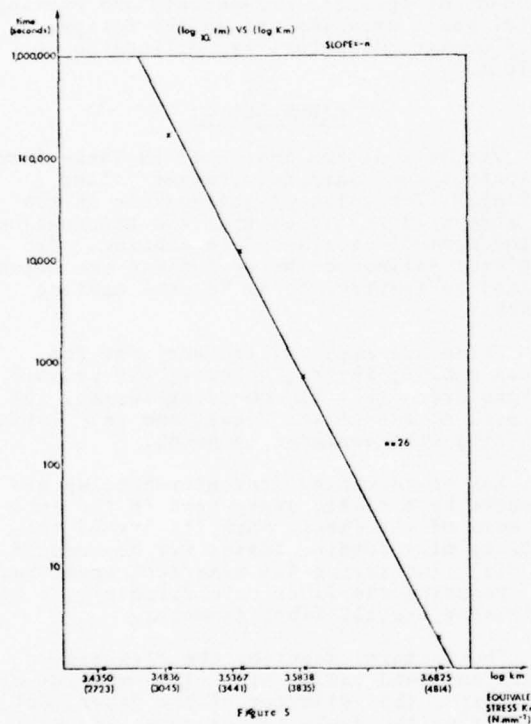


Figure 5

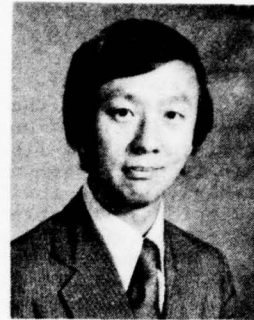
should suffer negligible degradation and can be employed safely.

Concluding Remarks

The extrapolation of fiber strength for a long length fiber from short length strength tests is reliable only if the flaw distribution is well characterized as in the case of a fiber made with special precautions. For a fiber with random flaws caused by several mechanisms, the extrapolation is unlikely to be reliable.

The test procedure which could be used to characterize fibers with specified

strength is to conduct short length test coupled with proof test at the required service strength. For fibers made for high strength this procedure allows high production yield as well as a guaranteed strength specification. For fibers made without special precautions this procedure could still be adopted but the fiber yield may be unacceptably low.



K. Charles Kao was born in China and received his BSc (Eng) and PhD degrees from London University. A pioneer of optical fiber communications, Dr. Kao has headed a team at STL, ITT's central research laboratory in England, engaged in optical fiber system research. More recently, while on leave of absence, he was Professor of Electronics Engineering at the Chinese University of Hong Kong. He is at present the Staff Scientist at ITT Electro-Optical Products Division, Roanoke, Virginia.

Dr. Kao is a Fellow of the Institution of Electrical Engineers, a Senior Member of the IEEE.



Dr. Maklad was born in Egypt and received a BS in Chemistry and Physics, and MS in Physics from Cairo University in Cairo. He held a scientist position with Egypt Atomic Energy Commission from 1962-1967 to study the radiation effects on glass and develop radiation shielding glass windows and glass dosimeters. In 1970 he received his PhD in Ceramic Engineering from the University of Missouri-Rolla. As a postdoctorate fellow, Dr. Maklad was engaged in fiber optic development at Catholic University in America from 1971-1974. Currently Dr. Maklad is with ITT-EOPD as a Principal Scientist heading the fiber optic R&D group.

Fiber Optic Cables for Local Distribution Systems

by

J. C. Smith and M. Pomerantz

ITT ELECTRO-OPTICAL PRODUCTS DIVISION
P. O. Box 7065
Roanoke, Virginia 24019

U.S. ARMY ELECTRONICS COMMAND
Ft. Monmouth, New Jersey 07703

INTRODUCTION

For the past four years, the US Army Electronics Command (ECOM) has been engaged in the development of ruggedized fiber optic cables for use in tactical communications systems. The cables utilize low loss multi-mode optical waveguides with attenuation under 20 dB/km at discrete wavelengths in the near infrared region. This new low-loss medium makes possible the transmission of digital data at rates up to 20 megabits per second for distances up to 8 kilometers without the use of repeaters. By way of comparison, the standard CX-11230 dual coaxial cable would require repeaters every ¼-mile at these data rates. In addition to the obvious benefits to be derived from these superior transmission properties, the fibers offer immunity from EMP, EMI, and crosstalk, are difficult to tap, and offer the potential of cable constructions which are many times smaller in size and lighter in weight than conventional metallic conductor cables. Such size and weight reductions are of crucial importance in the highly mobile Army tactical systems. For example,¹ a 64 km time division multiplex (TDM) system that uses CX-11230 weighs 8636 kg and requires four 2½ ton trucks for transport. The same 64 km system using fiber cable would weigh approximately 1815 kg and require only two 1½ ton trucks for transport. In local distribution systems which use cable assembly CX-4566, each 72.8m reel of cable weighs 34 kg, while the fiber cable replacement will weigh less than 2 kg, including the reel. This reduction in weight, for example, could mean replacing one 2½ ton truck of CX-4566 with a ¼ ton trailer. Replacement of the two standard cables, CX-11230 and CX-4566 with fiber optic cables represents the short time goal of ECOM's development activities in this area. Present plans call for initial systems operational tests in the early 1980's. The subject of this paper deals with the development of the fiber optic cable which is intended to replace the CX-4566 (26 pair) cable. A contract for this development was awarded to ITT Electro-Optical Products Division in May 1975. The work on the replacement for CX-11230 has been reported elsewhere.^{2,3}

The CX-4566 is currently used in local distribution telephone and data systems within Army command posts. The anticipated cable runs range from 100 meters to one kilometer. Consequently, the attenuation of the fiber optic cable replacement for the local distribution systems need not be as low as that for the long haul TDM system. This less severe attenuation requirement suggested the possible exploitation of a plastic clad/fused silica fiber which is potentially lower in cost than the doped silica fiber used in

the long haul TDM cable. Although the attenuation of the plastic clad/fused silica fiber cannot be consistently made as low as the doped silica, it seemed, it seemed reasonable to expect that 50 dB/km could be achieved. This was the maximum acceptable system limit. However, a program goal of 20 dB/km was established to provide additional system margin. The overall program goals are given in Table 1.

PROGRAM GOALS

To achieve the desired cable performance a number of optical, mechanical, and environmental goals were imposed on the design. These design parameters are delineated in Table 1.

CABLE DESIGN

The attenuation indicated in Table 1 represents a necessary requirement "after cabling." The value of attenuation in the end item will be higher than the attenuation of the optical fibers before cabling. The resultant difference between these two attenuations is referred to as "excess cabling losses."

There are numerous explanations for excess cabling losses, however, the primary reasons are: (a) microbending losses, (b) flexural stress of the fiber, and (c) losses resulting from designed in bends.

Losses resulting from microbending are produced by a small, sharp bend in the optical core of the fiber. Sensitivity of the fiber to microbending losses may be reduced by: (a) increasing the numerical aperture, (b) reducing the fiber core diameter, or (c) increasing overall fiber diameter.

The factors affecting the flexural stress and bend radius are: (a) modulus of elasticity, (b) diameter of the fiber, (c) diameter of the cable center core, (d) wall thickness of the fiber coating, and (e) length of the lay. For this design problem factors a, b, and d were considered constants. The remaining factors, i.e., center core diameter and length of the lay, represent the tools to control flexural stress and bend radius.

Tensile Strength

The elongation of optical fibers is very low when compared to the elongation of copper wire. The optical fiber cables were designed in such a manner so that the optical fibers will not stretch more than 1% when the cable is subjected to a maximum load. It was possible to achieve the required tensile

strength by utilizing strength members.

When considering strength member materials and configurations, it was first determined that a very high Young's modulus material was necessary. Since no metallic or conductive elements were allowed, steel wire and carbon fiber were eliminated. Consequently, the choice was Kevlar 49, a product of E. I. DuPont deNeumours & Company.

Two configuration approaches were explored, namely, a central strength member and an external strength member. The internal strength member is of contrahelically laid construction and is composed of 1-6-12 yarns of Kevlar 49. Since Kevlar 49 has a tendency kink, an outer braid of Kevlar 29 is added (see Figure 1). This construction makes up the central core of the cable around which the optical fibers are laid.

The external strength member cable consists of 18 yarns of Kevlar 49. This strength member is helically laid around the jacketed optical fiber core in the manner depicted in Figure 2.

Impact Resistance

The mechanical requirement for an impact resistance test, in accordance with MIL-C-13777, subjects the cable to very severe stress conditions. The apparatus utilized in this test is shown in Figure 3. To comply with the requirements of this test, two basic approaches were followed:

A. Fibers laid against a hard surface. The central strength member provides the hard supporting surface where the fibers will lay. It can be shown experimentally, that when an optical fiber is laid against a soft surface, like an eraser, and pressure is applied with a finger nail, the optical fiber will break. However, if the optical fiber is laid against a hard surface and the same pressure is applied, the fiber will survive. Because

of this phenomenon, it was felt that the cable would have high impact resistance.

B. Heavy Plastic Jacketed Cable Core.

Two plastic jackets and a layer of Kevlar 49 were utilized to reduce the effects of the impact. To provide additional protection, the optical fibers were cabled in a seven fiber bundle.

Cable Components

To achieve the desired cable performance, it was necessary to assure that all cable components were compatible with the design parameters of Table 1. The crucial cable components evaluated were: (a) optical fibers, (b) strength members, (c) fillers, (d) tapes, and (e) jackets.

A. Optical Fibers. Fiber optic waveguides consist of a pure silica core and a polymeric cladding with a lower refractive index than the silica core. The best commercial silica core available was utilized in this design. Since attenuation loss in a cable is much more affected by the type of polymeric cladding used than by the silica core, the evaluation of several cladding materials deserved special attention.

The most important cladding materials in this particular design were: (a) Teflon FEP, (b) Teflon PFA, and (c) clear silicones.

It was noted that Teflon PFA was superior to Teflon FEP, product of E. I. DuPont deNeumours & Company, since it was practically free of gel particles, but that optical losses were heavily dependent on the wall thickness of the coatings. Figure 4 shows the spectral loss curve of PFA cladded silica and silicone coated silica.

Experiments on cladding thickness revealed that the optical quality of PFA cladding varied inversely with cladding thickness, requiring a draw down ratio from

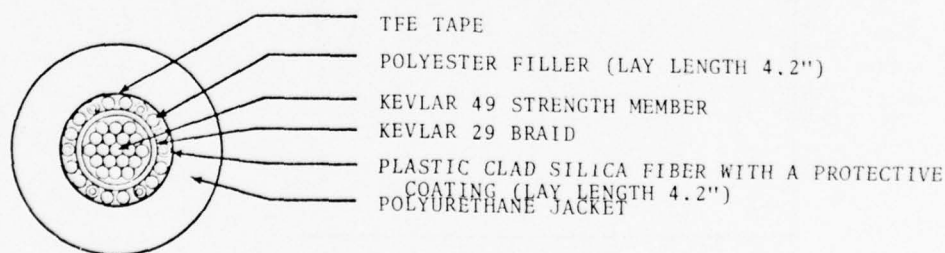


Figure 1. Central Strength Member Design (ECOM-1)

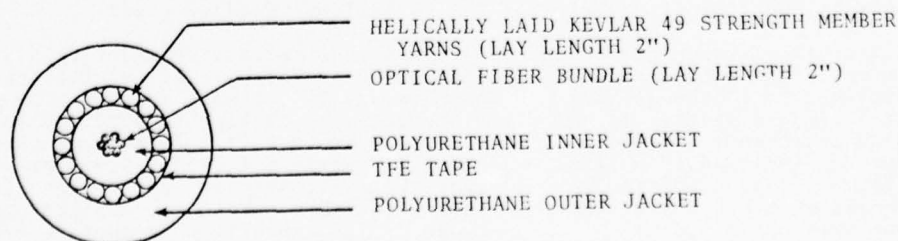


Figure 2. External Strength Member Design (ECOM-3)

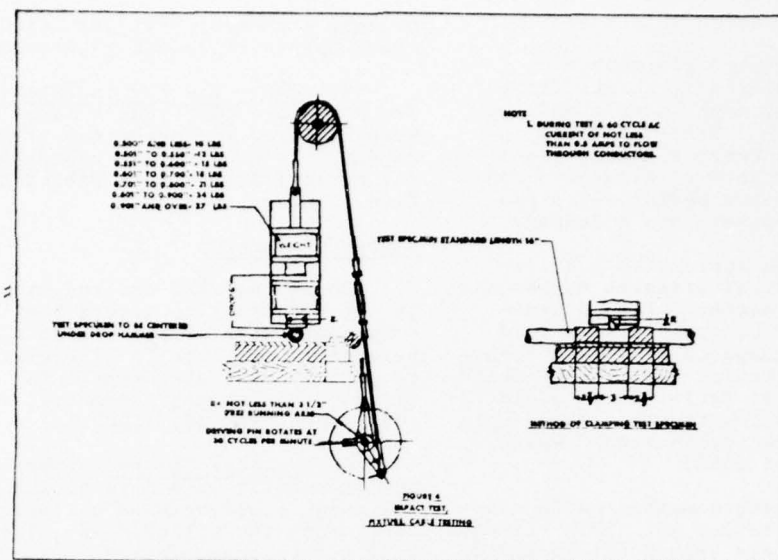


Figure 3. Impact Test Fixture

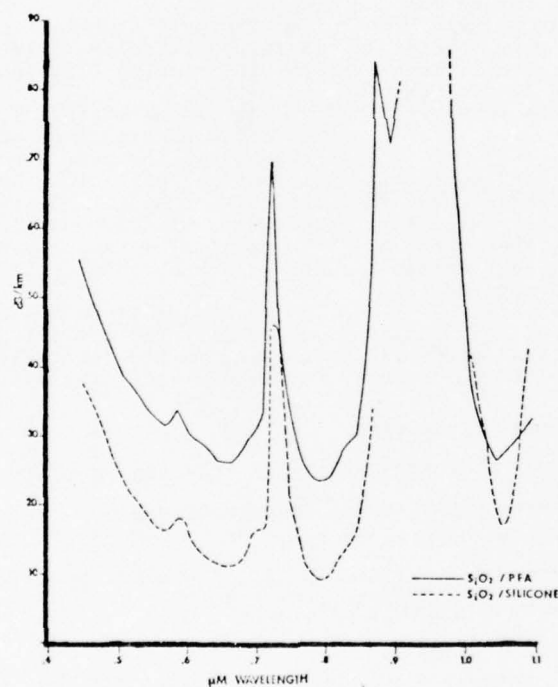


Figure 4. Optical Attenuation of PFA vs Silicone Cladded Fiber

900 to 2000:1. This extremely high draw down ratio led to pin holes in the extrudate which were found to be detrimental to the mechanical properties of the cladded fiber. In addition, an increase in attenuation was noted when the fiber was immersed in boiling water for several hours. This condition also led to cone breaks when not all of the extrusion conditions were optimized.

It was determined that RTV silicones

have a higher refractive index than either Teflon PFA or Teflon FEP, but that their performance is far more consistent. However, since silicone coating is soft, it is necessary to protect it. To resolve this problem, a jacket of Teflon PFA was provided over the silicone coating. Teflon PFA was chosen for this particular application because of its capability to operate over the required temperature range.

All fibers used in this program were proof tested at 50,000 psi to reduce the possibility of any weak spots in the optical fiber.

B. Strength Members. Since the design parameters specified that no metallic cable component would be allowed, graphite and carbon fibers were immediately ruled out because of their conductivity. This restricted the choice to: (a) highly oriented polymeric monofilament fibers, (b) glass fibers, and aramid fibers.

Kevlar 49, an aramid fiber, was selected because it has the highest Young's modulus of the commercially available non-metallic, non-conductive reinforcing materials.

Two types of Kevlar 49 strength members were used: (a) single yarn, 1420 deniers and (b) multiyarn, stranded and braided construction.

C. Fillers. Two polyester yarns were placed between each pair of optical fibers. a polyester filler was selected because it is fungus resistant and covers the entire operating temperature range.

D. Tapes. The original tape selected was of the uncured TFE type. This tape was chosen because of its ability to yield when stretched. This inherent ability relieves localized stresses on the optical fibers.

One cable (ECOM-1A), however, was designed utilizing a corrugated Mylar tape. This alternative later proved to have a much higher attenuation than the TFE tape when subjected to temperature cycling.

E. Jackets. A polyether grade of polyurethane jacket was selected because of its elastomeric properties, hydrolytic stability, operating temperature range, and fungus and radiation resistance.

Cable Evaluation

Six cables, of the composition indicated in Table 2, were produced.

The cables listed in Table 2 were subjected to the mechanical, environmental, optical, and nuclear survivability tests indicated in the following paragraphs.

Mechanical Evaluation

As a part of the mechanical evaluation, the cables were subjected to tests for tensile strength, bend, twist, and impact resistance.

A. Tensile Strength Test. Three samples of each type of cable were tested for fiber breakage utilizing a 400 pound load over a 24 inches gauge length. The total time to reach the required tensile strength required 26 to 30 seconds. The load was maintained for one minute, then released in 19 to 28 seconds. The results of the tensile strength test appear in Table 3.

From the data presented in Table 3, it

was concluded that all three cable designs were capable of sustaining the specified loading.

B. Bend Test. Three samples of each type were tested in accordance with the requirements of MIL-C-13777F. The test results for the bend test are delineated in Table 4.

As indicated in Table 4, all three cable designs meet the requirements of the bend test defined in MIL-C-13777F.

C. Twist Test. As in the previous tests, three samples of each cable type were subjected to the twist test of MIL-C-13777F. As may be observed in Table 5, all samples survived more than 2000 cycles without fiber breakage.

D. Impact Resistance. The impact resistance test was performed in accordance with the requirement defined in MIL-C-13777F, except that the impact loading was varied from 1 ft.-lb. to 5 ft.-lb. The test results for this test are shown in Table 6.

This test shows the superior impact resistance of ECOM-1 and ECOM-1A over ECOM-3.

Environmental Evaluation

The environmental evaluation consisted of a heat cycling test, a moisture resistance test, and fungus testing.

A. Temperature Cycling Test. One sample of each type of cable was subjected to temperature cycling from -55°C to +85°C in accordance with Method 102A, test condition D of MIL-STD-202D.

The average attenuation of the samples was measured at 7900 angstroms (injection NA of 0.124) before and after the temperature cycling. Table 7 summarizes the results of the test.

B. Moisture Resistance. Moisture resistance testing was performed on all three cable types. The results shown in Table 8 indicate a 4 to 5 dB/km increase in attenuation (at 7900 Å) after moisture cycling.

C. Fungus Testing. All three cable types were fungus tested in accordance with Procedure 1, Method 508 of MIL-STD-810B. Two of the samples (ECOM-1A and ECOM-3) showed no growth while the third showed significant growth. Efforts are presently being directed toward isolating the cause of this growth.

Optical Evaluation

The optical evaluation encompassed both attenuation and cable irradiation measurement.

A. Attenuation. The attenuation of the optical fibers was measured at 8200 angstroms. The average attenuation of the six cables tested is shown in Table 9.

The values indicated in Table 9 show

that the cables not only met the 50 dB/km requirement, but also met the 20 dB/km goal. It should be noted that all the cables with lengths $\frac{1}{2}$ km and $\frac{1}{3}$ km displayed an average attenuation lower than 12 dB/km at 8200 angstroms. Table 10 shows the individual fiber attenuation of these four cables.

B. Cable Irradiation. A short section of the ECOM-1 and ECOM-3 cable designs were exposed to a dose of 1.27×10^5 rads of gamma + 4.4×10^{10} neutrons/cm² and were visually inspected. No signs of degradation were observed.

Nuclear Survivability Test

Two fiber samples were tested under conditions simulating tactical field conditions. One sample was exposed to a dose of 10^5 rads while the other sample was irradiated to a level of 10^5 rads. The radiation induced optical losses were tested both at 10 seconds and 24 hours after irradiation.

The fibers were coiled around a 2 inch barrel spool with one flange cut off to expose the fiber to radiation.

The results of the two measurements follow:

A. Radiation Induced Optical Losses After 10 Seconds (Neutrons and Gamma Mixed Flux Irradiation). The non-radiated fiber optical loss is 6.9 dB/km at 0.79 μ m. After the sample received a dose of 5×10^4 rads, the induced loss after 10 seconds was 110 dB/km. Successive application of this irradiation resulted in progressively smaller attenuation increases.

B. Radiation Induced Optical Losses After 24 Hours (Gamma Irradiation). A total of 11 fibers were irradiated to doses ranging from 74 rads to 2.7×10^5 rads. It was observed that a total recovery of the optical properties of the fiber occurred within 24 hours even though doses as high as 2.7×10^5 rads were applied.

SUMMARY

This program represents an important advance in the Army's goal for replacement of metallic conductor cables with fiber optic cables. The results of the test program were sufficiently encouraging to warrant further consideration of the use of plastic clad/fused silica fibers in tactical field cable application. Indeed, the low attenuation values achieved were even better than the most optimistic goals established at the start of the program. This provides the added bonus of greater transmission distance in applications where pulse dispersion is not the primary consideration. Consequently, a significant system cost saving can be realized due to the lower cost of these fibers compared to the doped silica fibers.

The external strength member design (ECOM-3) appears to exhibit somewhat lower excess cabling losses than the central

strength member design (ECOM-1) although both designs are well within the program goals in this respect. However, the ECOM-1 design is substantially superior to ECOM-3 in impact resistance. Since the performance of both designs was substantially similar in all other respects, it would appear, from the work to this point, that ECOM-1 is the more favored of the two. Improvement in the impact resistance is possible, but at the expense of weight, flexibility, and cost. Further studies may be conducted to arrive at the optimum combination of these factors.

Determinations should still be made of the ultimate tensile strength of both designs, the effects of long time static load on attenuation, and the effects of long time high and low temperature storage.

REFERENCES

1. The Application of Fiber Optics to Army Communications by L. U. Dworkin, L. A. Coryell, CPT R. E. Dragoo, U. S. Army Electronics Command; Proceedings of 1975 SPIE/SPSE Conference.
2. Tactical Low Loss Optical Fiber Cable for Army Applications by R. A. Miller, Corning Glass Works; and M. Pomerantz, U. S. Army Electronics Command; Proceedings of 23rd International Wire and Cable Symposium.
3. Ruggedized Fiber Optic Cables for Army Communication Systems by M. Pomerantz, E. F. Godwin, U. S. Army Electronics Command; A. Asam, J. C. Smith, and M. Maklad, ITT Electro-Optical Products Division; Proceedings (Volume 77) of 1976 SPIE/SPSE East Conference.

Table 1. Program Goals

<u>A. Optical Requirements</u>	
1. Attenuation	50 dB/km (required) 20 dB/km (desired)
2. Numerical aperture	.27 minimum
3. Data transmission	
a. Bit rate	20 megabits/second
b. Rise and fall times	3 nanoseconds
c. Pulse flatness	3 dB peak to peak variation from voltage output level
<u>B. Mechanical Requirements</u>	
1. Tensile strength	400 lb
2. Vibration	MIL-STD-202
3. Flexing, impact and twisting	MIL-C-13777
<u>C. Environmental Requirements</u>	
1. Temperature cycling, moisture resistance, and immersion	MIL-STD-202
2. Fungus resistance	MIL-STD-810
3. Operating Temperature	-55°C to +85°C
D. Nuclear Survivability	10^3 to 10^5 roentgens level (cobalt 60)
	10^{12} to 10^{14} neutrons/cm ² (1 MeV equivalent)
E. Metallic Cable Components	Not allowed

Table 2. Composition of Final Cables

Cable Type	Composition
ECOM-1	1/3 km central strength member
ECOM-1	1 km central strength member
ECOM-1A	1/2 km central strength member (corrugated Mylar tape)
ECOM-3	1/3 km external strength member
ECOM-3	1/2 km external strength member
ECOM-3	1 km external strength member

Table 3. Tensile Strength Test

CABLE TYPE	LOAD	GAUGE LENGTH	BROKEN FIBERS IN GAUGE LENGTH
ECOM-1	400 lb	24 in	1 broke at 350 lb load
ECOM-1	400 lb	24 in	0
ECOM-1	400 lb	24 in	0
ECOM-1A	400 lb	24 in	0
ECOM-1A	400 lb	24 in	0
ECOM-3	400 lb	24 in	0*
ECOM-3	400 lb	24 in	0*
ECOM-3	400 lb	24 in	0*

*In ECOM-3, the central fiber broke in the clamp in all three samples. It is believed that this situation occurred when the clamps were tightened.

Table 4. Bend Test

CABLE TYPE	TOTAL # OF CYCLES TESTED	BROKEN FIBERS
ECOM-1	2030	None
ECOM-1	2020	None
EOCM-1	2170	None
ECOM-1A	2000	None
ECOM-1A	2000	None
ECOM-1A	2000	None
ECOM-3	2047	None
ECOM-3	2000	None
ECOM-3	2045	None

Table 5. Twist Test

CABLE TYPE	NUMBER OF CYCLES TESTED	BREAKS
ECOM-1	2201	None
ECOM-1	2198	None
ECOM-1	4017	None
ECOM-1A	2300	None
ECOM-1A	2200	None
ECOM-1A	2076	None
ECOM-3	2123	None
ECOM-3	2165	None
ECOM-3	4182	None

Table 6. Impact Test

CABLE TYPE	DESCRIPTION	IMPACT LOAD IN FT-LB			
		1	1.5	2	5
ECOM-1	Total no. of fibers tested	18	18	18	18
	Total no. of broken fibers	0	2	2	7
ECOM-1A	Total no. of fibers tested	18	36	18	18
	Total no. of broken fibers	0	1	3	13
ECOM-3	Total no. of fibers tested	21	-	21	21*
	Total no. of broken fibers	2	-	18	21

*ECOM-3 samples were tested at 4 ft.-lb.

Table 7. Temperature Cycling Test

CABLE TYPE	AVERAGE ATTENUATION (dB/km @ 7900 Å)	
	Before Heat Test	After Heat Test
ECOM-1	9.8	11.2
ECOM-1A	7.67	32.38
ECOM-3	10.5	12.0

Table 8. Moisture Resistance Test

CABLE TYPE	ATTENUATION BEFORE TESTING (dB/km)	ATTENUATION AFTER TESTING (dB/km)
ECOM-1	7.3	12.3
ECOM-1A	7.4	11.3
ECOM-3	6.0	10.3

Table 9. Attenuation of Final Cables

CABLE TYPE	LENGTH	ATTENUATION (dB/km)			
		6500Å	7900Å	8200Å	10500Å
ECOM-3	1140m	21.09	17.33	21.54	30.23
ECOM-1	1050m	21.68	17.75	21.90	31.98
ECOM-3	520m	9.71	7.25	11.30	16.38
ECOM-1A	506m	10.53	7.99	11.88	18.82
ECOM-3	336m	8.98	7.02	11.11	17.12
ECOM-1	324m	10.48	7.73	11.02	18.65

Table 10. Fiber Attenuation at 8200 Å in Final Models

CABLE TYPE	ECOM-1	ECOM-1A	ECOM-3	ECOM-3
CABLE LENGTH	324m	509m	336m	520m
FIBER #	ATTENUATION (dB/km)			
1	12.38	12.73	10.47	9.65
2	11.68	11.14	10.67	10.24
3	11.50	11.63	10.68	10.49
4	7.72	11.59	10.82	10.59
5	11.37	12.72	10.39	11.90
6	11.46	11.48	12.32	12.17
7	--	--	12.42	13.83



John C. Smith graduated from the Universidad Tecnica del Estado - Santiago, Chile in 1958.

He joined ITT Electro-Optical Products Division in 1974, where he is presently engaged in the development and design of fiber optic cables, including evaluation and selection of equipment and materials. He is also involved in the development of fiber optic coatings and related processes.

Prior to joining ITT, he was associated with General Cable Corp. (Philadelphia Insulated Wire) where he was Supervisor of Products Engineering.

Earlier, he was associated with Simplex Wire and Cable, Power and Control Division.

From 1960 to 1966, he held the position of Supervisor of Compounding Laboratory in MADECO, Santiago, Chile, where he was responsible for compounds development for wire and cable.



Morton Pomerantz served in the Army in World War II from 1943 to 1946. He received his BEE degree from New York University in 1955. He has been employed at the U. S. Army Electronics Command since 1952 as an Electronics Engineer. In that time he has been engaged in R&D activities principally in the areas of RF cables and connectors and tactical communications cables.

Mr. Pomerantz is a Member of IEEE and the IEEE Electromagnetic Compatibility Group. He serves as a Working Group Leader of the ANSI committee on RF cables, is a Department of Army advisor to the IEC National Technical Committee No. 46 on Cables, Wires, and Waveguides for Telecommunications Equipment, and is the current chairman of the Cable, Connector and Special Devices Working Group of the Tri-Services Fiber Optics Coordinating Committee.

He is currently engaged in development of fiber optic communication cable for tactical field army use.

OPTICAL FIBER CABLE FOR T1 CARRIER SYSTEM

J. A. Olszewski, A. Sarkar, Y. Y. Huang
General Cable Corporation
Union, New Jersey

Introduction

Recent rapid successes in development of low loss glass fibers and electro-optical components have changed the outlook of communications technology, including telephony. In the past ten years, attenuation of glass fibers was decreased from greater than 1000 dB/km to less than 4 dB/km (1,2,3) at 800 - 900 nm wavelength range and less than 2 dB/km at 1060 nm wavelength. Cables of various constructions (4,5,6) were produced using different approaches to protect the glass fibers. The attenuation of these constructions measured 6 - 20 dB/km and was considerably higher than attenuation of fibers prior to cabling. In the near future it is expected that the cabling loss and other fiber packaging losses will be virtually eliminated.

Although basic principles of cabling glass fibers were outlined (7,8) little emphasis was given to comparative evaluation of the characteristics of the cable constructions. What remains to be done at present is a practical verification of the performance of glass fiber cables and optical communication links under actual field conditions. In such field trials there is little difference whether the operating frequency is low or high. The study of installation and the effects of field environment should be done on relatively long installed links with a reliable commercial system as the final goal. For this purpose, General Telephone & Electronics, together with General Cable Corporation, selected the T1 PCM telephone carrier system which is at present a backbone of interoffice trunks. The test site was selected and General Cable undertook the development, production and joint installation of cable which will connect two telephone exchanges 10 kilometers apart. The system will carry commercial traffic and is scheduled to be operational in early part of 1977.

This paper discusses optical cable design criteria that governed our Laboratory development programs, as well as the results that were achieved. The work spanned the glass fiber development, fiber protection and cable prototypes construction. The main goal was low optical loss cable that could be installed by conventional methods and equipment.

Optical Glass Fibers

Bandwidth of step-index fibers of practical repeater spans is considerably wider than that of T1 system operated at pulse repetition rate of 1.544 megabits/second. The fiber development program was, therefore, concentrated on obtaining lowest, practically realizable attenuation.

Step-index fibers were produced in 1 km lengths. The physical and the optical characteristics of a batch of 20 coated fibers, produced under identical conditions, are shown in the table below:

	Average
Fiber diameter, μm	125
Fiber core diameter, μm	50
Attenuation at 825 nm, dB/km*	3.5
Pulse dispersion, ns/km**	8
Numerical aperture	0.16

* At 0.1 launch N.A.

** At half power level

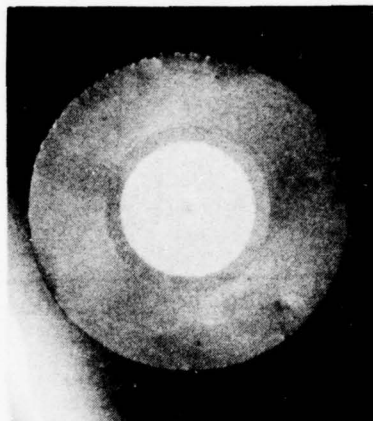


Figure 1: Cross-Section of a Typical Fiber

A typical fiber cross-section is shown in Figure 1 and the spectral attenuation data is plotted in Figure 2.

The shaded area shows the variation of attenuation from fiber to fiber within the batch. Since the light source selected for the system was an LED operating at 825 nm wavelength, the fiber attenuation at this wavelength was of primary concern. The average attenuation was found to be 3.5 dB/km. The lowest attenuation measured was 1.1 dB/km at 1060 nm wavelength. Attenuation of the same fiber measured at 1060 nm wavelength, but with an overloaded launch numerical aperture of 0.3, was 1.3 dB/km.

The apparatus for the spectral attenuation measurements utilized a tungsten lamp and a double monochromator with a lock-in feature to avoid errors due to external interferences.

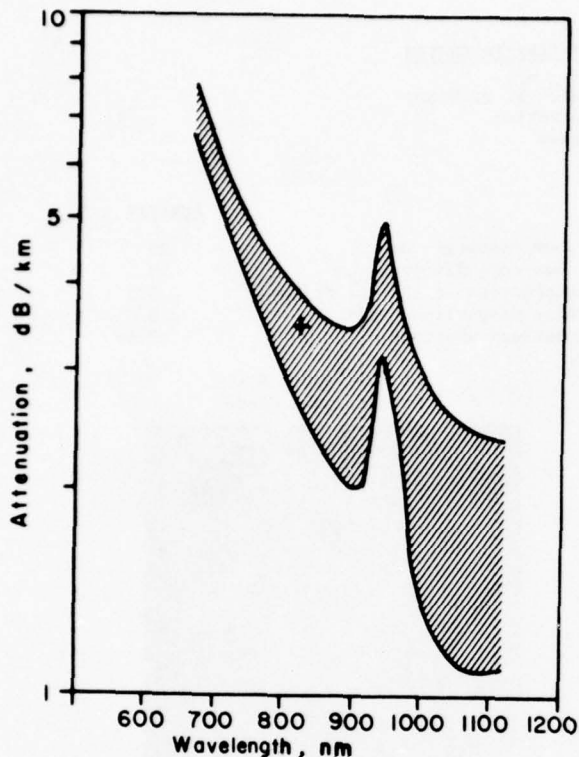


Figure 2: Spectral Attenuation of Glass Fibers with Kynar Coating

The pulse broadening of a typical fiber as a function of length is shown in Figure 3. Average pulse broadening of 8 ns/km, was obtained.

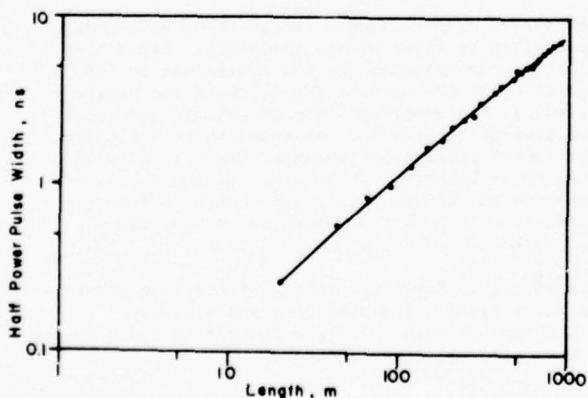


Figure 3: Pulse Broadening of a Typical Fiber

The pulse dispersion was measured with a specially designed and constructed set-up. The fiber was excited by a gallium arsenide laser diode emitting at 905 nm which was driven in a self-pulsing mode

by discharging a short section of coaxial line through a reed relay. The pulse obtained was 400 ps wide with 100 ps risetime and the repetition rate was 500 Hz. The emergent pulses were detected with a receiver consisting of an avalanche photodetector followed by wideband amplifier and a sampling oscilloscope.

The numerical aperture of the fibers was determined using a He-Ne laser with Gaussian optical power distribution and was calculated from $1/e^2$ power points of output radiation patterns of 1 km long fibers.

Since the strength of glass fibers is limited by flaw size and deteriorates rapidly with exposure to moisture, (9) a Kynar coating of 5-10 μ m was applied on the fibers. All fibers were also buffered, either by extrusion or by dip coating to a maximum overall diameter of 0.25 - 0.38 mm. Both buffering methods yielded fiber with minimal increase in attenuation. Special formulation materials were employed to minimize shrinkage, improve surface properties and control adherence of plastic to glass. The principal goals were minimal increase in attenuation, low temperature coefficient of attenuation and mechanical strippability.

Although tensile strength measurements on short gauge lengths of fibers indicated an average elongation of about 1%, a safe limit of elongation of long lengths of fibers was found to be about 0.2%. This performance characteristic imposes special demands on cable design from the point of view of installation.

Cable Design Criteria

The design of optical cable is governed by two major considerations, i.e.

- Mechanical requirements determined by necessary handling during installation and all the hazards that the cable is exposed to during its service life.
- Low optical attenuation and its temperature coefficient requirements.

From the mechanical point of view, the axial strength of the cable is of paramount importance. This characteristic controls the length of cable that can be safely installed. Conventional mechanical designs are inadequate because the optical fiber cables cannot be permitted to elongate more than about 0.2%. Similarly, fibers are sensitive to impact and consequently high cable impact and compression resistance is also required. Failure of glass also occurs under tensile stress due to torsion and bending. The stresses, therefore, have to be limited to a safe level. Appropriate safety factor (7) has to be taken into account for fiber life if residual stresses on fiber in cable are significant. Other mechanical design criteria remain the same as for conventional cables.

As far as control of optical attenuation is concerned, the problem is somewhat more complex. The two mechanisms that increase attenuation due to packaging are bending loss⁽¹⁰⁾ and microbending

loss.^(11,12) Since the attenuation of a glass fiber is an exponentially decreasing function of bending radius, the decision has to be made on a penalty that can be tolerated for bending and limiting the bending radius accordingly. In reality, the bending loss of fibers in cables of adequate flexibility can be made small compared to inherent attenuation of the fiber itself.

Microbending loss results primarily due to the fact that the glass fibers are very small and their axes can easily be distorted sharply by asymmetric forces of very small magnitude. Due to imperfections of almost all surfaces of cable components and necessary forces required for cable making, microbending losses cannot be totally eliminated.

Thus, glass fibers in cable form can stay with minimal increase in attenuation in one of the two following configurations:

- i. Placed loosely with no tension or lateral pressure in an oversized "channel" of very soft material such that the fiber can move when the cable is bent.
- ii. Embedded in a material that forms around the glass fibers without distorting their axes, forming a composite that is not as prone to distortion as the fibers are by themselves.

The temperature coefficient of attenuation of fibers in the cable is the last major concern. This is a function of all materials in intimate contact with the fibers; more specifically their differences in thermal expansion coefficients and the strength differential of the fiber and its coatings in a state of stress.

Design of Cable for Field Trial

Several cable prototypes were constructed and the design of two types* is discussed below in detail.

High axial strength at low elongation requirement can be met with a variety of materials and constructions, but metal reinforcement was selected for reason of:

- i. Impact and compression resistance.
- ii. Shielding and lightning protection of cable core incorporating power feed, order and fault locating metallic pair circuits.
- iii. Cable pressurization requirements.

The approach relied basically on building in sufficient metal of desirable temper and configuration which would guarantee about 200 kilogram tensile at 0.2% maximum cable elongation. This figure was determined from on site cable pulling experiments which were made on 1 km long polyethylene jacketed cable using lubrication and relatively low pulling speeds on practically straight runs. As a matter of interest, the type of pulling line was also found to have significant influence on the magnitude of pulling tension that

* These optical cable designs are subject of patent application.

can develop.

The overall cable sheath consisted of a welded metal tube, polyethylene jacket, corrugated steel longitudinally folded with overlap and flooded with asphaltic compound and polyethylene jacket overall. (Cable sections entering the telephone exchanges required flame retardant external jacket). This sheath was measured to have a tensile strength of 270 kg at 0.2% elongation and 440 kg at break. At 1300 kg a compressive force acting on a length of 1 m produced a 10% diameter deformation.

In developing the cable core construction, encapsulation of glass fibers into relatively rigid and mechanically stable assemblies was selected. The selection was based on previous cable manufacturing experience with loose fiber approach, where amongst other things it was found that within a year of fabrication several fibers in cables turned brittle.

Laminations of 1, 3 and 6 fibers were made in up to 300 meters lengths. The latest assemblies exhibited little, if any, increase in loss. Occasional increases in loss, however, still occur and efforts are continuing to control and stabilize the encapsulation process. The main advantage of this approach is the minimized proneness to microbending due to improved rigidity and reduced probability of fiber damage during construction of cable core.

Temperature coefficient of attenuation was measured in the range of 0°- 60°C and was found to average 0.2 dB/km/°C.

One cable core construction consisted of a torsionally preformed metal strip with a fiber assembly in contact with this tape. This placed the fibers at or close to the cable axis and, therefore, when suitable torsional lay is employed, the elongation of the fibers is kept to a low and safe level of 0.01 to 0.02% maximum. The cross-sectional view of this cable prototype is shown in Figure 4. Its attenuation was measured to be 6.2 - 12.7 dB/km at 825 wavelength.

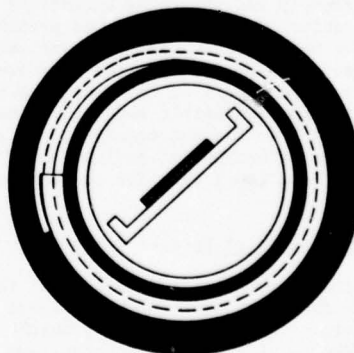


Figure 4: Cross-Section of Cable Prototype with Glass Fiber Assembly Placed in the Center of the Cable

Second cable prototype construction employed extruded plastic core with helical grooves and had a wire in the center for additional axial strength.

Fiber assembly was placed in one groove while the second groove was left for three No. 22 AWG plastic insulated metallic pairs - see Figure 5. The optical loss of this cable design was found to be 4.2 - 6.6 dB/km at 825 nm.

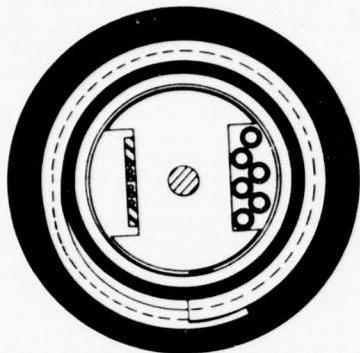


Figure 5: Cross-Section of Cable Prototype with Glass Fiber Assembly Applied Helically in a Grooved Core.

The advantages of fiber assembly placement in the grooves are numerous, i.e.

- i. Possible shifts in helix of fiber assembly are eliminated.
- ii. Compressive forces from binders, core tapes and cable sheath are avoided, even when cable is bent.
- iii. No restriction on fiber assembly movement when cable is flexed.
- iv. Improved fiber safety from impact and external compression.
- v. Greater separation from heat of cable sheathing operations.

No significant increase in attenuation was observed in cable core assembly and sheathing operations. The attenuation of cables of both designs was primarily a function of the degree of success that was achieved during encapsulation of fibers. The core construction of the above described cable designs was such that the minimum permissible bending radius for our fibers of about 7 cm was not exceeded. It also became apparent during mechanical evaluation of the cores that larger bend radii than for conventional cables are advisable.

System Aspects of Optical Cable Loss

All the attenuation figures quoted throughout this paper were determined with 0.1 launch numerical aperture and excluded the transient loss which is sometimes referred to as a non-equilibrium loss of the glass waveguide.

Measurements of transmitted power versus length of fiber was done with launch numerical apertures varying from 0.1 to 0.3. The non-linear length in all cases varied between 20-40 meters. Transient loss at 0.1 launch numerical aperture was 0.08 - 0.32 dB. Increase in transient loss due to increase

in N.A. to 0.3 was 0.2 dB average. The appropriate transient loss should only be considered once for each repeater span of any given system, i.e. at the output of the repeater. The increase in attenuation in the linear region was 0.8 dB/km average. Measurements with LED were not done because of anticipated variation in emitted pattern from manufacturer to manufacturer.

The launch N.A. of 0.1 was employed on the basis that it represented more closely the capabilities of our fiber waveguides as such and not the system, or more precisely, its light transmitter. The approach was not dissimilar to that which is commonly used with conventional lines when "cable attenuation" denotes true characteristics of the cable, while insertion of the cable in a specific system, changes its transmission performance as it becomes a function of source and termination impedance and is then referred to as an "insertion loss."

Optical cables in general have sizable fiber to fiber spread in attenuation and, therefore, loss averaging splicing technique will be required for each cable span between repeaters. Color coding of fibers, if employed, can only ease cable end to cable end identification of fibers, since color to color splicing cannot be practiced on current generation of cables.

Fiber Splicing

The subject of fiber splicing is rather complex and well beyond the scope of this paper. The list of publications on this subject is long with practically each publication, (13,14,15) describing different approach and the results that were obtained. General Cable's interest centers chiefly on factory splices and repairs. Fused splice is a prime candidate since the size of any mechanical splice cannot be tolerated. Fused splice also has a good potential for use in the field. The work is in progress under agreement with Corning Glass Works using principles described in reference 14. Splice losses as low as 0.05 dB were achieved in restoring continuity to broken fibers.

Summary and Conclusions

This paper lists the criteria of optical cable design in general and describes in considerable detail two designs that yielded average optical loss well under 10 dB per kilometer. Although the designs were made for T1 PCM carrier system application, the same approach should be valid in constructing optical cables for other applications. The true test of the system, of which a cable is a part, will come from an installation and operation of a reasonably long system in an actual field environment.

Acknowledgment

The authors wish to express their thanks to Dr. G. Bahder, Vice President and Director of Research for his guidance, and to personnel of the Facile Division, Sun Chemical Corporation for cooperation in making some of the encapsulations.

References

1. Kapron F.P., Keck D.B., Maurer R.D., Radiation Losses in Glass Optical Waveguides. Appl. Phys. Letters 10 (1970) 423-425.
2. MacChesney J.B., O'Connor P.B., DiMorcello F.V., Simpson J.R., Lazay P.D., Preparation of Low-Loss Optical Fibers Using Simultaneous Vapor Phase Deposition and Fusion. Proc. of Xth Internat. Congress on Glass, 1974, 40-45.
3. Payne, D.N. and Gambling, W.A., New Silica-Based Low-Loss Optical Fibre, Electron Lett. 1974, 10 (15) 289-290.
4. Slaughter, R.J., Kent, A.H. and Callan, T.R., "A Duct Installation of 2 Fibre Optical Cable", IEE Conf. Publ. 132, 1975, 84-86.
5. Nakahara, T., Hoshikawa, M., Suzuki, S., Shiraishi, S., Kurosaki, S., and Natsuda, S., "Step Index Type Optical Fibre Cable", IEE Conf. Publ. 132, 1975, 81-83.
6. Miller, R.A., and Pomerantz, M., "Tactical Low Loss Optical Fibre Cable for Army Application", Proceedings of the 23rd International Wire and Cable Symposium, Atlantic City, N.J., December 1974, 266-271.
7. Schwartz, M.I., Optical Fiber Cabling & Splicing, Topical Meeting on Optical Fiber Transmission, Williamsburg, Virginia, January 1975, Paper WA2-1.
8. Foord, S.G. and Lees, J., "Principles of Fibre Optical Cable Design", Proc. IEE. 123 (6), 1976, 597-602.
9. Kelly A., in "Strong Solids" (Clarendon Press 1966) Chap. 2, 36.
10. Marcatili, E.A.J., "Bends in Optical Dielectric Guides", Bell Syst. Tech. J., 1969, 48, 2103.
11. Olshansky, R., "Distortion Losses in Cabled Optical Fibers", Appl. Opt., 1975 (14), p. 20.
12. Gloge, D., "Optical Fibre Packaging and its Influence on Fibre Straightness and Loss", Bell Syst. Tech. J., 1975, 54, 245-262.
13. Kohanzadeh, Y., "Hot Splices of Optical Waveguide Fibers", Appl. Optics 15 (3) 1976, 793-795.
14. Chinnock, E.L., Gloge, D., Bisbee, D.L. and Smith P.W., "End Preparation and Splicing of Optical Fiber Ribbons," Topical Meeting on Optical Fiber Transmission, Williamsburg, Virginia, January 1975, paper WA6-1.
15. Murata, H., Inao, S., and Matsuda, Y., "Connection of Optical Fiber Cable", Topical Meeting on Optical Fiber Transmission, Williamsburg, Virginia, January 1975, Paper WA5-1.



A. Sarkar (Speaker)



Y. Y. Huang



J. A. Olszewski

The authors are with General Cable Corporation, Research Laboratories, at 800 Rahway Avenue, Union, New Jersey 07083. Dr. A. Sarkar is Research Group Manager, Fiber Optics; Dr. Y.Y. Huang is Senior Research Engineer in charge of optical measurements and J. A. Olszewski is Assistant Director of Research, Communication Cables.

A REVIEW OF OPTICAL FIBER CONNECTION TECHNOLOGY

by

J.F. Dalgleish, Bell-Northern Research, Ottawa, Canada

SUMMARY

Connections for bundle and single fiber cables are being developed. The theory of fiber-to-fiber coupling is reviewed and the sources of signal loss are identified. Techniques for making single fiber-to-fiber connections are discussed and the basic requirements for practical hardware outlined.

INTRODUCTION

The technology of optical fiber communications systems has advanced rapidly over the past few years. Experimental systems of significant size have been installed and are under evaluation on at least three continents. General review articles on fiber optic systems identify three essential elements which are new to most communications systems designers; a light source (light emitting diode or laser), an optical fiber and a light detector (photodiode). For practical systems, there is a fourth - fiber connections.

Two types of cables are used in optical communications, each having a distinct connection technology. One uses fiber bundles in which all fibers transmit the same optical signal and the other has single fiber cables in which each fiber is a separate transmission channel. Fiber bundles are currently employed for relatively short systems where high attenuation, low cost fibers can be used. Transmission through low-loss single fiber cables will be the dominant approach for intermediate and long length systems.

Bundle connection technology^{1,2} is based mainly on modifications to existing coaxial connector hardware. The fibers are inserted into a close-fitting ferrule and potted in place. After curing, the end is polished. To make a connection, two prepared ends are coupled together in an alignment sleeve.

The interconnection of single fibers requires the development of new connection concepts. The essential objective in making a single, fiber-to-fiber, connection is to create an accurate radial, longitudinal and axial alignment between the two fiber ends.

THEORY OF FIBER-TO-FIBER COUPLING

Figure 1 illustrates the basic principle of fiber-to-fiber coupling of step index fibers using a simplified geometrical ray analysis. Light exits from the transmitting fiber core according to the relationship;

$$NA = (n_1^2 - n_2^2)^{1/2} = n_3 \sin \theta \quad (1)$$

where

- NA = numerical aperture
- n_1 = core refractive index
- n_2 = cladding refractive index
- n_3 = refractive index of medium at the end of the fiber
- θ = maximum half-angle of radiation.

For example, a fiber with a silica-germania core ($n_1 = 1.464$) and a borosilica cladding ($n_2 = 1.450$) has a numerical aperture of 0.2 and a maximum half-angle, θ , of 11.7° in air ($n_3 = 1.0$). The receiving fiber core accepts light according to the same relationship, (1).

Provided that the transmitting and receiving fibers are identical, then any light striking the core of the receiving fiber at an angle of 11.7° or less (in air) will be transmitted along the fiber.

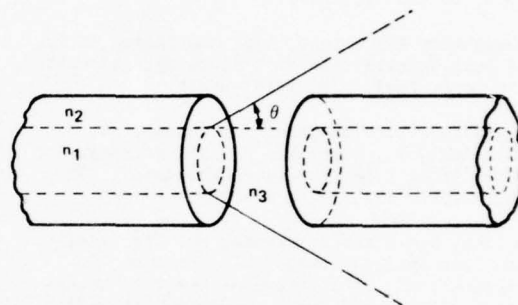


Figure 1 Radiation from a Step Index Fiber

The objective is to capture in the core of the receiving fiber as much of the cone of light radiated from the transmitting fiber as possible. (Some light may travel for a short distance through the cladding of the receiving fiber but this light attenuates very rapidly.) Figure 2 illustrates that transverse misalignment is relatively more critical than end separation. However, for efficient coupling the fiber ends must be in good radial alignment and be butted or nearly butted together.

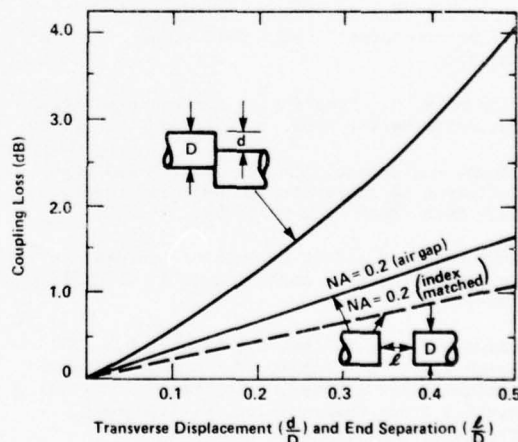


Figure 2 Coupling Losses of Step Index Fibers with Transverse Displacement and End Separation

Fresnel reflections are another source of loss. Light is reflected at the glass-air interface at the exit of the transmitting fiber and at the air-glass interface at the entrance to the receiving fiber. The reflectivity coefficients for each interface, R_{ga} and R_{ag} respectively, are defined by;

$$R_{ga} = R_{ag} = \frac{(n_1 - n_3)^2}{(n_1 + n_3)^2} \quad (2)$$

where n_1 and n_3 are as defined for equation (1). This relationship is valid for angles of incidence, θ , up to approximately 30° (i.e. $NA \leq 0.5$).

Using the above example of a step index fiber ($n_1 = 1.464$, $n_3 = 1$) then R_{ga} and R_{ag} are both equal to 3.5%. Therefore, the maximum coupling efficiency with an air gap between the fiber ends is approximately 93% (insertion loss of 0.3 dB).

Eliminating the air gap between the fiber ends by introducing an index matching medium (i.e. $n_3 = n_1$) has two effects. From equation (1), it can be seen that the maximum half-angle, θ , is reduced. For the example above ($NA = 0.2$), θ becomes 7.8° , thereby concentrating the transmitted radiation into a smaller cone and narrowing the acceptance cone of the receiving fiber. This reduces the sensitivity to end separation (as shown by the broken line in Figure 2). From equation (2), R_{ga} and R_{ag} both reduce to zero. Figure 3 shows the relationship between the reflected light and the refractive index of the matching medium. It illustrates that reflection losses are dramatically reduced with only an approximate match between the refractive indices of the core and matching medium.

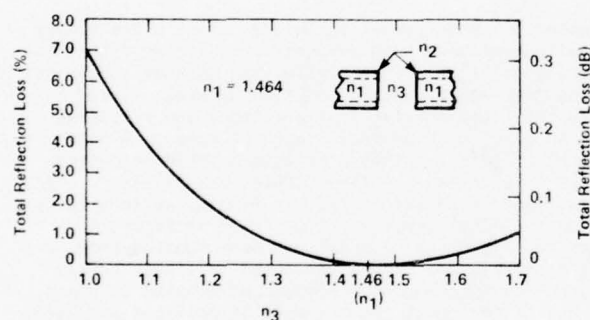


Figure 3 Reflection Loss

Axial misalignment also contributes to coupling inefficiency³. Figure 4 illustrates that coupling efficiency is less sensitive to axial misalignment than the sources of loss previously mentioned. Nevertheless, the angle between the axes of the fibers must be accurately controlled.

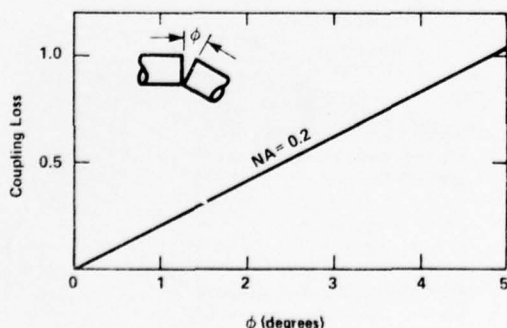


Figure 4 Coupling Loss of Step Index Fibers with Axial Displacement⁽³⁾

In all of the above analysis, it has been assumed that the ends of the fibers are smooth, flat and perpendicular to the fiber axis. Fiber end defects such as rough areas (hackle), scratches, or angled end surfaces (i.e. not perpendicular to the fiber axis) will contribute to scatter and reflection losses. These losses are difficult to quantify. However, the use of an index matching medium does reduce their effects.

Graded index fibers, which have a non-uniform refractive index across the core, have substantially less dispersion (i.e. lower pulse broadening) than step index fibers. This makes them attractive for long length, high capacity systems. The optimum refractive index profile to minimize dispersion is near-parabolic.

The radiation pattern from the end of a graded index fiber differs from that of a step index fiber. The maximum half-angle of radiation from the transmitting fiber is a function of distance from the center of the core as illustrated in Figure 5. Consider, for example, a graded index fiber having a silica-germania core with a refractive index (n_1) graded from 1.467 at the center of the core to 1.450 at the core/cladding interface and a borosilica cladding ($n_2 = 1.450$). Using equation (1) at the center of the core, the effective numerical aperture is 0.22 and the maximum half-angle, θ , is 12.9° (when $n_3 = 1$). At the edge of the core, where $n_1 = n_2$, the effective numerical aperture is zero and the maximum half-angle, θ , is also zero. Therefore, at the edge of the transmitting core, light is radiated parallel to the fiber axis and similarly at the edge of the receiving core, only light entering parallel to the fiber axis will be transmitted along the fiber.

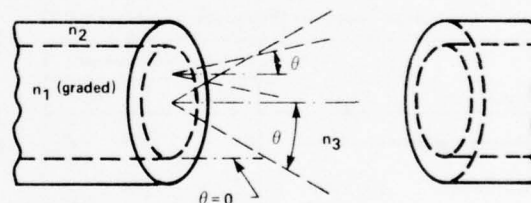


Figure 5 Radiation from a Graded Index Fiber

Consequently, the coupling of a graded index fiber is more sensitive to transverse misalignment than a step index fiber with the same core diameter as shown by the solid line in Figure 6⁴. Unlike step index fibers, a graded index fiber has the ability to transmit unbound or leaky rays (modes). Some of the unbounded rays will attenuate quickly while others will be transmitted over long distances. If the receiving fiber is short, unbounded rays can reach the detector and thereby reduce the apparent sensitivity to transverse misalignment as shown by the broken line in Figure 6⁴. Consequently, measurements made with short fiber will lead to an underestimation of the losses caused by transverse displacement.

The signal losses introduced by transverse misalignment, end separation, axial misalignment and Fresnel reflections are cumulative. Because there is some interdependence between these sources of loss, it is inaccurate to simply add the effect of each loss as though it were functioning independently. Nevertheless, in order to better appreciate the cumulative affect of coupling losses, it is useful to make the simplifying assumption that these sources of loss are independent and apply the results to typical fiber geometries. Table 1 summarizes the results for two step index fibers.

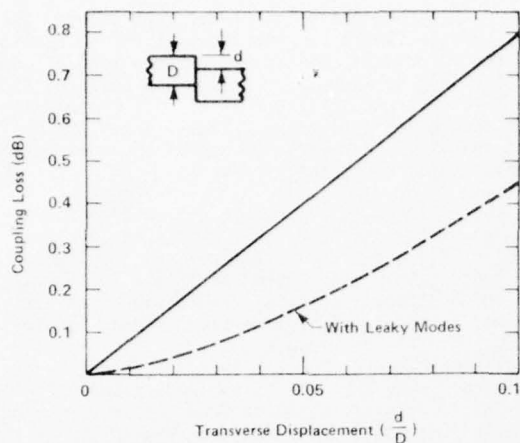


Figure 6 Coupling Loss of Graded Index Fibers with Transverse Displacement⁽⁴⁾

In practical applications, contamination represents another potential source of loss. A single particle, 10 μm in diameter, will block approximately 4% of the area of a 50 μm diameter core. This represents a loss of approximately 0.2 dB.

The fiber itself can contribute to the losses. Variations in outside diameter, core diameter and core/cladding eccentricity all create transverse misalignment.

Table 1 Cumulative Losses for Step Index Fibers (NA= 0.2)

Source of Loss		Fiber Core Diameter	
		50 μm	100 μm
Transverse Displacement	10 μm	1.3	0.6
	5 μm	0.6	0.3
End Separation	10 μm	0.7	0.4
	5 μm	0.2*	0.1*
Axial Displacement	3°	0.6	0.6
	1°	0.2	0.2
Reflections	Dry	0.3	0.3
	Matching Material*	0	0
Total Losses		2.9dB	1.9dB
		1.0dB	0.6dB

Two forms of optical fiber connection are required. A permanent fiber-to-fiber splice is needed to join cable into lengths that exceed the maximum single length that can be handled in the field and to provide a means of repairing damaged cable. Secondly, a remateable fiber-to-fiber connector is needed to permit quick, reliable attachment to transmitters, receivers and amplifiers (repeaters) and to facilitate the rearrangement of a system. There have been some promising experimental devices developed for both types of connection.

SPLICING

A loose-tube splice⁵ is illustrated in Figure 7. It consists of a glass tube with a square cross-section which is appreciably larger than the fiber diameter. A length of this tubing is prefilled with epoxy. The fiber ends are inserted into the tube and bent causing the glass tube to rotate and forcing the fibers into a corner. The fibers are then butted together and held in place until the epoxy cures. In addition to holding

the fibers in place, the epoxy acts as an index matching medium. Splicing losses averaging less than 0.1 dB per splice using graded index fibers with a 68 μm core diameter have been reported.

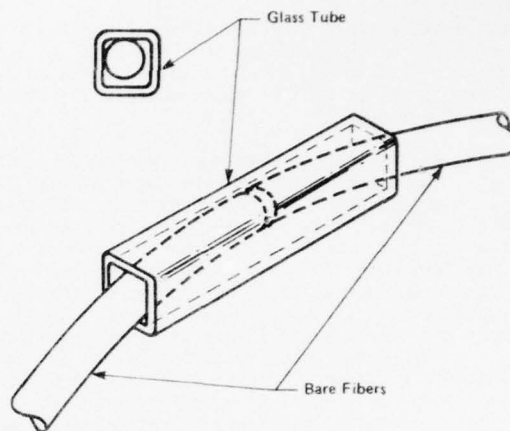


Figure 7 Loose-Tube Splice⁽⁵⁾

A number of experimental techniques using a Vee groove for alignment have been devised for splicing fiber ribbons (tapes)^{6,7,8}. Essentially, the methods consist of laying prepared fibers in parallel grooves, spaced to match the fiber spacing in the ribbon, and retaining them in place with an index matching epoxy. A "mass splice" of this type has been incorporated into each end of an experimental fiber cable installation⁹. The cable, containing 144 fibers, is terminated in a 12 by 12 "mass splice" array as illustrated in Figure 8. After the jacketing material has been removed from each of the fibers, they are interleaved in linear arrays between embossed aluminum plates and epoxied in place. The end of the completed assembly is polished and mated with an identical array to form a splice. Transverse alignment between the two polished arrays is controlled by grooves at the top and bottom of the half-splice assemblies. Careful control of plate thickness and embossing tolerances limit the maximum transverse positional error of any one fiber to a few microns. An index matching fluid is placed between the polished surfaces. Measurements on such splices in the laboratory produced average splicing losses of approximately 0.1 dB.

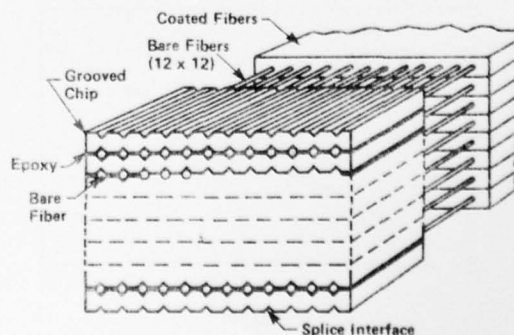


Figure 8 Mass Splice⁽⁹⁾

The use of a close-fitting alignment bore for single fiber splicing has also been used. An early experiment¹⁰ employs a fiber as an embossing tool to produce a close-fitting half-bore (i.e. groove) in which two fibers can be aligned. The use of a glass capillary with an inside diameter only slightly larger than the outside diameter of the fiber has been proposed¹¹ and experimental field tooling and techniques for using a close fitting glass capillary splice in conjunction with plastic coated fibers have been developed¹². A hole in the side of the sleeve is used to inject an index matching adhesive. Average splicing losses with an 85 μm diameter core, step index fiber are reported to be 0.3 dB.

A metal, single fiber splicing element has also been developed¹³ for use with plastic-coated multimode fibers. A stainless steel tube is preformed to have a center alignment bore which is a close fit to the bare fiber diameter (Figure 9). An index matching fluid is introduced into the splicing element before the fibers are installed. With the plastic coating stripped and the ends prepared, the fibers are inserted into the splicing element. The ends are guided by tapered sections into the alignment bore. The ends of the stainless steel splicing element are then crimped into the fiber's plastic coating to produce a permanent assembly. Insertion losses averaging 0.3 dB with a 125 μm diameter core, step index fiber have been reported.

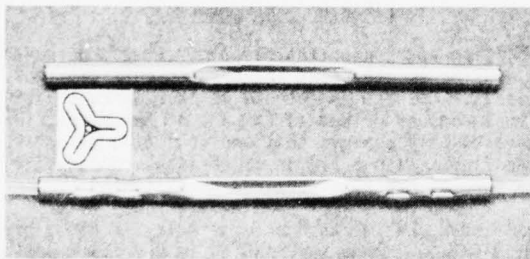


Figure 9 Single Fiber Splice⁽¹³⁾

Early fusion splicing techniques^{14,15} have used a nichrome wire heating element to soften and fuse low melting point glass fibers. The core diameters of these fibers were small (2 μm to 20 μm) and micromanipulation techniques were used to align the fibers before fusing. With the development of low loss, large core, multimode, silica fibers, several authors^{16,17,18} have successfully used an electric arc to fuse these high melting point fibers. Average losses of 0.3 dB to 0.1 dB have been reported.

CONNECTORS

The experimental techniques for making a remateable connector are more diverse than the splicing techniques. The first published device¹⁹ is an adjustable connector in which the fibers are eccentrically mounted. Accurate transverse alignment is achieved by rotating one fiber with respect to the other until the monitored signal through the connector is maximized. Insertion losses of less than 0.4 dB have been achieved with single mode fibers. Several improvements to the original design have been proposed^{20,21,22} and insertion losses of less than 0.1 dB have been reported with multimode graded index fibers and an index matching fluid.

Three experimental, remateable connectors involving the use of a close-fitting alignment bore have been proposed. In one method²³, shown in Figure 10, the fibers are centrally mounted in precision sleeves using epoxy. These sleeves are inserted into close-fitting alignment bores in the connector housings. Insertion losses averaging about 1 dB are reported for graded index fibers. Rotation of one fiber causes the insertion loss to vary between approximately 0.5 dB and 2 dB, which is an indication of the eccentricity caused by tolerance buildup between the machined sleeves and housings.

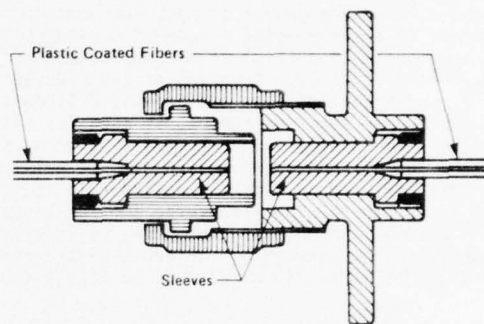


Figure 10 Concentric Sleeve Connector⁽²³⁾

A second approach²⁴ involves the use of jewellers bearings mounted inside a stainless steel ferrule. The small, centrally positioned hole in the center of the bearing is used to locate the fiber at the center of the bearing-ferrule assembly. The end of the assembly is potted and polished to produce the required end finish. Two such assemblies are held within a close fitting sleeve to form a connector. The eccentricity between the jewel hole and alignment tube is reported to have a worst case value of 10 μm . No experimental results have yet been published.

A third technique²⁵, illustrated in Figure 11, uses the concept of the formed splicing element¹³ to make a remateable connector. In the connector plug, the end of one fiber is located near the midpoint of the alignment bore which is filled with an index matching fluid. The second fiber floats freely in the connector jack. The

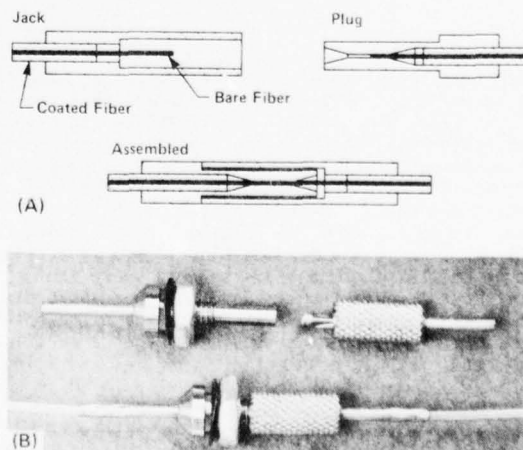


Figure 11 Formed Element Connector⁽²⁵⁾

Longitudinal position of each fiber end is accurately located with respect to a reference surface on each housing using an installation fixture. During assembly, the loose fit between the outside diameter of the plug and the inside diameter of the jack provides a rough transverse alignment which insures that the jack fiber enters the tapered opening of the plug. When fully mated, the reference surfaces are in contact and the fiber ends are separated by a small gap. Typically, the insertion loss of this connector is 1.0 dB with step index fibers having core diameters of 75 μm to 100 μm .

Experimental designs for multiple connectors are also being tested. The Vee groove concept has been combined with the use of a three-point alignment mechanism to produce a demountable multiple fiber connector^{26,27} as illustrated in Figure 12. A series of Vee grooves is cut into the circumference of two ceramic cylinders. One groove, deeper than the others, is used for alignment. Fibers are bonded into the remaining grooves and the ends of the cylinders are polished. Two metal supporting cylinders and an aligning cylinder in the connector housing provide the transverse and rotational alignment between the ends of the mating cylinders. Insertion losses of between 0.5 dB and 2 dB are reported using graded index fibers with 30 μm core diameters.

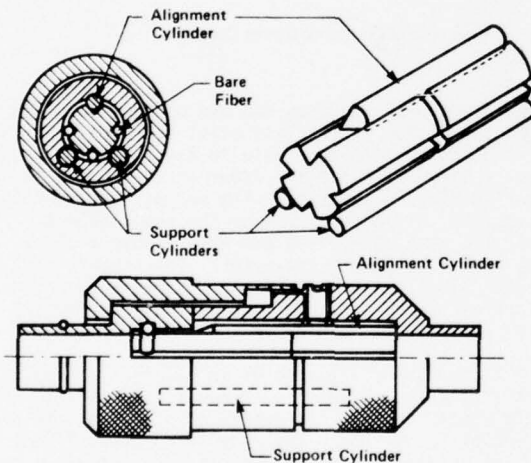


Figure 12 Multiple Connector^(26, 27)

A molded plastic multiple connector (which can also be used as a permanent splice) has been proposed²⁸ for use with fiber tapes and cables. As illustrated in Figure 13, the individual fibers in the tape are stripped of their jacketing material and aligned in a precision spacer within a molding block. The block is filled with resin and cured. After curing, the potted array of fibers is pulled from the molding block, leaving the precision spacer in the molding block. The slot left by the removal of the spacer is used to score the fibers. The potted array is then tensioned and bent, thereby breaking the fibers (as discussed in the following section). By mating two such potted arrays in an alignment channel, coupling efficiencies averaging approximately 0.1 dB have been achieved with 80 μm core diameter fibers.

Other single²⁹ and multiple^{30,31} connector designs have been proposed but at present do not appear to be as promising as the examples that have been discussed.

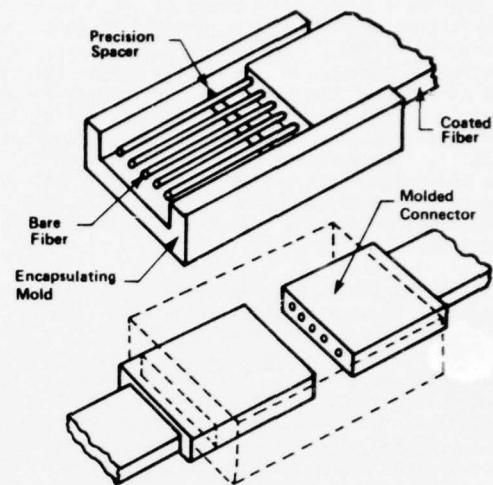


Figure 13 Molded Multiple Connector⁽²⁸⁾

FIBER END PREPARATION

All splicing and connecting techniques require that the fiber ends be smooth, flat and perpendicular to the fiber axis. Connection methods which require the fibers to be bonded or potted to part of the connection hardware usually achieve this end condition by polishing the fibers with a series of abrasive compounds. Fibers bundles are also prepared by polishing.

A "bend and score" technique for single fiber end preparation has been reported³² which is effective and easier to adapt for use in the field. In this method, the fiber is bent over a controlled radius and tensioned (to remove compressive stresses caused by bending). The surface of the fiber is then scored to initiate a crack which propagates across the fiber. The bending radius and tension required are a function of the fiber diameter and strength. Several authors^{5,33,34,35} have reported on experimental breaking tools which use this technique.

Other methods of preparing fiber ends, including thermal shock³⁶, have been reported but at present do not appear to be as convenient or reliable.

It is evident from the experimental techniques that the design principles of optical fiber connectors and splices differ substantially from their electrical counterparts. To assess the potential for developing practical hardware these techniques must be compared to the basic requirements for splices and connectors.

SPLICE REQUIREMENTS

1. **Insertion Loss.** The total splicing loss along a length of cable must be substantially less than the total cable attenuation. It has been suggested³⁷ that an insertion loss of less than 0.5 dB per splice will be required on long length systems. As most of the reported experimental results are comfortably below this value, this requirement should be achievable provided that the laboratory techniques can be adopted for field use.

2. Field Installation. Splices are a necessity caused by limitations on the length of cable that can be installed. The value of a splicing technique (electrical or optical) is judged largely by the ease and speed of field operation. Compared to copper, there are a large number of operations to be performed during fiber splicing. Consequently, more equipment will be required than for copper splicing. Because of the small size of fibers and the accurate alignment required, the equipment will be more sophisticated than that used with copper. The laboratory results to date indicate that tooling and techniques can be developed. However, it has yet to be established which of these techniques can be performed in the field using trained but not highly skilled labour.

3. Mechanical and Environmental Stability. Spliced fibers must be as easy to handle as unspliced fibers and they must maintain their efficiency over an extended period of time (for example, telephone cable splices are designed for operational periods of up to 40 years). The experimental fiber splicing techniques propose to use a number of components such as plastics, resins and fluids which will have to be carefully selected and thoroughly tested to insure splicing stability.

CONNECTOR REQUIREMENTS

1. Insertion Loss. Because connectors must be rematable and interchangeable, the insertion loss will be somewhat higher than that of a splice. A figure of less than 1.0 dB has been suggested³⁷. As illustrated by Table 1, this will only be achieved by careful control of the sources of loss and, in particular, transverse misalignment. The number and magnitude of manufacturing tolerances which contribute to transverse misalignment must be kept to a minimum. Relatively few results have been reported on connector insertion losses. Generally, the insertion losses have been at or above 1.0 dB, suggesting relatively large transverse misalignments.

2. Repeatability. The insertion loss with repeated matings of the connector must be constant. Most of the experimental results which are consistently equal to or less than 1.0 dB have used an index matching material. As with the splice, careful selection and thorough testing will be required to insure than repeatable connections can be made.

3. Handling Characteristics. Optical fiber connectors must have handling and environmental characteristics similar to electrical connectors. This implies, among other things, that the connector design must protect the fibers against accidental damage in the unmated condition and during mating. All of the reviewed connectors appear to afford some measure of protection to the fibers, although some of the concepts, particularly for multiple connectors, are not complete enough for a proper assessment. Thorough mechanical testing results (vibration, tensile and drop tests) have not yet been reported. A new handling factor is introduced with the use of an adjustable connector; that is, the necessity of monitoring transmission during mating of the connector.

In summary there are no major impediments to the development of practical connection hardware. At the present time, splices are closer to meeting their basic requirements than are connectors.

DRAWING SYMBOLS

To avoid confusion with electrical systems, particularly at interconnection points, a set of drawing symbols for optical components is required. These symbols must be;

- distinctive
- compatible with existing symbols
- applicable to all optical components
- simple in design.

Table 2 offers some suggestions. Existing electrical symbols, shown in the left-hand column, form the basis for the proposed symbols.

Table 2 Possible Drawing Symbols for Optical Components

Component	Electronic Symbol	Optical Symbols
"Conductor"		
Connector Plug		
Connector Jack		
Hermaphroditic Connector		
Splice		
Photodiode		
LED or Laser Diode		
Directional Coupler		

REFERENCES

- F.L. Thiel, R.E. Love and R.L. Smith, "In-Line Connectors for Multimode Optical Waveguide Bundles", *Applied Optics*, Vol. 13, No. 2, Feb. 1974, p. 240.
- R.L. McCartney, "Fiber Optic Connectors", 25th Electronic Components Conference, Washington, May 1975, p. 248.
- M. Young, "Geometrical Theory of Multimode Optical Fiber-to-Fiber Connectors", *Optics Communications*, Vol. 7, No. 3, March 1973, p. 253.
- M.J. Adams, D.N. Payne and F.M.E. Gladen, "Splicing Tolerances in Graded-Index Fibers", *Applied Physics Letters*, Vol. 28, No. 9, May 1976, p. 524.
- C.M. Miller, "Loose Tube Splices for Optical Fibers", *BSTJ*, Vol. 54, No. 7, Sept. 1975, p. 1215.
- E.L. Chinnock, D. Gloge, D.L. Bisbee and P.W. Smith, "End Preparation and Splicing of Optical Fiber Ribbons", *Topical Meeting on Optical Fiber Transmission*, Williamsburg, January 1975, p. WA6.
- A.H. Cherin and P.J. Rich, "A Splice Connector for Joining Linear Arrays of Optical Fibers", *ibid*, p. WB3.

8. E.L. Chinnock, D. Gloge, P.W. Smith and D.L. Bisbee, "Preparation of Optical-Fiber Ends for Low-Loss Tape Splices", BSTJ, Vol. 54, No. 3, March 1975, p. 471.
9. C.M. Miller and C.M. Schroeder, "Fiber Optic Array Splicing", Conference on Laser and Electrooptical Systems, San Diego, May 1976, p. 82.
10. C.G. Smeda, "Simple, Low-Loss Joints Between Single-Mode Optical Fibers", BSTJ, Vol. 52, No. 4, April 1973, p. 583.
11. D. Schicketanz, "Connectors for Multimode Fibers", Siemens Forsch.-u. Entwickl.-Ber. Bd. 2 (1973) Nr. 4, p. 204.
12. H. Murata, S. Inao and Y. Matsuda, "Connection of Optical Fiber Cable", Topical Meeting on Optical Fiber Transmission, Williamsburg, January 1975, p. WA5.
13. J.F. Dalgleish, H.H. Lukas and J.D. Lee, "Splicing of Optical Fibers", First European Conference on Optical Fiber Communication, London, Sept. 1975, p. 87.
14. D.L. Bisbee, "Optical Fiber Joining Technique", BSTJ, Vol. 50, No. 10, Dec. 1971, p. 3153.
15. R.B. Dyott, J.R. Stern and J.H. Stewart, "Fusion Junctions for Glass-Fiber Waveguides", Electronics Letters, Vol. 8, No. 11, June 1972, p. 290.
16. R. Jocteur, "Cabling of Low-Loss Optical Fibers", First European Conference on Optical Fiber Communication, London, Sept. 1975, p. 79.
17. Y. Kohanzadeh, "Hot Splices of Optical Waveguide Fibers", Applied Optics, Vol. 15, No. 3, March 1976, p. 793.
18. D.L. Bisbee, "Splicing Silica Fibers with an Electric Arc", *ibid.*, p. 796.
19. M. Borner, D. Gruchmann, J. Guttman and O. Krumpholz, "Detachable Connector for Monomode Glass-Fiber Lightwave Guides", Archiv.Fur Elektronische And Ubert., Vol. 26, No. 6, June 1972, p. 288.
20. M.L. Dakss and A. Bridger, "Plug-In Fiber-to-Fiber Coupler", Electronics Letters, Vol. 10, No. 14, July 1974, p. 280.
21. J. Guttman, O. Krumpholz and E. Pfeiffer, "A Simple Connector for Glass Fiber Optical Waveguides", Archiv.Fur Elektronische And Ubert., Vol. 29, No. 1, 1975, p. 50.
22. S. Zemon, D. Fellows and P. Sturke, "Eccentric Coupler for Optical Fibers: A Simplified Version", Applied Optics, Vol. 14, No. 4, April 1975, p. 815.
23. K. Miyazaki, M. Honda, T. Kudo and Y. Kawamura, "Theoretical and Experimental Considerations of Optical Fiber Connector", Topical Meeting on Optical Fiber Transmission, Williamsburg, January 1975, p. WA4.
24. J.D. Archer, "Current Status of Fiber Optic Interconnection", New Electronics, Vol. 9, No. 2, Jan. 1976, p. 37.
25. J.F. Dalgleish, "Connections: Well-Designed Splices, Connectors Must Align Fibers Exactly", Electronics, 5 Aug. 1976, p. 96.
26. J. Guttman, O. Krumpholz and E. Pfeiffer, "Multi-Pole Optical Fiber-Fiber Connector", First European Conference on Optical Fiber Communication, London, Sept. 1975, p. 96.
27. J. Guttman, O. Krumpholz and E. Pfeiffer, "Multi-pole Optical Fiber Connector", Electronics Letters, Vol. 11, No. 24, Nov. 1975, p. 582.
28. P.W. Smith, D.L. Bisbee, D. Gloge and E.L. Chinnock, "A Molded-Plastic Technique for Connecting and Splicing Optical Fiber Tapes and Cables", BSTJ, Vol. 54, No. 6, July-Aug. 1975, p. 971.
29. J.F. Dalgleish and H.H. Lukas, "Optical-Fiber Connector", Electronics Letters, Vol. 11, No. 1, Jan. 1975, p. 24.
30. "Fiber-Optic Cable Getting Connector for Use in Field", Electronics, 21 Aug. 1975, p. 29.
31. G. LeNoane and R. Bouillie, "Connections for Optical Cables: Design and Measurements", First European Conference on Optical Fiber Communication, London, Sept. 1975, p. 194.
32. D. Gloge, P.W. Smith, D.L. Bisbee and E.L. Chinnock, "Optical Fiber End Preparation for Low-Loss Splices", BSTJ, Vol. 52, No. 9, Nov. 1973, p. 1579.
33. Y. Toriyama et al., "Multimode Fiber Cable for Optical Transmission", Fujikura Technical Review, No. 6, Dec. 1974, p. 14.
34. H. Murata et al., "Splicing of Optical Fiber Cable on Site", First European Conference on Optical Fiber Communication, London, Sept. 1975, p. 93.
35. P. Hensel, "Simplified Optical-Fiber Breaking Machine", Electronics Letters, Vol. 11, No. 24, Nov. 1975.
36. R. Kersten, P. Mockel and D. Schicketanz, "Cutting of Glass Fibers by Temperature Shock", Siemens Forsch.-u. Entwickl.-Ber. Bd. 3, (1974) Nr. 3, p. 140.
37. M.I. Schwartz, "Optical Fiber Cabling and Splicing", Topical Meeting on Optical Fiber Transmission, Williamsburg, Jan. 1975, p. WA2.



J.F. Dalgleish received his B.A.Sc. in Engineering Science in 1965 and his M.A.Sc. in Engineering Materials in 1967, both from the University of Windsor, Windsor, Ontario, Canada. Since joining Bell-Northern Research in 1973, Jack has been involved with the development of optical fiber connectors, splices and associated equipment. Jack's current position is Manager of the Optical Connection Technology Department.

DEVELOPMENT OF A ROBUST OPTICAL FIBRE CABLE AND EXPERIENCE TO DATE WITH INSTALLATION & JOINTING

by

N.S. Dean

BICC Telecommunication Cables Limited,
Prescot, Merseyside, U.K.

R.J. Slaughter

BICC Research & Engineering Limited,
London, U.K.

1 Introduction

The studies undertaken to establish the feasibility of communication systems based on optical fibre are so recent and so well known as to need no recapitulation. However, feasibility having been established, the time taken to create practical working systems depends heavily on being able to realise system components capable of withstanding real work environments and of satisfactorily low cost. The overall criterion to be met, of course, is that the new system must be capable of providing the required service at a lower total cost than that of competing technologies. This does not necessarily mean that each component in the system must be cheaper than that of other systems although it is clearly advantageous that it should be so.

Component development, therefore, must be undertaken to meet two main objectives:

1. The component must satisfy the technical requirements of the system.
2. The installed cost must meet the overall system cost criterion.

With these objectives in mind approximately five years ago BICC established a small development team to investigate the problems of realising practical optical fibre cables. Work was first aimed at establishing basic design principles and later at the development and production of actual cables suitable for field evaluation.

This paper outlines the work undertaken to date, reports the very satisfactory field performance of installed cables, and suggests cable constructions which it is believed would be suitable for future, more ambitious, systems.

2 Cable Design Objectives

The design of an optical fibre cable for use in a telephone network involves solving the problem of protecting fibres for duct installation, i.e. avoiding breakage and increased attenuation arising from the form of distortion known as microbending. Individual fibres are normally provided with some form of plastics coating, which may be just a few micrometers thick, to prevent abrasion of the glass surface, or a much thicker ("buffer") coating of 0.3-0.5mm. The realisation of fully satisfactory buffer coatings, however, is not easy, and generally requires an extra production process. The

simple cable to be described does not incorporate buffer coatings.

3 History of PSP (Neutral Axis) Cable

The basic shape originated in designs worked out in 1972 and which were examined under a Post Office Corporation development contract. A first principles design study was made for a structure which would package almost inextensible glass fibre, and yet tolerate enough tension to pull 2km lengths into ducts, i.e. a cable which would be light, have a high Young's modulus at low tensile strain, and yet be flexible and adequately resistant to crushing. A simple construction satisfying these requirements was in essence a steel-reinforced plastic ribbon - a flat extrusion of polyethylene containing steel wires and optical fibres in line on the neutral axis for bending.

The concept was tried experimentally for the Post Office using glass fibre bundle, at a time when fibre breakage was the major consideration, and the problems of microbending had yet to be recognised.

In 1974, following an agreement between BICC, the Plessey Company, and Corning Glass Works, which made Corning fibre available to BICC, attention turned to the development of cables containing relatively few low-loss fibres. The first successful trial, in which isolation of the fibres to avoid the problem of microbending was provided by forming a cavity around them, was carried out in November 1974 (Fig.1).

This cable was cut and installed as two lengths in the grounds of Taplow Court in Berkshire the following month, and television signals were transmitted later the same day. Other details are shown in Tables 1 and 2. A normal cable installation team pulled the cable in by hand, and no difficulties were encountered. The cable has remained stable in attenuation as shown in Table 3, and is used for the experimental transmission of base-band television and PCM signals.

4 Hastings Cables

The first experience of pulling PSP cable over other cables in the same duct came from an order from Rediffusion Ltd., who wished to evaluate optical fibre cable in the Vision Trunk feeder of their TV distribution network at the British South Coast resort of Hastings. A two-fibre cable design was

selected, each fibre to carry one television channel on a carrier frequency of around 9MHz. These cables were successfully pulled through crowded ducts by the customer's own installation team (Fig.5).

This installation, which is believed to be one of the earliest installations of optical fibre cables in commercial service, is of particular interest since during installation many situations were encountered that were typical of a distribution network in an urban area. A full description of the installation is given in Appendix 1 together with a route diagram. No problems arising from the optical fibre cable were encountered and the installation undoubtedly proved the ease with which the cable can be handled, and its extremely uncritical nature. It is unlikely that any other wideband cable could have been installed in this environment as easily and without degradation of intrinsic performance.

5 Experience to date with Hastings Installation

Bearing in mind the difficulties experienced during installation from the congested nature of the ducts, that a significant part of the route is alongside a main road carrying heavy traffic, and has a gradient of 1 in 6 in parts, the very consistent performance of the cable must be regarded as encouraging. The simplicity of the design has not been shown to be a weakness, and the performance has, in every way, matched that of the traditional coaxial cable in its ability to resist its environment.

Since March 1976 the cable has carried BBC and ITA television programmes to over 34,000 subscribers in the Hastings area, without, in fact, many of the subscribers being aware that they are participating in a significant experiment. Indeed if there are any disappointments resulting from the Hastings experiment they can only be that the new technology has produced such an unremarkable result. Already from this field trial one can begin to draw the conclusion that system costs alone will determine the rate at which optical fibre cable systems can be absorbed into cable television networks.

6 Jointing

Our early experience suggested that a practical way of providing the necessary alignment at a butt joint between two fibres was to utilise an impressed groove in a malleable metal, tailoring the groove by using similar fibre as the forming tool. This approach is a development from the method described by C.G. Someda⁸ of Bell, which used an impressed groove in perspex.

The first outside installation was in May 1975, when the shorter of the Taplow cables was cut and jointed in an access box. The completed joint was protected by insertion in a standard Post Office jointing sleeve (Fig.6). Other field joints have subsequently been made, as indicated in Table 1.

Copper groove joints have been shown to be quite feasible to install in the field, although so far only by experienced laboratory personnel. No attempt has been made yet to semi-automate the process, but much could be done in this direction when the need arises.

Joint attenuation can be considered as a sum of two parts. One is the intrinsic mismatch loss between fibres which differ in size or n.a., and would be present even if perfect alignment were provided by the jointing technique. The other arises from lack of perfection in the joint, and would be present even if the fibres being joined were identical. In practice the joint loss is typically found to be the mismatch loss (where the fibres are different in size or n.a.) plus 0.1dB. Present joints include a drop of index matching liquid (liquid paraffin is used) at the fibre junction. No evidence of degradation with time has been seen to date.

No claim is made that this is a final solution to fibre jointing, but it appears to be at least a satisfactory interim solution for the early cable evaluations now being undertaken.

7 Exhibition Cable

At the time of the 1st European Conference on Optical Fibre Systems, September 1975, the Post Office, to show U.K. progress, arranged a small exhibition in a nearby building. The BICC/Plessey contribution was a demonstration of TV over a 6-fibre cable temporarily installed as a loop in and below the building. The route included a 30 metre vertical shaft and a horizontal tunnel. Installation was carried out by a Post Office team. After the exhibition the cable was recovered and redrugged. The redrugged cable was measured and found to have its original characteristics.

8 Gresham Street

By arrangement with the Post Office, a cable was laid in December 1975 between Wood Street exchange and a Post Office building in Gresham Street in the City of London, with the intention of providing an experimental link for vision signals (Fig.2). A second cable was added in July 1976. Four joints are present, including one in a footway box near the Bank of England (Fig.4).

The attenuation measurement record shows that no appreciable loss has been added by installation or jointing. It is intended by the Post Office to use the complete optical loop as an insert in a conventional cable network, in order to gain experience of the long term stability. Information available so far on attenuation stability in general suggests that cables which are made without introducing added attenuation are subsequently stable.

Environmental Testing

A short length of early PSP cable was subjected at Corning to a series of mechanical tests of the kind applied to military cables. The following were included :

1. Tension
2. Twists on tensioned cable
3. Repeated $\pm 90^\circ$ bends
4. Impact

The results are given in Table 4. Whilst some failures occurred the behaviour of the cable was generally encouraging. Post Office tests have included folding the cable back on itself and compressing in a vice until the loop was flattened. The fibres did not break.

Temperature cycling of a drum of recently-made cable between -10°C and $+60^\circ\text{C}$ showed no change in attenuation.

Certain of the mechanical tests, particularly those where tension is involved, appear irrelevant on short lengths; because of the loose mechanical coupling between the fibre and the cable sheath practically no load is transferred to the fibre in a typical case.

10 Round-Section Optical Cables

In parallel with the development of the flat cable, research here and elsewhere has been carried out to develop round-section optical cables, more closely resembling conventional telephone cables. Corguide is an example of an intermediate class of cable, superficially a round cable, but having a preferred direction of bend characteristic of a flat cable (by the use of 2 diametrically opposed reinforcement members).

Numerous designs for cables with true round-section symmetry have been proposed. One BICC design being developed for the Post Office comprises 6 fibres, individually coated by a soft buffer material (thermo-plastic rubber), laid up with hard polyethylene filaments around a central core which provides tensile strength.

11 Advantages and Disadvantages of Flat Cable

All the cable installations undertaken or planned to date have involved flat cable. The advantages of the design have already been outlined in Section 3 and it is fair to record that these advantages have been shown to be real under practical field conditions. No fibres have been broken during installation, even when cables have become jammed in blocked duct routes, or when, for purposes of exhibition or simply to make the best possible use of resources, individual cables have been installed, withdrawn and re-installed. The crush resistance of the design has been amply proved and one of the cable lengths installed

in London survived tramping underfoot by London's lunchtime shoppers as it lay 'flaked' on the pavement awaiting installation. However the flat design could have certain disadvantages. Although one can visualise it being developed to contain say 15 or 18 fibres it is more difficult to visualise a version containing say, 100 fibres, without returning to a fibre bundle concept. Also cable installation engineers believe that a flat cable may in certain circumstances be more prone to wedging when drawn into ducts containing other cables.

Finally, the design is asymmetrically compliant and this can make installation a little more difficult, and is not usually a characteristic of cables used in telephone networks. A round design of cable removes a number of these alleged disadvantages, but on the other hand it is difficult to visualise a round cable construction which enjoys the immunity of damage from crushing imparted by the flat design. A round cable will only have a symmetrical compliance if the strength members are suitably disposed circumferentially or are along the neutral axis. Moving the optical fibres away from the neutral axis demands that some provision is made for relative movement of the fibres when the cable is bent and probably will result in minimum bending radii being insignificantly greater than that of a flat design. However it is recognised that the simple flat design, having limited scope, will gradually be replaced by round designs or more symmetrical constructions which preserve, as far as possible, the good features of the flat design. This point is treated in further detail under Section 12.

12 Future Developments

To date production and field experience of the PSP cable have indicated its satisfactory design despite limited disadvantages which have been mentioned, and which in practice have proved to be more imagined than real.

It has been demonstrated so far that it is practicable to make and install PSP cable without raising the fibre attenuation, and that such cables can be jointed in the field.

The 'open' construction of PSP cable means that in the event of sheath damage water could gain access to a considerable length of cable. Some work has been done on filled or waterproof versions of the cable and this work is continuing. Such filling may also be useful in preventing creep in the presence of vibration, should this prove to be a problem.

Designs of cables are also being investigated in which small numbers of fibres are incorporated in plastic tubes, which are later stranded, to form a circular unit type cable. Strength members are incorporated either on the cable axis or in the cable sheath thereby preserving the symmetry of the design. Impact resistance of the design is expected to be satisfactory although it is not expected that the design will be able to

withstand large compressive forces for long periods. In parallel with this work further work is being carried out on 'buffered' fibre designs as noted in Section 10.

Some consideration is also being given to versions of cables suitable for overhead use. Two approaches are being considered, the first relying on a conventional catenary support, the second relying on a reinforced design of sheath. Experience to date suggests that successful cables can be evolved using the techniques indicated.

13

Conclusion

In this paper, work carried out by BICC in the development of optical fibre cables has been reported together with practical experience from cables installed in working systems. It is clear from the experience gained that practical transmission systems can be built employing optical fibre cables and that adequate techniques already exist for the installation of these cables. Their stability in service suggests that no long term problems are likely to develop, and that such systems can be confidently accepted into commercial use. The further work to be carried out must be aimed not only at realising the improved cables noted but also must be aimed at further reducing their cost. A significant factor in cable cost is the cost of the fibre, which can be expected to reduce as the volume of production increases. However, in the medium term optical fibre systems may well provide the lowest cost solution to certain network requirements and it is felt that the experience reported will contribute to the confident acceptance of the optical fibre cable solution in these cases.

14

Acknowledgements

The information presented in this paper is based on the work of many engineers from BICC Research & Engineering Ltd. and BICC Telecommunication Cables Ltd., in particular Mr. T.G. Murphy, who also contributed Appendix 1, and the following who have been closely involved in cable and jointing development :- J.E. Taylor, S.J. Stannard-Powell, D.J. Martin, and K. Lawton. Acknowledgement is made to the Directors of Rediffusion Ltd., and to Dr. A.E. Cutler of Rediffusion, for details pertaining to the installation of the Hastings cable, and to the Post Office Corporation and Corning Glass Works for the tests referred to in Section 9.

Thanks are due to the Directors of BICC Cables Ltd. for permission to publish.

15

References

1. K.C. Kao & G.A. Hockman, Proc.IEE 113 (7) 1151-8, 1966
2. R.J. Slaughter, A.H. Kent, and T.R. Callan, "A duct installation of 2-fibre optical cable", "Optical Fibre Communication", I.E.E. Conference Publication No.132, September 1975, p.84.

3. P. Fletcher, "Fibre optic TV link now in service", Electronics Weekly, 7 April 1976, p.24.
4. "Cable TV by piped light", Electronics & Power, August 1976, p.494.
5. Electronics, 5 August 1976, p.87.
6. C.G. Someda, Bell System Tech. J. 52 (4) April 1973, pp.583-596.
7. S.G. Poord & J. Lees, "Principles of fibre-optical cable design", Proc.IEE 123 (6) June 1976, p.597.

Figure captions

- (1) A 2-fibre PSP cable*
- (2) Installing cable in the City of London
- (3) Cross-section of the cable of Fig.1
- (4) Making foot-way box joint in the City of London
- (5) Hastings installation
- (6) Joint and protective sleeve

*This cable and its method of manufacture are the subjects of British & foreign patent applications.

TABLE 1
Installations of PSP Cable

Location	Date	Cable	Duct	Length (m)	Field Joints in cable*	Notes
Taplow	Dec 74	2-fibre	50mm PVC (empty)	740 200	0 1	Joint was added May 1975
Hastings	Oct 75	2-fibre	Glazed earthenware, P.O. type (with other cables)	800 650	1	Carrying commercial traffic since March 1976
London	Sep 75	6-fibre	None (cable on racks)	1000	0	Temporary, for exhibition purposes
City of London	Dec 75 Jul 76	4-fibre 2-fibre	P.O ducts (with other cables)	400 1000	1 1	Commissioned to CCTV Standard

(*For this purpose, a field joint is one in a footway box or kiosk. Joints located in buildings are not included)

TABLE 2
Optical path attenuations at
0.90µm wavelength

Location	Length (m)	Attenuation (dB)	Notes
Taplow	740	20	Loop attenuation(2 x 740 fibre metres)
	200	6	Loop attenuation(2 x 200 fibre metres)
Hastings	800 + 650	18	1427 metres route length
	800 + 650	22	1427 metres route length
London	1000	20	Temporary installation for exhibition purposes
City of London	380	12	Loop attenuation(2 x 380 fibre metres)
	930	8	Loop attenuation(2 x 930 fibre metres)

The fibres used were supplied by Corning Glass Works and ranged in attenuation from 18dB/km to 4dB/km

TABLE 3

Attenuation stability of installed cable
(Attenuation measured at 0.90 μ m with LED source)

Location	Length (m)	Date	Attenuation, dB			
Taplow	740	Dec.74 Apr.75 Nov.75 Feb.76	Fibre 1		Fibre 2	
			Measured	Expected	Measured	Expected
			13.6 13.3 12.2 11.6	- - - -	7.0 6.7 6.9 7.0	- - - -
Hastings	792	Oct.75	6.6	6.4	8.6	7.3
	635	Oct.75	13.0	12.6	11.5	11.1
	Calculated joint mismatch due to fibre differences		-	1.2	-	0
	792 + 635	Jan.76	19.4	20.2	19.5	18.4
Expected values calculated pro rata from measurements on original 1km manufactured length of cable.						
City of London	2 x 380 (instal- led Dec. 1975) 2 x 930 (instal- led Jul. 1976	Aug.76 Aug.76	Fibre loop			
			Measured		Expected	
			11.7		11.2	
			7.5		-	
Expected value from measurements immediately after installation						

TABLE 4

Mechanical Tests on 2-fibre cable

Test	Conditions	Number of cable samples	Fibre failures
Tensile	Up to 91kg load. Gauge length 0.61m	2	0
Twist	Plus and minus 90° under tensile load 2.3kg, 30 cycles/min. 2000 cycles total	3	0
Bend	Plus and minus 90° over 2.5cm mandrel, under tensile load 2.3kg, 30 cycles/min. Failure of strength member occurred at 200 to 270 cycles, and jacket at 740 to 2000 cycles	3	1
Impact	Impact 3 to 6 ft lb (0.4 to 0.8 m.kg) at 30 impacts/min. There was little dependence on impact magnitude in this range <u>No. of impacts</u> 3 4 10 200	30	0* 3* 6* 16*

*Cumulative total out of 60 fibres

Biographical Notes



NOEL S. DEAN
Director & Chief Engineer
of BICC Telecommunication
Cables Ltd.

He is responsible for the Technical policies of BTCL, which comprises manufacturing units in Prescott, Manchester, Belfast and London.

Joined BICC in 1944 as Electrical Engineering Graduate from Manchester University and holds post Graduate Diploma in Electronics from University College Southampton. He is a Member of the Institution of Electrical Engineers.



RAYMOND J. SLAUGHTER

Joined the cable industry as a laboratory assistant in 1942, subsequently graduating from London University, and is now a member of the Communications Department in BICC Research and Engineering Ltd. At different times he has been associated with development work on radio-frequency cables, submarine telephone cables, superconducting power cables, and millimetric waveguide, but since 1970 has worked mainly on optical fibres.

He is a Member of the Institute of Physics and a Member of the IEE.

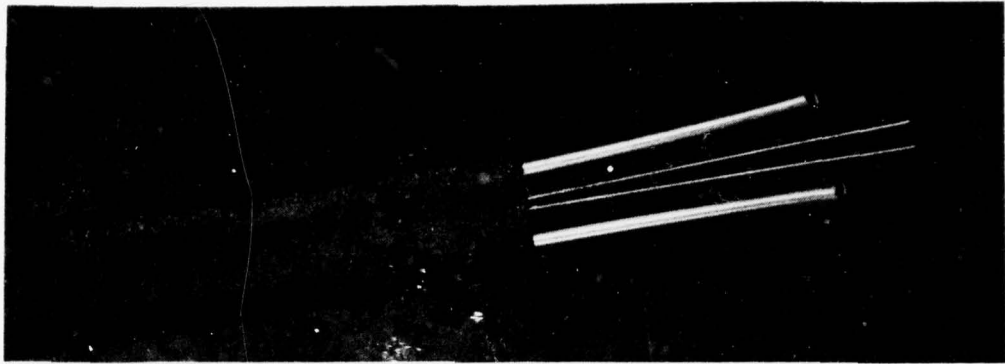


Fig.1

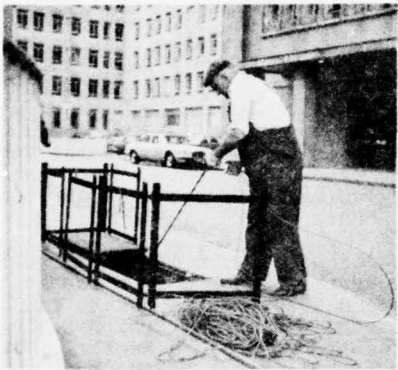


Fig.2

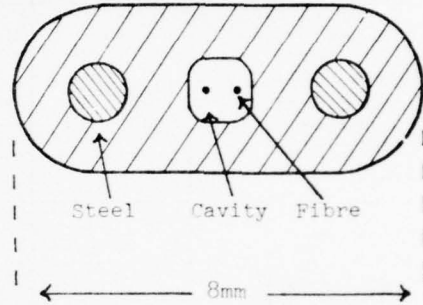


Fig.3

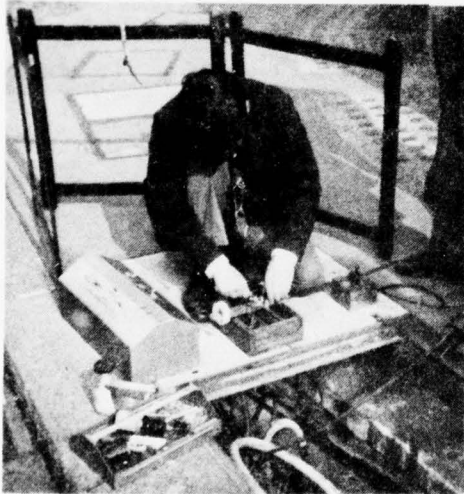


Fig.4



Fig.5

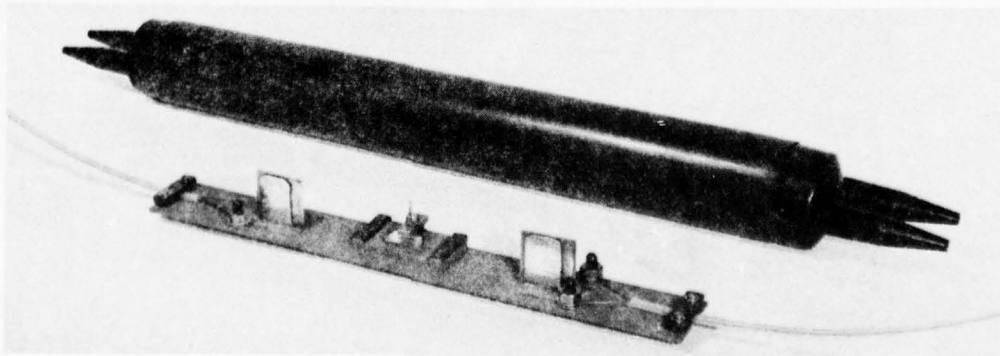


Fig.6

Appendix 1

The installation of a two-fibre optical cable by Rediffusion Ltd. at Hastings - 21 and 22 October 1975

1 Cable Installation

All ducts had been pre-rope with a $\frac{3}{4}$ " hessian rope, and a draw rope was also pulled in with the cable between each box. All pulling in was done by hand.

The first drum (Drum A) was set up at the surface box across the road from the Blackman Kiosk and the cable pulled towards the box at the junction of Marline Avenue a distance of 115 metres up a 1 in 18 slope. The pulling tension was 20lb, and the cable was lubricated with liquid paraffin at the entry box. The duct was of 4" diameter glazed earthenware and contained seven small diameter cables.

The cable was then pulled to the next box a further distance of 157 metres with a six foot rise and fall in the same type of duct containing six small diameter cables. The cable had lubrication applied at the intermediate box and the pulling tension increased to 35lb. The cable was then pulled a further 132 metres down a 1 in 20 slope in the same type duct containing 6 cables, lubrication being applied at the start and the two intermediate boxes. However, part way through this pull the pulling tension increased dramatically and the dynamometer registered at least 100lb tension. Pulling was stopped and it was assumed that the draw rope was wrapped around the existing cables. To overcome this problem it was decided to pull out a loop at the previous box and thereby eliminate any drag. This brought the pulling tension over this length down to 40lb.

The cable was then pulled 180 metres to the next box down a 1 in 30 slope. Lubrication was stopped at the first of the intermediate boxes but maintained at the second and third boxes. With the loop out at the second box, to relieve the tension over the third length, all the cable was pulled through at this point and flaked out onto the grass verge, leaving enough at the first box to be fed back across the road to the Blackman Kiosk.

Once all the cable had been pulled through, boxes 1, 2, 3, and 4 were closed down and the cable fed under Blackman Avenue to the box across the road. Men were stationed at these right angle boxes to keep a free loop in the cable and to lubricate it.

The cable passed through another intermediate box at 66 metres and onward 87 metres to a box on the corner of Stonehouse Drive where it was pulled out onto the pavement because the box was on a bend, and the duct entry and exit at this box caused rope fouling. The down gradient at this point was 1 in 40 and no high tensions were experienced. The cable was then back-fed 13 metres into the Hollington Kiosk where a cable joint was to be made at a later date by BICC.

The second drum (Drum B) was set up at a manhole 369 metres from Hollington Kiosk and the cable pulled towards the Kiosk.

The same procedure was followed as for Drum A. Men were stationed at the pull-through boxes, lubricating and easing the cable through and no hard pulls were experienced.

The cable was pulled 63 metres down a 1 in 25 slope through a 3 inch glazed duct containing 9 cables to a right-angled box, then 20 metres level to the next right-angled box, then 96 metres through an empty P.V.C. duct down a 1 in 6 gradient, then through a 3 inch steel pipe for 18 metres level to the next box where enough cable to reach the Hollington Kiosk was flaked onto the grass verge. The previous boxes were now closed down.

The next box was 46 metres away along Stonehouse Drive but trouble was experienced with the pulling rope. This was due to a collapsed duct caused by recent constructional work carried out nearby. The duct had to be exposed and two split sections of duct installed before cabling could continue.

The cable was pulled through 46 metres of duct in level ground to the next intermediate box, 12.5 metres at a 45° angle to the next box, then 69 metres, at which box the cable was again flaked onto a grass verge due to the awkward entry and exit of the ducts. The cable was then fed for 2.5 metres to another box in a 4 inch glazed duct containing 6 cables, then 39 metres into a box and finally 3 metres into the Kiosk.

The cable now remaining on the drum was flaked off along a footpath and back-fed through a 3 inch glazed duct containing 9 cables for 10 metres to a right angled box, then for 205 metres passing through three intermediate boxes on a slight curve and an up gradient of 1 in 40, and flaked onto a grass plot. It was then pulled 35.5 metres under Drury Lane through a 3 inch glazed duct containing 20 cables into Rediffusion House.

Tests were made on the fibre which was proved intact.

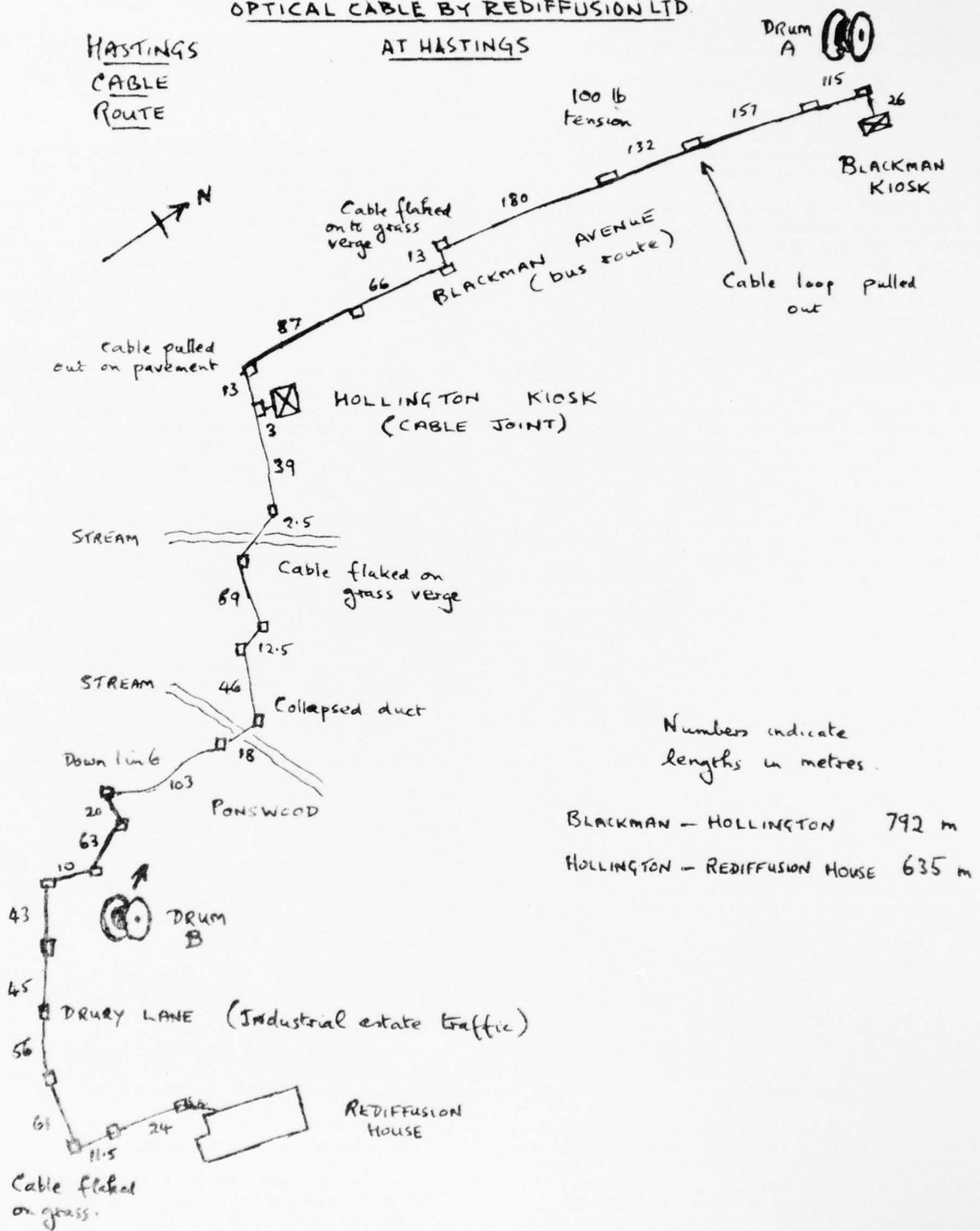
Blackman Avenue is a regular bus route and carries a lot of private car traffic at peak hours.

Drury Lane carries a fair amount of traffic, including lorries and private cars going to various parts of the Industrial Estate.

All other roads are residential.

On average the cable is 4 metres from the kerb in Blackman Avenue and 2 metres from the kerb in Drury Lane.

THE INSTALLATION OF A TWO-FIBRE OPTICAL CABLE BY REDIFFUSION LTD.



NOT TO SCALE.

WEATHERABILITY OF BLACK POLYETHYLENE - PREDICTABLE?

By

W. F. Jensen, Jr. and J. N. Jones

E. I. Du Pont De Nemours & Company
Plastic Products and Resins Department
Wilmington, Delaware

Summary

The history of the use of carbon blacks to provide UV stability in polyolefin resins is reviewed. The two methods of judging carbon black dispersion, visual and instrumental, are traced through their development to methods of test published by ASTM.

A comparison of these two tests is made. Data is presented comparing actual wire samples weathered 16 years outdoors to the dispersion test results.

Recommendations are made concerning dispersion ratings and required carbon content to provide adequate outdoor life for black polyethylene cable jackets.

The change from paper-lead exchange telephone cables to polyethylene insulated and jacketed cables started in earnest the years immediately following World War II. In the very early stages of this development it was recognized that polyethylene per se was rapidly changed when exposed to sunlight, resulting in dropping elongation values until crazing and cracking occurred. Work at Bell Telephone Laboratories and Western Electric (1) showed that the incorporation of carbon black of the proper particle size in the polyethylene matrix would effectively screen out ultraviolet rays. This combination would be expected to be able to maintain adequate physical properties to do its job for 20 or more years.

The need for producing a homogeneous mixture was recognized at the beginning. If a poor mixture existed, it was possible to have "windows" in the material that would allow penetration of the UV rays and thus brittle areas would develop leading to cracking and loss of the protective jacket.

The need to provide a rating system of the dispersion of the carbon black in the polyethylene resulted in the use of the optical microscope. As originally developed in the late 1940s, the test involved making a microscope slide containing a tiny slice of material which had been heated and flattened to a thin film. The resulting film was viewed at 100X and visually rated. Three criteria, agglomerates, background, and gel were considered. The visual appraisal was compared to some visual standard slides and a letter value of

excellence of dispersion resulted. Later, we will elaborate on this test.

The limitations of using human judgments were well known and a search for an instrumental method started early. Work during the 1950s led by ASTM and by the Electronics Command (2) did produce some test methods which were incorporated in some Federal specifications and also in some IPCEA standards. Work at Battelle Institute in cooperation with industry in the late 1950s (3) revealed such wide disagreement between various laboratories that the instrumental methods were generally discredited.

Work continued at Bell Labs, however, under the guidance of the late John Howard, and in the late 1960s a revised method was proposed which has now been generally accepted. Again, we will elaborate on this test later.

Along with the above tests, actual field experience was being generated over the past 30 years. The real question has been, have cables made from material rated acceptable by the above tests actually performed satisfactorily? Have we been overly critical in our tests and have we been spending more money for dispersion than necessary? A partial answer lies in the fact that an early sample of a dual conductor rural telephone wire hung on a pole in Florida for 20 years was still capable of being tied in knots without crazing or cracking (4).

Now, let's go back and review in some detail the two most widely used tests for carbon dispersion quality. First, the optical microscope test.

This test as applied to black polyethylene was the direct result of Bell Labs and Western Electric Co. specifications. In the mid to late 1940s producers of polyethylene were working very closely with these people in the development of a weatherable compound to replace the lead jackets then in use. Since these were totally new compounds, a new set of test parameters were required. Early researchers had established that a well dispersed carbon black in polyethylene should yield a compound which would give many years of outdoor life. The use of visual standards based on a microscopic examination was established very early.

In the beginning it was relatively simple for the seller to sit down with the buyer and agree on a set of observational standards, especially since at this time there was only one buyer and two sellers. At first there were only four grades of dispersion, A, B, C, and D. As usually happens, this soon expanded into a set that ran from A+, A, A- all the way down to D. The original grading of C was passing. Later this became C- and that is still the lower limit.

Also at the beginning a general rating of overall dispersion was determined. This changed also as we began to divide the dispersion into three categories, agglomerates, background, and gel, each of which was given a letter rating.

As can be seen from the foregoing discussion, the judgment of carbon dispersion was a very subjective process. Experienced laboratory technicians were vital to the resin producers. It was also necessary to have a "judge" available to adjudicate differences of opinion.

With this background, you can imagine the difficulties ASTM faced in attempting to translate this kind of a test into a standard procedure for use in many laboratories. Subcommittee D20.40 struggled with this test for many years. What finally resulted was a Standard Recommended Practice for Microscopical Examination of Pigment Dispersion in Plastic Compounds, ASTM D 3015-72. This is a general procedure for the study of many different polymers and pigments. It does have an appendix, however, which describes the specific task of observing the dispersion of carbon black in low density polyethylene. Even here the establishment of proper observational standards is left to agreement between the buyer and seller.

The current status of the microscope test is as follows: The only industry specification that still requires its use is the REA PE-200 specification. However, this specification also lists the new instrumental method as an alternate. Other industry specifications have used some form of an instrumental method (i.e., LP-390a, IPCEA S-61-402). There are still quite a few cable companies that use the microscope test in their in-house specifications. However, since the method is so subjective, the cable companies really have to rely on the judgment of the resin producer to deliver them a well dispersed black resin.

The major method now in use for specifying carbon dispersion is the one developed by John Howard, Harold Gilroy and Associates of Bell Labs. This method culminated many years of trials by many different researchers. It came into official use in 1969 and was proposed as an ASTM method in 1970. That same year John Howard presented a paper at the Wire and Cable Symposium (5) describing the test procedure.

The test method was studied by a task group of members of ASTM Committee D 20.12.03. The group consisted of 15 members

representing 13 companies or laboratories. The evaluation consisted of two round robin tests.

The first was designed by John Howard to permit us to compare the ability of various makes of spectrometers to measure the absorbance of a specially mounted test film of black low density polyethylene. Two reference materials, an optical filter made by Kodak and a film of black polyethylene, were mounted in fixed holders. Both of these samples had absorbance values of approximately one. A test sample film of black polyethylene containing about 2.5% carbon black was also mounted in a fixed holder. The above work was done at Bell Labs and these samples were measured on their instrument, a Beckman Model B. This original data is shown in Table I.

These three samples were passed between the participating laboratories. Each lab measured the absorbance of the test film in relation to each reference material. This data is shown in Table II. A preliminary study of the data indicated that different instruments gave slightly different levels of absorbance. The data was then sorted out by instrument and showed the results presented in Tables III and IV.

The results of the above work indicated that the various instruments give very reproducible values when measuring the same samples. This points up the fact that when a buyer and seller are judging a product they should both be using the same type of instrument. It is also possible that by multiple analyses of similar samples different instruments could be used to develop a correction factor. This could be used to report data on the same basis.

The most widely used instrument has been the Beckman Model B. This instrument also gives the lowest measured value of absorbance for those instruments studied. Since it is widely available, it has been used to establish numerical values for specification purposes.

The second round robin run by our task group consisted of performing the complete test starting with a uniform milled and molded plaque of a typical black resin. Each lab prepared their own films, mounted them in a holder, measured the absorbance, determined the thickness using the density and the weight of the film, and calculated the absorption coefficient according to the following formula:

a = absorption coefficient

$$a = \frac{-3 (2.303 \times \text{avg. absorbance value})}{10 \left(\frac{t}{t} \right)}$$

a = milli(absorbance/metre)

$$\text{Where } t(\text{thickness}) = \frac{W}{D \times A} \quad (\text{meters})$$

W = weight, g.

D = density, g./m³

A = area, m²

The results of the second round robin are shown in Table V. Those of you familiar with the test will note that ASTM is reporting data to three significant figures, whereas all previous data has been reported to four. It was our considered judgment that the experimental results showed that the precision of the test only warranted such values.

As you can see from Table V, the test is quite precise and is truly a great improvement over some of the early round robin work. However, a word of caution is appropriate here. The ASTM work was only with black low density polyethylene. Extrapolating this data to other polyolefins or polymers may or may not be justified. This test method has now been carried through the ASTM approval system and it appears in the 1976 Book 36 as D-3349-74.

Now let's take a look at how these test methods may relate to actual polymers that have been tested in weatherometers and in outdoor exposures.

First, we would like to show you some routine quality control data from our production unit in which we are measuring carbon content, absorption coefficient, and microscopic dispersion; Table VI. You will note that in the microscopic rating we report three items (5-N-1). The first and third are numerical conversions of the letter rating - 5 is a B and 1 is an A+. The second stands for N equals normal. The three parameters reported are agglomerates, background and gel. Since it has always been difficult to agree on shades of differences in the background rating, we call it either normal or abnormal. Therefore, the example cited above is rated:

Agglomerates	- 5 (B)
Background	N (Normal)
Gel	1 (A+)

The data in Table VI shows no distinct trends relating carbon content to either dispersion rating. It does, however, point out one important fact. Within the variation existing during this particular production run, the microscopic ratings were consistently uniform 4N2 or 5N2, whereas the instrumental numbers varied from 4096 to 4852. Since a 9 (C-) is considered passing in one test and a 4000 in the other, it appears we have greatly tightened our limits when we switched to the instrumental test.

Let us now take a look at some actual weathering data that we have developed over the past 17 years and compare it to the dispersion tests. Back in 1958, we decided it would be advantageous to obtain some long term weathering data on actual in-

sulated wire samples that were exposed in a severe, outdoor location. A series of compounds, Table VII, were extruded as a 30 mil coating on #14 AWG copper wire. At the Desert Sunshine Exposures Tests, Inc. site outside of Phoenix, Arizona, these wire samples were hung on pole crossarms spaced 40 ft. apart and oriented in a north-south direction. Periodically over the years we have had exposed lengths of each sample returned to our Chestnut Run, Delaware laboratories for testing. The last set of samples represented 16 years of exposure. Data on these wire samples as developed over the past 16 years are shown in Table VIII and Figures 1, 2, and 3. The resins evaluated are as follows:

Alathon® 4, BK-20 is an early version of the typical high molecular weight black jacketing resin for cables that is still used. Alathon® 5, BK-22 is a medium molecular weight resin with the same carbon black system as A-4, BK-20. The Alathon® 5, BN-07 is an early version of a brown pigmented TV wire compound. The Rulan 2, BK-48 was a flame retardant polyethylene with carbon black added to give it weatherability. The carbon black used in all compounds was a channel black with a 20 nm average particle size.

As shown in Figures 1 and 2, the A-4, BK-20 and A-5, BK-22 have survived the 16 years in great shape. The LTB data for the 16-year sample may be the start of a downward trend, but with the test variability present, this drop may not be significant. We will know more when the 20-year samples are tested.

The A-5, BN-07 shows that pigmentation alone is not very effective in giving weathering protection.

The Rulan® sample points out that carbon black does not always assure long life. The complete resin system must be considered. In this case, the presence of large amounts of additives for flame retardancy has changed the simple relation between polyethylene, carbon black, and weatherability.

Figure 3 shows that the insulating properties of all these compounds are still adequate after long exposure as long as the insulation layer is not physically cracked.

Reviewing the data in Table VII on carbon dispersion for A-4, BK-20 and A-5, BK-22, it appears that even though the absorptivity coefficients are well below the current limit of 4000 established in REA PE-200, the actual field performance is excellent. This further substantiates our belief that we have tightened our specifications in changing from the microscope to the spectrometer. We feel a more realistic value would be 3200 minimum or, expressed

in terms of the ASTM test, 320 min. This value already appears in the ANSI specification C8.35-1971; "Specification for Weatherproof Wire".

One other point is evident in Table VII. The actual carbon content of the two good samples was 2.0 percent. If in the future the cost of carbon black exceeds that of polyethylene, we may want to decrease the carbon level in weatherable resins. It appears that dropping the goal from 2.6% to 2.0% will be perfectly safe. This change would be further supported by the famous Bell Labs dropwire previously mentioned which had only 1% carbon.

One final set of data shows a comparison of weatherometer and outdoor exposure data. This data is detailed in Tables IX, X, and XI. The black resin is described in Table IX. Figures 4 and 5 show plots of LTB and elongation as a function of time. We have placed the weatherometer data and outdoor exposure data on the same graph, but this does not imply that we feel that this correlation exists. It is only plotted this way for convenience sake.

These graphs show a comparison between weatherometer data on molded plaques and wire samples along with outdoor exposure data on the same wire samples. After 10 years of outdoor exposure, we have seen only slight change in properties of the wire sample. The weatherometer data shows a long term drift downward in LTB for both samples, whereas, the elongation data is unchanged.

Perhaps the only conclusion that can be drawn from this data is that the black low density polyethylene jacket resins are so good that 10,000 hours in a weatherometer or 10 years outdoors cannot detect a significant change in properties.

Conclusions

1. The microscopic test for carbon dispersion has been largely supplanted in specifications by an instrumental method. However, for trained operators, it still yields valuable information for quality control during the compounding operation.
2. The instrumental dispersion test, ASTM-3349-74, is quite reproducible and precise. The physical dimensions of the different spectrometers do show evidence of machine bias.
3. Results of long term outdoor weathering experiments indicate that our current compounds are overdesigned.
4. It is recommended that the minimum value for carbon absorptivity coefficients be set at 320. This value is quite realistic to insure adequate service life.

- (1) V. T. Wallder, W. J. Clarke, J. B. De Coste, and J. B. Howard, "Weathering Studies on Polyethylene Industrial and Engineering Chemistry", 42, No. 11, 2330 (1950).
- (2) R. M. Schulken, Jr., G. C. Newland, and J. W. Tamblin, "Evaluation of Carbon Black Dispersions in Polyethylene to Predict Weatherability", Sixth Annual Wire and Cable Symposium, Dec. 1957, Asbury Park, N. J.
- (3) G. C. Cocks and A. P. Metzger, "Measurement of the Degree of Dispersion of Carbon Black in Polyethylene Using Absorption of Light", Seventh Annual Symposium on "Technical Progress in Communication Wires and Cables", Dec. 1958, Asbury Park, N. J.
- (4) J. B. Howard, and H. M. Gilroy, "Natural and Artificial Weathering of Polyethylene Plastics", Polymer Engineering and Science, July 1969, Vol. 9, No. 4, Pg. 292.
- (5) J. B. Howard, "Photometric Determination of Carbon Dispersion Quality in Polyethylene", Nineteenth International Wire and Cable Symposium, Dec. 1970, Atlantic City, N. J.

TABLE I

Absorbance of Kodak Standard A = 1.056
Absorbance of PE Standard No. 1 = 1.300
Absorbance values for Test Film at 375 nm:
Beckman Model B

Position Number	Using Kodak Std.	Using PE Std.
1	2.205	2.210
2	2.250	2.276
3	<u>2.306</u>	<u>2.294</u>
Avg.	2.254	2.260

TABLE II

ASTM D 20.12.03

ROUND ROBIN DATA - CARBON ABSORPTIVITY OF PE

LABORATORY	ABSORPTIVITY OF		AVG. OF SAMPLE USING		PHOTOMETER USED
	KODAK STD.	PE STD.	KODAK STD.	PE STD.	
Bell 1	1.056	1.300	2.254	2.260	Beckman - B
Du Pont 1	1.054	1.322	2.245	2.254	Beckman - B
Du Pont 2	1.056	1.320	2.245	2.244	Beckman - B
Phillips	1.233	1.426	2.311	2.327	Cary
Dow	1.056	1.345	2.245	2.246	Beckman - B
Allied	1.258	1.485	2.375	2.402	Beckman - DK2A
UCC	1.030	1.350	2.280	2.286	Beckman - B
Pict. Ars.	1.250	1.440	2.276	2.316	Beckman - DK1A
Eastman	1.218	1.498	2.366	2.381	Beckman - DK2A
USI 1	1.055	1.350	2.222	---	Beckman - B
USI 2	1.05	1.34	2.212	---	Beckman - B
N. Elect.	1.21	1.44	2.37	2.35	Unicas
Bell 2	1.061	1.310	2.243	2.239	Beckman - B
Hercules 1	1.070	1.350	2.224	2.440	Beckman - B
Hercules 2	1.222	1.455	2.373	2.414	Beckman - DK2A
Du Pont 3	1.253	1.502	2.402	---	Beckman - DK2A

SAMPLE: Pressed film of polyethylene containing approximately 2.65% of a furnace black of 20 nm average particle size. Film was mounted in a holder and tested by each laboratory without removing the film from the holder.

TABLE IV

ASTM D 20.12.03

ROUND ROBIN - CARBON ABSORPTIVITY OF PE
ANALYSIS OF DATA USING BECKMAN MODEL DK2A ONLY

LABORATORY	ABSORPTIVITY OF		AVG. OF SAMPLE USING		PHOTOMETER USED
	KODAK STD.	PE STD.	KODAK STD.	PE STD.	
Allied	1.258	1.485	2.375	2.402	Beckman DK2A
Eastman	1.218	1.498	2.366	2.381	for all samples.
Hercules	1.222	1.455	2.373	2.414	
Du Pont	1.253	1.502	2.402	---	
AVERAGE	1.238	1.485	2.379	2.399	
SIGMA	0.021	0.007	0.008	0.018	

TABLE III

ASTM D 20.12.03

ROUND ROBIN - CARBON ABSORPTIVITY OF PE

ANALYSIS OF DATA USING BECKMAN MODEL B ONLY

LABORATORY	ABSORPTIVITY OF		AVG. OF SAMPLE USING		PHOTOMETER USED
	KODAK STD.	PE STD.	KODAK STD.	PE STD.	
Bell 1	1.056	1.300	2.254	2.260	Beckman B
Du Pont 1	1.054	1.322	2.245	2.254	for all samples.
Du Pont 2	1.056	1.320	2.245	2.244	
Dow	1.056	1.345	2.245	2.246	
UCC	1.030	1.350	2.280	2.286	
USI 1	1.055	1.350	2.222	---	
USI 2	1.050	1.340	2.212	---	
Bell 2	1.061	1.310	2.243	2.239	
Hercules 1	1.070	1.350	2.240	---	
AVERAGE	1.054	1.332	2.243	2.255	
SIGMA	0.011	0.019	0.019	0.017	

TABLE V

ASTM D 20.12.03

ROUND ROBIN - CARBON ABSORPTIVITY COEFFICIENT

CARBON BLACK PIGMENTED ETHYLENE PLASTIC

USING KODAK A STANDARD

AS REFERENCE

LABORATORY	ABSORPTIVITY COEFFICIENT MILLI (ABSORBANCE/METER)
Du Pont	430
Bell	444
USI	440
Dow	456
UCC	467
AVERAGE	448
SIGMA	14

SAMPLE: Base polymer - ethylene - vinyl acetate copolymer
Carbon content - 2.65%
Carbon type - furnace black, 20 nm avg. size
Compound melt index - 0.4
Compound density - 0.934

Sample was prepared by milling and compression molding pellets. Molded sheet was cut into one inch squares which made up the test samples. Each laboratory pressed their own test films and measured same.

TABLE VI

% Carbon	Dispersion Ratings	
	Microscope	Absorption
2.45	4 N 2	4042
2.47	4 N 2	4652
2.53	4 N 2	4535
2.66	4 N 2	4312
2.53	5 N 3	4152
2.58	5 N 1	4354
2.61	4 N 2	4852
2.47	4 N 2	4307
2.57	5 N 2	4328
2.68	4 N 2	4271
2.72	5 N 2	4170
2.66	5 N 2	4539
2.76	4 N 2	4529
2.60	4 N 2	4096
2.65	4 N 2	4697
2.45	4 N 2	4152

Low Density, high molecular weight, black polyethylene.

TABLE VIII

30 Mil Coatings on #14 AWG Solid Copper Wire

Resin Code	Property	Unit	Test Values after Years in Arizona							
			Initial	1	2	5	8	12	16	
Alathon® 4-BK-20	Elongation	%	520	460	500	560	540	510	475	
	LTB	°C	-70	-66	-60	-72	-80	-82	-55	
	Diel. Strength	v/m	740	---	970	810	850	950	850	
5-BK-22	Elongation	%	480	540	510	480	470	480	480	
	LTB	°C	-65	-64	-60	-60	-65	-96	45	
	Diel. Strength	v/m	740	960	970	850	640	990	740	
5-BK-07	Elongation	%	530	55	60	40	10	20	15	
	LTB	°C	-80	-28	<-30	<-30	<-30	23	--	
	Diel. Strength	v/m	470	---	640	610	550	560	500	
Rulan® 2-BK-48	Elongation	%	250	---	80	50	---	---	---	
	LTB	°C	<-30	<-30	<-30	---	---	---	---	
	Diel. Strength	v/m	800	830	820	990	860	810	780	

NOTE: LTB is low temperature brittleness value for 50% failure point per ASTM D-746.

TABLE VII

Compound Code	Base Resin		Carbon Content-%	Dispersion Rating	
	Melt Index	Dens@25°C		Micro.	Abs. Coef. (1)
A-4,BK-20	0.25	0.92	2.0	B-	3680
A-5,BK-22	1.2	0.92	2.0	C	2912
A-5,BK-07(2)	1.2	0.92	0.0	NA(3)	NA
R-2,BK-48(4)	1.2	0.92	2.0	NA	NA
A-1000,BK-30	0.25	0.92	2.8	NA	NA

NOTE: (1) Absorption coefficient by the Western Electric test method.
 (2) Contains brown pigment (iron oxide) -- TV wire type.
 (3) NA - not available.
 (4) R-2 is Rulan® flame retardant compound.

TABLE IX

WIRE COATINGS EXPOSED IN ARIZONA
 Alathon 1000,BK-30
 30 Mils on #14 AWG Copper

Years Exposure	Tensile Strength, psi	Elongation	50% LTB(1) °C
Initial	2360	530	-73
1	2150	530	-60
2	2200	530	-67
5	2270	450	-68
10	2200	510	-72

A-1000,BK-30 - 0.26 Melt index, low density, with a carbon dispersion rating (microscope) of A and a carbon content of 2.8%.

NOTE: (1): 50% LTB °C means the temperature at which 50% of the specimens break using ASTM D-746.

TABLE X

WIRE COATINGS EXPOSED IN ATLAS WEATHEROMETER
Alathon 1000, BK-30
30 Miles on #14 AWG Copper

Hours Exposure	Tensile Strength, psi	Elongation, %	50% LTB °C
Initial	2360	530	-73
500	----	----	-72
2000	2080	540	---
3000	2370	480	-65
5000	----	---	-59
10000	2260	470	-52

TABLE XI

MOLDED PLAQUES EXPOSED IN ATLAS WEATHEROMETER
ALATHON 1000, BK-30

Exposure	Tensile Strength, psi	Elongation, %	50% LTB °C
Initial	2360	530	-96
2000	2080	540	-106
3000	1820	510	-79
5000	1800	470	-58
10000	----	---	-50

FIGURE 2

ELONGATION vs. WEATHERING

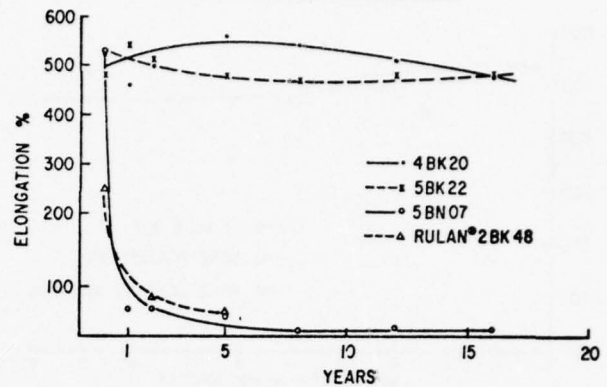


FIGURE 3

DIELECTRIC STRENGTH vs. WEATHERING

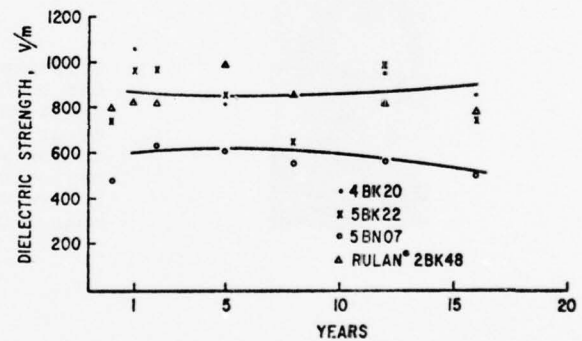


FIGURE 1

LTB vs. WEATHERING

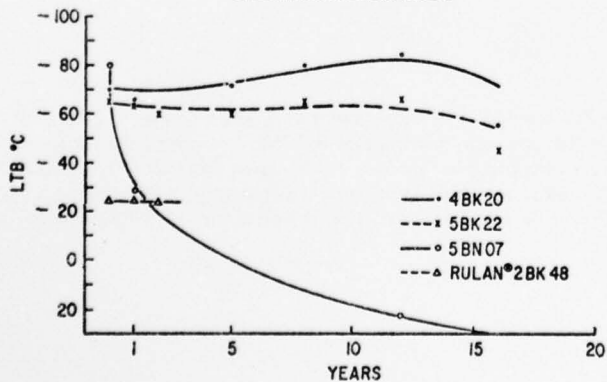


FIGURE 4

A1000 BK 30 - PE 2867

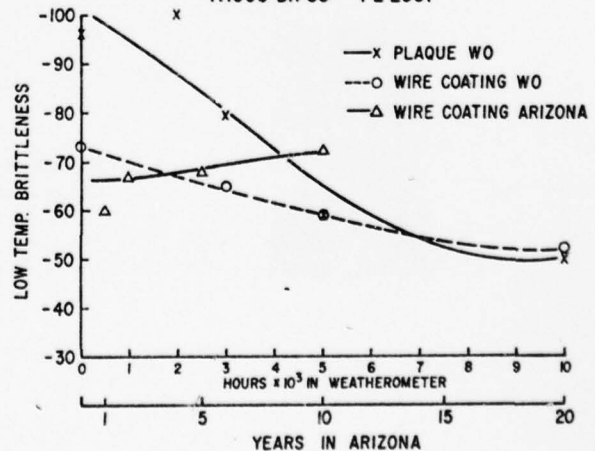
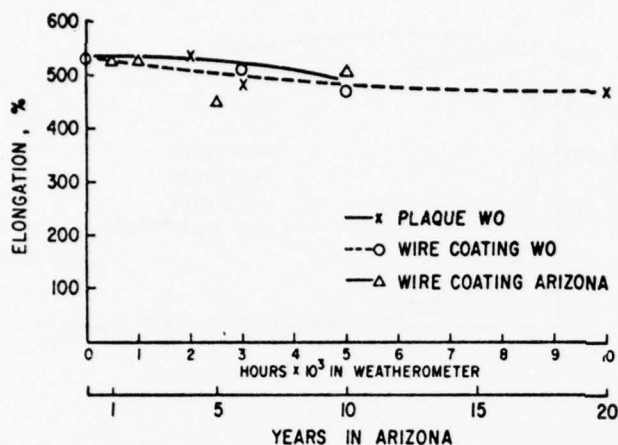


FIGURE 3
A 1000 BK 30 - PE 2867



Mr. Jensen is a graduate of the University of Virginia, with a degree in Chemistry. He has been with the Du Pont Company for the past 34 years. His assignments have been in manufacturing, technical and sales areas of the Plastics Department. He is currently a senior marketing specialist involved with polyolefins resins used by the wire and cable industry. He is an active member of ASTM, IEEE, SPE, and the National Research Council Conference on Dielectrics.



John N. Jones received a Bachelor of Science degree in Electrical Engineering from the University of Arkansas in 1951. He joined the Du Pont Company manufacturing plant in Orange, Texas, as an Electrical Engineer in 1951. He transferred to the Technical Services Laboratory in Wilmington, Delaware, in 1959. He is currently working in Polyolefins Division on wire and cable projects.

PREDICTION OF POLYETHYLENE AGING BY ISOTHERMAL DSC

By

Daniel L. Davidson
Union Carbide Corporation
Bound Brook, New Jersey 08805

SUMMARY

Empirical correlations have been established between isothermal differential scanning calorimetry (DSC) and accelerated heat aging tests in crosslinked low density polyethylene. For the first time, relationships are available which allow prediction of the effectiveness of antioxidant systems in polyethylene for practical heat aging tests by merely running an isothermal DSC experiment. The time saved is considerable since the DSC measurement takes only minutes whereas heat aging experiments require several days.

The method could be very useful as a quality control test for estimating the performance of vulcanizable polyethylene.

The empirical relationships determined and conclusions are discussed in detail.

INTRODUCTION

In the course of investigating potentially new antioxidants for vulcanizable polyethylene, isothermal oxidative stability studies at high temperature were conducted using differential scanning calorimetry (DSC). Although initially it was felt that useful information could easily be obtained by this technique, unusual thermal response of polyethylenes containing some thiophosphite antioxidants was found to complicate analysis.

Accelerated heat aging (air oven) tests are routinely used as quality control and specification tests for plastics throughout

the industry, but little is known about these in relation to DSC parameters. In the past, DSC has been used to show antioxidant effectiveness when relatively comparing plastics formulations, without regard for relationships which may routinely predict aging performance from DSC measurements. As the following discussion will show, it is believed that empirical correlations have been developed to allow one to practically predict long term oven aging behavior from DSC measurements. In order to more fully interpret these results in relation to the ability of the compound to withstand thermal aging, this report covers detailed findings of this research.

EXPERIMENTAL

The following antioxidants were used in this study; TP-93, CDP-1012, and 618 (thiophosphites from Borg-Warner, Weston Chemical Div.); Santonox R (hindered phenol from Monsanto Chemical); Irganox 1035 (hydroxycinnamate from Ciba-Geigy); and distearyl thiodipropionate (DSTDP from Evans Chemetrics, Inc.). Crosslinking agent was dicumyl peroxide, Di-Cup R, from Hercules, Inc. The polyethylene used was low density polyethylene of ~2.0 melt index (dg/min, ASTM D-1248), and density

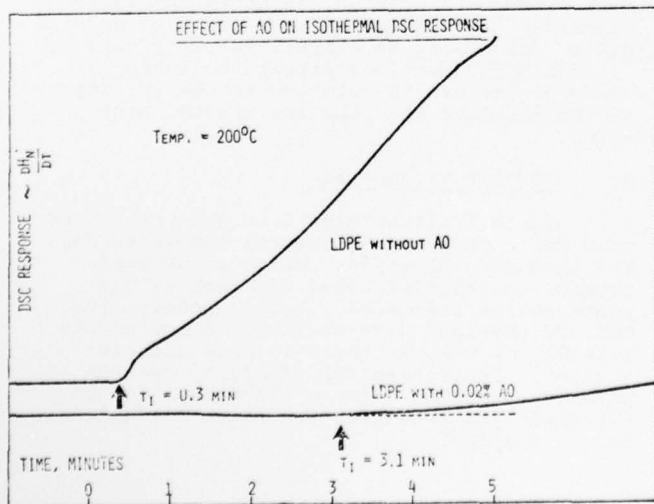


Figure 1

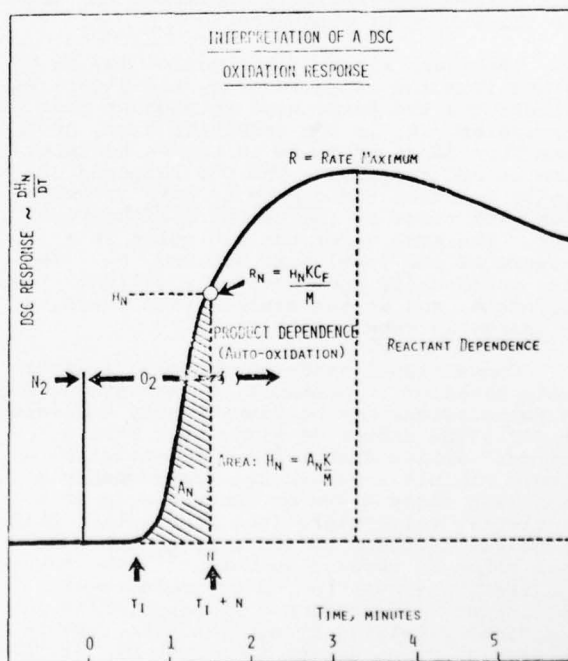


Figure 2

of 0.919 g/cm³. About 0.5% by weight of each antioxidant system and 2.1 weight % DiCup was compounded into the polyethylene using a Banbury intensive mixer at 110°C. Polymer flux was attained in three minutes after charging to the Banbury, after which the antioxidant and DiCup were added, and mixing was continued for another three minutes. The polymer was dumped, sheeted on a two roll mill, and granulated for further evaluation.

Aged physical properties were determined on 75 mil cured plaques prepared in an Elmes press at 180°C. Tensile strength, yield strength, and elongation were determined on original specimens and samples aged at 121, 136, 150 and 170°C for one week in an air oven.

Isothermal oxidation behavior was evaluated using cured 10 mil films and a DuPont 990 Thermal Analyzer with cell base operated in the DSC mode. Oxidation in a pure oxygen atmosphere (flow rate 100 cm³/min) on copper pans was followed at 150, 170, 180, 190, 200 and 210°C. Detailed analysis of the thermograms is described in the following discussion.

RESULTS AND DISCUSSION

Isothermal DSC is both a rapid and accurate method of determining differences in the ability of antioxidants to stabilize polyethylene against oxidative degradation. Experimentally, the sample is held at constant temperature under a controlled flow of oxygen, and the auto-oxidation response of the polyethylene is recorded by differential calorimetry. A typical thermogram is shown in Figure 1, which illustrates that low density polyethylene with an efficient antioxidant system substantially increases the time for initiation of oxidation.

Important kinetic information may be obtained from the isothermogram, and Figure 2 illustrates the terms used throughout this discussion. t_i is the induction time, or the time from first exposure to oxygen to initial rise in DSC response. The DSC response directly measures the change in rate of oxidation with time, or the second derivative of rate. The area under the DSC curve is a measure of the total heat evolved, H_n . The rate continually increases to a maximum, then decreases, and at the maximum rate there is no change in rate with time.

Conventional hindered phenolic antioxidants alone or in combination with synergists in polyethylene may be conveniently evaluated by DSC using induction time, t_i . Thus a "better" antioxidant system (relatively) should exhibit a longer t_i , and probably a much less steep slope on the DSC scan at a particular temperature (see Figure 1). This classical approach and interpretation has been taken by several authors,¹⁻⁵ who have qualitatively asserted that a measure of antioxidant effectiveness in polyolefins is kinetically related by studying the time to initiation of oxidation in a DSC, DTA or TGA apparatus.

In the course of investigating three thiophosphites as potential polyethylene antioxidants, unusual DSC responses were observed which did not correlate well with the antioxidant "goodness" by relative DSC when compared to thermally aged physical properties. In order to understand the "real" meaning of DSC oxidation measurements, the following discussion will treat each separate parameter of the DSC in an effort at correlation with heat aged physical properties.

A. Analysis of the DSC Thermogram

Figure 3 shows a comparison of the DSC oxidation behavior of the Irganox 1035/DSTDP and Weston TP-93 systems at 190°C in cross-linked polyethylene. It is clear that the thiophosphite TP-93 exhibits unusual induction time behavior, as there is an immediate rise in the DSC which is not observed for the conventional system. This behavior was observed at all temperatures studied for all the phosphite antioxidants. The induction times in these cases were therefore taken as the intersection of the tangents drawn for the second sharp transition, as shown in Figure 3.

Foster⁶ has proposed that the increase in oxidation rate to the maximum represents oxidation which is product dependent (auto-catalytic), and that after the maximum the decreasing rate is reactant dependent. This may represent a pathway in which the polyethylene is initially experiencing degradative crosslinking up to the maximum in the DSC curve, after which a decrease in oxidation rate is observed due to inaccessibility of unreacted polyethylene for further reaction and/or exhaustion of reactants. The question thus arises as to what part of the DSC thermogram is most related to drastic differences in physical heat aged properties. The illustrated parameters in Figure 3 are designed to determine this point. Induction time would measure the susceptibility of a particular compound toward initiation of oxidation. A point arbitrarily chosen for the most linear change in rate in the curves was 70% of the maximum rate, and also the time to achieve that stage of oxidation, as shown in Figure 3. Likewise, the maximum in rate and elapsed time may be important, as illustrated in Figure 3. The following sections attempt to interpret these parameters in relation to the ability of the compound to withstand thermal heat aging.

B. DSC Time Parameters

Table I illustrates time data extracted from DSC curves run at several temperatures, and includes values for retention of aged physical properties after one week at the temperatures indicated. Unfortunately, the DSC and physical data at 150°C do not correlate in any way, as there is considerable scatter. It is also impossible to use the physical property data at 170°C because of extremely low retention and small differences in the samples.

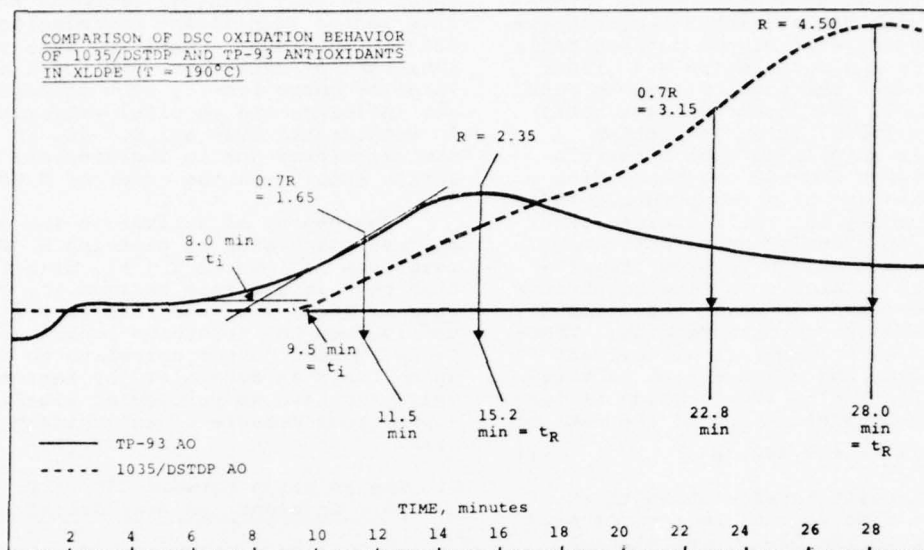


Figure 3

Table I

Comparison of DSC Time and Aged Physical Property Data
for a Series of Antioxidants in Crosslinked LDPE

Quantity Measured		Irganox 1035 DSTDP	TP-93	CDP-1012	618	Santonox
150°C	Induction Time, min (t_i)	42	47	68	3	-
	Time to 0.7R, min	455	800	210	89	-
	Time to R, min (t_R)	585	890	390	177	-
	Tensile Strength Retention, % (r)	76	54	44	33	84
	Elongation Retention, %	91	79	57	13	95
170°C	Induction Time, min (t_i)	42.5	38	21.5	0	17.5
	Time to 0.7R, min	101	56	38.4	13.5	80
	Time to R, min (t_R)	122.5	77	55	34	139
	Tensile Strength Retention, % (r)	33	45	-	30	36
	Elongation Retention, %	7	25	-	5	10
180°C	Induction Time, min (t_i)	21	15	8.4	0	10
	Time to 0.7R, min	46.5	22	12.1	4.9	68
	Time to R, min (t_R)	58	30	18.8	16.2	112
190°C	Induction Time, min (t_i)	9.5	8.0	0	0	1.40
	Time to 0.7R, min	22.8	11.5	6	4.8	19
	Time to R, min (t_R)	28	15.2	9.2	9.0	26.8

Therefore the only meaningful combination of data seems to be physical property retention at 150°C with DSC at higher temperatures. A detailed computer analysis of data in Table I was conducted, and revealed only a linear correlation between the time to maximum rate (t_R) for 170°C DSC and retention of tensile strength (r) at 150°C, which is plotted in Figure 4. It is surprising that a correlation exists between the DSC and heat aging for the phosphite and hindered phenolic antioxidants, especially for two different test temperatures. Apparently the effectiveness of a particular antioxidant system (regardless of kind) is related to a kinetic phenomenon (time dependence) on which retention of heat aged physical properties depends. Therefore the DSC reveals practical antioxidant effectiveness from the elapsed time to maximum rate of oxidation at 170°C, which is described by a least squares fit of the data to

$$r = 16.94 + 0.482 t_R \quad (1)$$

where r = % retention tensile strength at 150°C, and t_R = time to maximum rate of oxidation at 170°C on the DSC. (Correlation index = 0.9997).

C. DSC Kinetic and Thermodynamic Parameters

Some selected kinetic and thermodynamic data are listed in Table II, which have been calculated from the appropriate DSC thermograms using the analysis illustrated in Figure 3.

Regression analyses to find correlations between the aged physical property and DSC data revealed no significant correlations from the data in the table. Thus the rate change, maximum rate of oxidation, and total heat evolved (area of curve from t_i to R in Figure 3) do not influence the physical property behavior in accelerated oven aging. (H_n at 150°C was not calculated due to inordinately long oxidation times - on the order of 8 to 11 hours).

The energy of activation for oxidation, E_a , was calculated by plotting R (maximum rate from DSC) vs. $1/T$ (°K), with the assumption that at the rate maximum the change in rate is zero, i.e. the rate is first order and follows the Arrhenius equation. E_a 's in Table II also do not correlate to accelerated aging tests as determined by regression analyses, and have no particular significance as a practical measure of antioxidant effectiveness.

D. The Relation Between DSC First Order Rate Constant and Accelerated Aging

A detailed evaluation of the DSC curve allows one to calculate a first order rate constant at the maximum. It can be shown that

$$\frac{dH_n}{dt} = k_b (H_n)^n \quad (2)$$

$$\text{or} \quad \log k_b = \log \frac{dH_n}{dt} - n \log H_n \quad (3)$$

Table II

Comparison of DSC Kinetic, Thermodynamic and Aged Physical Property Data for a Series of Antioxidants in Crosslinked LDPE

		Irganox 1035 DSTDP	TP-93	CDP-1012	618	Santonox
150°C	0.7R, mcal/sec	0.500	0.195	0.175	0.588	-
	R, mcal/sec	0.715	0.278	0.250	0.840	-
	Tensile Strength Retention, %	76	54	44	33	84
	Elongation Retention, %	91	79	57	13	95
170°C	0.7R, mcal/sec	1.61	0.511	0.959	1.57	0.784
	R, mcal/sec	2.30	0.730	1.370	2.25	1.12
	H_n , Calories	3.14	2.74	6.20	0.74	7.38
	Tensile Strength Retention, %	33	45	-	30	36
180°C	Elongation, %	7	25	-	5	10
	0.7R, mcal/sec	2.32	1.00	1.28	2.34	0.952
	R, mcal/sec	3.32	1.43	1.83	3.35	1.36
	H_n , Calories	4.69	0.76	1.08	1.90	7.21
190°C	0.7R, mcal/sec	3.15	1.65	2.35	4.00	2.78
	R, mcal/sec	4.50	2.35	3.35	5.70	3.97
	H_n , Calories	3.42	0.750	0.469	0.849	4.58
	E_a , kcal/mole	23.6	27.0	32.4	24.6	-

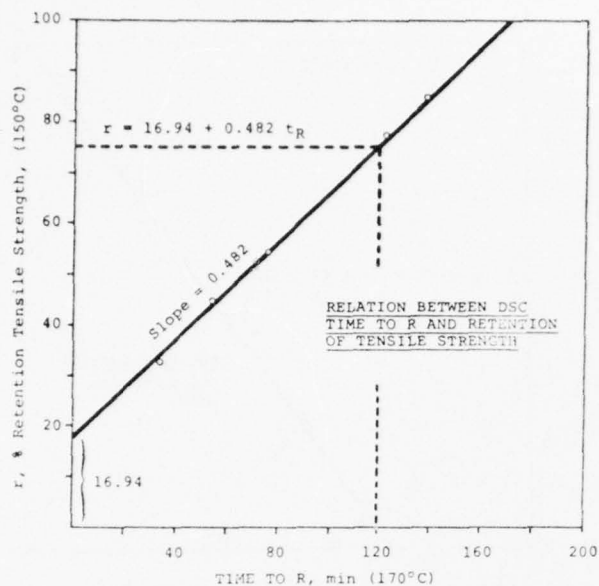


Figure 4

Using equation (3), one may calculate the first order rate constant, k_b , by knowing $\frac{dH_n}{dt}$ (area under DSC curve \div the elapsed time to maximum), H_n (area under DSC curve), and assuming $n = 1$. This analysis is based on the assumption that n does not change significantly with temperature. Using this approach, the data in Table III were generated, which includes a comparison of heat aging data.

Regression analysis indicates that the best mathematical fit to the experimental data follows the hyperbolic function:

$$r = 17.11 + \frac{7.98 \times 10^{-3}}{k_b} \quad (\text{index} = 0.9997) \quad (4)$$

where r = % retention of tensile strength at 150°C and k_b = DSC first order rate constant at 170°C. Figure 5 shows a plot of equation (4), where r vs. $1/k_b$ shows a perfectly linear correlation. Thus the DSC rate constant (at maximum rate), which encompasses both time and total heat evolved parameters, correlated significantly with massive loss in mechanical properties under accelerated heat aging.

E. Relation Between Energy Loss in Mechanical Properties and DSC Oxidation

The energy loss in physical properties upon heat aging should be important when an attempted correlation to DSC oxidation kinetic and thermodynamic parameters is desired. A convenient measure of mechanical energy exhibited by a vulcanizate is the area under the stress-strain curve. To eliminate time consuming area measurements, it has been found that the energy (area) may be closely approximated by the product of the tensile strength and elongation.⁷ Thus the retention of energy after aging $(TE)_f$ may be expressed as the ratio

$$(TE)_f = \frac{(\text{Tensile Strength} \times \text{Elongation})_{\text{Aged}}}{(\text{Tensile Strength} \times \text{Elongation})_{\text{Orig.}}} \quad (5)$$

This equation takes into account changes in both tensile and elongation, which in turn correlates in a relative way with the retained energy fraction after heat aging.

That $(TE)_f$ correlates with retention of aged tensile strength (r) is shown in Figure 6. The linear correlation has a confidence index of 0.996.

Since $(TE)_f$ correlates linearly with r , the data of Table IV were constructed to show relationships between $(TE)_f$ and DSC parameters. It is seen that the best fit to the experimental data is a linear plot of $(TE)_f$ vs. t_R , the time to maximum rate in the DSC; this exhibits a correlation coefficient of 0.987, with A and B constants indicated in

Table III

The Relation Between DSC First Order Rate Constant and Accelerated Aging for a Series of Antioxidants in Crosslinked LDPE

		1035 DSTDP	TP-93	CDP-1012	618	Santonox
r , % Retention Tensile Strength (150°C)		76	54	44	33	84
170°C	$k_b \times 10^4$	1.36	2.16	3.03	4.90	1.19
	for $r = A k_b^B$	Index = 0.9970;		A = 0.208;		B = -0.662
	for $r = A + B/k_b$	Index = 0.9997;		A = 17.111;		B = 7.985×10^{-3}
180°C	$k_b \times 10^4$	2.87	5.55	8.86	10.28	1.48
	for $r = A e^{B k_b}$	Index = 0.9845;		A = 98.90;		B = -1012
190°C	$k_b \times 10^4$	5.95	10.96	18.11	18.51	6.21

No Correlation

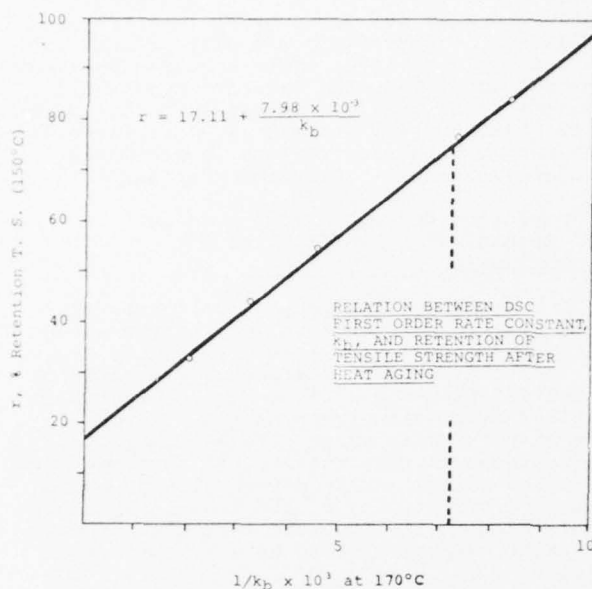


Figure 5

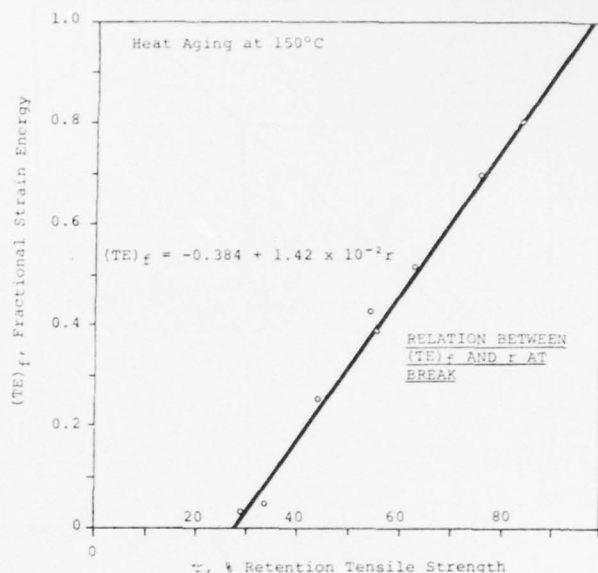


Figure 6

Table IV

The Relation Between $(TE)_f$ and DSC Oxidation Parameters

		1035 DSTDP	TP-93	CDP-1012	618	1035 DSTDP	Santonox	Santonox
(150°C)	$(TE)_f$	0.699	0.433	0.255	0.043	1.10	0.968	0.800
170°C:	t_R , min	122.5	77	55	34	157	225	139
	for $(TE)_f = A + B(t_R)$	Index = 0.987; $A = -0.1502$; $B = 6.97 \times 10^{-3}$						
	$k_b \times 10^4$	1.36	2.16	3.03	4.90	1.06	0.74	1.19
	for $(TE)_f = A + B/k_b$	Index = 0.986; $A = -0.417$; $B = 1.15 \times 10^{-4}$						
180°C:	$k_b \times 10^4$	2.87	5.55	8.86	10.28	1.61	1.01	1.48
	for $(TE)_f = A + B(k_b)$	Index = 0.984; $A = 0.922$; $B = -820.7$						

the table. Surprisingly, the fit is not as good for $(TE)_f$ vs. $1/k_b$ at 170°C as r vs. $1/k_b$, since the indices for fit are 0.987 and 0.997, respectively (calculated values of $(TE)_f$ and r using the equations show 0.997 correlation to give a more satisfactory fit than 0.987 correlation).

CONCLUSIONS

It has been observed that the effect of 150°C heat aging on physical properties and some kinetic DSC parameters determined at 170°C correlate nicely. This may be explained

by the fact that 150°C heat aging is most sensitive with more widespread differences in property retention than by aging at 170°C or lower temperatures. It may also be fortuitous that DSC at 170°C also reflects more sensitive thermal oxidation behavior, since at higher DSC test temperatures antioxidant volatility may complicate interpretation, and DSC at 150°C involves impractically long measurement times.

Thus, the practical "goodness" of the antioxidants studied has successfully been correlated with isothermal DSC measurements,

AD-A032 801

ARMY ELECTRONICS COMMAND FORT MONMOUTH N J
PROCEEDINGS OF INTERNATIONAL WIRE AND CABLE SYMPOSIUM (25TH) HE--ETC(U)
NOV 76

F/G 17/2

UNCLASSIFIED

NL

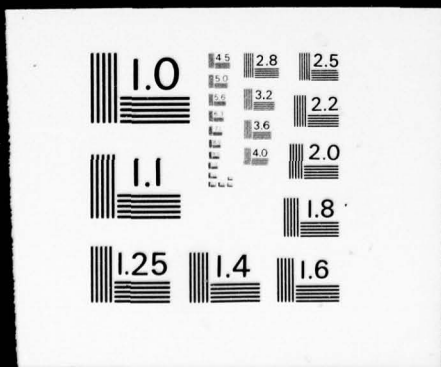
4 OF 5
ADA032801



4 OF

5

ADA032801



ac

an

wh
ta
ti
ag
ox
or
me

is
DS
re
15

me
ne
th
de
ce
th
ne
ic

be
an
ea
qu
vu
ty
DS
te
in
la
ne
a
pr

ma
an
as

1.
2.
3.

according to the following formulas:

Equation	Correlation Index
$r=16.94+0.428t_R$	0.9997 (6)
$r=17.11+.00798 (1/k_D)$	0.9997 (7)
$r=0.208k_D^{-0.662}$	0.9970 (8)
$(TE)_f=0.1502+.0069t_R$	0.9873 (9)
$(TE)_f=0.147+.000115 (1/k_D)$	0.9867 (10)
and $(TE)_f=-0.384+.0142r$	0.9960 (11)

where $(TE)_f$ = fractional strain energy retained after 150°C heat aging; r = % retention of tensile strength after 150°C heat aging; t_R = DSC time in minutes to reach oxidation rate maximum at 170°C; k_D = first order rate constant calculated from a DSC measurement at 170°C.

Hence, the best mathematical correlation is a simple measurement of t_R of the 170°C DSC, which allows empirical prediction of retention of tensile strength at one week 150°C heat aging.

Therefore, the most important DSC parameter for practical antioxidant effectiveness is the maximum rate (and time to get there) of oxidation, which relates to massive degradation of physical properties under accelerated heat aging tests. This may reflect the oxidative degradation (by crosslinking) necessary for nearly complete loss of mechanical properties.

The predictive power of this method could be further demonstrated by investigating other antioxidant/PE systems. The method could easily be extended to the development of a quick and convenient quality control test for vulcanizable polyethylenes. For example, a typical time measurement (t_R) in the 170°C DSC would translate to a predicted value of tensile strength retention for 150°C heat aging. Of course, a statistical analysis of a larger number and variety of samples would be needed, and reduction of the DSC analysis to a computer routine would significantly improve handling of the data.

ACKNOWLEDGEMENTS

The author thanks Dr. G. N. Foster for many helpful discussions on the mathematical analysis of DSC, and the excellent technical assistance of Mr. E. L. Brzezinski.

REFERENCES

1. J. B. Howard, Polymer Engineering and Science, **13**,429 (1973).
2. H. E. Bair, Polymer Engineering and Science, **13**,435 (1973).
3. D. I. Marshall, E. J. George, J. M. Turpinseed and J. L. Glenn, Polymer Engineering and Science, **13**,415 (1973).
4. J. P. Randino and J. R. Andreotti, Insulation, May, 24, (1964).
5. J. B. Howard and H. M. Gilroy, Polymer Engineering and Science, **15**,268 (1975).
6. G. N. Foster, private communication.
7. Exxon Technical Bulletin T1-52, 1975.



Daniel L. Davidson is a Research Chemist with Union Carbide Corporation in Bound Brook, New Jersey, and has been associated with Wire and Cable Materials research since joining the company in 1974. He has a B. A. in Chemistry from Earlham College (1968) and a Ph. D. in Polymer Science from the University of Akron (1975). His research interests include fundamental mechanisms of peroxide crosslinking and new crosslinking systems for polyolefins.

"PREDICTING FRACTURE, CREEP, AND
STIFFNESS CHARACTERISTICS OF CABLE
JACKETS FROM MATERIAL PROPERTIES"

by

G. M. Yanizeski, E. D. Nelson and
C. J. Aloisio

Bell Laboratories
Norcross, Georgia

ABSTRACT

Three methods are presented for predicting the fracture, creep, and stiffness performance of cable jackets. In each, tests on simple geometries combined with mechanical analyses enable a quick, meaningful estimate of jacket performance. The combined tests provide a rapid mechanical evaluation of plastic jacketing compounds. Low temperature fracture is related to the strain rate response of materials in notched impact tests; long term creep in pressurized cables is predicted from short term flexural creep tests, and jacket stiffness is determined from standard tensile tests.

I. INTRODUCTION

Simple, quick materials tests are essential in the selection and development of new materials. This is especially true in cable product development due to the variety of candidate materials and the expense and time required to test in product form.

Although the advantages are clear, the use of simple tests is often inhibited by difficulties in establishing a link between test results and product performance. This report describes three test methods in which mechanical analysis has been used to determine this link. In the first, a relationship is developed analytically between strain rates in a notched impact test, which is known to simulate product performance, and fundamental materials properties. In the second, analysis provides the link between simple flexural tests and the creep performance of cable jacket. In the third, an analysis of cable jackets under bending leads directly to the use of standard tensile tests to measure stiffness.

II. JACKET FRACTURE SENSITIVITY

The ASTM D746 impact test is widely used to determine the brittleness properties of cable jacketing compounds. However, it has been recognized for some time that the "brittleness temperature" determined in this test does not correlate with cable jacket brittle failures, which can occur at much higher temperatures. Efforts to develop a more representative test have involved

primarily the implementation of 1) biaxial states of stress and 2) surface imperfections or "notches."

Hopkins, Baker and Howard¹ established that polyethylene jacketing compounds are more brittle under biaxial stress than uniaxial stress, and Hoff and Turner² established that polyethylene is sensitive to brittle failure at notches. Okada and Utumi³ investigated the effects of biaxial stress and notches on a number of compounds. They found that notches generally had the strongest effect on brittleness temperature, but they recommended tests employing both notches and biaxial states of stress for evaluating cable jacketing compounds. Recently, Yamaguchi et al.⁴ using notched samples in the ASTM D746 test found that the notch depth and the notch position relative to the clamp affect the brittleness temperatures.

We have been using notched samples in the ASTM D746 test. The test can be performed quickly; notch geometry can be accurately controlled in molded samples to insure testing uniformity, and the notches simulate the surface character of cable jackets, which contain many scratches and corrugation imprints. By varying notch geometry and notch position relative to the clamp, a large range of strain rates can be obtained. An analysis of these strain rates, presented below, points to strain rate sensitivity as a controlling factor in the fracture performance of jacketing compounds.

Notch Tip Strain Rate Analyses

Two analyses are applied. In the first, elementary beam theory is combined with published concentration factors to establish a relationship between the velocity of the striker and the strain rate at the notch tip. In the second, finite element models are used to estimate the effect of the clamp on notch tip strain rates.

Beam Theory Analysis

The test configuration is shown in Figure 1a where W is the force applied by the striker. Initially, when the deflection is small, it is assumed that the material responds linearly. Viscoelastic effects are neglected for simplicity though

*Temperature at which 5 out of 10 samples fail

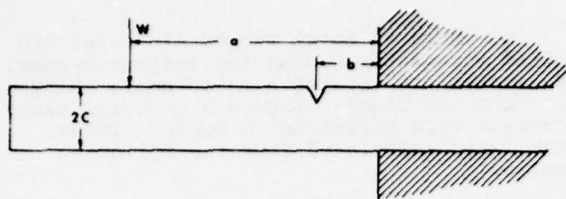


FIGURE 1a. TEST SAMPLE WITH NOTCH

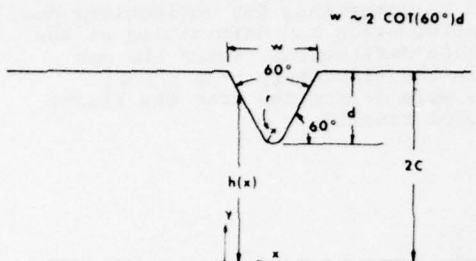


FIGURE 1b. CLOSE-UP OF MOLDED NOTCH

the correspondence principle⁵ permits transformation of elastic solutions to visco-elastic solutions. The deflection at W consists of the deflection due to curvature, which can be obtained from elementary beam theory, plus the deflection due to rotation at the notch. The total deflection is

$$\delta = -\frac{1}{3} \frac{Wa^3}{EI} + \theta(a-b) \quad (1)$$

where

E = modulus

I = area moment of inertia

θ = angular rotation at the notch

A rough estimate of θ can be obtained by treating the notched section of the sample as a beam with a variable moment of inertia subjected to a moment $M = -W(a-b)$. From beam theory,

$$\frac{d\theta}{dx} = \frac{M}{EI} \quad (2)$$

For a rectangular cross section of unit width the area moment of inertia is

$$I = \frac{1}{12} h(x)^3 \quad (3)$$

where $h(x)$ is shown in Figure 1b. Approximating the notch with a sharp "V" to obtain a linear relationship for $h(x)$, integrating (2), and substituting into (1) yields

$$\delta = -\frac{W}{EI} \left[\frac{a^3}{3} + \frac{wc(a-b)^2}{d} \left(\frac{1}{\beta^2} - 1 \right) \right] \quad (4)$$

where

$$\beta = \frac{2c-d}{2c}$$

For a notched beam subject to bending, the stress at the notch tip is

$$\sigma = K \left(\frac{Mc}{I} \right)_{\text{at notch}} \quad (5)$$

where K is the concentration factor. Using β as above,

$$\left(\frac{c}{I} \right)_{\text{at notch}} = \frac{1}{\beta^2} \frac{c}{I} \quad (6)$$

Substituting (6) and $M = -W(a-b)$ into (5) gives

$$\sigma = -\frac{K}{\beta^2} \frac{Wc(a-b)}{I} \quad (7)$$

For a condition of plane stress, the strain is

$$\epsilon = \frac{\sigma}{E} \quad (8)$$

Combining (4), (7), and (8), eliminating W , and differentiating with respect to time τ gives

$$\frac{d\epsilon}{d\tau} = \frac{KV(a-b)}{\frac{\beta^2 a^3}{3c} + \frac{w(a-b)^2}{d} (1-\beta^2)} \quad (9)$$

where $V = \frac{d\delta}{d\tau}$ is the velocity at which the striker impacts the sample.

Stress Concentration Factors

Concentration factors for notches in beams subjected to bending have been calculated by Neuber⁶ and measured photo-elastically by Leven and Frocht.⁷ For a notch with a 60° included angle, as shown in Figure 1b, the analytical and measured concentration factors differ by only 6%. Since Neuber's results cover the largest range of concentration factors, they have been used to calculate the strain rates that are presented later in this section.

Finite Element Analysis

The finite element meshes for notched LTB samples are shown in Figure 2. The notches are 0.010 and 0.020 inches deep with a 60° included angle. The base of the notch is 0.002 inches wide.

With the meshes shown in Figure 2, the notches were moved relative to the clamp by relocating 18 nodal points (intersections on the mesh) for the 0.010-inch notch and 24 nodal points for the 0.020-inch notch. Numerical solutions were obtained with the PALOS computer program.⁸

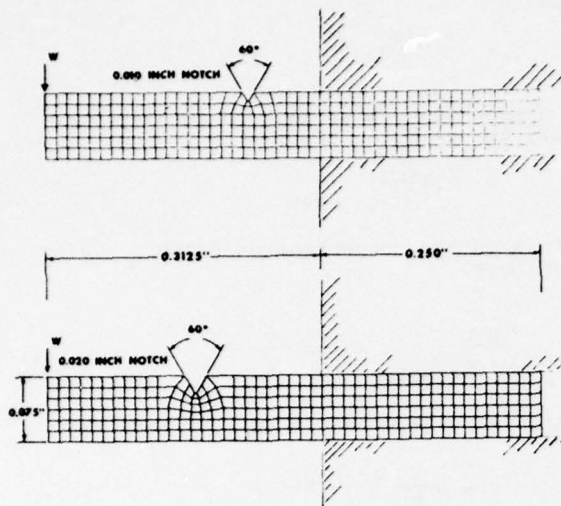


FIGURE 2. FINITE ELEMENT MESHES FOR NOTCHED LTB SAMPLES

Strain Rate Results

The effect of notch position on strain rate as determined from the finite element models is shown in Figure 3. Results are presented as a ratio of strain rates to eliminate the tip radius effect. The beam theory solution gives the same slope as shown in Figure 3 for notches located more than approximately a half thickness ($b/2c = 0.5$) from the clamp. For notches located closer to the clamp, clamp effects are significant, and the simple beam theory solution is not applicable.

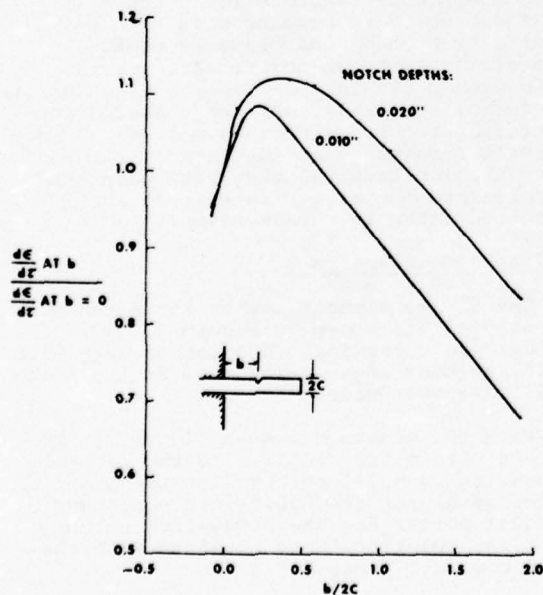


FIGURE 3. EFFECT OF NOTCH POSITION ON STRAIN RATE

In Figure 4, notch tip strain rates are plotted versus tip radius for various depths. The notches are located a half sample thickness from the clamp. Figure 5 contains plots of strain rate versus notch depth. These curves were calculated from the following equation:

$$\frac{d\epsilon}{dt} = \frac{KV(a-b)}{1.087 \frac{\beta^2 a^3}{3c} + \frac{w(a-b)^2}{d} (1-\beta^2)} \quad (10)$$

which is equation (9) with the 1.087 factor introduced to compensate for deflections due to shear deformation and deformation at the clamp. These deflections, which are not included in the elementary beam theory equations, were determined from the finite element model results.

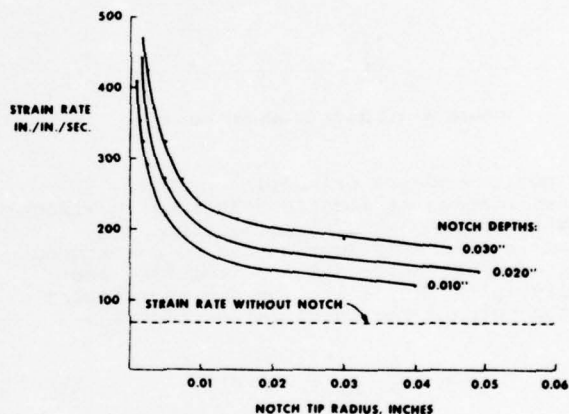


FIGURE 4. NOTCH TIP STRAIN RATES FOR 0.075-INCH THICK SAMPLES WITH NOTCHES LOCATED 0.0375 INCHES FROM CLAMP

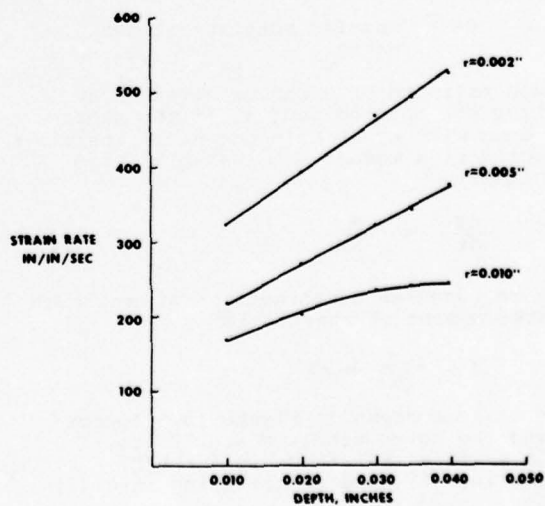


FIGURE 5. NOTCH TIP STRAIN RATES FOR 0.075-INCH THICK SAMPLES WITH NOTCHES LOCATED 0.0375 INCHES FROM CLAMP

Experimental Results and Discussion

The hypothesis presented here is that the strain rate at the notch tip is the major factor controlling failure. In order to test this hypothesis, notched brittleness temperatures, T_b , were determined for the following sets of experiments:

- 1) The distance, b , from the clamp was varied for a .010" deep, 0.0015" radius notch.
- 2) The notch radius was varied from 0.0015" to 0.024" for a 0.010" deep notch located at a distance $b/2c = 0.6$ from the clamp.

In experiment (1) the rate at the notch tip goes through a maximum with respect to position as shown in Figure 3 and, as shown in Figure 6, T_b varies in a similar manner for two low density polyethylene, LDPE, compounds. In fact, the maximum occurs near $b/2c = 0.5$ as in the analytical results of Figure 3. So that while one may argue that low temperature fracture is a complicated phenomenon involving many contributing variables, the data of Figure 6, when compared to the analytical results in Figure 3, indicate a strong contribution of strain rate.

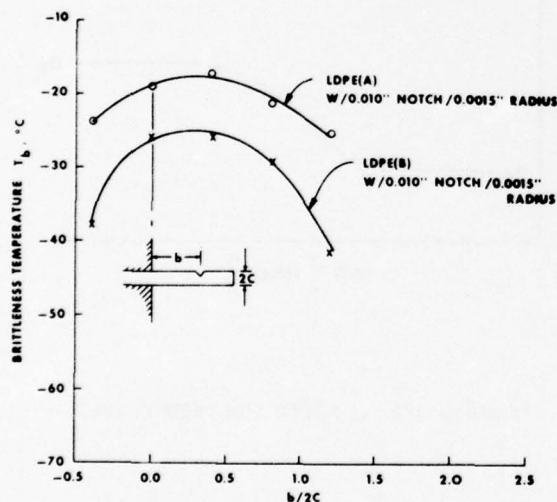
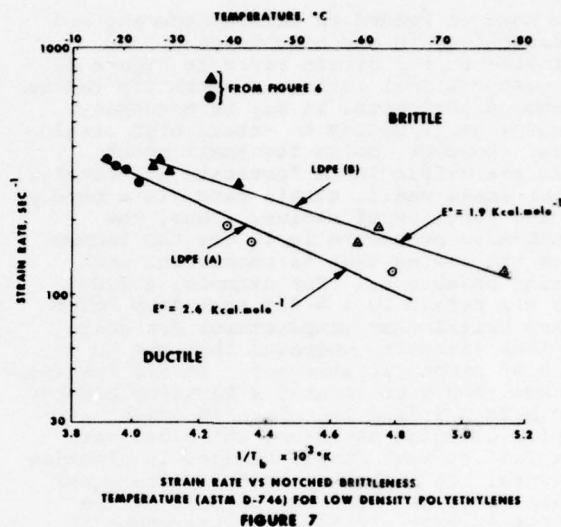


FIGURE 6
EFFECT OF NOTCH POSITION ON THE
BRITTLENESS TEMPERATURE.

The notch position variation method may now be compared to an alternative method of varying strain rate. In experiment (2), by varying the notch radius while maintaining its position constant, the strain rate may be varied as shown in Figures 4 and 5. The reciprocal of the T_b values obtained by experiment (1) and (2) are plotted versus the analytically determined strain rates in

Figure 7.* The brittleness temperature data from the two experiments fall on the same curve, further supporting the strain rate control of low temperature brittleness.



Consider now the engineering significance of Figure 7. Any points on the high temperature side of the lines represent temperature-strain rate combination at which the material will fail in a ductile mode. For example, at 100 sec^{-1} and -20°C both LDPE(A) and (B) will behave in a ductile manner. At a strain rate of 200 sec^{-1} and -45°C LDPE(A) will fail in a brittle mode while LDPE(B) will still be ductile. The temperatures at which failures occur during duct pulls of cables indicate that local strain rates of 300 to 400 sec^{-1} are operative.

The rate dependence exhibited in Figure 7 may be described by the following equation:¹²

$$\dot{\epsilon}_b = \dot{\epsilon}_0 e^{\frac{E^*}{R} \left[\frac{1}{T_b} - \frac{1}{T_0} \right]} \quad (11)$$

where R is the gas constant and $\dot{\epsilon}_b$ and $\dot{\epsilon}_0$ are the strain rates corresponding to T_b and T_0 respectively. The apparent activation energy, E^* , is a measure of the interaction between the rate of a mechanical process and the temperature at which the process occurs. The apparent activation energies 1.9 kcal/mole for LDPE(B) and 2.6 kcal/mole for LDPE(A), indicate that LDPE(B) will be somewhat more rate sensitive than LDPE(A).

*In Figure 7, LDPE(A) is a typical jacket compound and LDPE(B) is a commercial LDPE with dramatically improved low temperature performance on product.

Some of the molecular implications of these data have been discussed elsewhere^{11,12} Further discussion here is outside the intent of this paper.

Recommendations for the LTB Testing of Notched Samples

Some care is needed to insure accuracy and repeatability in the notched test. As indicated by the strain rates in Figure 4, the most critical factor is notch tip radius. In some experiments, it may be necessary to use a small radius to attain high strain rates. However, molds for small notch radii are difficult to fabricate accurately, and at small radii, strain rate is a rapidly varying function of radius. Thus, the recommended procedure is to use the largest notch tip radius that is consistent with testing objectives. For example, a 0.006 inch tip radius in a 0.010 inch deep notch yields brittleness temperatures for polyethylene jacketing compound that are in the range of practical interest. In all testing, notches should be located a distance greater than $b/2c \approx 0.5$ from the clamp to avoid complex clamping stresses, which can vary from test to test due to changes in clamping pressure. In repeated testing where equal strain rates are desired, notches can be located at $b/2c = 0.5$, where, as shown in Figure 6, brittleness temperatures are insensitive to small changes in position.

III. CABLE JACKET CREEP UNDER PRESSURE

In pressurized cable systems cable diameters increase with time. While it is desirable to limit the increase, the effect has been difficult to predict quantitatively without first making cables and subjecting them to pressure testing. By coupling laboratory characterization of plastics creep with simple analysis, design criteria for minimizing creep of polyolefin materials, such as high and low density polyethylene and polybutylene, in cable jackets have been developed. Also, the ability to more effectively screen plastic jacket material candidates is now available.

Jacket Creep Under Pressure

Creep is the time dependent deformation that occurs under constant stress. In plastics this deformation, which is also a function of temperature, is very often predictable in an engineering design using mechanical characterization data. A simple experiment involving three point bending¹³ permits the determination of the uniaxial creep compliance, $D(\tau)$. The beam deflection may then be calculated as a function of time from the elementary beam bending equation¹⁴,

$$x(\tau) = \frac{FL^3}{4cd^3} D(\tau) \quad (12)$$

where F is the midpoint load, L is the span between supports, c and d are the sample width and thickness respectively and $x(\tau)$ is the time varying deflection. For deflections smaller than the beam thickness, equation (12) is correct to within 3%. When

deflections become greater than the beam thickness, corrections for geometric nonlinearities must be made.¹⁵

The creep compliance versus time curve (shown in Figure 8 on a log-log plot) is typical of the shape of such curves for crystalline polymers below the melting temperature, T_m , and amorphous polymers below the glass temperature, T_g . The features are analogous to those observed for cross-linked amorphous polymers.¹⁶ At short times $D(\tau)$ approaches a value of the order of $D_g = 10^{-10} \text{ cm}^2/\text{dyne}$ ($7 \times 10^{-6} \text{ psi}^{-1}$). In amorphous polymers this region is called the glassy zone. Substitution of this value of $D(\tau)$ into

$$\epsilon_d = \frac{PD}{2t} D(\tau) \quad (13)$$

yields the initial diametral strain observed when pressurizing a cable. In Equation (13), ϵ_d is the diametral strain, t is the cable jacket thickness, P is the pressure and D is the mean diameter of the cable.

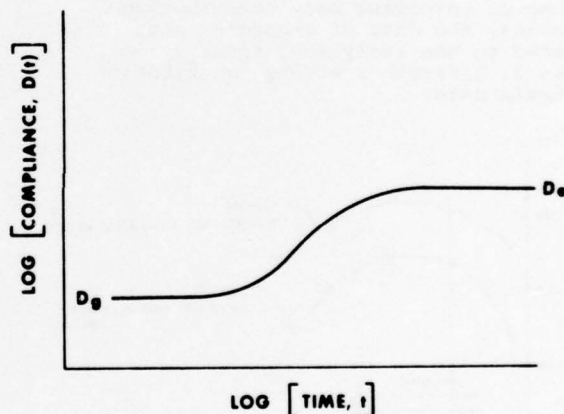


FIGURE 8. TYPICAL POLYOLEFIN CREEP CURVE

At long times $D(\tau)$ max. approach a limiting value D_e , the equilibrium compliance, of the order of

$$10^{-7} \frac{\text{cm}^2}{\text{dynes}} \quad (7 \times 10^{-4} \text{ psi}^{-1}).$$

The existence of an equilibrium value is strongly dependent on the proximity of the test temperature to T_g or T_m . For a semi-crystalline polymer details of the crystalline morphology, as T_m is approached, have a profound effect upon the existence of D_e . In a constant load application, such as pressurized cable jacket, the existence of D_e at the highest operating temperatures is a necessary but not sufficient condition for satisfactory

performance. If the magnitude of D_e is such that, under the typically applied pressure (10 psi in the Bell System), the cable diameter increases* excessively, then the material will be unacceptable. In addition the possibility exists for slow crack growth to occur even at low hoop strains.¹⁷

Equation (12) may be used to compare the cable performance under constant pressure with the flexural creep performance of the polymer. Figure 9 shows the comparison between flexural and pressurized cable derived compliance for a medium density polyethylene, MDPE, at 100°C. The similarity in shape of the two curves is encouraging. Once the equilibrium compliance at the maximum temperature is established the maximum allowable hoop stress may be calculated from the desired maximum strain, ϵ_{max} using

$$\sigma_{max} = \frac{\epsilon_{max}}{D_e} \quad (14)$$

and the minimum wall thickness as follows

$$t_{min} = \frac{PD}{2\sigma_{max}} = \frac{PDD_e}{2\epsilon_{max}} \quad (15)$$

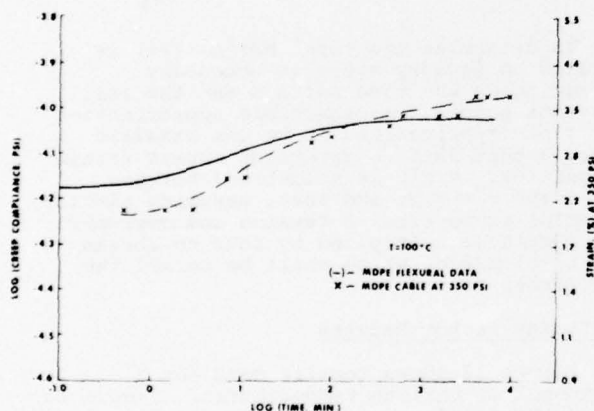


FIGURE 9. CREEP COMPLIANCE DERIVED FROM FLEXURAL CREEP EXPERIMENT AND PRESSURIZED CABLE EXPERIMENT

Key Result

The creep compliance, as shown in Figure 9, while applied herein to the diametral increases in pressurized cable, may be used to predict strains in any geometry where analysis indicates that the

*A cable diameter increase of up to 15% is considered acceptable. For some jacket materials increases of less than 10% are observed at 100°C.

linear viscoelastic uniaxial creep compliance is the primary material property controlling the material response. In some cases it may be necessary to determine additional time dependent properties. When comparing jacketing compounds, differences in the equilibrium creep compliance, D_e , at use temperatures will be reflected in differences in observed diametral increase unless jacket thicknesses are modified proportionately.

IV. CABLE JACKET STIFFNESS

Cable stiffness during installation is especially critical when cables are looped as, for example, during placement in cool weather in above-ground closures. This operation is shown schematically in Figure 10a where F and M_0 are the forces and moment applied by the craftsman.

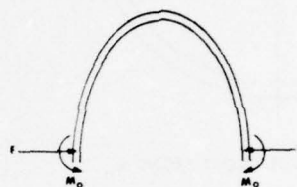


FIGURE 10a. FORCES AND MOMENTS APPLIED BY CRAFTSMAN WHEN LOOPING CABLE

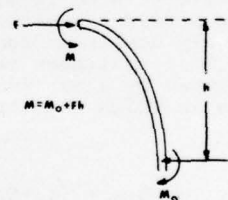


FIGURE 10b. FREE BODY DIAGRAM OF LOOPED CABLE

From the free-body diagram in Figure 10b, the cable at the top of the loop is under a compressive force F and a bending moment $M = M_0 + Fh$. M is relatively constant for a portion of the cable at the top of the loop, and the stresses due to M are generally large compared to the compressive stresses due to F alone. The net result is that the cable is essentially loaded in pure bending.

Stiffness: Resistance to Pure Bending

Figure 11 shows the cross section of a circular cable jacket of uniform thickness t . It is assumed that the cross section remains circular during bending and that the neutral surface is at the center of the cable (the x -axis). Under these conditions, the moment exerted by the differential area dA is

$$dM = \sigma y dA \quad (16)$$

or, from Figure 11,

$$dM = \sigma(R \sin \theta) (tR d\theta) \quad (17)$$

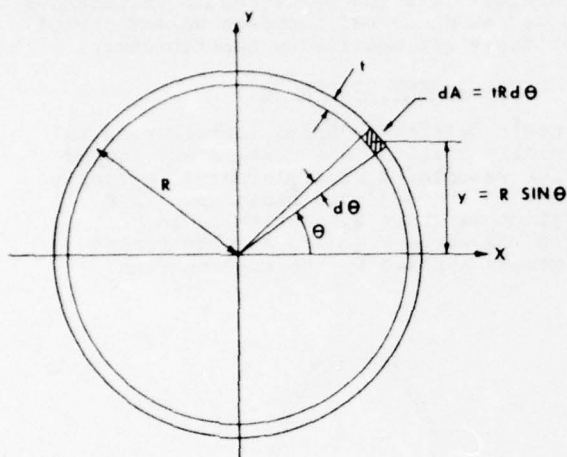


FIGURE 11. JACKET CROSS SECTION

During bending, cable jackets are subjected to relatively large levels of strain ($\sim 15\%$), and the stress σ exerted by the jacket is a highly nonlinear function of the strain ϵ . This nonlinear relationship can be approximated by a series of short linear segments in which the stress is given by

$$\sigma = E_i \epsilon + (\sigma_i - E_i \epsilon_i) \quad (18)$$

where

σ_i = Stress at the beginning of the i th segment

ϵ_i = Strain corresponding to σ_i

and

$$E_i = \frac{\sigma_{i+1} - \sigma_i}{\epsilon_{i+1} - \epsilon_i} \quad (19)$$

From elementary beam theory, the strain in pure bending is given by

$$\epsilon = \frac{y}{\rho + R} \quad (20)$$

where ρ is the radius of curvature measured to the inside surface of the cable on the

compressive side of the bend. Substituting $y = R \sin \theta$ and rearranging yields

$$\epsilon = \frac{\sin \theta}{1 + X} \quad (21)$$

where $X = \frac{\rho}{R}$ is the "bend ratio." Combining (17), (18) and (21) gives the following:

$$dM_i = R^2 t \left[\left(\frac{E_i}{1 + X} \right) \sin \theta + (\sigma_i - E_i \epsilon_i) \right] \sin \theta d\theta \quad (22)$$

which is applicable for strains between ϵ_i and ϵ_{i+1} . Solving (21) for θ yields

$$\theta = \sin^{-1} \left((1+X) \epsilon \right) \quad (23)$$

which can be used to obtain the angles θ_i and θ_{i+1} corresponding to the strains ϵ_i and ϵ_{i+1} . Integrating (22) between these angles and dividing by $R^2 t$ gives the following, which is independent of cable size R and jacket thickness t :

$$M_i / R^2 t = \left[\frac{E_i}{1 + X} \left(\frac{\theta}{2} - \frac{1}{4} \sin 2\theta \right) - (\sigma_i - E_i \epsilon_i) \cos \theta \right]_{\theta_i}^{\theta_{i+1}} \quad (24)$$

To determine the total $M/R^2 t$, (24) is applied in as many steps as necessary depending on the bend ratio X and the (ϵ_i, σ_i) data points. A reasonable approximation for cable applications is to use standard tensile test data to determine stress-strain properties. $M/R^2 t$ is calculated between $\theta = 0$ and $\theta = \pi/2$, and then, assuming similar material properties in tension and compression, the result is multiplied by four to obtain the total $M/R^2 t$, which shall be termed the "stiffness factor."

Stiffness Factor Results

Figure 12 shows tensile data for 5 compounds at various temperatures. Figure 13 shows the stiffness factor calculated for these compounds using Equation (24). The stiffness changes gradually with the bend ratio due to two factors: 1) jacket strains are relatively large with the maximum strain varying from 4% at $X = 25$ to 17% at $X = 5$, and 2) at these strains stresses tend to peak and level off. The net result is that a significant portion of the jacket is at a relatively constant level of stress. In addition, this portion of the jacket is located away from the neutral axis where the largest effect on stiffness is exerted.

Under the conditions described above, jacket stiffness for relatively tight bends (low X values) depends primarily on the maximum levels of stress exerted by the jacketing compounds. Below approximately $X = 10$, experience shows that cable jackets tend to buckle and stiffness decreases. Since

buckling is not included in the above analysis, stiffness factors below approximately $X = 10$ should be ignored. Therefore, from the curves in Figure 13, the maximum stiffness occurs at $X = 10$. In Figure 14, the stiffness factor M/R^2t at $X = 10$ is plotted versus the maximum stress exerted by the jacketing compound. The maximum stresses are taken from the Figure 12 curves between 0 and 10% strain, which is the range of jacket strains at $X = 10$.

Application to the Selection of New Compounds

As shown in Figure 14, maximum jacket stiffness is linearly proportional to the maximum stress exerted by the jacketing compound. This correlation has been established for a sufficient variety of compounds and temperatures that it can be safely applied to any new compound. Therefore, when comparing jacketing compounds, differences in maximum stress determined below 10% strain will result in differences in jacket stiffness, unless jacket thicknesses are changed proportionately.

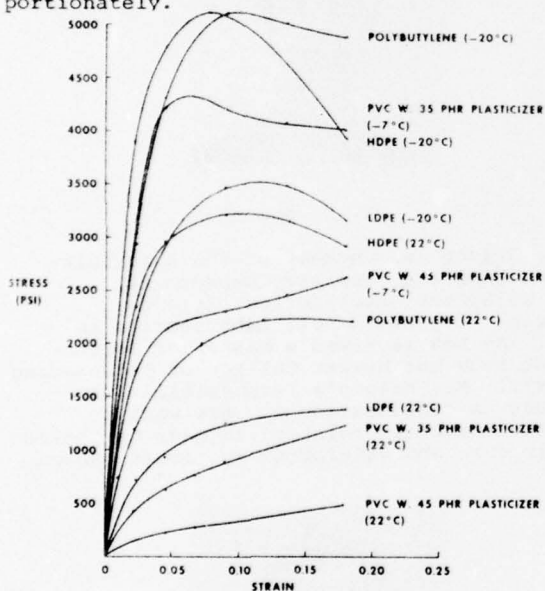


FIGURE 12 TENSILE DATA FROM MICROTENSILE SPECIMENS TESTED AT CROSS HEAD SPEEDS BETWEEN 2 AND 5 IN./MIN

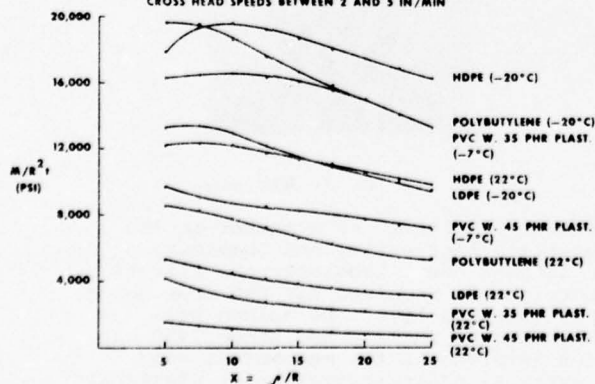


FIGURE 13. CABLE JACKET STIFFNESS FACTORS FOR COMPOUNDS IN FIGURE 12

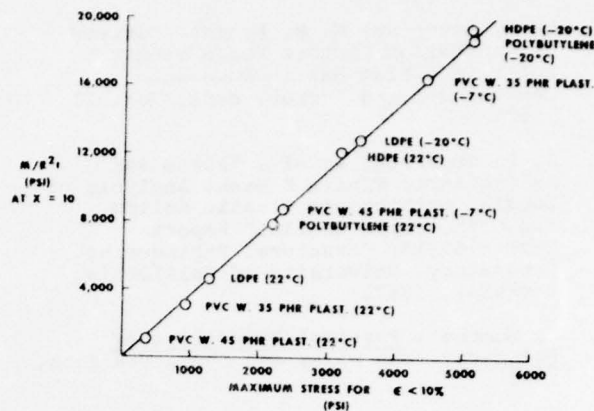


FIGURE 14. STIFFNESS IS DIRECTLY PROPORTIONAL TO MAXIMUM STRESS

V. SUMMARY

1. Strain rate is a controlling factor in the brittleness performance of low density polyethylene. A modified notched brittleness test gives data suitable for determining the low temperature performance of plastic in cable jacket.
2. The creep performance of plastic cable jacket under pressurization may be predicted from simple flexural creep experiments.
3. Cable jacket stiffness under pure bending can be determined from the maximum stress below 10% strain as measured in a standard tensile test. When comparing jacketing compounds, differences in maximum stress correspond to equal differences in jacket stiffness unless the thickness is changed proportionately.

REFERENCES

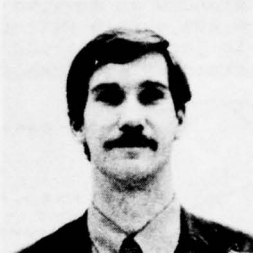
1. I. L. Hopkins, W. O. Baker, and J. B. Howard, "Complex Stressing of Polyethylene," *Journal of Applied Physics*, Vol. 21, 1950.
2. E. A. W. Hoff and S. Turner, *ASTM Bull.* 58, 1957.
3. M. Okada and A. Utumi, "Brittle Fracture of Polyethylene at Low Temperatures," 19th International Wire and Cable Symposium, December, 1970.
4. K. Yamaguchi, H. Kishi, H. Takashima and S. Otomo, "Low Temperature Brittleness of Low Density Polyethylene for Cable Jackets," 24th International Wire and Cable Symposium, November, 1975.
5. M. L. Williams, "Structural Analysis of Viscoelastic Materials," *AIAA Journal*, Vol. 2, 1964.

6. H. Neuber, Theory of Notch Stresses, 2nd Ed, Springer, 1958.
7. M. M. Leven and M. M. Frocht, "Stress Concentration Factors for a Single Notch in a Flat Bar in Pure and Central Bending," Proc. SESA, Vol. 11, 1953.
8. G. L. Goudreau, et al., "Plane and Axisymmetric Finite Element Analysis of Locally Orthotropic Elastic Solids and Orthotropic Shells," Report Number 67-15, Structural Engineering Laboratory, University of California, Berkeley, 1967.
9. F. Bueche, Physical Properties of Polymers, John Wiley and Sons, New York, 1962.
10. F. Schwaryl, "Molecular Theory of Linear and Non-Linear Relaxation", Kolloid - Feitschrift, 165, 1959.
11. S. Matsuoka, C. J. Aloisio, J. B. Daane, "Some Aspects of Brittle Failure in Polymers" Applied Polymer Symposia No. 5, 1967.
12. C. J. Aloisio and G. M. Yanizeski, "Molecular Interpretation of the Strain Rate Induced Brittle Transition in Polyolefins", American Physical Society Meeting, Atlanta, Georgia, March, 1976.
13. C. J. Aloisio and R. R. Cammons, "Rapid Flexural Creep and Engineering Analysis for Product Design of a Propylene Copolymer," Polymer Engineering and Science, Vol. 14, 1974.
14. R. J. Roark, Formulas for Stress and Strain, McGraw-Hill, 1965.
15. J. G. Williams, Stress Analysis of Polymers, Longman Group Limited, pp. 144-148, 1973.
16. J. D. Ferry, Viscoelastic Properties of Polymers, Wiley, 1970.
17. R. A. Schapery, "A Theory of Crack Growth in Viscoelastic Media," Texas A & M University Report MM-2764-73-1, March, 1973.



G. M. Yanizeski

George M. Yanizeski is a member of the Materials Engineering and Chemistry Department, Bell Laboratories, Atlanta, Georgia. He received his PHD from Carnegie-Mellon University in 1968. He joined Bell Laboratories in 1972 and since 1974 has been involved in the mechanical analysis and characterization of cable jacketing compounds.



E. D. Nelson

E. D. Nelson is a member of the Materials Engineering and Chemistry Department, Bell Telephone Laboratories, Atlanta, Georgia. He joined Bell Laboratories in 1967. He has received a Master of Science Degree from the Newark College of Engineering in 1973. Mr. Nelson's responsibilities include a continuation of his work in plastic materials relating to many varieties of air core and waterproof multipair cables.



C. J. Aloisio

Charles J. Aloisio is a member of the Materials Engineering and Chemistry Department, Bell Laboratories, Atlanta, Georgia. He received his PHD from Purdue University in 1970. He joined Bell Laboratories in 1952 and since 1959 has been involved in the mechanical and electrical characterization of plastics.

HIGHLY FIRE-RETARDANT NAVY SHIPBOARD CABLES

by

Michael A. DeLucia

David W. Taylor Naval Ship Research & Development Center
Annapolis, Md. 21402

Summary

Ships cableways have been identified as a major problem area during fire emergencies. Fire propagation, smoke, toxic and corrosive gas generation are primary concerns. The state of fire technology in the Wire & Cable Industry was surveyed with major advances noted. A comprehensive evaluation of thirty-two candidate cables was conducted.

Introduction

Recent shipboard fire experience has focused attention on electric cableways and the part they play in a ship's conflagration. Major fires aboard the USS FORRESTAL (CVA-59) and the USS SARATOGA (CVA-60) are examples of the concern generated. Damage reports in each case appear to blame electric cableways for spreading a relatively small and confined fire thereby directly contributing to the substantial time loss and dollar damage incurred (3 to 4 months unscheduled ship availability at a shipyard and millions of dollars in repair costs). In the recent collision between the USS JOHN F. KENNEDY (CVA-67) and USS BELNAP (DLG-26) in the Mediterranean the damage survey team again cited the electric cables as contributing to the severity of the post-collision fire. In addition to the propagation of fire, there is increasing concern for the dense black smoke and potentially toxic and/or corrosive gases generated by burning electric cables which incorporate relatively large quantities of various plastic and elastomeric compounds as insulation and jacketing components.

Since most electrical shipboard cables are designed and certified to be "non-propagating" and "self-extinguishing" there appeared to be a conflict between certification procedures and the real life shipboard fire conditions. A discussion of present Navy cable fire performance requirements is presented here as background material.

Most electric cables installed on Navy ships are specified under MIL-C-915E.¹ There are two basic fire performance requirements contained in that document. Readers are referred to the specification for detailed descriptions of the procedures. The first requirement, the Gas Flame Test (paragraph 4.8.17) is cited for critical cables which must maintain circuit integrity during shipboard fire conditions. Briefly, a single completed cable is subjected to a 2-foot horizontal ribbon burner for 3 hours with voltage applied to its conductors. Cables designed to provide this degree of protection incorporate combinations of silicone rubber and fiberglass insulation (in extruded or taped form) which provide the silica ash decomposition insulation necessary to maintain circuit integrity without shorting during fire exposure. The evaluation therefore does not (and was never intended to) evaluate the burning or non-burning characteristics of the cable but only its ability to perform electrically during fire emergency conditions.

The second fire performance requirement, the Flammability Test (paragraph 4.8.16), attempts to address the propagation and self-extinguishing characteristics of cables more directly. In this procedure a single, 18-inch length of completed cable is exposed to a heater

coil/spark gap ignition source in the vertical configuration. Gases generated from the cable by the hot coil are ignited by the spark. The source of ignition is then removed and the degree to which the cable is self-extinguishing and non-propagating is evaluated. This test has been employed by the Navy as a production screening test for over 25 years and was originally designed to prevent accidental ignition of switchboard and electric panel wiring by welding torches and not to simulate the cableway fire situation.

Recent shipboard fire experience however, indicated that standard Navy cables are not self-extinguishing and will propagate fire for appreciable distances when grouped in typical ships cableways and subjected to a high heat fire source. As a result of this conflict between laboratory qualification results and real fire performance, a review of the state-of-the-art of cable flammability standards (military and commercial) was included in the scope of this investigation. In this way, candidate fire-retardant cable materials could be evaluated under laboratory conditions which would most nearly simulate a real fire situation.

Background

Fire has emerged as a major national problem to such an extent that a special presidential commission was established to study the facts and recommend possible solutions. After 2 years of investigative hearings the National Commission of Fire Prevention and Control issued its final report² "America Burning" detailing the size of the nation's problem. Over 12,000 deaths and \$11 billion in wasted resources was directly attributed to destructive fires each year, placing the United States tragically as the world leader in both statistical categories.

As a result of increased awareness of the fire problem, a number of agencies and universities have initiated fire research programs. The National Bureau of Standards³; The National Academy of Sciences⁴; The Flammability Research Center, University of Utah⁵; and the Federal Aviation Administration⁶ are among the many national organizations, universities and agencies with major fire research programs in progress. Some of this work has already improved consumer product performance through the development of new industry standards of fire performance. Most notable are fire-retardant clothing (particularly children's sleepwear), carpeting and interior fabrics standards all now nationally accepted.

The wire and cable industry has also developed a new family of highly fire retardant materials and constructions in response to stringent performance requirements demanded in nuclear power generation. These requirements were developed by the Insulated Conductor Committee of the IEEE (Institute of Electrical/Electronic Engineers) and published as IEEE Standard 383-1974.⁷ Among the cable requirements of that standard is the Vertical Tray Fire Test which represented an attempt to simulate a real cableway fire situation in evaluating propagation and extinguishment parameters of completed cables installed in typical tray fashion. With this newly developed, industry-recognized, standard as a guide, many cable manufacturers developed highly fire-retardant cable product lines employing new or improved

polymer materials and construction techniques aimed at the expanding nuclear power generating market. It was the goal of the Navy's program to determine if these materials and constructions could be employed in the Naval shipboard environment without substantial compromise to other performance requirements. Two reports were issued during the course of this study; a preliminary report⁸ outlining the approach and presenting initial findings and a final report.⁹ This paper is a summary of the work presented in this final report and readers are referred to it for more detailed information.

Candidate Cable Selection

An industry wide survey was conducted to determine the variety of highly fire-retardant cable materials and constructions being developed for the nuclear generating station and other markets. The survey included major Navy cable manufacturers and material suppliers as well as those known to be active in the fire-retardant field. One fear was that only a single-source proprietary material would provide the additional fire protection required. This would cause problems in supply and logistics for the naval shipboard application. It was discovered, however, that a wide variety of insulation and jacket materials would meet the new requirements for fire retardation. The range of materials was from sophisticated irradiation cross-linked polyolefins to commonly used polyvinyl chlorides compounded with improved fire-retardant additives. The broad extent of this survey is demonstrated by the following listing of most of the companies involved:

ALLIED CHEMICAL, MORRISTOWN, N.J.
ANACONDA CONTINENTAL, WIRE & CABLE CO., YORK, PA.
BOSTON INSULATED WIRE & CABLE CO., BOSTON, MASS.
BRAND REX, WILLIMANTIC, CONN.
CERRO WIRE & CABLE, NEW HAVEN, CONN.
CITIES SERVICE CORP., CHESTER, N.Y.
COLLYER INSULATED WIRE, LINCOLN, R.I.
CYPRESS WIRE & CABLE, ROME, N.Y.
E.I. DUPONT de NEMOURS CO., WILMINGTON, DEL.
GENERAL CABLE CORP., BAYONNE, N.J.
B.F. GOODRICH CHEMICAL CO., CLEVELAND, OHIO
GREAT AMERICAN CHEMICAL CORP., FITCHBURG, MASS.
ITT, SURFRENANT DIVISION, CLINTON, MASS.
MOBAY CHEMICAL CO., PITTSBURG, PA.
OKONITE, PASSAIC, N.J.
PLASTOID CORP., HAMBURG, N.J.
RAYCHEM CORP., MENLO PARK, CALIF.
TIMES WIRE & CABLE CO., WALLINGFORD, CONN.
U.S. STEEL, ELECTRIC CABLE DIVISION, WORCESTER, MASS.
UNIROYAL INC., NAUGATUCK, CONN.

Six standard Navy cable types were selected to represent the variety of power, control, communications and telephone cables contained in MIL-C-915E. These six types were: TSGU-50; MSCU-7; MHOF-19; TTRS-8; 2SU-19 and TTSU-20. These types were suggested as a guide to manufacturers in the hope of obtaining a degree of continuity of samples. Industry response to the program was enthusiastic. Many companies supplied commercial variations of Navy types. All samples were welcomed in order to include the widest variety of highly fire-retardant materials in the evaluation program.

Sample Description

Thirty-two samples of highly fire-retardant designs have been received and evaluated during the course of this investigation. Each sample (identified FR-1 to FR-32) is described in detail in the report⁹ including materials description and dimensions for each sample. For convenience the following brief description of the 32 samples, including the primary insulation and jacket

materials employed, general functional description of types and size and manufacturer (coded), is presented.

FR-1, -2 & -3 were manufactured by Code A and represent 15, 38 and 48 conductor respectively, 16 AWG control cables marketed to the nuclear generating industry. Dual conductor insulation of Ethylene-Propylene Rubber/Chlorosulfonated Polyethylene and a Chlorosulfonated Polyethylene jacket are employed.

FR-4 was manufactured by Code B and employs a fire-retardant Polyurethane jacket over a standard Navy TTRS-8 core.

FR-5, -6 & -7 were manufactured by Code C and employed specially developed highly fire-retardant Polyvinyl Chloride compound (supplied by Code B) as a jacket over standard Navy TTSU-20, 2SU-19, 2SWU-30, respectively, cores.

FR-8 and -10 were manufactured by Code E and employed a fire-retardant Polyurethane jacket over a single twisted pair insulated with Thermal Plastic Rubber (Unshielded and shielded, respectively).

FR-9 was manufactured by Code B and employed a fire-retardant Polyvinyl Chloride jacket over a standard Navy TTSU-20 core.

FR-11 was manufactured by Code F and employed a fire-retardant Polyurethane jacket over a standard Navy TTSU-8 core.

FR-12, -13, -15, -16 & -17 were manufactured by Code G. All samples employed the dual-conductor insulation system specified in MIL-W-81044¹⁰ and a highly fire-retardant modified Polyolefin jacket, except FR-16 which employed a proprietary irradiation cross-linked Polyolefin jacket. FR-12 was a 7-conductor control, FR-13 a twenty pair telephone communications, FR-15 & -16 were 10 conductor waterblocked control and FR-17 was a 10 shielded twisted pair waterblocked communication cable.

FR-14 was jacketed by Code H with an Ethylene-Fluorocarbon Copolymer over a standard Navy TTSU-20 core (purchased from Code C).

FR-18 was manufactured by Code C and employed a second generation of Code D Polyvinyl Chloride jacket over a standard Navy TTSU-20 core (see FR-5, -6 and -7).

FR-19, -20, -21 & -22 were all 7-conductor/#12 AWG cables manufactured by Code H. FR-19 employed Silicone Rubber insulation and Fluorinated Ethylene Propylene jacket; FR-20 employed Silicone Rubber insulation and as Ethylene-Fluorocarbon Copolymer jacket; FR-21 was all Ethylene-Fluorocarbon copolymer (insulation and jacket) and FR-22 was all Fluorinated Ethylene Propylene (insulation and jacket).

FR-23, -24 & -25 were manufactured by Code I and employed a proprietary fire-retardant Cross-linked Polyolefine compound. FR-23 and -25 were standard Navy MHOF-19 and 2SU-19 cables, respectively employing the proprietary fire-retardant Cross-linked Polyolefine as insulation and jacket while FR-24 was a standard Navy 2SU-19 core (Polyethylene insulated) with the proprietary fire-retardant Cross-linked Polyolefine material employed as a jacket.

FR-26 & -27 were manufactured by Code J and were standard Navy MSCU-14 and TSGU-50 designs employing a highly fire-retardant Thermoplastic Rubber jacket compound.

FR-28, -29, -30, -31 and -32 were manufactured by Code K. FR-28 & -29 were standard Navy TSGU-75 and TSGA-

100 cables with no modifications. FR-30 was a merchant marine power cable designated TVAIB-168 in Specification IEEE-45.¹¹ It is a 3-conductor 168 MCM power cable with an Asbestos insulation, Polyvinyl Chloride jacket and bronze armor. FR-31 and -32 were 7-conductor #12 AWG cables. FR-31 employed Cross-linked Polyethylene insulation and Chlorosulfonated Polyethylene jacket and FR-32 a dual Ethylene-propylene Rubber/Polychloroprene insulation and Polychloroprene jacket.

Selection of Fire Performance Evaluation Method

As stated previously, a review of the state-of-the-art of flammability standards (military and commercial) was included in the scope of this development program. The objective of this review was to determine whether a satisfactory standard method for simulating shipboard cableway fire performance already existed.

The survey produced a vast number of recognized flammability standards used throughout the plastic industry to evaluate the burning parameters of the polymeric materials comprising the bulk of an electric cables mass. The reader's attention is called to References 12 to 17 for detailed descriptions of a representative sample of these methods. Generally each method evaluates one or more combustion parameters and attempts to rate materials or constructions for specific applications. The most common parameters include:

- (a) Time to ignition
- (b) Time to self-extinction
- (c) Distance of fire propagation
- (d) Rate of flame spread
- (e) Amount of heat released
- (f) Rate of heat released
- (g) Nature of burning (i.e. sparking, flaming droplets, afterglow, etc.)
- (h) Limiting Oxygen Index required to sustain burning

In an effort towards better correlation of laboratory test results and real-life cable performance, a recent trend in the Wire and Cable Industry has been to employ full-scale cable tray tests. Even in this limited category seven tray test methods were revealed during the survey to be employed in the industry. They are:

- (a) Baltimore Gas and Electric Test¹⁸
- (b) Philadelphia Electric Test¹⁹
- (c) General Electric Test²⁰
- (d) Detroit Edison Test²¹
- (e) IEEE Standard 383 Test⁷
- (f) Okonite Test¹⁹
- (g) Raychem Test²²

After discussions with industry leaders and experimental testing of standard Navy cables the IEEE Standard 383 Vertical Tray Cable Test Method was selected as most nearly fulfilling our two major requirements. These requirements were: first, simulation of a real life Navy cableway fire and second, being widely accepted by the wire and cable industry. As an initial screening test, three standard Navy cables were exposed to this evaluation method employing a ribbon burner ignition source. The cables selected, representing a variety of standard Navy cables specified in MIL-C-915E, included a small boat control, a large communication, and a fire-proof telephone cable type.

The method requires the cables to be mounted in vertical trays and exposed to a specified ribbon burner flame for a period of 20 minutes. Fire propagation along the cables to the top of the eight foot tray (i.e. six feet above the burner) is considered failure. Results of this screening test were as follows:

STANDARD NAVY TYPE

3SU-24
TTSU-30
3SJ-14

RESULTS

Failure - 8 minutes
Failure - 6 minutes
Failure - 5 minutes

As a result of this screening test, and with the knowledge that a wide variety of cable designs which offer this increased degree of fire protection were being marketed, the prospect for improving the degree of fire protection afforded by Navy cables was bright.

The next phase of the screening process was to determine which of the variations of this IEEE Standard 383 Method would be employed in our program. As written, the Standard offers two choices for ignition source. The first is a burlap cloth, folded and soaked in a measured quantity of transformer oil. The second is the propane/air or natural gas/air ribbon burner source which is nominally rated at "70,000" BTU/Hr. Additionally, there is a proposed variation of this test which employs a nominal "210,000" BTU/Hr. burner rating. In an effort to select a variation, the following screening test was conducted. A standard Navy cable was selected from stock which displayed a superior degree of fire retardation when subjected to the Flammability Test of MIL-C-915E. The particular sample selected was a MSCU-61 (fire-proof control type) displaying a 5-15 second burn time (of an allowable 120 seconds) and a 1/2" flame propagation (of an allowable 2"). This sample was then exposed to the three variations of the IEEE Standard 383 Method described above. The results were as follows:

Burlap Cloth Ignition - The cloth burned for 25 minutes and never appreciably ignited the cables in the tray. Damage was limited to the immediate area of the cloth. The sample passed the test.

"70,000" BTU/Hr. Burner

Source - The cables in the tray propagated the fire to the top of the tray in 14 minutes. The sample failed.

"210,000" BTU/Hr. Burner

Source - The cables in the tray propagated the fire to the top of the tray in 8 minutes. The sample failed.

It was apparent that the oil soaked burlap cloth was insufficient to ignite the cables (which have burned under actual ships fire conditions). The "210,000" BTU/Hr. Burner Source caused the cable to fail in a shorter time but added no new insight over the recognized, industry wide standard method. As a result of this series of screening tests the IEEE Standard 383 Vertical Tray Method with ribbon burner as written, was selected for evaluation of candidate cables under this program.

A Cable Fire Test Facility was established at the Nike Site area of the Center. This area is actively used to perform fire evaluations for other programs at the Center. The Cable Fire Test Facility consists of an 8 X 8 X 8 foot steel burning chamber with an adjacent observation room. Draft in the burning room is controlled by means of an exhaust blower and damper set at a level so that no measurable draft is present on the cable tray for at least 4 feet above the burner. Experience has taught that cables which propagate to this level usually will propagate to the top of the tray (6 feet above the burner) and fail the evaluation. In addition to monimeters and flow-meters in

the propane and air lines to the burner, the tray is fully instrumented with thermocouples at 1 foot intervals. A multi-channel recorder is employed to provide a temperature profile of the fire propagation. A view port for photographically recording each burn is also present. Photographic slides are taken at 1 minute intervals during each burn to record the rate of fire spread and give some insight into the amount of smoke, sparks, and dripping (if any) displayed. The burner flame is standardized by controlling the propane and air pressure at the mixer as described in the document⁷ (i.e. propane pressure of -26 ± 3 mm H₂O; air pressure of 43 ± 5 mm H₂O at mixer input ports). It is emphasized that the flame is controlled by setting the propane and air pressure levels as described in the IEEE Standard. There is wide controversy about the term "70,000 BTU/Hr." which is generally associated with this pressure level. For that reason all references to BTU/Hr. levels will be placed in quotation marks. They are included only because of their wide use in industry but their validity is suspected and caution is advised in using this descriptive term.

Procedures

A comprehensive laboratory program was established to evaluate the physical, electrical and chemical performance of the highly fire retardant candidate samples received in the course of this investigation. The primary consideration was improved fire retardance; therefore all samples were exposed to the IEEE Standard 383 Vertical Tray Flammability Method using the ribbon burner ignition source. These evaluations were performed at the Cable Fire Test Facility of the Center under fully controlled and instrumented laboratory conditions. As a general rule, this evaluation was performed first and those samples which demonstrated insufficient fire retardation to successfully pass were eliminated from further evaluation. In some instances additional data was gathered on failing samples in order to provide engineering data for comparison purposes.

Due to the large number of samples received and the wide variety of military and commercial types represented, the primary objective of the evaluations performed was to determine the performance parameters of the materials employed rather than the construction. In some instances, a number of samples were submitted by one manufacturer, each employing the same jacket and/or insulation. As an example FR-1, -2 and -3 were identical in all respects except the number of conductors present. Evaluations of jacket material performance (as in compatibility with common ships' fluids) could therefore be limited to FR-1 only. In other samples, the number of parameters evaluated was limited by the short length of sample supplied.

In addition to the IEEE Standard 383 flammability evaluation, samples were generally subjected to those portions of MIL-C-915E consistent with their use and/or construction. For non-Navy samples the requirements of the closest Navy type were employed.

Results

Data gathered during the comprehensive laboratory evaluation phase of this development effort are detailed in the following paragraphs and tables:

Vertical Tray Flammability

Results of the IEEE Standard 383 evaluation are presented in Table 1. The number of specimens of each sample in the tray was determined by loading the tray (using a 1/2 diameter spacings) with enough lengths of each cable to fill at least the central 6-inch

section of the tray as specified in the standard. The number of lengths of a particular sample, therefore, was a function of the overall diameter of the sample. Table 1 indicates the number of lengths in the tray for each sample, the cable type and the general material class designation for the insulation and jacket employed. Propagation to the top of the tray (6 feet above the burner) indicated failure in the time noted. Most samples that did not propagate to the top of the tray (passing) would extinguish immediately when the burner was turned off (at the 20 minute mark). In some instances the samples continued to burn after the burner was turned off (afterburn) but did not propagate. The time these samples self-extinguished is also noted. It is noted that sample FR-7 was not evaluated since it was a larger version of FR-6 incorporating a larger number of polyethylene insulated pairs. The fire-retardant PVC jacket on FR-7 was identical to that which already failed on FR-5 and FR-6. Evaluation of FR-7 was therefore not performed.

Visual and Dimensional

Visual observations and constructional dimensions for each sample are presented in the report⁹ in complete detail for readers desiring this information. A brief description of each sample, including manufacturer (Coded), type and general materials employed is presented in the "Sample Description" section of this paper. It is noted, that in general the performance of a particular sample does not represent the manufacturer's ability to produce fire-retardant cables since all cable manufacturers can process a variety of formulations of many basic insulation and jacket materials.

Physical Properties and Compatibility

The results of tensile strength and elongation measurements on selected jacket samples in the "as received" condition as well as after 10-day, room-temperature exposure to common ships' fluids (distilled water, fuel oil, hydraulic fluid and battery electrolyte) are presented in Tables 3 & 4. For comparison purposes typical requirements of current standard Navy jackets are 1800 psi minimum tensile strength and 225% minimum elongation in the "as received" condition. There are no current requirements for compatibility with ships' fluids but data was obtained to provide insight in the event of a "spill" situation aboard ship.

Bending and Twisting Endurance

Low temperature bending and twisting endurance results are presented in Table 5. Of the 32 samples received, samples FR-6, FR-23, FR-24 and FR-25 employed essentially cores of standard Navy cable type (2SU or MHOF) designed for flexing service. These samples were therefore subjected to this evaluation. In addition sample FR-17 was included since it is similar to a Navy type TTRS which would require bending and twisting endurance. Sample FR-18 was included as a comparison to sample FR-6 which are both manufactured by the same company. Sample FR-6 failed the Vertical Tray Flammability Evaluation and the manufacturer modified the compound of the jacket material and resubmitted it on sample FR-18 which passed the flammability evaluation. Information on the effect of the recompounding on the low-temperature flexing properties was desired. Two specimens of each cable sample were evaluated. For comparisons purposes, standard Navy cables designed for the low-temperature flexing service require a minimum of 2000 cycles to failure at -30°C.

TABLE 1
Vertical Tray Flammability Data

Sample No.	Type	General Material Class*		No. In Tray	Results (Comments)
		Insulation	Jacket		
FR-1	Control	EPR/H	H	6	Passed (extinguished at 30 minutes)
FR-2	Control	EPR/H	H	4	Passed (extinguished at 36 minutes)
FR-3	Control	EPR/H	H	4	Passed (extinguished at 38 minutes)
FR-4	Communications	PE	PU	5	Failed (11 minutes)
FR-5	Telephone	S	PVC	6	Failed (11.5 minutes)
FR-6	Communications	PE	PVC	5	Failed (10 minutes)
FR-7	Communications	PE	PVC	-	(not tested; see text)
FR-8	Control	TPR	PU	11	Failed (6 minutes)
FR-9	Telephone	S	PVC	5	Passed (extinguished at 25 minutes)
FR-10	Control	TPR	PU	11	Failed (8 minutes)
FR-11	Communications	PE	PU	5	Failed (10 minutes)
FR-12	Control	PA/K	PO	10	Passed
FR-13	Telephone	PA/K	PO	8	Passed
FR-14	Telephone	S	ETFE	5	Passed (extinguished at 30 minutes)
FR-15	Control	PA/K	PO	9	Passed
FR-16	Control	PA/K	PO	10	Passed
FR-17	Communications	PA/K	PO	7	Passed
FR-18	Telephone	S	PVC	5	Passed (extinguished at 27 minutes)
FR-19	Control	S	FEP	5	Passed
FR-20	Control	S	ETFE	7	Passed
FR-21	Control	ETFE	ETFE	7	Passed
FR-22	Control	FEP	FEP	7	Passed
FR-23	Control	PO	PO	7	Passed
FR-24	Communications	PE	PO	5	Failed (27 minutes)
FR-25	Communications	PO	PO	5	Passed
FR-26	Control	S	TPR	6	Failed (7 minutes)
FR-27	Power	S	TPR	5	Failed (14 minutes)
FR-28	Power	S	PVC	4	Passed (extinguished at 34 minutes)
FR-29	Power	S	PVC	4	Passed (extinguished at 25 minutes)
FR-30	Power	AV	PVC	3	Passed
FR-31	Control	XLP	H	4	Passed
FR-32	Control	EPR/N	N	4	Passed

(*) See Table 2
General material class designations employed in the data tables are identified in Table 2.

Watertightness

Ten of the thirty two candidate samples employed watertight constructions and were evaluated. Results are presented in Table 6. Leakage (in cubic inches) is reported for each sample after a 6 hour, 25 psi exposure. The percent of full contract price¹ is based on the total circular mil area of the conductors.

Scrape-Abrasion Resistance

Results of scrape-abrasion resistance evaluations performed on 21 candidate fire-retardant constructions are presented in Table 7. Present Navy standard for conductors insulated with silicone rubber employing a polyamide insulation jacket (for mechanical protection of the individual insulated conductor) require an average minimum of 200 scrapes to failure. Table 7 lists the primary insulation and insulation jacket (if any) employed as well as the basic copper conductor size since the evaluation procedure yields results that are a function of geometry with smaller conductors (i.e. 16 AWG and Navy 3/5 (7) sizes) receiving more severe treatment compared to larger sizes (12 AWG sizes and Navy 2 1/2 (19)).

RF Communications Characteristics

The mutual capacitance, capacitance unbalance and characteristic impedance of the 5 shielded twisted pair candidate communication cables were determined at 1 MHz and is presented in Table 8. The candidates

were generally constructed to either Navy Type TTRS or 2SU specifications. Current requirements for Standard Navy TTRS cables are:

Mutual Capacitance - 28 pf/ft max.
Capacitance Unbalance - 10% max.
Characteristic Impedance - 75-90 ohms.

Similar requirements for Standard Navy 2SU types are:

Mutual Capacitance - 30 pf/ft max.
Capacitance Unbalance - 8% max.
Characteristic Impedance - 75 ± 5 ohms.

It is noted that FR-17 was not constructed to either Navy standard type but was a general purpose shielded twisted pair communication cable. Its characteristics are presented for informational purposes.

Flammability (MIL-C-915E)

Results of flammability evaluations on 19 candidate samples are presented in Table 9. Data includes time to ignition, burning time and flame travel distance. Present requirements for unarmored standard Navy cables are for a minimum of 30 seconds to the time of ignition, a maximum of 120 second burning time and a maximum flame travel of 2 inches.

TABLE 2

General Material Class Designations

Designation	Material
AV	Asbestos - Varnished Cambric
EPR	Ethylene - Propylene Rubber
ETFE	Ethylene - Fluorocarbon Copolymer
FEP	Fluorinated Ethylene Propylene
H	Chlorosulfonated Polyethylene
K	Polyvinylidene Fluoride
N	Polychloroprene
PA	Polyalkene
PE	Polyethylene
PO	Polyolefin
PU	Polyurethane
PVC	Polyvinyl Chloride
S	Silicone Rubber
TPR	Thermoplastic Rubber
XLP	Crosslinked Polyethylene

Gas Flame

Four of the candidate samples employed a Navy Type TTSU basic core and were subjected to the 3 hour gas flame evaluation to determine their ability to maintain electrical integrity during fire conditions. Sample FR-9 passed the 3-hour evaluation while samples FR-5, FR-14 and FR-18 failed at 15, 9 and 49 minutes, respectively.

Cold Bend

A cold-bend evaluation was conducted on the following nineteen selected candidate samples: FR-1, -2, -3, -5, -8, -9 and -12 through -23 inclusive. Each sample was conditioned at -20°C and then wrapped around a mandrel of 12X its overall diameter. All samples passed this evaluation with no cracking or derangement of the jacket or core materials.

Permanence of Printing

The legibility of printed identification on 9 candidate insulated conductors and 9 candidate jackets (not necessarily the same nine samples) was evaluated and results are presented in Table 10. Printing legibility on current standard Navy cables must be maintained for a minimum of 50 cycles on an insulated conductor and a minimum of 250 cycles on outer jacket printing.

DISCUSSION

In reference to the IEEE Standard 383 Flammability performance of the candidate samples, it is noted that a wide variety of materials and constructions can be formulated to perform satisfactorily. This eliminates the fear that only special proprietary materials will provide the increased degree of fire retardancy required. Among the jacket materials passing this evaluation were fire retarded chlorosulphonated polyethylene, polyvinyl chloride, crosslinked polyolefin, ethylene-fluorocarbon copolymer, fluorinated ethylene-propylene and polychloroprene.

As expected, the cable core played a large part in the fire-retardant nature of the overall design in some construction types. The most critical primary insulation was the polyethylene employed in twisted pair communications cables. Consider the results of Samples FR-24 and -25. Both samples were manufactured by the same company. Sample FR-24 employed a standard Navy Type 2SU-19 core (19 twisted pairs insulated with polyethylene) and a highly fire-retardant crosslinked polyolefin jacket. Fearing that the fire-retardant jacket would not protect the highly flammable core, the manufacturer also submitted Sample FR-25 which employed the same highly fire-retardant crosslinked polyolefin as insulation and jacket. As expected the standard core cable failed although its fire retardant jacket slowed the propagation to such an extent that it took 27 minutes (7 minutes after the burner was turned off) to propagate to the top of the tray. Sample FR-25, with the improved core would not propagate and as shown in the RF Characteristics section of the Results, possessed characteristic impedance and capacitance parameters at 1 MHz within the limits of the specification. Sample FR-17, employing a polyalkene/polyvinylidene fluoride dual insulation on a communication cable, is another possible approach to the solution of the flammable polyethylene-insulated communications cable problem.

A major problem area revealed during this evaluation was the poor low-temperature twisting and bending performance of the highly fire-retardant cables. As shown in Table 5 none of the fire-retardant samples performed to recognized levels of acceptance during the -30°C endurance evaluations (note that sample FR-6 did not pass the vertical tray flammability evaluation). While bending endurance failures appear regularly during standard Navy inspections, twisting endurance is very rarely a problem and all candidate samples exhibited poor twisting and bending endurance properties. It is

TABLE 3

Tensile Strength Data

Sample	Material*	Tensile Strength, Psi				
		As Received	Distilled Water	Fuel Oil	Hydraulic Fluid	Electrolyte
FR-1	H	2290	1865	1290	1930	2110
FR-4	PU	3401	2645	2065	1900	2970
FR-5	PVC	2150	2120	2150	1975	2185
FR-9	PVC	1340	1385	1260	1360	1335
FR-11	PU	2200	1155	960	675	1405
FR-16	PO	1770	1800	1370	1515	3365
FR-17	PO	2330	2350	1390	2380	2200
FR-18	PVC	1860	1830	1955	1775	1885
FR-24	PO	2395	2046	1415	2320	2440
FR-25	PO	1545	2425	1530	2275	2350
FR-26	TPR	1760	1880	1185	950	1966
FR-27	TPR	1965	1990	1155	1045	1835
FR-28	PVC	3030	3045	2965	3220	3135
FR-29	PVC	3150	3185	2760	2925	3010
FR-31	H	2285	2325	1255	1595	2240

*See Table 2.

TABLE 4
Elongation Data

Sample	Material*	Elongation, %				
		As Received	Distilled Water	Fuel Oil	Hydraulic Fluid	Electrolyte
FR-1	H	355	370	425	365	345
FR-4	PU	480	495	515	390	445
FR-5	PVC	335	345	265	325	360
FR-9	PVC	245	240	170	295	245
FR-11	PU	300	280	310	245	385
FR-16	PO	50	25	395	212	110
FR-17	PO	410	420	345	425	355
FR-18	PVC	270	285	260	335	295
FR-24	PO	330	250	280	305	310
FR-25	PO	365	275	310	225	295
FR-26	TPR	405	445	430	335	450
FR-27	TPR	425	460	395	335	445
FR-28	PVC	345	335	345	395	365
FR-29	PVC	330	365	340	360	350
FR-31	H	305	385	475	355	385

*See Table 2.

TABLE 5
Flexing & Bending Endurance Data

Sample	Cycles to Failure			
	Bending		Twisting	
	Specimen 1	Specimen 2	Specimen 1	Specimen 2
FR-6	870	450	---	2000+
FR-17	110	1	190	100
FR-18	960	660	1085	365
FR-23	430	805	1130	1225
FR-24	310	345	---	380
FR-25	310	40	400	330

TABLE 6
Watertightness Data

Sample	Leakage, in. ³	Contract Price Category, (%)
FR-9	0.4	100
FR-14	26.1	Rejection
FR-15	0	100
FR-16	0	100
FR-17	2.4	95
FR-18	38.7+	Rejection
FR-26	58.0	Rejection
FR-27	311.	Rejection
FR-28	7.1	95
FR-29	0	100

possible that some compounding changes may improve this performance level, but it appears that low temperature flexibility is the major material performance parameter to be traded off against superior fire retardance in cable design. For the shipboard application though this may not be a serious problem since those cables requiring low temperature flexibility are generally in exposed (weather deck) locations where fire risks may not be as critical as in passageways and internal compartments and spaces. It is emphasized that the problem is with flexibility (i.e. repeated flexing) and not bendability since all samples passed the -20°C Cold Bend evaluation.

Minor problems were discovered in watertightness, scrape abrasions, permanence of printing, and gas flame

performance evaluations. These are not considered major problem areas in that careful attention during manufacturing can correct these deficiencies without adversely affecting fire performance. As an example, Samples FR-5, -14 and -18 all employed Standard Navy Type TTSU-20 telephone cores manufactured by the same company and all exhibited gas flame, permanence of printing and watertightness (sample FR-5 not evaluated) failures. This is unusual performance in light of previous experience with this manufacturer and cable type and it may well be that suppliers chose to use a standard Navy core which had been rejected as a basis for the evaluation of fire retardant jacket materials rather than discard the core.

All other data gathered appears within the acceptable tolerance for current standard Navy cables of similar construction.

A question has been raised recently about the relative affect of removing the braided aluminum armor on the fire retardancy of Navy shipboard cables. While no conclusion can fairly be drawn from one comparison, it is of interest to consider the fire performance of samples FR-29 and -30. Both were manufactured by the same supplier and employed the same insulation and jacket compounds. Sample FR-29 was a three conductor, 75 MCM unarmored power type while Sample FR-29 was a slightly larger three conductor, 100 MCM armored type. Both passed the vertical tray evaluation.

CONCLUSIONS AND COMMENTS

As a result of this investigation, the following conclusions are drawn and limitations are discussed.

- Improved fire-retardant performance in standard ships cabling is feasible without major sacrifice to other required physical, electrical, or chemical properties with exception of low temperature flexibility.

- A wide variety of cable insulation and jacket materials can be employed to provide this increased fire retardancy, thus insuring adequate supply.

- The IEEE Standard 383 Vertical Tray Flammability procedure employing a ribbon burner ignition source and draft controls represents a suitable laboratory tool for the evaluation of fire propagation along a cableway. It is limited in that it does not attempt to evaluate the smoke, toxic and/or corrosive products generated during the fire.

TABLE 7

Scrape Abrasion Data

Sample	Material Designation*		Conductor Size	Average Scrape Cycles to Failure
	Primary Insulation	Insulation Jacket (if any)		
FR-1	EPR	H	16 AWG	25
FR-2	EPR	H	16 AWG	30
FR-3	EPR	H	16 AWG	25
FR-5	S	N	Navy 3/5 (7)	65
FR-8	TPR	-	16 AWG	170
FR-9	S	N	Navy 3/5 (7)	55
FR-10	TPR	-	16 AWG	50
FR-12	PA	K	Navy 3/5 (7)	175
FR-13	PA	K	22 AWG	10
FR-14	S	N	Navy 3/5 (7)	55
FR-15	PA	K	Navy 2 (7)	155
FR-16	PA	K	Navy 2 (7)	320
FR-17	PA	K	Navy 3/5 (7)	45
FR-18	S	N	Navy 3/5 (7)	105
FR-19	S	N	14 AWG	500+
FR-20	S	N	14 AWG	500+
FR-21	ETFE	-	12 AWG	500+
FR-22	FEP	-	14 AWG	500+
FR-23	PO	-	Navy 2 1/2 (19)	500+
FR-24	PE	N	Navy 3/5 (7)	500+
FR-25	PO	-	Navy 3/5 (7)	55

*See Table 2.

TABLE 8

Communications Data (1 MHz)

Sample	Basic Navy Type	Capacitance (pf/ft)	Capacitance Unbalance (%)	Characteristic Impedance (ohms)
FR-4	TTRS	23.2	4.5	78.4
FR-6	2SU	23.9	5.3	79.6
FR-17	---	37.7	6.3	60.2
FR-24	2SU	23.5	1.4	83.2
FR-25	2SU	25.3	1.2	79.8

TABLE 9

Flammability (MIL-C-915E) Data

Sample	Ignition Time (sec.)	Burning Time (sec.)	Flame Travel (in.)
FR-4	70	95	4 1/4
FR-8	59	14	3 1/4
FR-9	110	36	1 1/2
FR-10	68	56	2
FR-11	64	56	2 1/4
FR-12	84	21	1/4
FR-13	110	12	1
FR-14	**	**	**
FR-15	120	32	1
FR-16	88	27	3/4
FR-17	81	31	3/4
FR-18	92	18	1/4
FR-19	**	**	**
FR-20	**	**	**
FR-21	**	**	**
FR-22	**	**	**
FR-23	82	46	1 1/2
FR-24	70	5	1/4
FR-25	72	42	1/2

**Sample failed to ignite after 200 second exposure.

TABLE 10

Permanence of Printing Data

Sample	Cycles to Illegibility	
	Insulation	Jacket
FR-1	>50	---
FR-2	>50	---
FR-3	>50	---
FR-5	<10	---
FR-8	---	<50
FR-9	<50	>250
FR-10	---	<50
FR-12	---	<200
FR-13	---	>250
FR-14	<25	---
FR-15	---	>250
FR-16	>50	<20
FR-17	>50	>250
FR-18	<20	>250

While the conclusions drawn are encouraging, they must not be interpreted as the final answer to the very serious Navy cableway fire problem. It is noted that the accompanying problems of smoke generation and toxic products of combustion of cable materials when burned has not been addressed and no safe performance levels are presently required. Smoke and toxic gases

generated during the ship's fire (particularly in a submarine) directly affect the safety, health, and lives of the crew and impede the mission capability of the ship. In addition, corrosive products of combustion can greatly increase the damage caused even by a small fire.

It should be pointed out that changing one of the characteristics of a cable insulation and/or jacket material can not be done without substantially affecting other characteristics. For example, in the chemical structure a change to reduce the rate of fire spread will also change the electrical properties of the insulating materials and its toxic properties when the cable is ignited and does burn. If one of the halogen family, such as chlorine, is added to the insulation of the cable, it is found that the flame spreadability rate is substantially lessened but the toxic production rate when the cable is ignited is often increased and many of the toxic products are lethal to personnel. The final solution to the cable fire problem must consider the overall problem since the physical, electrical, chemical, and toxic properties of the material are not mutually independent. At best only a solution that strikes a good balance among these characteristics can be found, especially when dealing with the hydrocarbon type of insulation. It is suggested that the best solution would be one in which the insulating and jacketing materials would not smoke, smolder, nor burn and in which good electrical insulating and other characteristics were to be found. Hope for such a material may be found in inorganic materials.

RECOMMENDATIONS

It is recommended that the Flammability requirements of MIL-C-915E be superseded by a new vertical tray flammability procedure modeled after the ribbon burner variation of IEEE Standard 383-1974.⁷ This new performance requirement should be enforced for all cable types except those requiring low-temperature flexibility performance (the bending and twisting endurance requirements).

It is recognized that this change will have major impact on Navy cable suppliers and a transitional period may be in order. To aid in the transition it is recommended that Naval Ship Engineering Center, Hyattsville, Md. (NAVSEC) conduct an industry-wide meeting or series of meetings to discuss the proposed changes and remedy any problems which arise.

FUTURE WORK

Work discussed in this paper completes Center efforts on the first of four areas related to the shipboard cable fire problem, that of propagation of fire along cableways. Work will continue within funding limitations on methods of evaluation and reduction of the smoke, and toxic and corrosive products generated during the combustion of ships cable materials. The implementation of stricter flammability requirements recommended herein will have an immediate direct impact on the smoke, toxic and corrosive products problem by reducing the amount of cable consumed during any conflagration.

In addition, work is continuing on a related task, with the U.S. Coast Guard, seeking to extend the impact of improved fire retardant cable technology to the merchant marine fleet and oil rig applications.

REFERENCES

1. MIL-C-915E, Military Specification, Cable and Cord Electrical, for Shipboard Use, General Specifications for, Dated 1 Aug 1972.
2. National Commission of Fire Prevention and Control, America Burning, Dated 4 May 1973.
3. Gross, D., et al, Smoke and Gases Produced by Burning Aircraft Interior Materials, National Bureau of Standards, Building Science Series 18, Dated Feb 1969.
4. National Academy of Sciences, Directory of Fire Research in the United States 1971-1973, Seventh Edition Dated 1975.
5. Einhorn, I.N., et al, The Physiological and Toxicological Aspects of Smoke Produced During the Combustion of Polymeric Materials, Flammability Research Center, University of Utah, Annual Report 1973-1974.
6. Lopez, Edward L., Smoke Emission From Burning Cabin Materials and the Effect on Visibility in Wide-Bodied Jet Transports, Federal Aviation Administration Report FAA-RD-73-127, Dated March 1974.
7. Institute of Electrical and Electronics Engineers, Inc., IEEE Standard for Type Test of Class IE Electric Cables, Field Splices, and Connections for Nuclear Power Generating Stations, IEEE Standard 383-1974, Dated 15 April 1974.
8. DeLucia, Michael A., Preliminary Investigation of the Shipboard Cableway Fire Problem, Report 27-784, Dated 25 Feb 1974.
9. DeLucia, Michael A., Development of Highly Fire-Retardant Shipboard Electric Cables, Report PAS-75-72, Dated July 1976.
10. MIL-W-81044B, Military Specification, Wire, Electric, Crosslinked Polyalkene, Crosslinked Alkane-Imide Polymer, or Polyarylene Insulated, Copper or Copper Alloy, Dated 31 Dec 1973.
11. Institute of Electrical and Electronics Engineers, Inc., Electric Installations on Shipboard, Recommended Practice for, IEEE Standard 45, Dated Feb 1967.
12. Benjamin, I. and Gross, D., Naval Shipboard Fire Risk Criteria, Final Report Phase 1, Evaluation of Fire Test Requirements, National Bureau of Standards Report No. 10-159, Dated 26 Jan 1970.
13. Berry, F. and Bogner, C., Testing Materials for Fire Performance, Naval Ship Systems Command Technical News, Dated March 1974.
14. Emmons, Howard W., Fire and Fire Protection, Scientific American, Vol. 231, No. 1, Dated Jul 1974.
15. Brown, J.R., and Dunn, P., The Combustion of Organic Polymeric Materials-Evaluation of Flammability by the Oxygen Index Method, Australian Defence Scientific Service, Defence Standards Laboratories Report No. 561 Dated Jun 1973.
16. Fenimore, C.P. and Martin, F.J., Candle-Type Test for Flammability of Polymers, Modern Plastics, Dated Nov 1966.
17. Gaffney, J., The Significance of the New FR-1 Flame Test, Wire Journal, Dated Oct 1973.

18. Bhatia, P. et al, Flame Propagation Tests on 600 Volt Control and Power Cables in Trays for Calvert Cliffs Nuclear Power Plant, Presented at IEEE Summer Power Meeting, Portland, Oregon, July 1971.
19. McAvoy, F.M., Flame Tests-A Systems Approach for Power and Control Cable, Presented at IEEE Winter Meeting, New York, N.Y., Jan 1972.
20. Robertson, J.W., New Flame Tests for Control and Power Cable, Presented at the Conference on Electrical Insulation and Wire Technology, New York, N.Y., June 1971.
21. Detroit Edison Specification 498, Specification for 600 Volt EPR Insulated Nuclear Power Plant Cable.
22. LaPetra, F.E., Flame Retarded Cables for Power Plant Usage, Presented at the Symposium on Fire Protection of Cables, sponsored by the Electrical Research Association, London, England, May 1972.



Biography

Mr. Michael DeLucia graduated from Pratt Institute with a Bachelor of Electrical Engineering degree in 1964. He continued his education and earned a Master of Science in Electrical Engineering degree from New York University in 1968.

While attending college Mr. DeLucia worked at the New York Naval Shipyard as part of a Navy Cooperative Work/Study program. After graduating he worked at the Naval Applied Science Laboratory primarily on electromagnetic shielding problems relating to shipboard cables. He is presently employed at the David W. Taylor Naval Ship Research and Development Center (DTNSRDC) as a Senior Project Engineer concentrating on problems relating to ship's cableway fires.

A Test Method for Measuring and Classifying
the Flame Spreading and Smoke Generating
Characteristics of Communications Cable

by

J. R. Beyreis
J. W. Skjordahl

Underwriters Laboratories
Northbrook, Illinois

S. Kaufman
M. M. Yocum

Bell Laboratories
Norcross, Georgia

Abstract

A test method to characterize flame spread and smoke production of cables has been developed, and a classification scheme for grouping and reporting the test results is proposed. The method uses the Steiner Tunnel as the test facility and is similar to ASTM E-84 with the exceptions that a cable rack is used for mounting the samples in the upper part of the tunnel and the test time has been extended to twenty minutes.

Introduction

The widespread use of plastic insulated communications cable in plenums over the past 20 years has been recognized in the National Electrical Code. As of 1975, it contained a provision that "Conductors having inherent fire-resistant and low smoke producing characteristics approved for the purpose, shall be permitted for ducts, hollow spaces used as ducts, and plenums..."¹ The Code stops at that point and does not define either the procedure for measuring flame and smoke properties, or the acceptable levels of performance. Some localities have attempted to utilize existing tests and have specified minimum flame spread and smoke ratings per ASTM E-84, "The Surface Flame Spread of Materials Test." E-84 is a building materials test which is not intended to apply to cable.

This lack of standards has been a source of confusion and controversy. To an architect designing a minimum cost office building, the plenum is an attractive area to place communications cable, for it saves the expense of under-the-floor conduit (which is the installation method generally recommended by the telephone companies). Some localities have permitted cable installations in plenums while others have not.

In cooperation with Bell Laboratories and manufacturers of wire and cable, Underwriters Laboratories has undertaken to develop a method and a classification scheme for flame spread and smoke production of wire and cable. This effort has resulted in a test method which uses the Steiner Tunnel² (the ASTM E-84 facility) as the test apparatus. The test method is similar to ASTM E-84 except a cable rack has been introduced and the test duration is twice as long.

Objectives

Two objectives in developing a test method for communication wire and cable were:

1. To provide a numerical rank ordering of the flame spread and smoke producing characteristics, and
2. To provide a test condition that would be meaningful with respect to actual fire conditions.

For rank ordering flame spread characteristics, it is necessary that the test specimens be sufficiently long. Quantification of smoke requires that there be a means for confining the smoke and making appropriate measurements.

For the test to be meaningful with respect to actual fire conditions, the following provisions are necessary:

1. A high heat flux characteristic of actual fires³ (6-7 watt/cm²) is needed.
2. Large flame coverage of the test samples is needed in order to provide a high heat input to the cables.
3. The test sample should be mounted horizontally in order to simulate actual conditions in a plenum.

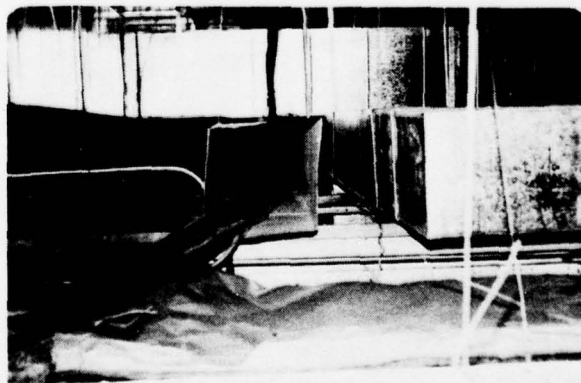


Figure 1. A Cable Installation in a Plenum

4. Multiple cable samples of sufficient length should be tested in order to simulate actual installation (Figure 1) and to provide a realistic amount of combustibles.
5. The test facility should be insulated in order to provide conservation of heat energy.
6. A movement of air over the test samples is needed to provide oxygen for combustion and to promote flame propagation.
7. The test must be of sufficient duration to allow the flame spread to achieve a peak value.

The requirements for a test facility are met by the Steiner Tunnel, the test facility used in ASTM E-84. There are 15 Steiner Tunnels in North America. Utilization of this well-known facility has several advantages. Since it is widely used and well characterized^{2,3,4} one has confidence in having a reproducible environment and test facility.

Test Method and Classification Scheme

The fire test method for characterization of flame spread and smoke production of communications cable employs the Steiner Tunnel, Figures 2 and 3, operated in accordance with ASTM E-84 with two basic operational differences, and a variation in reporting of results.

The first of the operational differences is the use of a cable rack for sample support, as shown in Figure 3. The second difference is that the test is conducted for a 20-minute period rather than the 10-minute period indicated in ASTM E-84. The standard flame and draft conditions of ASTM E-84 were maintained, i.e., a draft of 240 feet/minute in the direction of flame growth, and a 300,000 BTU/hour 4-1/2 foot long methane igniting flame. The ignition source subjects the test samples to approximately 6 watt/cm² heat flux.

The use of a cable rack provides for total flame engulfment of the cable specimen, in contrast to limited exposure that was observed in earlier tests in which the cable specimens were supported in the normal E-84 ceiling test position.⁵ Separation of the cable from the ceiling also provides for a reinforcement of the heating of the upper surfaces of the cable as the tunnel lid surface heats and reradiates energy to the specimen. The cable rack supports the cable high in the tunnel furnace so that it remains in the zone of maximum temperature and heat concentration. The resultant proximity of the cable specimens to the windows spaced along one wall of the furnace permits easy observation of fire development and flame spread from a close range. This test exposure mounting technique uniquely provides fire conditions which simulate the building service environment with respect to fire energy confinement, radiative feedback, large area flame coverage, and cable flame engulfment.

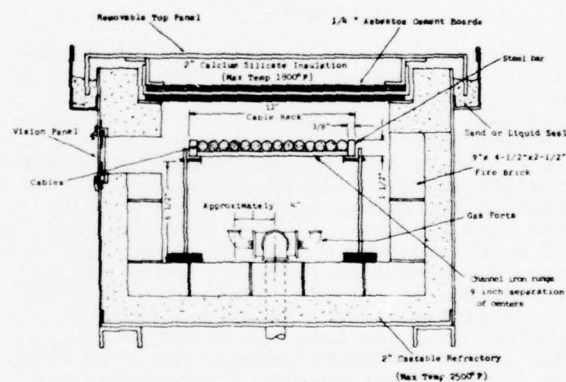


Figure 3. Cross Section of Tunnel Showing Mounting of Cable Rack

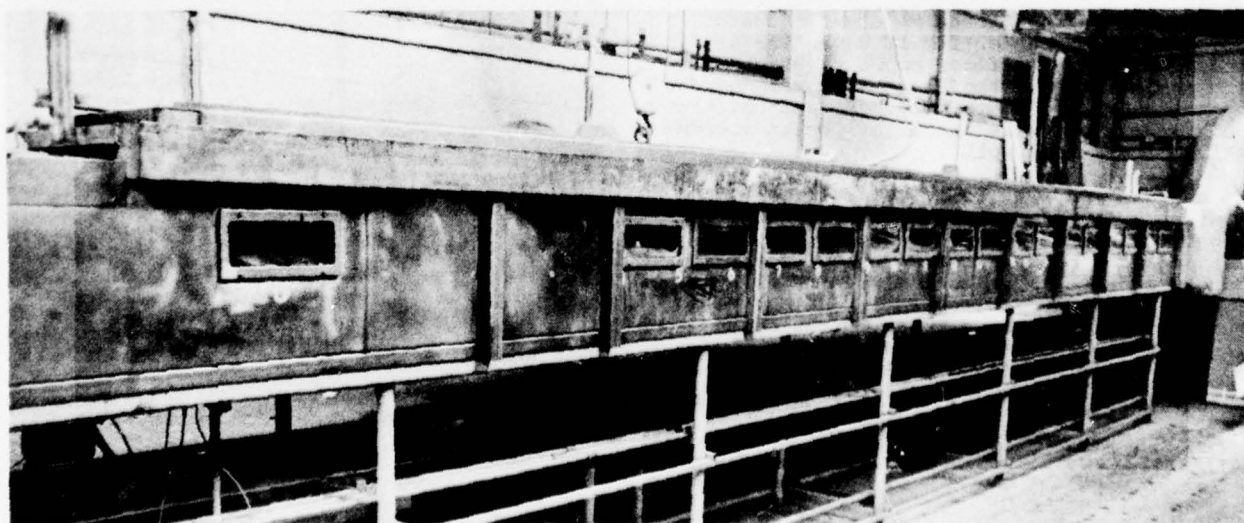


Figure 2. The Steiner Tunnel

A twenty-minute test duration was chosen after it was determined that significant fire involvement of some cables did not occur until late in the standard 10-minute E-84 test period, and in some cases not until after the 10-minute test period. In tests of 30 minutes or more, it became apparent that most cable constructions would reach their maximum flame spread within a twenty-minute test period.

A proposed classification scheme has been developed to convert the recorded test observations into flame spread and smoke-developed groupings. Since limitation of flame spread is considered the chief objective, the proposed flame spread grouping is predicated solely on distance without giving credit to time. These groupings are:

Flame Spread Class	Flame Travel Distance, Feet
I	<5
II	5½ to 15
III	15½ to 19½
IV	>19½

Class I represents a situation in which the cable ignites and burns under direct, intense exposure, but fails to propagate significantly beyond the exposure fire.

Near the opposite end of the scale, cables which propagate flame in the test to near, but not past, the end of the tunnel are assigned to Class III. These cables would be recognized as having desirability of use in some less hazardous occupancies, but where there is still an interest in limiting fire growth potential.

Class IV simply designates cables which result in flame propagation beyond the end of the tunnel. The ultimate flame growth potential for such cables is unknown. Class II characterizes those cables which fall between Class I and Class III.

Smoke development is monitored by a photometer system installed across the furnace exhaust duct. The photocell output is reduced as smoke passing through the duct reduces the intensity of light reaching the photocell. The output of the photocell is recorded for the 20-minute test period and the area under the resultant curve is obtained by integration over the entire 20-minute test period. This area is divided by the area developed by untreated red oak lumber during a 10-minute ASTM E-84 calibration test and multiplied by 100 to arrive at the smoke-developed value.

The resultant smoke values are assigned a Class in accordance with the scheme:

Smoke Class	Smoke Value
A	<50
B	50 - 500
C	>500

Class A denotes a low smoke-producing cable. Class B indicates cable having a marked, though limited capacity for smoke production, while Class C indicates a capacity for a high level of smoke production.

Characterization of Inside Wiring Cable

The test development work was carried out primarily with inside wiring cable (Figure 4). The core is made up of twisted pairs of 24 gauge copper conductors insulated with 6 mils of semirigid poly(vinyl chloride) (PVC) compound. Inside wiring cables do not have a core wrap or a shield. The jacket is a flexible PVC compound. Switchboard cable is of similar construction and uses identical materials.

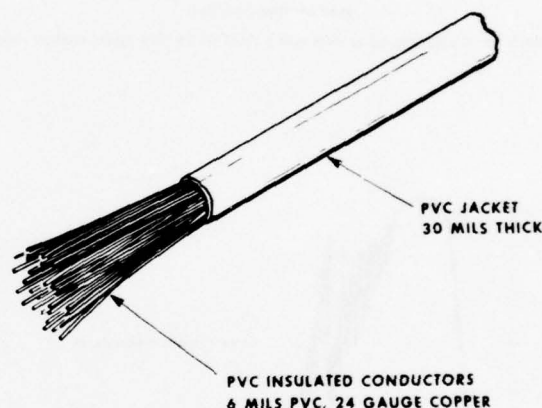


FIGURE 4. 25 PAIR INSIDE WIRING CABLE

Figure 5 shows flame spread versus time curves for five tests of 25 pair inside wiring cable. These curves are typical of well flame-retarded cable; the flame spreads to a peak value and then recedes for the duration of the test. Figure 5 shows good test reproducibility. Good test reproducibility has been found to be a characteristic of cables that are either very well or very poorly fire retarded.

Figure 6 shows a typical smoke curve for 25 pair cable. The smoke rating, which is calculated from the area under the smoke curve, increases with the amount of cable tested and with increasing flame spread.

Using the proposed classification scheme, these inside wiring cables are classified Class II in flame spread and Class C in smoke production.

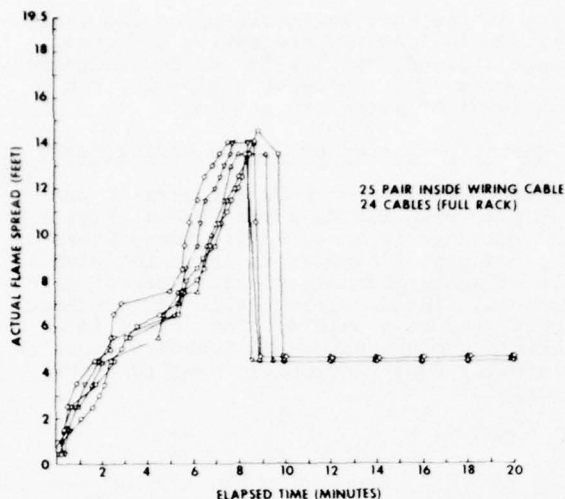


FIGURE 5. FLAME SPREAD RESULTS FOR 5 TESTS OF 25 PAIR INSIDE WIRING CABLE

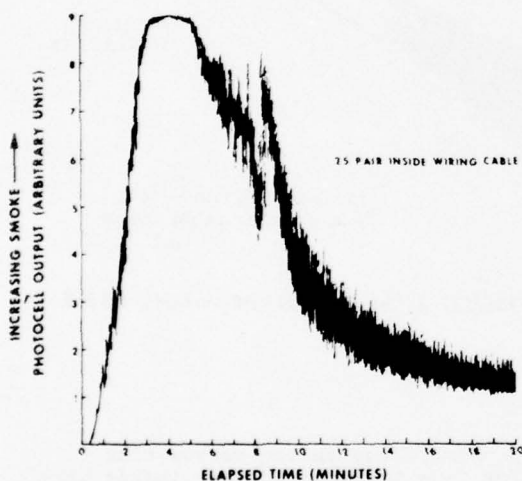


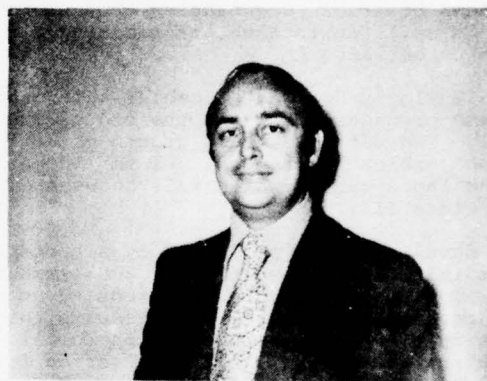
FIGURE 6. A TYPICAL SMOKE CURVE FOR 25 PAIR INSIDE WIRING CABLE

Conclusion

The test method meets the design objectives of providing numerical values for flame spread and smoke production and therefore provides a basis for rank ordering of cables. The fire exposure conditions provided by a diffusion flame exposure, totaling engulfing horizontally mounted cables under conditions of controlled air flow, are expected to be meaningful under building fire conditions where fire growth and smoke production are of concern. It is expected that the significance and limitation of the method will be explored further in large scale fire tests.

References

1. National Fire Protection Association, National Electrical Code 1975, Section 800-3d.
2. A. J. Steiner, "Fire Hazard Classification of Building Materials," UL Bulletin of Research No. 32, September 1944.
3. G. T. Castino, J. R. Beyreis, W. S. Metes, "Flammability Studies of Cellular Plastics and Other Building Materials Used for Interior Finishes," June 13, 1975, UL Report.
4. L. E. Endicott, R. B. Bowhay, "A Statistical Evaluation of the Fire Hazard Classification Furnace (ASTM E-84-68)," Materials Research and Standards, 10, No. 5, P. 19 (1970).
5. S. Kaufman, C. A. Landreth, "Development of Improved Flame Resistant Interior Wiring Cables," Proceedings of the 24th International Wire and Cable Symposium, 1975, P. 9.



J. R. Beyreis

J. R. Beyreis is Associate Managing Engineer in the Fire Protection Department of Underwriters Laboratories, Inc. He has been responsible for numerous projects involving both large scale and laboratory scale fire tests of building materials and systems. A member of several technical fire testing committee activities, Mr. Beyreis is also a 1966 graduate of Valparaiso University with a BSCE Degree.



J. W. Skjordahl

J. W. Skjordahl is a Project Engineer in the Fire Protection Department of Underwriters Laboratories, Inc. He has carried responsibility for numerous activities associated with development of fire test methods and performance data for wire and cable. Prior to joining Underwriters Laboratories in 1974, Mr. Skjordahl was involved in plastics manufacturing. He is a 1970 graduate of Rose Polytechnic Institute.



M. M. Yocum

Mary Margaret Yocum is a Western Electric employee who is assigned to Bell Laboratories in the area of flame retardant material development. She attended Cottey College and the State University of Iowa. Before joining Western Electric she was employed by Continental Oil Company.



S. Kaufman

Stanley Kaufman is a Member of Technical Staff at Bell Telephone Laboratories. He received a B.S. in Physics from the City College of the City University of the City of New York, and a Ph.D. in Chemistry from Brown University. Before joining Bell Laboratories in 1970, he was a research scientist at the Uniroyal Research Center.

THE NATURE OF WATER IN SUBMARINE CABLE CORE AND ITS RELATIONSHIP TO DIELECTRIC LOSS

J. H. Daane
H. E. Bair
G. E. Johnson
E. W. Anderson

Bell Laboratories
Murray Hill, New Jersey 07974

ABSTRACT

The effect of water trough cooling of extruded, large diameter, polyethylene coaxial cable core on the resultant dielectric loss of the cable has been found to relate to the amount and nature of water present and its radial distribution in the dielectric core. Techniques were developed to sample, measure and characterize the water present from the core cooling operation in both factory and laboratory simulation samples.

The effect of various parameters such as water trough temperatures, time of drying and sample preparation was assessed. An explanation for the nature of the dielectric loss behavior is set forth. Practical suggestions are given as to the utilization of the information obtained in this study for the operating extrusion engineer involved with the production of low dielectric loss cables.

I. Introduction

In the manufacture of submarine coaxial cable, a series of water troughs, maintained at decreasing water temperatures, are utilized to cool the extruded polyethylene dielectric core. Earlier work has shown the desirability of cooling the large cross-section of crystallizing polyethylene as uniformly as possible to achieve good gripping and to prevent the formation of voids at the inner conductor.¹ This cooling consideration thus leads one to use as high an initial trough temperature as practically possible and to use slow line speeds as well.

The use of initial trough temperatures approaching or exceeding the boiling point of water through the use of pressurized systems can lead to a situation where an anomalous dielectric loss behavior can be noted in the finished cable. Laboratory experiments and manufacturing trials were used to ascertain the nature and extent of this anomalous loss. Techniques were developed to sample, measure and characterize the water present from the core cooling operation which was found to be responsible for the anomalous loss.

II. Anomalous Loss

Cable attenuation values, as measured on finished submarine coaxial cables, can be predicted from a consideration of the material and geometric parameters involved in the cable design. The following equation has been found to apply for the frequencies currently of interest in submarine cables²:

$$\alpha = K_1 \sqrt{f} \left(\frac{1}{d\sigma_i} + \frac{1}{D\sigma_o} \right) \frac{\sqrt{E}}{\log D/d} + K_2 f F_p \sqrt{E}$$

where

K_1 and K_2 are constants

d and D are the inner conductor and dielectric diameters respectively

E is the permittivity of the dielectric

f is the frequency of the signal

F_p is the dissipation factor of the dielectric

σ_i , σ_o are the conductivities of the inner and outer conductors

Cables are regularly manufactured where prediction of their attenuation is possible and stable values are measured close to the expected. However due to the evolution of larger diameter and consequently higher capacity coaxial cables, a movement to the use of higher water trough temperatures to achieve good gripping and to minimize void formation has been shown to produce higher attenuation values than expected. These higher values have also been found to be unstable in some cases.

The frequency dependence of the cable attenuations produced under these conditions indicated that the excess attenuation is associated with the dielectric rather than with the copper conductors. Initial results of 30 MHz loss tangent values extracted from cable attenuation values showed losses of twenty microradians above the accepted limit of fifty-three microradians for the dielectric material. Consequently the dielectric loss of plaques, molded from dielectric core freshly cut from high loss cable, was measured at several frequencies within 0.5 hours of molding. The results are shown in Figure 1 where they are compared to measurements made on the starting polyethylene. Initially plaques from the high loss cable had an excess loss at 30 MHz comparable to that extracted from cable attenuation.

A decay phenomenon was also noted with the plaques molded from the cable. After twenty hours the loss tangent values returned to those of the starting material as shown in Figure 2. Further, the decay of loss could be accelerated by placing the plaques under vacuum between measurements. A plaque molded from a low loss core or pellets and subjected

to a simulated cable water cooling treatment in the laboratory produced the same effect with the same level of excess loss and decay characteristic as that of a high loss cable sample. Thus water has been shown to be directly responsible for the excess loss.

III. Total Water Measurement

The samples described in the preceding section were checked for water content by a coulometric type instrument, the DuPont Moisture Analyzer Model 26-321A. High loss cable plaques or simulated cable cooling plaques were found to contain significantly more water than plaques from pellets or low loss cable. Further it was found that the high loss plaques lost water with time.

At this point a significant amount of work was done to obtain a procedure to determine the level of water in polyethylene to an accuracy of $\pm 5\%$ and for small amounts of water to ± 2 parts per million (ppm).³ This was done so as to seek a correlation between excess loss and water content. Equilibrium solubility values were determined by determining the maximum amount of water a freshly molded plaque would absorb independent of time after soaking in isothermal water baths. Above 100°C, all samples were subjected to high pressure steam. In every case the samples were quenched in a 23°C water bath, removed, and the surfaces dried with a cloth before water analysis. The results are shown in Figure 3 where the saturation value for water in polyethylene melt at 100°C is 30 times that found at room temperature.

Another concern was to measure the radial distribution of the water in cable core. Consequently a cable core cutter was designed and built to allow one to cut and remove a cylindrical plug from a section of submarine cable core as shown in Figure 4. It should be noted that the design of this cutter allows one to extract a sample without affecting the distribution of water. The cutter is pressed in a radial direction into the core and has a cutting edge shaped to fit the inner conductor. In order to measure the radial distribution of water, six or more plugs of 0.40" diameter were removed from the cable and then sliced into thin slices usually 80 mils thick. To minimize loss of water during cutting, coordination between several people was utilized for the various operations with alternate sections being discarded so that freshly cut specimens were measured each time. The total elapsed time between sectioning a new sample of cable and measurement of water was kept below fifteen minutes.

IV. Clustered Water Determination

As much as 160 ppm of water have been found in the outer area of the SG core after extrusion into water troughs maintained at 100°C (see details in Section V). However, the room temperature solubility of the polyethylene is only 12 ppm. This leads to excess water being trapped in the polyethylene cable core. Thus, we decided to

see if we could observe the excess water by phase transition studies in a DSC. If the excess water exists in the polyethylene in an associated state it should be possible to form ice crystals by quenching below room temperature.

Quenched samples containing high levels of water were placed in a Perkin-Elmer Differential Scanning Calorimeter, Model DSC-2, and cooled to -55°C. Subsequently the samples were heated to 30°C. A typical melting peak observed at 0°C is shown in Figure 5. Using the sample weight, the measured heat absorbed in the 0°C transition and a heat of fusion of 79.7 cal/gm for ice, we calculated the amount of water in the clustered form. Combining this result with the total water measurement from the Moisture Analyzer, it thus became possible to differentiate between water sorbed in the polyethylene and that associated in clusters. This has been done over a range of temperatures using isothermal water baths to condition the samples to equilibrium sorption. The samples are then quenched at room temperature prior to measuring. The results of this work are shown in Figure 6.

Early attempts to observe the clusters microscopically failed, apparently because of their submicron size. However after high pressure steam treatment at 208°C for 60 seconds followed by a cold water quench, clusters were observable under a light microscope as shown in Figure 7. The clusters are about 2 microns in diameter, are fairly uniformly distributed and the sample was found to contain approximately 5600 ppm water. Essentially all of the water is in the clustered state.

Plaques containing clusters were dried out and subsequently re-exposed to water at a temperature much lower than that at which the clusters were formed. It was found that the cavities refill partially and one then has a sample whose water content far exceeds its saturation level at the temperature soaked. For instance a sample originally treated at 100°C and dried was found to contain 65 ppm water after soaking at 40°C for 10 days. This is >3 times its equilibrium saturation at 40°C.

V. Radial Distribution of Water

Both the type and amount of water content of several cables which had excess dielectric loss were determined using the tool and the techniques described earlier. For a cable exhibiting approximately 20 microradians excess loss at 30 MHz, the outer 160 mils of the approximately 600 mil thick core was found to contain 50 ppm total water (these measurements were made approximately four months after production). The rest of the core was near or below the room temperature saturation value of 12 ppm. In order to isolate the key parameters which control the ingress of water during cable production, we designed a series of experiments to simulate the water trough portion of the cable extrusion process.

A one foot length of cable core was heated to 175°C in an oven and then cooled in a series of circulating isothermal water baths with temperature chosen to equal those of the manufacturing plant troughs. The residence times in the baths were chosen to match those for cable passing at a given line speed in known trough lengths. Results obtained on a simulated cooling cycle sample are shown in Figure 8. The bulk of the water, with a concentration as high as 140 ppm, was concentrated in the outer 160 mils of the dielectric. From this 160 mils to the inner conductor, the level of water was near or below the room temperature (23°C) saturation value of 12 ppm. A large fraction of the water in the outer layer was in the clustered form for this sample held in the first bath at 100°C for 12 minutes. When the initial water bath temperature was lowered from 100°C to 70°C in four steps, the water profile was found to decrease from a maximum of 157 ppm and 133 ppm of total and clustered water respectively to only 25 ppm total and no detectable clusters as shown in Figure 9.

It appears that the temperature of the initial water bath plays a critical role in controlling the final concentration of water in the cable. These results were confirmed at cable factories where virtually the same distributions were obtained at the same initial water trough temperatures.

VI. Water Content Versus Dielectric Loss for Plaques

Dielectric loss measurement were made on plaques brought to equilibrium saturation with water at various temperatures. A linear relationship between $\tan \delta$ at 30 MHz to the total concentrations of water was found up to 80 ppm as in Figure 10. As $\tan \delta$ measurements were made on plaques containing larger amounts of water (up to 300⁺ ppm for plaques treated in 100°C water), it was noted that the increase in loss was not proportional to water content. Measurement of $\tan \delta$ over the frequency range of 0.1 to 30 MHz for samples containing large amounts of water showed Maxwell-Wagner type behavior. A calculation using literature data indicated that spherical particles of water imbedded in polyethylene could give a Maxwell-Wagner loss peak in the MHz region³, which agrees with the results obtained (Figure 11).

VII. Water Content Versus Loss for Cables

In discussing this subject we must bear in mind the fact that the high concentration water profiles found in laboratory simulated cooling of cores discussed earlier were obtained on unshaved specimens. The measurements of water content were gotten as quickly as possible after the core was cool. For a cable, the core is first shaved, after having stood for a while on a drum, by a servo-controlled head with cutters to achieve concentricity of the outer surface with the inner conductor. The amount of material removed, the heat involved in the operation

and the time before application of the outer conductor and jacket will affect the amount of water trapped in the finished cable. Thus a significant portion of the originally sorbed water in the core may be eliminated before the cable is finished. Another concern will be whether the cooling sequence has generated clusters and whether the shaving operation leaves any in the core.

The results for a cable extruded into a cooling system with an initial pressurized 105°C cooling trough were as follows: The extracted loss tangent at 30 MHz for the cable at 23°C was 24 microradians above that expected from the pellets used. A plaque molded from the total core material had an initial loss of 75 microradians which decayed to 50 microradians within 24 hours. The outer 160 mils initially contained 60 ppm water and for our earlier correlation of 1 microradian per 2.3 ppm water, this would mean 26 microradians excess loss. However in a cable neither the electric field nor the water distribution is uniform and calculations seeking to relate the profile of water to the effect on cable attenuation have not been totally successful. By keeping the initial water trough temperature below 92°C however the problem is avoided and cable attenuation values are what is expected.

VIII. Conclusion

Experiments conducted in the laboratory and at submarine cable plants have shown that unexpectedly high cable attenuations result from the entrapment of cooling water in the dielectric core during manufacture. This entrapment is strongly dependent on the first water trough temperature and may result in water being present in two forms, i.e. as dissolved and as clusters generated by the rapid lowering of the solubility of water in the melt as it is cooled.

The shape and magnitude of the dielectric loss of polyethylene containing water has been shown to depend on whether the water is present in the clustered form. Cable that has been dried but contains voids left by clustered water can reabsorb more than its equilibrium amount of water upon immersion in water and thus exhibit instability as regards cable attenuation. The use of lower initial water trough temperatures, consistent with the maintenance of good gripping of the dielectric on the inner conductor, is called for to produce cable attenuations as designed.

IX. Acknowledgments

The authors wish to thank S. Matsuoka for many helpful discussions during the course of this work. We have also had the benefit of numerous discussions with our colleagues at Bell Laboratories, Holmdel, N. J. and Western Electric, Springfield, N. J. We also would like to thank M. C. Biskeborn and his associates at the Phelps Dodge Cable and Wire Company for the use of their high pressure steam facility to produce high water content films.

REFERENCES

1. Daane, J. H., Proceedings of the 24th International Wire and Cable Symposium, p 75-82, Cherry Hill, N.J. 1975
2. Bowker, M. W., W. G. Nutt and R. M. Riley, Bell System Technical Journal, 43, 1197 (1964)
3. Bair, H. E. and G. E. Johnson, Analytical Calorimetry, Vol. 4, R. S. Porter and P. F. Johnson, eds., Plenum Press, New York, 1976
4. Progress in Dielectrics, Vol 7, J. B. Birks, editor, CRC Press (1967)
5. Johnson, G. E., H. E. Bair, E. W. Anderson and J. H. Daane, Annual Report, Conference on Electrical Insulation and Dielectric Phenomena (1976)

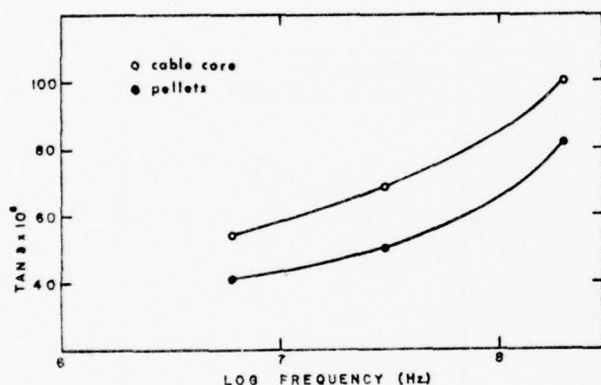


Fig. 1 Comparison of the dielectric loss of plaques molded from pellets and high attenuation cable core

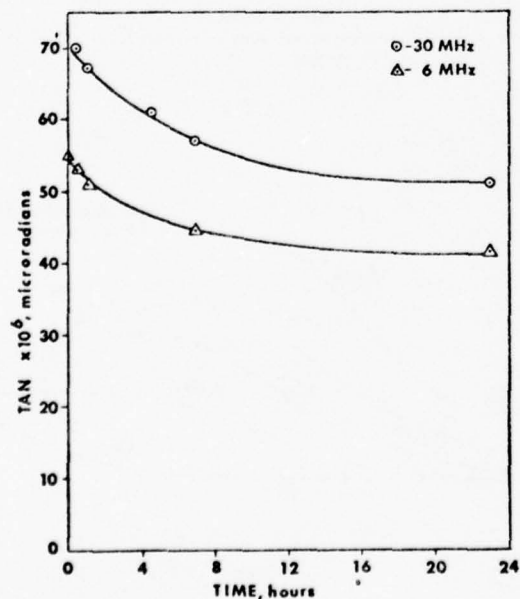


Fig. 2 6 and 30 MHz loss data as a function of time, from molding, on a plaque from high attenuation cable core

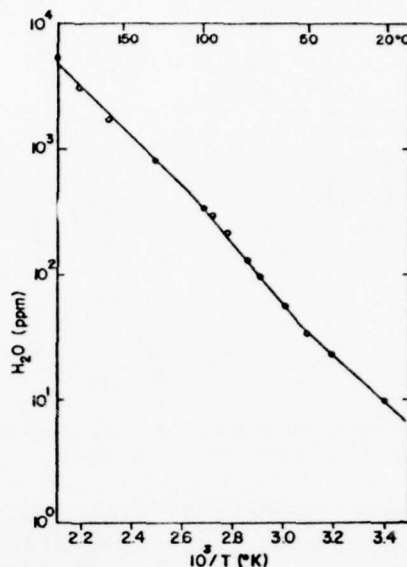


Fig. 3 Log of saturation water concentration in polyethylene versus reciprocal absolute temperature

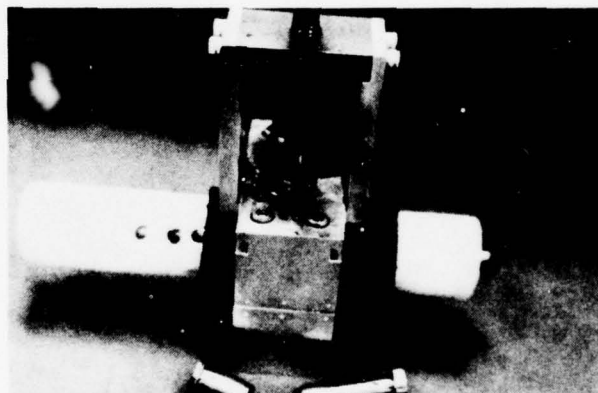


Fig. 4 Photograph of submarine cable cutter

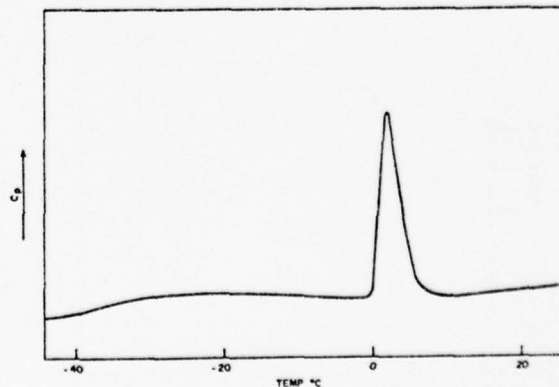


Fig. 5 Below room temperature DSC trace of polyethylene after soaking in water at 100 deg C and held at -55 deg C for one hour

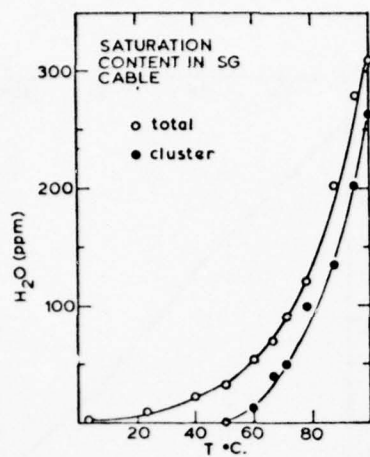


Fig. 6 Total and clustered water in polyethylene plotted against isothermal temperature of conditioning

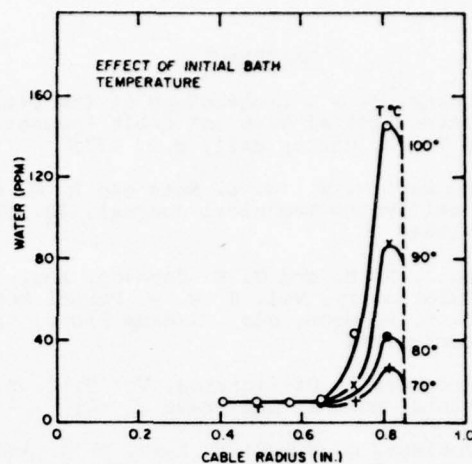


Fig. 9 Effect of initial water trough temperature on the radial distribution of water in SG cable core

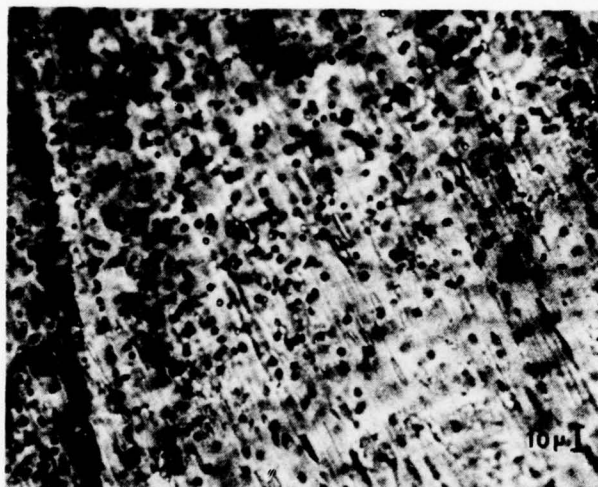


Fig. 7 Photomicrograph of cavities created in SG polyethylene by water (transmitted light)

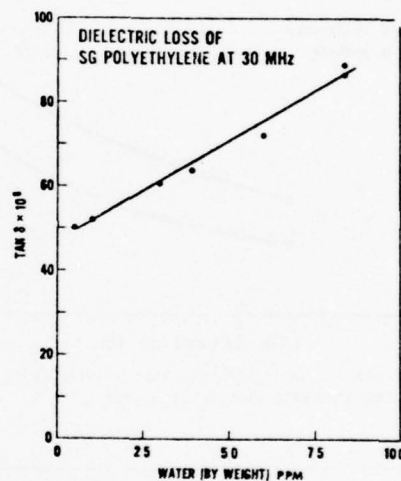


Fig. 10 Dielectric loss of polyethylene containing water versus total water content at 30 MHz

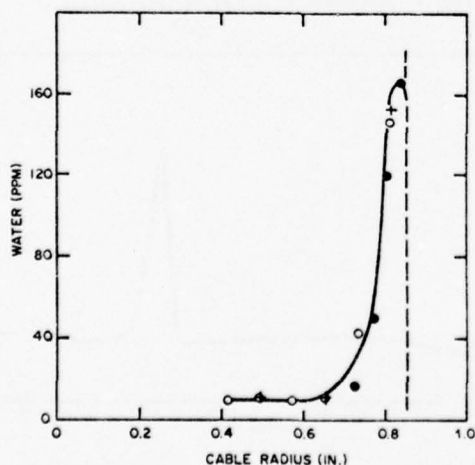


Fig. 8 Radial distribution of water in cable core cooled in 100 deg C initial water trough system

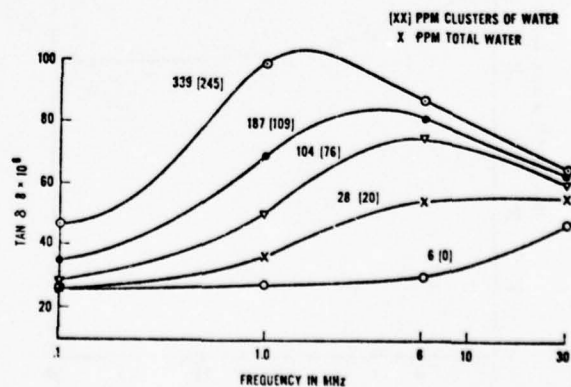
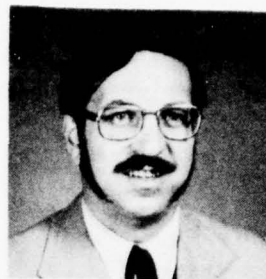


Fig. 11 Dielectric loss versus frequency for polyethylene plaques with different amounts of water (bracketed numbers represent clustered water)



John H. Daane

Mr. Daane received a B.S. in Science from Adelphi University in 1962 and a M.S. in Chemistry from Union College, Schenectady, New York, in 1966. He has been a member of the Plastics Research and Development Department at Bell Laboratories, Murray Hill, New Jersey, since 1966. Prior to that time he was employed by the General Electric Co. at their Research Center in Schenectady and their Silicone Products Department, Waterford, New York. For the past seven years, he has been engaged in the study of polymers for use in submarine cable systems.



G. Edward Johnson

Mr. Johnson received a B.S.E.E. in 1966 and a M.S. (Physics) in 1970 from the New Jersey Institute of Technology. He has worked in the field of dielectrics at Bell Laboratories since 1960. During that time he has been involved in the development of test methods for dielectric properties of polymers used in submarine cable systems.



Harvey E. Bair

Mr. Bair is a member of the technical staff in the Plastics Research and Development Department at Bell Laboratories in Murray Hill, N.J. During the last 14 years he has published over 70 papers which have been primarily concerned with the development and utilization of thermoanalytical techniques to characterize plastics. Prior to joining BTL in 1965 he was employed at the General Electric Research Laboratory in Schenectady, N.Y. and the Johns Hopkins University Applied Physics Laboratory in Maryland. Mr. Bair has received a B.S. degree in Chemistry from Dickinson College, Carlisle, Pa. and a M.S. in Chemistry from Penn State University, University Park, Pa.



E. W. Anderson

A member of the Plastics Research and Development Department at Bell Laboratories, Mr. Anderson joined the firm in 1957. He received a B.S. degree in Physical Science from Seton Hall University in 1953. His current activities include the evaluation of insulating materials, processes, and electrical properties of polymers with emphasis on the requirements of the ocean cable systems. He is a member of A.S.T.M. Committee D-9 and A.N.S.I. Committee C-59.

CORROSION STUDIES ON SHIELDING MATERIALS FOR UNDERGROUND TELEPHONE CABLES

PART II: CORROSION PROTECTION FOR FILLED CABLES

K. E. Bow and L. G. Colter
Dow Chemical U.S.A.
Freeport, Texas

Abstract

In Part I, electrochemical test methods were used to provide data on the corrosion behavior of telephone cable shielding materials. The purpose of this paper is to apply these techniques to the study of the plastic and floodant coated shielding systems of buried, filled cables. The mechanisms whereby coatings provide corrosion protection are investigated and a discussion of the breakdown mechanisms observed with floodant coatings is given. Data showing the need for adequately protecting aluminum from galvanic corrosion in aluminum-steel sheath designs are presented.

Introduction

Background

Part I of this paper was presented at the 24th Wire and Cable Symposium.¹ In that paper, an attempt was made to define a realistic corrosion test methodology based on electrochemical techniques. The electrolytes chosen for test environments had substantially the same chemical compositions as the water extracts from test sites utilized in the joint National Bureau of Standards/Rural Electrification Administration (NBS/REA) soil burial evaluation of shielding materials.^{2,3,4,5} Reasonable agreement between the laboratory studies and the soil burial tests was obtained. Examination of the test results indicated that a comprehensive evaluation of shielding materials for their resistance to corrosion required that more be considered than the chemical composition of the electrolyte. Therefore, the mechanisms of galvanic corrosion due to dissimilar metals, differential aeration, and mechanical stress were investigated. For almost every shielding material studied, the data indicated that these mechanisms often constituted the main factors in determining the service life of a shielding material. It was concluded that all the common shielding materials in use today experience varying degrees of corrosion. Plastic clad metals were found to have a significantly better resistance to corrosion than the corresponding bare metals.

Test Methodology from Part I

An essential and important part of all corrosion testing is the electrolyte chosen for the test medium. To supply a realistic point of comparison, soil water solutions were synthesized with substantially the

same chemical make-ups as the soil waters in three of the sites chosen for the NBS/REA field tests of shielding materials.⁶ The compositions of the solutions as shown in Table I represent the soil waters of NBS/REA Site A (sandy loam, pH 8.8), Site C (acidic clay, pH 4.0), and Site G (tidal marsh, pH 7.1).

A Petrolite® Corrosion Rate Meter, M-1010 CIY, was chosen to directly measure the electrochemical corrosion rates. Polarization curves were determined with a Petrolite Potentiodyne® Analyzer, M-4100, and galvanic corrosion currents were measured with a zero resistance ammeter. Corrosion rates were measured weekly for five weeks. The galvanic currents, due to bimetallic couples, were measured for eight weeks. From the galvanic corrosion currents and Faraday's law, corrosion rates in mils per year were calculated.

Additional Analysis of Part I Data

On several occasions during the studies reported in Part I, the laboratory and soil burial results did not agree. The most notable of these was observed with copper in the alkaline solution A: in the laboratory test solution, copper had a very high corrosion rate while in the actual soil at Site A, copper was not severely attacked. This behavior may be explained by a consideration of the mechanism whereby copper achieves its corrosion resistance and an analysis of the corrosive waters to which copper is known to be susceptible. The corrosion resistance of copper stems from the presence of a surface oxide film. Soil waters high in carbonic acid can be particularly harmful to copper because the carbonic acid dissolves this protective oxide film.⁷ Synthetic solution A contains a high concentration of bicarbonate ion which can react to form carbonic acid. The attack of the copper by this acid results in a pitting type corrosion. Indeed, examination of the copper sample from the electrochemical test revealed the presence of dark orange spots of localized corrosion on its surface.

Other types of anomalies occurred within the laboratory data. For example, with most samples tested, differential aeration increased corrosion. The reverse occurred for copper in synthetic solution A. This reversal may be explained as follows: the presence of the flowing oxygen restricted the amount of carbonic acid available to

TABLE I: PROPERTIES OF SYNTHETIC SOLUTIONS REPRESENTING SOIL WATERS

Solution Identification	Soil	pH	Ca ⁺⁺	Mg ⁺⁺	Chemical Composition (parts per million)				
					Na ⁺	HCO ₃ ⁻	SO ₄ ⁼	Cl ⁻	NO ₃ ⁻
A	Sandy Loam	8.8	7	20	2420	4207	215	314	7
C	Clay	4.1	598	716	2200	0	6480	3413	116
G	Tidal Marsh	7.1	166	152	2350	0	1776	3212	35

attack the protective oxide layer on the surface of the copper. Without oxide dissolution, the corrosion rate of the copper can decrease.

Guidelines which rate a soil's corrosiveness by its value of soil resistivity have been established for pipelines.⁸ Using these guidelines, one would have expected aluminum to be viciously attacked in the 400 ohm-cm soil at Site A during the NBS/REA studies. To the contrary, excellent results were obtained through six years of burial with bare, flooded, and plastic coated aluminum.⁹ In this instance, the laboratory data of Part I indicated a good performance of aluminum in this soil which was explained as follows: a polarization study revealed that the aluminum formed a protective, or passive, layer in the synthetic solution representing the soil water at Site A. This layer gives the aluminum a natural resistance to corrosion. Therefore, solution A was not used in the corrosion studies of Part II because: first, the variables affecting the lack of corrosion observed for aluminum at the actual Site A could not be easily identified and second, in the synthetic solution A, where the variables were controlled, a natural protective coating was formed on the aluminum which greatly reduced the corrosive attack.

Protection for Filled Cables

Sheath damage of buried cables is a common occurrence.¹⁰ This damage often allows the entry of electrolyte which can lead to subsequent loss of the electrical continuity of the shield due to corrosion. This problem was recognized very early in the trend to bury cables. Steps were taken to mitigate shield corrosion through the use of copper for shielding due to its substantially lower deterioration rate when compared to aluminum in ASTM studies of corrosion.¹¹ The development of adhesive copolymer coatings substantially reduced the susceptibility of aluminum to corrosion and allowed the use of plastic clad aluminum as a more economical alternative to copper.¹² With the advent and growth of filled cables, the bare metal shields and armor have been flooded with grease-like materials to provide a water block. The ability of these materials to inhibit corrosion has become a topic of interest to the cable industry. There have been several no-

table efforts to assess the degree of corrosion protection afforded by these materials. Shick, using polarization techniques, determined that petrolatum flooding compounds could be worse than no coating.¹³ He subsequently showed that inhibitors added to the floodant could be rendered ineffective due to leaching by the soil water.¹⁴ However, since the type of floodant he used is obsolete today, and since there has been an advancing technology in flooding compounds,¹⁵ it was deemed appropriate to reexamine the ability of these types of coatings to provide corrosion protection and compare their behavior to commonly used plastic coatings.

Sample Preparation

Sample preparation is one of the key considerations in the study of grease-like materials as protective coatings for metal. Corrosion protection supplied by these materials was generally believed to be thickness dependent.¹⁶ Therefore, for a comprehensive evaluation, it was necessary to prepare coatings of various thicknesses. Also, for reproducible results, a uniform coating is required on any given test specimen. After much experimentation, the following procedure was adopted to fulfill these criteria: the metal strip to be coated was weighed, dipped in flooding or filling compound at 240°F for 10 seconds, and then suspended vertically in a circulating air oven heated to 240°F. The specimen was removed from the oven, cooled, reweighed, and coating thickness calculated. The oven treatment remelts the coating causing it to flow to a uniform thickness dependent on the oven residence time. This procedure was adopted because flooding compounds in cable manufacturing are applied above their melting points and are then exposed to higher temperatures during extrusion of the cable jacket.¹⁷ It should be noted that the edges of the specimens did not coat due to the surface tension of the hot liquid.

Many types of filling and flooding compounds were evaluated. A typical representative of each type was selected for the in-depth investigation to be reported herein. The filling compound is a commercially available material consisting of 92% petrolatum and 8% polyethylene. The floodant is a commercially available mixture of 75% petrolatum and 25% atactic polypropylene. These materials were applied to bare 8 mil thick aluminum, 1145 alloy, and bare 6 mil black plate steel.

Commercially available plastic coated metals were used which had both sides of an 8 mil thick 1145 aluminum alloy and a 6 mil thick electrolytic tin plated steel coated with an adhesive copolymer of ethylene. This copolymer has the chemical resistance and general characteristics of low density polyethylene with the additional attributes of adhesiveness to metals and increased mechanical strength. A more detailed description of the nature of this material has been given in a previous Wire and Cable Symposium paper.¹⁸

Experimental Procedure

Galvanic couples of plastic coated aluminum and black plate steel, plastic coated aluminum and plastic coated tin plated steel, and flooded aluminum and flooded black plate steel were selected for testing. Strips of each respective material were placed in corrosion cells, each containing about 900 cc of the synthetic solutions, and coupled electrically. The solutions were kept at room temperature without agitation. Galvanic corrosion current readings were made at various time intervals for up to 4 months using a zero resistance ammeter.

To simulate actual cable practice, the solutions were allowed to contact bare metal exposed at the specimen edges. Though the function of a coating on metal is to provide a total environmental barrier, it must be expected that bare metal areas will exist in the coating as the result of design, defect, or damage. The edges of bare metal could represent the cable seam, for example, which is an exposed area that exists because of design.

The actual area of exposure for an 8 mil (0.203 mm) coated aluminum specimen was the bare edge along a three inch (7.62 cm) section of a one inch (2.54 cm) wide by seven inch (17.28 cm) long strip, or an area of about 0.024 square inches (0.393 cm²). For the 6 mil (0.152 mm) steel, the exposed bare area on the coated specimen was again the edge, an area of 0.018 square inches (0.294 cm²).

It should be noted that an effective coating must limit corrosive attack only to these exposed areas of bare metal. Therefore, a basic difference in symmetry exists between bare and coated metals. The service life of a coated metal system in which the coating is permanent is dependent on the width of the shielding tape as shown in Figure 1. For bare metals, service life becomes thickness dependent as shown in Figure 2.

Qualitative Results

A description of the galvanic couples after 18 weeks of testing is given in Table II. In all cases, some type of corrosive attack was observed on at least one metal in the couple. The corrosive attack of flooded aluminum began in localized areas on the bare

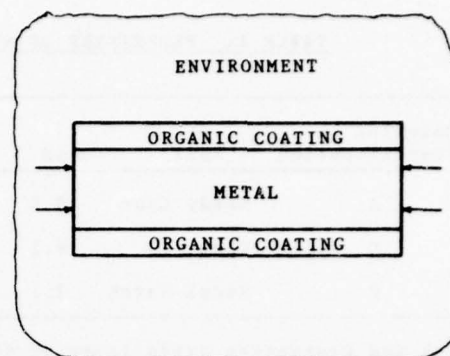


FIGURE 1

ILLUSTRATION OF LIMITING THE AREA OF CORROSIVE ATTACK WITH COATED METALS

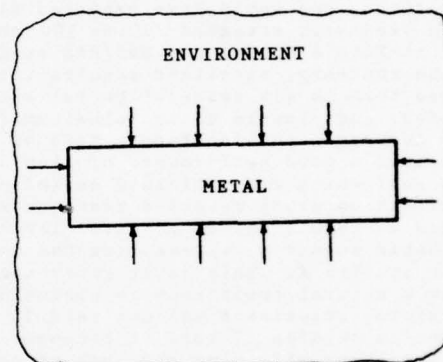


FIGURE 2

ILLUSTRATION OF THE CORROSIVE ATTACK ON ALL SURFACES OF BARE METALS

edges of the sample generating a white corrosion product. The attack then moved progressively inward with the corrosion product completely destroying the integrity of the coating. Two types of corrosion damage were observed with the flooded steel: a progressive attack from the sample edges and localized corrosion cells that appeared to originate beneath the coating. A hard red corrosion product was generated in both cases moving progressively inward from the edges or progressing outward in all directions from the points of localized attack.

It appeared that the same corrosion process was at work irrespective of coating thickness. The corrosion process destroyed thick coatings as well as thin, the difference was that the rate at which the metal was consumed appeared to be reduced with increased coating thickness.

For the plastic coated aluminum, some corrosion product was observed at the bare edges but the corrosive attack was not nearly as severe as that observed on flooded aluminum.

TABLE II. DESCRIPTION OF GALVANICALLY COUPLED TEST SAMPLES AFTER 18 WEEKS

A. Filler Coated Aluminum/Filler Coated Black Plate Steel

System Number	Test Solution	Coating Thickness (mils)		Extent of Corrosion			
		Aluminum	Steel	Aluminum		Steel	
				Amount*	Type**	Amount*	Type**
1	Acidic (C)	11.1	10.9	5%	Edge	50%	Heavy pitting
2	Neutral (G)	12.1	10.6	7%	Edge	5%	Small pits
3	Acidic (C)	2.0	2.0	Slight	Edge	100%	All surfaces
4	Neutral (G)	2.2	2.4	70%	Edge	Slight	Extensive pitting

B. Floodant Coated Aluminum/Floodant Coated Black Plate Steel

5	Acidic (C)	15.6	15.2	10%	Edge	5%	Edge
6	Neutral (G)	15.8	15.9	20%	Edge	5%	Edge
7	Acidic (C)	3.1	3.1	20%	Edge	40%	Edge and pitting
8	Neutral (G)	3.1	3.1	25%	Edge	5%	Pitting

C. Plastic Coated Aluminum/Plastic Coated Tin Plated Steel

9	Acidic (C)	2.3	2.3	None	Edge	9%	Edge
10	Neutral (G)	2.3	2.3	None	Edge	10%	Edge

D. Plastic Coated Aluminum/Bare Black Plate Steel

11	Acidic (C)	2.3	None	None	Edge	100%	All surfaces
12	Neutral (G)	2.3	None	None	Edge	60%	All surfaces

* Amount of metal attacked

**Type or location of corrosive attack

The physical integrity of the coating and the bond of the coating to the aluminum were retained. The plastic coated tin plated steel showed an increased amount of edge attack when compared to the plastic coated aluminum. The plastic coating retained its integrity and the bond of coating to metal appeared to restrict the corrosion process only to edge attack. No areas of localized attack were observed under the plastic coatings.

Quantitative Results

Table III shows the galvanic corrosion currents for the systems described in Table II. Note that for systems 1 through 8, which have coatings of floodant or filler on both metals, corrosion current generally increases with time. Systems 9 and 10 with adhesive copolymer coatings show a constant level of corrosion current versus time. Figure 3 graphically illustrates this behavior for samples in the acidic synthetic solution C. Though the effect of increasing floodant thickness initially tempers the corrosion current, as time passes, the level of corrosion current flowing in the couple approaches that of the thinner coating. Figure 4 illustrates that there is a correspondence between the amount of aluminum destroyed (data of Table II) and the amount of current flowing at the end of the test (data of Table III).

The behavior of System 3, a couple of aluminum and black plate steel in which a thin coating of filler is on both, and System 11, a couple of aluminum with adhesive copolymer coatings and uncoated black plate steel, is of particular interest. As can be seen from Table III, the role of the aluminum and steel in these couples switched from the normal galvanic order with the steel becoming the anode. This behavior only occurred in the acidic synthetic solution C when the steel was bare or coated with a thin coating of filler. To investigate the role of the aluminum in these two systems, couples were prepared with bare aluminum and bare black plate steel and exposed to the acidic and neutral solutions. Again the reversal of polarity occurred only in the acidic solution. After one week, the steel was anodic, and 9 microamperes of corrosion current were recorded for this cell. The tendency toward reversal of polarity appears to be independent of the presence or effectiveness of the coating on aluminum and solely dependent on the effective amount of bare black plate steel exposed to the acidic solution. The amount of bare steel is dependent on coating thickness as shown in Figure 5. As mentioned earlier, corrosion rates were lower with thicker coatings. This reduction in corrosion rate can be attributed to the greater mechanical resis-

TABLE III. ALUMINUM/STEEL COUPLES IN SYNTHETIC SOLUTION

A. Filler Coated Aluminum/Filler Coated Black Plate Steel

System Number	Test Solution	Coating Thickness (mils)		Galvanic Corrosion Current, Microampres, Weeks									
		Aluminum	Steel	1	2	3	4	5	6	7	9	18	
1	C	11.1	10.9	1.6	1.9	0.7	1.5	1.6	2.8	3.3	5.4	14.5	
2	G	12.1	10.6	14.9	15.3	13.6	14.1	14.5	14.3	14.8	14.9	17.4	
3	C	2.0	2.0	0.6	0.7	0.5	(1.2)	(0.5)	(0.1)	(0.1)	0.2	0.2	
4	G	2.2	2.4	45.5	53.1	55.1	69.6	97.6	105.4	113	118.6	158	

B. Floodant Coated Aluminum/Floodant Coated Black Plate Steel

5	C	15.6	15.2	14.9	9.6	9.9	11.6	10.8	14.6	16.7	21.6	34.6
6	G	15.8	15.9	18.9	25.2	21.6	25.3	22.6	25.4	21.8	26.4	50.1
7	C	3.1	3.1	9.1	8.5	13.8	21.6	27.8	38.9	41.2	42.8	46.3
8	G	3.1	3.1	29.6	33.9	27.9	28.5	34.1	24.8	24.5	35.1	43.6

C. Plastic Coated Aluminum/Plastic Coated Tin Plated Steel

9	C	2.3	2.3	16	--	13	16	--	--	--	14	15
10	G	2.3	2.3	16	--	19	25	--	--	--	27	25

D. Plastic Coated Aluminum/Bare Black Plate Steel

11	C	2.3	none	(.11)	(.11)	(.11)	(.08)	--	(.01)	(.07)	--	(.02)
12	G	2.3	none	2.8	3.4	1.8	1.1	--	.29	.03	--	.04

() Steel anodic to the aluminum

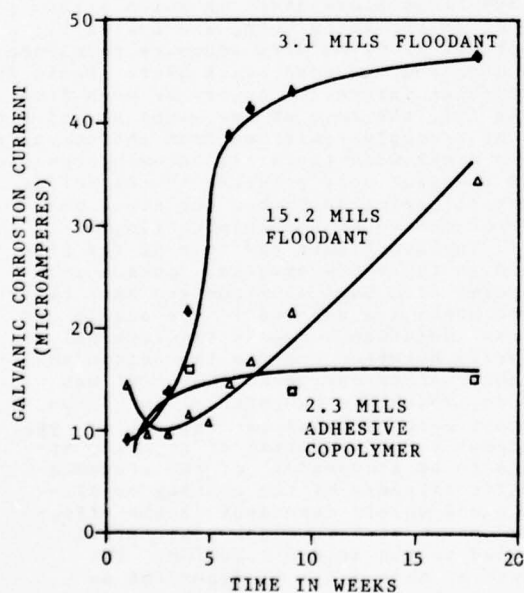


FIGURE 3

GALVANIC CORROSION CURRENT VERSUS TIME
IN ACIDIC SOLUTION C FOR COUPLES OF ALU-
MINUM AND STEEL HAVING VARIOUS COATINGS

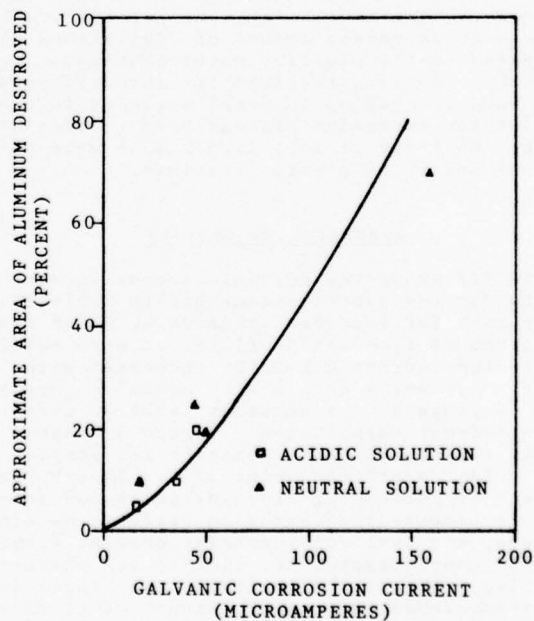


FIGURE 4

RELATIONSHIP BETWEEN FLOODED ALUMINUM DE-
STROYED AND GALVANIC CORROSION CURRENT

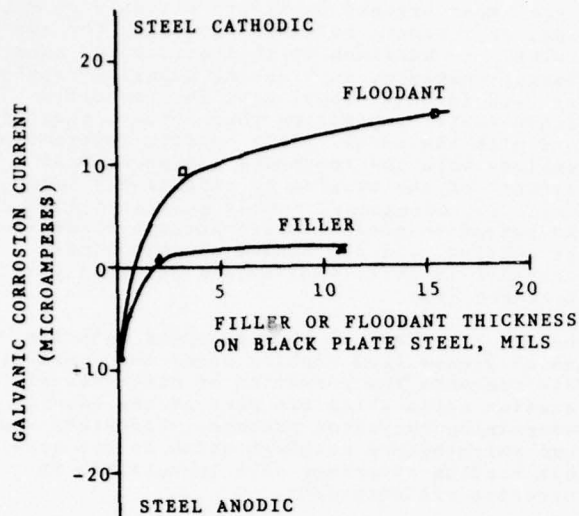


FIGURE 5

EFFECT OF FLOODANT AND FILLER THICKNESS ON POLARITY OF ALUMINUM-STEEL COUPLE ONE WEEK AFTER COUPLING ALUMINUM AND BLACK PLATE STEEL

tance of thicker coatings to destruction by the corrosion processes. With less coating destruction, less steel is exposed to the electrolyte, and the corrosion reactions are insufficient to effect a polarity change. In addition, since floodants have a greater cohesive strength than fillers,¹⁵ they are more resistant to destruction.

It should be pointed out also that the inability of a floodant or filler material to provide corrosion protection to a metal in no way reflects on the water block properties of these materials.

Discussion

The use of galvanic couples of steel and aluminum, for testing the effectiveness of coatings, can accelerate the corrosion rate. This procedure appears to be a realistic test in that shields of telephone cables are bonded and grounded at intervals along their length. The types of metals used for bonding and grounding clamps and grounding rods are often different from the shielding materials. Also, certain designs of cable sheaths incorporate dissimilar metals in order to provide both electrostatic shielding and mechanical armoring protection. In these circumstances, the potential for galvanic corrosion exists and must be considered.

Corrosion Mechanisms with Flooded Aluminum

A discussion of the nature of the corrosive attack of bare aluminum in soil waters is essential to understand the experimental results with coated systems. Aluminum is subject to a pitting type corrosion. It has been shown

that aluminum pitting occurs in the pH range of about 4.5 to 9.0.¹⁹ Outside this range corrosion takes place by a uniform surface attack as the surface oxide film is dissolved. Pitting results from the action of local cells on the surface of the metal. The point of initiation becomes the local anode while the surrounding metal surface forms the local cathode. The development of acidity within the pits has been reported by many workers. The acid may in turn cause the metal within the pit to be dissolved, enlarging the pit. The local cells which lead to pitting may be attributed to differences in the environment in or on the metal surface. The most common causes of local cell formation are local scratches or abrasion, differential concentration, or differential aeration.

The increasing corrosion current with time, as shown in Figure 3 for flooded aluminum, exemplifies a corrosion mechanism called anodic undermining corrosion. Similar behavior has been described by Koehler who considered it as one of the most significant types of failure mechanisms for metals with organic coatings.²⁰ The mechanism follows the pattern shown in Figure 6. Corrosion begins at the bare edge or any other defect in the coating. The corrosion products grow, detach the weakly adhered coating from the aluminum substrate, and force the fragile coating to break up. The area of fresh metal at the advancing edge of the detached coating serves as the anode in a crevice type corrosion cell. As more corrosion product is generated on the newly bared metal, more coating is detached, continuing the process across the width of the metal at an accelerated rate.

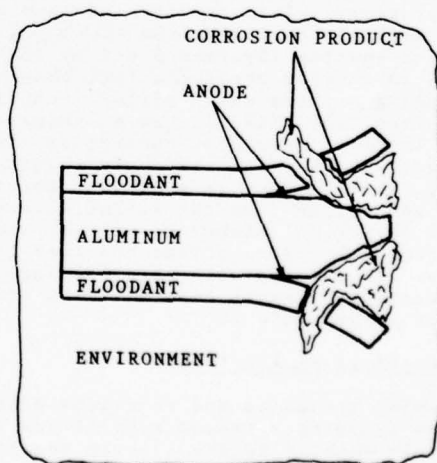


FIGURE 6

MECHANISM OF ANODIC UNDERMINING CORROSION FOR ALUMINUM COATED WITH FLOODANT

The corrosion mechanism observed with the flooded aluminum systems bears a close relationship to pitting, but the undermining occurs preferentially to pitting because the coating over the anodic area acts as a greater barrier to diffusion than the corrosion products at the anodic area in the bottom of the pit. Though the corrosion mechanisms involved in pitting and crevice corrosion are similar, with crevice corrosion a foreign substance usually restricts the access of electrolyte to, or traps electrolyte on, the metal's surface.

Corrosion Reactions During Undermining Corrosion

At least two types of corrosion reactions may be proceeding concurrently at the anodic area during the anodic undermining process. The difference in oxygen concentration between the major portion of the test solution and solution trapped in the anodic area under the coating produces an oxygen concentration cell. The areas having the greater degree of oxygen starvation become anodic to those of higher oxygen concentration (cathodic areas). When the oxygen is depleted by the corrosion reactions, a second process can dominate which causes the anodic area to become more acidic. This in turn can intensify the attack. Many investigators consider differential aeration mechanisms to be one of the most widespread and important reasons for corrosion damage in soils.²¹

Another factor that must be considered as important to the overall intensity of the corrosion reaction is the relative effectiveness of the coating as a barrier to diffusion of water and oxygen. As the barrier property of the coating improves, the intensity of the corrosion mechanisms can increase. Both composition and thickness of the coating affect this barrier property. Evidence for this can be seen in Table II where aluminum with the thicker floodant coating (Systems 5 and 6) in both solutions is showing greater attack than the corresponding systems using filler (Systems 1 and 2). From Table III, it can be observed that the level of corrosion current is also significantly higher for the systems using floodant. The floodant is a greater barrier to water and oxygen than the filler allowing a greater oxygen deficiency to prevail under the coating. This intensifies the rate of corrosion. In systems with thin coatings, reduced coating strength overrides the effect of barrier properties.

Plastic Coatings on Aluminum

The corrosion mechanism and reactions described for the flooding compound type of coating should apply equally to the plastic coatings on aluminum. Yet, as shown in Table III, aluminum coated with the adhesive copolymer sustained no corrosion damage from edge attack. There are four differences that contribute to this superior performance by adhesive copolymer coatings.

First, most organic coatings rely only on wetting, or intimate molecular contact, for adhesion. In addition to this attribute, some plastic coatings, such as the adhesive copolymer used in this study, have functionality within their composition that forms a chemical bond with the metal. This bonding interaction combines with the toughness and mechanical strength of the coating to effectively counteract the mechanical forces generated during the corrosion process which attempt to detach the coating. (A discussion of this bonding mechanism is quite complex and has been given elsewhere.²²)

Second, the chemical bond prevents moisture and chemicals from wicking under the coating. This prevents the formation of differential aeration cells which are part of the anodic undermining corrosion process. Floodants and pure polyethylene coatings which do not have this bonding advantage show instability in corrosion resistance.²³

Third, the mechanical strength of the coating is retained during the corrosion process. The volume of corrosion product generated does not destroy the integrity of the coating as with the floodants.

Fourth, the retention of corrosion products by the coatings reduces the corrosion process by restricting the rate of ion transfer.

Flooded Steel Corrosion Mechanisms

There are several corrosion mechanisms that can occur with the flooded steel. First, there is the familiar mechanism of cathodic detachment. Since the steel surface is easily attacked by water and oxygen to form metallic ions of iron, the surface to which the coating is attached corrodes away thereby disbonding it. This appears to be the main mechanism at work in the acidic synthetic solution C. Here the corrosion process began at the edges and progressed inward. An area of detached coating could be seen advancing ahead of the voluminous corrosion product.

A second mechanism appeared to be at work in the neutral solution G. The corrosion process appeared to start under the coating and manifest itself in local action cells which grew into pits. To have local cells beneath the coating, an electrolyte must be present. If a soluble salt residue were on the surface of the steel, it could draw water to it. The water in turn could combine with the salt forming an electrolyte and initiating corrosion. Indeed, it has been found with paints over steel that failure of the paint was related to ferrous sulfate and chloride residues beneath the surface.²⁴

A third mechanism whereby the corrosion process can begin under the coating results from permeation of aggressive ions through the coating. Much work has been done to confirm the diffusion of ions through organic coatings^{25,26} and define the factors which in-

fluence their transfer.^{27,28} Once the ions and water reach the steel surface, the electrolyte requirements are satisfied and a corrosion cell can be formed beneath the coating.

A fourth mechanism comes into play when the local action cell proceeds sufficiently to generate enough corrosion product to rupture the fragile coating of the floodant. The corrosion mechanism may now change strictly to that of differential aeration. A difference will exist between the oxygen level in the corrosion product in contact with the bulk electrolyte and that under the coating. The oxygen starved areas beneath the coating become anodic, and the corrosion rate is accelerated.

It should be pointed out that black plate steel contains all the requirements for anodic and cathodic areas on its surface. During the production of low carbon steel, a microstructure is created which consists of iron carbides in a ferrite matrix. In the presence of an electrolyte, the ferrite regions are anodic and therefore corrode releasing metal ions. If enough ferric ions accumulate in the electrolyte, they can actively participate in the corrosion process by being reduced to ferrous ions.

An interesting phenomenon occurred with bare and coated black plate steels in acidic solution C. As shown in Figure 5, the bare steel became anodic and corroded preferentially to the aluminum. When only the bare edge was exposed on coated samples, the steel remained the cathode. This would tend to indicate fundamental differences between the surface and edges of a metal coupon. A similar observation was made in Part I for bare versus coated aluminum. These differences were explained in terms of the energy states of the exposed areas. For example, slit edges, having been stressed, are at a higher energy level as compared to flat surfaces and are therefore less resistant to corrosion. It appears that in the case of black plate steel, these differences could be due to impurities on the surface.

Plastic Coatings on Tin Plated Steel

The behavior of the plastic clad tin plated steel in the corrosive environments is quite complex in that the tin plate is a protective coating for the steel. At the edge, the tin and steel are exposed to the aerated aqueous solutions. The steel corrodes because of the bimetallic couple. This preserves the integrity of the tin plate which, in turn, allows the bond of tin and adhesive copolymer coating to be retained. The tin plated steel surface is also less prone to the formation of local action cells under the coating. However, tin plate coatings are very thin and naturally porous. It is therefore necessary to utilize an adhesive copolymer coating with its chemical bond and high mechanical strength to prevent the underfilm corrosion processes to which the flooded steels are prone.

Practical Considerations

For buried cables, it can be expected that the sheath will be subject to damage from mechanical sources, rodents, and lightning. Every point at which damage occurs becomes a potential shield corrosion problem by allowing the entry of soil water. The presence of filler and floodant in filled cable will tend to localize the soil water at the damage site. If bare metals coated with filler or floodant are used in the sheath, these coatings cannot be expected to provide corrosion protection. They are unable to resist destruction by abrasion or corrosion processes. In fact, as discussed previously, the coatings may accelerate corrosion. Unfortunately, the direction in which the accelerated corrosion can take place, especially in corrugated shield designs, is the circumferential direction. (This is due to the fact that the coating is thinnest on the crests of the corrugations which extend circumferentially around the cable.) This is the most undesirable direction for corrosion to propagate. A break in longitudinal conductivity of the shield will destroy its protective electrical functions. Therefore, suitable corrosion protection must be provided to the shield to limit corrosive attack at the point of sheath damage. In the case of the steel/aluminum sheath designs, the additional factor of galvanic corrosion must be considered. The test data indicate that these requirements for corrosion control can be met through the use of adhesive plastic coatings.

The performance of a cable utilizing bare aluminum coated with filling compound was recently reported as part of the six year data from the joint soil burial studies conducted by the National Bureau of Standards and the Rural Electrification Administration.²⁹ This system, in both Site C, the acidic clay soil, and Site G, the neutral tidal marsh soil, was completely destroyed after 3 years of burial. Bare aluminum actually out-performed the flooded aluminum in these sites while plastic coated aluminum significantly out-performed the bare aluminum in the neutral Site G. These results tend to support the corrosion behavior described herein for flooded aluminum systems in that the flooded aluminum exhibited an accelerated rate of corrosion.

As shown in Figure 3, there is some slowing of the corrosion process when the floodant coating is 15 mils or more in thickness. However, to prevent circumferential corrosion, this thickness must be maintained over the crest of the corrugation. From the cable manufacturing standpoint, it is impractical to provide or maintain such heavy coverage of the shield. Examination of commercial and experimental cables in our laboratory has shown that the floodant coating is so thin on the crests as to be practically nonexistent. Moreover, whether thick or thin, floodant coatings are soft, fragile, and lack abrasion resistance. Damage to the sheath will physically remove or thin the coating irrespective of thickness. If cable diameter were increased to accommodate ultra-thick coatings, this would

adversely affect the economics. At the same time, the ability of the cable to resist jacket slippage would be reduced.

Conclusions

1. The potential for corrosion exists in buried, filled cables in spite of the use of water blocking materials over the metallic components of the sheath. Coatings used to provide corrosion protection to metallic shielding and armoring materials require adhesive and mechanical properties that can resist the forces generated during the corrosion process by volume changes, hydrogen evolution, and the growth of corrosion products under the coating. Mechanically tough, adhesive copolymer coatings which develop chemical bonding to the metallic components provide these properties. Coatings based on the floodant and filler compositions tested do not.
2. The mechanism observed for bare aluminum coated with a flooding compound appeared to be anodic undermining corrosion. This can be described as a form of crevice corrosion in which the anodic area occurs between the bare metal and the detached coating above this metal at the advancing edge of the corrosion process.
3. Several corrosion mechanisms were noted for flooded steel. Cathodic disbondment appeared to initiate anywhere bare metal was exposed. Other corrosion processes appeared to initiate beneath the coating. When the corrosion products generated by these processes grew to the point where the coating was ruptured, differential aeration appeared to be the dominating corrosion mechanism.
4. The potential for accelerated galvanic corrosion exists in couples of flooded aluminum and flooded steel. Galvanic corrosion of the aluminum due to the dissimilar metals, anodic undermining corrosion of the aluminum, and cathodic disbondment of the steel all occur simultaneously.
5. In the flooded aluminum and black plate couples, the steel normally is the cathode and accelerates the corrosive attack of the aluminum. Under certain limited circumstances, the steel can become anodic. This behavior appears to have no practical significance.
6. As the resistance of the coating to the diffusion of water and oxygen was improved through compositional changes and/or increased thickness, the intensity of the corrosive attack on the aluminum increased. This is because the corrosion mechanism at work obtains its driving force from relative differences in the concentrations of ions and oxygen. The destruction of the floodant

coating by the corrosion process aids in establishing these differences. No accelerated effect was noted with adhesive copolymer coatings since they retain their mechanical properties.

7. The studies of coated metal systems by electrochemical test methods are more complex than that of bare metal systems. However, these methods do appear useful for determining the degree of corrosion protection provided by coatings when relatively long term tests are undertaken.

References

1. T. S. Choo, "Corrosion Studies on Shielding Materials for Underground Telephone Cables, Part I: Development of Test Methodology," 24th International Wire and Cable Symposium, 1975.
2. G. A. Lohs and M. Romanoff, "Corrosion Evaluation of Shielding Materials for Direct Burial Telephone Cables," 17th International Wire and Cable Symposium, 1968.
3. G. A. Lohs and M. Romanoff, "Progress Report on Corrosion Evaluation of Shielding Materials for Direct Burial Telephone Cables," 18th International Wire and Cable Symposium, 1969.
4. W. F. Gerhold, J. P. McCann, and W. E. Williamson, "Report on Corrosion of Underground Telephone Cable Shielding Materials in Soil Environments after Exposure for Four Years," Paper No. 87, National Association of Corrosion Engineers, Chicago, Illinois, March, 1974.
5. W. F. Gerhold, J. P. McCann, "Corrosion Evaluation of Underground Telephone Cable Shielding Materials," Paper No. 31, National Association of Corrosion Engineers, Houston, Tx., 1976.
6. *Ibid.*, p. 31/26.
7. H. H. Uhlig, Corrosion and Corrosion Control, John Wiley & Sons, Inc., New York, 1963, p. 287.
8. Recommended Practice, Control of External Corrosion on Underground or Submerged Metallic Piping Systems, National Association of Corrosion Engineers Standard (RP-01-69).
9. Reference No. 5, pp. 31/28, 31/29, 31/32.
10. R. C. Brooks, J. D. Kirk, D. G. Saul, "Progress and Pitfalls of Rural Buried Cable," 18th International Wire and Cable Symposium, 1962.
11. C. R. Ballard, P. M. Emmons, "Engineering and Material Considerations in Buried Plant," 11th International Wire and Cable Symposium, 1962.
12. C. L. Cox, L. Jachimowicz, I. Kolodny, and H. Pulliam, "Improved Telephone Cable Sheathing," presented at the National Electronics Conference, Conference Paper

No. 68CP532-COM, December, 1968.

13. G. Schick, "Effect of Inhibitors on Aluminum Shield in Telephone Cable Sheaths," 28th Conference of National Association of Corrosion Engineers, Paper No. 107, St. Louis, Missouri, 1972.
14. G. Schick, "Corrosion Inhibitor Studies on Aluminum," Paper No. 67, National Association of Corrosion Engineers, Chicago, Illinois, 1974.
15. J. J. Kaufman, T. E. Luisi, "Evaluation of Adhesive and Cohesive Characteristics of Petrolatum Based Flooding Compounds," 24th International Wire and Cable Symposium, 1975.
16. K. E. Bow, T. S. Choo, T. H. Lyon, "A Review of Corrosion Protection for Shields in Buried Telephone Cable," Private Communication, 1973.
17. K. E. Bow, T. S. Choo, "Corrosion Resistance of Plastic Clad Aluminum for Cable Shielding," Paper No. 88, National Association of Corrosion Engineers, Chicago, Illinois, 1974.
18. G. E. Clock, G. A. Klumb, R. C. Mildner, "Adhesive Thermoplastic Copolymers for the Wire and Cable Industry," 12th International Wire and Cable Symposium, 1963.
19. H. P. Godard, W. B. Jepson, M. R. Bothwell, R. L. Kane, The Corrosion of Light Metals, John Wiley & Sons, Inc., New York, 1967, p. 51.
20. E. L. Koehler, "Corrosion Under Organic Coatings," National Association of Corrosion Engineers, presented at the U. R. Evans International Conference on Localized Corrosion, Williamsburg, Va., 1971.
21. E. Schaschl and G. A. Marsh, "Some New Views on Soil Corrosion," Materials Protection, Vol. 2, No. 11, p. 8.
22. H. G. Frank, M. C. McGaugh, and W. E. Ropp, "A Study of the Effect of Time, Temperature, and Moisture on Bonded Interfaces in 'Bonded Jacket' Cable Constructions," 17th International Wire and Cable Symposium, 1968.
23. Reference No. 12, p. 4.
24. U. R. Evans, Corrosion and Oxidation of Metals, St. Martin's Press, New York, 1960.
25. C. A. Kumins and A. London, J. Polymer Science, Vol. 46, 395, 1960.
26. G. Menges, W. Schneider, "Which Service Life Can Be Expected from Plastics-Metal Composites Attacked by Aggressive Media," 31st Annual Technical Conference, Society of Plastic Engineers, Montreal, Quebec, Canada, 1973.
27. W. W. Kittleberger and A. C. Elm, Ind. & Eng. Chem., Vol. 44, 326, 1952.
28. B. D. Craig, D. L. Olson, "Corrosion at a Holiday in an Organic Coated-Metal Substrate System," Corrosion, Vol. 32, No. 8, August, 1976.
29. Reference No. 5, pp. 31/17, 31/44, 31/60.

Acknowledgements

The authors wish to thank S. Kottie, G. D. Schwank, and B. H. Brooks for their helpful suggestions, W. G. Lewis and D. O. Plunkett for the experimental work, and M. Black and J. Jackson for typing.

Biographies



L. G. (Les) Colter is a Research Engineer in the Specialty Products R&D Laboratory, Olefin Plastics Department, Dow Chemical U.S.A. He is an active member of the National Association of Corrosion Engineers and is vice-chairman of the task group, T-10-C3, on Corrosion of Lead and Other Metallic Sheaths. He is also a member of the teaching staff of the Appalachian Underground Corrosion Short Course held annually at West Virginia University. Mr. Colter received a B.S. (1972) and M.S. (1974) in Metallurgical Engineering from the University of Texas at El Paso.



K. E. (Ken) Bow is a Senior Research Engineer in the Specialty Products R&D Laboratory, Olefin Plastics Department, Dow Chemical U.S.A. He is a member of the Institute of Electrical and Electronic Engineers, the Wire Association International, the Society of Plastics Engineers, and the National Association of Corrosion Engineers. Mr. Bow received his B.S. in Electrical Engineering from Michigan State University (1962).

M. Azuma, Y. Oishi, K. Fuse and M. Oda

The Furukawa Electric Co., Ltd., Tokyo, JAPAN

Summary

Development of Gas-stoppage Dam, which forms a very important part of gas pressurized telephone cable system, has been tried by a completely new manufacturing process, that is, polyethylene molding.

The point of the development is to obtain complete packing in a mold containing very sophisticated inserts without any contact between conductors.

Gas-stoppage dams in the form of polyethylene blocks as large as about 120mm are successfully commercialized by this method.

I. Introduction

The gas pressurized system of telephone cables in Japan has contributed greatly to the reliability of telephone services. This system is shown schematically in Fig. 1. The main features of this system are the gas supplying equipment, gas pressure monitoring system and gas-stoppage dam. As shown in Fig. 1, the gas-stoppage dam is installed at the boundary point between the feeder cable and distribution cable. Multipairs insulated by color coded polyethylene are used for the distribution cable and local paper-insulated stalpeth cable for the feeder.

In the conventional type of gas-stoppage dam, a process of injecting epoxy resin into the lead sleeve and curing at laying site has been used, but complete gastightness could not be achieved by the following defects. 1). 2).

- (1) Cracking or void formation due to temperature change or vibration during the curing process of epoxy resin.

- (2) Cracking due to the difference of thermal expansion of epoxy resin, insulator and lead sleeve.
- (3) Poor adhesive property of epoxy resin to polyethylene.
- (4) Ununiformity of thermal conductivity of epoxy resin during curing process.

Hence, when a gas-stoppage dam became defective due to these causes, it was necessary either to make another gas-stoppage dam or to replace the cable with the defective dam to a new one.

Therefore, increased reliability of gas-stoppage dams and reduction of labor cost in the field have been aimed at by developing a cable with a gas-stoppage dam in a pre-scribed position assembled in a factory with good working environment.

II. Approach to Production

A completely new process has been tried for the development of a cable with gas-stoppage dam, instead of improving conventional resins cured in room temperature such as epoxy resin.

Setting aside the formation of defects during the curing process, the most important problem of the gas pressurized system using epoxy resin is the gas leakage which occurs with time in the longitudinal direction of the cable, due to the poor adhesive property of epoxy resin to polyethylene.

The idea is that since the cable in which the gas-stoppage dam is to be made is multipair color corded polyethylene (polyethylene insulated and stalpeth sheathed) cable, higher

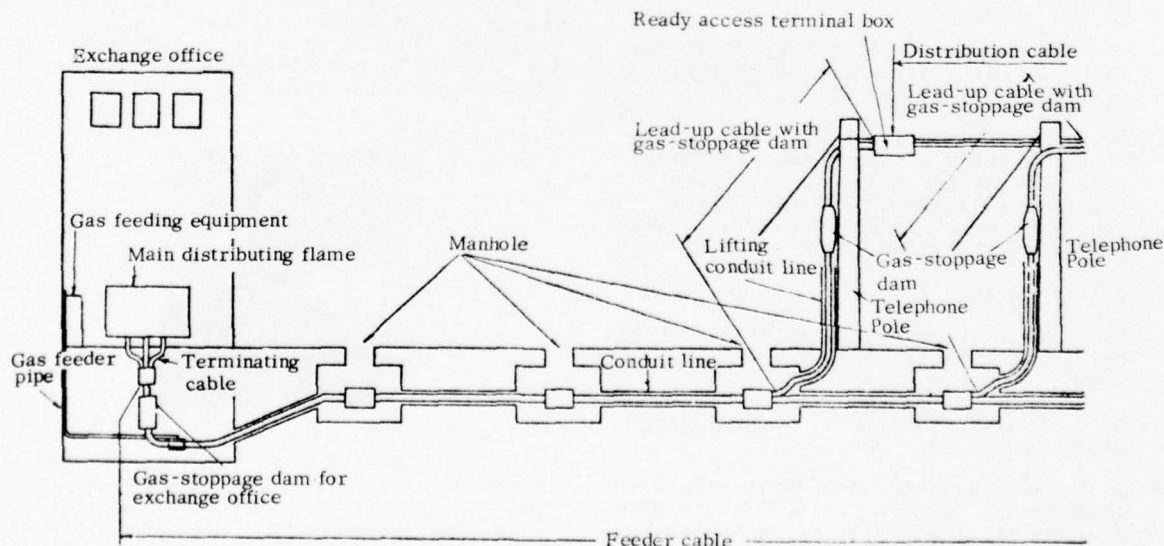


Fig. 1 Gas Pressurized System for City Cable

gastightness must be obtained by molding the gas-stoppage dam with plastic material of the similar property as the cable insulator and sheath.

It is reported that the process of molding polyethylene into a cut-open portion of cables was used for submarine coaxial cable junctions.

However, there has been no precedent reports of molding thermoplastic substance like polyethylene instead of room-temperature cured resin into a cable, which consists of sophisticated inserts such as a group of 800 - 2400 insulated conductors, steel tapes and sheath.

Viewing from general plastic molding technology, it may safely be said that there are few plastic products more than 100mm thick. Some molded products such as plastic containers, bath tubs and so on are so bulky but their wall thickness is several tens of millimeters at most.

Furthermore these molded goods are completely enclosed in the molding process.

On the other hand, our molding cannot be completely enclosed since the part of the cable where the gas-stoppage dam is to be made is connected to the outer environment in the longitudinal direction through the cable core.

Hence, different mold configuration and molding technique are required.

Since the gas-stoppage dam should not degrade the function of the telephone cable, we must pay careful attention to maintain conductor insulation during the molding process. This imposes a temperature restriction on the process.

III. Design and Manufacture

If it is possible to construct a gas-stoppage dam based on the similar properties between polyethylenes, much better gastightness than epoxy resin must be achieved.

However, as mentioned before, a great number of technical difficulties were found in the process of molding polyethylene into a cut-open portion of mutipair cable.

III-1 Filling Compounds and Insulation Materials

The properties required for the filling compound used to form the gas-stoppage dam are: the mechanical properties fundamental to the gas-stoppage dam; fluidity enough to penetrate into the all insulated conductors to ensure complete gastightness; and strong adhesiveness to insulators.

On the other hand, insulation materials must have good heat resistance which can withstand the injection temperature during the polyethylene molding process.

Certain special compounds which can satisfy the requirements described above have been obtained as a result of investigations of fundamental properties of every obtainable kinds of polyethylene including blended matrices. During this research work, heat resistance and adhesiveness of insulators and the adhesiveness between insulators and conductors were also studied, reaching the optimal solution.

III-2 Molding

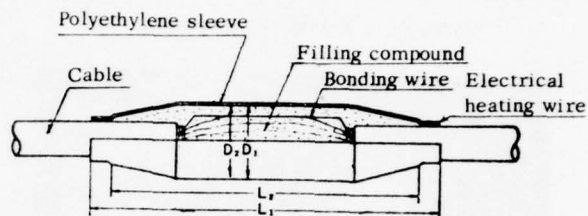
When a gas-stoppage dam is to be manufactured, there are three important factors: form of the cut-open portion of the cable, mold configuration and molding methods (Careful selection of filling compounds and insulation materials is of course essential.). The processing of the cut-open portion involves cutting the sheath open, removing the binding tapes untying the bundle and inserting a spacer of the same material as the filling compound to facilitate filling injection.

A special mold and cooling process is employed since the mold is open type unlike the shut-tight mold of usual plastic molding.

The resin injection gate is so designed that the resin can be injected completely and uniformly around the insulation conductors.

Furthermore, it is well known that various problems generally arise during the processing of this kind of plastic molding and our gas-stoppage dam processing is no exception.

However, a simple application of the usual molding technique has been found to be quite inadequate for filling polyethylene around such a large group of insulated conductors, in order to get complete gastightness and other necessary properties for gas-stoppage dams.



	Total dimension		Dam dimension	
	L1(mm)	D1(mm)	L2(mm)	D2(mm)
400P	480	85	410	80
800P	500	105	430	100
1200P	520	125	450	120

Fig. 2 Dam Structure

Therefore, "flow molding" technology has been studied and complete gas-stoppage dams in any part of the cable have been made possible, by the development of the following molding process: preheating of the cable - resin injection - first stage pressuring - second stage pressuring - cooling.

Photo.1 shows the entire gas-stoppage dam manufactured as the result of this technical development. Fig. 2 shows its dimension: 120mm diameter for 1200 pair cable. Photo.2 shows a cross-sectional view of the gas-stoppage dam, in which very uniform dispersion of 2400 insulated



Photo. 1 Dam structure

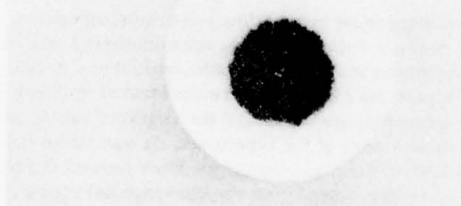


Photo. 2 Cross-sectional view of Dam

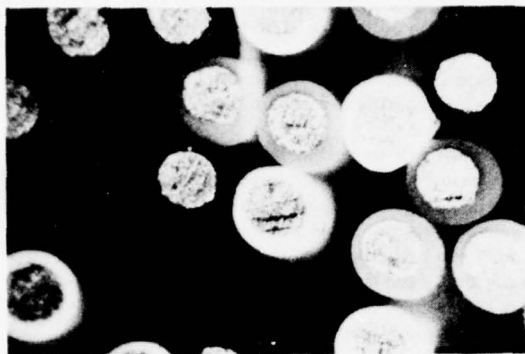


Photo. 3 Enlarged microscopic view

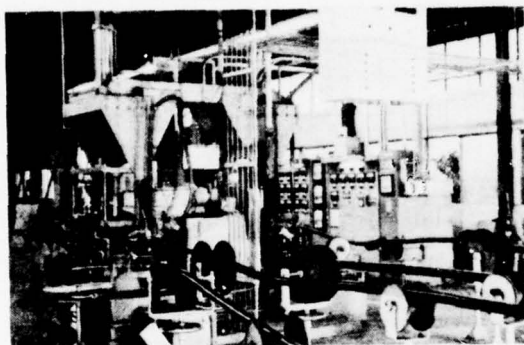


Photo. 4 Molding Equipment

conductors can be seen. Photo. 3 shows an enlarged microscopic view of this part: complete dispersion of the filling compound in the quad can be seen. Photo. 4 shows the gas-stoppage dam manufacturing equipment which is used by us in practise. Since this extruder has a rotating head, enabling alternative filling of two molds, one may be preheated during the cooling period of the other. Temperature control of the molds and the extruder is possible from a central controle panel.

Presently, completely automatic control of the whole molding process by computer is under study, intending to reduce molding faults due to human error in the operation and increase the reliability of gas-stoppage dams.

In addition, completely gastight dams for plastic insulated stalpeth cable (full size; 0.32mm x 3600 pairs) has been achieved by the same process as described above.

The cables with gas-stoppage dams manufactured by this method are wound onto drums, with mean cable length of about 30m, for shipment.

IV. Properties of Polyethylene-Molded Gas-stoppage Dams

In stead of improving conventional gas-stoppage dams using epoxy resin, a completely new manufacturing process, that is, polyethylene molding, has been studied and developed. A series of type tests (Table 1) were performed to check whether the gas-stoppage dams had the required functions. Photo. 5-6 show a part of the type tests. It was found that the polyethylene-molded gas-stoppage dams passed the test completely and were superior to the conventional epoxy resin type processed in the field.

Table 1 Testing Items of Lead-up Cable with gas-stoppage dam

Testing Items	Test Conditions	Test Results	Remarks
Heat Cycle Test	(1) Temperature: -30°C - $+70^{\circ}\text{C}$ Internal temperature of dam is held at -30°C and $+70^{\circ}\text{C}$ for 30 min. (2) Gas pressure: Gas corresponding to 700 g/cm^2 (at -30°C) is enclosed. (3) Test piece: 50cm + Dam + 50cm (4) Number of cycles: 100 cycles	No gas leakage at 100 cycles	Example of gas pressure: Initial: 700 g/cm^2 Final: 695 g/cm^2 Measured at -30°C
Vibration Test	(1) Amplitude of vibration: $\pm 10\text{mm}$ (2) Number of vibration: 600 rpm (3) Test piece: same as above (4) Part where vibration is excited: Dam center (one end fixed, the other end half fixed) (5) Number of cycles: 1,000,000 times (6) Gas pressure: same as above	No gas leakage in 1,000,000 cycles	Example of gas pressure: Initial: 1.05 kg/cm^2 Final: 1.04 kg/cm^2 Measured at normal temperature
Low Temperature Test	(1) Test piece: samples after 50 cycles of temperature cycle test (2) Temperature cycle: -30°C - $+70^{\circ}\text{C}$ as one cycle (3) Vibration test: 100,000 times (4) Number of tests: 5 cycles taking (2) + (3) as one cycle (5) Gas pressure: same as above	No gas leakage in 5 cycles	Example of gas pressure: Initial: 1.05 kg/cm^2 Final: 1.03 kg/cm^2 Measured at normal temperature
Static Load Test	(1) Load: 0.4 kg - 400 kg 0.4 kg - 1200 kg (2) End: using a pulling eye (3) Gas pressure: same as above	Normal after 2 years	Example of gas pressure: Initial: 1.05 kg/cm^2 Final: 1.04 kg/cm^2 Measured at normal temperature
Impact Test (A)	(1) Test piece: 50cm + Dam + 50cm (2) Height: natural falling from a height of 2.5m (3) Gas pressure: same as above (4) Temperature: normal temperature	No abnormality found in appearance or gas pressure	Example of checking gas pressure: Initial: 1.05 kg/cm^2 Time length of the test: 24 hours Final: 1.06 kg/cm^2
Impact Test (B)	(1) Load: 2.2 kg iron lump (2) Height: Falling from the height of 5 m (3) Gas pressure: same as above (4) Temperature: Normal temperature	No abnormality found in gas pressure or appearance	Example of checking gas pressure: Initial: 1.05 kg/cm^2 Time length of the test: 2 hours Final: 1.04 kg/cm^2
Bending Test	(1) Test piece: 1m + Dam + indeterminate part (2) Bending angle: 1200 kg $\pm 45^{\circ}$ 600 kg $\pm 90^{\circ}$ (3) Gas pressure: same as above (4) Fixing point: 1/6 of the dam length (5) Number of bendings: 5 each way (6) Temperature: Normal temperature	No abnormality found in gas pressure or appearance	Example of checking gas pressure: Initial: 1.05 kg/cm^2 Time length of the test: 24 hours Final: 1.04 kg/cm^2 Measured at normal temperature
Tension Test	(1) Test piece: 50cm + Dam + 50cm (2) End: Wire net (3) Tension speed: 100 mm/min (4) Max. tension: up to 500 kg (5) Gas pressure: same as above	No abnormality found in gas pressure up to the tension of 500 kg No abnormality found in the appearance of dams	Example of gas pressure: Initial: 1.05 kg/cm^2 Tension of gas leakage start: 550 kg



Photo. 5 Impact test

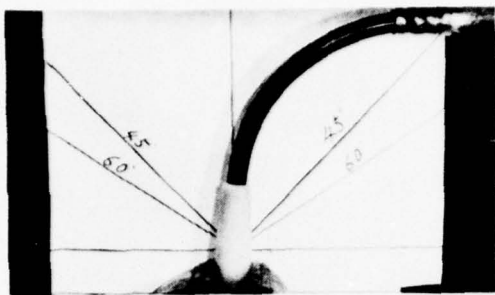


Photo. 6 Bending test

As another type test, a low temperature impact test was performed, confirming that the properties are almost equal to those of the cable sheath.

For a severer outdoor exposure test, a gas-stoppage dam under gas pressure and without a protecting cover has maintained excellent gastightness after more than 5 years' exposure. Gas-stoppage dams are now widely used in Japan. Eversince more than 35,000 gas-stoppage dams by this process have been supplied for commercial circuits, giving firm proof of their high reliability.

V. Conclusion

Production of the gas-stoppage dam, which occupies a very important role in telephone cables as a gas pressurized system, has been studied by a completely new manufacturing process, namely the polyethylene molding process and the following conclusions was obtained.

- (1) The utilization of strong adhesiveness between polyethylenes is very effective to solve the difficulties associated with the conventional epoxy resin.
- (2) A molded polyethylene products having very complicated inserts and thickness of more than 100mm has been commercialized successfully.
- (3) The cable with gas-stoppage dams developed by this method has been found to have very high reliability in practical application.

VI. Reference

- 1) N. Niimura, K. Ogawa, M. Watanabe,
Cable with gas-stoppage dam, Shisethu, Vol. 23,
No. 1
- 2) H. Fukutomi, K. Ogawa, J. Egashira,
Prefabricated Pressure Dam for Telephone Cable,
The 20th I.W.C.S.

(AUTHORS BIOGRAPHIES)



MASAO AZUMA

The Furukawa Electric
Co., Ltd.
6-1 Marunouchi, 2-Chome,
Chiyoda-ku, Tokyo,
Japan

Mr. Azuma graduated from Tokyo Institute of Technology with a B. SC. in chemical engineering in 1959. Then, he joined The Furukawa Electric Co., Ltd. and has been engaged in research and development of plastic materials and manufacturing methods for telephone cables. He is now a Manager of the Production Engineering Department of Telecommunication Division of The Furukawa Electric Co., Ltd., and a member of the Society of Polymer Science of Japan.



YOSHIAKI OISHI

The Furukawa Electric
Co., Ltd.
6-1 Marunouchi, 2-Chome,
Chiyoda-ku, Tokyo,
Japan

Mr. Oishi graduated from Kyoto Univ. in 1968 with a M. SC. degree in Petro chemical engineering. He joined The Furukawa Electric Co., Ltd. and has been engaged in research and development of plastic materials and manufacturing methods for telephone cables. He is now a Deputy Chief of the Production Engineering Department of Telecommunication Division of the Furukawa Electric Co., Ltd.



KENICHI FUSE

The Furukawa Electric
Co., Ltd.
6-1 Marunouchi, 2-Chome,
Chiyoda-ku, Tokyo,
Japan

Mr. Fuse graduated from Keio Univ. 1971 with a M. SC. degree in mechanical engineering. Then he joined The Furukawa Electric Co., Ltd. and has been engaged in research and development of plastic material and manufacturing methods for telephone cables. Mr. Fuse is now a member of the Material Research Department of Telecommunication Laboratory of The Furukawa Electric Co., Ltd. and a member of the Society of Rheology, Japan.



MIKIO ODA

The Furukawa Electric
Co., Ltd.
6-1 Marunouchi, 2-Chome,
Chiyoda-ku, Tokyo,
Japan

Mr. Oda graduated from Osaka Univ. with a B. SC. in chemical engineering in 1971. Then he joined The Furukawa Electric Co., Ltd. and has been engaged in research and development of plastic material and manufacturing methods for telephone cables. Mr. Oda is a member of the Production Engineering Department of Telecommunication Division of The Furukawa Electric Co., Ltd.

THE USE OF BLOWING AGENT CONCENTRATES IN THE MANUFACTURE OF TELECOMMUNICATIONS CABLES

BY: T.C. HODGSON, D.B. CAREFOOT, G.F. GOUTHRO (SANTECH INC. TORONTO) S.M. BEACH (PHILLIPS CABLES LTD. VANCOUVER)

SUMMARY

When Blowing Agent Concentrates are used in the proper extrusion equipment a cellular product can be made which compares well with the product which is being made with fully compounded materials.

Considerable savings are possible in raw material costs. Problems of pre-decomposition of the Blowing Agent are avoided and at the same time excellent dispersion and cell structure can be achieved.

The Wire & Cable manufacturer is given the ultimate in flexibility in choice of resin and foam density to suit any property particular to his end product.

This paper will discuss (1) The manufacture of non-plating blowing agent concentrates, (2) Quality control and analytical methods involved, (3) Choice of base resin, (4) Comparison of foam insulation properties using the concentrate method and the fully compounded method.

INTRODUCTION AND DISCUSSION

The use of foamed insulation in place of solid polyethylene or polypropylene has been popular in Canada, parts of Europe and Japan for 5-10 years. More recently foamed insulation has made its appearance in the United States. Not only does the foam use less resin as would be expected but since the capacitance of the foam more nearly approaches the ideal, i.e. that of air, a smaller diameter insulation is used. Telephone distribution cables can be smaller, lighter or more pairs can be used in a given bundle. The usual method of manufacture is to extrude the insulation from a full letdown of blowing agent i.e. typically 0.5 to 1% azodicarbonamide in the polyethylene or polypropylene. Medium or high density polyethylene is used since lower densities suffer more from the problem of the cable filler entering the cells. Unless a special cable filler is used which prevents cell filling high density polyethylene or polypropylene is used.

One difficulty of this is that the high density polyethylene and polypropylene process at temperatures above the start of decomposition of the blowing agent. Therefore preparation of the "full-letdown" resin is very difficult for the resin supplier who must prevent pre-decomposition taking place. A full let-down resin can only be used to produce foams in a narrow range of densities. In some cases considerably different densities are required.

An alternative method which will be discussed in this paper is to use a concentrate of the blowing agent with a natural resin. Colour can be added as a concentrate as is the usual practice today.

The second stage of this work involves the addition of colour-blowing agent multi-pellets. Thus the colour and blowing agent are added from the metering device at one time in one pellet. This method makes the concentrate system as simple to use as the present one.

It will be shown how the concentrate method gives control of foam density, prevents premature decomposition of the blowing agent, provides a lower cost insulation, allows the processor a choice of base resin and allows more than one density of foam to be produced. Physical and electrical properties of the insulation can be produced on suitable process equipment in the manufacturing facility.

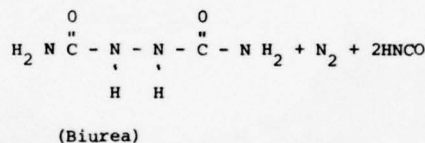
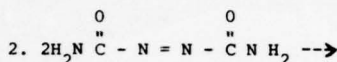
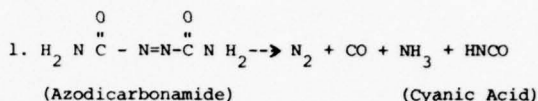
MANUFACTURE OF THE CONCENTRATE

The most commonly used blowing agents are the non-plating azodicarbonamides. These have been described by Roulstone et al. They contain a filler which releases water at decomposition temperature.

NON PLATING AZODICARBONAMIDE

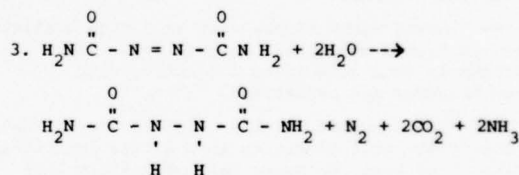
Suggested decomposition mechanism is as follows.

There are three probable reactions.

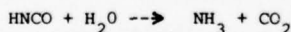


The Biurea may lose ammonia to form a urazole

In the presence of acid or base at high temperatures azodicarbonamide can hydrolyse as follows.

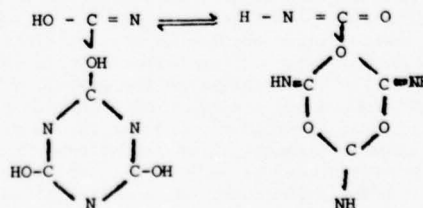


The cyanic acid from 1 or 2 may react with water as follows:



UNTREATED AZODICARBONAMIDE

In this case the Cyanic acid trimerises to cyanuric acid, and isocyanic acid to cyamelide. The equilibrium may be represented by:-



The cyanuric acid forms a white plateout on the extruder screw and die. This results in increased head pressure and greater variance in extrudate diameter. Capacitance can also be affected.

A method of making the cyanuric acid soluble in these polymers to prevent plateout has been reported by Yanagisawa et al. That method may well be suitable for the concentrate system although at this time our work has been only concerned with the treated azodicarbonamides.



Fig. 1 Effect of Volatiles on Concentrate

Figure 1 illustrates pellets of the concentrate which are controlled for volatiles compared with uncontrolled compound.

The blowing agent is prepared as a high quality dispersion from a compatible polymer base. This dispersion is then reduced to 20% active with polymer, extruded and pelletized.

Care must be taken at this point to ensure that the concentrate melt viscosity is a little lower than the final host resin to be certain of uniform let-down and dispersion. This whole process is done at temperatures below 150°C. Since the blowing agents begin to decompose at approx 170°C, no predecomposition occurs during this process.

When compounding colour with blowing agent the procedure is identical to ensure ultimate let-down and dispersion of the colour as well.

QUALITY CONTROL OF THE DISPERSION

After preparation, samples of the concentrate are tested for gas yield and activation temperature on an instrument known as a Cell-U-Corder[®]. In this instrument a sample of foamable polymer is loaded into a sealed mixing chamber at a temperature below initial decomposition. The temperature is then programmed to 220°C, during which the polymer viscosity, and melt temperature are measured. The gas produced by the blowing agent in the polymer is led from the mixing chamber through a mass-flowmeter. There an accurate measurement is made of gas evolution rate and this information recorded on a travelling chart. A totaliser is used to count the total volume of gas evolved.

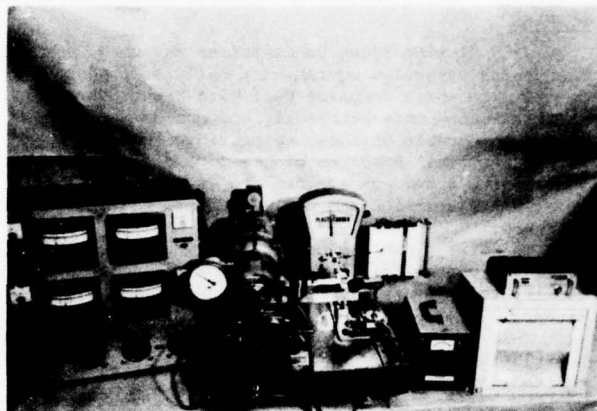


Fig. 2. The equipment used in the Quality Control Procedure.

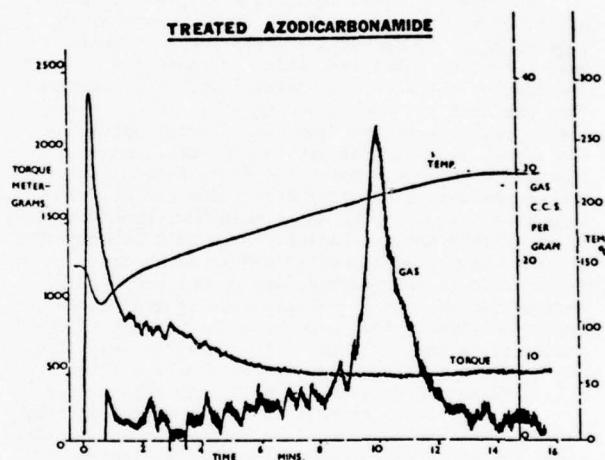


Fig. 3 Non Plating Azodicarbonamide in Polyethylene

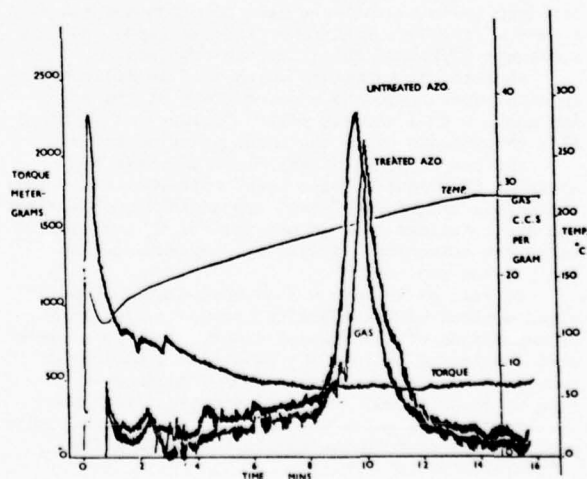


Fig. 4 Comparison of Regular and Treated Azodicarbonamide

Figure 4 shows there is a slight difference between treated and untreated Azodicarbonamide. It should be noted that the treated material is only about 65% active ingredient. It is suspected that in the treated version some gas comes from the breakdown of the cyanic acid to NH_3 and CO_2 . It will be appreciated that this instrument can be used to show if any predecomposition has occurred or if the incorrect quantity of active ingredient has been used.

CHOICE OF RESIN

The concentrate method does allow some choice in final insulation resin. If the electrical requirements can be met and the resin can tolerate speeds of 5000 ft/min., then the next step is to run a viscosity check to make sure the resin is similar to present commercial products.

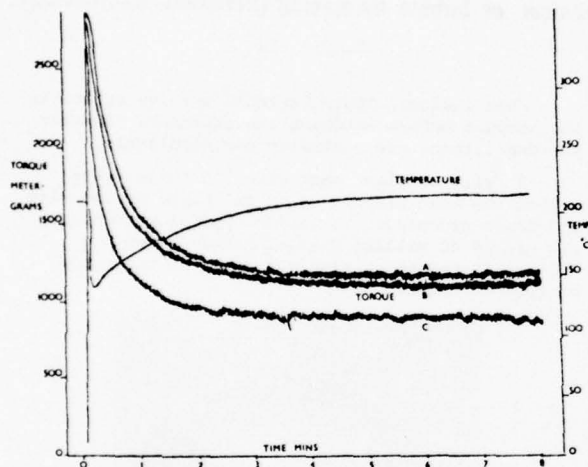


Fig. 5 Viscosity Comparison of Three Resins.

Samples of foamed extrudate are made from resins that show promise at this stage. It has been found that a Brabender 3/4" lab extruder can be successfully used to evaluate resin and blowing agent or colour concentrates. Using the current commercial "full letdown" resin as reference, samples are run through a 1/8" diam. rod die. Thin slices or microtomed sections of the foam are then examined under a microscope. Particular attention being paid to cell size and uniformity. The number of breaks are noted.

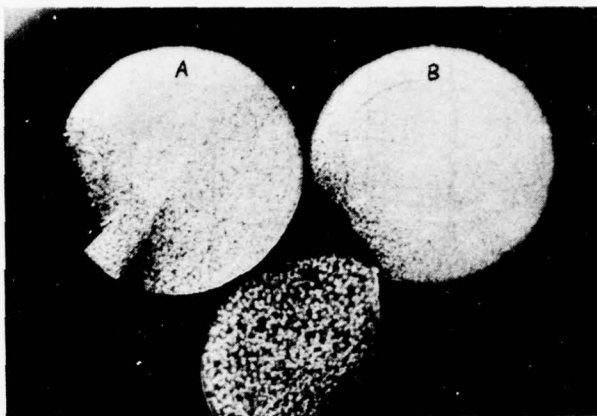


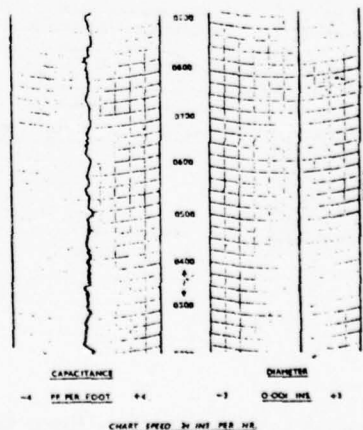
Fig. 6 Foam Quality with different Resins

Resin "A" is a current commercial foamable resin. "B" is a similar resin with the concentrate added. "C" is a different resin with the concentrate which is unlikely to be suitable for this type of insulation, e.g. this resin may have an unsuitable melt viscosity at blowing agent decomposition temperatures. Resins that have been successful usually show a high melt strength in the decomposition range (see fig. 5).

METHODS OF USE

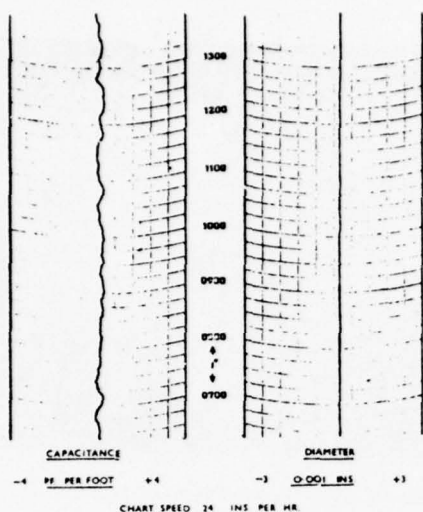
The usual practice heretofore in the telephone industry for cellular polyethylene insulation has been the use of a fully letdown blowing agent in resin without colour. The colour is added in the form of a masterbatch at the feed zone of the extruder producing the insulation. The insulation usually contains about 30-35% void.

Telephone singles are now being produced using the blowing agent colour masterbatch in the range of 30 to 60% void. With satisfactory temperature and mixing control during processing the product so produced compares very well with the full letdown system. Existing two component metering devices such as the Wilson colormeter* can be successfully used to feed this masterbatch.



Commercial resin with colour/blowing agent concentrate. Approx. 40% void.

Figure 7.

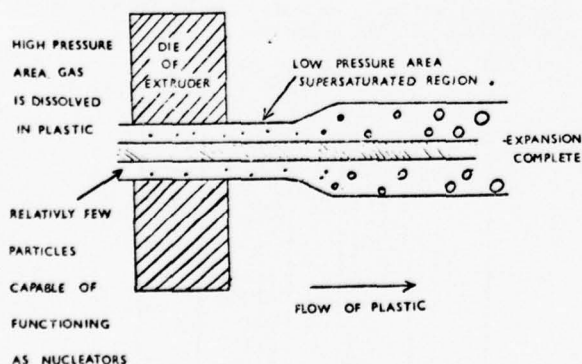


'Full letdown resin'
Insulation with approx. 40% void.

Figure 8.

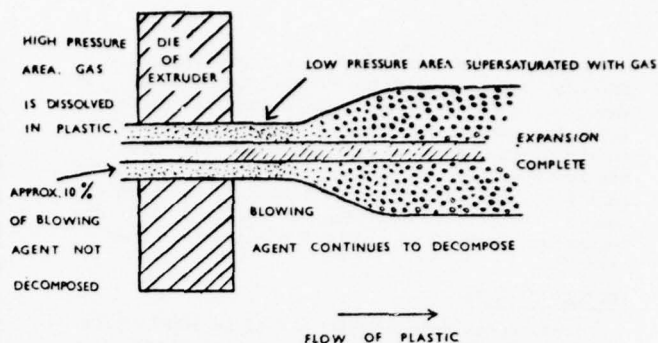
Competitive forces which will always be our lot have clearly indicated that the higher levels of blow are desired. To obtain these higher levels certain alterations in resin viscosity may be required but certainly higher levels of blowing agent must be used. In attempts to reach 60% void via the full letdown technique one difficulty has been the presence of preblow. This affects the cell nucleation and causes poor cell structure.

In order to produce a fine cell structure it is accepted that cell formation should occur between the exit die and the water/wire interface in the mobile cooling trough. Approximately 90% of the blowing agent should be decomposed in the extruder head and the gas remain in solution in the polymer. The remaining 10% decomposes as the material leaves the die creating "hot spots" which provide sites for nucleation.



Mechanism of bubble formation (poor nucleation).

FIGURE 9



Mechanism of bubble formation (efficient nucleation).

Figure 10.

When indiscriminate variable preblow exists in the product before entering the extruder, diameter and capacitance are virtually uncontrollable.

It will be clear that with the concentrate method the heat history is in the hands of the wire and cable processor. A recent typical concentrate run was of 40 million feet of highly blown (60% void) telephone single for use in the manufacture of DUCTCEL[®].

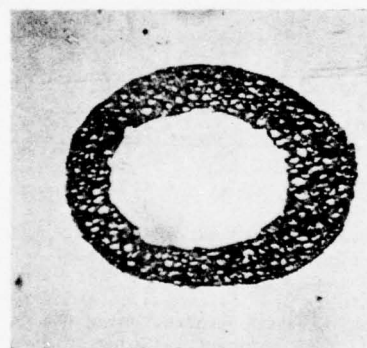


Figure 11. Sample of the 55% Void Insulation

At the 35% void level the concentrate method gives virtually no change in physical properties. It will be recognized that as the percentage void increases physical properties of the insulation change. The overall insulation diameter decreases. The fragility of the insulation sleeve increases and the tensile and elongation decrease.

Whether the full cost saving of this 55% void type can be utilized depends on the particular processor and the market he must satisfy. It is his choice to obtain the degree of blow that is technically and commercially acceptable to him.

	DUCTCEL		CELSEAL		CELSEAL	
TYPE	CONC. TYPE		FULLY COMPOUNDED		CONC. TYPE	
COLOUR	RED		ORANGE		WHITE	
% VOID	55		31		35	
GAUGE NO.	22		24		19	
INS. PER MIN.	20	2	20	2	20	2
GAUGE LENGTH	1"	1"	1"	1"	1"	1"
INS. ELONG.	1.6	1.6	2.8	2.8	3.6	3.9
O.D.	0.0397	0.0397	0.0347	0.0347	0.0620	0.0620
I.D.	0.0251	0.0251	0.0200	0.0200	0.0358	0.0358
AREA	0.00074	0.00074	0.00063	0.00063	0.00201	0.00201
LBS.	1.09	1.09	1.47	1.40	4.04	4.03
TENSILE LBS./SQ. INS.	1470	1470	2330	2220	2010	2000
% ELONG.	160	160	280	280	360	390

Figure 12 Physical Properties

CONCLUSION

When proper care is taken to control volatiles and attention is paid to ultimate dispersion, a concentrate can be produced which has been used in many millions of feet of telephone singles.

The concentrate can be controlled from batch to batch to ensure the correct amount of gas will be produced at the right temperature when it is required.

The wire and cable processor using suitable extrusion equipment and existing retreating facilities can produce high quality telephone singles, vary his base resin within certain limits and adjust insulation density to meet the needs of his market and at the same time obtain considerable cost advantages.



THOMAS C. HODGSON

Thomas C. Hodgson was born in Yorkshire, England in 1940. Educated at Constantine Poly-Technical College, Teesside. He spent 7 years in quality control and development labs at the Billingham and Wilton I.C.I. plants. The majority of this time he was involved in the analytical department of dystuffs division, in particular with Nylon 6:6 manufacture.

Emigrated to Canada in 1968 and joined Ware Chemical of Canada, later called Santech Inc.

Mr. Hodgson worked for sometime in product development and is presently responsible for the company's marketing efforts. He is located in Toronto, Ontario, Canada.



DONALD B. CAREFOOT

Donald B. Carefoot was born in Collingwood, Ontario in 1943. He was educated at Ryerson Polytechnical Institute of Technology in Toronto, in the polymer sciences.

He spent three years at Firestone Tire & Rubber Co. in Hamilton, Ontario, in quality control and development associated with the tire curing department.

In 1971 Mr. Carefoot joined Ware Chemical of Canada (later called Santech Inc.)

At present he is product development and quality control manager of Santech Inc., located in Toronto



EUGENE G. GOUTHRO

Eugene G. Gouthro was born in Toronto in 1954. Educated at Central Technical School.

Joined Santech Inc. in 1972 and is employed in product development.

Mr. Gouthro has completed courses in rubber and plastics technology.

He is a member of the Ontario Rubber Group and S.P.E.



S. M. (MIKE) BEACH

Mr. Beach was educated in Brockville, Ontario and has been employed by Phillips Cables Limited principally since 1936. He has been employed in both administrative and technical capacity relating to rubber and plastics technology and processing. During this period he has attended a number of courses provided by the industry related to the rubber and plastics industry.

REFERENCES

1. Canadian Patent No. 982804
Phillips Cables Ltd.,
2. British Patent No. 56562/72 Fisons Ltd.
3. Reed-Plastics Progress 1955
4. C.J. Benning Plastics Foams I and II (published
by Wiley & Sons)
5. Technology of Celogen Blowing Agents.
(Uniroyal Chemical Div.)
6. An Instrument for Analytical Control of the
Chemical Blowing of Cellular Polymers.
(Journal of Cellular Plastics Nov/Dec.1973)
7. Cellular Polyethylene for Telephone Cables -
J.J. Helbling & R.A. Houben - 31st annual S.P.I.
conference, Vancouver B.C.
8. Yanagisawa et. al. U.S. patent 3,882,209
(Furukawa Electric Co. Ltd.)

A NEW METHOD FOR RING COLOR CODING
OF PLASTIC INSULATED WIRES

by

Klaus Kimmich

STANDARD ELEKTRIK LORENZ AG (ITT)

Stuttgart, Germany

SUMMARY

The increasing use of plastic insulated cables with color ring marking and the production of plastic insulated wires with take-up speeds of 2000 m/min (6500 feet/min) or even more demand the introduction of very fast and economically operating marking equipment. A method is described, by which an electrically charged, colored ink jet is deflected by a high voltage electrical field. Deflection frequencies of more than 1500 cycles per second are possible. Furthermore a digital phase shifting method is demonstrated, by which the synchronisation of single and multi-ring marking is achieved. Finally a machine is presented, by which the described new technique is realised.

INTRODUCTION

Plastic insulated wires are marked with colored rings to allow an easy identification of the wires in a cable. Nowadays, it is possible to extrude plastic insulated wires with speeds far above 1000 m/min, while the actual production speed of color-ring marked wires is in most cases limited by the operating speed of the marking system.

The presently known methods, which allow a fast change between two different colors or marking codes, are limited to speeds much less than 1000 m/min. Other methods, which are running faster than 1000 m/min, will need an excessively long converting time and are normally to be used for rings of one color only. This situation led to the development of a new type of marking equipment, which had to fulfill the demands as follows:

Requirements:

- * Marking speed up to 2000 m/min for ring distance larger than 10 mm
- * time interval for the change of colors or marking code should be less than 20 seconds
- * universal application for different marking codes (e.g. single ring, double ring, twin color marking)
- * compactness of set-up; simplicity of control
- * low expense for maintenance

THE METHOD, ITS FUNCTION AND THEORETICAL BASE

The available methods for the ring marking of insulated wires have the common disadvantage of using a mechanically oscillating or rotating device. The mechanically oscillating system is limited by the oscillating mass while the rotating system with its high centrifugal forces causes a sedimentation of the color pigments, which leads to frequent blocking of the bore holes. In addition, the life time of rotating or oscillating machine parts decreases exponentially with increasing speed.

Therefore the research activities were directed towards a method, which eliminates the above mentioned disadvantages and allows the introduction of additional feature. The principle function of this method is demonstrated in fig. 1.

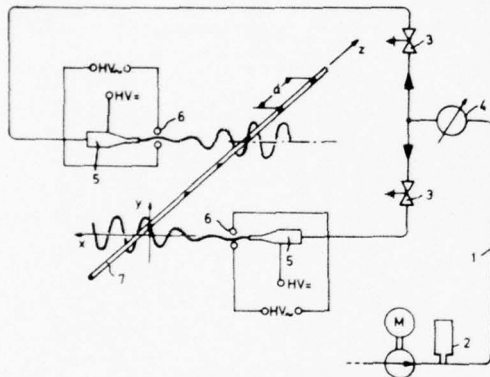


Fig. 1 Schematic diagram of novel method for ring marking

A cog-wheel pump, which is driven by a motor with continuously variable rotating speed, transports the marking ink through the pipe system (1). The irregularities in the ink flow are equalised by a buffer tank (2). Before reaching the grounded magnetic valves (3), the ink pressure is measured (4) and electronically compared with an adjustable threshold value. This allows the valves to open automatically after reaching a preset operating pressure and to give access to the unmoved nozzle (5). The ink jet leaves the nozzle horizontally with a pressure of about 1 bar and a diameter of about 0.5 mm.

The ink jet then passes the deflecting system, consisting of two very good insulated cylindrical electrodes (6). This deflecting system is comparable with the one of an electron beam oscilloscope. A marking ink with special physical properties is charged with electric carriers by application of a high tension direct current between the grounded valves and the insulated ink nozzle. The deflecting force on the charged ink jet passing the electrical field between the deflecting electrodes is given by the Coulomb relationship:

$$\vec{F} = n \cdot e \cdot \vec{E} \quad (1)$$

with \vec{F} = force vector
 n = number of carriers per unit of volume
 e = elementary electrical charge
 \vec{E} = electrical field vector

The electrical field between the deflecting electrodes causes a vertical acceleration of the ink particles. They leave the deflection system in that direction which they momentarily reach during their acceleration within the alternating electrical field. Using a sine-wave deflecting voltage and watching the jet with a stroboscopic flashlight the image of the oscillating jet is to be seen very clearly. An extruded wire (7), running into z-direction will be marked by the touch of the wave shaped ink jet at every zero passing with one half of a ring. The completing half of the ring is made by a second ink jet, which comes from a nozzle located in a z-shifted position on the opposite side. Both halves are joined by using the proper phase relation between the two ink jet modulations.

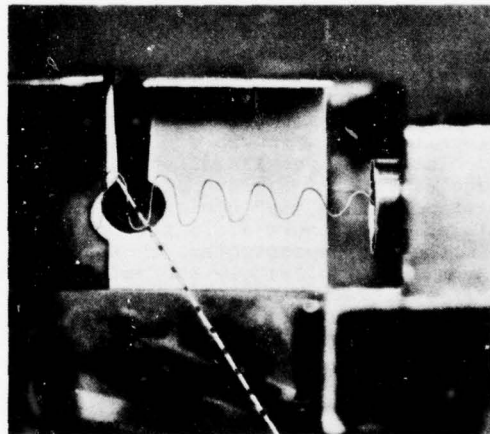


Fig. 2 The oscillating ink jet at a frequency of 1000 cps with the ring coded wire

Figure 2 shows the wedge shaped enlarging deflection of the ink jet, which is modulated by a sine wave deflection high voltage with a frequency of 1000 cycles per second. This corresponds at a mean ring distance of 15 mm with a line take-up speed of 1800 m/min. The ink collecting trough is cut on the sidewalls to allow the passing of the extruded hot wire. The amplitude of the ink jet oscillation at this point is about 15 mm.

The shape of the modulated ink jet oscillation in the x-y plane against the wire is given by the following equation:

$$y = a_x \cdot \sin \left(\frac{\omega}{v_x} \cdot x \right) \quad (2)$$

with a_x = amplitude of the jet oscillation depending on the x-value

ω = circle frequency

v_x = x-component of ink velocity

The quality of the ring marking is determined by the slope of the oscillating ink jet at the location of the wire, i.e. at the x-axis crossing point of the curve given in equation (2). This slope is described by

$$\frac{dy}{dx} = \pm \frac{a_0 \cdot \omega}{v_x} \quad (3)$$

with a_0 = amplitude at the marking point.

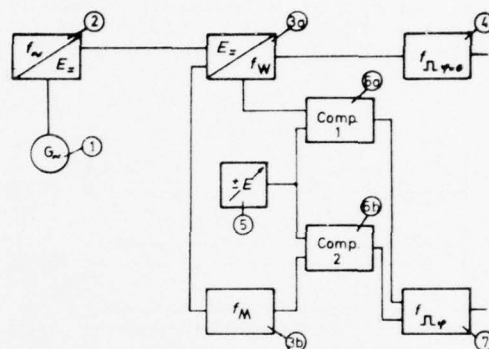
Equation (3) shows, that the slope of the ink jet in the marking area will decrease with decreasing modulation frequency, if the ink velocity is kept constant. That means, that the ring halves have an inclination which increases at greater ring distance or lower take-up speed. This negative effect is totally compensated by using a modulation voltage with a sine wave form, that is approximated to a slightly rounded rectangular shape with decreasing frequency.

The operating limit of this method is presently at a deflection frequency of about 1500 cps. A further increase of this frequency limit seems to be possible. But the inertia of the ink jet is the reason for its behaviour like a low pass RC-filter, which leads to a decrease of the deflection amplitude with increasing frequency. However, it is essential that a minimum amplitude in the marking area shall not be exceeded in order to achieve good quality of marking.

Another restricting factor is the relation between the speed of wire v_z and the horizontal speed of ink particles v_x . An increasing value of this relation $\frac{v_z}{v_x}$ means an increasing sickle-shape of the ring halves.

SYNCHRONISATION OF RINGS, MULTI-RING MARKING

The marking of a wire with one closed ring needs two deflecting units as shown in fig.1. A certain phase relation between the two oscillating ink jets is necessary to achieve the jointing of the two ring halves. This can be done either by adjustment of the mechanical set-up or by pressure control. A completely electronic method was developed to allow an even easier adjustment combined with a simple set-up of the deflecting units and furthermore the possibility of remote control. This was also favoured because of the high operating speed.



- 1 frequency generator
- 2 frequency converter
- 3a, 3b VCO, triangle ni, ii
- 4 rectangular pulse, $\varphi=0$
- 5 DC voltage, variable
- 6a, 6b comparator
- 7 flip-flop, output E_φ

Fig. 3 Blockdiagram of a digital phase shifting method

Figure 3 shows a block diagram of this electronic ring synchronisation. Its main task is to generate two electrical oscillations according to the following equations:

$$\text{oscillation 1} \quad E_1 = E_0 \sin \omega t$$

$$\text{oscillation 2} \quad E_2 = E_0 \sin (\omega t + \varphi)$$

with φ = phase angle

The phase shift angle must be independent of the frequency, because the synchronisation of the both ring halves must be stable even for small deviations of the take-up speed. As conventional phase shifting circuits have a frequency depending shift, a frequency independent solution on a digital basis was developed. The block diagram of this method is contained in figure 3.

The extrusion line drives a frequency generator (1) which supplies a velocity proportional frequency. This is fed to a D/A-converter (2), supplying a frequency proportional DC-voltage, which controls a voltage controlled oscillator (VCO). This oscillator generates a rectangular signal (4) and by integration of this signal a triangular signal (3a) is obtained, which is inverted in (3b) with equal amplitude. The comparators (6a), (6b) compare the two triangular signals with a DC-voltage (5), the level of which is variable within the amplitude range of the triangular functions. The comparators supply pulses the width of which is dependent upon the adjusted DC-level and get to the inputs of a flip-flop (7). The rectangular signal at its output is phase-shifted by the frequency-independent angle φ against the signal of the output (4). The angle is adjustable from nearly 0 to 180 degrees.

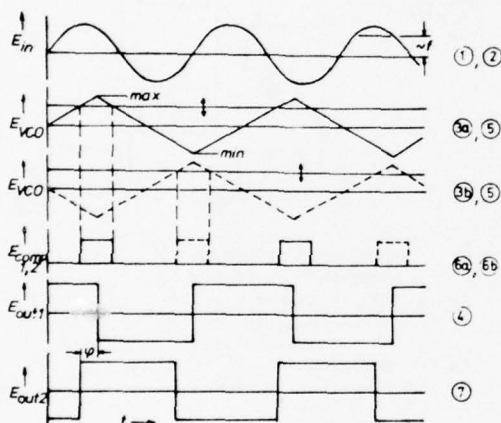


Fig. 4 Time chart of digital phase shifting pulses

Figure 4 shows the sequence of the processes in form of a pulse diagram. Both rectangular signals with equal pulse width are converted by low pass filters into sine-wave voltages, which control a B-amplifier. The amplifier outputs are connected to high tension transformers, which supply the voltage for the deflection of the ink jet.

The method for the generation of phase locked rectangular signals is not only used for the synchronisation of the ring halves, but also applied for the distance control for double ring or twin color marking. In this case two complete marking units are needed, each one consisting of two deflecting units (fig. 5).

The exact adjustment of the phase angles φ_{12} and φ_{34} generates two closed single rings, the distance of which is controlled by adjusting the phase angle φ_{13} . The twin color marking with equidistant rings of two alternating colors is therefore only a special case of the general double ring marking using a phase angle φ_{13} of 90 degrees.

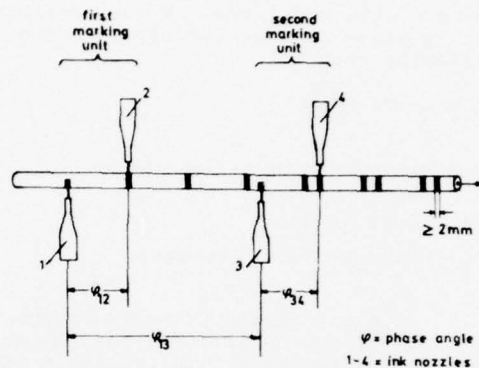


Fig. 5 Phase shifting for double ring and twin color marking

PERFORMANCE OF THE EQUIPMENT

The new method for ring marking of plastic insulated wires as described above is realised by the equipment shown in fig. 6. It consists of a frame with the central plug-in unit for power supplies, pressure controls, amplifiers for high voltage generation, and printed circuits for the entire electronic control system. The instrument panel with separate control elements for the two marking units is also furnished with a test arrangement for the deflecting procedure of the ink.

Two separate marking units with the ink circuits are mounted on the frame and can be levered or lowered independently. This allows cleansing the unused system while it is down and marking in the meantime with the lifted system in order to minimise idle times and scrap on wire production. Each marking system is provided with a three way valve allowing an undisturbed switch over from operating to cleansing and vice versa.

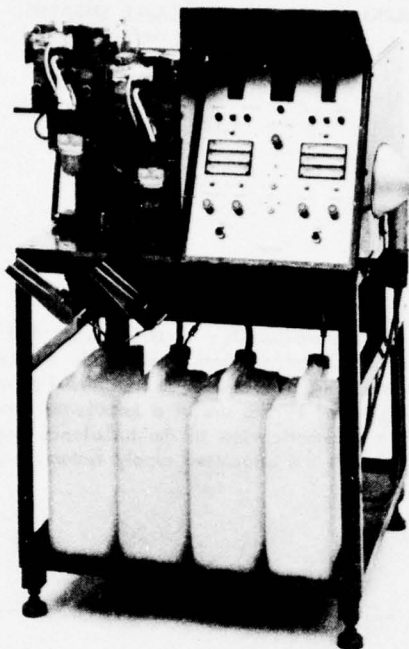


Fig. 6 Total view of the novel ring marking equipment

The two-fold arrangement of the marking units not only allows double ring and twin color marking technique, but also a very fast change of the ring color of single rings in a few seconds. The range of application for this equipment is primarily the marking of PVC insulated wires with diameters from 0.5 to 1.5 mm with single rings at a distance of 4 to 40 mm. Presently 10 different colors are available. Using a ring distance of ≥ 15 mm allows wire speeds of up to 2000 m/min. Secondly the equipment is able to mark PE-insulated wires of 0.8 to 1.6 mm diameter with colored single or double ring marking. Additionally it is possible to use further markings with single or multiple ring programs.

The universal application in a wide range of wire velocities, the low volume of scrap wire during the exchange of colors or ring codes, the outstanding ring quality, as well as the low maintenance costs designate this equipment a most economic means for the production of ring marked plastic insulated wires on high speed extrusion lines.



K. Kimmich

STANDARD ELEKTRIK
LORENZ AG (ITT)

Product Line Cables
and Wires
Development Dept.

H.Hirth-Str. 42
D-7000 Stuttgart 40
Germany

K. Kimmich received his Dipl.-Phys. degree from the Technische Hochschule Stuttgart in 1969 and immediately joined SEL Kabelwerk in Stuttgart. Since then he is engaged as a development engineer in the department of telecommunication cables.

Acknowledgements

This paper is partly based on preceding activities on this topic. The author wishes to thank O. Grießer, H.J. Haise and H. Harbort for their valuable contributions.

A NEW TECHNIQUE FOR PERMANENT AND NON-ABRASIVE MARKING OF PLASTIC CABLE SHEATHS

by

Jörg Hennig

STANDARD ELEKTRIK LORENZ AG (ITT)
Stuttgart, Germany

Summary

A new technique has been developed for the application of combined symbols and footage markings on polyethylene cable sheaths. The marking medium is a plastic powder, which sinter-fuses into the surface of the jacketing material and results in a raised, permanent, and non-abrasive mark.

The process is performed on the hot cable sheath immediately after the extrusion head by the use of a new type of machine consisting essentially of two marking wheels of exact circumference and driven by stepper motors. The marks are engraved into the contact surface of the wheels, and one of the wheels is, additionally, equipped with a footage counter. Plastic powder is loaded into the engravings by a special filling device and is then transferred upon the hot cable jacket to achieve a permanent bond with the jacket material.

In contrast to conventional marking methods using raised symbols on the cable, the machine precludes any risk of reducing the wall thickness, thus permitting the economical production of cable sheaths.

The use of plastic powder is a simple solution under the aspect of today's manufacturing practices and offers substantial advantages as compared with the application of colored inks.

Introduction and Task

Outdoor communication cables with polyethylene sheath for the German PTT must be provided with embossed marking in the form of symbols (telephone receivers, danger arrows). Additional interest was expressed in the exterior footage marking of the cable sheath. For this, the cable industry uses separate equipment for embossing the symbols and for marking the length with ink.

The present arrangement, whereby two machines are required at different locations along the jacketing line, is difficult to supervise by one operator alone. Moreover, the use of inks was a time-consuming process and did not result in the desired durability of the markings. Therefore, it was necessary to look for an improved production method eliminating these substantial disadvantages.

The following is a description of the marking equipment designed for marking in one or two lines and the practical use of which has been approved by the German PTT.

Operating Principle

The marking medium is a plastic powder that is applied to the hot cable sheath immediately adjacent to the sheath extruder. The powder is transferred to a rotating marking wheel by the use of a turbulence chamber. Figure 1 is a schematic view of the turbulence chamber (Figure 1, a) with the associated supply system.

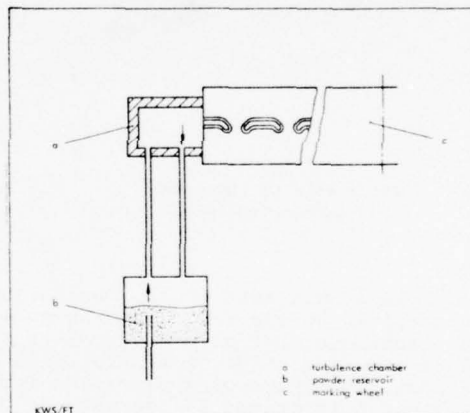


Figure 1
Plastic powder transfer to
marking wheel (schematic)

The plastic powder is stored in a reservoir (Figure 1, b) from where it is conveyed into the turbulence chamber. Inside the chamber the powder is continuously kept in motion by a large volume of turbulent air. One side of the stationary turbulence chamber is terminated by the marking wheel (Figure 1, c), which has the shape of a cylindrical drum. The surface of the wheel is provided with engravings (figures, contours of symbols, etc.) that are filled with plastic powder while passing through the turbulence chamber to transfer that powder to the surface of the cable sheath when the marking wheel subsequently contacts the cable. There, the powder fuses with the plastic cable sheath in a permanent and resistant bond.

Design of Marking Machine

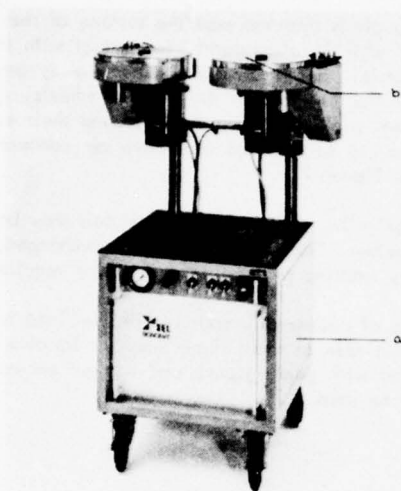


Figure 2
Front view of marking machine

The machine shown in Figure 2 is suitable for single-line and double-line marking and consists of a box-shaped base (Figure 2, a), accommodating electronic and pneumatic controls, and an upper part for carrying out the marking operation by means of the marking wheels (Figure 2, b).

Figure 3 is a backview of the machine in direction of movement of the cable.

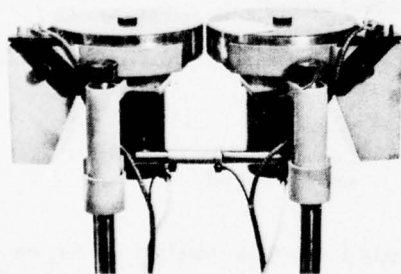


Figure 3
Backview of marking part

Figure 4 shows a section of a marking wheel and the supply unit for the plastic powder, looking down upon the machine from above.

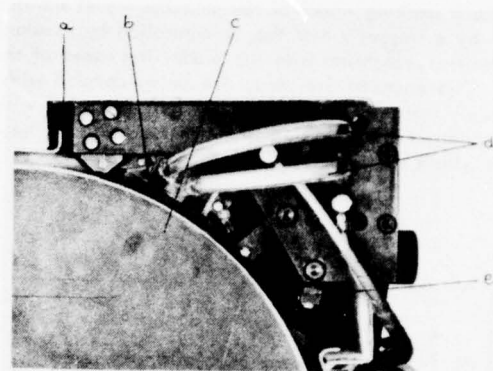


Figure 4
Powder supply unit

The powder is kept in a large-volume storage container (Figure 4, a) above which the turbulence chamber (Figure 4, b) is located. The chamber is made of plexiglass to permit the flow conditions inside the chamber to be watched. The side of stationary turbulence chamber that is in contact with the marking wheel (Figure 4, c) has a steel facing which accurately conforms to the shape of the wheel. A drawspring assures sufficient contact pressure between the chamber and the wheel surface and thereby a tight seal. The problem of wear between the marking wheel and the turbulence chamber has been solved by choice of suitable materials. The inlet and outlet lines (Figure 4, d) for the powder-and-air mixture consist of flexible hoses. A stripper plate (Figure 4, e) operating in opposite direction to the rotating wheel, returns any surplus powder directly to the storage container, whereas the powder required for marking is contained in the surface engravings and subsequently transferred to the cable sheath.

Plastic powders that are suitable for this marking method have poor flow characteristics. By injecting compressed air pulses into the powder storage container this drawback is overcome.

For marking cables with consecutive precise length indications, one of the marking wheels, the circumference of which must coincide with the desired length marking, is provided with a numeral printer with engraved numerals (Figure 5).

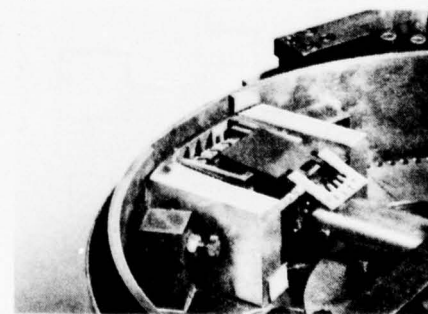


Figure 5
Marking wheel with footage counter

The printer is mechanically operated; for the numbering operation the printer is moved out of the numeral openings and retracted again after the numbering operation.

Each marking wheel of the machine model shown is driven by a stepper motor that is controlled by a rotary encoder in synchronism with the production speed of the cable. Two encoders are used, one being coupled with an accurately operating footage counter and the other with the capstan of the extrusion line. The location of the encoders within the line is shown in Figure 6.

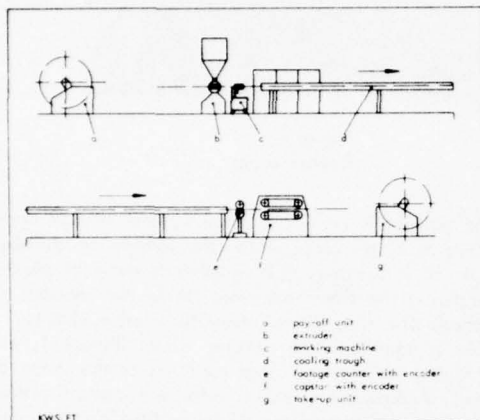


Figure 6
Schematic representation of a jacketing line with marking machine

The principle of control of a stepper motor is shown in Figure 7. The encoders are connected to the electronic stepper motor control unit through a switch-over device.

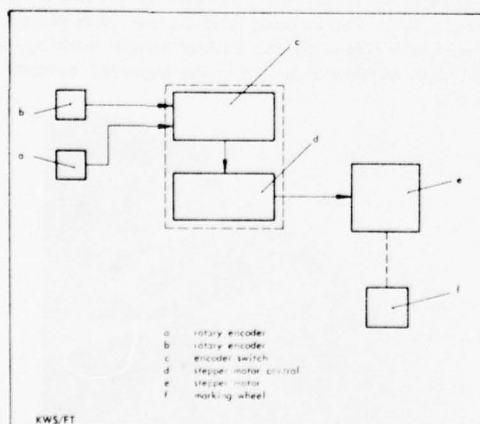


Figure 7
Block diagram of electronic control unit

The switch-over device includes an electronic circuit which automatically applies one of the signals arriving from the encoders to the stepper motor control unit as preset. This is done at a time when both signals are in phase so that smooth operation of the stepper motor without jerks is assured.

Cooling air is directed past the surface of the marking wheels, which are constantly in contact with the hot extruded material, and also serves to carry away any excess powder. The covering of the marking wheels, which assures uniform cooling of the wheels around their entire circumference, as well as the respective air connections are shown in Figure 2.

Pneumatically, the two marking wheels may be operated together. The wheels are easily exchanged, and the necessary marking pressure may be set as required.

In case of unilateral marking with combined length indications (in case of small diameters, for instance), a counter-wheel with guide groove and without engraved surface will be used.

Test Results

During the practical use of the machine described in the production of polyethylene-insulated communication cables it was found that a comparatively low pressing force of the marking wheels upon the cable jacket is needed because elevated characters are being applied.

	necessary pressing force of marking wheel N
new marking method with plastic powder	5 to 20
conventional method (elevated stamping)	30 to 45

Table 1
Comparison with conventional marking method

In Table 1 the figures obtained for the new system, which are dependent on the wheel diameter and the production conditions, are compared with those of the conventional stamping method (raised stamping of telephone receiver symbols).

The cable maker is thus enabled to save jacket material because, unlike in the past, it is no longer necessary to overdimension the jacket in order to obtain the wall thickness required on the marking line.

The effectiveness of the air cooling system used for the marking wheels is shown in Figure 8.

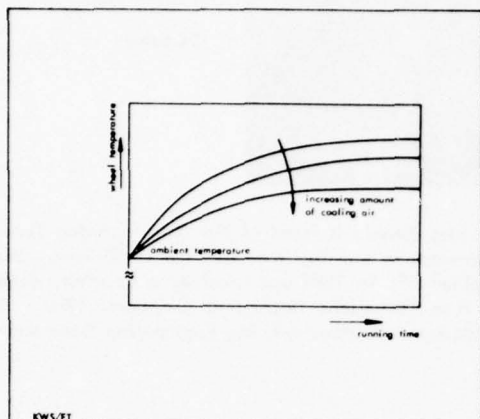


Figure 8
Surface temperature of marking wheel
as a function of running time

Depending on the manufacturing conditions, a thermal equilibrium is achieved with a constant supply of cooling air after 10 - 20 minutes running time. Starting from the ambient temperature, the wheels are heated by their contact with the hot extruded material. The wheel temperature is essentially determined by the temperature of the extruded material, the contact area between the wheel and the cable sheath, and the speed of production. To achieve perfect marking results it has been found advisable to operate at a surface temperature of below 50° Centigrade.

The plastic powder used must be of a type that will sinter-fuse with the cable jacket before entering the cooling trough to assure a permanent and abrasive-resistant bond. For testing the abrasive-resistance on polyethylene the test equipment shown in Figure 9 is being used.

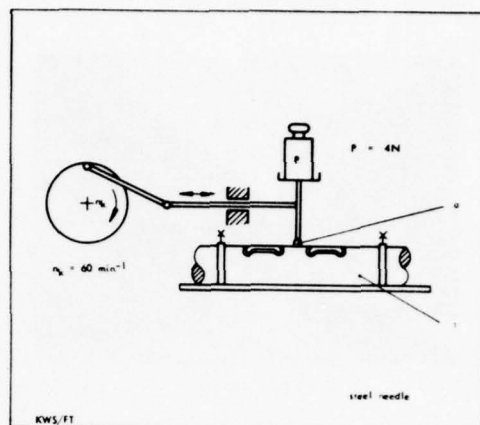


Figure 9
Test equipment for abrasive resistance
of marking on cable sheaths (schematic)

A ground steel pin of 1 mm (.04") diameter (Figure 9, a) is moved along the cable (Figure 9, b) at a load of 4 N by a crank drive operating at 60 rpm. The number of double strokes causing complete abrasion of the marking along the line of contact of the steel pin is measured. Test with various types of powder at differing manufacturing conditions have resulted in 500 to 6000 double strokes.

The marking speed is limited by the fact that centrifugal forces tend to fling the powder out of the wheel engravings or even prevent it from entering the engravings out of the turbulence chamber. However, this may be influenced by adapting the width and depth of the engravings to the grain size distribution and the type of the powder. The machine is now used at speeds up to 131 feet per minute (40 m/min).

The marking medium has not been found to affect the cable sheath characteristics. Further marking has no influence on the production and the quality of cable splices.

Field of Application

Apart from its use for marking communication cables with polyethylene jackets (Figure 10),

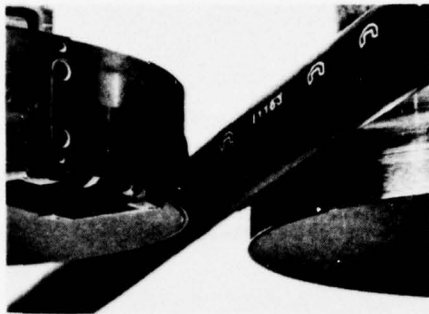


Figure 10
Marking of a telephone cable

the machine may be used for marking similar extruded plastics with numerals, letters, and symbols, singly or in any combination, with more than two lines of marks also being conceivable.

The plastic powder may have different colors to permit marking in a color contrasting with the color of the jackets.



Dr. Jörg Hennig
Standard Elektrik Lorenz AG
EG Kabel und Leitungen
D-7000 Stuttgart
Germany

Jörg Hennig is Head of the Manufacturing Technique Departments in the SEL Wire and Cable Division, Stuttgart. He joined SEL in 1965 and received a Dr.-Ing. degree in 1970 from Technische Hochschule Stuttgart. 1970 - 76 he was Manager of Manufacturing Engineering Department.

Acknowledgements

The developed machine is a result of team work. The author acknowledges the contributions of Mr. O. Griebler, Mr. H. Kaiser, Mr. G. Kramer, and Mr. K. Maisel.

DEVELOPMENT OF FIRE-STOPPING MATERIALS FOR WIRING SYSTEM

M. ISHIBASHI, H. KOBAYASHI, M. MAKIYO
THE FUJIKURA CABLE WORKS, LTD.
TOKYO, JAPAN

Summary

In most case of fires, the spread of fire through cables leads to great damages to buildings, telephone exchanges, etc. There is a technical limit in developing fire-proof wires and cables. It is essential therefore to stop the fire at openings and holes of floor, wall and ceiling through which telephone and electric power cables pass.

We have successfully developed fire-stopping materials to be used at these penetration points, and have carried out fire tests using the materials. Two hundred PVC insulated and PVC sheathed cables in bundle were suspended vertically, and a newly developed fire-stopping putty was applied to the opening between cables and hole. A flame of temperature exceeding 1000°C was applied for two hours duration.

The results show that the putty has an excellent fire resistance.

This paper describes the characteristics of the newly developed fire-stopping putty and paint and the results of fire tests.

1. Introduction

Many reports have been published about fires,^{1,2} fire test methods,^{3,4,5} improved fire-proof wires and cables⁶ and fire protective procedures. There are fire protective procedures as follows:

- (1) One of fire protective procedures is a well planned detection and alarm system.^{7,8}
- (2) The other procedure is constructive fire protection using fire-stopping materials.^{9,10,11,12}

In a building, bundled cables pass from floor to floor through openings and holes of floor, wall and ceiling. So, when a fire occurs, there is nothing to stop the fire from spreading at these penetration points. Fire resistant mineral fibers or cure-type putty are commonly used to seal the openings and holes. But it is a problem that the seal of mineral fibers can not be adequately smoke- and water-tight due to gaps caused by uneven packing density.¹¹ Also it is slightly difficult to remove the cured seal.

The newly developed fire-proof putty is smoke- and water-tight and can be removed easily as required. When the putty and paint are used together, they show an excellent fire resistance.

2. Characteristics of fire-proof putty

Characteristics of two kinds of putty are described in this paper. One putty (Type A) is water-base and becomes thoroughly cured in 2-3 days at room temperature and has 41 Shore "D" hardness.

The other putty (Type B) keeps its original softness after application and never drops down by the fire. The putty (Type B) is properly pressure-fitted into openings and gaps, and can be removed easily

whenever necessary. The typical characteristics of two kinds of putty are given in Table 1.

Table 1 Characteristics of Putty

Properties	Type A	Type B	Test method
Type	Cure-type	Non cure-type	
Specific gravity	1.4	2.0	
Shrinkage of volume [%]	25	0	80°C-4 days
Penetration [1/10 mm] original	81	76	JIS K 2530
after 2 months exposure	—	76	Needle type
Flame resistance	No propagation (Fig. 2)	No propagation (Fig. 2)	Horizontal flame test (Note 1)
Effect on plastics	No deterioration	No deterioration	60°C-6 months (Note 2)
Effect on metals	No discoloration	No discoloration	60°C-6 months (Note 2)
Main content	Mineral fiber Inorganic filler Water emulsion of polymer Flame retardant materials	Mineral fiber Inorganic filler Plasticizer Flame retardant materials Synthetic rubber	

Note 1: Horizontal flame test

A 30 cm length of 0.5 mm x 100 pairs PVC insulated and PVC sheathed cable was used for the test. Two thermocouples were placed as shown in Fig.1.

Note 2:

PVC and polyethylene sheets of 100 mm x 200 mm with 1 mm thick were used for samples. Plates of plain copper, tin plated copper and iron with size of 50 mm sq. and 0.2 mm thick were used for samples. The test samples, shown in Fig.3, were heated in a forced circulating-air oven at 60°C for 1,2,3 and 6 months. Tensile properties of the plastic sheets and discoloration of the metal plates were measured and observed respectively.

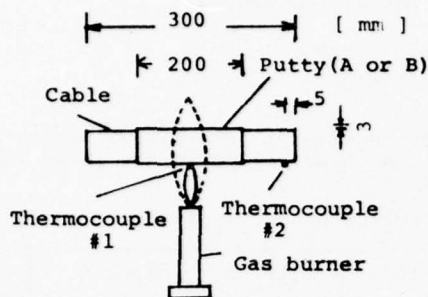
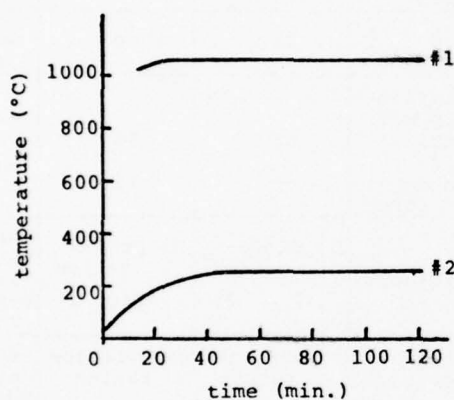


Fig.1 Horizontal flame test



An example of Type B
Fig.2

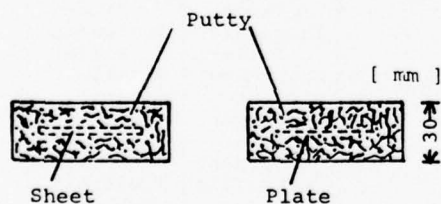


Fig.3

3. Characteristics of fire-proof paint

There are two types in the newly developed fire-proof paints; blowing-type and non-blowing type. The former (Type A), when heated, expands more than ten times and forms rigid carbonized layer. A minimum coating thickness of 0.5 mm is necessary for fire protection. The latter (Type B) is water-base and a minimum coating thickness of 3 mm is necessary for fire protection. Both paints can be applied on cables by brush and spray. Table 2 shows the typical characteristics of the paints.

Table 2 Characteristics of Paint

Properties	Type A	Type B	Test method
Type	Blowing type	Non-blowing type	
Specific gravity	1.11	1.35	
Flexibility	No crack	No crack	Bending test (Note 1)
Accelerated weathering test	No crack	No crack	Weather O Meter 2500 hours
Water immersion test	No leaching	No leaching	20°C-6 months
Flame resistance	No propagation (Fig. 4)	No propagation (Fig. 4)	Horizontal flame test (Note 2)
Effect on plastics	No deterioration	No deterioration	60°C-6 months (Note 3)
Effect on metals	No discoloration	No discoloration	60°C-6 months (Note 3)
Main content	Acrylic resin Blowing agent Flame retardant materials	Acrylic resin Mineral fiber Flame retardant materials	

Note 1: Bending test

PVC sheathed cables having diameter of 15 mm with paint coating were tested.

Sample 1---0.5 mm coating thickness of Type A

Sample 2---3 mm coating thickness of Type B

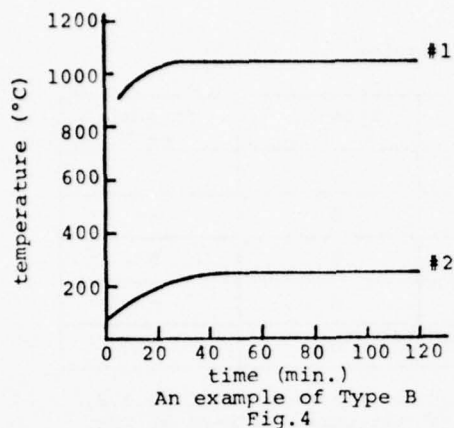
The cables were bent one time around 150 mm mandrel at room temperature and the coating was examined to see if cracks had occurred.

Note 2: Horizontal flame test

Same as Note 1 in Table 1 except for coating thickness. Coating thickness of Type A and B were 0.5 mm and 3 mm respectively.

Note 3:

See Note 2 in Table 1.



4. Fire tests

Vertical and horizontal fire tests were carried out taking into consideration the bundled cables installed in telephone exchanges.

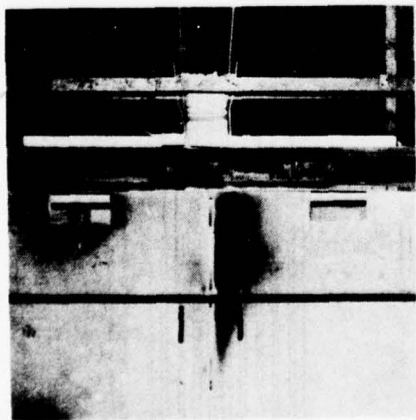
Fire test facility

(1) Furnace

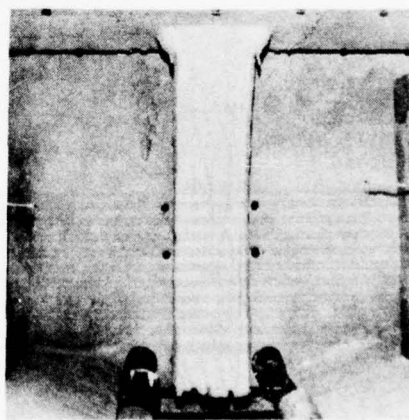
The furnace used for fire tests has dimensions 2 meter wide x 1 meter long and 1.2 meter high with 250 mm x 1050 mm x 150 mm thick ceiling hole as shown in Fig. 5.

(2) Flame source

Four propane gas burners with 40 mm diameter were used as the flame source because of their high output.



(outside)



(inside --- Sample No.3)

Fig. 5 Furnace

Fire test samples

Two hundred numbers of 0.5 mm x 100 pairs PVC insulated and PVC sheathed cables were tested. Putty of Type A or B were sealed or not sealed into gaps among the cables. The test samples with 175 cm length were intimately bundled by waxed hemp threads and two thermocouples were inserted in the gaps before sealing the putty, and test samples were suspended or positioned vertically or horizontally in the center of the hole and a horizontal hole of firebrick respectively. Figs. 6,7,8,9 and 10 show construction of the samples. Fig. 11 is a photograph of sample No. 2. The location of thermocouples are shown in Figs. 12 and 13. Calcium silicate boards were stuffed in the hole, and finally the putty was sealed into gaps between boards and outer surface of test samples (Figs. 6,7,8,9 and 10). Details of the samples are given in Table 3.

Procedure

Air/gas combination was adjusted and the temperature (thermocouples #3 and #4 in Figs. 12 and 13) was controlled according to the curve of Fig. 14 and the flame was applied for two hours duration. After the flame was extinguished, a fresh area of bundled cables was observed and measured to investigate the degree of flame propagation.

The following were also observed and measured.

- (1) Dropping down of the putty by the fire
- (2) Leakage of smoke from opposite sides
- (3) Temperature

Table 3 Detail of the Samples

Sample number	Number of cables	Length [cm]	Type of putty	Type of paint
Sample 1	200	175	A	-
Sample 2	200	175	B	-
Sample 3	200	175	B	B
Sample 4	200	175	B	-
Sample 5	200	175	B	-

The putty was sealed into gaps among the cables for samples of No.1,2, 3 and 4 except No.5. The paint was coated on the outer surface of the cables of sample No.3 only

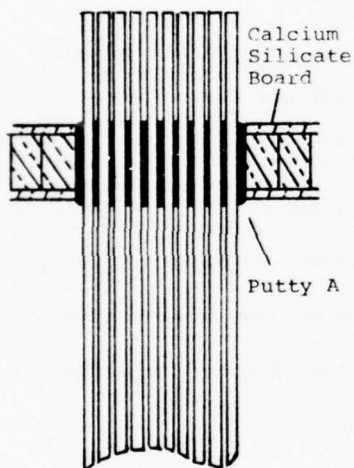


Fig.6 Sample No.1

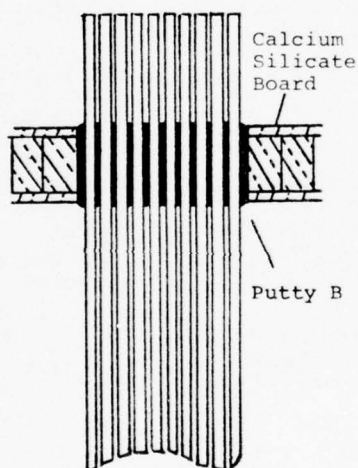


Fig.7 Sample No.2

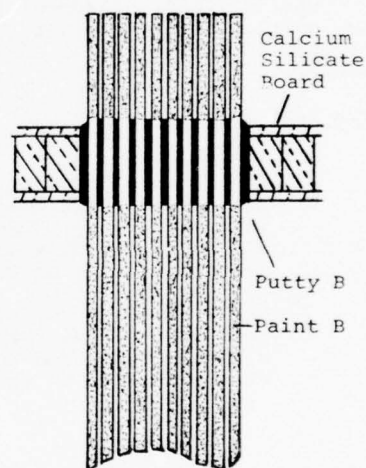


Fig.8 Sample No.3

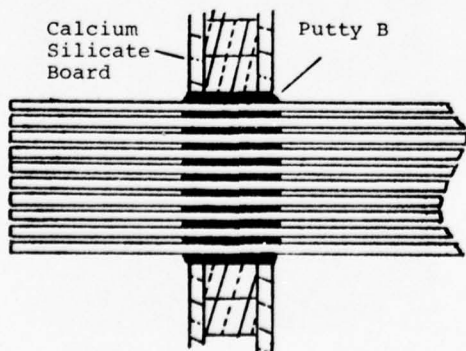


Fig.9 Sample No.4

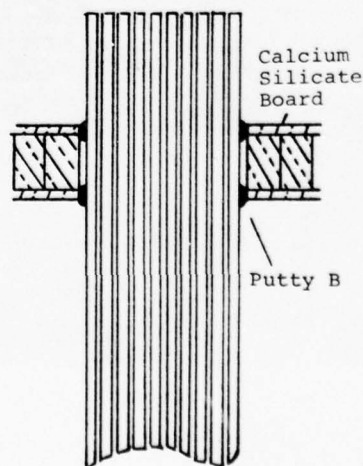


Fig.10 Sample No.5

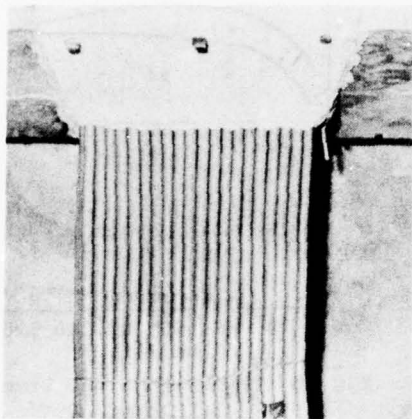


Fig.11 A photograph of Sample No.2

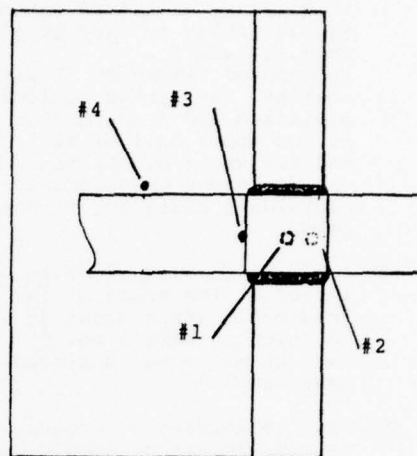


Fig.13 Location of thermocouples
(Horizontal fire test)

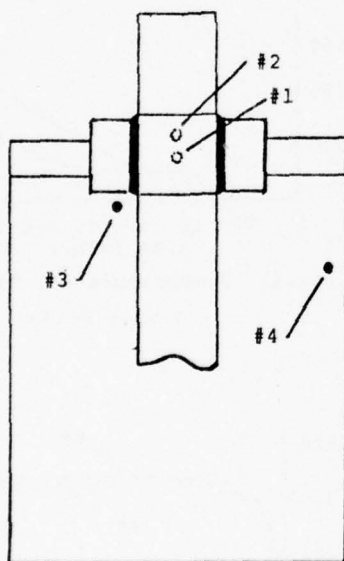


Fig.12 Location of thermocouples
(Vertical fire test)

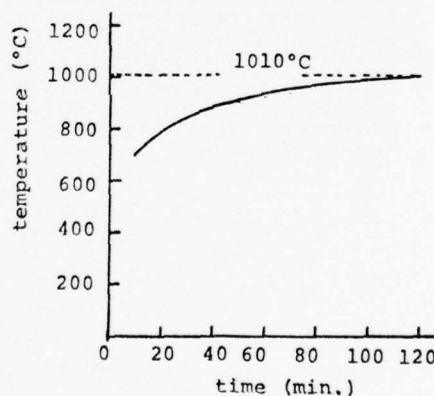


Fig. 14 Target Curve

5. Result

The following test results were obtained concerning propagation of the fire and leakage of smoke.

- (1) Temperature is shown in Figs. 15, 16, 17 and 18. Difference of temperature is big between thermocouples #3, 4 and thermocouples #1, 2 in all test samples. Excellent fire protection was observed by fire-proof putty and paint.
- (2) Equivalent results were observed between putty A and B (Fig. 15) concerning the propagation and the leakage of smoke. Therefore, only results obtained by Type B are mainly described in this paper.

- (3) Spread of fire was nearly reached to boundary of sealed and non-sealed cables in case of samples No.1,2,4 and 5
In case of sample No. 3 with paint coating, the spread of fire was minimized and a fresh area remained at the upper half of sealed part and the smoke of the burning cables was decreased considerably by using additional effective fire-proof paint.
- (4) A slight leakage of smoke was observed at the start of the test but it stopped after about 20 minutes ignition in sample No. 5. No leakage of smoke was observed in other four samples.

(5) Fig. 18 shows the temperature of various points of sample No. 5. The result as to propagation was, unexpectedly, nearly the same regardless of whether the putty was sealed or not sealed into gaps among the cables. It is considered that high heat conductivity of copper conductors caused decomposition of PVC whether the gaps were sealed or not. Concerning the stopping of leakage of smoke, it is considered that PVC insulations and sheaths were melted or decomposed by flame and by heat conduction through copper conductors, resulting in the sealing of the gaps.

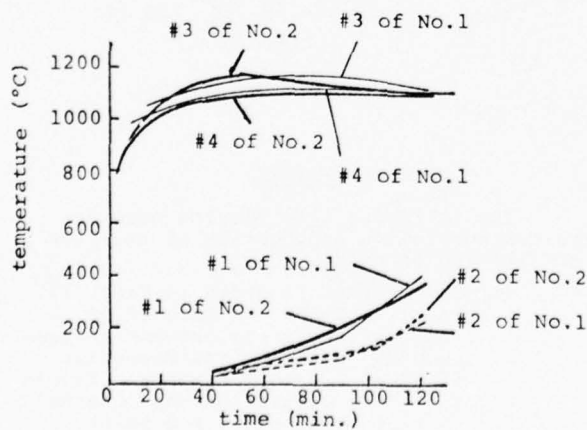


Fig.15 Temperature vs. Time
(Sample No.1,2)

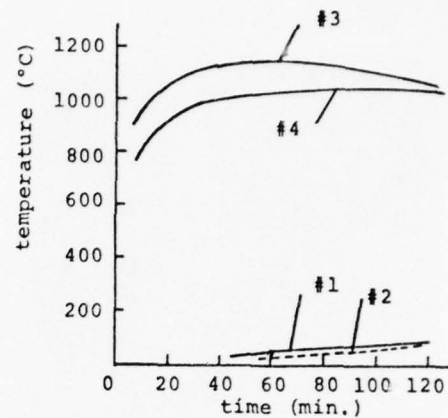


Fig.16 Temperature vs. Time
(Sample No.3)

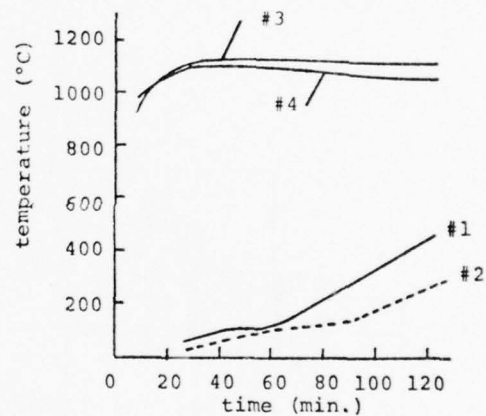


Fig.17 Temperature vs. Time
(Sample No.4)

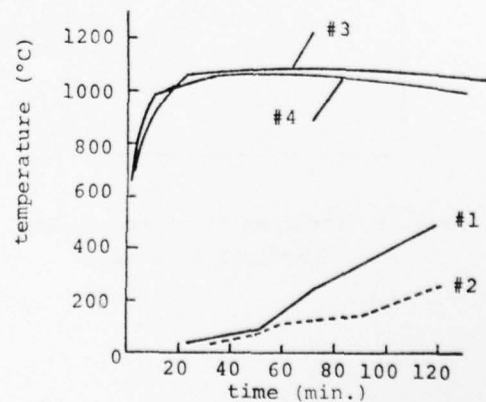


Fig.18 Temperature vs. Time
(Sample No.5)

6. Conclusion

The putty, which keeps its original softness after sealing, has been successfully developed. It shows excellent fire-proof characteristics under vertical and horizontal fire tests at temperature exceeding 1000°C for two hours duration and it does not influence the cable composition and frames, for example, PVC, polyethylene and metals. The putty can be removed when required. Better fire resistance is confirmed when a fire-proof paint is used together with the putty.

7. Acknowledgement

The authors wish to thank our associates who contributed to the development of fire-stopping materials and various fire tests.

References

- 1) V.A. Sielert : "How GT of California snuffed out a fire before it started" March 8, 1976. Telephony
- 2) L. Stolzman : "New York Tel transforms disaster into triumph" April 14, 1975. Telephony
- 3) "Fire-resisting characteristics of electric cables" IEC Recommendation, publication 331, 1970
- 4) F.M. McAvoy : "Flame tests-A Systems Approach for Power and Control Cable" Conference Paper of IEEE, 1972
- 5) G.R. Woollerton : "Fire hazard evaluation of cable & materials" The 24th International Wire and cable Symposium
- 6) S. Kaufman : "Development of Improved Flame Resistant Interior Wiring Cables" The 24th International Wire and cable Symposium
- 7) N. Chergotis : "Fire in CO!" December 15, 1975. Telephone Engineer & Management
- 8) R. Blain : "Early fire detection system protects Bell Canada offices" May 31, 1976. Telephony
- 9) "Fiberglass sheet blocks cable fire in Detroit Edison test" Volume 53, June 23, 1975. Electric Light & Power
- 10) Al. Schuman : "How to contain a fire" February 9, 1976. Telephony
- 11) "Silicone foam fills the gap in fire and smoke protection" March 29, 1976. Telephony
- 12) S. Sehested : "A Way to Stop Fires Cold" April 5, 1976. Telephony

Authors



Masashi Ishibashi
Chief, Telecommunication Cable Research & Development Dept.
The Fujikura Cable Works, Ltd., 1440 Mutsuzaki, Sakurashi, Chibaken, Japan

Mr. Ishibashi was born in 1937. He joined the Fujikura Cable Works, Ltd. after his graduation from Saitama University in 1959 and has been engaged in research and development of plastic materials and manufacturing methods for telephone cables. Mr. Ishibashi is a member of the Society of Polymer Science of Japan.



Hirotada Kobayashi
Engineer, Telecommunication Cable Research & Development Dept.
The Fujikura Cable Works, Ltd., 1440 Mutsuzaki, Sakurashi, Chibaken, Japan

Mr. Kobayashi was born in 1943. He joined the Fujikura Cable Works, Ltd. after his graduation from Tohoku University in 1967 and has been engaged in research and development of plastic materials for telephone cables. Mr. Kobayashi is a member of the Society of Polymer Science of Japan.



Minoru Makiyo
Engineer, Telecommunication Cable Research & Development Dept.
The Fujikura Cable Works, Ltd., 1440 Mutsuzaki, Sakurashi, Chibaken, Japan

Mr. Makiyo was born in 1951. He joined the Fujikura Cable Works, Ltd. after his graduation from Gumma Technical College in 1972 and has been engaged in research and development of plastic materials for telephone cables. Mr. Makiyo is a member of the Society of Polymer Science of Japan.

New Types of Intumescent Materials and Their Application to Fire Protection of Cables

By

T. Yabuki, Y. Koide, T. Kaide, M. Takada
Dainichi-Nippon Cables, Ltd.
Osaka, Japan

Abstract

The new intumescent flame retardant materials have been developed. They are divided into three types; Compound A(thermoplastic), Compound B(rubber-like), Compound C(putty-like). They consist of a base material which differ from intumescent coating and a component which form a carbonaceous layer like in the coatings such as ammonium polyphosphate, polyhydric alcohol and amino compound. Compound A and B contain chlorinated polymer and Compound C contains oil, oligomer and inorganic filler as base material. Flame tests according to IEEE Std-383 revealed that cables covered with Compound A extrudate and Compound B-tape show satisfactory flame retardancy, while cable-through-hole models sealed with Compound C exhibit high fire resistance when subjected to a two-hours fire resistance test as directed in JIS A 1304.

1. Introduction

The increasing need for preventing fire spreading through electric wire and cable lines has focused great attention on fire-retardant materials. As one aspect of fire prevention, intumescent flame retardant coatings are applied because they reduce very effectively the flame spread, and smoke generation of plastic cables.¹⁻² However, intumescent coatings are usually not sufficiently flexible and have poor impact strength and low water resistance³. Fire proof walls are also provided where cables extend from one area to another. In those areas all cable ducts or cable through-holes should be sealed to prevent the spread of fire and the ingress of smoke from fire areas into unaffected areas.⁴ Those suggest that more effective fire prevention for electric cable lines is not attainable with such coating materials alone. An improved material is strongly required for this purpose.

New type of intumescent materials have been developed which are applicable to alternative method of fire protection.

The materials are combination of three kinds of compounds, i.e., Compound A(thermoplastic), Compound B (rubber-like) and Compound C(putty-like).

This paper describes the development and properties of these compounds, flame testing of the cables covered with Compound A(intumescent extruded layer) and Compound B(wrapping layer of intumescent self-bonding tape), and flame testing of the cables installed in a model cable-through-hole where inlet and exit are sealed with Compound C(intumescent putty) as well as some applications of the compounds.

2. Materials Development

The first objective of the materials development was to design a thermoplastic (or extrudable) compound which had the same intumescent flame retardancy as intumescent coating and favorable flexibility, impact strength, and water resistance superior to those of intumescent coatings.

The second objective was to design a putty-like sealing compound which could be packed into cable through-hole, and which would bubble up when heated to form a porous carbonaceous layer having outstanding fire retardancy.

2.1 Development of the Thermoplastic Intumescent Compound

Typical intumescent coating contains five basic components as follows⁵:

1. Carbonaceous residue source ; polyhydric alcohols such as pentaerythritol and starch.
2. Blowing agent ; such as dicyandiamine, melamine and chlorinated paraffin.
3. Dehydrating agent ; ammonium polyphosphate and melamine phosphate.
4. Resinous binder(or Base Material) ; polyvinyl acetate and cellulose derivatives.
5. Solvent ; water or mineral spirit.

In order to obtain an extrudable compound, many kinds of polymers were investigated as base material in view of compatibility of the polymer with the ingredients for forming the foamed carbonaceous layer by means of two roll mill at each optimum temperature. Selected formulations which showed excellent compatibility were adopted for test compounds.

Each of the test compounds was subjected to Bunzen burner test to assess the intumescent flame retardancy. The test compounds were evaluated to estimate tensile strength, elongation at break, thermal aging resistance, water resistance and oil resistance. Balancing between the flame retardancy and other properties determines acceptable compounds which could be divided into two types : Compound A and Compound B.

2.2 Bunzen Burner Test

A 600 Volts rating cable of 13.5mm outside diameter which was insulated with cross-linked PE and sheathed with PVC was employed as a sample cable in 250mm length. Each compound was shaped into a tape and was wrapped around the sample cable to form a layer of 2mm thickness. The sample cable was then heated by two Bunzen burners at about 1,020°C for 30 minutes as illustrated in Figure 1.

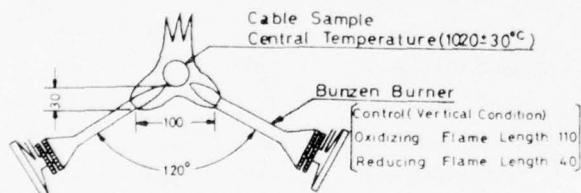


FIGURE 1
Bunzen Burner Test

At the same time the sample cable was stressed at AC 1,200 Volts of 60 Hz for 30 minutes, and insulation resistance of the sample cable was measured at intervals of 1 to 5 minutes by means of a DC 500 Volts megger. In the case of the resulting cable sample did not break down under the test condition, the corresponding compound could be acceptable in flame retardancy.

A sample cable with a 1 mm thick intumescent coating showed good insulation resistance when evaluated by the flame test. Such intumescent coating was found to be correspond to a 2mm thick the tape wrapping.

2.3 Development of the Intumescent Putty-Like Compound

In the case of the second objective, various oligomers, oils and inorganic filler were investigated for use as the putty-like base material. Those condidative formulations which showed advantageous compatibility of base materials with ingredients were mixed to obtain a test compound with a 1 liter mixer which has two agitator blades at room temperature.

Each putty-like compound was also subjected to Bunzen burner flame test. The foregoing test was carried out on a 250mm long sample cable whose sheath was coated with the putty compound to a thickness 3mm.

Other properties of the sealing compound were procedingly tested for mixing compatibility, cone-penetration, moisture resistance, thermal aging resistance and air tightness. An acceptable compounds, named Compound C, was determined in balancing between the flame retardancy and other properties.

2.4 Properties of each Intumescent Compound

The all acceptable compounds selected from the results on foregoing tests can be classified into three types : Compound A, Compound B, Compound C. Each compound contains ammonium polyphosphate, polyhydric alcohol and amino compounds as components for forming the foamed carbonaceous layer like intumescent coatings. Characteristic of the base materials are responsible to that of the compounds. Compound A contains PVC and another chlorinated polymer as base materials and can be extruded with usual extruder. The properties of Compound A are shown in Table 1 and 2.

Compound B containing chlorinated elastomeric polymers as base materials shows poor thermoplasticity, but it has excellent flame retardancy due to the foamed carbonaceous layer. It also exhibit a excellent flexibility and a self-bonding property additionally. Therefore, the Compound B was applicable to cable in the form of a tape which was made from calendered sheat. The properties of the Compound B are shown in Table 1 and 2.

Non hardening type, putty-like Compound C contains mineral oils, synthetic oils, and inorganic filler as base materials. Compound C is free from any volatile component such as water or organic solvent unlike conventional intumescent coatings, consequently it shows no shrinkage and excellent air tightness. The properties of Compound C is shown in Table 3.

Nevertheless appearances, constitutions and mechanical properties of Compound A, B and C are entirely different to those of conventional intumescent coatings, these compounds easily bubble and foam at about 300°C to form a multicellular carbonaceous layer. This foamed carbonaceous layer shows an excellent heat insulating effect as shown in the Bunzen burner test results, Figure 2.

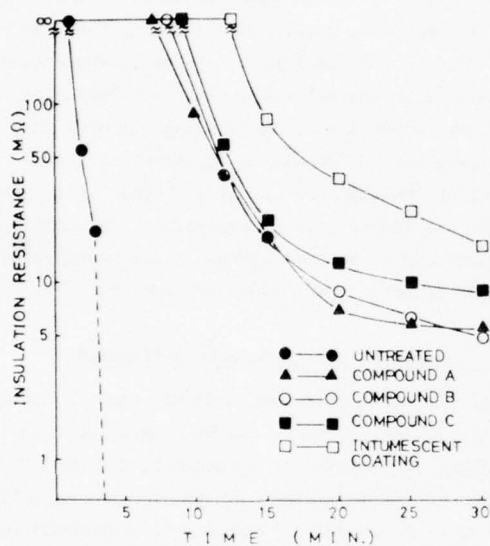


FIGURE 2
Results of Bunzen Burner Test

3. Flame Testing

Flame protecting effects of Compound A, B and C in more practical scale were tested in following manner.

3.1 Vertical Tray Flame Test (IEEE Std-383-1974)

3.1.1 Preparation of Cable Samples

The sample cable of 2.4m long, 13.5mm outside diameter with XLPE insulation and PVC sheath (600Volt, 3 x 3.5sq.mm.) was employed. The flame retardant material applied over PVC sheath was varied as follows.

Flame Retardant Material

Sample-1	Compound A extruded over the PVC sheath with 2mm thickness.
Sample-2	Compound B-tape 0.7mm in thickness and wrapped 2 times.
Sample-3	Intumescent coating of 1mm thickness.
Sample-4	None.

Table 1. Properties of Compound A and B

Items	Compound A	Compound B	Intumescent coating
Specific gravity, at 25°C	1.4	1.4	1.4
Oxygen Index*	50	50	70
Original properties			
TS (kg/mm ²)	0.6	0.25	—
EL (%)	180	800	—
Thermal aging(100°C, 96hrs.)			
TS(% retained)	100	100	—
EL(% retained)	95	90	—
Water resistance			
Water Immersion(RT, 60 days)			
TS(% retained)	95	100	—
EL(% retained)	100	95	—
Chemical resistance			
10% HCL, Immersion(RT, 14 days)			
TS(% retained)	100	120	—
EL(% retained)	95	70	—
10% NaOH, Immersion(RT, 14 days)			
TS(% retained)	100	120	—
EL(% retained)	100	70	—
Cable oil resistance			
Cable oil Immersion(RT, 30 days)			
TS(% retained)	100	100	—
EL(% retained)	90	85	—

* JIS K 7201

TS : Tensile strength
EL : Elongation at break
RT : Room temperature

Table 2. Properties of Compound A and B
- Environmental Resistancy of Heat Insulating Effect -

Items	Applied State to the Sample Cable	Bunzen Burner Test (minimum insulation resistance-MΩ)		
		Compound A	Compound B	Intumescent coating
		2mm thick, extruded	2mm thick, wrapped	1mm thick, coated
Initial		5	5	9
Thermal aging**(100°C, 96 hrs.)		3	3	3
Water resistance				
Water immersion (RT, 60 days)		4	4	*
Chemical resistance				
10% HCL, immersion (RT, 14 days)		4	4	*
10% NaOH, immersion (RT, 14 days)		3	3	*
Cable oil resistance				
Cable oil immersion (RT, 30 days)		3	2	2

* Coating layer disappeared.

** Each sample cable was exposed to the environmental test condition and subjected to Bunzen burner test.

Table 3. Properties of Compound C

Items	Value	Test Method
Specific gravity, at 25°C	1.4	at 25°C
Appearance	Light yellow putty like	
Loss on heating (%)	0.12	JIS A 5752 (105°C x 3 hrs)
Cone penetration at		JIS A 5752
-20°C	21	
0°C	53	
20°C	74	
40°C	83	
60°C	90	
90°C	102	
Oxygen index	70	JIS K 7201
Flame retardency(minimum insulation resistance-MΩ)		Bunzen burner test
Initial	15	The sample cables which were coated with Compound C to 3mm thickness were exposed to the test condition and then, subject- ed to Bunzen burner test.
Thermal aging(100°C, 15 days)	1	
Moisture exposure (100% R.H., RT, 90 days)	1	
Radiation exposure (5 x 10 ⁷ R)	12	

3.1.2 Test Procedure

The flame test was conducted in a spontaneous ventilated room as shown in Figure 3. A 75mm deep, 300mm wide, and 2.4m long ladder type metallic tray was set vertically. The cable samples, each 2.4m long, were arranged in a single layer apart from each other by approximately 1/2 of cable diameter. A 250mm wide ribbon type burner with a venturi air/gas mixer was a flame source. The flow rate of fuel gas(propane) and compressed air were adjusted to give a flame length of 450mm and a temperature of 815°C at vicinity of the cable surface.

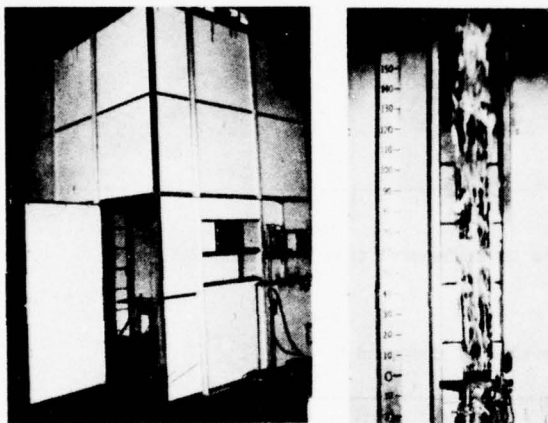


FIGURE 3

IEEE Std-383 Verticaltray

Left : Combustion Room

Right : Verticaltray and Burner

3.2 Flame Tests to Assess the Sealing Materials

Since no standard test method has been elucidated for this purpose, we developed the following methods.

3.2.1 Horizontal Cable-Through-Hole Test

Figure 4 shows the details of the test furnace and a model cable-through-hole. This furnace was specified in the Fire-Service Law of Japan for testing of fire-proof cables which are used for emergency power service cables.

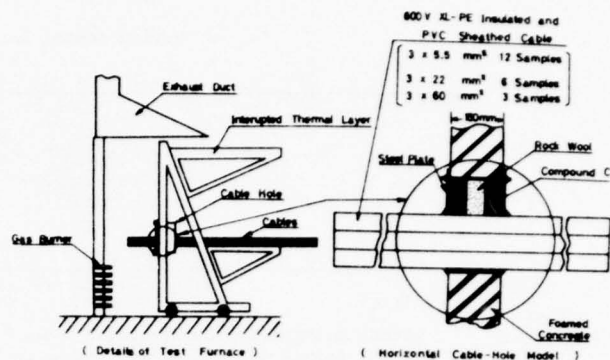


FIGURE 4

Horizontal Cable-Through-Hole Test

Experiment - 1

Model cable-through-holes were sealed with the intumescent putty(Compound C) and rock wool as shown in Figure 5 with no cables installed in the holes. The putty seals had varying thickness of 30mm, 50mm and 70mm, respectively, and the rock wool thickness was fixed. Then the model-hole was placed into the furnace and then heated for 2 hours while the temperature raised according to the indoor fire heat curve specified in JIS A 1304 "Method of Fire Resistance Test for Structural Parts of Buildings" as illustrated in Figure 9 (Curve 1). The temperature at each position shown in the Figure 5 was recorded during the heating.

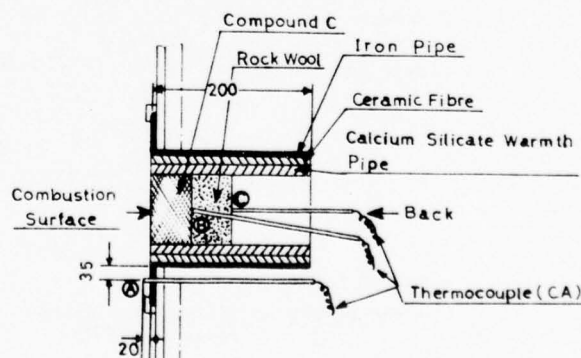
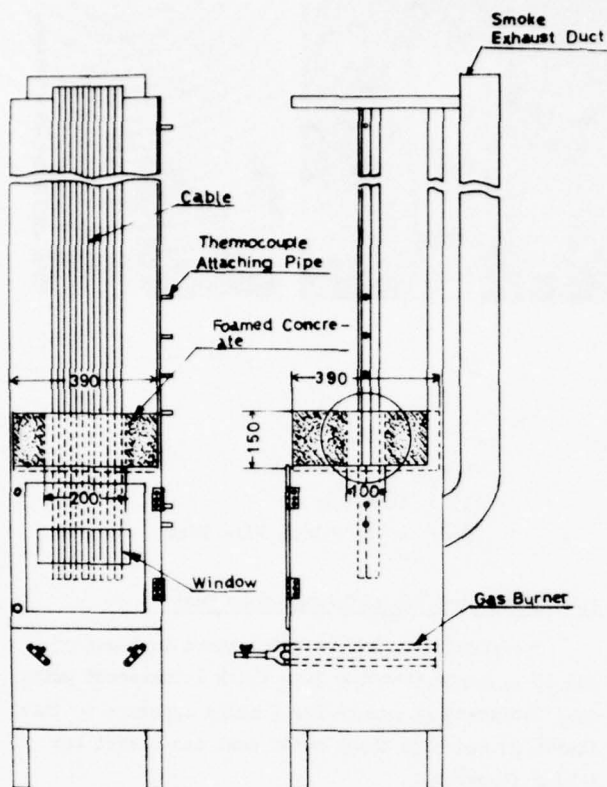


FIGURE 5

Experiment-1, Model Cable-Hole and Temperature Mesuring Point

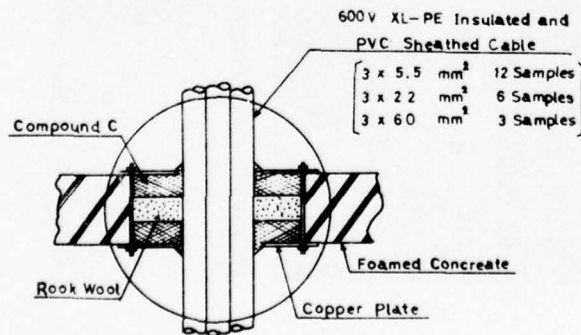
- ① Furnace Temperature Control Point
- ② Compound C Surface Temperature Measuring Point
- ③ Rock Wool Back Surface Temperature Measuring Point



(Details of Test Furnace)

FIGURE 6

Vertical Cable Hole Test



(Vertical Cable Hole Model)

FIGURE 7

Vertical Cable Hole Test

Experiment-2

The model cable hole in which twenty-one cable samples of 1.5m length were installed was sealed with the 50mm thickness of intumescent putty and rock wool as shown in Figure 4. Then the model cable-hole was placed into the furnace and heated for 2 hours while raising of the temperature was accorded to indoor fire test curve specified in JIS A 1304 (maximum 1040°C).

3.2.2 Vertical Cable-Through-Hole Test

In order to test the fire resistance of the vertical cable-through-hole, we designed a furnace as shown in Figure 6.

Experiment-3

A concrete model cable-hole in which 21 cable samples of 1.5m length were installed was placed in the furnace. The model cable-hole was sealed with the 50mm thickness of intumescent putty and rock wool, respectively, as shown in Figure 7. Then heat was applied from beneath the model hole for 2 hours while the temperature raised according to the indoor fire heat curve specified in JIS A 1304.

4. Test Results

4.1 Vertical Flame Test (IEEE, Std-383-1974)

The flaming characteristics and the PVC sheath char distances are shown in the Figure 8. The Figure 8 shows that, in the case of sample-4, the flame have spreaded over the full length of the cable tray only 6 minutes exposure to the burner flame and all the PVC sheath have also been charred. In contrast, Sample-1 shows a suppressed flame height of 1m at the maximum spread after 8 minutes after the exposure to flame and then receded, and PVC sheath char distance is only 65cm. In the case of Sample-2, a flame height at the maximum spread, and PVC sheath char distance are 0.7m after 10 minutes and 50cm, respectively. The result on Sample-3 exhibit the flame height of 0.6m at maximum spread after 12 minutes exposure and PVC sheath char distance of 45cm.

These results shown that the 2mm thick extruded layer of Compound A and the wrapping layer of Compound B-tape are equivalently as effective as the intumescent coatings in flame spreading resistance.

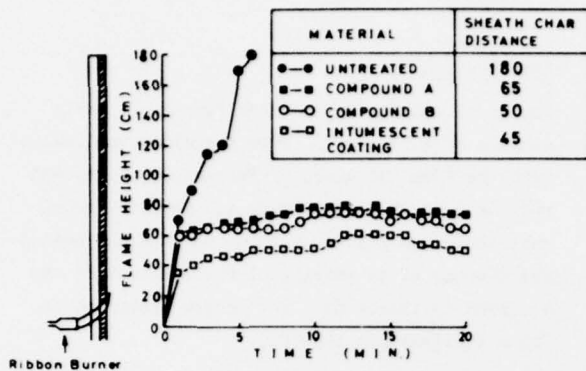


FIGURE 8
Results of IEEE-Std-383 Flame Test

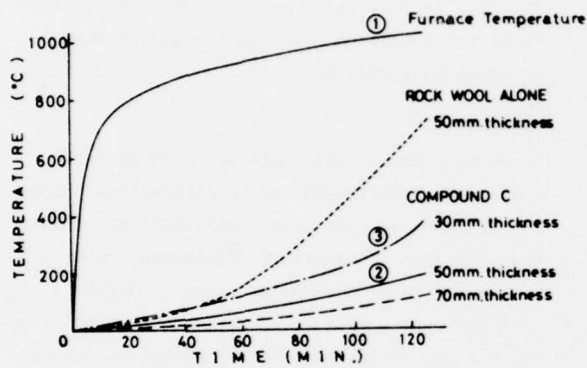


FIGURE 9
Results of Experiment-1

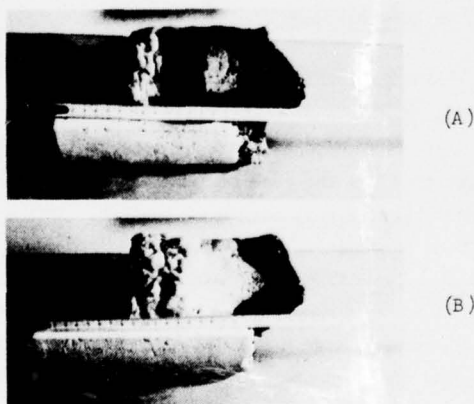
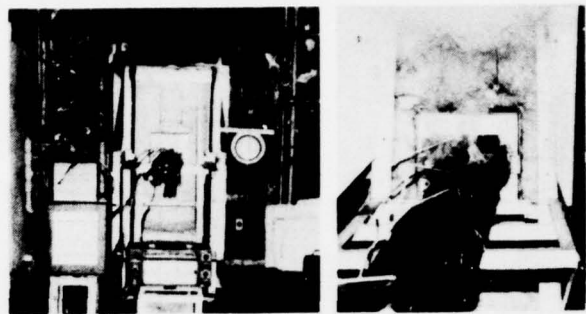


FIGURE 10

Results of Experiment-1

- (A) 50mm Thickness Filled Compound C x 2hrs. Fire Test
(B) 50mm Thickness Filled Compound C x 1hr. Fire Test



(A) (B)

FIGURE 11

View of Experiment-2

- (A) : Test Furnace
(B) : After 2 hrs. Fire Test

4.2 Horizontal Cable-Through-Hole Test

The results on Experiment-1 shown in Figure 9 and 10 indicate that the 50mm thick intumescent putty seal satisfactory endure for 2 hours exposure to fire (Curve 2) and 30mm thick putty seal can resist for 1 hour (Curve 3).

Results of Experiment-2 are shown in Figure 11. The flame spreading along the cable sample is completely prevented at the sealed cable-through-hole.



(A) (B)

FIGURE 12

View of Experiment-3

- (A) : Test Furnace
(B) : After 2 hrs. Fire Test

4.3 Vertical Cable-Through-Hole Test

Figure 12 illustrates the results of Experiment-3 in which it is also revealed that the flame spreading along the cable sample is perfectly prevented at the sealed cable-through-hole in the vertical test.

5. Applications

Compound A, in the form of an extrudate has already found application to the Leaky Coaxial Cable (or LCX) which is insulated and sheathed with PE used for police radio system for under ground street in great city. LCX cables are usually installed in the ceiling where the space is greatly limited for the application of coatings. Therefore, the cable construction including a Compound A extrudate is easily installable and can overcome the disadvantage of conventional coatings. Investigations are progress on the application of a Compound A-sheet as a wrapping material for a group of cables and also on the application of Compound A-tube, "C" shaped in cross section for a certain cable as illustrated in Figure 13 and 14.

It is found that Compound B-tape is applicable to large diameter cables such as Oil-Filled cables, and also suitable for a small group of cables as illustrated in Figure 15 and 16.

Compound C putty has already been used in nuclear power generating stations in Japan. Other examples of applied state of Compound C is shown in Figure 13.

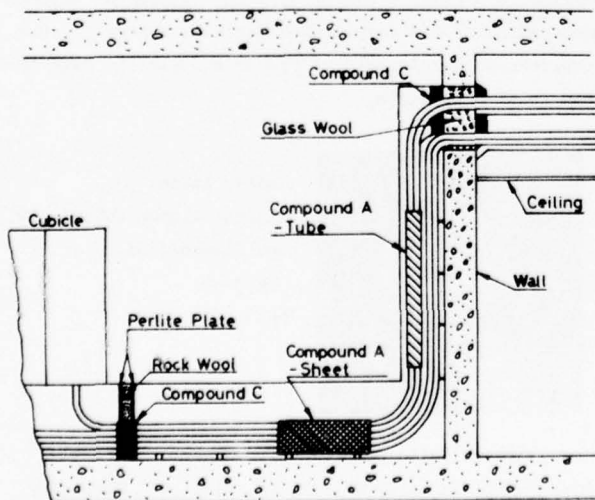


FIGURE 13

Example of Line with Compound A, B, and C

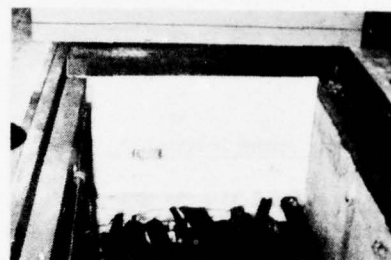


FIGURE 14

Example of Applied State of Compound A-sheet and Compound C

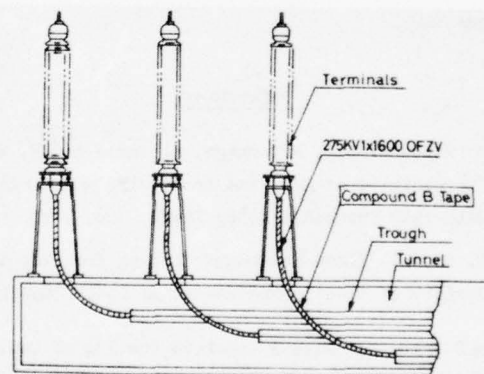


FIGURE 15

Oil-Filled Cable with Compound B Tape



FIGURE 16

275kV Oil-Filled Cable with Compound B

6. Conclusions

The development of new intumescent materials which are classified into three types ; i.e. the thermoplastic compound, the rubber-like compound and the putty-like compound, has resulted in the new fire preventing methods for cable lines.

Those materials can be used in every forms, as extrude over cable sheath, as wrapping layer with rubber-like self-bonding tape or as putty seal packed into a cable-through-hole or other cavities. They have been already used preferably in police radio system for under ground streets and in nuclear power generating stations and in substations.

Acknowledgements

The authors would like to express their thanks to Mr. Hiroshi Inoue and Dr. Hideo Fujita for helpful discussion and for giving them an opportunity to publish this paper. The authors also wish to express sincere thanks to Mr. Keiji Ichikawa, Mr. Kazunori Terasaki, Mr. Yasuo Ijiri, for their devotion to the present work.

References

1. H. Matsubara, C. Matsunaga, A. Inoue and N. Yasuda "Development of New Fire-Proof Wire and Cable", 24th IWCS Proceedings, pp 15-25, Nov. 1975.
2. R. Slysh, "Flame-Retardant Coating for Plastics", Society of Plastic Engineers, pp 13-16, May 1974.
3. M.D.Sympson, "Fire Protective Coating of Cables", Symposium on Fire Protection of Cables, pp 18-21, 1972.
4. N. Foulsham, "The design of Power Station Cable Installations to Limit the Effects of Fire" Symposium on fire protection of cables, pp 25-27, May 1972.
5. Vandersall, H.L. J. Fire and Flammability, Vol 2, p. 97, 1971.



Takahiko Yabuki
Dainichi-Nippon Cables, Ltd.
3-4-1, Marunouchi,
Chiyoda-ku,
Tokyo, Japan

Takahiko Yabuki graduated from Morioka Technical College majoring Electrical Engineering in 1945 and immediately joined Dainichi-Nippon Cables Ltd. where he had been mainly engaged in the designing of the insulated wires and cables. He is now a sales manager of those wires and cables.



Yooichi Koide
Dainichi-Nippon Cables, Ltd.
Higashimukaijima,
Amagasaki,
Japan

Yooichi Koide graduated from Shizuoka University majoring industrial chemistry in 1959 and immediately joined Dainichi-Nippon Cables Ltd. where he was initially engaged in manufacturing section of wires and cables. Now he is a Senior Research Engineer in Material Laboratory of his company and has been engaged in the research and development of rubber and plastic materials and related products.



Tamotsu Kaide
Dainichi-Nippon Cables, Ltd.
Higashimukaijima,
Amagasaki,
Japan

Tamotsu Kaide graduated from Hyogo Technical High School in 1958 majoring in Industrial Chemistry and immediately joined Dainichi-Nippon Cables, Ltd. He has been engaged in research and development work on rubber and plastic materials for cables.



Mitio Takada
Dainichi-Nippon Cables, Ltd.
Higashimukaijima,
Amagasaki,
Japan

Mitio Takada graduated from Hyogo Technical High School in 1964 majoring in Industrial Chemistry and immediately joined Dainichi-Nippon Cables, Ltd. He has been engaged in research and development work on rubber and plastic materials for cables.

RADIATION CURABLE POLYOLEFIN COMPOUNDS
FOR FLAME RETARDED WIRE AND CABLE INSULATION

M. F. Maringer, J. W. Biggs
Research Department
U.S. Industrial Chemicals Company
Cincinnati, Ohio

P. E. Pinnow
Marketing Department
U.S. Industrial Chemicals Company
Cincinnati, Ohio

Summary

Increased energy costs for thermal crosslinking and the greater processing flexibility of radiation curing have resulted in a trend towards radiation curing of Wire and Cable insulation in the last three years. Growth for flame retardant polyolefin insulation has been limited by the availability of acceptable materials. Porosity and low strength properties are the two principal problems encountered with radiation curing. Tailoring of compound formulations specifically for radiation curing is required. Data for commercial compounds are provided.

Introduction

The high versatility and large volume applications of polyolefins are well known and strongly established. This growth has been principally with unmodified polymers or with limited modification to obtain stability, or a desired color or to change surface properties. One application area which is rapidly growing and extending the range of commercial polyolefin based products is filled compounds, especially fire retardant compounds. However, for many applications the thermoplasticity of polyolefins leads to serious temperature limitations. Their inherent mechanical toughness at room temperature is due to their high level of crystallinity which is lost at elevated temperatures. To preserve the toughness and resistance to deformation above the crystalline melt point, it is necessary to convert the polymer from a thermoplastic to a thermoset structure through crosslinking of the polymer chain. Crosslinking eliminates the important reprocessing characteristics of polyolefin resins resulting in the loss of recyclability. However, some applications such as wire and cable insulation, demand performance properties and long life requirements which far exceed any advantages of resin reuse.

Low density polyethylene and ethylene copolymers may be crosslinked either by thermal treatment (1) using a peroxide or by excitation with a high energy source such as radiation, (2) or ultraviolet light. For polyolefin based compounds in nonthin film applications, thermal crosslinking using peroxides has been the principal commercial method employed. In the past three years, radiation curing has been experiencing rapid growth. With this growth, there has been an increasing demand for application of radiation curing to polyolefin compounds.

Crosslinking Processes

Thermal crosslinking provides a degree of flexibility in selection of the chemical curing system and its concentration. However,

this selection prescribes the time and temperature of cure to a large degree. It requires heat to obtain curing and pressure to prevent void formation. Steam is generally the best heat transfer medium to provide these requirements. Production rate is limited by the length of the Continuous Vulcanizer (CV) Tube and the rate of curing of the compound. Thus, considerable production space is required since product curing is carried out in line after the product fabrication process. Maintenance requirements common to a steam system and air pollution problems of a steam generation plant are other disadvantages.

Radiation curing offers increased flexibility in product processing. For example, the formed product can be cured at a later date or cured to varying degrees without a change in compound formulation. Without temperature limitations in the compound, fabrication and extrusion may be performed at a faster rate. It has been reported that 80% of the radiation equipment in operation has been installed in the last three years. Space requirements for equipment are reduced and are more flexible without the need for in-line extrusion and curing. Maintenance and equipment problems are reduced with the elimination of the need for steam. However, radiation processing requires more stringent safety procedures and it can introduce employee concern for safety. Overall, growth in radiation curing is due principally to lower unit product cost compared to the cost for thermally cured products. Table I provides a summarization of data from several sources comparing radiation and thermal curing in 1972. Relative cost with each process will depend on many factors related to plant location, equipment available and company product line. For many applications, radiation curing may not be as favorable as indicated by these data. However, the recent rapid growth indicates a more advantageous position for radiation curing at the present time.

Polyolefin Compounds

The growth of radiation curing for polyolefin compounds is related to the availability of materials which can be processed to finished products with acceptable performance properties. Here there has been a deficiency, especially for flame retardant compounds. Modification of the curing system of a thermally curable compound by peroxide removal does not provide a suitable compound for curing by radiation. In our developmental program, initial property evaluations on radiation treated wire insulation indicated insufficient crosslinking. Formulation modification and variation of the radiation dose in an attempt to

increase curing failed to provide acceptable insulation properties. Generally, physical properties were low, solvent extractables were high and heat distortion resistance was deficient. Often, the insulation did not pass the Underwriter's Laboratory FR-1 flame test. Density measurements led to microscopic observations and the detection of a very fine cell porosity which was also found in the uncured insulation and ultimately traced back to the pelletized compound. Therefore, formation of voids is a problem which may occur during compound preparation, extrusion onto wire or radiation curing.

The effect of porosity is illustrated by a comparison of the performance properties of porous and nonporous wire insulations (Table II). This porous wire insulation was obtained about half way through the development program. At this point, compound and processing improvements provided acceptable heat distortion properties and passage of the flame test. Porosity in the uncured material increases the radiation dose required for crosslinking. The best balance of properties obtained with radiation curing of porous wire insulation still shows inadequate tensile strength, solvent extractables and wet electrical properties. In contrast, nonporous insulation provides excellent performance properties with a low radiation dose.

To the naked eye, both porous and nonporous pellets of compounded material appear to be similar. At a magnification of 85 power, porosity is evident in the porous pellet, as shown in Figure 1. Extrusion of this material to a strand or insulation on wire results in a porous texture which, on magnification, appears as shown in Figure 2. The same magnification of an extruded strand from nonporous pellets is shown in Figure 3. The noted density data indicate the degree of porosity present and confirm that extrusion of a porous compound does not remove the voids. Porosity caused by entrapped moisture is illustrated with 85 power magnification in Figure 4. This type of porosity is detected by the naked eye. Generally, moisture absorbing pigments produce this condition.

The effect of total radiation dose on uncured porous and nonporous wire insulation is graphically illustrated in Figure 5, and the corresponding properties data are listed in Table III. Porous insulation becomes more porous at all doses while nonporous insulation develops significant porosity only at high levels of radiation. Generally, the radiation dose for initiation of porosity in nonporous insulation exceeds the dose required for optimum cure of properly formulated flame retardant polyolefin compound. Porosity formation during radiation curing is illustrated by photomicrographs taken at an 85 power magnification. Figure 6 shows slightly porous insulation after curing at 12.5 Megarads. A 20 Megarads dose produces significantly greater porosity in the same insulation (Figure 7). From these and other results, the following ideas were derived concerning the successful formulation of radiation curable polyolefin compounds.

Radiation curing requires no pressure. As noted above, this contributes economic

advantages. Also, it avoids the development of chemical compounds, such as peroxide residues, which can contribute to polymer degradation with heating or aging. However, hydrogen formation during irradiation is a strong factor in porosity formation. The dose rate is another important factor since the rate of application of radiation determines the temperature generated in the material which affects the melt strength of the compound. Thus, a combination of lack of pressure, hydrogen formation and heat generation provide favorable conditions in radiation curing for porosity formation and expansion of porosity present.

Therefore, elimination of porosity must originate at compound preparation. Compound formulation must be tailored to provide mixed materials without porosity or ingredients which will not generate porosity during processing. The combination of flame retardant additives, stabilizers, pigments, fillers, etc. employed in flame retardant polyolefin compounds can provide ideal conditions for efficient dispersion of absorbed air, moisture and other volatiles resulting in a porous composition of very fine cells. Removal of this type of porosity during fabrication is very difficult. Raw materials which liberate volatiles during processing or which are susceptible to absorbing moisture during storage can initiate or amplify porosity. Complete elimination of all absorbed volatiles and sources of volatiles is frequently not economically feasible. Often, performance properties required in the finished product necessitate such ingredients. Therefore, the production compounding process must be tailored to remove volatiles. Careful control of the degree of mechanical shear on the polyolefin polymer throughout the compounding process results in dispersion of all ingredients with a continual removal of volatiles through a breakdown of the fine cell porosity. Accurate density measurements provide a quality control measure for obtaining the desired nonporous material.

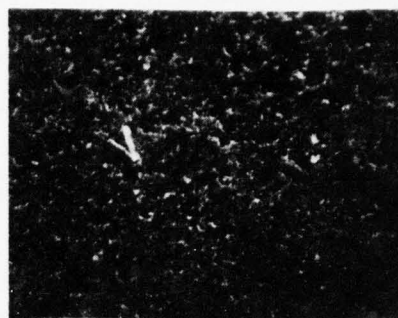
These procedures were used to produce a compound which cures efficiently with radiation to a wire insulation exhibiting excellent performance properties as noted in Table II. Photomicrographs of this nonporous wire insulation exhibit no voids with a 12.5 Megarad dose (Figure 8) and only slight porosity at 20 Megarads (Figure 9).

FIGURE 1



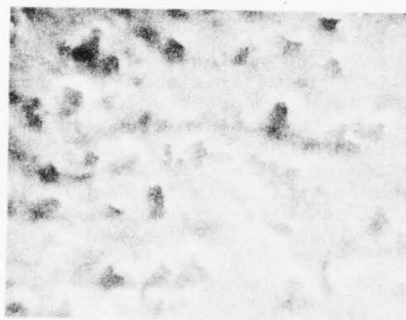
Porous - Cube
Density = 1.137 g./cc.
Max. Density = 1.258 g./cc.

FIGURE 4



Compound Containing Moisture

FIGURE 2



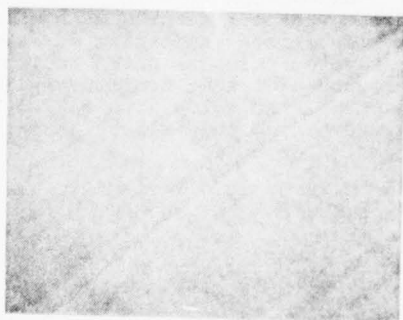
Extruded Strand - Porous
Density = 1.228 g./cc.
Max. Density = 1.258 g./cc.

FIGURE 6



12.5 MR Wire Insulation - Slightly Porous
Density = 1.205 g./cc.
Max. Density = 1.258 g./cc.

FIGURE 3



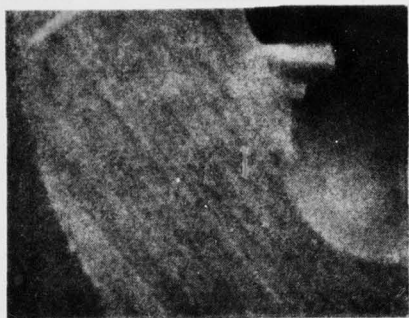
Extruded Strand - Nonporous
Density = 1.297 g./cc.
Max. Density = 1.297 g./cc.

FIGURE 7



20 MR WIRE Insulation - Porous
Density = 1.136 g./cc.
Max. Density = 1.258 g./cc.

FIGURE 8



12.5 MR Wire Insulation - Nonporous

Density = 1.292 g./cc.

Max. Density = 1.297 g./cc

FIGURE 9



20 MR Wire Insulation - Very Slight Porosity

Density = 1.284 g./cc.

Max. Density = 1.297 g./cc.

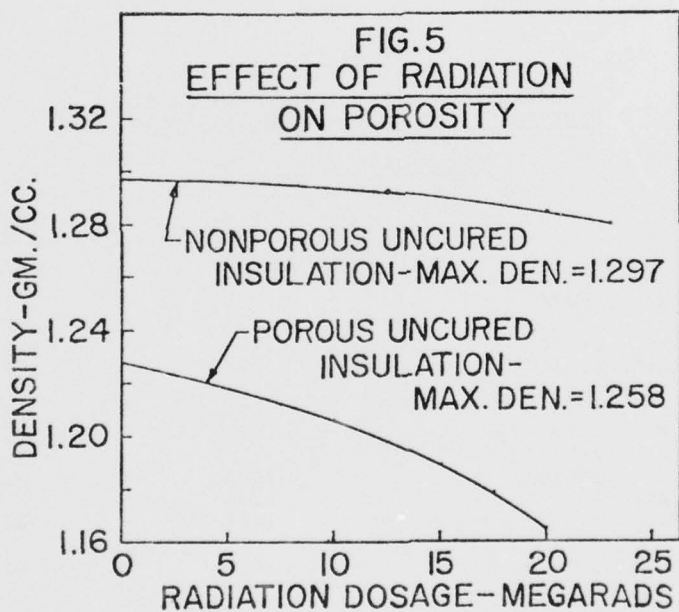


TABLE I

Radiation Curing vs. Thermal Curing
Equipment and Operational Cost (1972)

Unit	Radiation	Thermal
Compounds	1.0 MEV 25 MA Accelerator PVC, PE, Rulan, Kynar, FEP,	3-1/2 Horiz. CV Line XLPE, Silicone, Neoprene
Total Cost of Line	\$260,000	\$200,580
Amortization (5 Yr.)	\$ 52,000	\$ 40,000
Direct Labor	\$ 24,000	\$ 36,000
Overhead	\$ 24,000	\$ 36,000
Utilities	\$ 6,000	\$ 40,000
Insurance	\$ 2,000	\$ 1,110
Maintenance	\$ 12,000	\$ 16,000
Operating Supplies	-	\$ 15,000
Scrap Loss	\$ 3,600 (3%)	\$ 18,400 (10%)
Hourly Operational Cost (6000 Hrs./Yr.)	\$ 20.60	\$ 33.60
Annual Output	300 x 10 ⁶ Ft.	180 x 10 ⁶ Ft.
Cost Per Ft.	\$.00412	.00112

TABLE II

Radiation Curing - Optimum Dosage
Porous Vs. Nonporous Wire Insulation

Performance Properties

	Nonporous 12.5 Mrads Cure	Porous 15 Mrads Cure	Spec.*
Density-Cured Insulation, g./cc/	1.292	1.187	
Max. Density, g./cc.	1.297	1.258	
Density-Compound Pellet, g./cc	1.286	1.137	
Density-Uncured Insulation, g./cc	1.297	1.228	
Tensile Strength, psi	2000	1420	1800 min
Tensile Elongation, %	430	370	250 min
Heat Aging - 7 days @ 121°C			75 min
% Retention of Tensile Strength	>100	>100	75 min
% Retention of Elongation	>100	97	
Xylene Extractables, Wt. %	10.4	24.0	30 max
Heat Distortion-121°C., 500 gm. load - %	25.5	25.7	30 max
Electrical Moisture Absorption			
SIC after 24 Hrs. -75°C H ₂ O, 40 V./mil.	3.2	3.2	6.0 max
Increase in Capacitance			
1-14 Days, %	0.6	33.0	3.0 max
7-14 Days, %	0.6	12.9	1.5 max
Stability Factor after 14 Days	0.24	2.3	1.0 max
Flame Test, UL FR-1	Pass	Pass	Pass
Limiting Oxygen Index	28.5	26.5	-

Extruded as 1/32" wall insulation on #12 AWG Wire Irradiated with High Energy Electron Beam

* Insulated Power Cable Engineers Pub. No. S-66-524

TABLE III

Effect of Radiation Dose on Properties of Wire Insulation

Performance Property	Condition of Uncured Insulation	Radiation Dose in Mrads						
		0	10	12.5	15	17.5	20	23
Density, g/cc	Porous	1.228	1.204	1.202	1.187	1.174	1.147	-
	Nonporous	1.297	-	1.292	1.290	1.284	1.284	1.282
Tensile Strength, psi	Porous	960	1350	1460	1420	1395	1365	-
	Nonporous	1100	1840	2000	1980	1750	1740	1680
Elongation, %	Porous	570	400	405	370	345	325	-
	Nonporous	570	410	430	400	350	320	300
Heat Distortion	Porous	-	-	37.2	25.7	29.4	27.0	31.2
	Nonporous	-	30.9	25.5	25.7	27.7	23.9	23.5
UL FR-1 Flame Test	Porous	Pass	Pass	Pass	Pass	Pass	Pass	-
	Nonporous	Pass	Pass	Pass	Pass	Pass	Pass	Pass



Melvin F. Maringer received a Ch.E. degree in Chemical Engineering in 1952 from the University of Cincinnati and pursued process development work with the Container Corporation of America and industrial finishes development with Inmont Corporation. Joined the Central Research Laboratories of the U.S. Industrial Chemicals Co. in 1956 and has carried out product and applications development work; presently a Research Associate for flame retardant compounds. Member of the Society of Plastics Engineers, American Chemical Society, Rubber Division and Polymer Division of ACS.

James W. Biggs received a B.S. degree in Education from Eastern Illinois State College in 1954. Joined U.S. Industrial Chemicals Co., Polymer Service Laboratory, in 1956. Held various positions as Research Engineer in the Pilot Plant development of polyethylene and ethylene vinyl acetate copolymers. Worked extensively in process development in synthesis and finishing processes in polyethylene. Joined U.S. Industrial Chemicals Research in Cincinnati in 1974 as a Senior Chemist in the Polyolefins Compounding Group.



Paul Pinnow received a B.S. degree in Chemical Engineering in 1968 from Case-Western Reserve University, Cleveland, Ohio. He joined U.S. Industrial Chemicals Co. in 1969 at the Tuscola, Ill. Technical Services Laboratory as an Applications Engineer and Technical Services Engineer for Wire & Cable, Tubing and Profile Extrusion, Extrusion Coating Products. In 1973 he became the Market Development Specialist for flame retarded polyolefin compounds.

FILLED VINYL JACKET COMPOUNDS

J. A. Falter
P. C. Warren
Bell Laboratories
Murray Hill, New Jersey 07974

Abstract

Alumina trihydrate and calcium carbonate were added to a vinyl jacket compound up to 0.25 volume fraction to study the effects on processing, mechanical and flammability properties. The results were obtained under conditions of constant plasticizer and constant low temperature impact (variable plasticizer). The most useful compounds emerged from the latter category. The highest filled formulations appropriately compensated with extra plasticizer were slightly cheaper, had good elongation and processed reasonably well. They were twice as flexible as the unfilled formulations. On the negative side, the tensile, shear and tear strengths were roughly halved over those of the control. Alumina hydrate-filled materials burned at a constant oxygen index when maintained at constant low temperature brittleness, while the calcium carbonate-filled vinyl was considerably more flammable.

Introduction

One way to reduce costs and extend vinyl jacket materials is to incorporate inorganic fillers into them as efficiently as possible. An added incentive is to use functional additives such as alumina hydrate (for improved fire resistance) or calcium carbonate (for absorption of acidic gases during pyrolysis or combustion). While many commercial vinyl compounds currently use either of these inorganics in moderate amounts (up to 0.1 volume fraction), we decided to measure the effects of loadings as high as 0.25 volume fraction on mechanical, electrical, low temperature impact, processing and flammability properties under two conditions: constant 40 phr plasticizer and constant low temperature brittleness (variable plasticizer). The results would allow us to document the advantages of highly filled vinyl as applied to wire and cable jackets. We were particularly interested in identifying those properties that might give a nonlinear response to increasing filler and/or plasticizer concentrations.

Experimental

All vinyl compounds were initially blended in a Henschel mixer, followed by fluxing in a Banbury mixer and then sheeted on a two-roll mill. A summary of the standard tests run on compression molded .075" thick samples is included in Table 1.

Processing

Early experiments utilized an initial dry mix on a two roll mill only, but the low temperature brittleness performance of the resulting filled samples suffered by as much as 3-5° compared to more efficiently mixed compounds.

We have concluded that a filler study must include adequate processing to achieve optimum performance of the material. The high speed Henschel mixer served to disperse all components evenly as well as break up the inevitable agglomerates in the filler, while the Banbury assured wetting of all surfaces.

Filler Description

Any discussion of filler performance must characterize the inorganic material as completely as possible since the final properties of the vinyl compound are highly dependent on filler shape and surface chemistry as well as particle size and distribution. Based on earlier work in this laboratory, we narrowed our study to two functional fillers, calcium carbonate and alumina hydrate. Commercial calcium carbonates are available in a wide range of particle sizes and distributions, and Omyalite 90T (Pleuss-Stauffer), a calcium stearate coated calcium carbonate, was eventually selected as the best example of the lot.¹ Similarly, Hydral 710 (Alcoa) was picked over several candidates of alumina hydrate.² Sedigraph analyses are shown in Figure 1 for these materials, both are shown to be small particle size inorganics with very narrow distributions. Finally, both fillers showed low oil absorption, a characteristic that encourages plasticizer to interact with resin rather than the filler surface.

Results and Discussion

Mere addition of large amounts of inorganic filler to an existing vinyl formulation to cheapen it or to improve physical, electrical, processing and/or flammability properties would probably give undesirable material. On the other hand, controlled compensation with appropriate amounts of plasticizer would hopefully produce useful compounds. We chose to maintain constant the low temperature brittleness (LTB) property as both filler and plasticizer gradually dominated the compound and study the effect on the overall performance of the material. Adding equivalent amounts of filler to a constant 40 phr plasticized vinyl served as our control. Two separate studies were conducted, one incorporating alumina hydrate (Hydral 710) and the other utilizing calcium stearate-coated calcium carbonate (Omyalite 90T).

Low Temperature Brittleness

Figure 2 compares the low temperature performance of constant plasticizer compounds with that of constant LTB materials. Both alumina trihydrate and coated calcium carbonate had only a relatively moderate effect on this property in the former case but it accumulated to a 10-15° deterioration at 0.25 volume fraction of solids. The constant LTB formulations were empirically determined and are listed for

each filler in Table 2. The two inorganics were remarkably similar in LTB performance, the calcium carbonate being slightly more efficient than alumina hydrate -- 16 additional phr plasticizer were necessary to compensate for 0.25 volume fraction of the former filler while 20 phr plasticizer were necessary for the latter, as illustrated in Figure 3. Furthermore, it is obvious that increasing amounts of filler required ever-increasing amounts of plasticizer. For instance, the first 20 phr of calcium carbonate necessitated just 2 phr of plasticizer, but the last 25 phr filler demanded over twice that amount.

Elongation

Either filler added directly to the 40 phr plasticized formulation gave a precipitous drop in elongation as shown in Figure 4. Constant LTB formulations, however, gave only minor negative responses -- the alumina hydrate-filled materials stabilized at about 70% of the unfilled value, while the coated calcium carbonates gave essentially no deterioration. Clearly the maintenance of the LTB property also guarantees acceptable elongations for jacket materials.

Tear, Tensile, Shore A Hardness, and Shear

Quite the opposite results were apparent from other commonly measured mechanical properties such as tear, tensile and shear strengths, and hardness, summarized in Table 3. In all cases the constant 40 phr plasticized formulations gave only minor (0-20%) reductions relative to the unfilled material, but the constant LTB compounds eroded linearly with increasing filler/plasticizer additions such that each property at 0.25 volume fraction (of either filler) was approximately half of the original. Since the shear and tear performance is very relevant to jacket applications, it is primarily here that the designer has to decide how much filler can be tolerated and still have a useful product.

Flexural Modulus

Additions of filler to constant plasticized formulations had a stiffening effect resulting in doubled flexural moduli (8300 psi) at 0.25 volume fraction over the unfilled control (4100 psi). Constant LTB materials, however, had half the original value (2200 psi) for the heaviest filler loadings. Two facts were thus apparent: plasticizers soften much faster than fillers stiffen at room temperature and they also are relatively inefficient at preserving impact properties at lower temperatures. As a result, highly filled vinyl jacket formulations with good low temperature properties are very flexible materials indeed.

Melt Flow

If a material cannot be manufactured in commercial equipment it is of little practical use. The relative processing characteristics of the constant plasticizer and constant LTB materials were examined at one shear stress, shown in Figures 5 and 6. An almost straight line deterioration of melt flow described the

constant plasticizer materials. The constant LTB compounds, however, initially dropped to half the unfilled flow rate but at higher loadings regained and, in the case of coated calcium carbonate, surpassed the initial value. (This latter case is presumably due to the lubricant effects of calcium stearate on the surface.) Constant LTB compounds would therefore be expected to show only minor differences in processing relative to the unfilled control.

Dielectric Constant and Volume Resistivity

While this investigation was primarily concerned with jacket formulations, we did examine two electrical properties; dielectric constant and volume resistivity. The former property increased linearly with filler content in both constant plasticizer and constant LTB materials for both fillers. For instance, the constant LTB vinyl increased from 3.93 to 5.85 and 5.31 for the highest filled alumina hydrate and calcium carbonate compounds, respectively. Volume resistivities showed a mixed response -- the dry and wet values for the constant plasticizer materials increased while those for the constant LTB formulations decreased (due to the increased plasticizer concentration), in some cases up to an order of magnitude.

Flammability

Burning properties of cable jackets have become extremely important in recent years and we have accordingly determined oxygen index on our formulations, shown on Figure 7. The alumina hydrate-filled constant plasticizer compounds showed a steadily increasing oxygen index. For instance, the 0.25 volume fraction vinyl gave a value of 38, up 7.5 units over the unfilled control. In epoxy systems alumina hydrate is reported³ to become increasingly more effective at higher loadings, but this observation was only slightly evident in our work. The constant LTB material gave a constant oxygen index. Apparently LTB and oxygen index are about equally sensitive to plasticizer and alumina hydrate, and maintenance of the first property also tends to maintain the second. A practical corollary is that it is probably better not to use alumina hydrate at all for maximum mechanical performance at maximum fire resistance. (Such a statement does not, however, consider that oxygen index might not model a true fire situation, that the filler might be economically advantageous or that low smoke benefits might accrue from its use.)

Coated calcium carbonate lowered the oxygen index in a linear manner. Constant plasticizer mixtures dropped by about 3.5 units at 0.25 volume fraction filler and constant LTB compounds decreased by twice that amount. On the plus side, however, the calcium carbonate at loadings of 0.2 volume fraction or higher absorbed about three-quarters of the corrosive HCl gas emitted during combustion,⁴ as shown in Figure 8. (In separate experiments it was determined that very small particle size precipitated calcium carbonates increased the absorption to 90%. These high surface area fillers are not currently practical, however, because of very poor mechanical properties at the higher loadings.) While the acid-absorbing fillers have not been utilized to

any great extent commercially, it is noteworthy that calcium carbonate is probably the most economical and practical of all the basic salts that might be incorporated into vinyl jackets for this purpose.

Economics

Based on August 1976 bulk prices, the lb-vol cost of all components in the unfilled control would be \$0.387 as shown in Figure 9. Both alumina hydrate and coated calcium carbonate give cost benefits amounting to about 6% for the highest loaded alumina hydrate constant LTB compound and 15% for the calcium carbonate analogue. The lesser filled materials exhibit proportionately lower benefits. Recent price increases have indeed rendered the cost saving virtues of alumina hydrate meager. Even coated calcium carbonates are not as cheap as they might appear when one considers they are used on a volume basis - the meaningful lb-vol cost is almost half that of the unfilled compound. Therefore, both fillers should be considered primarily as functional additives and only secondarily as cost reducing extenders.

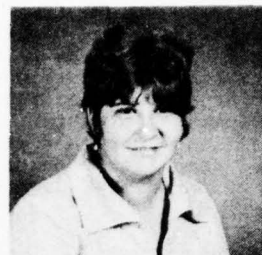
Conclusions

Addition of inorganic filler to vinyl jacket compounds must be accompanied by appropriate amounts of plasticizer to maintain a selected low temperature brittleness property. Only minor reductions in elongation result but other important mechanical properties such as shear, tensile, tear and hardness deteriorate significantly at high loadings. The resulting materials are all noticeably more flexible than the unfilled control. The filled compounds can all be processed on commercial equipment, albeit less easily in some cases. Flammability properties will either be just maintained (alumina hydrate) or will deteriorate (calcium carbonate) depending on the filler, but in the latter case the potential for reducing corrosive smoke during combustion exists. Based solely on oxygen index results, alumina hydrate is a useful but only mildly effective fire retardant for vinyl jacket applications. There are definite cost saving advantages in using fillers, but only up to a maximum of about 15% savings. The decision of when and how much to use fillers is thus the usual complex one that rests on a careful analysis of the end use of the material and then compromising on the best cost/performance design.

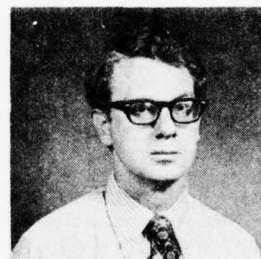
References

1. Earlier unpublished work by E. Scalco helped determine the selection of Omyalite 90T over other calcium carbonates.
2. This decision was based in part on a report by S. Kaufman and M. M. Yocum, "Balancing Flame Retardancy and Low Temperature Properties in PVC," in Fire Retardants: Proceedings of 1975 International Symposium on Flammability and Fire Retardants, ed. V. M. Bhatnagar, Technomic Press (Westport, Conn., 1976), p. 238.
3. F. J. Martin and K. R. Price, J. Appl. Polym. Sci., **12**, 143 (1968).

4. We are indebted to M. M. O'Mara for his advice on the use of the Schoeniger Combustion Apparatus for measuring HCl absorptions.



Julia A. Falter received a B.S. in Plastics Technology from Lowell Technological Institute in 1971 and is now a graduate student in the field of Chemical Engineering at Steven's Institute of Technology. She joined the Plastics Chemistry Research and Development Department at Bell Laboratories, Murray Hill, New Jersey in 1974 where she was engaged in a study of fillers for PVC jacketing formulations. She is presently involved in reclamation of polyolefin scrap.



Paul C. Warren is a Member of Technical Staff at Bell Laboratories, Murray Hill, New Jersey. He received an A.B. degree in Chemistry from Wesleyan University and a PhD in Organic Chemistry at Cornell in 1969. His main interest at Bell Labs has been flammability of plastics materials, most recently in PVC wire and cable applications.

Table 1 - Test Methods

Tensile Strength and Ultimate Elongation	ASTM D-412, Specimen Die C and speed of 20 in./min.
Tear Resistance	ASTM D-624, Specimen Die B and speed of 20 in./min.
Shear Strength	Western Electric Material Specification test. Force required to drive a one inch 45° wedge with a 0.30 inch flat through a 0.075 inch thick plaque.
Hardness	ASTM D-2240, Shore A Durometer.
Stiffness in Flexure	ASTM D-747.
Low Temperature Brittleness	ASTM D-746, 20 specimens per temperature, only complete breaks counted as failures.
Oxygen Index	ASTM D-2863, 0.075 inch thick specimens.
Volume Resistivity (Dry & Wet)	ASTM D-257-75.
Dielectric Constant	ASTM D-150-74.
Melt Flow	ASTM D-1238 at 170°C and 20,000 gram load using a one inch die with 45° entry angle.
HCl Absorption	Method utilizing Schoeniger Combustion Apparatus. ⁴

Table 2 - Test Formulations

		<u>Constant Plasticizer</u>	<u>Constant LTB</u>
Resin	- GP5-00003 (Geon 103EP)	100 phr	100 phr
Plasticizer	- Mixed Dialkyl Phthalate (Santicizer 711)	40 phr	As specified in Figure 3
Stabilizer	- Tribasic Lead Sulfate (Tribase)	5 phr	5 phr
Fire Retardant	- Antimony Oxide	3 phr	3 phr
Lubricant	- Stearic Acid	0.5 phr	0.5 phr
Filler	- Calcium Stearate Coated Calcium Carbonate (Omyalite 90T) or Aluminum Oxide Trihydrate (Hydral 710)	0,25,50,75 or 100 phr	0,25,50,75 or 100 phr

Table 3 - Mechanical Properties

<u>Filler</u> <u>phr Filler/phr Plasticizer</u>	<u>Volume</u> <u>Fraction</u> <u>Filler</u>	<u>Tensile</u> <u>Strength</u> <u>(psi)</u>	<u>Tear</u> <u>Resistance</u> <u>(lb/in)</u>	<u>Shear</u> <u>Strength</u> <u>(lb)</u>	<u>Hardness</u> <u>Shore A</u>
None 0/40	0	3175	880	990	91
Hydral 710					
25/40	0.083	2921	827	970	91
50/40	0.154	2710	817	877	90
75/40	0.214	2695	778	813	89
100/40	0.267	2580	747	810	87
25/41.5	0.081	2795	704	810	90
50/47	0.145	2426	649	746	85
75/53.8	0.195	1951	568	650	83
100/60	0.236	1755	489	572	83
Omyalite 90T					
25/40	0.075	2881	835	957	90
50/40	0.139	2751	794	857	88
75/40	0.195	2404	785	790	87
100/40	0.244	2374	770	733	86
25/42	0.074	2631	835	893	90
50/46	0.133	2467	736	730	87
75/51	0.181	2284	581	650	84
100/56	0.220	1898	552	533	80

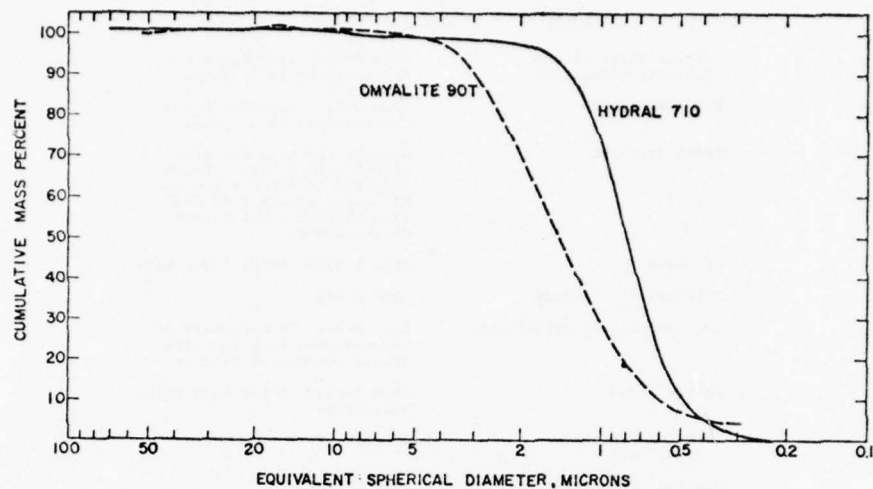


Figure 1 - Sedigraph Analyses of Filler Particle Sizes

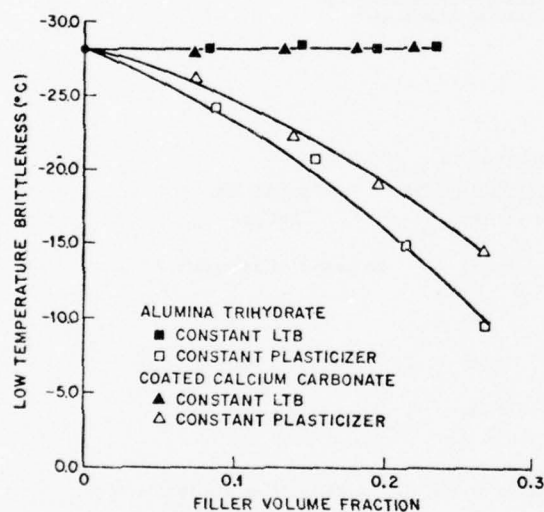


Figure 2 - Effect of Fillers on Low Temperature Brittleness

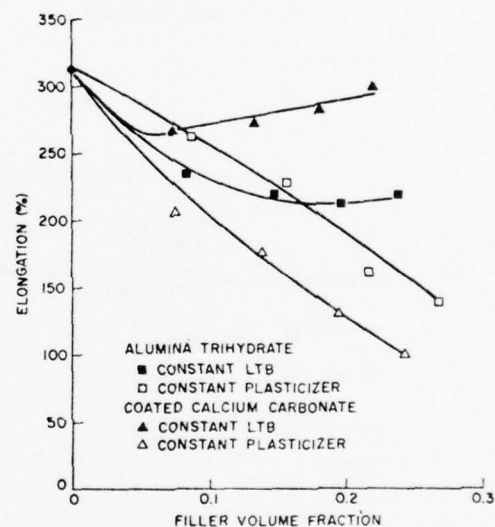


Figure 4 - Effect of Fillers on Elongation

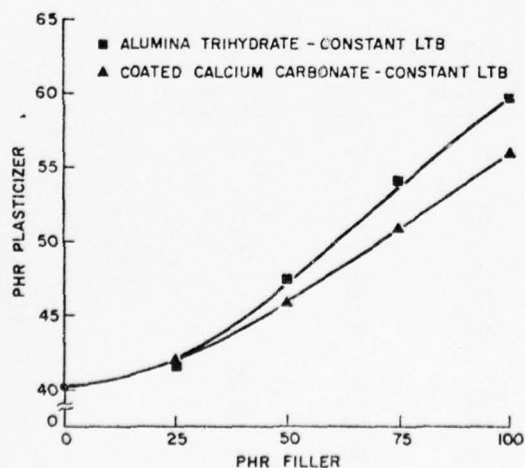


Figure 3 - Plasticizer Compensation for Added Filler

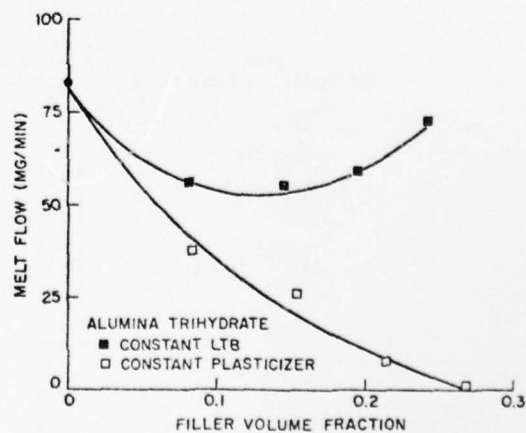


Figure 5 - Effect of Alumina Trihydrate on Melt Flow

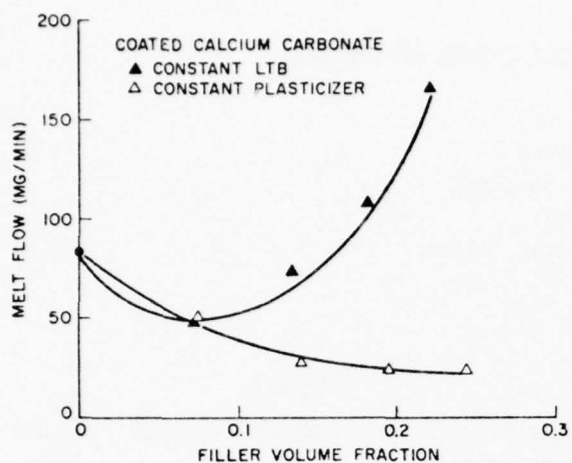


Figure 6 - Effect of Coated Calcium Carbonate on Melt Flow

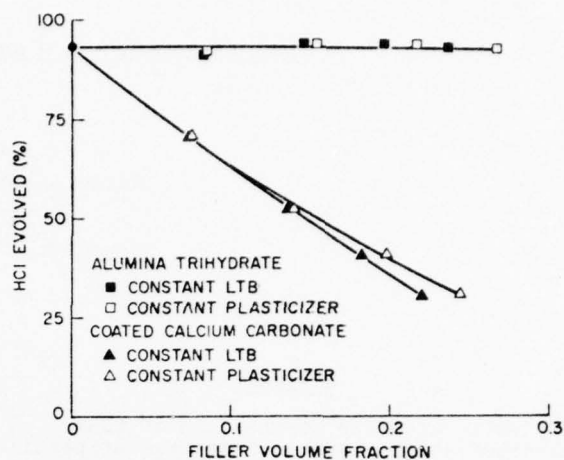


Figure 8 - Effect of Filler on HCl Absorption

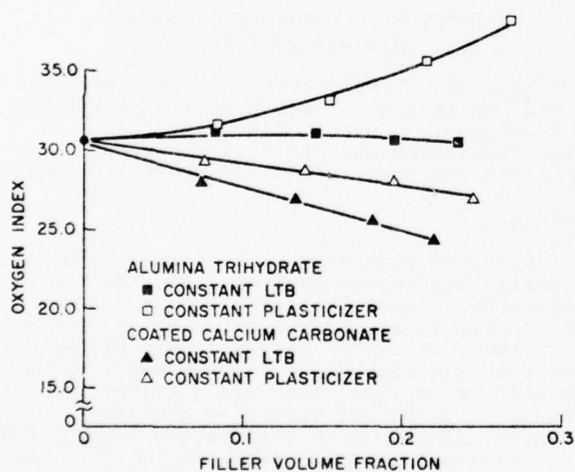


Figure 7 - Effect of Filler on Oxygen Index

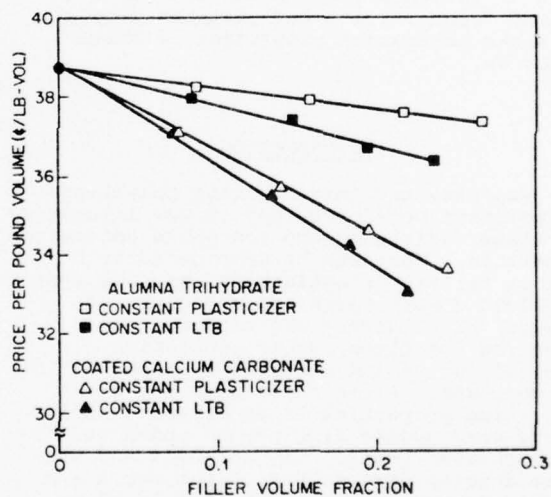


Figure 9 - Effect of Filler on Pound-Volume Cost

FLAME RESISTANT - LOW SMOKE CABLE JACKET DEVELOPMENTS

by

William D. Jones
UNIROYAL Chemical Division
UNIROYAL, Inc.
Naugatuck, Connecticut 06770

ABSTRACT

Cables with the combination of flame resistance and low smoke generation properties are required in many applications. UNIROYAL's Research Center has developed technology to reduce smoke generation while maintaining flame resistance. This paper presents the results of applying this technology to thermosetting cable jackets. Jacket compounds based on experimental thermosetting compounds are presented. Flame resistance and smoke generation were judged from NBS smoke chamber, oxygen index, UL 44 flame and IEEE 383 flame tests on laboratory compounds and jacketed cables. Test results and pictures show the low smoke generation properties of these compounds.

INTRODUCTION

Experimental thermosetting polyblends and polymers were developed in our laboratory for flame resistance and low smoke generation properties. They can be compounded with various fillers, plasticizers and cure systems. Polyblend combinations and the types of fillers, plasticizers and cure systems determine the flame, smoke generation, physical, aging and mechanical properties of the compound. Flame resistance and smoke generation properties of experimental polyblends were judged from oxygen index and NBS smoke chamber tests. Oxygen index and NBS smoke density (Dm) values of Polymer A and Polymer B compounds are compared to chloroprene, chlorosulfonated polyethylene and nitrile/PVC compounds in Table I. The Dm values are from 3" x 3" x .075" slabs using the flaming exposure. Although these compounds are in an oxygen index range which is generally regarded to be flame resistant, there is a wide range in the smoke density (Dm) values. Chloroprene's smoke density was too high to measure in our test unit. Chlorosulfonated polyethylene and nitrile/PVC values are equal within experimental error and are significantly lower than the chloroprene value. These Dm values are consistent with test results from commercial chloroprene, chlorosulfonated polyethylene and nitrile/PVC compounds. Dm values of Polymer A and Polymer B are dramatically lower than chloroprene and are 35 and 60% lower than chlorosulfonated polyethylene and NBR/PVC values.

TABLE I

<u>Polymers</u>	<u>Oxygen Index %</u>	<u>NBS Dm</u>
Chloroprene	31	700+
Nitrile/PVC	34	450
Chlorosulfonated Polyethylene	34	420
Polymer A	34	300
Polymer B	30	180

EFFECT OF COMPOUND INGREDIENTS ON SMOKE DENSITY

Fillers, plasticizers and cure systems, as well as polymers, determine the properties of a compound. Several flame retardant filler-additives and plasticizers were evaluated for their effect on smoke generation.

Fillers:

Hydrated aluminum oxide and organohalogen materials are recommended for improved flame resistance. These fillers were compared to a hard clay in an NBR/PVC formulation (Table II). Their Dm values were slightly higher than the hard clay value but are equal within experimental error. They did not improve the oxygen index but did lower tensile strength values. Hard clay is the best choice on a cost/performance basis.

TABLE II

	<u>Hard Clay</u>	<u>Hydrated Aluminum Oxide</u>	<u>Organo- halogen</u>
Smoke Density DM	450	480	510
Oxygen Index %	34	33	32
Tensile Strength, psi	2000	1440	1490

Plasticizers:

Chlorinated and phosphate plasticizers are recommended to improve flame resistance. Dioctyl phthalate (DOP), a general purpose plasticizer, was compared to a DOP/chlorinated paraffin blend, a DOP/phosphate blend and tricresyl phosphate in a polyblend compound. The DOP/chlorinated paraffin blend increased the oxygen index and reduced smoke density. These phosphates increased the oxygen index but also increased the smoke density. Physical, aging, flame, smoke generation and mechanical requirements will determine the plasticizer or blend of plasticizers for a compound. Chlorinated paraffin may be the best choice for flame resistance and smoke generation but phosphates provide better heat resistance and DOP better low temperature properties.

TABLE III

Plasticizers	NBS Dm	Oxygen Index %
DOP	350	30
DOP/Chlorinated Paraffin	300	34
Tricresyl Phosphate	380	33
DOP/phosphate	390	32

SMOKE DENSITY VS SAMPLE THICKNESS

Smoke emission is affected by the thickness of the material. A significant temperature gradient would be expected for thicker samples and smoke emission could be expected not to increase significantly beyond a certain thickness. M. I. Jacobs¹ found this "thermal thickness" is approached asymptotically for some materials.

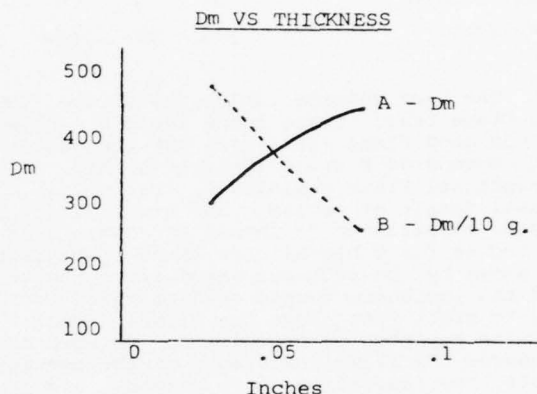
NBS smoke chamber samples are usually 3" x 3" slabs but the thickness varies. To measure the thickness effect in a typical cable jacket thickness range, 3" x 3" x .030" to .075" slabs of an NBR/PVC compound were tested in the NBS chamber. Dm results, Curve A, in Figure 1 increase significantly from .030" to .060" but tend to level off. The exposed area of the .030" samples burned to ashes but the .075" sample did not burn through.

Our data agreed with M. I. Jacobs' conclusion. Sample thickness is an important factor when reporting or comparing smoke density results.

Some smoke density values are reported on a weight basis, usually 5 to 10 grams. Curve B in Figure 1 is Curve A converted to a 10 gram basis. These data would lead to a conclusion opposite to that reached from Curve A, i.e. for Curve B smoke density decreases with increasing sample thickness.

Comparing smoke density values of thin samples to thick samples can lead to wrong conclusions. Converting Dm values of thin and thick samples to a weight basis can lead to an opposite conclusion. Our data indicate that to have meaningful Dm values for comparison, the sample thickness should be standardized at a thickness beyond the "thermal thickness" and values should not be calculated on a weight basis.

FIGURE 1



CABLE FLAME TESTS

Flame resistance and smoke generation properties of compounds must be proven in flame tests conducted on jacketed cables. Polymer A, Polymer B and the NBR/PVC compounds in Appendix A were selected for evaluation in the UL 44 vertical and IEEE 383 flame tests. The NBR/PVC and Polymer A compounds (A and B) meet heavy duty oil resistant jacket requirements. Polymer B compounds (C and D) meet medium duty general purpose jacket requirements. Polymer B compounds (C and D) are the same except for the plasticizer blend. Both compounds have low smoke density values but "D" has a higher oxygen index value. These compounds have sulfur cure systems because the cables were pan cured. The four compounds were extruded on these cable samples for flame testing:

1. No. 14 solid tinned copper .047" wall
2. Four conductor control cable (3 cond. No. 10 and 1 cond. No. 9) Cable OD .720"

No. 14 samples passed the UL 44 vertical flame test. All samples had fast flame extinction and low flame propagation (Table IV). Flames did not reach the paper flag indicator.

TABLE IV

UL 44 Vertical Flame Test

No. 14 Sample	A	B	C	D
Burn time, seconds after application				
1	1	1	0	0
2	1	1	0	0
3	0	0	1	43
4	0	0	1	0
5	0	0	1	0
Flag, % burn	0	0	0	0
Pass Test	yes	yes	yes	yes

The four control cables passed the IEEE 383 flame test. Cable A and Cable B (Polymer A) had good flame resistance but the cables with compounds C and D (Polymer B) had exceptional flame resistance. The total visual damage of Cables C and D was 22 and 25 inches compared to 36 inches for Cable B and 61 inches for Cable A. Low flame propagation is shown by the pictures taken after the test and the low thermocouple reading taken from two to eight feet above the flame. Test results reported in Appendix B. As this test measures the flame resistance of the complete cable, the insulation, core assembly and the jacket must be flame resistant.

The U.S. Navy Ship Research Center (NSRDC) confirmed our results on Cable B and Cable C in their IEEE 383 flame test.

Smoke generation during the IEEE 383 test was judged by pictures and visual observation of a doctor's eye chart through the test chamber window. The chart was six feet from the window. The smoke exhaust fan was shut off during the test.

Lower smoke generation of Cable B (Polymer A) and Cables C and D (Polymer B), especially Cables C and D, was quite obvious. After three minutes of burning Cable A (NBR/PVC), I could not read the eye chart. After three minutes of burning Cable B (Polymer A), I could read the chart but could not read the chart after six minutes. During the burning of Cables C and D (Polymer B), I could read the small print on the chart to the end of this 20-minute test. Pictures A3, B3, C3, C20, D3 and D20 show the improved visibility with Polymer B compounds. This low smoke generation was noted during the NSRDC IEEE 383 test.

CONCLUSION

These experimental polymer compounds have good flame resistance and low smoke generation properties. The Polymer A compound combines these properties with good ozone and oil resistance. Polymer B compounds offer the best flame resistance and lowest smoke generation with good ozone and low temperature properties. Polymer B compounds are not recommended for applications that require oil immersion but the oil resistance should be satisfactory for many applications.

Visual Observations

Minutes*	Cpd A NBR/PVC	Cpd B Poly A	Cpd C Poly B	Cpd D Poly B
3	no	yes	yes	yes
6	no	no	yes	yes
12			yes	yes
20			yes	yes

*Read chart after burning

The properties of these compounds will vary with the type of polyblend, polymer, fillers, plasticizers and cure systems. These thermosetting compounds will process on standard production equipment and are being evaluated for cable insulation, hose and mechanical goods applications.

ACKNOWLEDGMENT

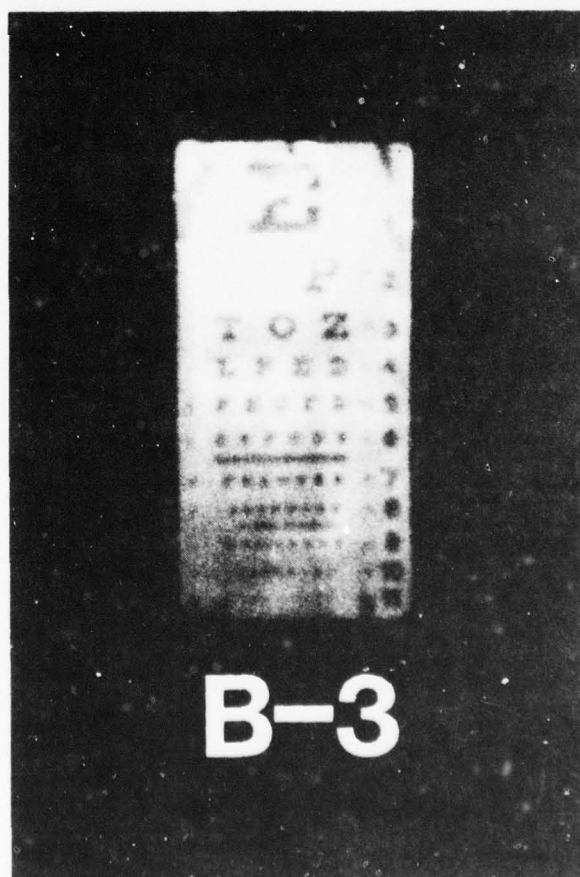
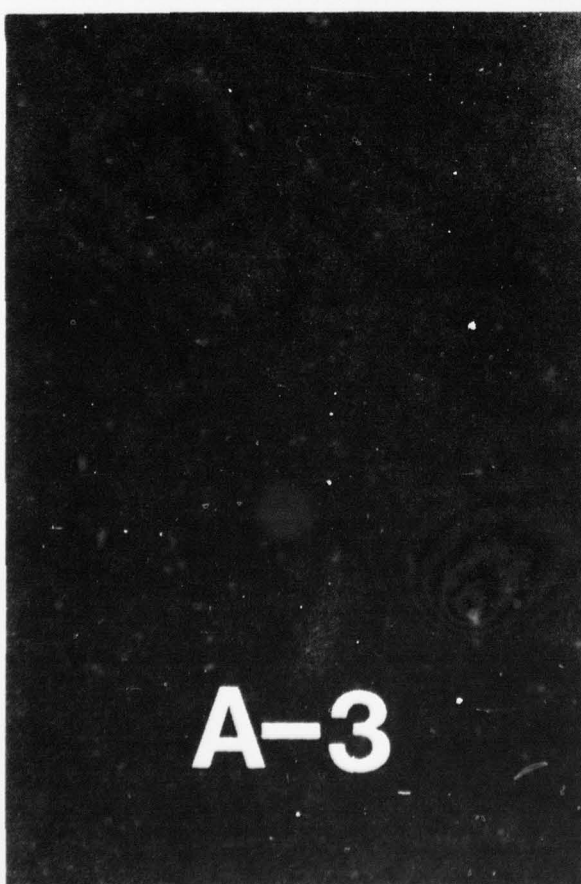
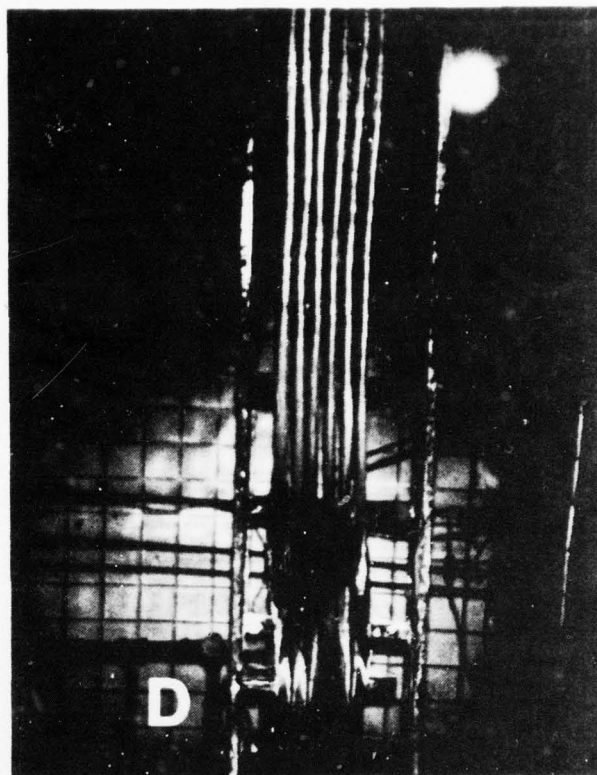
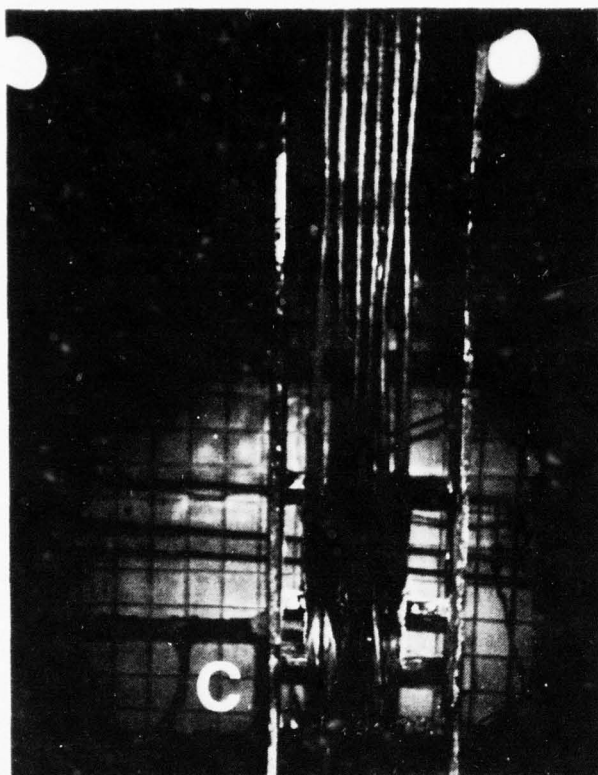
I greatly appreciate the cooperation of the Kerite Company, especially Alex McAuley, in making and flame-testing the cable samples. I thank our laboratory personnel, especially L. E. Mace, for their assistance in developing the laboratory data.

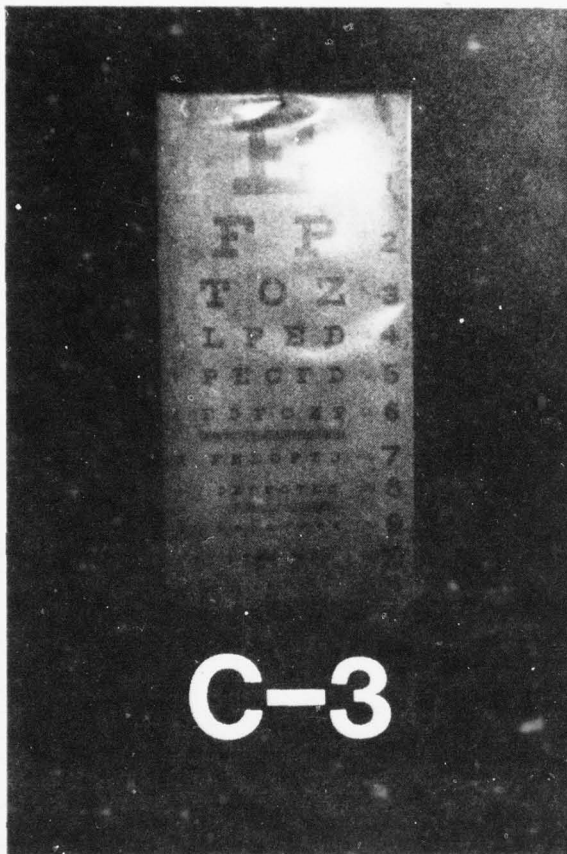
REFERENCES

1. M. I. Jacobs, "Factors Affecting the Measurement of Smoke Generation by Burning Polymers", J. FIRE AND FLAMMABILITY, Vol. 6 (July 1975).

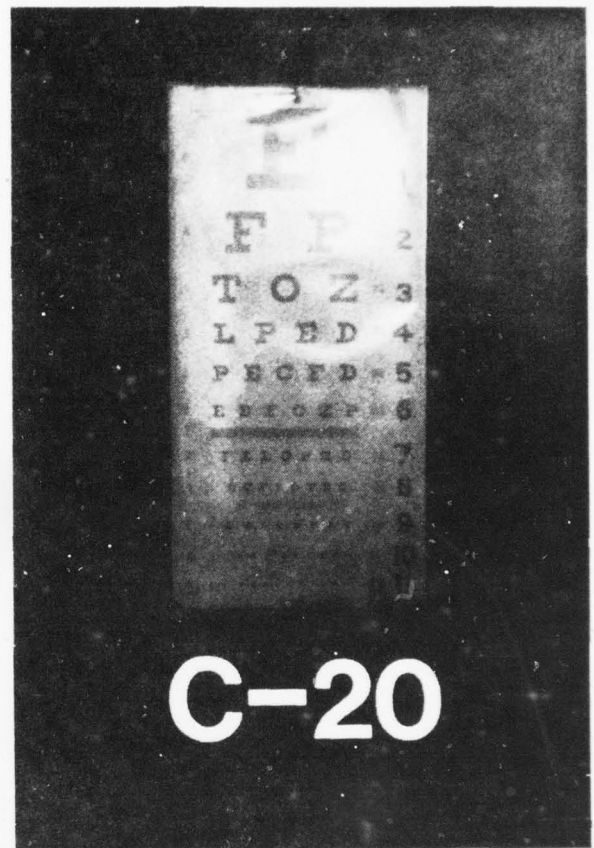
BIOGRAPHY

William D. Jones is a Research Scientist in the Technical Sales Service for wire and cable applications. His twenty years wire and cable experience includes eleven years with the Okonite Company and nine years with UNIROYAL. He received his B.S. degree in Chemistry from Wilkes College in Pennsylvania.

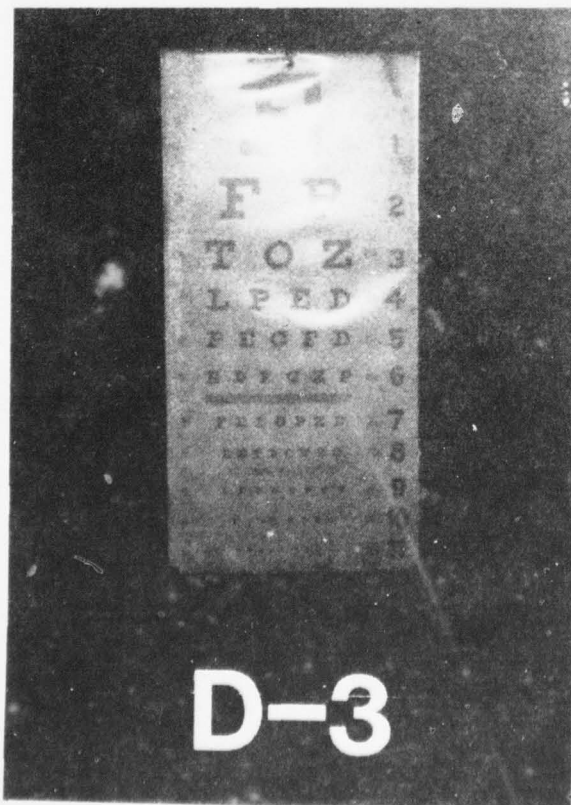




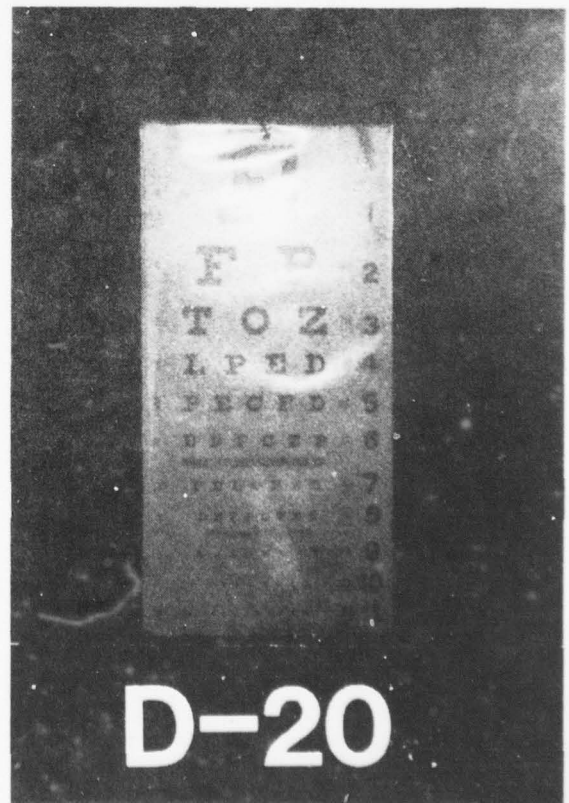
C-3



C-20



D-3



D-20

AD-A032 801

ARMY ELECTRONICS COMMAND FORT MONMOUTH N J
PROCEEDINGS OF INTERNATIONAL WIRE AND CABLE SYMPOSIUM (25TH) HE--ETC(U)
NOV 76

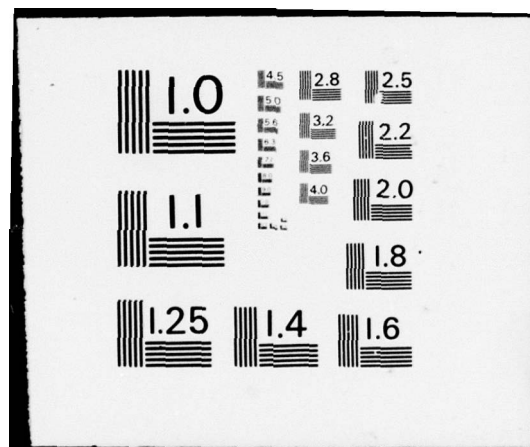
F/G 17/2

UNCLASSIFIED

NL

5 of 5
ADA032801





APPENDIX A

<u>Compound</u>	<u>A</u>	<u>B</u>	<u>Compound</u>	<u>C</u>	<u>D</u>
NBR/PVC	100.0	-	Polymber B	125.0	125.0
Polymer A	-	125.0	Black N550	110.0	10.0
Black N550	25.0	25.0	Hydrated Silica	20.0	20.0
Hard Clay	70.0	70.0	Hard Clay	50.0	50.0
Zinc Oxide	3.0	3.0	Litharge	8.0	8.0
Antimony Oxide	5.0	5.0	Antimony Oxide	5.0	5.0
Antioxidant	1.0	1.0	Antioxidant	1.0	1.0
Dioctyl Pthalate	10.0	10.0	Stearic Acid	1.0	1.0
Chlorinated Paraffin	20.0	20.0	CBS	1.0	1.0
Stearic Acid	1.0	1.0	BODITS	1.5	1.5
Lead Stabilizer	3.0	3.0	ZODIDC	1.0	1.0
MBTS	2.5	2.5	Sulfur	2.0	2.0
TMTDS	1.5	1.5	Paraffinic Oil	10.0	-
TETDS	1.5	1.5	Chlorinated Paraffin	-	25.0
Sulfur	.5	.5	Phosphate Plasticizer	10.0	10.0
NBS Dm	490	350	NBS Dm	260	220
Oxygen Index, %	35	35	Oxygen Index, %	28	35
<u>Physical Properties</u>			<u>Physical Properties</u>		
Tensile Strength, psi	2100	1850	Tensile Strength, psi	1660	1500
Elongation, %	390	325	Elongation, %	490	475
M200%, psi	1290	1390	M200%, psi	510	430
Shore A	77	83	Shore A	77	71

SUPPLIERS

<u>Material</u>	<u>TRADE NAME</u>	<u>Supplier</u>
Nitrile/PVC	PARACRIL® OZO	UNIROYAL CHEMICAL
Chloroprene	Neoprene	E. I. duPont
Chlorosulfonated Polyethylene	Hypalon	E. I. duPont
Antioxidant	OCTAMINE®	UNIROYAL CHEMICAL
Antioxidant	AMINOX®	UNIROYAL CHEMICAL
Lead Stabilizer	Dyphos	National Lead Company
TMTDS	TUEX®	UNIROYAL CHEMICAL
TETDS	Ethyl TUEX®	UNIROYAL CHEMICAL
Chlorinated Paraffin	Chlorowax 40	Diamond Alkali Company
Phosphate Plasticizer	Santicizer 140	Monsanto Chemical Company
Hydrated Silica	HiSil 215	PPG Industries
Hard Clay	Suprex Clay	J. M. Huber
CBS	DELAC® S	UNIROYAL CHEMICAL
BODITS	ROYALAC® 139	UNIROYAL CHEMICAL
ZODIDC	ROYALAC® 140	UNIROYAL CHEMICAL

APPENDIX B

IEEE 383 FLAME TEST DATA

Cable size - Four conductor OD - 0.720 inches
 Number of cables - 6 x 8 feet
 Gas - Propane
 Flame length - 15 inches
 Flame time - 20 minutes
 BTUs - 70,000

Nitrile/PVC Jacket - Compound A

Did cable pass test? - Yes
 Length of visual damage- 61 inches
 Burn time after removal of flame - 0 seconds

Thermocouple Location Readings °F

1. Flame Start 1462

1 min. <u>1172</u>	6 min. <u>1432</u>	11 min. <u>1378</u>	16 min. <u>1456</u>
2 min. <u>1166</u>	7 min. <u>1422</u>	12 min. <u>1395</u>	17 min. <u>1496</u>
3 min. <u>1175</u>	8 min. <u>1363</u>	13 min. <u>1409</u>	18 min. <u>1512</u>
4 min. <u>1229</u>	9 min. <u>1349</u>	14 min. <u>1419</u>	19 min. <u>1499</u>
5 min. <u>1329</u>	10 min. <u>1378</u>	15 min. <u>1411</u>	20 min. <u>1487</u>

	<u>Start</u>	<u>5 min.</u>	<u>10 min.</u>	<u>15 min.</u>	<u>20 min.</u>
2. 2' above flame	<u>78</u>	<u>1287</u>	<u>1282</u>	<u>867</u>	<u>729</u>
3. 4' above flame	<u>91</u>	<u>337</u>	<u>417</u>	<u>1068</u>	<u>354</u>
4. 6' above flame	<u>97</u>	<u>265</u>	<u>307</u>	<u>630</u>	<u>267</u>
5. 8' above flame	<u>106</u>	<u>185</u>	<u>206</u>	<u>288</u>	<u>195</u>

Polymer B Jacket - Compound B

Did cable pass test? - Yes
 Length of visual damage - 36 inches
 Burn time after removal of flame- 30 seconds

Thermocouple Location Readings °F

1. Flame Start 1450

1 min. <u>1411</u>	6 min. <u>1454</u>	11 min. <u>1474</u>	16 min. <u>1471</u>
2 min. <u>1440</u>	7 min. <u>1447</u>	12 min. <u>1473</u>	17 min. <u>1470</u>
3 min. <u>1475</u>	8 min. <u>1446</u>	13 min. <u>1460</u>	18 min. <u>1472</u>
4 min. <u>1475</u>	9 min. <u>1446</u>	14 min. <u>1469</u>	19 min. <u>1477</u>
5 min. <u>1478</u>	10 min. <u>1465</u>	15 min. <u>1468</u>	20 min. <u>1486</u>

	<u>Start</u>	<u>5 min.</u>	<u>10 min.</u>	<u>15 min.</u>	<u>20 min.</u>
2. 2' above flame	<u>85</u>	<u>1089</u>	<u>1165</u>	<u>1307</u>	<u>1261</u>
3. 4' above flame	<u>99</u>	<u>268</u>	<u>309</u>	<u>445</u>	<u>338</u>
4. 6' above flame	<u>112</u>	<u>206</u>	<u>225</u>	<u>260</u>	<u>223</u>
5. 8' above flame	<u>119</u>	<u>164</u>	<u>178</u>	<u>204</u>	<u>187</u>

APPENDIX B

(continued)

Polymer B Jacket - Compound C

Did cable pass test? - Yes
Length of visual damage - 22 inches
Burn time after removal of flame - 11 seconds

Thermocouple Location Readings °F

1. Flame Start	1430				
1 min.	1213	6 min.	1201	11 min.	1272
2 min.	1154	7 min.	1229	12 min.	1277
3 min.	1171	8 min.	1237	13 min.	1275
4 min.	1178	9 min.	1248	14 min.	1279
5 min.	1193	10 min.	1265	15 min.	1283
		16 min.	1285	17 min.	1304
		18 min.	1299	19 min.	1294
		20 min.	1293		
		Start	5 min.	10 min.	15 min.
		20 min.			
2. 2' above flame	100	451	465	484	510
3. 4' above flame	113	243	258	272	272
4. 6' above flame	121	211	222	229	231
5. 8' above flame	131	167	175	183	184

Polymer B Jacket - Compound D

Did cable pass test? - Yes
Length of visual damage - 25 inches
Burn time after removal of flame- 0 seconds

Thermocouple Location Readings °F

1. Flame Start	1425				
1 min.	1373	6 min.	1165	11 min.	1206
2 min.	1224	7 min.	1170	12 min.	1207
3 min.	1195	8 min.	1177	13 min.	1205
4 min.	1179	9 min.	1192	14 min.	1203
5 min.	1171	10 min.	1205	15 min.	1204
		16 min.	1205	17 min.	1215
		18 min.	1210	19 min.	1211
		20 min.	1211		
		Start	5 min.	10. min.	15 min.
		20 min.			
2. 2' above flame	97	616	657	650	651
3. 4' above flame	112	284	299	315	314
4. 6' above flame	121	242	246	257	259
5. 8' above flame	131	177	189	196	198

Data extracted from the Kerite Company test reports.

PLASTIC INSULATING OF TELEPHONE CONDUCTORS AT 10,000 TO 15,000 FPM

A. Cueto

M. Cubero

A. Garvalena

Cables de Comunicaciones, S.A.
Zaragoza, Spain

1. SUMMARY

Most of us recall when the so-called *high speed* insulating lines were running at something like 1000 FPM. The advancements in the past few years have been spectacular and presently there are lines operating at speeds of 6500 to 8000 FPM. The race for ultra high performance continues and recent papers have discussed speeds of 10000 FPM and the problems arising from physical laws and limitations which place a practical limit on further advancement.

There is no question that such insulating speeds are extremely difficult to obtain on a day in day out basis in production.

Ultra high speeds place a high premium upon raw materials, equipment and the people who operate and maintain the machines.

The authors therefore have been experimenting with alternative methods which would not be dependant upon sheer speed and its many limiting factors. As a result of these studies a successful method was developed for insulating two wires simultaneously in the same line at "normal" speeds, thereby doubling output without the attendant problems normally related to an increase of this magnitude.

The paper discusses the prototype two conductor line itself and the problems associated with ultra high insulating speeds. A photograph of the "heart" of the prototype line is shown below.

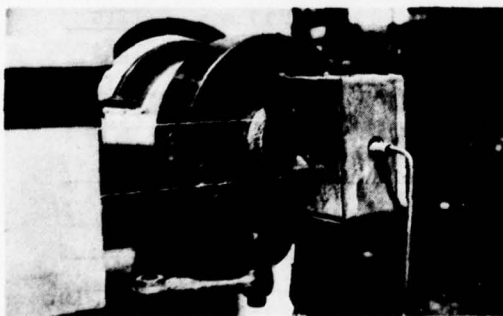


Fig. 1
Closeup view of double conductor crosshead insulating two wires of 0.64 mm (22 AWG)

2. PROBLEMS RELATED TO SPEED

The problems related to ultra high speed have been discussed in detail by many authors. Although our initial objective was to increase output without changing speeds, the following summary of speed related problems is an

important consideration to determine the ultimate potential of the two conductor insulating line.

2.1 Wire Drawing, Annealing

Incorporation of the wire drawing and annealing process on a tandem basis with insulating is the most common arrangement in modern installations. Wire drawing and annealing are the cause of up to 70% of the downtime experienced in this process. Die alignment, die design and/or condition, drawing solution, cones, etc., are critical factors which can cause wire breaks, however, the raw material itself is the principal source of most breaks.

While wire drawing equipment is available which can operate at speeds up to 12000 FPM, the uncertainty regarding the quality of the raw materials and other limitations which will be discussed later make it difficult to take advantage of such speeds when operating on a tandem basis.

Resistance annealing has inherent limitations which are primarily the result of centrifugal force (fig. 2). Since centrifugal force is a function of speed, this also limits the drawing-annealing portion of the line to about 12000 FPM.

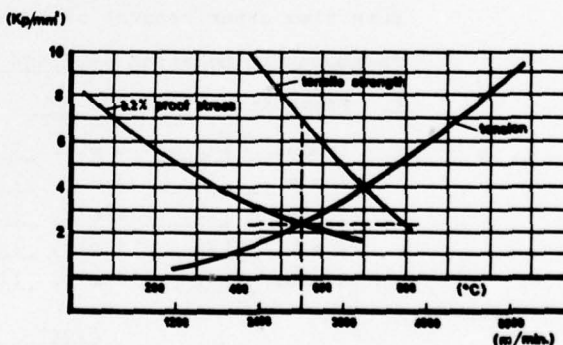


Fig. 2
Mechanical strength of copper at various temperatures and wire tension due to centrifugal force

2.2 Dual Flyer Cones

In the case of the two conductor line it is impractical to install two drawing machines and annealers especially where one must expect an average of up to 2 wire breaks per 1000 lbs of drawn wire in finer sizes.

The alternative is to use dual flyer (flip cones) for each wire. Operating in this manner the defects have largely been eliminated at wire drawing. The conductor is already

annealed and any wire breaks will require a fraction of the time which is required to string up a drawing machine before the line can be restarted.

Furthermore, keeping in mind the factor of interference (i.e. downtime of both conductors where only one is broken) all steps must be taken towards eliminating duplicate installations and additional sources for problems and downtime.

With dual flyers one must accept the fact that changeovers at speeds above approximately 4000-8500 FPM are unreliable.

Recent dual flyer designs however claim 8000-8500 FPM.

2.3 Extrusion

Plastics extrusion experts are always seeking an equilibrium between three factors: output, quality and low temperature. Output is measured in volume or weight extruded per hour. In the case of telephone wire insulating the cross sectional restriction of flow reduces this output. Quality is a product of suitable raw materials and a smooth, homogeneous and regular extrusion. In order to increase speeds (and output) with a given extruder design, one must increase the RPM of the screw. Increasing the revolutions of the screw will elevate temperatures and can affect the quality of the product. Therefore, it is obvious that a lack of equilibrium between the three factors can negatively affect the quality of the end product.

Another primary consideration in the extrusion process with respect to speed is the crosshead. As an oversimplification, the extrusion process in telephone singles can be described as pulling a fragile wire through a puddle of molten plastic at high speeds. Despite divergent opinions in the various papers which have been published in the past concerning design, ideal pressure, etc., all agree that wire back tension increases considerably as line speed is increased. The order of increase has often been reported at about 70% to 100% in a speed increase from 3300 to 10000 FPM.

A typical graph showing the increased back tension and elastic limits of copper wire is shown in figure 3.

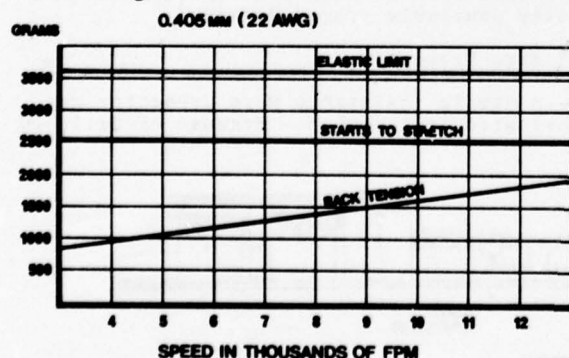


Fig. 3

Wire back tension in the crosshead at different speeds and limits of 0.405 mm (26 AWG) wire

2.4 Cooling

Early attempts to increase insulating speeds often encountered wire pull down in the cooling area because the insulated conductor will pull a "column of water" along with it in a conventional trough. As speeds increased to the current levels wire back tension reached critical limits and new designs of cooling troughs have become a necessity. Improperly cooled insulated wire will later shrink while on the bobbin and render it almost impossible to pay off or rewind. Since the cooling phenomenon requires a specific constant time regardless of speed (see figure 4), lengthening of water troughs must be considered in any increase of lineal output. The length requirement in turn also poses problems in regard to available space and the most common solution has been multi-loop troughs. As is usually the case in any such development, eventually the multi-loop troughs also led to problems with wire tension and wire stretching due to friction caused by the pulleys.

While all of the above problems have already been solved, we are still faced with the familiar problem of centrifugal force and the increased wire tensions necessary to overcome it. The speed limitation in the cooling portion is therefore in the order of approximately 12000 FPM.

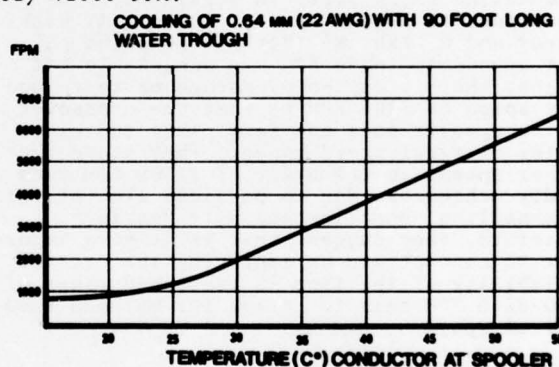


Fig. 4

Insulation Cooling Curves

2.5 Capstan

Most capstan models are capable of operating at speeds similar to the limits we have discussed for wire drawing, etc. Some equipment suppliers however have combined the capstan unit into the multi-loop portion of the water trough to reduce the overall number of pulleys and loops required in the line.

2.6 Spooling

The modern automatic dual parallel shaft spooler is one of the most complex production units in the cable industry. While great advancements have been made in their design and reliability, this equipment, next to wire drawing, produces most of the incidences of downtime. Usually the cause of this downtime is due to missed crossovers.

The theoretical maximum speed for spoolers is approximately 13000 FPM resulting from the now familiar problem of centrifugal force. However the spooler has a further limitation

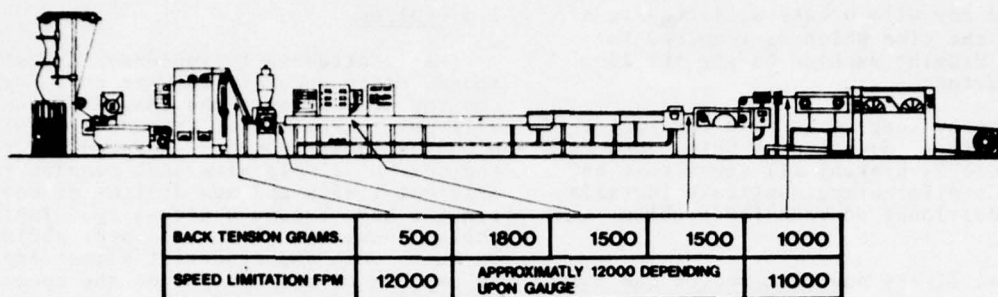


Fig. 5 Typical tandem line indicating back tension (at 10000 FPM) and theoretical speed limitation for the various components

of 10000-12000 FPM at crossover due to a perpendicular acceleration phenomenon.

2.7 Summary

The information discussed previously is summarized in figure 5 which establishes that the limitation of a tandem insulating line is theoretically 10000 FPM during crossovers and up to approximately 12000 FPM at other times. More important than speed is, of course, the total output of the process. It is possible that at higher speeds reliability factors and raw materials limitations will cause increases in downtime which serve to offset such improvements in lineal speed. Authors A. Riekkinen⁵ and R. Ekholm⁵ (24th IWCS) point out that speeds to 10000 FPM are achievable but suggest that it may be advantageous to reduce line speed to 8200 FPM so that the crossover in the spooler does not take place too close to the critical speed range. They state that higher speeds in the order of 11500 FPM seem hardly achievable due to physical limitations in annealing, spooling and wire tensions. Therefore, they suggest that it is more important to concentrate on improving the overall reliability of the line in the speed range of 6500-8200 FPM than to strive for maximum theoretical speed.

3. AN ALTERNATIVE SOLUTION

Assuming one can insulate two conductors simultaneously on a single line then the lineal speed required to match the maximum theoretical speed of prototype lines under current development is only 5000-6000 FPM. We have already seen that such speeds are now commonplace in the industry and it is generally agreed that reasonably high reliability and corresponding net output in production condition can theoretically be obtained for speeds of approximately 8000 FPM with the flyer cones as the primary limitation.

In such an installation, each of the two conductors can operate well within the safe limits of physical laws which limit further speed gains.

In principle, there are other gains to be realized which are summarized in the following list:

- Requires less floor space (see fig.6).
- Reduction of energy and manufacturing expenses (electric, water, etc.).
- Labor costs are substantially reduced.
- Reliability can exceed that of ultra high speed lines i.e. 10000 FPM or more.
- Output per extruder, which is a problem in telephone conductors insulating due to its thin wall application, is increased.
- Capital outlays for such installations are greatly reduced since the extruder, capstan, water trough, etc., are common for both wires.

4. PROTOTYPE DOUBLE INSULATING LINE

4.1 Flyer Cones

To save space, two sets of dual flyer cones were fabricated in "piggy-back" fashion (see figure 7). This particular unit has a speed limitation of 5000-6000 FPM. To operate at higher speeds this component of the prototype line must be substituted for a commercially available proven design.

4.2 Wire Preheat

A simple resistance wire preheater was fabricated in the shop. Because of delivery

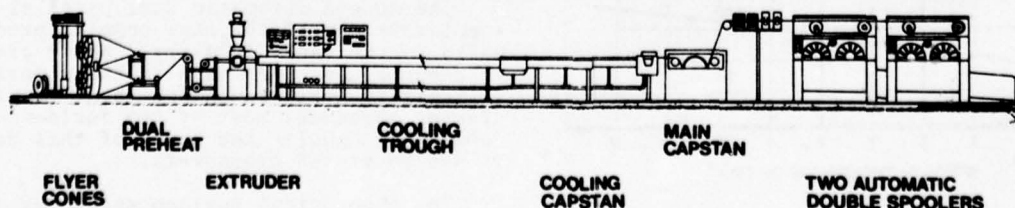


Fig. 6
The Double Insulating Line - An Alternative Solution

lead times it was not possible to obtain a commercially available model in time for the trials. In addition to an effective preheat limit of about 5000 FPM the unit is adjustable only via a variable transformer on a manual basis.

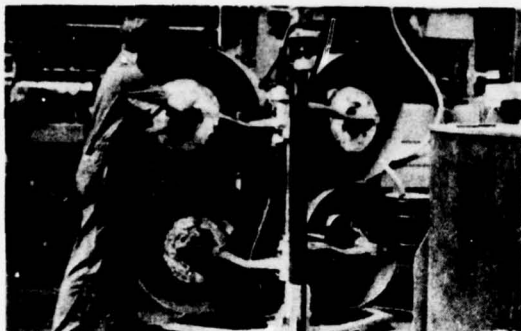


Fig. 7
Photograph of two dual flyers installed "piggy-back" fashion

4.3 Water Trough

To avoid the problems discussed in section 2.4, a spray cooling system was installed. Two tiers were employed to adequately initiate the cooling of each conductor during the first third of the trough. At this point both wires come together and are cooled in a common system (see figure 8).

The cooling system consists of short "V" sections with closely spaced holes in the valley which allows water to bubble upwards under the insulated conductor. Spray heads are installed above the troughs and are oriented in the same direction as the wire travels (see figure 9).

The final cooling is a multi-pass system with a helper capstan unit. Four to six loops are usually made around the drum type capstan and cooling is obtained in two short lateral troughs (see figure 10).

The cooling portion of the prototype line was effective and should be adequate up to speeds of 10000 FPM or more in the case of the smaller gauges.

4.4 Capstan

The main capstan is a belt type which has been found to be the most effective for two conductor pulling. At the exit end of the capstan the individual wires are oriented towards each spooler with directional sheaves (see figure 11).

4.5 Spooling

Two dual, automatic, parallel shaft takeups were used. These particular takeups have a design speed limitation of 5000 FPM which, along with the flyers and conductor preheater, were the principal speed limitations of the prototype line. However, speed trials were carried out up to 6500 FPM to develop the necessary data.

A practical consideration of high speed



Fig. 8
Photograph of water trough with two initial cooling levels

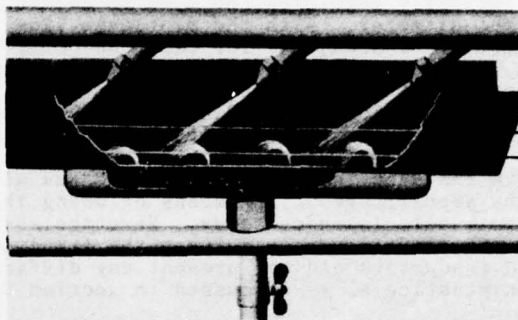


Fig. 9
Drawing showing modified spray cooling method

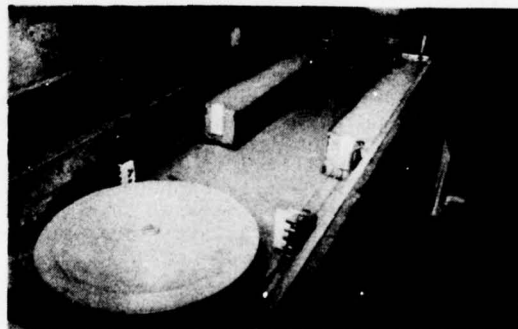


Fig. 10
Photograph of helper capstan cooling trough

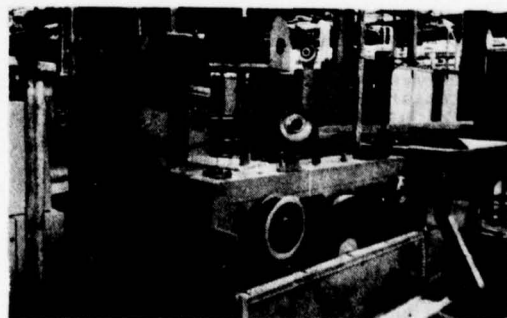


Fig. 11
Photograph of the capstan showing directional sheaves. Individual sparkers and diameter control units can be observed in the background

operation is bobbin unbalances. These can be the result of the bobbin itself or of the level winding unit in the spooler. The level winding must be nearly perfect to avoid peaks and valleys which often will result in a "loping" effect due to the uneven distribution of the mass of insulated conductor in the bobbin. In addition to the excessive vibration which can take place, the spooler must rapidly accelerate and decelerate as it encounters peaks and valleys in the bobbin package. Small differences in the dimensions of the spools can also cause this condition as the traverse stops must be readjusted with each bobbin.

4.6 Diameter Monitoring Equipment

Normally, the tandem insulating lines have been operated in our plant in the automatic diameter mode. That is, the optical diameter monitor measures the insulated conductor and automatically regulates the line to obtain the desired diameter. With the prototype line two monitors were used, one for each conductor (see figure 11). Obviously, both monitor units cannot be set to control the line as the necessary regulation may be diametrically opposed. Therefore, the units were used as displays only and operator attention was required to ensure that the "smallest conductor" was within the specifications. A means of doing this automatically is under study. Nevertheless, dimensional differences between the two insulated conductors did not present any difficulty in practice as is discussed in section 5.

4.7 Extrusion

Whereas extrusion would normally be described earlier in a report of this type, in this case we have left it for last for obvious reasons.

The extruder crosshead is clearly the most novel and critical element in the subject line.

The extruder utilized in this line is a stock model and in reality happens to be the only one which could be released from production to conduct trials. It was by no means special in any sense.

The crosshead, however, is a different matter. Over the past three years three different concepts have been tried each with numerous modifications before arriving at the present design (see figures 1 and 14).

The objectives which were established for the design of the head were:

- A Should be interchangeable with other crossheads in the plant to facilitate the application of this development to other existing lines.
- B Cartridges with selfcentering tips and dies would be used to speed changes and reduce variables and operator error. Preferably they should be interchangeable with those in the "conventional" tandem lines.
- C Quality requirements with regard to diameters, eccentricity, etc. should be met with the same order of tolerances obtained on single conductor lines.

D Surface smoothness and general appearance levels should be equal to normal production.

E Back tension on the conductor passing through the head should be comparable to that which exists in conventional insulating lines.

The final head design is shown schematically in fig. 14 and a photograph of the crosshead in operation can be seen in figure 1. The results of the trials were successful and the objectives stated above have been achieved.

As stated previously, the output of an extruder in this type of application is restricted by the small cross section of thin wall telephone conductor insulation (see figure 12).

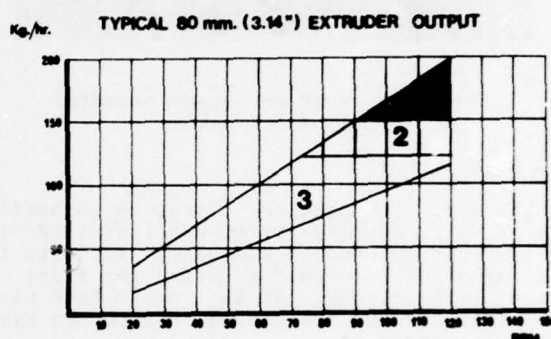


Fig. 12
Typical graph showing output obtained by an 80 mm extruder. Field III represents the extrusion of small cross sections at high speed. Fields I & II represent applications of successively higher cross section extrusion

From the above it is apparent that with the two conductor head we increase the cross section, reduce output constriction and get some "free" additional output (see below).

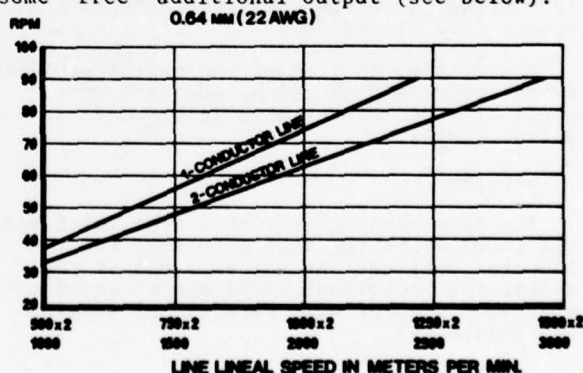
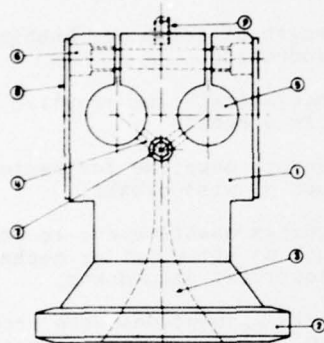


Fig. 13
Graph showing performance comparison of an 80 mm extruder operating with single and double 0.64 mm (22 AWG) conductors

The above data provides the basis for some interesting observations concerning facilities utilization. It is well known that the selection of an extruder for high speed insulating is a "compromise" decision. If one purchases a small extruder the effective utilization

with smaller gauges is good, however, output with the larger gauges is extremely low. If one selects a larger extruder the production output of larger gauges is improved but one finds that he is using only a fraction of the installed capacity with the smaller gauges keeping in mind that theoretically a lineal speed of 25000 FPM would be needed to operate at 100%. As we have seen, these speeds are impossible to achieve giving rise to a situation whereby manufacturers are utilizing perhaps half of their installed capacity depending on product mix. The two conductor concept not only provides some "free" additional output but also permits a theoretical utilization of nearly all of the installed capacity.

An initial area of concern was the wire back tension in the head. In practice, however, this has posed no problem whatsoever. The back tension recorded for the two conductor line is quite similar to that experienced with conventional single wire lines. (Fig.15)



- 1 MAIN HEAD BODY
2 COLLAR HEAD CLAMP
3 ENTRANCE EXTRUDATE
4 FEED CHANNEL TO CARTRIDGE
5 RECEPTACLE/CARTRIDGE
6 RETAINER BOLT/CARTRIDGE
7 FLOW REGULATION
8 RESISTANCE
9 THERMOCOUPLE

Fig. 14

Schematic drawing of double wire crosshead

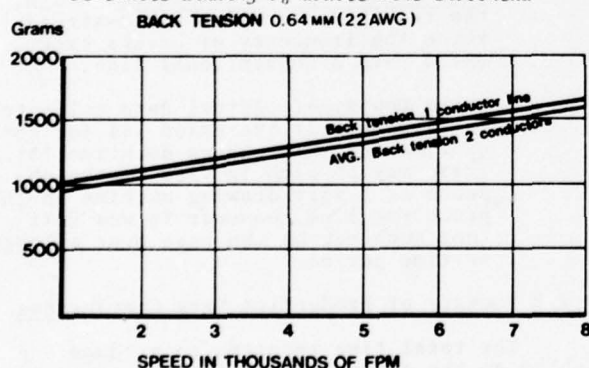


Fig. 15

Back tension at various speeds for one and two conductor crossheads

With a two conductor crosshead a far greater sensitivity to leveling of the crosshead during installation was noted than with conventional extrusion.

Thus far, work has been restricted to rigid PE although indications exist that PVC

can be extruded with equal success. Logically, foam extrusion should present additional problems which will be evaluated with respect to feasibility at a later date.

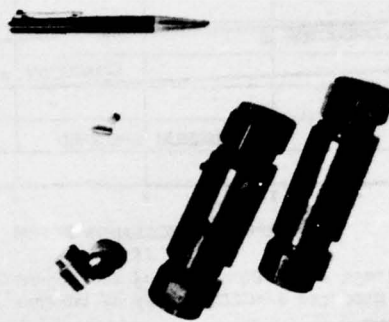


Fig. 16

Closeup of crosshead tooling

5. RESULTS OF TRIALS

Although the concept has been in development for over three years, the trials reported in this paper were conducted over the previous 8 months. During the latter part of this period, the line, having performed successfully, was released for production and scheduled as any other insulating line in the plant. While this increased the data which could be collected, it also restricted the possibilities of improving some components.

5.1 Quality

This factor is perhaps the most important consideration in this project towards determining if the two conductor insulating line is a practical alternative to conventional single wire installations. The following data should clear up any questions in regard to quality.

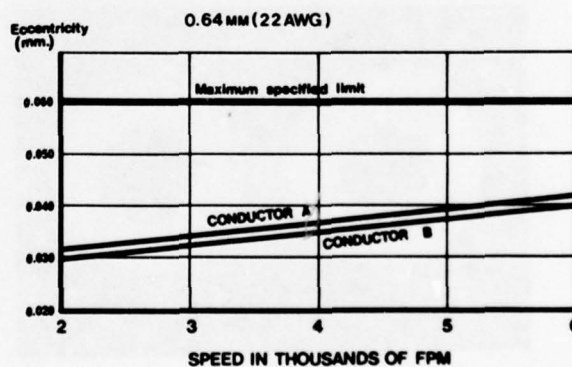


Fig. 17

Eccentricity characteristics of the two conductors (A&B) produced simultaneously on the two conductor line at various speeds compared with specified limits

The differences in the wall thickness of the two conductors insulated simultaneously is comparable to the best results obtained in conventional tandem lines producing the same gauge. In fact, the tendency of the two wire line was for the two conductors to become "more identical" dimensionally as speeds were increased.

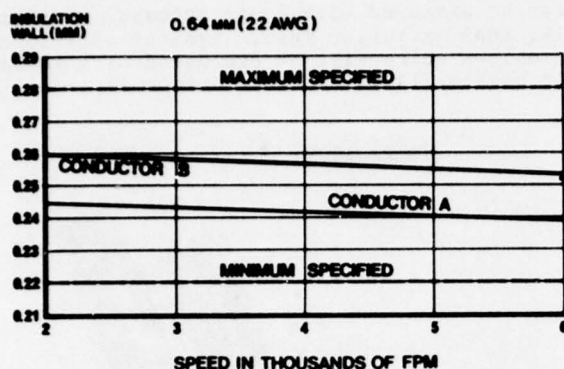


Fig. 18
Average insulation wall of two conductors (A&B)
produced simultaneously at various speeds

The differences in the overall diameter of the two conductors produced in the prototype line varied between 0.005 and 0.018 mm depending upon gauge and line speed.

The sample size was fortunately large enough (4000) to ensure that the following conclusions are reliable:

- 1 The insulated conductors produced in the two conductor line easily passed all of the specified requirements.
- 2 The differences observed in quality levels or average test values between the single and double conductor lines is acceptable.
- 3 The two conductors produced in the prototype line were "identical twins", in that any differences between them were comparable to those obtained from two separate conventional tandem lines (see figure 19).

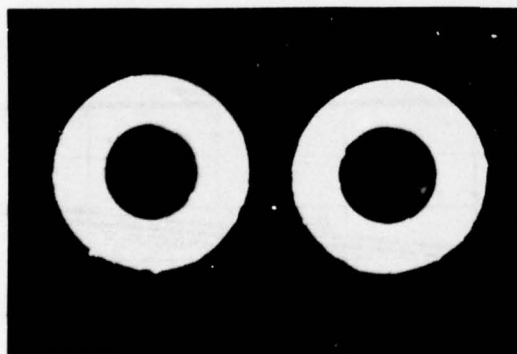


Fig. 19
Micrograph of cross section of two 0.6 mm conductors produced on prototype line

5.2 Economic Considerations

The economic study of the two wire line is based upon a comparison with a conventional tandem line. As we have already seen the principal differences between the two lines are:

- The prototype line insulates two conductors and the conventional line one.

- The two conductor line is fed by flyers while the conventional line has a wire drawing machine with annealer.

- There are small differences such as the water trough design and in the monitoring controls.

In our initial economic considerations we will compare the two lines and later add a correction factor to the results of the two conductor line to compensate for wire drawing being a separate process.

5.2.1 Production Data

The time required to produce a given quantity of good production in relation to line speed is required to complete our cost study. The parameters which were studied for various speeds are:

- Length of insulated conductor per bobbin.
- Length of scrap per bobbin of good production.
- Theoretical time required to manufacture a bobbin.
- Average downtime for various causes such as wire breaks.
- Average downtime due to other causes such as set up time, mechanical or electrical breakdowns.

Certain assumptions were necessary where the data collected was more favorable to the two conductor concept than would logically be the case. Some of these were:

- **Missed Crossovers:** The two conductor line was assigned twice the downtime for this cause as is common with single wire lines.
- **Wire Breaks in the Crosshead:** Again, the two conductor line was assigned twice the frequency of breaks experienced with a conventional line.
- **Other Downtime:** Actual data collected was arbitrarily increased 15% for set up time and maintenance downtime 10%. These may be high in view of the absence of a wire drawing machine in the prototype line, however it was felt that such may be the case over a longer time period.

5.2.2 Summary of Production Data Conclusions

The total time required to produce one bobbin on the conventional line was approximately the same as for two bobbins on the prototype line at speeds up to 5000 FPM. At speeds beyond this point, the two conductor line requires less time to produce two bobbins compared to one bobbin for normal tandem lines.

The principal reason for this is the frequency of breaks in relation to speed and the wire drawing element in the tandem line with its substantial downtime caused by the subsequent string up of the machine.

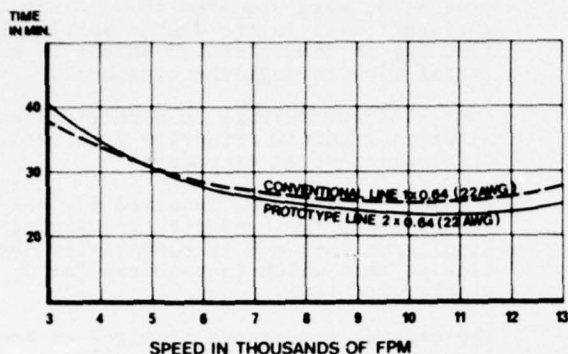


Fig. 20
Time required to produce one bobbin on conventional line and two bobbins on prototype line (solid line)

The actual speeds which can be obtained in practice depend upon wire gauge (extruder output) and the other limiting factors discussed in previous sections.

If we accept the conclusions given in figure 20 we see that the ideal theoretical speed for the single conductor line is approximately 9000 FPM compared to 10500 FPM for the two conductor line. Keeping in mind that the prototype line is producing two conductors at any given speed the differences in output are substantial. According to the results of our studies it would appear that if the conventional line could operate at 13000 FPM the prototype line would only require 8200 FPM to produce more than twice as many bobbins per day. The use of the term *ideal theoretical* speed is arbitrary in that problems such as spooler crossover make such speeds impractical at present.

5.3 Cost Study

Using the production data described above as a base, the usual factors which are utilized to determine costs were calculated.

These include:

- Direct Labor
- Indirect Labor
- Amortization
- Manufacturing expense
- Energy consumption

The proportional costs related to the drawing operation as a separate process were added to the prototype line to make the conclusions comparable.

As indicated in figure 21, it is obvious that the two conductor line is more economical at all line speeds with an average saving of 30% at "normal" speeds and over 60% at ultra high speeds excluding raw materials costs.

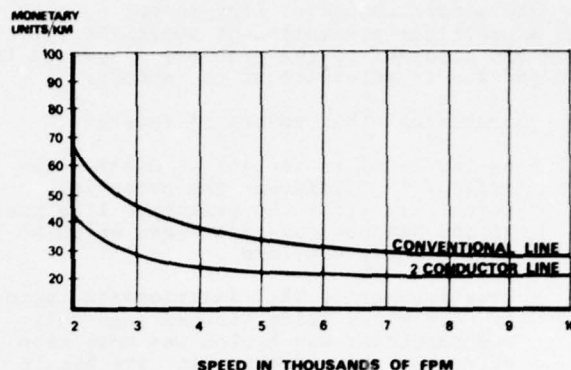


Fig. 21
Cost in monetary units per km at various speeds for conventional line vs double conductor line

6. OTHER THEORETICAL APPLICATIONS

Assuming that the practical considerations have been resolved for the two conductor insulating concept the next logical step may be the insulation of "pairs". A theoretical evolution could be a line which has two extruders, one producing the ring and the other the tip color. Each is insulating two conductors.

At the exit end of the capstan the "pairs" would be led via sheaves to the respective spoolers. In effect, each bobbin would contain equal lengths of the ring and tip colored conductors wound on a parallel basis. The bobbins could later payoff (probably on a roll off basis only) into a conventional pairing machine for twisting. Our early trials were performed in a similar manner. Disposing of only one spooler both of the wires produced were wound on the same bobbin and the individual conductors were later rewound onto individual bobbins. Trials demonstrated that both conductors could be paid off into a pairing machine without any difficulty whatsoever. If one were to produce small pair count layless cable it would be possible to install rotating payoffs behind the sheathing extruder and produce the pairs as they were paid off thereby eliminating all manufacturing steps between insulating and sheathing. Such rotating payoffs already exist in Europe but are used for combination pairing/stranding machines.

7. CONCLUSIONS

It should be pointed out that a project such as this receives limited support because, after all, if it is feasible why isn't everyone else doing it?. Such doubts are reasonable and a very limited budget was established for development of the prototype line.

Most of the special components were fabricated in the shop from obsolete parts. Some of the limitations therefore are not the result of the process itself but are largely due to self-imposed budget restrictions. Having determined that this concept is completely feasible the next step is to replace the weaker elements with sound, commercially available components.

Nevertheless we can observe that the current practical limitation of the two conductor line might be 8000 FPM x 2 = 16000 FPM (flyer and spooler limitation).

The single conductor line in our opinion, has a practical limitation of approximately 8000 FPM also due to the problems discussed in 2.6 and 4.5 in reference to the spooler.

Summarizing other points of interest:

- As indicated in section 6 -Other Theoretical Applications- the potential which exists for the prototype line goes beyond the obvious advantages which we have already examined.
- Downtime due to the interference factor of both wires being stopped when only one conductor was broken was more than offset by the reduction in wire breaks and downtime due to wire drawing and annealing.
- Average production output was equal to, or exceeded, two single tandem lines.
- In the two conductor process the drawing operation must be performed separately. Despite this additional cost, the prototype line is substantially less costly overall. This fact would seem to support the argument for separating wire drawing now that there are machines capable of 12000 FPM, speeds which we may have difficulty in taking full advantage of in a tandem line.
- This type of line particularly suits the production of heavier gauges or special thick wall insulation designs which reduce a tandem's output considerably.
- Once released for production the quality level of the subject line was comparable to that of the tandem insulators.
- Tensions, tip and die wear, maintenance attention, etc., was comparable to that of conventional lines. While the two conductor line has an additional spooler that can potentially give additional maintenance problems, this is offset in that the single conductor lines have the drawing machine and annealer.

- Different heats, particularly in the crosshead, were required to maintain surface finish in the double insulating line due to the increased amount of material flow through the crosshead.
- A significant savings in electrical consumption resulted primarily from the elimination of an extruder.
- The additional space required for conversion to a two conductor insulating line is minimal and is essentially the same as that which is required for a single wire line.
- The capital investment required to modify a conventional insulating line to run two conductors simultaneously is approximately 1/4 to 1/3 of the capital investment required for a conventional line.

ACKNOWLEDGEMENTS

The authors wish to thank all of the operators, mechanics, electricians, technicians and others who enthusiastically participated in a common project. The authors also wish to acknowledge Mr. J. Justiss who several years ago commented upon the feasibility of such a project thereby creating the necessary interest.

BIBLIOGRAPHY

- 1 J.C. Calhoun and W.M. Flegal, "The Cooling Process in Plastic Insulated Wire", 23rd IWCS Proceedings pp 330-336, Dec. 1974.
- 2 E. Kertscher, "Recent Developments in the High Speed Insulation of Quality Telephone Wires", 22nd IWCS, Proceedings pp 315-335, Dec. 1973.
- 3 A. Riekkinen and R. Ekholm, "Plastic Insulating of Telephone Wires at Ultra High Speeds", 24th IWCS, Proceedings pp 43-51, Dec. 1975.
- 4 M. Rokunohe, M. Oxada, U. Ueno, J. Konishi, "Ultra-High Speed Extrusion of Foamed Polyethylene Insulation for use in Multi-Pair Telephone Cables", 24th IWCS, Proceedings pp 53-61, Dec. 1975.

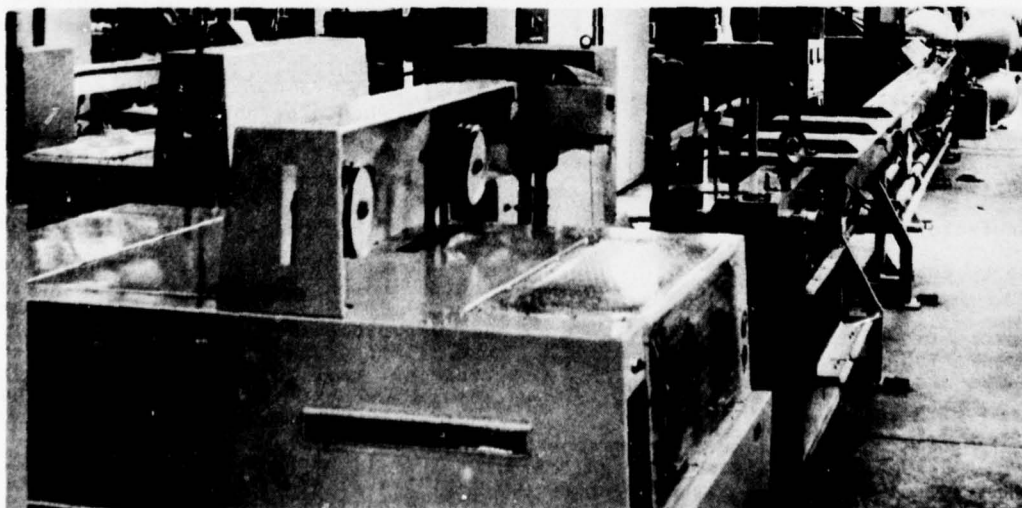


Fig. 22 - Photograph of the two conductor prototype line in operation

Agustin Cueto is General Manager of Cables de Comunicaciones, S.A. in Zaragoza, Spain. He started his career in the industry over 20 years ago with General Cable Corporation. Since that time he has worked in almost all phases of the business and was Manager of General Cable's telephone cable plant in Tampa, Florida before his transfer to Spain in 1970. Mr. Cueto has a Bachelor of Science degree from the University of Tampa and studied for his MBA in Connecticut.



Manuel Cubero has a PhD in telecommunications engineering and is Assistant Director of Research and Development for Cables de Comunicaciones, S.A. His prior experience includes four years as a professor of physics and electronics and 12 years in the electronics and telecommunications industries in R&D and engineering management. In 1972 he was awarded the CNES Space Program Contribution Medal by the French Government for his work in satellite tracking.



Antonio Garvalena is currently Manager of Process Engineering for Cables de Comunicaciones, S.A. in Zaragoza, Spain. Mr. Garvalena has a degree in mechanical and electrical engineering and joined CCSA in 1972 immediately after graduation as a Process Technician. Currently he is responsible for the development of production equipment and process engineering.



MAILING ADDRESS

Cables de Comunicaciones, S.A.
Apartado de Correos 581
Zaragoza, Spain

COMPUTER CONTROL OF HIGH SPEED WIRE COATING LINES

by

V. LeNir
NORTHERN TELECOM LIMITED
Montreal, Quebec

1. SUMMARY

This paper describes the development of a computerised control system for a high speed wire insulating line. It resulted in a substantial improvement of the transmission characteristics of the final product and, in addition, there will be savings in material and labour costs. Software was developed which paved the way for a similar system to be installed on a bank of insulating lines.

2. INTRODUCTION

It was realised soon after the introduction of filled telephone cables that capacitance unbalance to ground levels were not comparable to those obtained in air core cables. Based on theoretical considerations, levels up to 65% higher were estimated (reference 1). This incompatibility with system noise level objectives becomes a serious concern where filled cables are used in long loops. It is important therefore to restore the performance of the cable to that of air core PIC cables. Since capacitance unbalance to ground is mainly caused by non-uniformity of dimensional and dielectric properties of the individual conductors, the required improvement can be achieved by a much higher degree of manufacturing control.

The route of computerisation was followed by Northern Telecom to obtain better coaxial capacitance and/or diameter control of foam skin and solid insulated conductors.

The first phase of the project involved a study of rheological properties of insulating materials as related to processing behaviour. A number of computer programs were written to analyse various aspects of the wire insulating process -- for instance programs were developed for extrusion, for melt flow in the die, and for cooling of the insulated conductors. This approach enabled a more systematic analysis of process problems to be carried out, and provided a background for computerisation of the extrusion process.

An experimental high speed wire insulating line and computer control system were then installed with the objective of developing skills in a production environment without any of the associated pressures. This phase lasted about one year. Based on the results, the decision was made to install a similar system in a strictly production environment (at the Kingston Cable Works) for 12 PIC insulating lines. This installation is underway at the present time.

3. EXPERIMENTAL INSULATING LINE

A schematic of the line is shown in Fig.(I). The line was used to evaluate different types of resins and insulations. In addition, results were obtained from "simulation" programs to provide information relative to "optimised" steady state line operating conditions. In parallel with these activities, problems pertaining to computerisation, such as operator acceptance and system reliability, were resolved.

4. COMPUTER CONTROL SYSTEM

Various systems to achieve closed loop control of process parameters can be rather loosely categorised as follows:

- (1) Hardwired dedicated per line (analog).
- (2) Minicomputer/microprocessor dedicated per line.
- (3) Minicomputer shared ("multi-line"), with analog backup.
- (4) Supervisory minicomputer plus microprocessor dedicated per line.

Examples in category (2) can be found in references (2) and (3).

Costs of the different systems vary widely depending on the degree of flexibility and features offered.

A number of systems were evaluated and the FOX 2/30 control system, manufactured by The Foxboro Co., was selected (1973) because it best satisfied the following requirements:

- (a) Flexibility - The system can be applied to different and evolving processes in cable making.
- (b) Support of high level program languages - it is time consuming to handle problems in assembler language.
- (c) Ease of on-line program development - the foreground/background mode of operation enables programs to be developed on-line while control functions are being executed.
- (d) Expandability - The system is easy to expand and distance between lines does not pose any problem.
- (e) Reliability/ease of maintenance - The system had been field proven for two years.

5. CONTROL SYSTEM HARDWARE CONFIGURATION

The system hardware configuration is comprised of the following components:

Central Control

- Central Processor
- Core memory 28K 16 bit words
- Bulk storage (fixed head disk) 496K
- High speed paper tape reader and punch
- Magnetic tape

Process Interface

- Digital input module (up to 1200 digital inputs)
- Digital output module (up to 1200 digital outputs)
- Pulse count module (up to 60 counters)
- Interspec Communication Module (ISCM)
 - Interfaces with controllers and analog inputs)

Operator Interface

- Operator's console (CRT for display of functional blocks)
- Engineering display unit (CRT for program development, trending)
- System teletype (KSR 35 teletype for program development, hard copy trending).
- Logging teletype (KSR 35 teletype for production reports, alarm messages etc.).

Fig. (II) illustrates the computer-process communication hardware. Up to 3 Interspec Communication Modules (ISCM) can be incorporated into the computer, giving a maximum of $3 \times 16 \times 16 = 768$ control loops or mixture of control loops and inputs (3 inputs \equiv 1 control loop). Our control system had one Controller Communication Module (CCM) and one Analog Input Module (AIM) to handle requisite controlled and monitored points (listed later).

6. OPERATING SYSTEM SOFTWARE

The operating system provides a foundation on which user oriented application software may be developed - via IMPAC process control language and FORTRAN.

Impac

Impac (Industrial MultiLevel Process analysis and Control) is a package of programs providing a means by which different types of functional blocks (e.g. scan, control or computational) may be constructed and linked if required to provide a control strategy. Each block is identified by 5 characters, the first being an alphabetic and the next four digits. Once the block is built (via a series of questions at the terminal), its characteristics may be displayed at the operator's console (Fig. (iii)). Blocks may be modified easily and control schemes rapidly rebuilt. Typical data acquisition features such as signal conditioning, amplifier drift compensation, alarming, etc. are provided.

Fortran

Programs may be written, compiled and debugged on-line without interfering with any control functions (foreground/background mode of program execution). They communicate with the IMPAC system via system subroutines, thus providing considerable flexibility in developing control strategies. In addition a number of system subroutines allow time based functions to be executed (e.g. periodic cycling, or scheduling) - in otherwords real time FORTRAN is implemented in the system.

7. COMPUTER - PROCESS INTERFACE

Interfaced inputs and outputs for the control system are shown in the following table:

Parameter	Inputs Process to Computer	Outputs Computer to Process
<u>Analog Points</u>		
Diameter	X	-
Capacitance	X	-
Preheat	X	-
Melt Temperature	X	-
Main screw RPM	X	X
Secondary screw RPM	X	X
Line Speed	X	X
Movable Trough	X	X
Zone Temperature 1-5	X	X
Head Temperature	X	X
Worm Motor	X	X
Annealer, preheat current	X	-
Reheat current	X	-
<u>Digital States (on/off)</u>		
Product Type	X	-
Start/stop	X	X
Line reset	X	-
Reel changeover	X	X
Line Reset	X	-
Line Status lights	-	X
(Plus) Spark Count	X	-

8. USER DEVELOPED SOFTWARE

Control schemes can be developed via IMPAC blocks on a per process basis. Fortran is used to activate block linkages, insert tuning constants to blocks, cycle relevant programs and satisfy other product/process oriented requirements. The program system developed provides the following features:

- Operator selectable product type.
- Line check prior to startup (e.g. is the barrel temperature profile correct?).
- Automatic startup to line running operating conditions - line startup modes can be reasonably flexible.
- Automatic switch over to predefined control strategy, if "line running" conditions are acceptable.
- Ease of on-line change of control strategy.

(f) Line condition printout.

Additional features available are production reporting and parameter trending, and automatic loop tuning is under development.

As an example Fig. (iv) illustrates the control block diagram constructed for our insulating line. The following steps are taken to "close the loop" for foam skin insulated and for solid insulated conductors:

(a) Foam skin insulated product (selected via control panel switch):

Diameter and coaxial capacitance are simultaneously controlled. Switches 1, 5, 6 and 7 could be closed, tuning constants relevant to the product inserted to the Integral and PID (Proportional-Integral-Derivation) blocks, and a program or programs could be cycled. The PID and Integral blocks are examples of control blocks in which an algorithm is provided to generate an output. For instance the output from the Integral control block has the following form:

$$\Delta M = \frac{\Delta t}{T_r} E$$

where Δt is the point scan period, T_r is a constant, and E is the difference between set-point and measurement.

Thus, in this example, any difference between measured diameter and its required value would allow an output to pass downstream to regulate line speed. Simultaneously, a difference between measured capacitance and its required value generates an output which regulates trough position. Trough position, in its turn, is compared to a required trough position and any resulting output regulates the extruder metering zone set-point.

(b) Solid insulated product: If coaxial capacitance is required to be controlled via screw RPM regulation, switches 4 and 7 would be closed and a program cycled to determine eccentricity from diameter and capacitance.

9. START-UP PROCEDURE

Fig. V shows a simplified panel for the purpose of illustrating start-up, which would proceed in the following manner:

(1) PRODUCT SELECT

The operator switches to the product to be run.

(2) LINE RESET

The Line Reset button is pressed which informs the computer to;

(a) check all the blocks associated with the line to ensure that they are in correct condition (e.g. are they on scan? or are they on control?).

(b) check the selected product against available file data.

If either (a) or (b) is not satisfactory, the "LINE CANNOT RESET" light is activated, otherwise line parameters such as required barrel temperatures are set. The barrel temperature profile which is set at this point is a "LINE STOPPED" profile, which is 10 - 15°F lower than a "LINE RUNNING" profile.

(3) LINE RUN

When line conditions are at adequate values for start-up, the "LINE READY" light is energised indicating to the operator that he can start-up. He presses the RUN button and the line ramps to speed. At this point the barrel temperature set points are raised to the "LINE RUNNING" set points' profile, since viscous heating of the melt drives up temperatures. This procedure facilitates rapid control of the line at start-up for cellular insulated conductor. Line conditions are again checked to ensure that closed loop control can be activated. If it cannot, the line automatically ramps down to stop with an appropriate message and alarm light on the panel. There is some flexibility in start-up. The line can be ramped directly up to operating speed, or in two stages if required - first ramp to slow speed, then ramp to operating speed. Control strategies can be changed on-line via the system terminal.

10. RESULTS

One of the main objectives of computerisation was to reduce the average capacitance unbalance to ground levels of filled cable by improving control of the coaxial capacitance of single conductors. Long term variations of ± 1 pF/ft or more are typical when an insulating line is run manually. As line speeds are increased, long term variations are more difficult to control. When the loop is closed under computer control, long term coaxial capacitance variations were reduced to better than ± 0.2 pF/ft (Fig. VI), and this resulted in a significant improvement of average capacitance unbalance to ground of finished cables. It is not unusual to have average values worse than 200 pF/1000 ft when conductors are produced under manual control. Values better than 100 pF/1000 ft have been regularly attained with the insulating process under computer control.

Another benefit of computerisation is derived from savings associated with reduced start-up scrap. Since tight control can be much more rapidly obtained by the computer at start-up, a reduction of scrap conductor from about 4 reels (half telephone reel size) to better than 1 reel is possible (for cellular insulations).

The results obtained from this "prototype" computerised control system provided justification for the installation of a multiline computer control system in our Kingston Cable Works. It is envisaged that a minimum of supervision of the computer and peripherals will be required, with all required functions being available at the line on a simple control panel. In other words the computer connection will be transparent to the operator.

11. CONCLUSIONS

The objectives which were outlined initially for the development of a computerised control system on a single process line as a prelude to more comprehensive automation of cable plant processes have been satisfied. Software, adaptable to different product/process line requirements, was developed and enabled us to proceed with the implementation of a multiline computerised monitoring and control system.

12. ACKNOWLEDGEMENT

The author would like to acknowledge the efforts of two people closely associated with the project

- Mr. G.D. Baxter, for his part in the initiation of the project and subsequent supervision of the experimental line.

- Mr. P. Schmidt, who was involved in the instrumentation and interfacing of the line to the computer.

13. REFERENCES

1. J.A. Olszewski. "Capacitance Relationships in Filled Telephone Cables and Equilibrium Prediction from Water Immersion Tests." Proceedings 24th International Wire & Cable Symposium.
2. E. Kertscher. "Automatic Process Control in the Insulating of Telephone Cables." Wire Journal. January 1976.
3. S. Yumoto, K. Masuda, K. Matsubara, T. Hiroshima. "Computer Control of Insulation Extrusion Line." Wire Journal, September 1973.



Victor L. LeNir graduated with a B.Sc. in Physics from Manchester University, England in 1960. After 2 years with Standard Elektrik Lorenz in Germany, he joined Northern Electric Cable Division, Lachine, in 1963 and was involved until 1967 in Process Analysis and Modelling in cable processes. In 1968 he took an M.Sc. at London University, England, in Computer Science, and since then has been involved in software development for computerised process control, first with English Electric Co. in England, and since 1970 with Northern Telecom Cable Division, Lachine, Quebec, Canada.

FIG. I EXPERIMENTAL WIRE INSULATING LINE

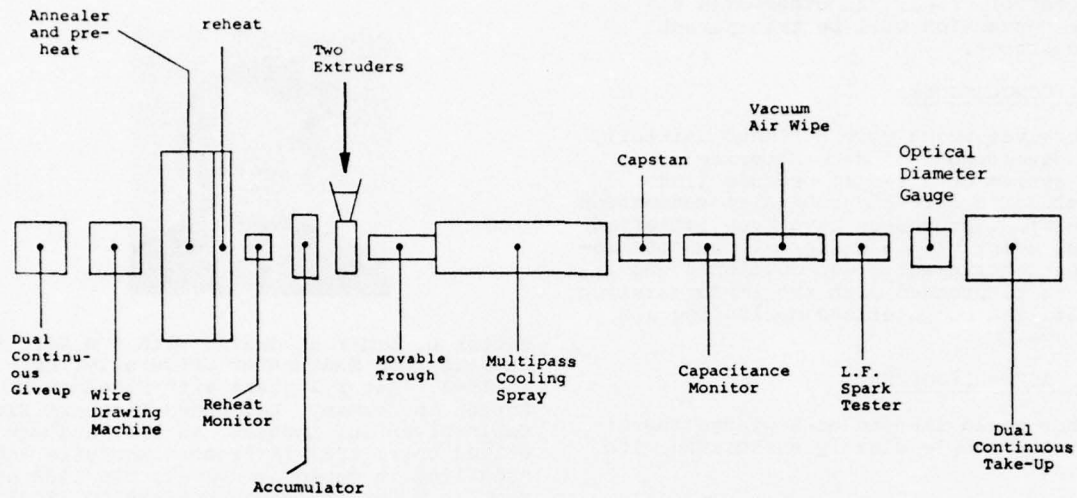


FIG. II PROCESS INTERFACE

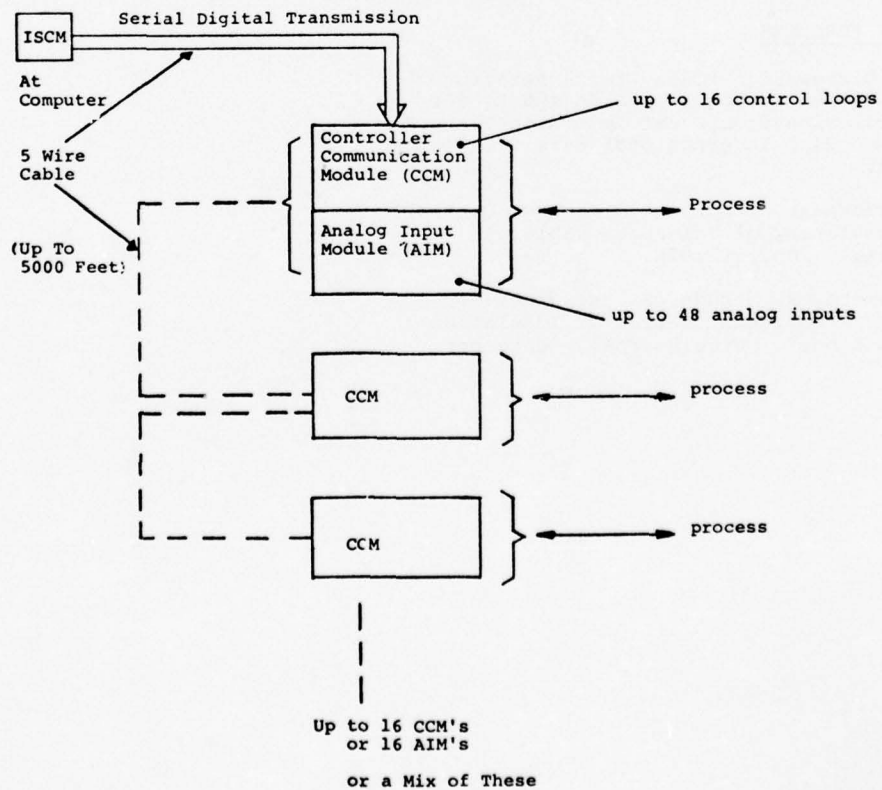
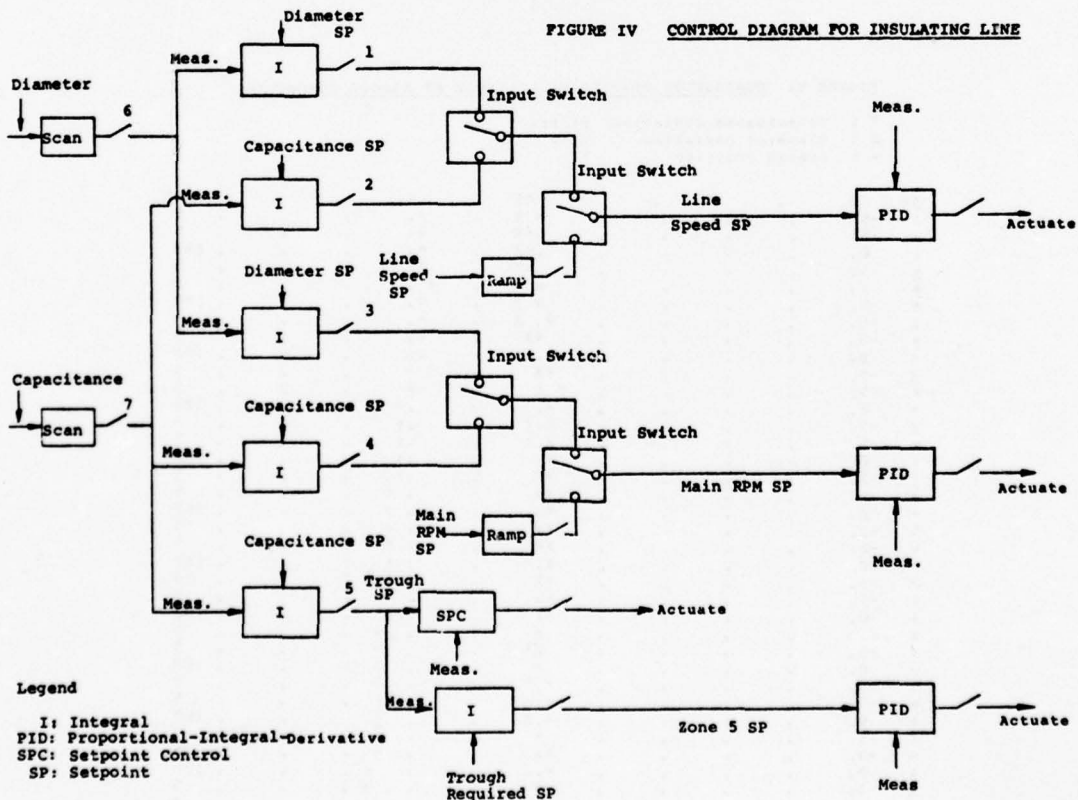


FIGURE III OPERATOR'S CONSOLE

02/04/00 07:11

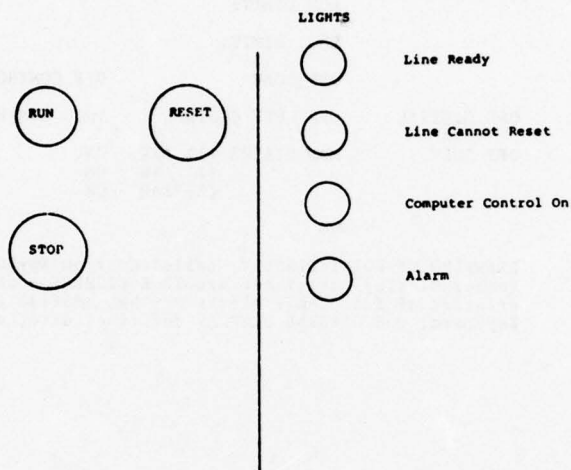
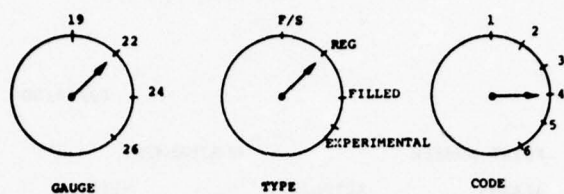
POINT NUMBER	MEASUREMENT	
ALARMS	SETPOINT:	SETP
	HIGH LIMIT:	
	LOW LIMIT:	
	DEV. LIMIT:	
	OFF SCAN	OFF CONTROL
OFF DIGITAL	OFF SUPV CONTROL	LOCL CONTROLLER
OFF SUPV	MSG STATUS (1) DEV	ON
	(2) ABS	ON
	(3) BAD	ON

EXAMPLES OF POINT DISPLAY, called up from Keyboard
(other displays available are TUNE DISPLAY - characteristics of functional blocks may be modified from Keyboard, and GENERAL DISPLAY for time, date, etc.).



The figure shows three circular diagrams, each representing a different part of a code system:

- GAUGE:** A circle with four tick marks labeled 19, 22, 24, and 26. A pointer is positioned between 19 and 22.
- TYPE:** A circle with three tick marks labeled REG, FILLED, and EXPERIMENTAL. A pointer is positioned between REG and FILLED. Above the circle is the label "F/S".
- CODE:** A circle with six tick marks labeled 1, 2, 3, 4, 5, and 6. A pointer is positioned between 4 and 5.



* : Capacitance deviation pF/ft.
X : Diameter Deviation Mils
+ : Trough Position %

[illegible]

A UNIQUE MONITORING SYSTEM FOR EXPANDED WIRE INSULATIONS

T. S. DOUGHERTY
Western Electric Company, Inc.
Norcross, Georgia

Abstract

A unique monitoring system is described for use in the manufacture of expanded wire insulations. The system makes use of coaxial capacitance versus DOD plots to allow the on-line measurement of insulation expansion and weight. The monitor is used to demonstrate the effectiveness of process variables in controlling the expansion process. It is also used to compare the processibility of dual expanded insulation and single layer expanded insulation.

Introduction

Expanded insulations have been under development in the Bell System for approximately 20 years, but widespread introduction of such insulations has not occurred. This was primarily due to the difficulty of efficiently manufacturing quality expanded insulations at high speed. However, technical solutions to many of the problems which have retarded the growth of expanded insulations are now in hand. The development of non-plating chemical blowing agents, and methods of compounding blowing agents into pellets or blending them into flake are several areas where breakthroughs have occurred in the industry to improve process stability.

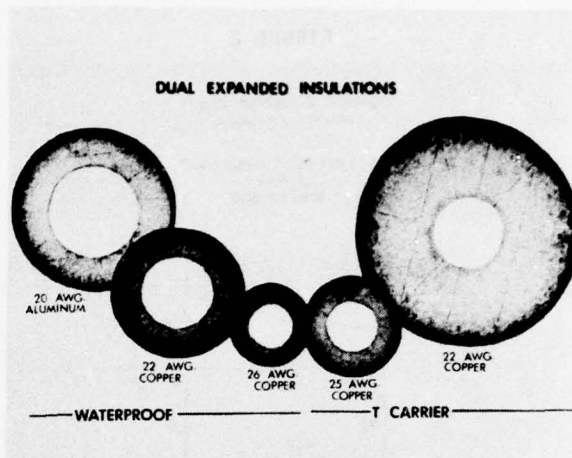
Within Western Electric process development has been concentrated in the following key areas:

1. Insulating tool design
2. Extrusion screw design
3. Raw material inspection
4. Bare wire temperature measurement
5. Insulation cooling studies
6. Process monitoring
7. Process control

The result of this effort has been the development of an efficient high speed process for the manufacture of Dual Expanded Plastic Insulated Conductors (i.e. DEPIC). Cross sections of a variety of DEPIC insulations are shown in Figure 1 and include waterproof designs and low capacitance designs for T carrier applications. They were manufactured at line speeds varying from 1600 to 6000 feet per minute.

Previous papers presented at the International Wire and Cable Symposium discussed the development of an insulation cooling model,¹ and raw material inspection procedures for expandable polyolefins.² A third paper discussed applications for DEPIC insulations in telephone cable.³

FIGURE 1



The purpose of this paper is to describe a unique insulation monitoring system which was developed to provide an improved understanding of the insulating process. It has been found to be a valuable tool in the specification of insulation capacitance and DOD requirements, and has been used in the laboratory to interpret experiments on the effects of process variables.

Foam Versus Solid

The foam insulating process is sensitive to raw materials, hardware design, and to all operating variables. Screw speed, line speed, barrel zone temperatures, wire temperature, water trough position and water temperature either affect the insulation weight per unit length or the degree of expansion or both. These independent process variables must be controlled to simultaneously meet insulation specifications on two dependent variables, coaxial capacitance and DOD. By contrast the solid plastic insulated conductor (i.e. PIC) process involves the control of one independent variable, either line speed or screw speed to meet a specification on one dependent variable, coaxial capacitance or DOD. The complexity of the foam process is caused by the additional degree of freedom.

When manufacturing expanded insulations both coaxial capacitance and DOD are usually monitored on separate channels of a strip chart recorder to assure that they are within specification limits. Typical traces

are shown in Figure 2 for 22 AWG DEPIC manufactured at 5000 ft/min for waterproof cable. A cross section of this insulation is shown in Figure 3, and consists of a 2 mil skin of colored high density polyethylene over a 45% expanded core of natural high density polyethylene. Also shown is an equivalent single layer Expanded Plastic Insulated Conductor (i.e. (EPIC).

FIGURE 2

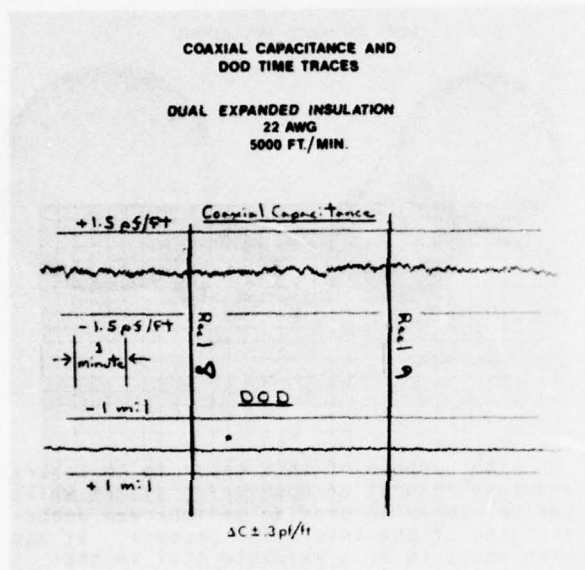
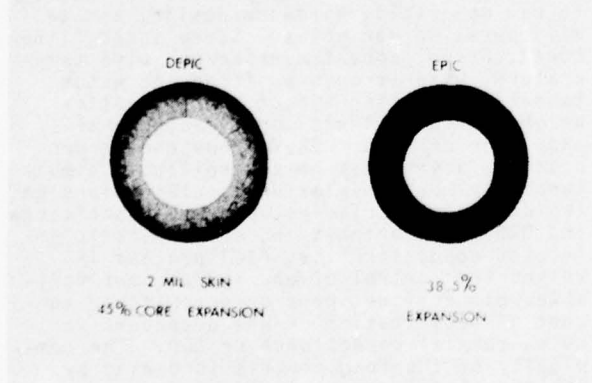


FIGURE 3

22 AWG FILLED CABLE



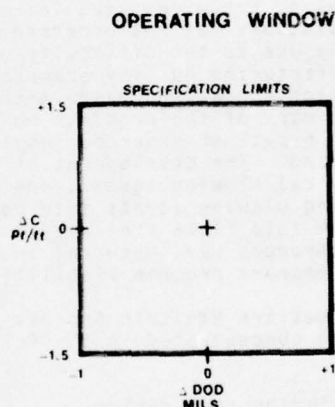
The capacitance and DOD traces are interpreted to determine which process variables require adjustment to approach the nominal condition. This decision process is not easy, but it can be supplemented by off-line measurements of percent

expansion and insulation weight per unit length. Screw speed can then be adjusted to control insulation weight, and air gap or barrel temperature to control expansion. A system which would allow the on-line measurement of insulation expansion and weight per unit length would facilitate this decision making process.

The Capacitance-DOD Display

Since expanded insulations must meet specifications on both capacitance and DOD, it is proposed to display capacitance directly against DOD on-line using an X-Y recorder or X-Y scope. The capacitance and DOD limits can be superimposed on such a display as shown in Figure 4. The capacitance-DOD trace must lie inside this operating window to be within specification.

FIGURE 4

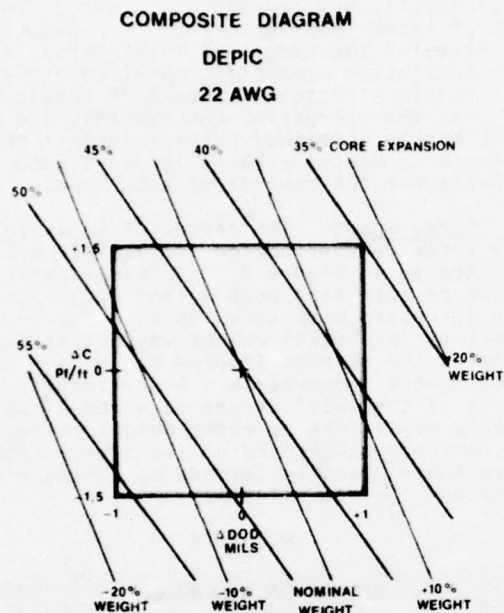


Additional information can be gained from this type of display by superimposing lines of constant plastic expansion (i.e. core expansion in the case of DEPIC), and lines of constant insulation weight per unit length as shown in Figure 5. The lines of constant expansion and weight were calculated from standard equations for coaxial capacitance and insulation weight. The coaxial capacitance equation for DEPIC follows:

$$C = \frac{7.36 \epsilon_s \epsilon_f}{\epsilon_f \log_{10} \left(\frac{DOD}{DOD-2t} \right) + \epsilon_s \log_{10} \left(\frac{DOD-2t}{d} \right)} \quad (1)$$

where C=coaxial capacitance-picofarads per ft.
DOD=diameter over dielectric
t=skin thickness
d=conductor diameter
 ϵ_s =skin dielectric constant
 ϵ_f =foam dielectric constant

FIGURE 5



Several assumptions were made in these calculations. First, perfect insulation concentricity was assumed. Second, the skin thickness for DEPIC insulation was either assumed to be constant and independent of DOD, or the cross sectional area of the skin was assumed constant and the skin thickness determined as a function of the DOD and the nominal dimensions. The constant skin thickness assumption is used in design problems where the nominal DOD is unknown. The constant cross sectional area assumption is used when simulating experiments, where the extruder output for the skin is relatively constant. Finally, an effective foam dielectric constant was calculated as a function of percent expansion from an empirical equation which was developed by performing a series of experiments at known coaxial capacitances, insulation dimensions, and expansions. This improved the accuracy of the coaxial capacitance calculation, because radial variation of expansion causes the effective dielectric to be lower than that calculated from the usual linear relationship.

Now referring back to Figure 5, note that the insulation weight is a minimum (18 percent below nominal) and expansion a maximum (55 percent) at the lower left corner of the operating window. Likewise, weight is a maximum (18 percent above nominal) and expansion a minimum (35 percent) at the upper right corner. If it is necessary to avoid high or low values of expansion, the shape of the specification limits on the capacitance-DOD display could be redefined to limit extreme values of expansion.

This composite diagram has proven to be a useful tool in the specification of capacitance and DOD requirements for expanded insulations, since all insulation characteristics are presented on a single chart. Once the nominal capacitance and DOD are chosen, the effect of allowable capacitance and DOD variations on the ranges of expansion and insulation weight can be easily studied by varying the size of the operating window.

Effect of Process Variables

The capacitance-DOD display is also a useful laboratory tool. Though previous papers have discussed effects of process variables^{4,5}, several experiments were performed on a high speed production type insulating line to illustrate the use of the display in studies of the effect of operating variables on capacitance, DOD, insulation weight and percent expansion. Both the 22 AWG DEPIC insulation already mentioned and the equivalent EPIC insulation were studied for comparison. It must be emphasized that the magnitude of the effects will depend upon the type product being manufactured, the raw materials, and the characteristics of the insulating line such as extruder size, screw design and tool design. A 2½" 24/1 extruder was used for the foam, and an additional 2½" 20/1 extruder was used for the skin in the case of the DEPIC insulation.

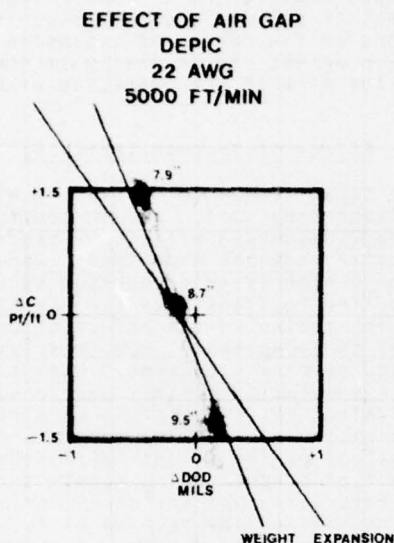
An underwater diameter gauge, which measures diameter by direct contact with the wire, was used to allow the measurement of DOD as close to the capacitance monitor as possible. This minimized the time delay between the measurement of capacitance and DOD to achieve a good correlation between these two variables. In addition the capacitance monitor and DOD gauge were located in a tank between the capstan and the take-up to assure that measurements were made on cold insulation. An optical diameter gauge could have been used instead of the underwater gauge. In such a case, the capacitance monitor and the DOD gauge would be separated by an air wipe which would introduce a longer time delay. This would not be a problem for small fluctuations or for gradual changes in capacitance or DOD. The deviations of capacitance and DOD from their nominal values were amplified and sent to an X-Y recorder to obtain a permanent record of the traces.

DEPIC Experiments

Air Gap. The effect of air gap is illustrated in Figure 6 for DEPIC insulation at 5000 ft/min. Each trace was recorded for one minute. An approximate 10% change in air gap was necessary to move the trace from the nominal condition to the specification limit. Note that the trace followed a line of constant weight since only the expansion was varied. Also note the narrow trace with the DEPIC insulation. For thin wall ex-

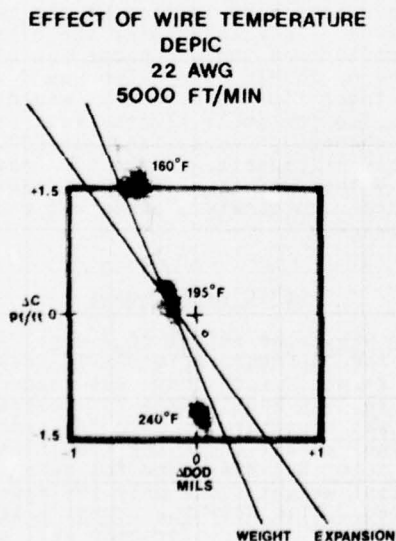
panded insulations (ex. 5 - 20 mils) the air gap was a very effective means of achieving an immediate change in expansion.

FIGURE 6



Conductor Temperature. The effect of conductor temperature is shown in Figure 7. In this case the slope of the trace movement was slightly steeper than a line of constant weight, because conductor temperature not only affected expansion but also the radial distribution of expansion. Hence increased expansion near the wire caused the trace at 240°F to be lower than predicted. The opposite was true for the trace at 160°F.

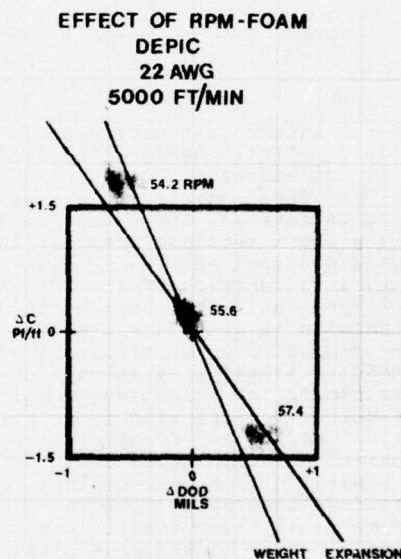
FIGURE 7



Conductor temperature cannot be varied indiscriminately. It must be kept as high as possible to meet insulation elongation requirements, but low enough to avoid formation of large bubbles against the conductor. For example, the sample at 195°F passed a 300% insulation elongation requirement with good bubble structure. The 160°F sample did not pass the elongation requirement, and the 240°F sample contained bubbles against the conductor. Hence, preheat is not a good variable for the control of expansion.

Screw Speed. The effect of an approximate three percent change in foam screw is illustrated in Figure 8. In this example, it can be seen that both weight and expansion increased with screw speed. The response to this small change was not as immediate as the changes induced by the air gap or conductor temperature. Approximately two-thirds of the total change occurred almost immediately as the extruder output increased. The remaining one-third of the change took approximately thirty seconds as a result of transient thermal effects.

FIGURE 8



Though line speed was not examined during this series of tests, it had been studied previously and found to have the same type of response as screw speed. That is to say there was an initial rapid response as insulation weight changed followed by a short interval of drift which was a result of transient thermal effects induced by a change in head pressure.

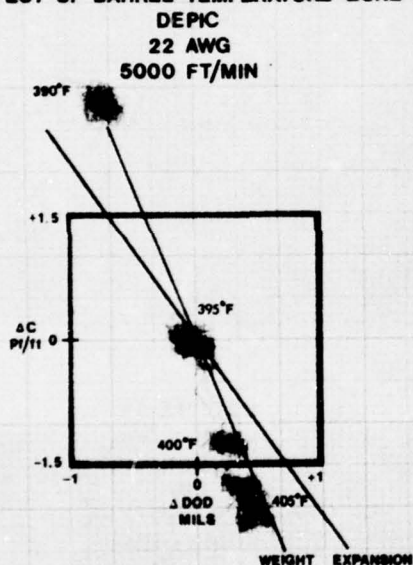
Because small line and screw speed changes appear equivalent, screw speed is the preferred method of controlling insulation weight, especially since this allows a constant production rate. A constant line

speed also facilitates maintenance of constant conductor temperature, resistance and elongation.

Barrel Temperature. The effect of the metering zone temperature closest to the screw tip is illustrated in Figure 9. Note that the trace closely follows a line of constant weight indicating that a 15°F change in barrel temperature had little effect on extruder output. In addition, as the temperature was increased in 50°F steps, the reductions in capacitance or increases in expansion became successively smaller. The expansions derived from this diagram were plotted in Figure 10 as a function of barrel temperature. Had the barrel temperature been increased further, expansion would have begun to decrease while the variation in expansion would have increased due to a loss of effective nucleation at high temperatures.

FIGURE 9

EFFECT OF BARREL TEMPERATURE-ZONE 5



EPIC Experiments

The previous series of experiments was repeated with EPIC insulation, which was expanded 38.5% to maintain the same capacitance and DOD as the DEPIC insulation. Because the same 2½" 24/1 extruder was used for the foam, the line speed was reduced to 3500 ft/min to maintain a foam output of 55 lb/hr for a fair comparison.

Air Gap. The effect of air gap is shown in Figure 11. Note that the scatter was approximately twice as great as with the DEPIC insulation. The scatter occurred primarily along a line of constant insulation weight indicating that variations in expansion were occurring.

FIGURE 10

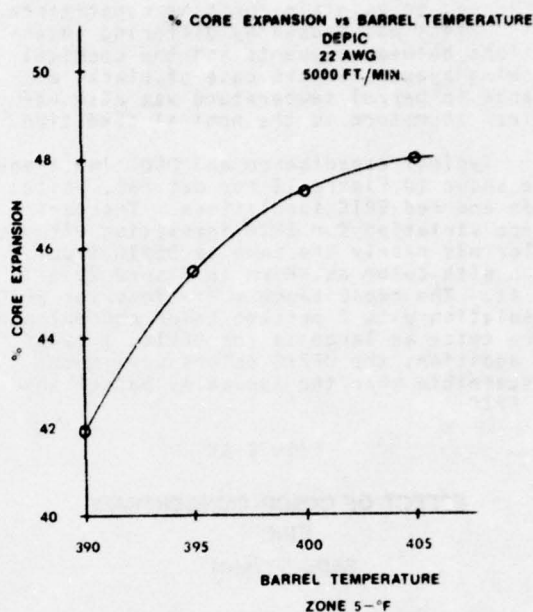
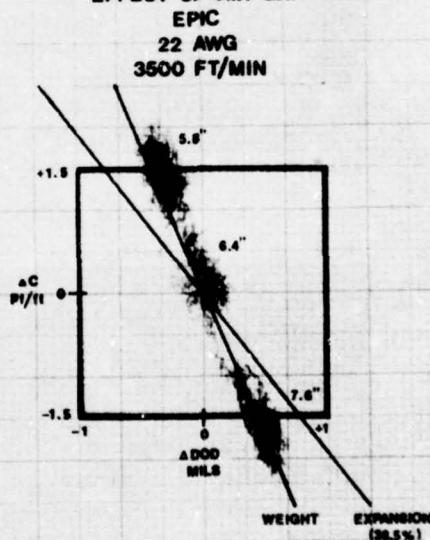


FIGURE 11

EFFECT OF AIR GAP



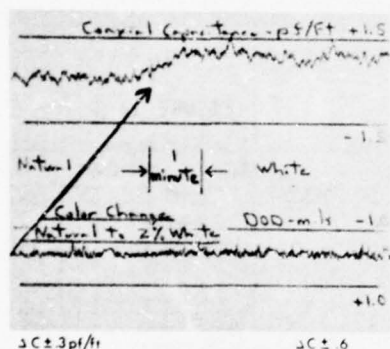
Color Concentrate. To resolve the question of expansion variation a short series of color concentrate experiments were performed with EPIC insulation. The trial was begun with natural insulation (i.e. without color) and proceeded through the standard colors using 2 percent concentrate.

The changes in color concentrate necessitated adjustments in the air gap from 8 to 15 inches to maintain constant capacitance. This effect was caused by differing interactions between pigments and the chemical blowing agent. In the case of black, a change in barrel temperature was also required to return to the nominal condition.

Typical capacitance and DOD time traces are shown in Figure 12 for natural, white, blue and red EPIC insulations. The capacitance variation for EPIC insulation without color was nearly the same as DEPIC insulation with color as shown in Figure 2, $\pm .3$ pf/ft. The capacitance variations for EPIC insulation with 2 percent color concentrate were twice as large as for DEPIC, $\pm .6$ pf/ft. In addition, the DEPIC colors were more discernible than the typically pastel shades of EPIC.

FIGURE 12

**EFFECT OF COLOR CONCENTRATE
EPIC
3500 FT/MIN**

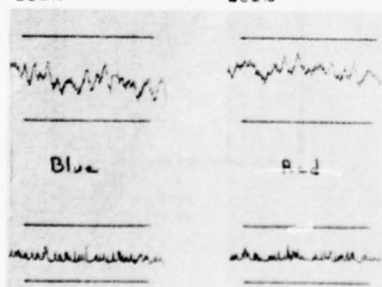


$\Delta C \pm 3 \text{ pf/ft}$

$\Delta C \pm 6$

$\Delta C \pm 6$

$\Delta C \pm 6$



Remaining Process Variables. The magnitude of the effects of conductor temperature, screw speed and barrel temperature were the same as for DEPIC insulation, as shown in Figures 13-15. The primary processing difference between the DEPIC and EPIC insulations was the line speed and the trace

scatter. When the EPIC line speed was increased to 5000 ft/min, the scatter became four times greater than the scatter for DEPIC insulation, as shown in Figure 16. A larger extruder would have reduced this scatter but it would not have approached the narrow scatter of DEPIC insulation because of the effect of color pigments.

FIGURE 13

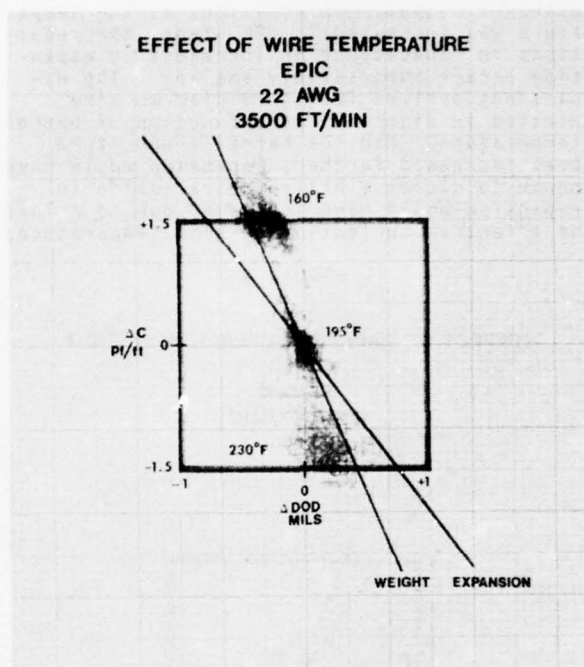


FIGURE 14

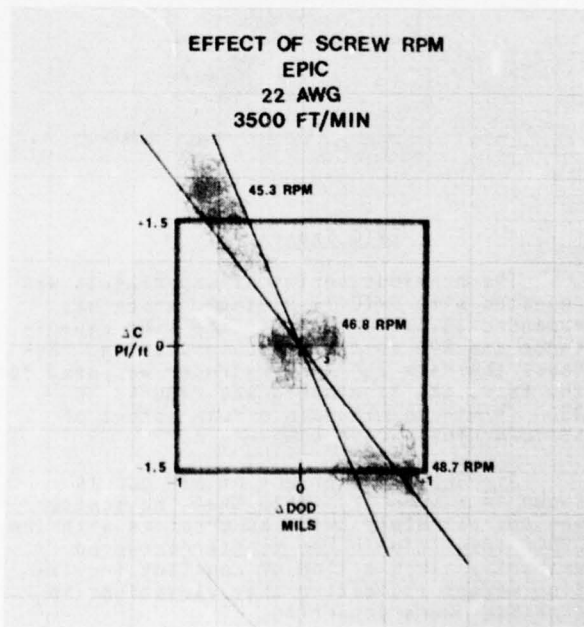


FIGURE 15

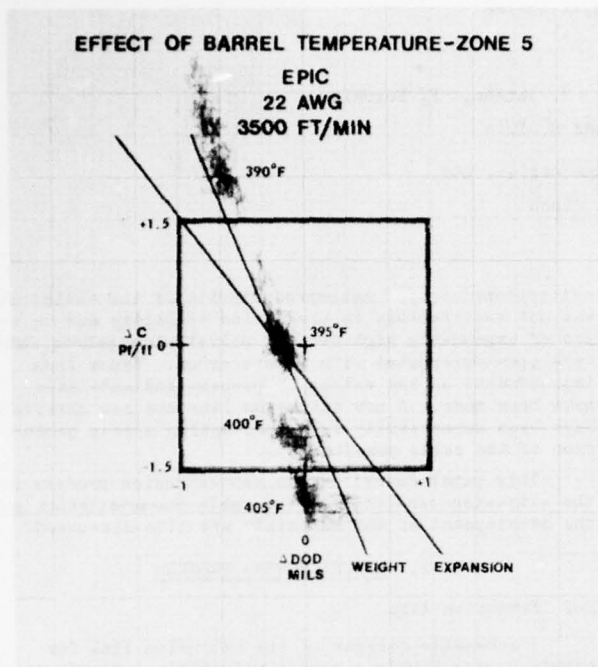
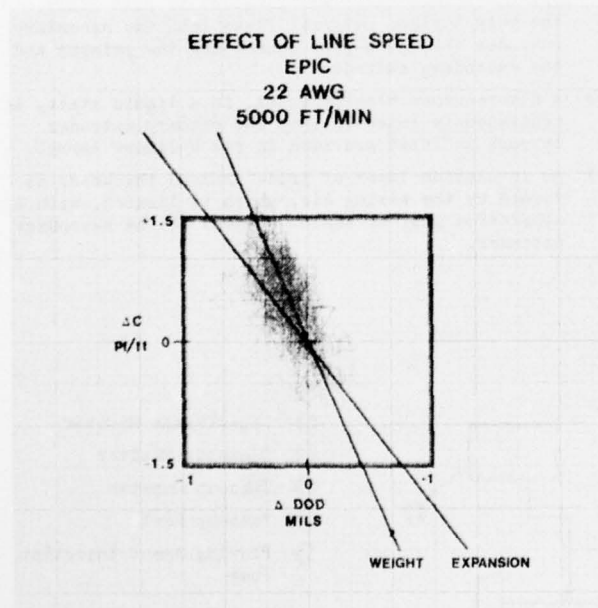


FIGURE 16



Conclusions

The capacitance-DOD insulation monitoring system has proven to be a valuable laboratory tool since it allows the on-line measurement of insulation weight and expansion. The previous examples illustrated the use of the capacitance-DOD monitor to interpret experiments. They demonstrated the ability of the monitor to distinguish small changes in in-

sulation weight or expansion on-line. Because all pertinent characteristics of expanded insulations can be presented on a single display, a greater understanding of the expansion process can result. This is especially true in the specification of insulation capacitance and DOD requirements.

Acknowledgments

The author gratefully acknowledges the contributions of Mr. W. K. Miller, Western Electric Company, and Prof. M. R. Cereijo, Florida International University. The guidance of Mr. C. B. Heard and assistance of Messrs. L. E. Field and E. C. Akins is also appreciated.

References

1. J. C. Calhoun, W. M. Flegal, "The Cooling Process in Plastic Insulated Wire." Proceedings 23rd International Wire and Cable Symposium, p. 330, 1974.
2. D. I. Marshall, J. M. Turnipseed, F. R. Wright, "Raw Material Inspection for Expandable Polyolefin Insulations." Proceedings 23rd International Wire and Cable Symposium, p. 63, 1974.
3. D. M. Mitchell, G. H. Webster, "Material Savings by Design in Exchange and Trunk Telephone Cable." Proceedings 23rd International Wire and Cable Symposium, p. 216, 1974.
4. E. J. Gouldson, M. Farago, G. D. Baxter, "Foam-Skin, A Composite Expanded Insulation for Use in Telephone Cables." Proceedings 21st International Wire and Cable Symposium, p. 158, 1972.
5. E. Kertscher, "Recent Developments in the High Speed Insulations of Quality Telephone Wires." Proceedings 22nd International Wire and Cable Symposium, p. 315, 1973.



Timothy S. Dougherty received a B.S. in Mechanical Engineering from the University of Connecticut and a M.S. and Ph.D. in Mechanical Engineering from Rensselaer Polytechnic Institute. He joined Western Electric's Engineering Research Center in 1968 and worked in the area of plastic extrusion. In 1971 he transferred to the Cable and Wire Product Engineering Control Center where he has worked on expanded insulation process development. He holds four patents in the manufacture of expanded insulations.

NOVEL EXTRUSION PROCESS FOR ROBUST HIGHLY EXPANDED POLYETHYLENE

INSULATED COAXIAL CABLES

T. Nakahara, A. Tsukamoto, H. Shimba, F. Suzuki,
T. Miyaziri and M. Yuto

Sumitomo Electric Industries, Ltd.

Yokohama, Japan

SUMMARY

An extrusion process for the mass production of coaxial cable with approximately 85% expanded polyethylene insulation has been successfully developed. The process provides a stable production of cable at a line speed equal to that of a conventional extrusion process using a chemical blowing agent. The extrusion line is provided with specially designed equipment and the extrusion materials are carefully selected. The cables have proved to be satisfactory in all applications. This paper describes the extrusion process and discusses the cable characteristics.

1. INTRODUCTION

With the increasing expansion of the bandwidth and the increase of CATV and CCTV facilities, broad band and low loss transmission lines have become an important consideration. Although lower transmission loss in a conventional coaxial cable, with approximately 50% expanded polyethylene insulation, can be obtained through an increase in the conductor and insulation diameter, a cable of larger diameter is inconvenient for installation and maintenance. However, if a larger cable is not adopted, the transmission facilities cost increases due to the increased number of amplifiers necessary.

In order to solve these problems, a new coaxial cable with approximately 85% expanded polyethylene insulation was developed. The primary manufacturing technology, including the development of the materials, was presented in 1973. However, the primary technology was

not appropriate for mass-productivity of the cable; and was not satisfactory in production stability due to the use of expandable high density polyethylene pellets which were pre-impregnated with fluorocarbon. Since then improvements on the extrusion process and materials have been made. A new extrusion line and new materials have been successfully developed making a mass production of the cable possible.

This paper describes the new extrusion process and the extrusion conditions. The cable characteristics and the development of the materials are also discussed.

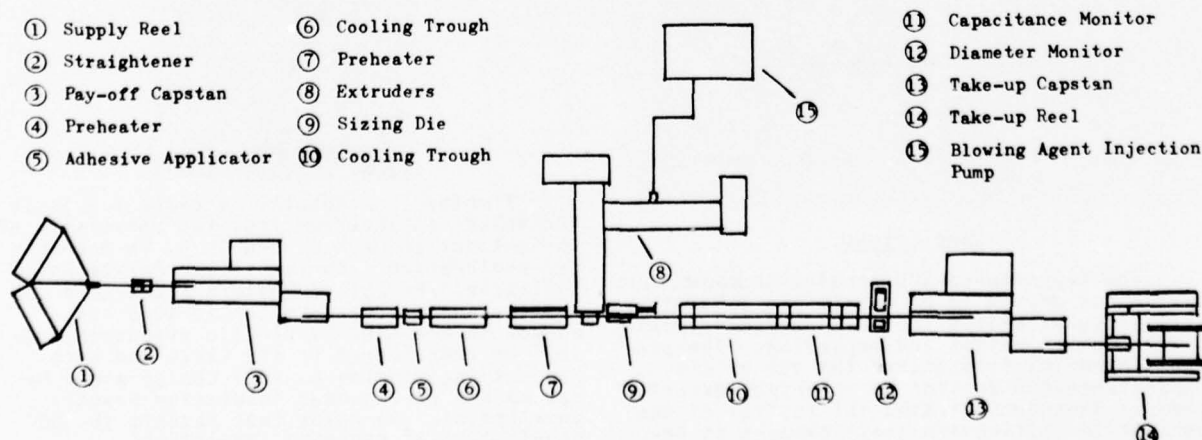
2. MANUFACTURING PROCESS

2-1 Extrusion line

A schematic diagram of the extrusion line for manufacturing highly expanded polyethylene insulation cores is shown in Figure 1. The prominent features of this process are as follows ;

- 1) The extrusion facility consists of tandem type extruders whose axes are parallel to each other. The polyethylene material flows into the secondary extruder through a pipe connecting the primary and the secondary extruder.
- 2) A fluorocarbon blowing agent, in a liquid state, is continuously injected into the primary extruder through an inlet provided in its cylinder barrel.
- 3) An insulation layer of predetermined thickness is formed by the sizing die, which is located, with a separation gap, at the cross-head of the secondary extruder.

Fig. 1 Extrusion Line



4) An adhesive coating is applied to the surface of the inner conductor so as to provide good adhesiveness between the inner conductor and the insulation layer.

The primary extruder functions to melt the polyethylene compound and thoroughly mix it with the liquid blowing agent, which is directly injected into the primary extruder through the inlet. The mixture is advanced to the secondary extruder where additional mixing is accomplished and the material is cooled to a temperature which is suitable for making highly expanded polyethylene insulation.

The inlet is located about two-thirds of the distance down the barrel and is equipped with a special valve which prevents the molten polyethylene from flowing back into the injection pipe from the extruder. During extrusion, the blowing agent is continuously supplied from its storage tank by a metering pump which is designed to control its flow rate.

The primary extruder has functions which are different from those of the secondary extruder. In order for each extruder to perform its functions, a special screw design is required. The primary extruder screw is provided with zones of metering and mixing at its exit. In addition, it has a compression relief zone near the inlet where the pressure of the molten polyethylene is reduced to provide a continuously stable injection of the blowing agent. The secondary extruder screw is a common metering type but is characterized by a deeper screw depth and larger screw diameter than the primary screw. This design reduces the heat from friction in the molten polyethylene without decreasing the output capacity of the secondary extruder. In this process, the extrusion temperature must be strictly controlled. Therefore, stepless controllers using SCRs are used for regulating the temperature of the cylinder barrel, the cross-head, and the extrusion die of the secondary extruder.

The sizing die, located near the cross-head, is indispensable in the production of satisfactory cable cores in the extrusion line. The polyethylene on the conductor expands at the exit of the extrusion die, and then passes through a cooled sizing die where its expansion is restricted, and a predetermined core diameter is formed. The cable core has a smooth surface and satisfactory uniformity in diameter and expansion ratio along its entire axis.

Coatable plastics, such as low density polyethylene with a high melt index, are applied to the conductor at the adhesive applicator by a floating die. This process is immediately followed by the extrusion of expanded insulation at the cross-head. The adhesive coating insures good adhesiveness between the conductor and the expanded insulation. If it was not applied, the pullout strength between them would be weak and fluctuate due to the formation of voids caused by the diffusion of the gasified blowing agent on the surface of the conductor.

Other equipment is the same as that installed in a conventional extrusion line for producing coaxial cable cores with 50% expanded insulation using a chemical blowing agent.

2-2 Extrusion of coaxial cable core

Insulation Material : A modified polyethylene, with high processability, is now in use as an insulating material. Its physical properties are presented in Table 1. The polyethylene is formulated with a small amount of antioxidant and nucleating agent. A robust, highly expanded, insulation material of modified polyethylene (which is different from conventional low density or high density polyethylene) has been developed. High density polyethylene has a high

Table 1 Properties of Polyethylene

Density	, g/cm ³	0.927	ASTM D1505 - 68
Melt Index	, g/10min.	2.32	ASTM D1238 - 70
Yield Strength	, kg/mm ²	1.22	ASTM D 638 - 72
Ultimate Strength	, kg/mm ²	1.30	"
Elongation	, %	545	"

compression strength. However, its performance in sharp bending is rather poor, but better than that of polystyrene foam. Another shortcoming of high density polyethylene is its low processability which leads to production difficulties in the stable extrusion of uniform cores. The basic shortcoming of low density polyethylene is its low compression strength.

Blowing Agent : Volatile liquids such as dichlorotetrafluoroethane (CF₂Cl·CF₂Cl), trichlorotrifluoroethane (CF₂Cl·CFCl₂), dichlorodifluoromethane (CF₂Cl₂), trichloromonofluoromethane (CFCl₃) and their blends can be used for this purpose. According to our extrusion tests, dichlorotetrafluoroethane or blends of dichlorotetrafluoroethane and trichloromonofluoromethane or trichlorotrifluoroethane produce excellent results in the production of cable cores.

Nucleating Agent : The cell structure of the foamed insulation depends greatly on the type of nucleating agent used. Therefore, the selection is very important in making uniform and highly expanded insulation. Materials selected from several kinds of inorganic compounds, such as fine talc and chemical blowing agents such as sodium bicarbonate, were tested in our extrusion experiments. It was found that a chemical blowing agent was the most preferable nucleating agent with concentration levels of 0.1 to 0.5 parts per 100 parts polyethylene.

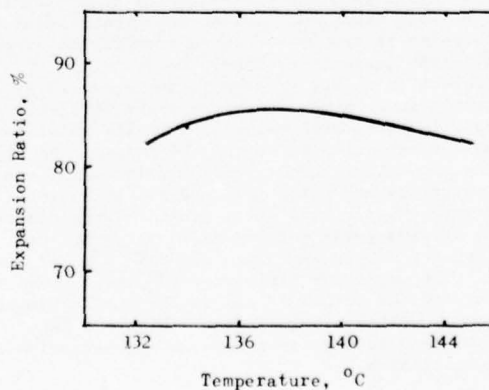


Fig. 2 The Effect of Stock Temperature on Expansion Ratio of the Insulation.

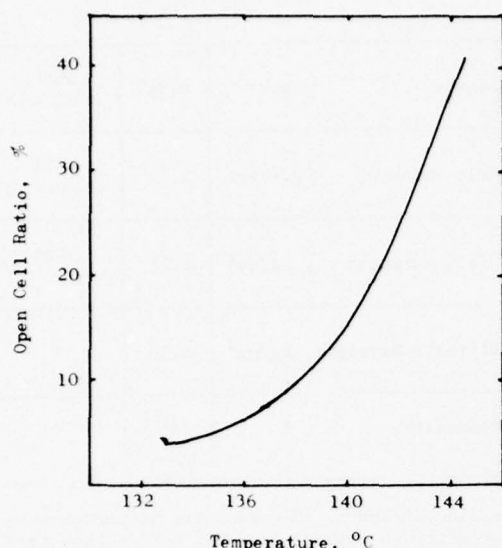


Fig. 3 The Effect of Stock Temperature on Open Cell Ratio

Adhesive Material : Low density polyethylene, with a melt index of approximately 20, was formulated with a small amount of antioxidant and used as the adhesive material.

To investigate the relationship between the extrusion (stock) temperature and the expansion ratio of the insulation, extrusion tests were carried out. Results of tests, using predetermined constant conditions of screw revolution, line speed, and the rate of the blowing agent, are shown in Figure 2. The inclination of the curve in Figure 2 is remarkably different from that of a conventional extrusion process using a chemical blowing agent. The expansion ratio of the insulation is less dependent on the extrusion temperature in our novel extrusion process than in the conventional process. This is due to the use of the sizing die and the physical blowing agent. Figure 3 shows that the extrusion temperature has great influence on the open cell ratio of the expanded insulation. The open cell ratio is defined as the ratio of open cells to total cells. From the view point of moisture penetration into the expanded insulation, the desired value of the ratio should be less than 10%. Taking this requirement into consideration it can be concluded from Figure 3 that the extrusion temperature should be below 138°C. The core production in our process is now operated at 138°C or slightly lower since it proved to be difficult to make satisfactory cores below 135°C. The relationship between the expansion ratio and the rate of the blowing agent is shown in Figure 4. The blowing agent was injected by the injection pump under a pressure of 70~100 kg/cm². Figure 4 illustrates that the addition of 8 parts blowing agent per 100 parts polyethylene is necessary for making approximately 85% expanded insulation. The expanding efficiency (%) is defined as the ratio of the volume of gas in the insulation to the volume of supplied blowing agent. Figure 5 shows the effect of the blowing agent rate on the expansion ratio of the insulation.

Four standard sized CATV cables, with about 85% expanded insulation have been successfully manufactured for the commercial market. The diameters of the outer conductors are 19.0mm(0.75 inch), 12.7mm(0.5 inch), 10.5mm(0.412 inch) and 9.5mm(0.374 inch). The extrusion speeds are approximately equal to those of the conventional process using a chemical blowing agent. For example, the 0.5 inch size cable has an extrusion speed of 25~30 m/min. In this case, the core diameter and capacitance are controlled within $\pm 1.0\%$ and $\pm 0.8\%$, respectively. The fluctuations are shown in Figure 6 and Figure 7. Cross sections of the foamed insulations are shown in Figure 8 and Figure 9.

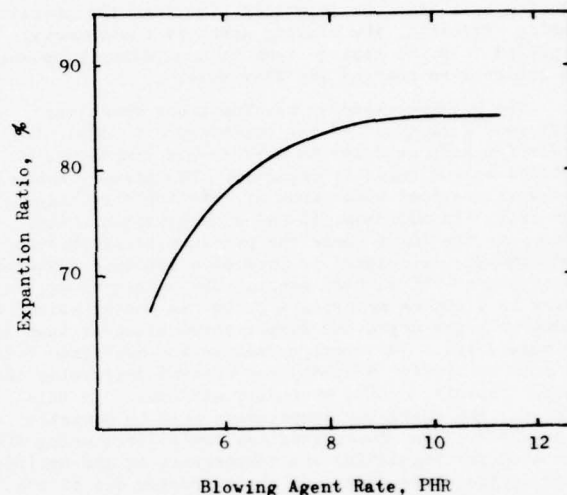


Fig. 4 The Effect of Blowing Agent Rate on Expansion Ratio of the Insulation

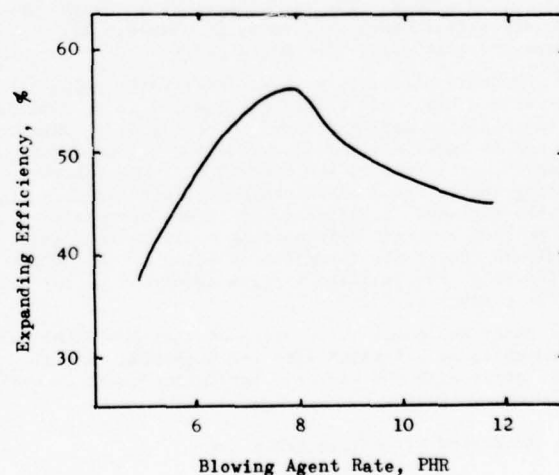


Fig. 5 The Effect of Blowing Agent Rate on Expanding Efficiency

Fig. 6 Diameter Fluctuation of 12.7mm(0.5") Cable Core

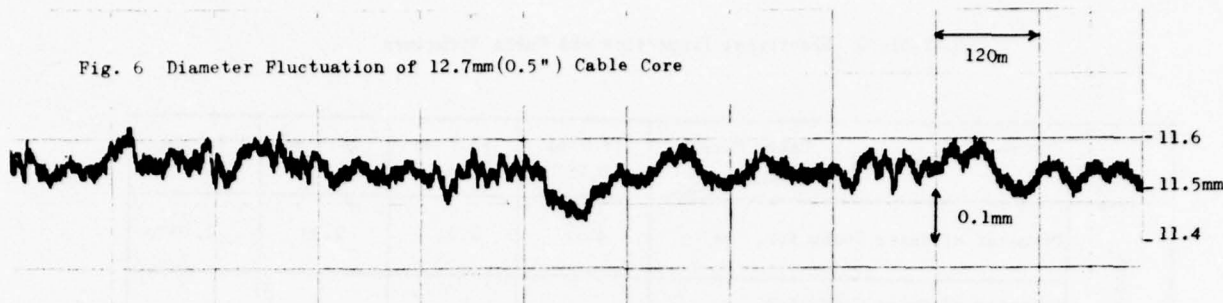
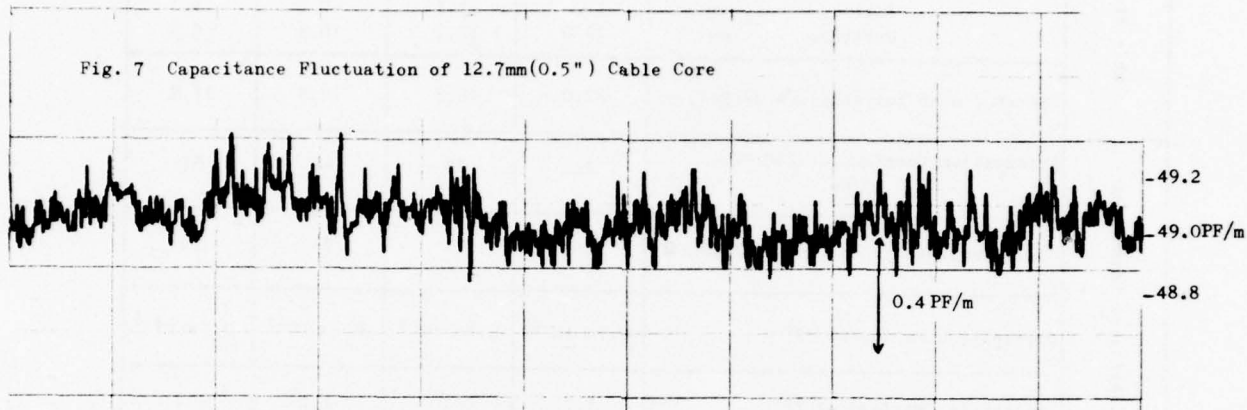


Fig. 7 Capacitance Fluctuation of 12.7mm(0.5") Cable Core



3. PROPERTIES OF CATV CABLES

3-1 Electrical properties

Table 2 shows the electrical properties of four standard sized CATV cables and their cable structures. The frequency characteristics of attenuation constants are shown in Figure 10. The typical S.R.L. frequency characteristics for the four standard sized cables are shown in Figures 11 through 14.

In a comparison of the attenuation constant of the new cable with that of conventional cables (50% expansion ratio), of the same size, the former are lower by approximately 14%. When the attenuation constant is the same, the cable diameter of the new cables is approximately 20% smaller when compared to conventional cables. This clearly indicates that the new cables are more economical than conventional cables.

3-2 Mechanical properties

The properties of minimum bending radius, and pull-out strength are tabulated in Table 3. The bending radius is defined as the minimum bending radius when the characteristic impedance is changed 0.75% (1%) by a bend in the cable.

3-3 Field evaluation

In order to evaluate the practical applications of the new coaxial cables, they were aerially installed in our test field and their electrical properties were measured at regular intervals. No changes in electrical properties have been observed since the installation in July, 1975. This data is provided in Table 4.

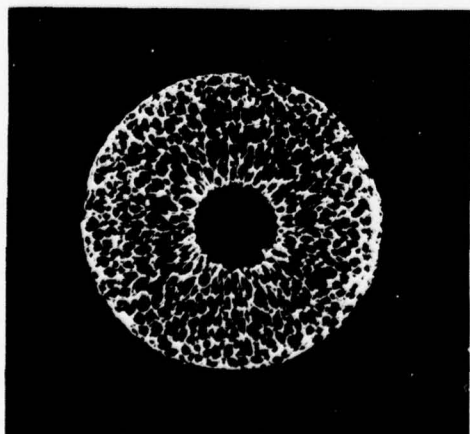


Fig. 8 Cross Section of 0.5" Insulation

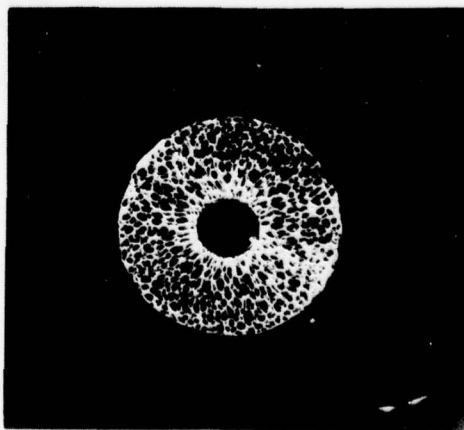


Fig. 9 Cross Section of 0.374" Insulation

Table 2 Electrical Properties and Cable Structure

Items		Cable Size	19.0 mm (0.75")	12.7 mm (0.5")	10.5 mm (0.412")	9.5 mm (0.374")
Cable Structure	Diameter of Inner Conductor, mm		4.32	2.85	2.34	2.10
	Diameter of Outer Conductor					
	Inside, mm		17.2	11.3	9.1	8.3
	Outside, mm		19.0	12.7	10.5	9.5
	Diameter over Polyethylene Jacket, mm		22.0	15.3	12.9	11.9
Electrical Properties	Attenuation Constant at 250 MHz, dB/km		26	38	46	51
	Characteristic Impedance at 10 MHz, Ω		75	75	75	75
	Dissipation Factor at 23°C		0.7×10^{-4}	0.7×10^{-4}	0.7×10^{-4}	0.7×10^{-4}
	Dielectric Constant at 23°C		1.2	1.2	1.2	1.2

Fig. 10 Attenuation Constants vs. Frequency Characteristics

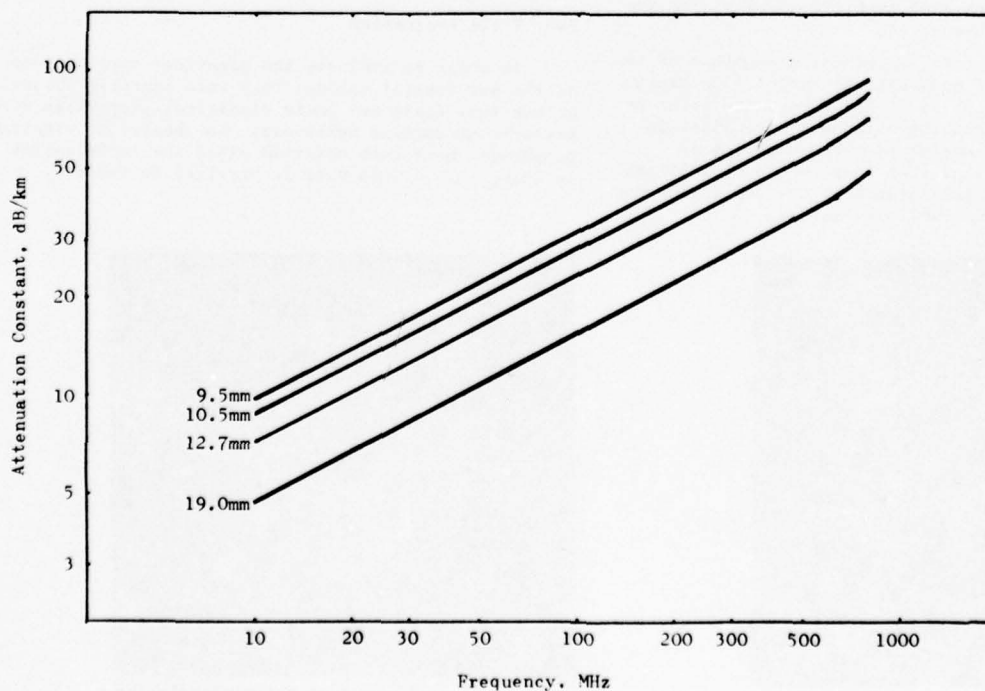


Fig. 11 S.R.L. Frequency Characteristics of 0.75" Cable

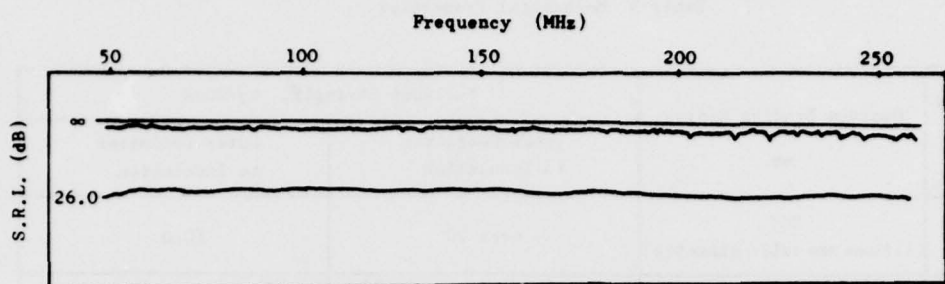


Fig. 12 S.R.L. Frequency Characteristics of 0.5" Cable

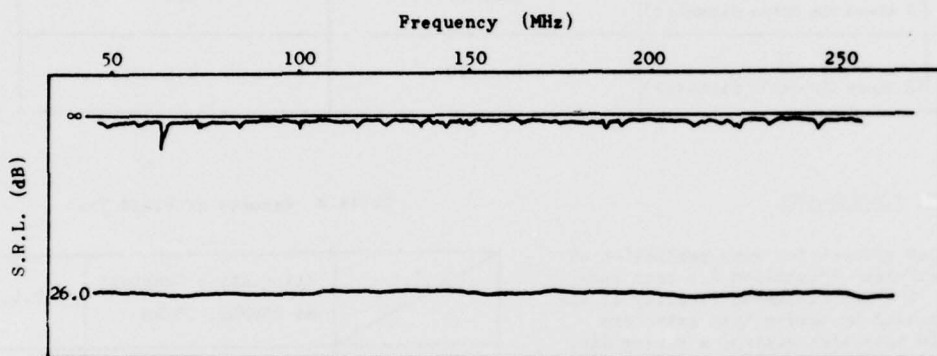


Fig. 13 S.R.L. Frequency Characteristics of 0.412" Cable

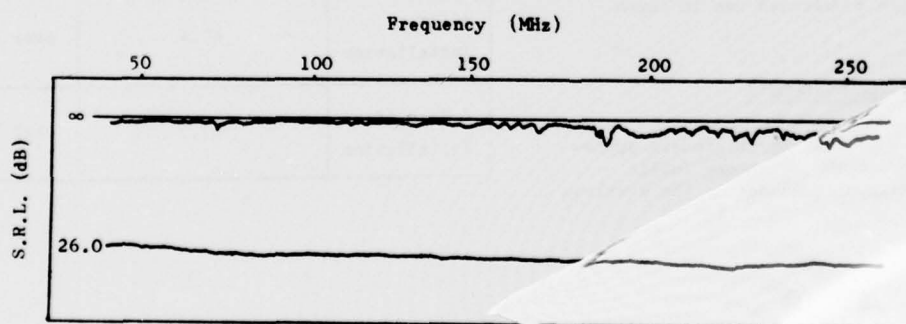


Fig. 14 S.R.L. Frequency Characteristics of 0.374" Cable

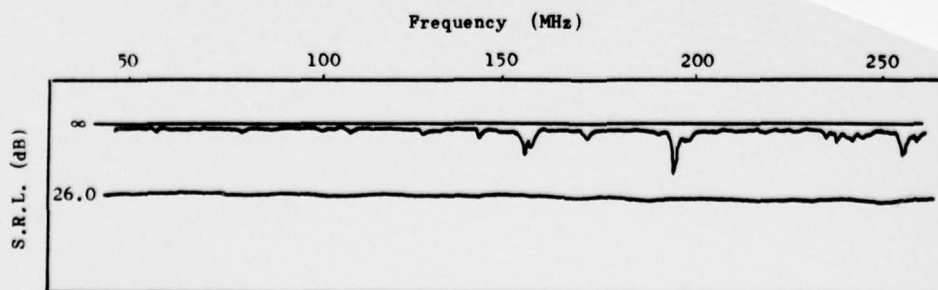


Table 3 Mechanical Properties

Items Size	Minimum Bending Radius, mm	Pull-Out Strength, kg/20cm	
		Inner Conductor to Insulation	Outer Conductor to Insulation
19.0mm (0.75")	207 (11 times the cable diameter)	over 20	10.0
12.7mm (0.5")	119 (9 times the cable diameter)	over 20	7.0
10.5mm (0.412")	86 (8 times the cable diameter)	over 20	5.0
9.5 mm (0.374")	76 (8 times the cable diameter)	over 20	4.5

4. CONCLUSIONS

A stable extrusion process for mass production of highly expanded polyethylene insulation has been successfully developed. The manufacturing facility of the new cable is characterized by tandem type extruders provided with a liquid injection system, a sizing die, and an adhesive applicator. This extrusion line can produce new cable insulation at the equal extrusion speed to that of 50% expanded insulation using a chemical blowing agent.

This cable is now in commercial use in Japan.

5. ACKNOWLEDGMENTS

The authors wish to express their sincere appreciation to Nippon Telegraph and Telephone Public Corporation for its continual guidance in the development of this cable.

6. REFERENCE

1. Y. Toda and T. Nakahara, et al., "A Highly Expanded Polyethylene Insulated CATV Coaxial Cable" 22nd International Wire and Cable Symposium, 1973.

Table 4 Results of Field Test

	Attenuation Constant at 250MHz, dB/km	S.R.L., dB
Before Installation	48.2	over 26.0
After Installation	47.4	over 26.0
A Year After Installation	47.7	over 26.0



Tsuneo Nakahara

Sumitomo Electric
Industries, Ltd.
1 Taya-cho,
Totsuka-ku, Yokohama
Japan

Tsuneo Nakahara received a B.S. degree in electrical engineering and a Ph. D. in engineering from the University of Tokyo in 1953 and 1961 respectively. In 1953, he joined the Research and Development Laboratories of Sumitomo Electric Industries, Ltd. He has worked in the field of microwaves, cybernetics and electronics. He is now General Manager of R & D Group. Dr. Nakahara is a member of the IEE and the Institute of Electronics and Communication Engineers of Japan and the IEEE of the U.S.A. as well as a member of the Japan Technoeconomics Society.



Fumio Suzuki

Sumitomo Electric
Industries, Ltd.
1 Taya-cho,
Totsuka-ku, Yokohama,
Japan

Fumio Suzuki finished the Chemical Engineering Course of Arai High School in Niigata Prefecture in 1958. He joined the Research Division of Sumitomo Electric Industries, Ltd. in 1958, and worked on application research of high polymers especially polyvinyl chloride for wire and cables. Mr. Suzuki is now a staff member of Communications R & D Department, and a member of the Society of Polymer of Japan.



Akiyoshi Tsukamoto

Sumitomo Electric
Industries, Ltd.
1 Taya-cho,
Totsuka-ku, Yokohama,
Japan

Akiyoshi Tsukamoto received his B.S. and Ph. D. degree from Tokyo Institute of Technology in 1952 and 1962 respectively. In 1952, he joined in Electrical Communication Laboratories of NTT pC., where he has worked on development of carrier systems and high speed PCM system. In 1969, he changed to Sumitomo Electric Industries, Ltd. Dr. Tsukamoto is now a Deputy Manager of the Communications Division as well as Manager of the Communication Systems Departments, and a member of the Institute of Electronics & Communications Engineers of Japan.



Tetsuo Miyaziri

Sumitomo Electric
Industries, Ltd.
1 Taya-cho,
Totsuka-ku, Yokohama,
Japan

Tetsuo Miyaziri received his B.S. degree in mechanical engineering from Tokyo University in 1972. He then joined Sumitomo Electric Industries, Ltd., and engaged in development of communication cable manufacturing process. Mr. Miyaziri is now a member of Communications R & D Department and a member of the Japan Society of Mechanical Engineers.



Hiroshi Shimba

Sumitomo Electric
Industries, Ltd.
1 Taya-cho,
Totsuka-ku, Yokohama,
Japan

Hiroshi Shimba received his B.S. degree in applied chemical engineering from Osaka Prefectural University in 1960. He then joined Sumitomo Electric Industries, Ltd., and engaged in research and development of plastic materials for telephone cables, and in manufacturing of plastic cables. Mr. Shimba is now a Chief Research Associate of the Communications R & D Department.



Masao Yuto
(Speaker)

Sumitomo Electric
Industries, Ltd.
1 Taya-cho,
Totsuka-ku, Yokohama,
Japan

Masao Yuto received his B.S. degree in applied chemical engineering from Kyushu University in 1971. He then joined Sumitomo Electric Industries, Ltd., and engaged in research and development of plastic materials, and in manufacturing of plastic cables. Mr. Yuto is now a member of Communications R & D Department.

EXTRUSION OF FLAT MULTI-WIRE COMPUTER CABLE

Charles J. Fetner, Jr.

IBM Corporation
Research Triangle Park, N. C.

Summary

This paper describes a continuous extrusion process used for the production of flat, multi-wire computer cable. The two types of cable extruded are polyethylene and ETFE (ethylene-tetrafluoroethylene). The extrusion equipment, special crosshead, and the process controls used to ensure the extrusion of quality cable are described.

An extrusion process is used at the IBM Research Triangle Park facility for the production of flat-multi-wire computer cable. This cable, used exclusively for signal transmission, is continuously extruded to very close tolerances at speeds up to 50 ft./min. The cross section of a typical flat cable is shown in Figure 1. The plastic materials extruded are polyethylene and ETFE (ethylene-tetrafluoroethylene).

Extrusion Equipment

The cable extrusion complex is shown in the schematic layout of Figure 2 and consists of the following equipment:

Wirerack

The wirerack stores up to 66 spools of wire and feeds the even-tensioned pre-aligned strands to the extrusion crosshead. Each wire is guided from spool to crosshead by a series of guide rolls. The final guide roll is a precision roll that accurately spaces the wires as they are fed into the crosshead. The wire is also cleaned as it passes over the final roll by a directed stream of pressurized air.

Each wire spool rotates on a spindle as the wire is drawn off. An adjustable brake is provided for each spindle to maintain proper tension and is attached to the spindle through a torsion spring so that minor variations in the braking force are dampened.

Extruder System

The extruder system consists of a pellet-storage hopper, an extruder, and an SCR-controlled drive system. The storage hopper, which is automatically vacuum loaded, incorporates a hot-air drying system that allows the feeding of dry, heated pellets to the extruder.

The extruder is of the single-screw type with a 1.5-inch-diameter, 24/1 L/D barrel. Strap-on electric heaters are used to heat the barrel in three zones. Because heat is generated from the shearing action of the feed screw when extruding polyethylene, it is also necessary to be able to cool the barrel. This is accomplished in each zone by pumping water through tubing rolled into the barrel surface. Solenoid valves control the water flow in each zone. Control of the heating and cooling is provided by bidirectional, temperature con-

trollers featuring time proportioning and automatic reset on both heating and cooling. High-precision, platinum-wire resistance sensors are located in the three zones. Temperature of the barrel is maintained within $\pm 1.5^\circ$ C of the set point. The extruder feed screw is a specially designed "Barrscrew". Its significant features are modified flight widths and a flight melt channel. Performance of this screw is excellent. Only the lowest possible melt temperature is required, and melt temperature and pressure is very uniform. The screw is not internally cooled.

The feed screw is driven by a 15 HP, SCR-controlled DC motor. The drive motor is a shunt-wound DC motor, the speed of which may be adjusted over a wide range by controlling the armature voltage.

A screen pack is used not only to filter contaminants but also to increase back pressure over the screw. The higher pressure tends to level out the inherent screw surges, particularly with lower viscosity melts. A pneumatically operated changer is used so that a new screen pack can be inserted without disassembly.

Crosshead

The crosshead accurately guides the wires into two convergent, extruded streams and gives final shape to the cable prior to quenching. It is machined to extremely close tolerances. The construction and design of the crosshead is schematically presented in Figure 3. A particularly salient feature of the crosshead is the hinged, book-opening type of construction that allows easy access for cleaning and wire loading. Lateral alignment of the upper and lower crosshead sections is possible through adjustment of the hinge pin, which has 0.006-inch eccentricity.

The internal sprue path is so designed that uniform melt flow is attained through the crosshead. As seen in Figure 3, helically grooved sprue pins are positioned at a 45-degree angle to the initial melt flow paths and divert the melts parallel to the wire. The melts and wire meet at the front of the crosshead. A spatial representation of the melt flow paths between the inlet and exit of the crosshead is shown in Figure 4.

Construction and design of the internal wire guides and profile dies can be seen in Figure 5. The grooves in the lower wire guide are precision machined to a tolerance of ± 0.0004 inch to provide the wire-spacing accuracy required. The profiling grooves are located between the wires to assure that the shaped cable shrinks toward the wires during quenching.

The crosshead used for extruding polyethylene was fabricated essentially from hardened Type 420 stainless steel. Some warpage was encountered after several years service,

but this problem was solved by flame spraying the affected areas with molybdenum and grinding to shape. The higher extrusion temperature and corrosive nature of ETFE required the use of Hastelloy for the crosshead. Screws and dowels were fabricated from Duralnickel.

Appropriately located calrod heaters are used to heat the crosshead. Temperature controllers are again time proportioning with automatic reset and use platinum resistance sensors.

Quench Tank

The quench tank provides controlled cooling for the cable after it leaves the crosshead. As shown in Figure 2, the tank is in two sections: the initial quench section containing flowing hot water and the last section flowing cold water. The water is heated by a submerged electrical heater. The temperature controller has true time proportioning with automatic reset and uses a resistance-type sensor.

A gauge and metering station is mounted on the exit end of the tank to continuously monitor cable footage, width, and thickness. The gauging is accomplished by two dial indicators and the metering by a wheel-activated micro-switch.

Haul Off

The commercial haul off pulls the extruded cable at a controlled speed from the crosshead through the quench tank. The two endless rubber belts that pull the cable are driven by a variable-speed DC motor. Power for the motor is supplied by a power module, which also serves as a speed regulator. The voltage delivered to the armature is determined by the reference voltage from the operator's control potentiometer, the tachometer output, and the power-amplifier output in such a way as to maintain motor speed within 1% for any potentiometer setting.

Rewind

The rewind continuously winds the cable onto cardboard reels. Two separate capstans are provided to facilitate changing reels without causing unnecessary interruption of the process. The eddy-current drive consists of an AC, constant-speed induction motor with an integral, variable-torque, eddy-current clutch. In the particular speed range for this application, the unit delivers essentially a constant torque.

Control Station

The control station centrally locates the main-power input and shutdown systems, extruder and haul-off drive controls (10-turn potentiometers), and the following indicators: melt-pressure, melt-temperature, drive-motor-load, extruder-screw-rpm, haul-off-speed, crosshead-and-extruder-temperature, hot-water-quench-temperature, and cable-footage.

Cable Raw Materials

The polyethylene used is a high-density, flame-retardant type with a melt index of 0.40 to 0.75 g/10 minutes (190 C) and a melt point of 118.0 ± 3.0 C. It is supplied in the form of diced pellets of a specified density and size.

ETFE is supplied as flat pellets with a melt-index range of 6.0 to 11.0 g/10 minutes (297 C) and an endotherm peak of 267 C. Pellet density and size are also controlled.

The wire is silver-plated, oxygen-free copper with a diameter of 0.0071 ± 0.0001 . Minimum elongation is 15%.

Process and Quality Controls

For a certain die size, the physical dimensions of extruded polyethylene cable are determined principally by melt-flow and quench rates, and haul off speed. These are in turn affected by screw speed, melt viscosity, pellet density, melt temperature, length of air quench, and temperature of hot-water quench. However, by using accurate screw-drive and uniform extrusion-temperature controls, along with specification-grade polyethylene, cable dimensions are readily maintained by adjusting the quench water temperature. Cable width and thickness are continually measured in-line with dial indicators and additional checks are made with a hand micrometer and optical comparator.

Quench characteristics of extruded ETFE are somewhat different from those of polyethylene. Dimensional control depends more on die size and extrusion speed and is more difficult to maintain. Flattening of the cable just prior to water quench (see Figure 2) is required for ETFE to prevent excessive curling.

Parallel- and horizontal-wire alignment are controlled mainly by the wire guides. Excessive wear to either the lower or upper wire guide allows the wires to float to an out-of-tolerance position. A sample from each reel of extruded cable is checked for alignment with an optical comparator or by visually examining a cross-section. Wire guides are replaced as required.

Normally, the extruder is operated in "manual mode". In this mode, the operator will manually shutdown the operation to correct an out-of-tolerance condition. However, an error-detection system is available to automatically shutdown the extruder when such a condition occurs in "automatic mode". Feedback is provided by the in-line gauging station.

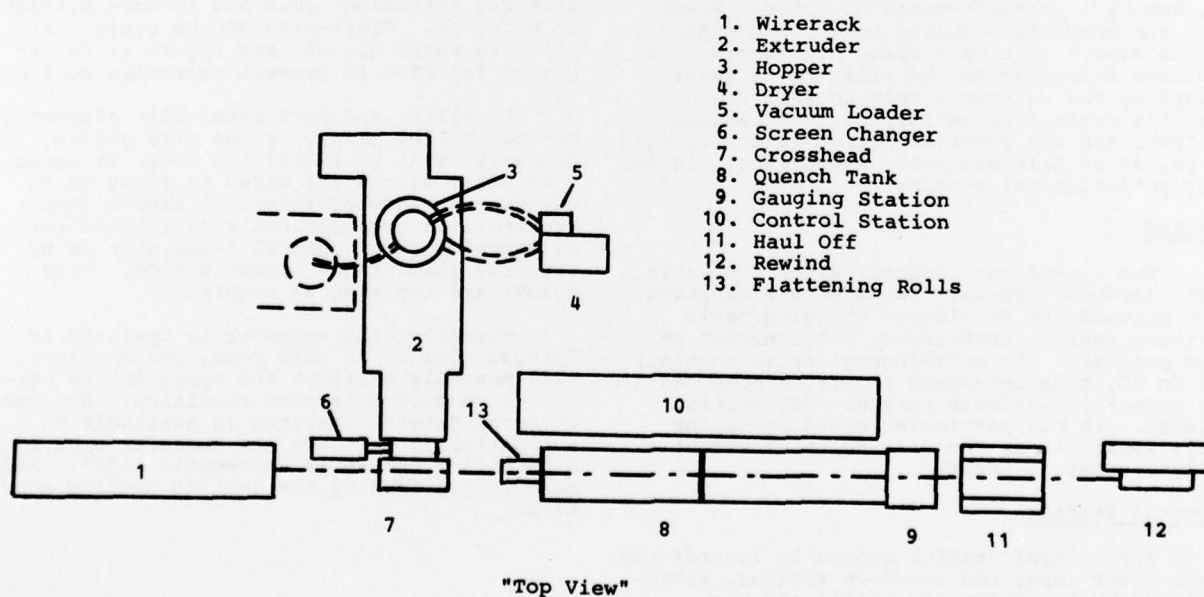
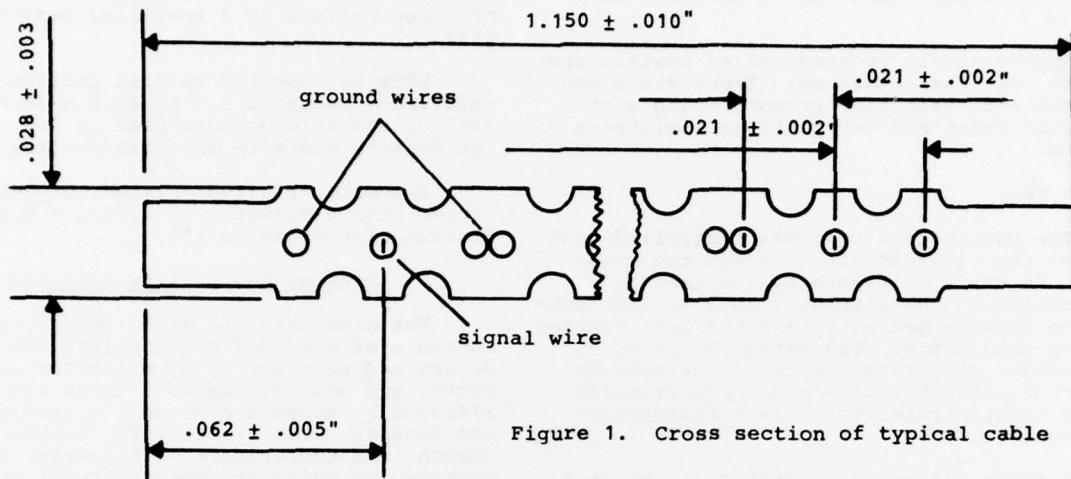


Figure 2. Schematic layout of extrusion complex

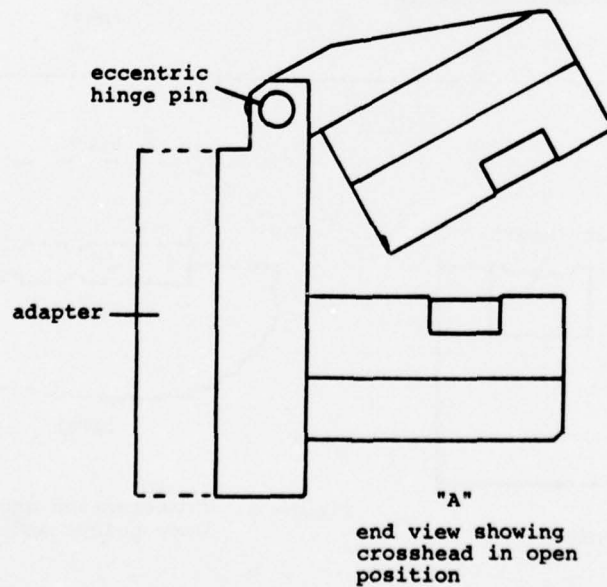
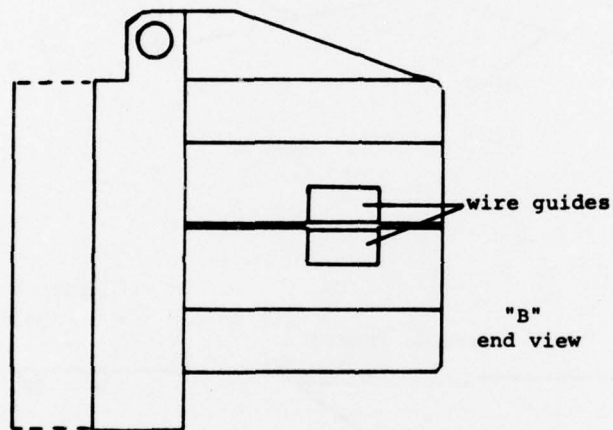
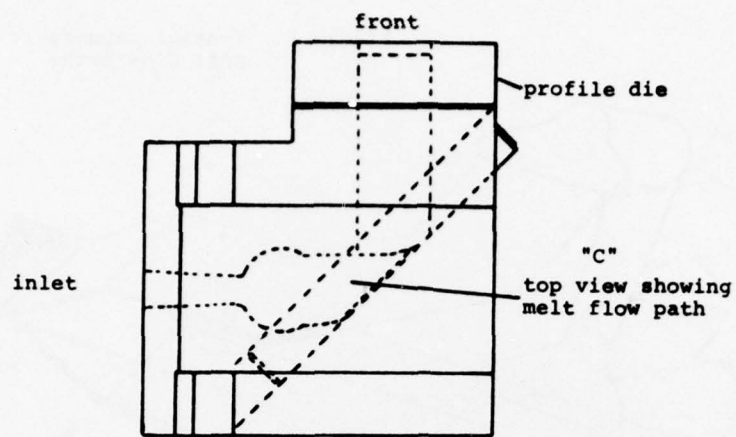


Figure 3. Construction and design of crosshead

Figure 4. Spatial representation of melt flow paths

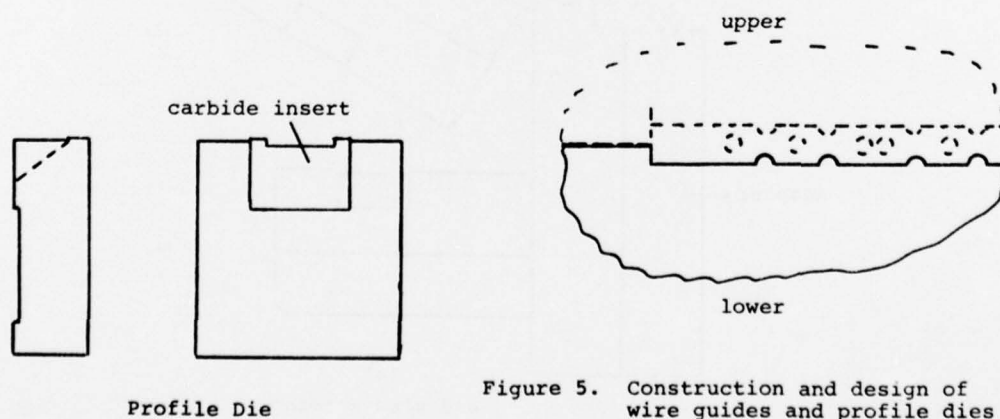
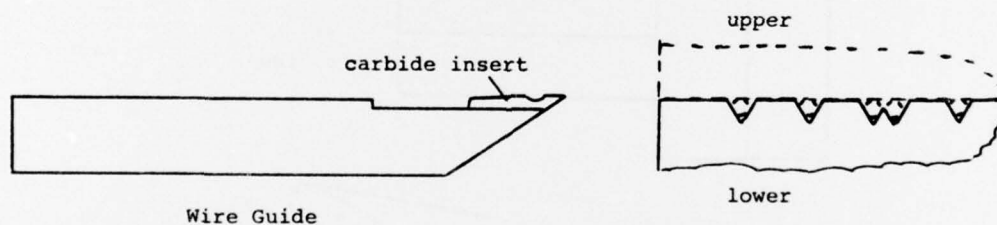
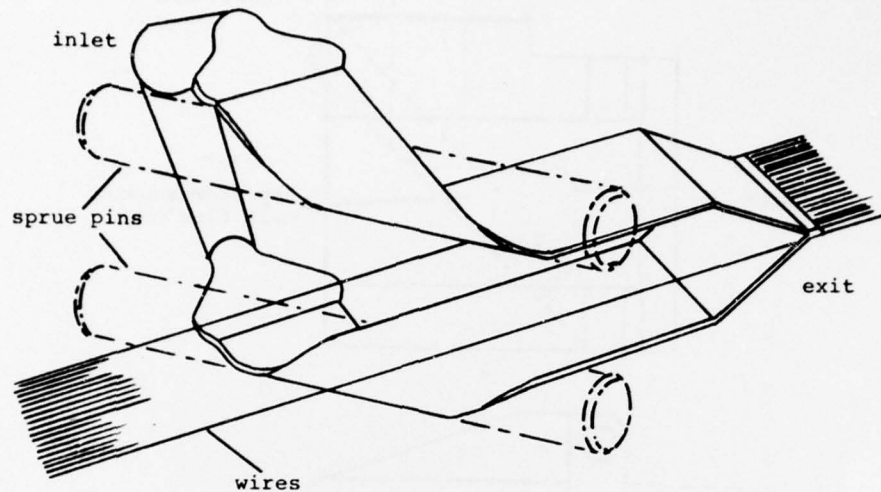


Figure 5. Construction and design of wire guides and profile dies



Charles J. Fetner, Jr.
Dept. 327/S904
IBM Corporation
P.O.Box 12195
Research Triangle Park, N.C. 27709

Charles J. Fetner, Jr. is employed by IBM Corporation, Systems Communication Division, Research Triangle Park, N.C. A staff engineer in process engineering, he has a BS and MS in chemical engineering from North Carolina State University. His present work is in computer cable manufacturing.

SPACE-SAVING TELEPHONE WIRE EXTRUSION LINES WITH VERTICAL COOLING AND SHARED AUTOMIZED REEL TAKE-UP

Sigurd Nordblad

Telefonaktiebolaget LM Ericsson
Telephone Cables Division
Älvsjö Sweden

Summary

An extrusion system is described where the cooling trough is arranged vertically which saves a considerably big amount of floor space. At the same time the cooling can be achieved in an effective way by using a combination of water mist and air streams.

The reel changing is made by a device which can serve up to ten extrusion lines simultaneously. The device can also be programmed to deliver full reels at different locations, and catch empty reels at a centralized storing place.

Introduction

In conventional extrusion lines for telephone wires, the cooling trough is arranged horizontally, occupying a considerable floor space. The walking distance along a line and between adjacent lines limits for the operator the possibilities of simultaneous watching the processing units of a line or a group of lines.

In the currently used types of dual take-up, the automatized reel changing system works only for a rather short period of time. Though this part of the take-up unit represents a big part of the costs, it is inactive during the reel filling time, and the investment cost is multiplied by the number of lines. The take-up deliver the full reels just outside the unit and a transportation and distribution operation must be done before the reel is ready for next operation.

A vertical arrangement of the cooling trough is a drastic step for saving floor space. The idea is based on a moderate speed system where the components of the line are designed accordingly.

Optimal extrusion speed

When thermoplastic insulation for telephone wires came in use, it was found that extrusion permitted a rather high production speed compared to, for instance, paper lapping machines. The investment cost for an extrusion line is high and efforts to increase the economy has therefore been concentrated towards even higher speeds. Increased speed is not only a question of solving technical problems, it is also a question of rapidly increasing costs for the machines. More scrap is produced and the product will suffer in quality due to variations in wire elongation etc. Increased speed is not necessarily the only way to improved economy, another way is to match speed, machine-complexity, scrap, quality etc, and thus find an optimal solution.

An investigation of speed used in the factories today throughout the world, indicates

that for ordinary telephone wires, a speed of 1000-1500 m/s is usually used, even if the lines are designed for higher speed.

It is difficult to say if there exists a theoretical upper limit in speed, but friction in cooling trough, ballbearings, vibration etc certainly not are possible to completely overcome.

An extrusion line consists of many different components. Let us study just one of them according to fig 1. A pulley is fixed on a springloaded swing arm and the wire is taken up on a reel, which has one flange not exactly perpendicular to the rotating shaft. This causes an eccentricity of the material taken up on the reel. Due to the eccentricity of the take-up, the pulley will be accelerated and decelerated, and the mass reaction of the pulley will cause a tension in the wire. As can be seen from fig 1, the tension very rapidly reaches values, where permanent elongation of copper conductor occurs.

Even if the reel is perfect, the layers of the conductor cannot be perfect. This is illustrated in fig 2. With a diameter of about 1,5 mm of the insulated conductor an eccentricity of 3-4 mm easily arises, and also under these circumstances a notable tension will occur.

The simplified example above indicates that unavoidable difficulties already begin at a speed of about 1000 m/min. This corresponds fairly well with a general experience.

Vertical extrusion

If a high quality extrusion is wanted, a max speed of 1000 m/min is reasonable. To make this speed competitive to faster running lines the components of the line must be designed for that speed and not more, and some other approaches must also be done. Vertical extrusion is one. The cost for the cooling trough is low as long as the height up to the factory ceiling is used. This length is generally fairly short, but sufficient for extrusion speeds up to about 1000 m/min because the comparatively short length can be compensated by a special cooling system, which only the vertical arrangement permits. The cooling is achieved in a closed system by air streams and water mist.

The extruder in a vertical extrusion system can be the same as in a conventional, horizontal line and the extruder head is also the same, but turned 90° upwards. Only small modifications of the die may be done. The cooling trough, however, must be designed in another way which also gives a more efficient cooling effect.

In a vertical system the insulated conductor is completely free-running between the extruder die and the upper pulley. The cooling trough consists of two concentric tubes according to fig 3.

The space between the tubes is connected to an air pressure system, and air is pressed into the inner cooling tube through a number of dies with small diameter. The inner surface of the cooling tube is flooded with water, coming from the top of the tube. The water is covering the air dies and thereby converted to mist. Air streams and mist are cooling the wire effectively and no heat insulating water film can develop on the wire surface.

The air pressure and the die dimension are chosen so that the air temperature after expansion is approximately -20°C . Therefore the water mist also will have a low temperature. The water is circulated in a closed system according to fig 4. Since the total water quantity is fairly low, the temperature of the water rapidly reaches an operational temperature of about $+5^{\circ}\text{C}$, regardless the ambient temperature. The water temperature is held constant by adding water from an outer source, and loss of water is compensated from the same source.

The cooling system is not only an efficient one, it is also efficiently controlling water temperature. It is therefore well suited for use in tropical areas or places with big difference in night and day temperature, as well as in areas with big seasonal temperature difference.

No common cooling device and big water tanks are necessary. The air stream has two functions; first the cooling effect of the plastic material and second to absorb the developed heat in the system and keep the system at a low temperature level. Since the air is an important part of the cooling system, it is necessary that the air pressure is kept at a constant level.

Take-up system

Today most take-ups for extruded telephone cable wire have a fully automatized dual system. They have a reel changing system, which is in operation a very short time compared to the total working time of the line. In a moderate speed line the disadvantage of an expensive change-over device is even more pronounced.

The take-up design has drawn advantage of the moderate speed and no extra costs are built in by foreseeing high speeds, which in practice never will be used. A tendency to claim the possibility of high speeds is today sometimes presented, but the user mostly do not use the high speed. Our take-up has the wire-change-over system built in, but no reel-changing arrangement. Instead, a shared reel distributor device is developed. The reel distributor can serve up to ten extrusion lines, and it also distributes full reels to storing places according to a given programme and picks up empty reels from another place. When only a few lines are in use, the reel distributor is probably not justified and the reels are changed manually. Later, when the

number of lines may have increased, the reel distributor can be installed. In this case, the take-up system not only delivers full reels, it also participates in transportation and sorting reels according to a predetermined programme. The cost for this device is shared by the participating lines. It is foreseen that even after installing the reel distributor, the manual handling can be made if the distributor fails. Maintenance of take-up can also be made during fully automatized operation of the other lines. A take-up with reel distributor in action is illustrated in fig 5.

Economy of vertical extrusion

The vertical extrusion line is working with a moderate speed, which gives the product a high quality. Variations and amount of permanent elongation is low and plastic material performs better at low speed. Those circumstances are difficult to evaluate in economical terms, but they must be considered when comparison is made to high speed systems.

There are, however, other costs that can be calculated and a comparison is made in fig 6, with a conventional line where wire drawing and annealing in tandem are included. In the vertical line system conductor drawing and annealing are included, but as a separate operation with a wire speed obtainable for single working drawing machines.

A comparison cannot be generalized, local conditions must always be considered. Factory building costs, workers cost, energy cost etc are unlike from place to place. Fig 6 gives not only relation to costs between vertical line system and tandem line, it also presents the relation between the different cost sources within each system. The cost relation is presented as relative cost per produced equal quantity. Under these circumstances fig 6 indicates the following:

Machine cost

The lower speed of vertical extrusion is compensated by low cost for the take-up system as well as by higher efficiency of the conductor drawing section.

Floor cost

Here arises a considerable reduction of costs, about 55 %. Floor cost is of special interest concerning existing buildings. An extension of the building can be comparatively expensive since very often space not only for an extrusion line but a whole section must be built.

Working cost

A cost reduction of about 50 % can be reached. In conventional tandem lines an operator can control up to two lines, partly because big working area and partly because complicated start up work after wire break etc. With vertical extrusion the working area is compacted, lack of drawing machines and easiness of starting up combined with less disturbances makes it possible for one operator to operate five lines simultaneously.

As an example of the convenience of the line can be mentioned that feeding the cooling trough with a new conductor is achieved with a plastic ball to which the conductor is fastened, and then shot through the cooling tube system with air pressure. For this operation the worker needs not to take one step!

In working cost is also wire drawing included with high efficiency drawing machines.

Power cost

The electric power is needed mainly for plasticizing the material and extrude it over the conductor. The need is therefore more or less equal, but lower speed and lower power consumption in the take-up reduce the total power cost slightly.

Air cost

The consumption of air in the vertical extrusion line is higher, but air is an essential part of the cooling system and replaces other cost consuming water cooling arrangements.

Water cost

Water consumption and circulation are in both cases comparatively low but is of pronounced favour to the vertical system.

Scrap cost

Scrap represents an essential part of the economy. In fact, the scrap is the most important problem concerning the development of high speed lines, especially in tandem systems. A problem lies also in the fact that even if exact costs can be calculated for machine investments, floor cost etc, the calculation of scrap costs is a rather uncertain estimation. Very often the calculated figures for high speed lines are too optimistic.

Total cost

Considering all costs it is found that the vertical system can be run about 20 % cheaper compared to horizontal tandem lines.

Conclusion

Vertical extrusion has for some time been in full operation in our factory at Piteå, Sweden, and has proved to work satisfactorily in practice. The production cost is lower, at the same time due to the moderate speed, a high quality product is achieved.

Almost in every respect the cost is lower for vertical extrusion compared to tandem lines and the system solves very often investment problems, both when new factories are designed as well as in existing plants where costs for extended floor space very often is prohibitive.



S.S. Nordblad
Technical Manager
Telefonaktiebolaget LM Ericsson
Telephone Cables Division
S-125 20 Älvsjö
Sweden

S.S. Nordblad, graduated in 1947 at the Royal Institute of Technology, Stockholm, whereafter he joined Sieverts Kabelverk, Sweden. In 1956 he joined as technical manager IKO Kabelverk, Sweden and 1966 Latinoamericana de Cables S.A., Mexico, a company operating with the LM Ericsson group.

Since 1968 at LM Ericsson in the Telephone Cables Division, Stockholm.

S.S. Nordblad presented CROSS STRANDING at the Wire and Cable Symposium, Atlantic City, 1971.

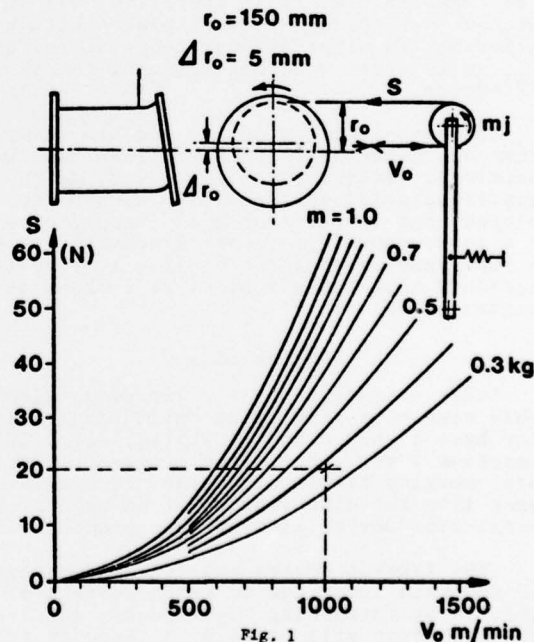


Fig. 1

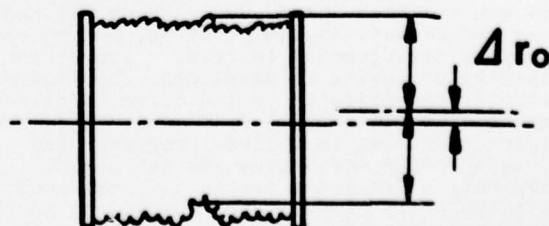


Fig. 2

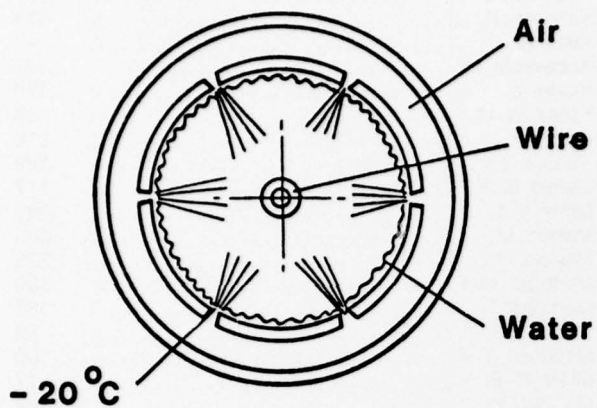


Fig. 3

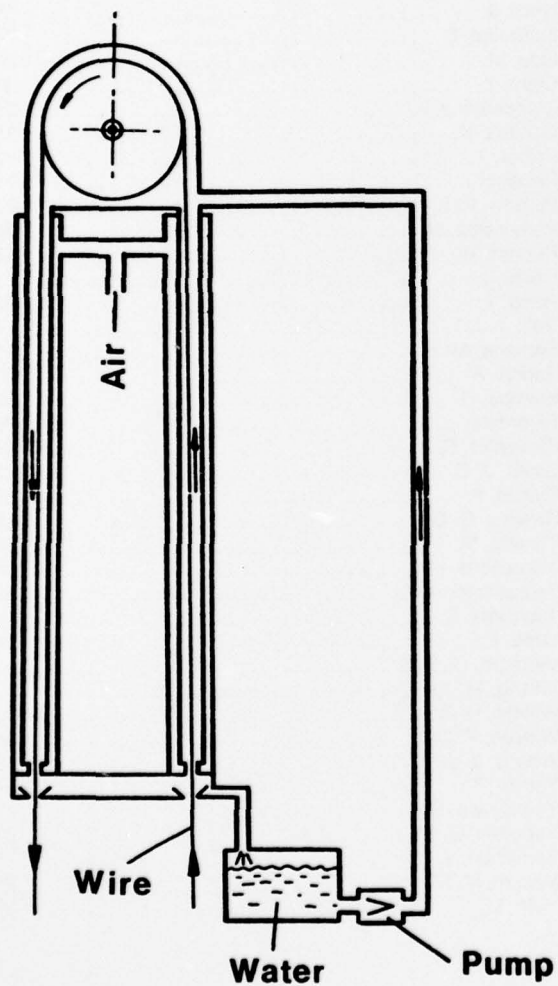


Fig. 4

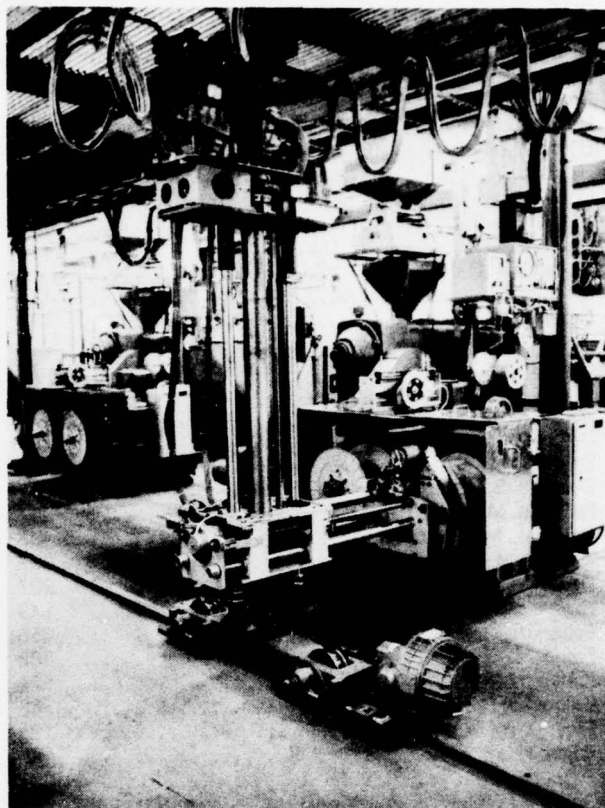


Fig. 5

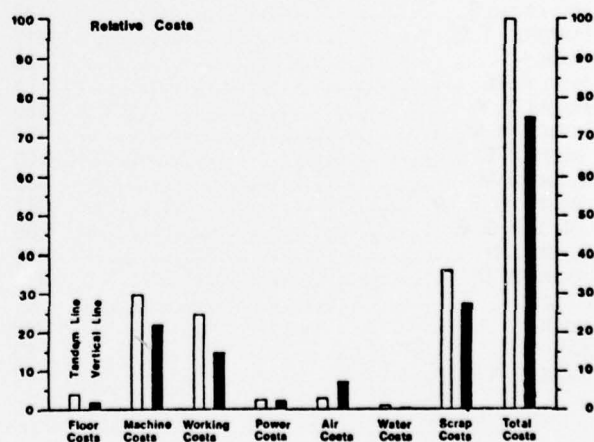


Fig. 6

AUTHOR INDEX

Aloisio, C. J.	272	Kaufman, S.	291
Ance, L.	138	Kimmich, K.	323
Anderson, E. W.	296	Kishi, H.	47
Azuma, M.	312	Kobayashi, H.	333
Bair, H. E.	296	Koide, Y.	340
Bayles, F. D.	207	Korez, W. H.	56
Beach, S. M.	317	Krahn, F.	216
Beyreis, J. R.	291	Kubota, Y.	129
Biggs, J. W.	350	Lavoie, G. K.	117
Bow, K. E.	302	LeNir, V. L.	380
Brewer, M. L.	108	Makiyo, M.	333
Carefoot, D. B.	317	Maklad, M.	223
Carlson, A. D.	12	Maringer, M. F.	350
Calzolari, P.	174	Maruoka, T.	185
Cogelia, N. J.	117	Mathieu, R.	82
Colter, L. G.	302	McIntosh, T. F.	100
Cubero, M.	370	Miller, H. E.	17
Cueto, A.	370	Miyaziri, T.	394
Daane, J. H.	296	Molleda, L.	158
Dagleish, J. F.	240	Nagasawa, T.	47
Davidson, D. L.	265	Nakahara, T.	394
Dean, N. S.	247	Nantz, T. D.	100
DeLucia, M. A.	281	Nelson, E. D.	272
Dembia, M. R.	32	Niwa, J.	185
Dougherty, T. S.	387	Nordblad, S.	408
Dudley, M. A.	207	Oda, M.	312
Evans, M. N.	143	Oishi, Y.	312
Falter, J. A.	356	Olszewski, J. A.	235
Fetner, C. J.	402	Oshima, K.	185
Forleo, M. B.	174	Peltier, Y.	82
Franey, J. P.	63	Peveler, J.	199
Frey, D. R.	125	Pinnow, P. E.	350
Fujita, H.	47	Pomerantz, M.	226
Fuse, K.	312	Purkert, W.	32
Gabriel, A. P.	199	Radar, L.	74
Garvalena, A.	370	Reed, T.	223
Ghazi, A. J.	82	Refi, J. J.	91
Glahn, J. F.	117	Santana, M. R.	152
Godts, J. E., Dr.	149	Sarkar, A.	235
Gonthro, G. F.	317	Shimba, H.	394
Graedel, T. E.	63	Skjordahl, J. W.	291
Hale, A. L.	152	Slaughter, R. J.	247
Hardee, A. G.	125	Smith, J. C.	226
Hennig, J.	328	Suzuki, F.	394
Hiramatsu, S.	185	Swasey, C. C.	68
Hodgson, T. C.	317	Takada, M.	340
Holte, N.	25	Takashima, H.	47
Horn, F. W.	1	Tsukamoto, A.	394
Huang, Y. Y.	235	Tsurutani, S.	47
Hutson, H. M.	138	Used, E.	158
Isaacs, J. C.	100	Vermont, G. S. B.	21
Ishibashi, M.	333	Villarig, M.	1
Jensen, W. F., Jr.	257	Walker, H. D.	36
Johnson, G. E.	296	Warren, P. C.	356
Jones, J. N.	257	Woods, J. J.	199
Jones, W. D.	362	Yabuki, T.	340
Judy, A. F.	91	Yamakawa, S.	129
Kaide, T.	340	Yaniziski, G. M.	272
Kao, C.	223	Yamazaki, Y.	47
Karst, K. A.	42	Yocum, M. M.	291
		Yuto, M.	394



INTERNATIONAL WIRE & CABLE SYMPOSIUM

SPONSORED BY U.S. ARMY ELECTRONICS COMMAND

15, 16 & 17 November 1977

Cherry Hill Hyatt House, Cherry Hill, N.J.

Please provide in the space below a 100-500 word abstract (12 copies) of a proposed technical paper on such subjects as design, application, materials, and manufacturing of Communications and Electronics Wire & Cable of interest to the commercial and military-aerospace industries. Such offers should be submitted no later than 4 April 1977 to the Commanding General, U.S. Army Electronics Command, Att: DRSEL-TL-ME, Ft. Monmouth, NJ 07703.

Title: _____

Authors: _____

Company: _____

Address: _____